PART 1: DEVELOPMENT TOWARDS A POTENTIAL ANTI-PERTUSSIS
GLYCOCONJUGATE VACCINE; PART 2: BINDING AND MITIGATION OF
CYTOTOXICITY OF AMYLOID BETA AND TAU OLIGOMERS BY HEPARIN

By

Peng Wang

A DISSERTATION

Submitted to
Michigan State University
in partial fulfillment of the requirements
for the degree of

Chemistry−Doctor of Philosophy

2018

ABSTRACT

PART 1: DEVELOPMENT TOWARDS A POTENTIAL ANTI-PERTUSSIS
GLYCOCONJUGATE VACCINE; PART 2: BINDING AND MITIGATION OF
CYTOTOXICITY OF AMYLOID BETA AND TAU OLIGOMERS BY HEPARIN

By

Peng Wang

Despite massive vaccination, the world has been experiencing a resurgence of pertussis, a highly contagious respiratory disease. Current acellular vaccines lack sufficient bactericidal activity and there is an urgent need of better vaccines aiming at clearing the pathogen, *Bordetella pertussis*. Oligosaccharide on the surface of the bacteria has been proven to be a promising protective antigen that elicits antibody-mediated complement-dependent cytotoxicity against *Bordetella pertussis*. However, obtaining the saccharide on a large scale with high purify remains one of the main obstacles. Herein, we report the first total synthesis of a pentasaccharide antigenic determinant from *Bordetella pertussis*. Immunization of mice with a conjugate of the pentasaccharide with a carrier protein, bacteriophage Qβ, elicited high titers of IgG antibodies. An IgG subclass study showed that it induced Th1-weighted immune response. The antibodies were able to bind *Bordetella pertussis* in flow cytometry and induced complement-dependent cytotoxicity. Further study will be focused on the epitope mapping on the pentasaccharide and optimization of the antigen structure.

Accumulation of amyloid β in the brain is believed to play a key role in the pathology of Alzheimer's disease and it is one of the most important biomarkers in the early diagnosis of AD. Glycosaminoglycans have been found to participate in the process of Aβ aggregation. Herein, we

report the study on the interaction between Aβ and superparamagnetic iron oxide nanoparticles coated with heparin, a member of the GAG family. The interaction between Aβ and nanoparticle was studied through enzyme-linked immunosorbent assay, gel electrophoresis and thioflavin T assay. Furthermore, the nanoparticle showed no toxicity against neurons and effectively protected neurons from Aβ, which made it a potential tool in the detection of Aβ *in vivo*.

Neurofibrillary tangles formed by intracellular aggregation of tau proteins are another important hallmark of Alzheimer's disease. However, recent studies have suggested that tau oligomers, rather than neurofibrillary tangles, are playing a key role in the progression of the disease. Glycosaminoglycans can mediate the intercellular propagation of tau proteins. Herein, we report the synthesis of heparin-like oligosaccharides with different lengths and sulfation patterns. Binding assays with tau oligomers revealed that longer backbones and higher sulfation degrees resulted in stronger binding affinity. The oligosaccharides promoted aggregation of tau oligomers and effectively protected SH-SY5Y cells against tau oligomers.

Suttipun Sungsuwan, for all they have done for me, which has helped me greatly in adapting to the experiments and the new life in the United States. I also want to thank the current members, Qian, Weizhun, Xuanjun, Jicheng, Zeren, Mehdi, Sherif, Jia, Shuyao, Zibin, Changxin, Yuetao, Kedar, Tianlu, Zahra, Mengxia, Hunter, Setare, Shivangi, Kunli. As I said before, I would never have made it through the difficult times without your company and friendship over the years. It is also true for all my friends at MSU including Yubai, Xiaopeng, Yi, Jun, Wei, Xinliang, Hadi, Yukari, Xiaoxiao, Wenjing, Chengpeng, Yongle and many more people.

Finally, I want to thank my family, especially my parents, for their unconditional support and love throughout my life. I am so excited to have a chance to go back to China and share my success with them, before I depart again from home and step onto the next stage in my career.

Thank you,

Peng Wang

TABLE OF CONTENTS

LIST OF TABLES

LIST OF FIGURES

concentrations of Hep-SPION. The percentage was calculated by dividing the intensity of the low molecular weight   oligomer band by the sum of the intensities of all bands in the specific lane.

LIST OF SCHEMES

KEY TO ABBREVIATIONS

7-AAD	7-aminoactinomycin D
AAT	2-acetamido-4-amino-2,4,6-trideoxygalactose
ACT	adenylate cyclase toxin
Ac_2O	acetic anhydride
AcOH	acetic acid
AD	Alzheimer's disease
AFM	Atomic force microscopy
AgOTf	silver trifluoromethanesulfonate
aP	acellular pertussis
APC	antigen-presenting cells
ATCC	American Type Culture Collection
BAIB	bis(acetoxy)iodobenzene
$BF_3 \cdot Et_2O$	boron trifluoride etherate
Bn	benzyl
BSA	bovine serum albumin
Bz	benzoyl
Cbz	benzyloxycarbonyl
CDC	Centers for Disease Control and Prevention
COSY	correlation spectroscopy

CSA	camphorsulfonic acid
DBU	1, 8-diazabicyclo[5.4.0]undec-7-ene
DCM	dichloromethane
DDQ	2, 3-dichloro-5, 6-dicyanobenzoquinone
DIAD	Diisopropylazodicarboxylate
DIPEA	diisopropylethylamine
DLS	dynamic light scattering
DMAP	4-dimethylaminopyridine
DMEM	Dulbecco's Modified Eagle Medium
DMF	dimethylformamide
DMSO	dimethyl sulfoxide
DTPads	diphtheria, tetanus toxoids and whole-cell pertussis vaccines on alum
DTT	dithiothreitol
EDC·HCl	1-ethyl-3-(3-dimethylaminopropyl) carbodiimide hydrochloride
ELISA	enzyme-linked immunosorbent assay
ESI-MS	electrospray-ionization mass spectrometry
Et_3N	trimethylamine
FAB	fast atom bombardment
FACS	fluorescence-activated cell sorting
FBS	fetal bovine serum
$Fe(acac)_3$	ferric acetylacetonate

$FeCl_2 \cdot 4H_2O$	ferrous chloride tetrahydrate
$FeCl_3 \cdot 6H_2O$	ferric chloride hexahydrate
FHA	filamentous hemagglutinin
FPLC	fast protein liquid chromatography
Fuc2NAc4NMe	2-acetamido-4-*N*-methyl-2,4,6-trideoxy-galactose
GAGs	glycosaminoglycans
GlcA	glucuronic acid
GlcN	glucosamine
GlcNAc	2-acetamidoglucose
HCl	hydrochloric acid
Hep-SPION	heparin-coated superparamagnetic iron oxide nanoparticles
H_2O_2	hydrogen peroxide
HPLC	high performance liquid chromatography
HRMS	high resolution mass spectrometry
HRP	horseradish peroxidase
HS	heparan sulfate
HSF-LPF-IAP	histamine-sensitizing, lymphocyte-leukocyte-promoting and islet-activating
HSQC	heteronuclear single quantum correlation
IACUC	Institutional Animal Care and Use Committee
IdoA	iduronic acid

IgG	Immunoglobulin G
kDa	kilo-dalton
Kdo	3-deoxy-D-manno-2-octulosonic acid
KLH	keyhole limpet hemocyanin
KPB	potassium phosphate buffer
LDH	lactate dehydrogenase
LevOH	levulinic acid
LiAlH$_4$	lithium aluminum hydride
LiOH	lithium hydroxide
LOS	lipooligosaccharide
LPS	lipopolysaccharide
mAb	monoclonal antibody
MALDI-TOF	matrix assisted laser desorption ionization-time of flight
ManHep	mannoheptose
Man2NAc3NAcA	2,3-diacetamido-2,3-dideoxy-mannuronic acid
MD	molecular dynamics
MeI	methyl iodide
MPLA	monophosphoryl lipid A
MS	mass spectrometry
NaN$_3$	sodium azide
NFTs	neurofibrillary tangles

NH$_4$OH   ammonium hydroxide

NHS   *N*-hydroxysuccinimide

NIS   *N*-iodoxuccinimide

NMO   4-methylmorpholine *N*-oxide

NMR   nuclear magnetic resonance spectroscopy

OD   Optical density

OsO$_4$ osmium tetraoxide

PAGE   polyacrylamide gel electrophoresis

PBS   phosphate buffered saline

PBST   PBS/0.5% Tween-20

Pd(OH)$_2$ palladium hydroxide

PGs   proteoglycans

Ph   phenyl

PHF   paired helical filament

PMB   *p*-methoxybenzyl

PRN   pertactin

PT   pertussis toxin

p-TolSCl   *p*-toluenesulfenyl chloride

p-TolSH   *p*-toluenethiol

Py/Pyr   pyridine

Qβ   bacteriophage Qbeta

SA	streptavidin
sat.	saturated
SDS	sodium dodecyl sulfate
SEC	size exclusion chromatography
SPION	superparamagnetic iron oxide nanoparticles
SSM	Stainer-Scholte media
STD-NMR	saturation transfer difference NMR
TauO	tau oligomers
TBAF	tetrabutylammonium fluoride
TBAI	tetrabutylammonium iodide
TBDPS	*t*-butyldiphenylsilyl
TBS	*t*-butyldimethylsilyl
t-Bu	*t*-butyl
TCT	tracheal cytotoxin
TEM	transmission electron microscopy
TEMPO	2, 2, 6, 6-tetramethyl-1-piperidinyloxyl
TFA	trifluoroacetic acid
Tf_2O	trifluoromethanesulfonic anhydride
TGA	thermogravimetric analysis
Th	helper T cell
THF	tetrahydrofuran

ThT	thioflavin T
TLC	thin layer chromatography
TMB	3,3',5,5'-tetramethylbenzidine
TOCSY	total correlation spectroscopy
TrocCl	trichloroethyl chloroformate
TT	tetanus toxoid
TTBP	2,4,6-tri-*t*-butylpyrimidine
WHO	World Health Organization
wP	whole-cell pertussis

Chapter 1. A Review of Developing Vaccines against *Bordetella pertussis*

1.1. Introduction

Pertussis, commonly known as whooping cough or 100-day cough, is a highly contagious acute respiratory disease of which the most characteristic symptom is uncontrollable violent coughing. Severe coughing fits followed by gasping for breath of pertussis patients result in the "whooping" sound, hence its name. Although severity of syndromes of pertussis is usually mild and not life-threating to adults, this disease can be particularly harmful and fatal for infants.[1-2] According to the surveillance and reporting by the Centers for Disease Control and Prevention (CDC), most pertussis incidents have been reported for babies less than one year old for the last 20 years in the United States, with an incident rate at about 60 per 100,000 persons in 2016.
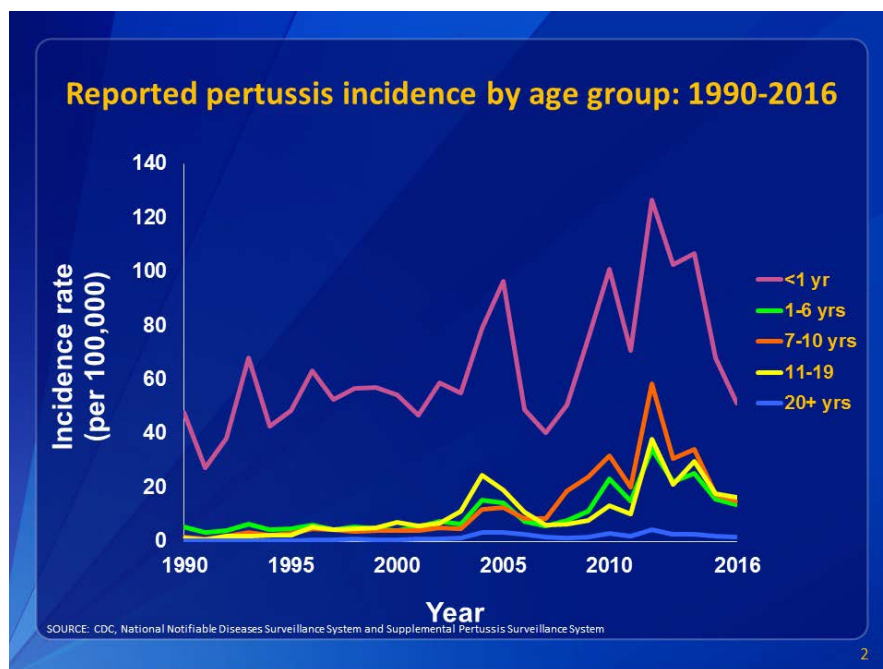
Figure 1.1. **Reported pertussis incidence (per 100,000 persons) by age group in the United States from 1990–2016**. Infants aged <1 year, who are at greatest risk for serious disease and death, continue to have the highest reported rate of pertussis. This figure is adapted and reproduced from reference[3] (free of copyright restrictions).

The etiological agent of pertussis, *Bordetella pertussis*, was isolated and identified by Bordet and Gengou in 1906.[4] It is a Gram-negative, aerobic encapsulated coccobacillus of the genus *Bordetella*. As defined by World Health Organization (WHO), the course of pertussis is consisted of the catarrhal, paroxysmal and convalescent phases. The infection of pertussis is through aerosol transmission of droplets emitted in coughs or sneezes, which mostly happens during the catarrhal phase. After being inhaled into the respiratory system, *B. pertussis* colonizes ciliated cells of mucosa and produces an array of virulence factors that play a key role in the establishment of infection, including pertussis toxin (PT), adenylate cyclase toxin (ACT), filamentous hemagglutinin (FHA) and pertactin (PRN).[5] PT is known to be main exotoxin which elicits a number of deleterious consequences including leukocytosis, splenomegaly and histamine sensitization, while both FHA and pertactin are presumed as adhesins.

The best way to prevent infection of *B. pertussis* is vaccination and it is recommended for routine use by the WHO and CDC. The first vaccine was prepared as early as in 1929 by T. Madsen, which was composed of a suspension of *B. pertussis* in rabbit blood.[6] Efficacy of the vaccine was proven by the decreased death rate of vaccinees compared to that of nonvaccinees, according to a two-year period of surveillance. The more well-known tri-functional vaccine, which combined whole-cell pertussis vaccines with diphtheria and tetanus toxoids onto alum (DTPads) was then invented and applied throughout the United States. The number of deaths caused by *B. pertussis* infection dropped dramatically since the introduction and standardization of whole-cell pertussis vaccines.[7] However, the vaccine itself raised safety concerns as it occasionally results in serious adverse effects such as local reactions, fever and seizures.[8]

With the increasing public scrutiny on vaccine safety, a safer acellular vaccine composed of pertussis toxin and filamentous hemagglutinin was invented in Japan and now adopted in most developed countries.[9] Although widespread vaccination has greatly reduced the morbidity, the world has been experiencing a resurgence of pertussis in recent decades with more and more reported cases of pertussis patients, especially after the introduction of acellular vaccine (**Figure 1.2**).
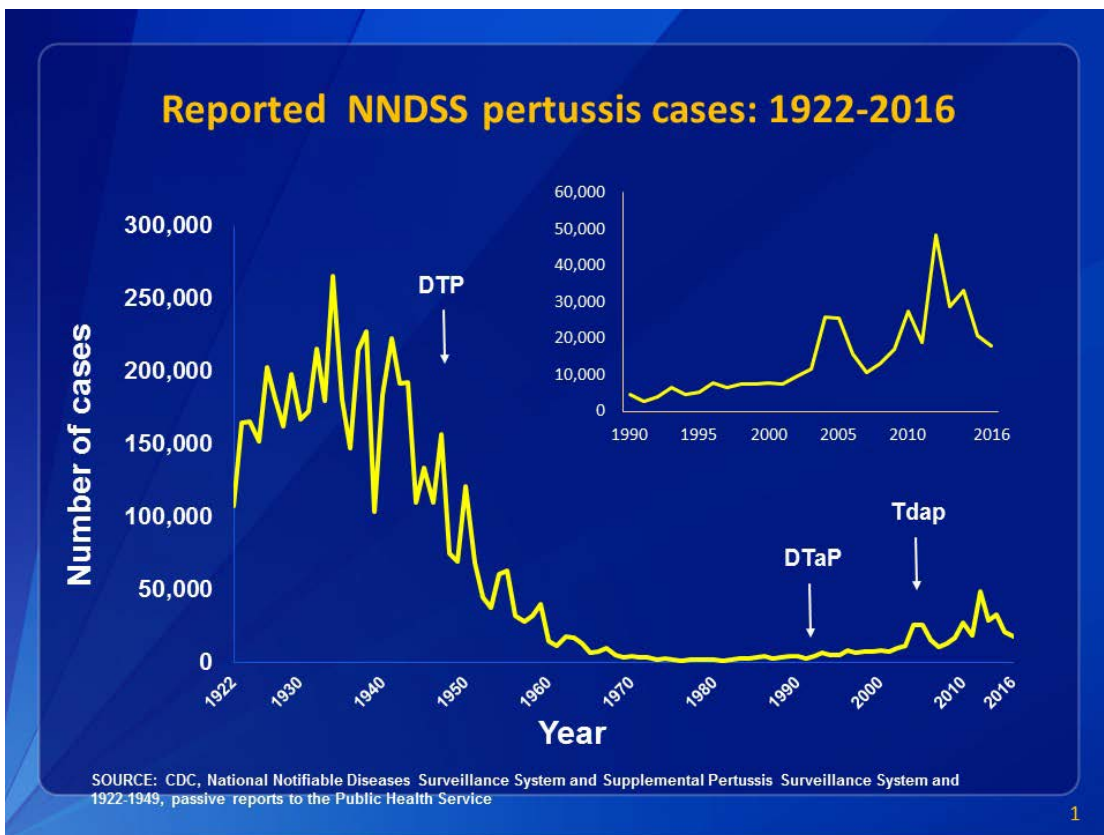
Figure 1.2. **The number of pertussis cases reported to CDC from 1922 to 2016.** Following the introduction of pertussis vaccines in the 1940s when case counts frequently exceeded 100,000 cases per year, reports declined dramatically to fewer than 10,000 by 1965. During the 1980s pertussis reports began increasing gradually, and by 2015 more than 20,000 cases were reported nationwide. This figure is adapted and reproduced from reference[3] (free of copyright restrictions).

1.2. Hypotheses for Resurgence of Pertussis

Although the introduction of acellular pertussis vaccine appeased safety concerns of vaccination, it has been noticed that a widespread resurgence of pertussis is occurring. Around the world, there are about 260,000 deaths due to pertussis infection annually. Even in developed countries where the vaccination rates are high, the number of reported cases of pertussis has markedly risen during recent decades,[10-11] reaching a 60 year high in countries such as US and Australia.[12] The infection rate of pertussis was reported to be 1-6%,[13-14] which became the most prevalent vaccine-preventable disease in developed countries. The reasons proposed for the resurgence of pertussis includes pathogen adaption and conversion from whole-cell vaccines to acellular vaccines.

Virulence factors contained in the acellular pertussis vaccines, including pertussis toxin, filamentous hemagglutinin, pertactin and other components, can elicit protective antibodies against the pathogen. However, strain differences and mutations in those virulence factors have resulted in the antigenic divergence between vaccine strains and the currently circulating strains, which rendered the vaccines ineffective. The dramatically increasing fraction of pertactin-deficient strains have been discovered in the recent outbreak of pertussis,[15-17] presumably due to the selection of bacteria under the immune pressure. It turned out to be advantageous for *B. pertussis* since the deficiency in the expression of pertactin conferred more invasive infection on patients.[18] Polymorphism in pertactin region 1 also limited the efficacy of vaccines since the antibodies were found to be type-specific and shown little cross reactivity.[19] The emergence of strains that overproduced pertussis toxin and led to more severe syndromes

further proved the importance of pathogen adaption of *B. pertussis*.[20] A phylogenetic analysis of a worldwide collection of 343 *B. pertussis* strains isolated from 1920 and 2010 was performed by Marieke J. Bart and coworkers.[21] Comparative genomics indicated that the genotype population and diversity of *B. pertussis* had increased a lot since the introduction of vaccination, consistent with the suggestion that the vaccine was the main driving force of pathogen adaption. Several changes in the gene coding of the proteins included in acellular vaccines were also discovered, which might have contributed to the "vaccine escape" in the resurgence of pertussis.

1.3. Acellular Pertussis Vaccines

It was proposed by Margaret Pittman of National Institute of Health (NIH) in 1979 to name the histamine-sensitizing, lymphocyte-leukocyte-promoting and islet-activating (HSF-LPF-IAP) antigen as "pertussis toxin" that had caused harmful effects and prolonged immunity of pertussis.[22] She also suggested that an antitoxin against pertussis toxin would be a good defense against the disease. An acellular pertussis vaccine (aP vaccine) composed of pertussis toxin and filamentous hemagglutinin was invented in Japan in 1981 and evaluation of the vaccine showed excellent efficacy as well as much lower reactogenicity compared to whole-cell pertussis vaccine (wP vaccine).[23] The current commercial aP vaccine may contain up to five virulence factors from *B. pertussis*, including pertussis toxin, filamentous hemagglutinin, pertactin, and fimbriae 2&3. Although debates are still going on about the necessity of including more virulence factors, there has been agreement that pertussis toxin is an essential component in the aP vaccines.[24]

Early clinical trials of aP vaccines appeared to be comparably effective as wP vaccines.[25-26]

However, recent studies revealed that aP vaccines are actually not as durable as initially thought. Epidemiological data show that aP vaccines induce shorter term immunity compared to wP vaccines. The anti-pertussis immune responses from acellular vaccines tend to drop with reduced efficacy after 3-5 years and only 10% of the children vaccinated with aP vaccines would still have protection by the time of the next adolescent booster.[27] To better understand the different protection stimulated by wP and aP vaccines, it is essential to know the difference in the immunological responses. It was found that wP and aP vaccines induce different skewing of immune responses. Similar to natural infection, wP vaccines mainly induce a cellular-immunity-related Th1-dependent immune response, eliciting IgG2 antibody subclass as well as IgG1 and IgG3. On the contrary, aP vaccines induce Th2/Th1 mixed or more Th2-skewed responses.[28-30] Although Th2 cells were thought to be important for promoting antibody responses against extracellular pathogens such as bacteria, Kingston H. G. Mills and coworkers[31] recently found that this immune response was actually dispensable for protection against *B. pertussis*. Knockout of the gene of the cytokine IL4 that was important for inducing differentiation of naïve T helper cells to Th2 cells did not affect clearance of bacteria. On the contrary, much slower clearance of bacteria was observed in IL17$^{-/-}$ mutant mice. They also found that the clearance of bacteria was mainly mediated by Th17 cells that were associated with recruiting macrophages and neutrophils to the lungs and promoting the killing of *B. pertussis*. The immune protection can be improved by substituting the commonly used adjuvant alum in aP vaccines with an adjuvant that promotes Th1 cells. The redundant Th2 component in immune responses against aP vaccines may have even caused the rare type hypersensitivity reactions seen

in children after a fourth or fifth injection.[32-33] Protection by wP vaccines mainly depends on the production of IFN-γ by Th1 cells. Although the role of Th17 response upon immunization with wP vaccines is not well understood yet, the induction of Th17 cells via IL-1 might explain the better protection provided by wP vaccines.

To better understand the mechanism of immune responses as in humans, a recent study by Tod J. Merkel and coworkers was performed on nonhuman primate model using baboons.[34] The baboons were immunized with wP or aP vaccines on the same schedule as infants before being subjected to direct challenge with *B. pertussis*. Although post-vaccination serum analysis indicated comparable levels of antibodies against four main virulence factors and aP also successfully prevented leukocytosis, more persistent colonization of bacteria were found in aP vaccinated baboons according to the analysis of nasopharyngeal washes. To mimic the transmission through cough illness in human disease, they either cohoused challenged animals with aP vaccinated animal or naïve animals with challenged animals that had been pre-immunized with the aP vaccine. Surprisingly, transmission of bacteria was observed in both cases despite vaccination. Their results indicated that aP vaccines failed to prevent colonization of *B. pertussis* in the respiratory tract or transmission to healthy individuals. This compromised herd immunity might be another mechanism leading to the resurgence of pertussis.

The endotoxins included in the aP vaccines have different biological functions and contribute synergistically to the pathology of pertussis. Pertussis toxin secreted by *B. pertussis* impedes the antigen processing and presentation by inhibiting the migration and phagocytosis of antigen-presenting cells (APC).[30, 35] Both FHA and pertactin carries the RGD motif and are

presumed as adhesins that help cell attachment.[36-37] Although people expected by targeting those antigens, especially the outer-membrane bound proteins, to confer complement-mediated bactericidal killing, it has been found that immunization with aP vaccines did not improve bactericidal activity.[38] In a survey of 34 pairs of pre- and post-immunization serum samples from adults by Alison A. Weiss and coworkers, no significant increases in bactericidal activity at high serum concentrations were observed after vaccination in spite of elevated titers of IgG against all three exotoxins (pertussis toxin, FHA and pertactin) in the vaccine.[39] Those results suggested that antibodies induced by aP vaccines might neutralize the exotoxins and reduce related syndromes, rather than directly kill the pathogens.

The failure of aP vaccines in providing prolonged protection urges the development of better vaccines for pertussis. However, returning to wP vaccines will not be an acceptable choice due to the potential side effects for adolescents and adults. Improvement of the current pertussis vaccines should be focused on discovery of antigens that are able to elicit bactericidal antibodies and optimal adjuvant that correctly tunes the adaptive immune arm. Kingston H. G. Mills and coworkers identified and characterized an endogenous lipoprotein BP1569 from *B. pertussis*, which was able to activate macrophages and dendritic cells via TLR2.[40] A synthetic lipoprotein of the N-terminus was capable of activating both Th1 and Th17 responses and conferring protection against *B. pertussis*. The same group also demonstrated the capability of infection clearance by activating TLR4, which is the receptor of lipopolysaccharide.[41]

1.4. Pertussis Lipooligosaccharide

Lipopolysaccharide (LPS) is the major component of the outer membrane of Gram-negative bacteria, which protects the bacteria from the surroundings by serving as a physical barrier. It is commonly comprised of three parts: lipid A, core oligosaccharide and *O*-specific antigen.
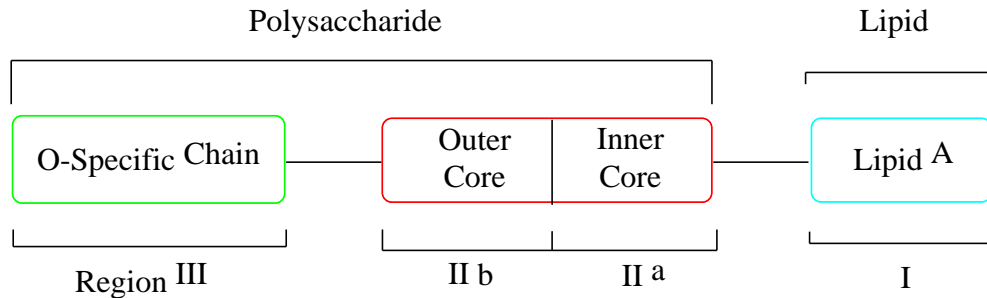
Figure 1.3. Common structure of lipopolysaccharide of Gram-negative bacteria.

Unlike two other bacteria in the same genus, *B. bronchiseptica* and *B. parapertussis*, which both contain a homopolymer of 2,3-dideoxy-2,3-diacetamidogalactosaminuronic acid, the LPS of *B. pertussis* is devoid of such *O*-specific chain, thus commonly referred to as lipooligosaccharide (LOS). The LOS of *B. pertussis* was first isolated by Eldering in 1941 with an acid method, and later a more commonly used hot phenol-water method was applied to the extraction of *B. pertussis* LOS, as reported by MacLennan.[42] SDS-PAGE analysis of *B. pertussis* LOS depicts two separate bands. The more abundant, slowly migrating band, which is referred to as band A, represents a LOS containing a dodecasaccharide core, while the minor, fast-migrating band B lacks a distal trisaccharide.

The biological activity of *B. pertussis* LOS is similar to those of the endotoxins isolated from other Gram-negative bacteria. It was found that LOS worked synergistically with tracheal

cytotoxin (TCT) inducing epithelial NO production exclusively in non-ciliated cells, which eventually caused the disruption of ciliated cells in respiratory mucosa.[43] LOS also protects *B. pertussis* from the innate immunity in respiratory tract mediated by surfactant proteins A and D, which bind to the lipid A region and core saccharide region respectively, inducing aggregation and acting as opsonins for macrophages and neutrophils.[44-45] The interaction was shielded mainly by the distal trisaccharide in LOS, as mutants lacking the trisaccharide can be aggregated and permeabilized by the innate defense mechanism.

1.4.1. Structure Elucidation of Pertussis LOS

Detailed elucidation of the structure of pertussis LOS was pioneered by Martine Caroff and coworkers.[46-48] They extracted the LOS from *B. pertussis* strain 1414 following the hot phenol-water method and cleaved lipid A from LOS with the mild sodium dodecyl sulfate (SDS) condition. Selective hydrolysis of fatty acids from the major component of lipid A with hydroxylamine or sodium hydroxide pinpointed the linkage of fatty acids, while the distribution of fatty acids on the β-(1→6)-linked glucosamine disaccharide backbone was resolved by analyzing the fragmentation pattern in fast atom bombardment (FAB) data.[46] The ensemble of those results defined the only structure for lipid A, as shown in **Figure 1.4**. A minor species was less in molecular weight by 226 Da, presumably by losing a hydroxytetradecanoic acid.
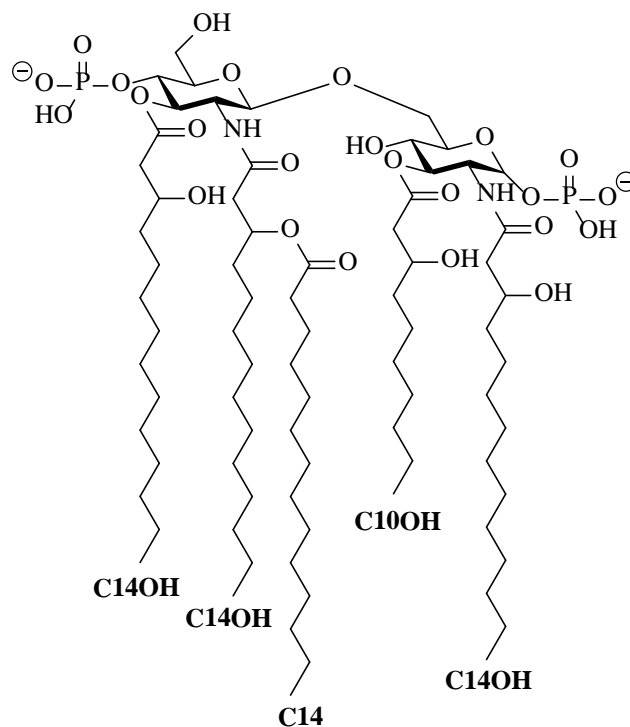
Figure 1.4. Structure of the major molecular species present in *B. pertussis* lipid A.

Structural characterization of the heptasaccharide that is adjacent to lipid A was first attempted by Richard Chaby and coworkers.[49-52] By hydrolysis with hydrochloric acid of different concentrations, di- or trisaccharide subunits at the non-reducing end of the heptasaccharide were harvested in low yields. These di- or trisaccharides were further digested into monosaccharides, which were then subjected to chemical modifications such as reduction or acetylation and comparison with standard samples in HPLC. The structure of the heptose was proven to be L-glycero-D-mannoheptose by chemical degradation. Enzymolysis by stereochemistry-specific enzymes revealed the correct configuration for glycosidic linkage. Eventually, the substitution positions of glucosamine and glucuronic acid on heptose were determined to be 7 and 2 respectively by analyzing fragments from the reduction with NaB^3H_4

11

and cleavage with $NaIO_4$.[49-50] Similarly, the structure of another trisaccharide purified from the acidic hydrolysis was characterized as the 4-*O*-(2-amino-2-deoxy-α-D-glucopyranosyl) -6-*O*-(2-amino-2-deoxy-α-D-galactopyranuronyl)-D-glycopyranose configuration.[51] Due to the lability of 3-deoxy-D-manno-2-octulosonic acid (Kdo) in strong acid, they applied a nitrous acid-cleavage protocol and successfully separated an Kdo-containing oligosaccharide that was claimed to be a tetrasaccharide with the configuration of D-glucopyranosyl-β-(1→3)-D-glycopyranuronyl-β-(1→2)-L-glycero-D-mannoheptopyranosyl-α-(1→5)-3-deoxy-D-manno-2-octulosonic acid. By overlapping the shared monosaccharide units in all fragments, they proposed the structure of the reducing end heptasaccharide as in **Figure 1.5**:
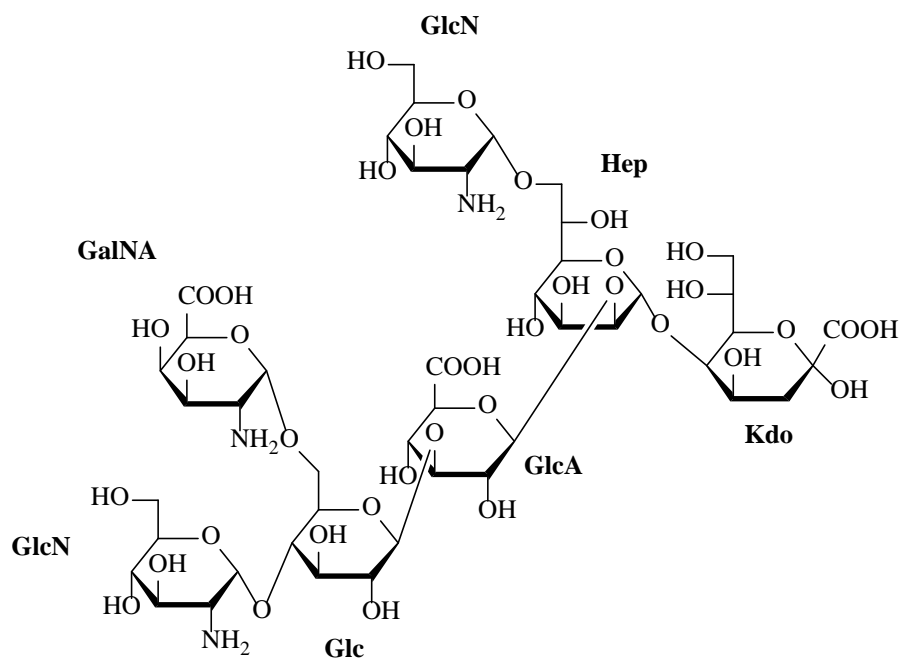
Figure 1.5. Proposed structure of the heptasaccharide present at the reducing end of LOS-1 isolated from *B. pertussis* endotoxin.

However, exactness of the structure of the last claimed-to-be tetrasaccharide relied heavily on the colorimetric estimation of monosaccharides. They failed to notice that the ratio of hexoses to heptoses was actually 1:2 rather than 1:1 and therefore the wrong structure was proposed. After sequential dephosphorylation with hydrofluoric acid, deamination with nitrous acid and hydrolysis promoted by sodium dodecyl sulfate, Ladislas Szabo and coworkers isolated a hexasaccharide from the *B. pertussis* endotoxin.[47] Methylation analysis revealed another mannoheptose in the structure, which was 3, 4-disubstituted and not detected in the previous research. Although anomeric configuration was not easy to assign in the hexasaccharide due to overlapped signals, exhaustive Smith degradation with $NaIO_4$ truncated all but the non-reducing end disaccharide and the glycosidic linkage was determined to be α by NMR analysis. The anomeric stereochemistry of the glucuronic acid was also determined to be α by NMR, which was incorrectly assigned to be β by cleavage reaction with a commercial β-D-glucuronidase.

Nitrous acid deamination afforded the distal pentasaccharide from the LOS of *B. pertussis* stain 1414. Relative structures of the five subunits in the pentasaccharide were resolved by NMR analysis, which suggested the existence of α-2-acetamidoglucose (α-GlcNAc), β-2-acetamido-4-*N*-methyl-2,4,6-trideoxy-galactose (β-Fuc2NAc4NMe), β-2,3-diacetamido-2,3-dideoxy-mannuronic acid (β-Man2NAc3NAcA), α-mannoheptose (α-ManHep) and anhydromannitol. By hydrolyzing the pentasaccharide with hydrochloric acid, the α-GlcNAc and α-Hep subunits were isolated and the absolute configuration was determined to be D and L, D by GC-MS.[48] Potential energy calculation in combination with NOE measurements helped determining the absolute structures of the other three monosaccharides.

Based on all data obtained, the complete structure of *B. pertussis* LOS was proposed as in **Figure**

1.7.
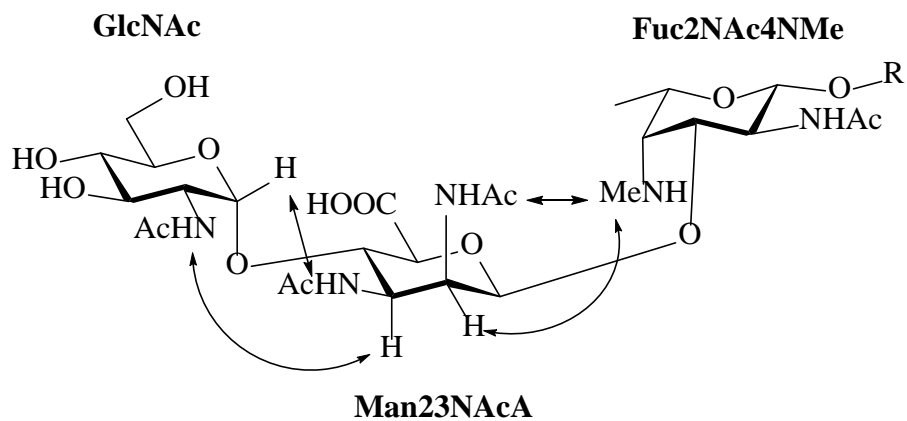
Figure 1.6. Structure of the trisaccharide present in the distal pentasaccharide from *B. pertussis*. Some short interproton distances that could be observed in the NOE experiments and used to determine the absolute configuration of the sugars are shown.
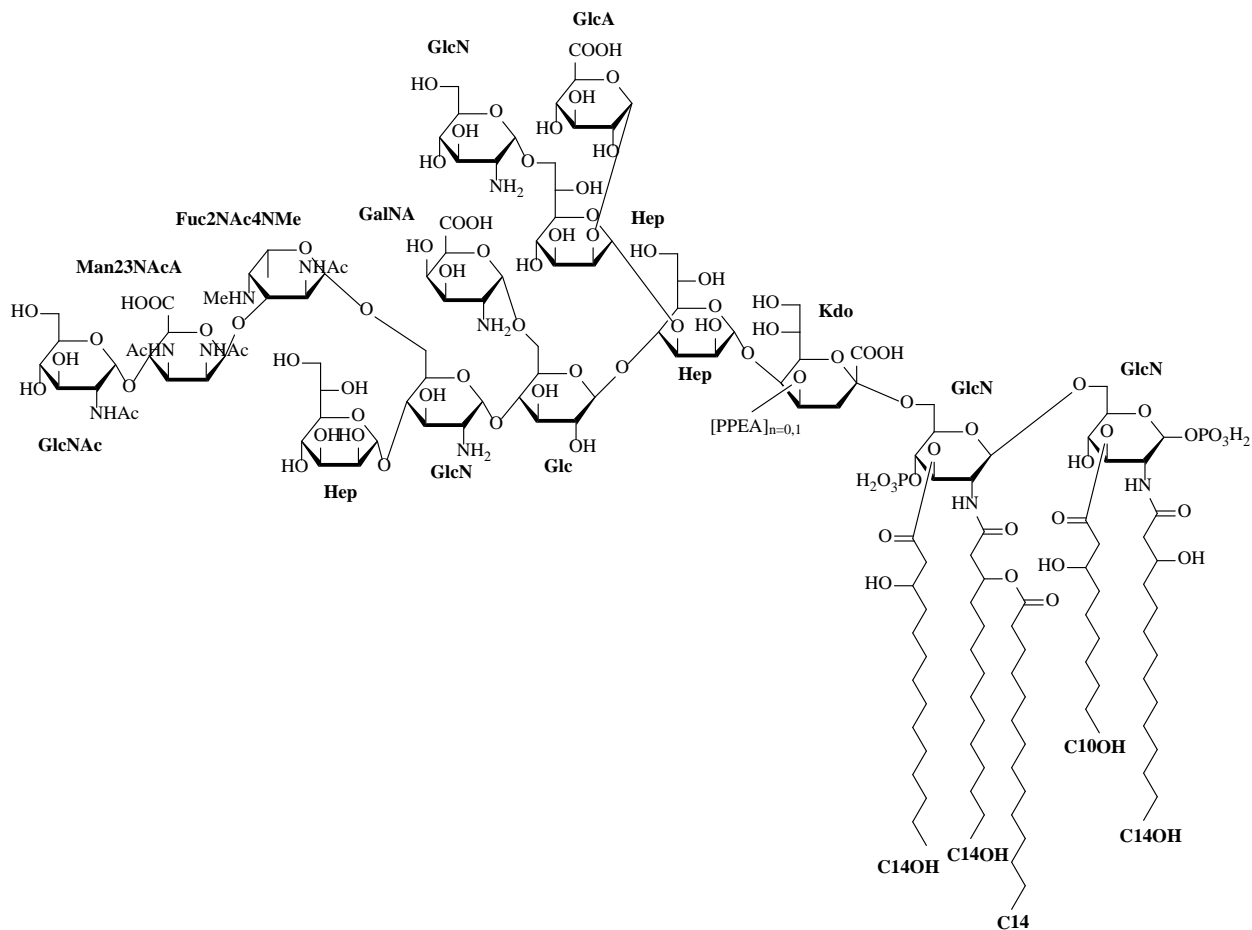
Figure 1.7. Complete structure of the LOS of *B. pertussis* strain 1414.

1.4.2. Immunology of Pertussis LOS

Early failure in wP vaccines gave impetus to research that aims at identifying the key factors in the protective immunogenicity for pertussis. Jean M. Dolby and coworkers characterized fractions of antibodies in the *B. pertussis* antisera and identified a complement-mediated bactericidal antibody capable of killing *B. pertussis*.[53-54] However, the bactericidal activity pattern did not correlate well with any of the titers for agglutinin, antihaemagglutinin or anti-histamine sensitizing factors, suggesting that the antibody was stimulated by a complete

different antigen, which was referred to as "the bactericidal antigen". Extraction of the endotoxin LOS from six strains of *B. pertussis* and immunization at multiple doses of the LOS coupled with carrier protein elicited bactericidal antibodies, which suggested that the antigen was actually LOS.[54]

There has been a significant amount of research done to further identify antigenic determinants on the lipooligosaccharide of *B. pertussis*. Bernard R. Brodeur and coworkers described the preparation of both monoclonal antibodies specific for band A or band B by the hybridoma cell line protocol.[55-56] The LOS band A-specific antibodies were found to react well with strains of LOS AB phenotype but not the atypical strain 134 of LOS B phenotype. At least two antigenic epitopes were discovered, with five out of the seven LOS band A-specific antibodies found to recognize the same epitope.[55] Although band B-specific antibody BL-8 bound to strain 134 and led to moderate lytic activities, it failed to affect predominant strains that express both LOS band A and B, presumably due to the limited expression and accessibility of epitopes on the cell membrane.[56]

Structure elucidation of the pertussis LOS significantly helped epitope mapping for antigen design. Richard Chaby and coworkers immunized mice with strain 1414 which carried a majority of band A LOS.[57] Three monoclonal antibodies were tested against LOS from *Bp*1414, *Bp*A100, *B. bronchiseptica*, *B. parapertussis* and different subparts of band A LOS. All three monoclonal antibodies bound to the terminal pentasaccharide, which was located far from lipid A, but recognized GlcNAc-Man2NAc3NAcA, Fuc2NAc4NMe-GlcN and Hep-GlcN respectively. The carbohydrate region which was proximal to lipid A was considered as poorly immunogenic

16

because of the failure in generating an antibody that bound to strain A100. Tomasz Niedziela and coworkers conjugated the pentasaccharide cleaved from band A LOS with nitrous acid to tetanus toxoid for mouse immunization to generate polyclonal antibodies.[58] Those antibodies failed to bind with strain 606 in western blot, which carries only band B LOS and was included in the wP vaccines in Poland. It implies that the immunogenic epitopes were mainly located on the distal trisaccharide. Saturation transfer difference NMR experiments (STD-NMR) were also employed to investigate the structural elements on the pentasaccharide that contributed to the binding epitope. Although information provided by STD-NMR supported that major components of antigenic epitopes were on the trisaccharide, weak signals on the ManHep suggested that the heptose unit may also play a role in the immunogenicity of LOS. It was further confirmed by the research done by John Robbins and coworkers, in which they found that repetitive expression of the distal trisaccharide from a *B. brochiseptica* mutant led to a decreased binding affinity with anti-LOS antibodies.[59] Molecular modeling of the LOS from *B. pertussis* strain 1414 also revealed that those epitopes were exposed at the extremities regardless of the existence of PPEA on Kdo, as illustrated in **Figure 1.8**.
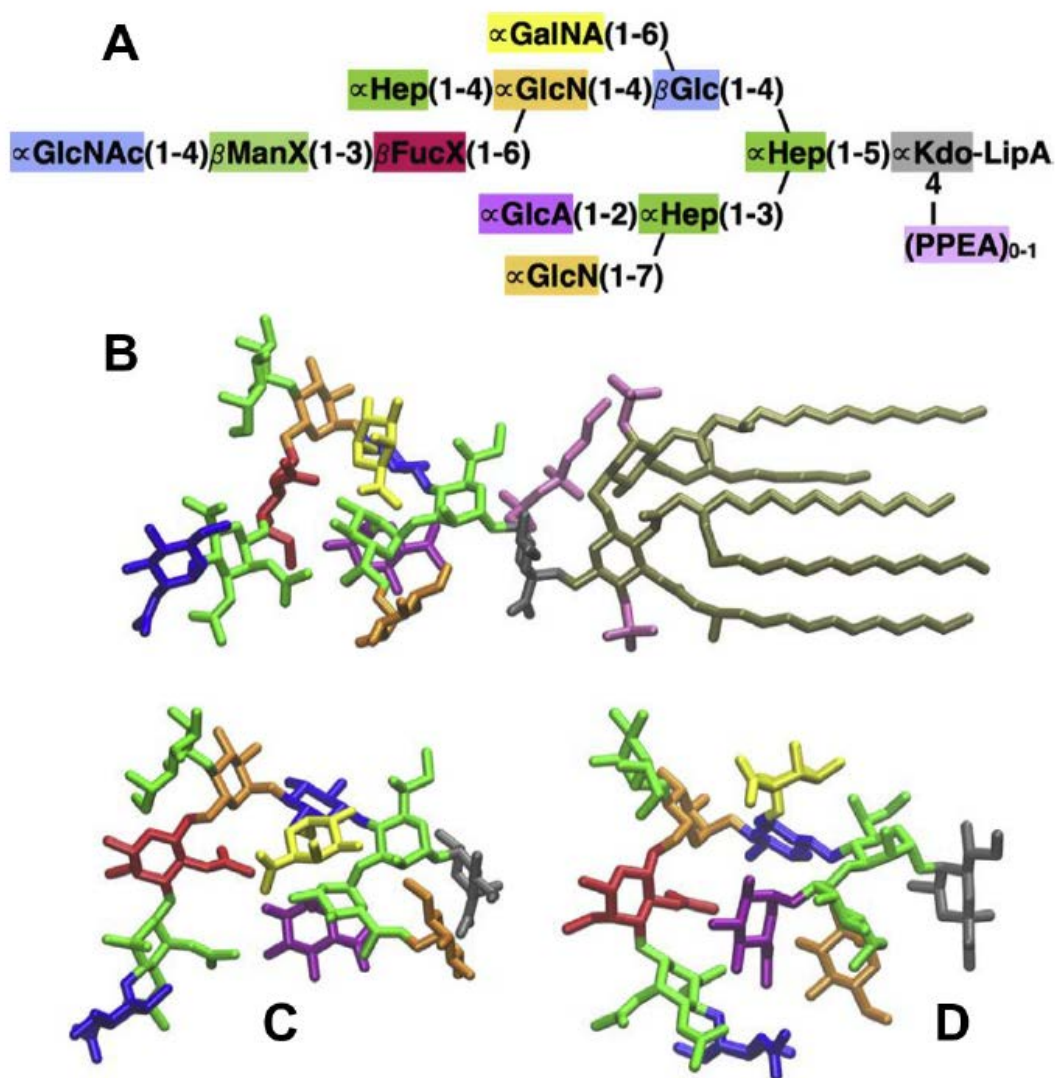
Figure 1.8. **Structure and molecular models of *B. pertussis* BP1414 LOS.** (A) Structure of the LPS where ManX represents Man2NAc3NAcA and FucX represents Fuc2NAc4NMe. (B) Molecular model with PPEA showing lipid A. Models for (C) and (D) did not include PPEA and lipid A. Conformers in (C) and (D) show the flexibility about the GlcN(1–7)Hep and Fuc (1–6)GlcN linkages. The dihedral angle (O7–C7–C6–O6) of the (1–7)Hep residue is -78° for models (B) and (C) and 55° for model (D). The dihedral angle (O6–C6–C5–O5) of the (1–6)GlpN residue is 64° for model (B) and -60° for models (C) and (D). The residues are colored gray for Kdo, green for Hep and ManX, blue for Glc and GlcNAc, orange for GlcN, purple for GlcA, yellow for GalNA, red for FucX, mauve for PPEA and PO4 of lipid A and tan for lipid A. Hydrogen atoms are not shown in the molecular models. This figure is adapted and reproduced with permission from reference.[60]

1.5. Pertussis LOS-based Glycoconjugate Vaccines

Despite the antibodies elicited from LOS in wP vaccines, it is not feasible to directly use *B. pertussis* LOS as a vaccine. Many lipopolysaccharides from Gram-negative bacteria have been reported to be highly immunogenic, but *B. pertussis* LOS was poorly immunogenic when injected alone, probably due to the low molecular weight. Unlike proteins, the LOS is only a T-independent antigen and triggers B cells to secret predominantly IgM with low binding affinity. Moreover, LOS was suspected to be the main culprit for side effects of wP vaccines because of its endotoxin activity.[61] Therefore, it is necessary to remove the lipid A part, which is the endotoxin determinant. Covalent conjugation of the immunogenic carbohydrate region with a carrier protein results in uptake by B cells and antigen presentation through MHC II to $CD4^+$ T cells. Cytokines secreted by the activated T cells will stimulate the maturation of B cells and cause the class-switching from IgM to high-affinity IgG, which helps achieve the optimal immune responses. Although the relative abundance of two bands of oligosaccharides may vary across different strains, such as band B being the major component in strain A100, the structure of *B. pertussis* core saccharide remains relatively conserved, which is different from exotoxins included in the current aP vaccines. This conclusion was supported by an investigation on the structure of *B. pertussis* LOS from pre- and post- vaccination era,[60] suggesting that those antigens may be good potential vaccine components.

Tomasz Niedziela and coworkers cleaved the pentasaccharide from *B. pertussis* LOS by nitrous acid and conjugated it with tetanus toxoid (TT) through reductive amination with the free aldehyde group on the reducing-end anhydromannose. They found that the mouse polyclonal

antibodies against such a conjugate bound strongly with the whole wild-type LOS of *B. pertussis* as well as the live *B. pertussis* bacteria. It was reported previously that LOS worked synergistically with tracheal cytotoxin and induced the release of NO from secretory epithelial cells.[43] Such effect was significantly inhibited by the polyclonal antibodies against the pentasaccharide-TT conjugate along with lower production of IL6 and TNF-α, which are both proinflammatory cytokines involved in the inflammatory process stimulated by LOS.

Instead of choosing the most immunogenic distal pentasaccharide as the antigen, John R. Robbins and coworkers cleaved the whole dodecasaccharide from LOS with 1% acetic acid and conjugated it with BSA. A mutant of *B. bronchiseptica* which lacked the complete *wbm* locus and did not express the *O*-specific chain was used as an alternative source of LOS, due to the ease in culturing compared with *B. pertussis*. The purified dodecasaccharide shared the same structure as that in *B. pertussis*, except that ~50% of the non-reducing end GlcNAc was replaced by GalNAc. The glycan-BSA conjugate successfully induced antisera that were bactericidal against *B. pertussis* Tohama I strain.
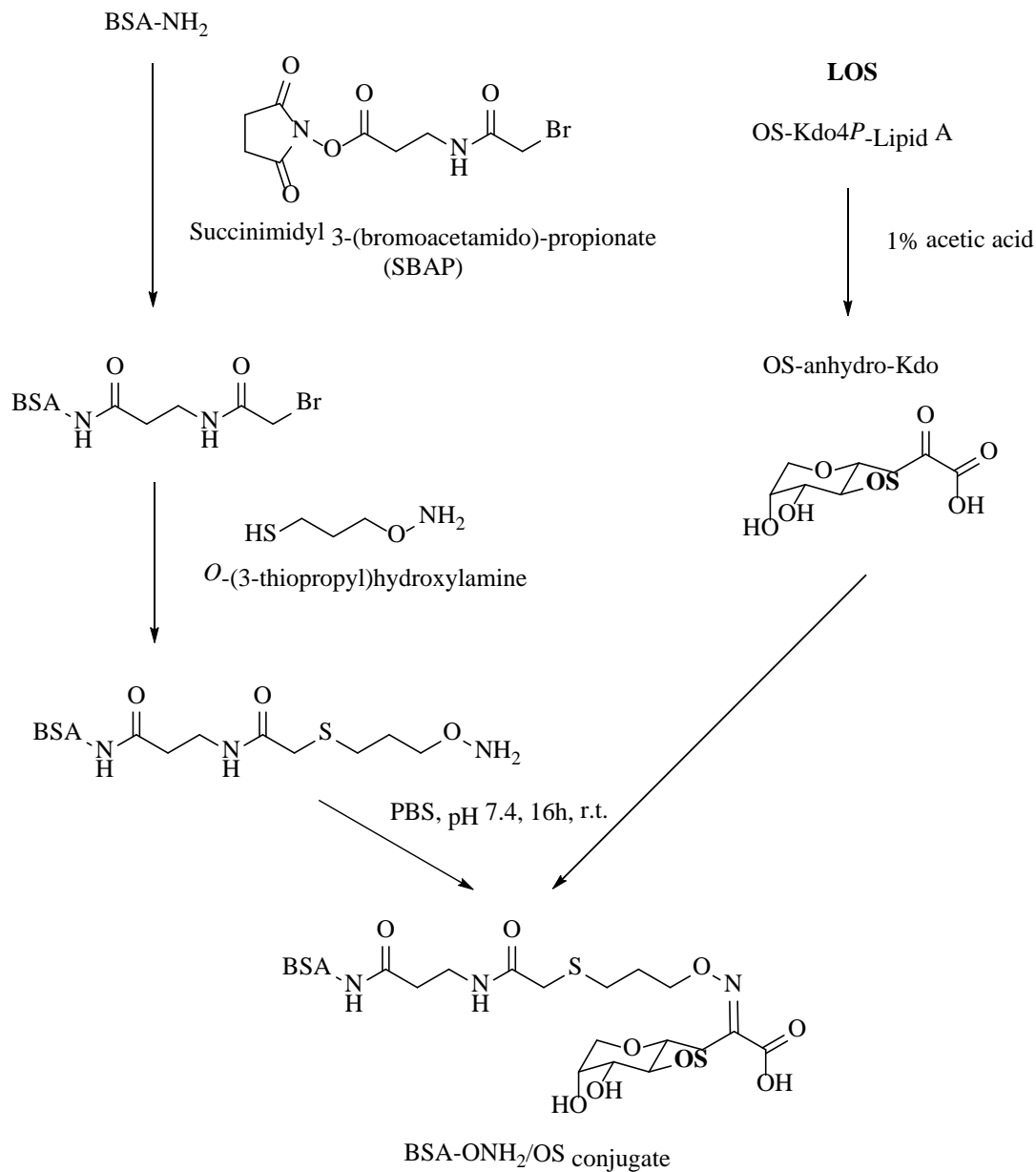
Figure 1.9. Scheme of conjugation of *B. pertussis* and *B. bronchiseptica* core OS.

1.6. Future Outlook

The failure of aP vaccines in inducing durable protection urges the development of new vaccines that are able to elicit long-term robust bactericidal immune responses. Carbohydrates present on the surface of bacteria have been used as immunogens to develop carbohydrate-based

vaccines against many pathogens such as *Streptococcus pneumoniae*, *Neisseria meningitides* and *Haemophilus influenza*.[62] Conjugates of *B. pertussis* LOS with a carrier protein elicit bactericidal antibodies, which were reported to overcome the BrkA protein-induced resistance against complement-dependent bactericidal pathway.[24, 63] This along with the highly conserved structure of LOS across strains renders LOS an appealing target for vaccine development. However, isolating LOS in abundance from the highly aerosol transmissible pathogen remains a big obstacle, while the alternative way of expressing LOS in a mutant *B. bronchiseptica* results in heterogeneity in the desired structure. The obtainable sequences of oligosaccharides limited by LOS processing methods also impose restrictions on screening for the optimal immunogenic epitope and understanding the adaptive immunity against LOS. Synthetic carbohydrate chemistry provides the flexibility in accessible antigen structures and can add to the arsenal for combating bacteria with higher quality control compared to natural sources.

REFERENCES

REFERENCES

1. Kerr, J. R.; Matthews, R. C., *Bordetella pertussis* infection: pathogenesis, diagnosis, management, and the role of protective immunity. *Eur. J. Clin. Microbiol. Infect. Dis.* **2000,** *19* (2), 77-88.

2. Kilgore, P. E.; Salim, A. M.; Zervos, M. J.; Schmitt, H.-J., Pertussis: microbiology, disease, treatment, and prevention. *Clin. Microbiol. Rev.* **2016,** *29* (3), 449-486.

3. CDC National Notifiable Disease Surveillance System and Supplemental Pertussis Surveillance System, https://www.cdc.gov/pertussis/surv-reporting.html.

4. Cherry, J. D., Epidemiological, clinical, and laboratory aspects of pertussis in adults. *Clin. Infect. Dis.* **1999,** *28* (Supplement_2), S112-S117.

5. Marzouqi, I.; Richmond, P.; Fry, S.; Wetherall, J.; Mukkur, T., Development of improved vaccines against whooping cough: current status. *Hum. Vaccin.* **2010,** *6* (7), 543-553.

6. Madsen, T., Vaccination against whooping cough. *J. Am. Med. Assoc.* **1933,** *101* (3), 187-188.

7. Warfel, J. M.; Edwards, K. M., Pertussis vaccines and the challenge of inducing durable immunity. *Curr. Opin. Immunol.* **2015,** *35* (Supplement C), 48-54.

8. Linnemann, C. C.; Perlstein, P. H.; Ramundo, N.; Minton, S. D.; Englender, G. S.; McCormick, J. B.; Hayes, P. S., Use of pertussis vaccine in an epidemic involving hospital staff. *The Lancet* **1975,** *306* (7934), 540-543.

9. Robbins, J. B.; Schneerson, R.; Keith, J. M.; Miller, M. A.; Kubler-Kielb, J.; Trollfors, B., Pertussis vaccine: a critique. *Pediatr. Infect. Dis. J.* **2009,** *28* (3), 237-241.

10. Celentano, L. P.; Massari, M.; Paramatti, D.; Salmaso, S.; Tozzi, A. E., Resurgence of pertussis in Europe. *Pediatr. Infect. Dis. J.* **2005,** *24* (9), 761-765.

11. Control, C. f. D.; Prevention, Summary of notifiable diseases-United States, 2010. *MMWR. Morb. Mortal. Wkly. Rep.* **2012,** *59* (53), 1-111.

12. Rumbo, M.; Hozbor, D., Development of improved pertussis vaccine. *Hum. Vaccines Immunother.* **2014,** *10* (8), 2450-2453.

13. de Melker, H. E.; Versteegh, F. G. A.; Schellekens, J. F. P.; Teunis, P. F. M.; Kretzschmar, M., The incidence of *Bordetella pertussis* infections estimated in the population from a combination of serological surveys. *J. Infect. 53* (2), 106-113.

14. Ward, J. I.; Cherry, J. D.; Chang, S.-J.; Partridge, S.; Keitel, W.; Edwards, K.; Lee, M.; Treanor, J.; Greenberg, D. P.; Barenkamp, S.; Bernstein, D. I.; Edelman, R., *Bordetella pertussis* infections in vaccinated and unvaccinated adolescents and adults, as assessed in a national prospective randomized acellular pertussis vaccine trial (APERT). *Clin. Infect. Dis.* **2006,** *43* (2), 151-157.

15. Lam, C.; Octavia, S.; Ricafort, L.; Sintchenko, V.; Gilbert, G. L.; Wood, N.; McIntyre, P.; Marshall, H.; Guiso, N.; Keil, A. D., Rapid increase in pertactin-deficient *Bordetella pertussis* isolates, Australia. *Emerging Infect. Dis.* **2014,** *20* (4), 626-633.

16. Pawloski, L.; Queenan, A.; Cassiday, P.; Lynch, A.; Harrison, M.; Shang, W.; Williams, M.; Bowden, K.; Burgos-Rivera, B.; Qin, X., Prevalence and molecular characterization of pertactin-deficient *Bordetella pertussis* in the United States. *Clin.Vaccine Immunol.* **2014,** *21* (2), 119-125.

17. Otsuka, N.; Han, H.-J.; Toyoizumi-Ajisaka, H.; Nakamura, Y.; Arakawa, Y.; Shibayama, K.; Kamachi, K., Prevalence and genetic characterization of pertactin-deficient *Bordetella pertussis* in Japan. *PLoS One* **2012,** *7* (2), e31985.

18. Martin, S. W.; Pawloski, L.; Williams, M.; Weening, K.; DeBolt, C.; Qin, X.; Reynolds, L.; Kenyon, C.; Giambrone, G.; Kudish, K.; Miller, L.; Selvage, D.; Lee, A.; Skoff, T. H.; Kamiya, H.; Cassiday, P. K.; Tondella, M. L.; Clark, T. A., Pertactin-negative *Bordetella pertussis* strains: evidence for a possible selective advantage. *Clin. Infect. Dis.* **2015,** *60* (2), 223-227.

19. He, Q.; Mäkinen, J.; Berbers, G.; Mooi, F. R.; Viljanen, M. K.; Arvilommi, H.; Mertsola, J., *Bordetella pertussis* protein pertactin induces type-specific antibodies: one possible explanation for the emergence of antigenic variants? *J. Infect. Dis.* **2003,** *187* (8), 1200-1205.

20. Mooi, F. R., *Bordetella pertussis* and vaccination: The persistence of a genetically monomorphic pathogen. *Infect., Genet. Evol.* **2010,** *10* (1), 36-49.

21. Bart, M. J.; Harris, S. R.; Advani, A.; Arakawa, Y.; Bottero, D.; Bouchez, V.; Cassiday, P. K.; Chiang, C.-S.; Dalby, T.; Fry, N. K.; Gaillard, M. E.; van Gent, M.; Guiso, N.; Hallander, H. O.; Harvill, E. T.; He, Q.; van der Heide, H. G. J.; Heuvelman, K.; Hozbor, D. F.; Kamachi, K.; Karataev, G. I.; Lan, R.; Lutyńska, A.; Maharjan, R. P.; Mertsola, J.; Miyamura, T.; Octavia, S.; Preston, A.; Quail, M. A.; Sintchenko, V.; Stefanelli, P.; Tondella, M. L.; Tsang, R. S. W.; Xu, Y.; Yao, S.-M.; Zhang, S.; Parkhill, J.; Mooi, F. R., Global population structure and evolution of *Bordetella pertussis* and their relationship with vaccination. *mBio.* **2014,** *5* (2).

22. Pittman, M., Pertussis toxin: the cause of the harmful effects and prolonged immunity of whooping cough. A hypothesis. *Rev. Infect. Dis.* **1979,** *1* (3), 401-412.

23. Aoyama, T., Acellular pertussis vaccines developed in Japan and their application for disease

control. *J. Infect. Dis.* **1996,** *174* (Supplement_3), S264-S269.

24. Robbins, J. B.; Schneerson, R.; Kubler-Kielb, J.; Keith, J. M.; Trollfors, B.; Vinogradov, E.; Shiloach, J., Toward a new vaccine for pertussis. *Proc. Natl. Acad. Sci., U. S. A.* **2014,** *111* (9), 3213-3216.

25. Taranger, J.; Trollfors, B.; LagergÅrd, T.; Lind, L.; Sundh, V.; Zackrisson, G.; Bryla, D. A.; Robbins, J. B., Unchanged efficacy of a pertussis toxoid vaccine throughout the two years after the third vaccination of infants. *Pediatr. Infect. Dis. J.* **1997,** *16* (2), 180-184.

26. Lugauer, S.; Heininger, U.; Cherry, J. D.; Stehr, K., Long-term clinical effectiveness of an acellular pertussis component vaccine and a whole cell pertussis component vaccine. *Eur. J. Pediatr.* **2002,** *161* (3), 142-146.

27. McGirr, A.; Fisman, D. N., Duration of pertussis immunity after DTaP immunization: a meta-analysis. *Pediatrics* **2015**, peds. 2014-1729.

28. Ryan; Murphy; Nilsson; Shackley; Gothefors; Øymar; Miller; Storsaeter; Mills, Distinct T-cell subtypes induced with whole cell and acellular pertussis vaccines in children. *Immunology* **1998,** *93* (1), 1-10.

29. Edwards, K. M.; Berbers, G. A. M., Immune responses to pertussis vaccines and disease. *J. Infect. Dis.* **2014,** *209* (Supplement_1), S10-S15.

30. Higgs, R.; Higgins, S.; Ross, P.; Mills, K., Immunity to the respiratory pathogen *Bordetella pertussis*. *Mucosal Immunol.* **2012,** *5* (5), 485-500.

31. Ross, P. J.; Sutton, C. E.; Higgins, S.; Allen, A. C.; Walsh, K.; Misiak, A.; Lavelle, E. C.; McLoughlin, R. M.; Mills, K. H. G., Relative contribution of Th1 and Th17 cells in adaptive immunity to *Bordetella pertussis*: Towards the rational design of an improved acellular pertussis vaccine. *PLoS Path.* **2013,** *9* (4), e1003264.

32. Ryan, E. J.; Nilsson, L.; Kjellman, N. I. M.; Gothefors, L.; Mills, K. H. G., Booster immunization of children with an acellular pertussis vaccine enhances Th2 cytokine production and serum IgE responses against pertussis toxin but not against common allergens. *Clin. Exp. Immunol.* **2000,** *121* (2), 193-200.

33. Rennels, M. B.; Black, S.; Woo, E. J.; Campbell, S.; Edwards, K. M., Safety of a fifty dose of diphtheria and tetanus toxoid and acellular pertussis vaccine in children experiencing extensive, local reactions to the fourth dose. *Pediatr. Infect. Dis. J.* **2008,** *27* (5), 464-465.

34. Warfel, J. M.; Zimmerman, L. I.; Merkel, T. J., Acellular pertussis vaccines protect against disease but fail to prevent infection and transmission in a nonhuman primate model. *Proc. Natl. Acad. Sci., U. S. A.* **2014,** *111* (2), 787-792.

35. Meade, B.; Kind, P.; Ewell, J.; McGrath, P.; Manclark, C., In vitro inhibition of murine macrophage migration by *Bordetella pertussis* lymphocytosis-promoting factor. *Infect. Immun.* **1984,** *45* (3), 718-725.

36. Relman, D.; Tuomanen, E.; Falkow, S.; Golenbock, D. T.; Saukkonen, K.; Wright, S. D., Recognition of a bacterial adhesin by an integrin: Macrophage CR3 (αMβ2, CD11bCD18) binds filamentous hemagglutinin of *Bordetella pertussis*. *Cell* **1990,** *61* (7), 1375-1382.

37. Leininger, E.; Roberts, M.; Kenimer, J. G.; Charles, I. G.; Fairweather, N.; Novotny, P.; Brennan, M. J., Pertactin, an Arg-Gly-Asp-containing *Bordetella pertussis* surface protein that promotes adherence of mammalian cells. *Proc. Natl. Acad. Sci., U. S. A.* **1991,** *88* (2), 345-349.

38. Weingart, C. L.; Keitel, W. A.; Edwards, K. M.; Weiss, A. A., Characterization of bactericidal immune responses following vaccination with acellular pertussis vaccines in adults. *Infect. Immun.* **2000,** *68* (12), 7175-7179.

39. Weiss, A. A.; Patton, A. K.; Millen, S. H.; Chang, S.-J.; Ward, J. I.; Bernstein, D. I., Acellular pertussis vaccines and complement killing of *Bordetella pertussis*. *Infect. Immun.* **2004,** *72* (12), 7346-7351.

40. Dunne, A.; Mielke, L.; Allen, A.; Sutton, C.; Higgs, R.; Cunningham, C.; Higgins, S.; Mills, K., A novel TLR2 agonist from *Bordetella pertussis* is a potent adjuvant that promotes protective immunity with an acellular pertussis vaccine. *Mucosal Immunol.* **2015,** *8* (3), 607-617.

41. Higgins, S. C.; Jarnicki, A. G.; Lavelle, E. C.; Mills, K. H., TLR4 mediates vaccine-induced protective cellular immunity to *Bordetella pertussis*: role of IL-17-producing T cells. *J. Immunol.* **2006,** *177* (11), 7980-7989.

42. Maclennan, A. P., Specific lipopolysaccharides of *Bordetella*. *Biochem. J.* **1960,** *74* (2), 398-409.

43. Flak, T. A.; Goldman, W. E., Signalling and cellular specificity of airway nitric oxide production in pertussis. *Cell. Microbiol.* **1999,** *1* (1), 51-60.

44. Schaeffer, L. M.; McCormack, F. X.; Wu, H.; Weiss, A. A., Interactions of pulmonary collectins with *Bordetella bronchiseptica* and *Bordetella pertussis* lipopolysaccharide elucidate the structural basis of their antimicrobial activities. *Infect. Immun.* **2004,** *72* (12), 7124-7130.

45. Schaeffer, L. M.; McCormack, F. X.; Wu, H.; Weiss, A. A., *Bordetella pertussis* lipopolysaccharide resists the bactericidal effects of pulmonary surfactant protein A. *J. Immunol.* **2004,** *173* (3), 1959-1965.

46. Caroff, M.; Deprun, C.; Richards, J.; Karibian, D., Structural characterization of the lipid A of *Bordetella pertussis* 1414 endotoxin. *J. Bacteriol.* **1994,** *176* (16), 5156-5159.

47. Lebbar, S.; Caroff, M.; Szabó, L.; Mérienne, C.; Szilégyi, L. s., Structure of a hexasaccharide proximal to the hydrophobic region of lipopolysaccharides present in *Bordetella pertussis* endotoxin preparations. *Carbohydr. Res.* **1994,** *259* (2), 257-275.

48. Caroff, M.; Brisson, J.-R.; Martin, A.; Karibian, D., Structure of the *Bordetella pertussis* 1414 endotoxin. *FEBS Lett.* **2000,** *477* (1-2), 8-14.

49. Chaby, R.; Szabo, L., 7-O-(2-Amino-2-deoxy-α-D-glucopyranosyl) L-glycero-D-manno-heptose. *Eur. J. Biochem.* **1976,** *70* (1), 115-122.

50. Chaby, R.; Moreau, M.; SzabÓ, L., 2-O-(β-D-Glucuronyl)-7-O-(2-amino-2-deoxy-α-D-glucopyranosyl)-L-glycero-D-manno-heptose :a constituent of the *Bordetella pertussis* endotoxin. *Eur. J. Biochem.* **1977,** *76* (2), 453-460.

51. Moreau, M.; Chaby, R.; Szabo, L., Isolation of a trisaccharide containing 2-amino-2-deoxy-D-galacturonic acid from the *Bordetella pertussis* endotoxin. *J. Bacteriol.* **1982,** *150* (1), 27.

52. Moreau, M.; Chaby, R.; Szabo, L., Structure of the terminal reducing heptasaccharide of polysaccharide 1 isolated from the *Bordetella pertussis* endotoxin. *J. Bacteriol.* **1984,** *159* (2), 611-617.

53. Dolby, J. M.; Vincent, W., Characterization of the antibodies responsible for thebactericidal activity patterns' of antisera to *Bordetella pertussis*. *Immunology* **1965,** *8* (5), 499.

54. Ackers, J.; DOLBY, J. M., The antigen of *Bordetella pertussis* that induces bactericidal antibody and its relationship to protection of mice. *Microbiology* **1972,** *70* (2), 371-382.

55. Archambault, D.; Rondeau, P.; Martin, D.; Brodeur, B. R., Characterization and comparative bactericidal activity of monoclonal antibodies to *Bordetella pertussis* lipo-oligosaccharide A. *Microbiology* **1991,** *137* (4), 905-911.

56. Martin, D.; Peppler, M.; Brodeur, B., Immunological characterization of the lipooligosaccharide B band of *Bordetella pertussis*. *Infect. Immun.* **1992,** *60* (7), 2718-2725.

57. Le Blay, K.; Caroff, M.; Blanchard, F.; Perry, M. B.; Chaby, R., Epitopes of *Bordetella pertussis* lipopolysaccharides as potential markers for typing of isolates with monoclonal antibodies. *Microbiology* **1996,** *142* (4), 971-978.

58. Niedziela, T.; Letowska, I.; Lukasiewicz, J.; Kaszowska, M.; Czarnecka, A.; Kenne, L.; Lugowski, C., Epitope of the vaccine-type *Bordetella pertussis* strain 186 lipooligosaccharide and antiendotoxin activity of antibodies directed against the terminal pentasaccharide-tetanus toxoid conjugate. *Infect. Immun.* **2005,** *73* (11), 7381-7389.

59. Kubler-Kielb, J.; Vinogradov, E.; Lagergård, T.; Ginzberg, A.; King, J. D.; Preston, A.; Maskell, D. J.; Pozsgay, V.; Keith, J. M.; Robbins, J. B.; Schneerson, R., Oligosaccharide conjugates of *Bordetella pertussis* and *bronchiseptica* induce bactericidal antibodies, an addition to pertussis vaccine. *Proc. Natl. Acad. Sci., U. S. A.* **2011,** *108* (10), 4087-4092.

60. AlBitar-Nehme, S.; Basheer, S. M.; Njamkepo, E.; Brisson, J.-R.; Guiso, N.; Caroff, M., Comparison of lipopolysaccharide structures of *Bordetella pertussis* clinical isolates from pre- and post-vaccine era. *Carbohydr. Res.* **2013,** *378* (Supplement C), 56-62.

61. Dias, W. O.; van der Ark, A. A. J.; Sakauchi, M. A.; Kubrusly, F. S.; Prestes, A. F. R. O.; Borges, M. M.; Furuyama, N.; Horton, D. S. P. Q.; Quintilio, W.; Antoniazi, M.; Kuipers, B.; van der Zeijst, B. A. M.; Raw, I., An improved whole cell pertussis vaccine with reduced content of endotoxin. *Hum. Vaccin. Immunother.* **2013,** *9* (2), 339-348.

62. Khatun, F.; Stephenson, R. J.; Toth, I., An overview of structural features of antibacterial glycoconjugate vaccines that influence their immunogenicity. *Chem. Eur. J.* **2017,** *23* (18), 4233-4254.

63. Weiss, A. A.; Mobberley, P. S.; Fernandez, R. C.; Mink, C. M., Characterization of human bactericidal antibodies to *Bordetella pertussis*. *Infect. Immun.* **1999,** *67* (3), 1424-1431.

Chapter 2. Synthesis and Immunological Evaluation of Pertussis Pentasaccharide Bearing Multiple Rare Sugars as Potential Anti-pertussis Vaccines

2.1. Retrosynthetic Analysis and Rare Sugar Building Block Preparation

In Chapter 1 we demonstrated that the pertussis pentasaccharide could be a key component in designing a new potential bactericidal vaccine. The pertussis pentasaccharide has multiple unique structural features, which include three rare monosaccharides, i.e., 2,3-dideoxy-2,3-diamino-D-mannuronic acid (B), 2,3,6-trideoxy-4-methylamino-2 -acetamido-L-galactose (C), and L-glycero-D-manno-heptose (E). In addition, it contains three 1,2-*cis* glycosyl linkages and a 1,2-*trans* linkage between units C and D, which is found to be surprisingly challenging to form (*vide infra*). The structure of the pentasaccharide cleaved from pertussis LOS is illustrated in **Figure 2.1**. The reducing end, 2,5-anhydro-mannose, is converted from glucosamine by reacting with nitrous acid, and the deamination reaction also adds an additional nitroso on the methylamino group of the unit C. To best represent the native structure of the epitopes on pertussis LOS, we choose compound **2** as our target structure with a C3 linker at the reducing end for carrier protein conjugation. Unit E is not a free glucosamine as in the pertussis LOS since converting it to anhydromannose did not affect the antibody binding and saturation transfer difference NMR (STD-NMR) did not locate the key epitopes on it.[1]
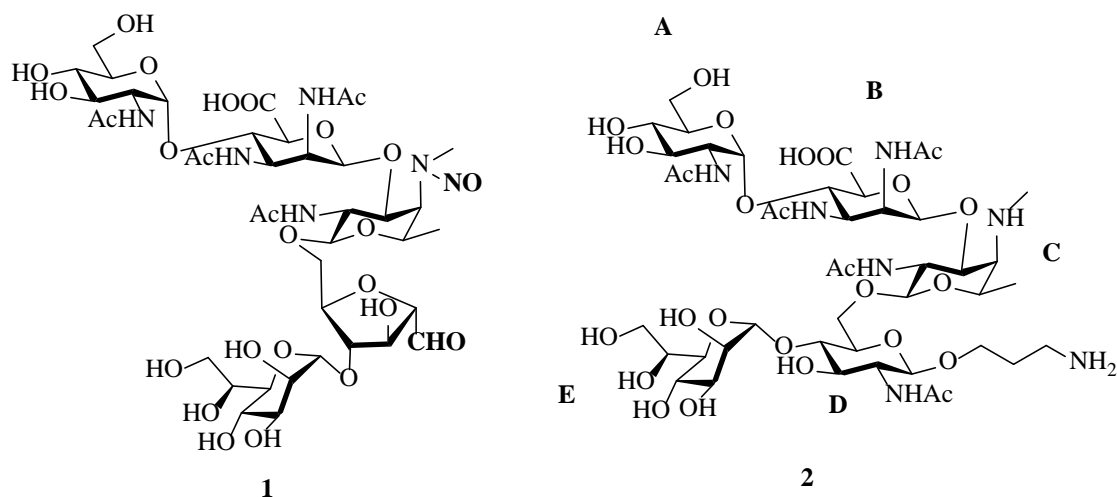
Figure 2.1. Structures of the pentasaccharide **1** cleaved by deamination and our synthetic target pentasaccharide **2**.

The synthetic design of the target pentasaccharide **2** was based on several considerations (**Scheme 2.1**). For the CDE branching trisaccharide, we envision the E unit should be installed onto D first before C as the 4-OH of D may be too hindered if the 6-OH of D is glycosylated first. To facilitate the formation of the 1,2-*trans* linkage between C and D, Troc, which is known to be a participating neighboring group, was used as the *N*-protecting group for 2-amine of unit C (building block **5**). The 1,2-*cis* linkage between amino-mannuronic acid B and fucosamine C is challenging to form directly. Instead, we opted for an indirect route using the 3-amino glucose derivative **6**, the 2-*O* stereochemistry of which could be stereospecifically inverted following glycosylation. The 2-*O* Bn and 2-N$_3$ bearing building blocks **3** and **7** were designed to facilitate the formation of α- glycosyl linkages.
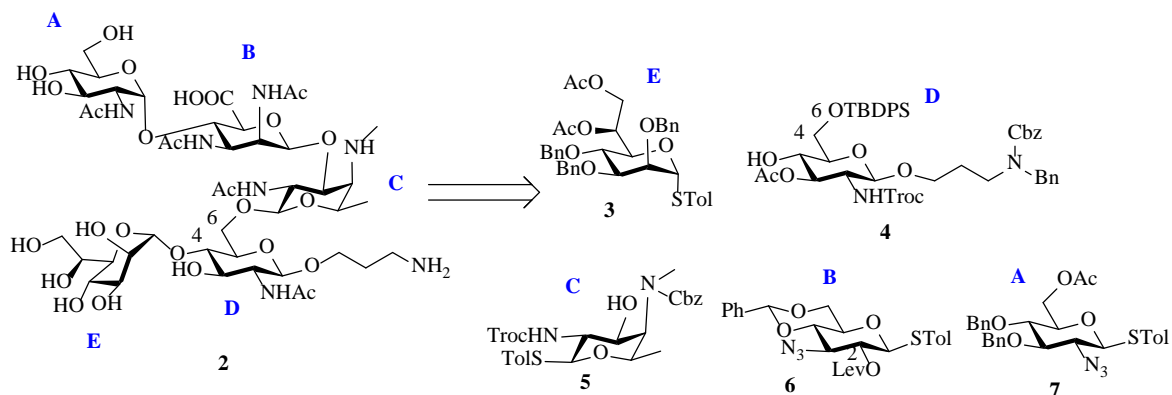
Scheme 2.1. Retrosynthetic analysis of target pentasaccharide **2**.

Our synthesis commenced with preparation of building blocks for the rare sugars (**3**, **5** and **6**) in the pentasaccharide. Acid-catalyzed ketal hydrolysis of the known 3-azido glucose derivative **8**[2] followed by global acetylation and treatment with *p*-toluenethiol (*p*-TolSH) and boron trifluoride etherate (BF$_3$·Et$_2$O) gave the thioglycoside **9** in 54% yield over 3 steps (**Scheme 2.2**). All *O*-acetyl groups of **9** were removed with NaOMe and 4, 6-benzylidene was installed to afford **10** in 81% yield. Protection of the free 2-OH with levulinic acid (LevOH) aided by 1-ethyl-3-(3-dimethylaminopropyl) carbodiimide hydrochloride (EDC·HCl) and 4-dimethylaminopyridine (DMAP) yielded the first rare sugar building block **6**.[3-4]
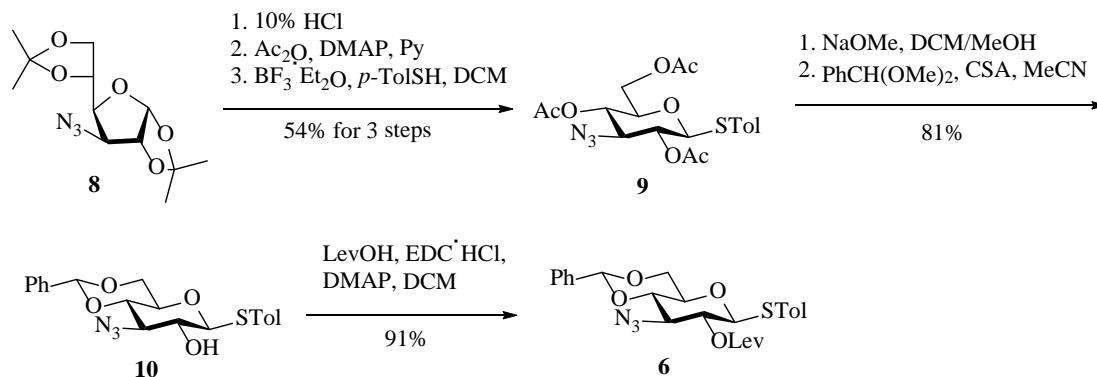
Scheme 2.2. Preparation of building block **6**.

Preparation of 2-acetamido-4-amino-2,4,6-trideoxygalactose (AAT) presented significant difficulties. The first route we undertook started with bis-triflation of α-rhamnoside **11**[5-6] to be followed by S_N2 displacement of *O*-triflates with sodium azide (**Scheme 2.3**). However, triflation resulted in a low yield of the desired bis-triflate with a major side product isolated containing the STol migrated to C-2 presumably due to the 1,2-*trans* arrangement of the α-STol and the purported intermediate bearing 2-OTf. To overcome this, the corresponding β-rhamnoside **12** was prepared, which was selectively protected at the 3-OH with benzoyl (Bz) and triflated at the 2- and 4-OH. Sequential displacement of the two triflates by sodium azide and potassium phthalimide gave the fucosamine analog **14** in a moderate 30-50% yield. Deprotection of the phthalimide and Bz groups with hydrazine produced the free amine **15**, but with a low 30% yield.

α-rhamnoside **11**

β-rhamnoside **12**

13

PhthN **14**

15
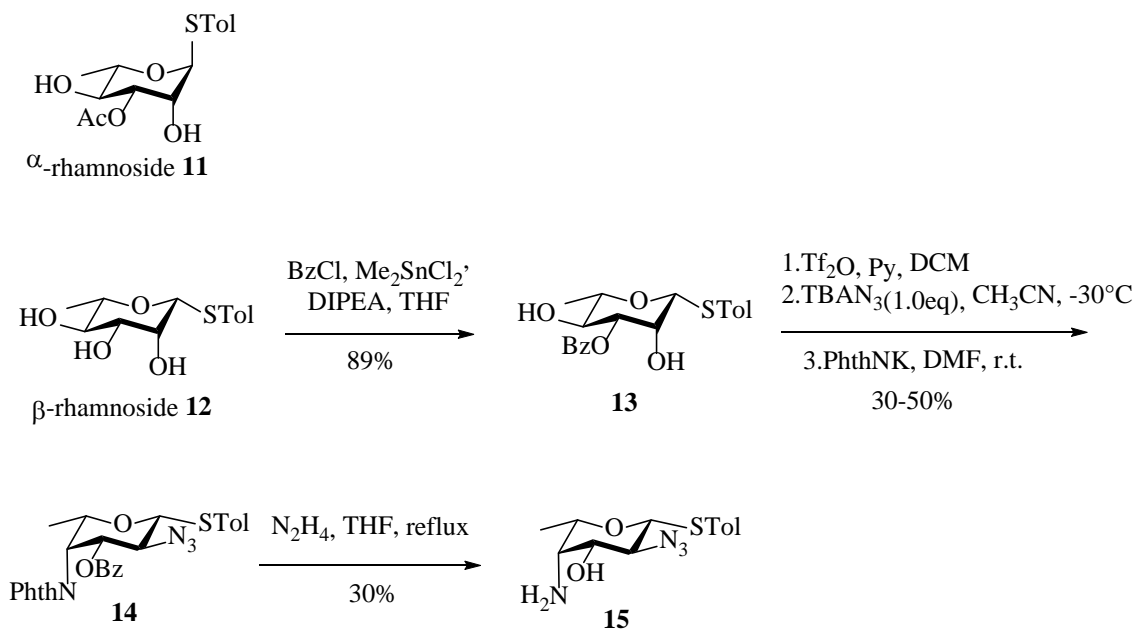
Scheme 2.3. Preparation of fucosamine building block by following the previously reported route.[5-6]

To improve the yield, we explored trichloroacetimidate as the protecting group[7-8] of 3-OH of β-rhamnoside **12** rather than Bz so that C4 inversion could be achieved *in situ* upon triflation (**Scheme 2.4**). The thioglycoside **12** was treated with trichloroacetonitrile and 1, 8-diazabicyclo[5.4.0]undec-7-ene (DBU), giving **16** in a yield of 90%. The imidate **16** was subjected to trifluoromethanesulfonic anhydride (Tf$_2$O) and pyridine at -30 °C, which formed 3, 4-oxazoline ring spontaneously following nucleophilic displacement of 4-OTf by the neighboring imidate. Displacement of the 2-OTf with sodium azide (NaN$_3$) in DMF at 50 °C afforded **17** in an excellent yield of 85% over 2 steps. Refluxing **17** in 4M hydrochloric acid (HCl) opened the oxazoline ring and gave **15** in 89% yield with the two N moieties on the ring differentiated. Among multiple methods investigated, monomethylation of 4-NH$_2$ was best performed by refluxing **15** in ethyl formate and trimethylamine (Et$_3$N) followed by treatment

with lithium aluminum hydride (LiAlH$_4$), which was accompanied by simultaneous reduction of the 2-N$_3$ to the amine. Selective protection of the equatorial primary 2-NH$_2$ with trichloroethyl chloroformate (TrocCl) yielded **19**, which was then treated with benzyl chloroformate giving the fucosamine building block **5** in 75% yield.
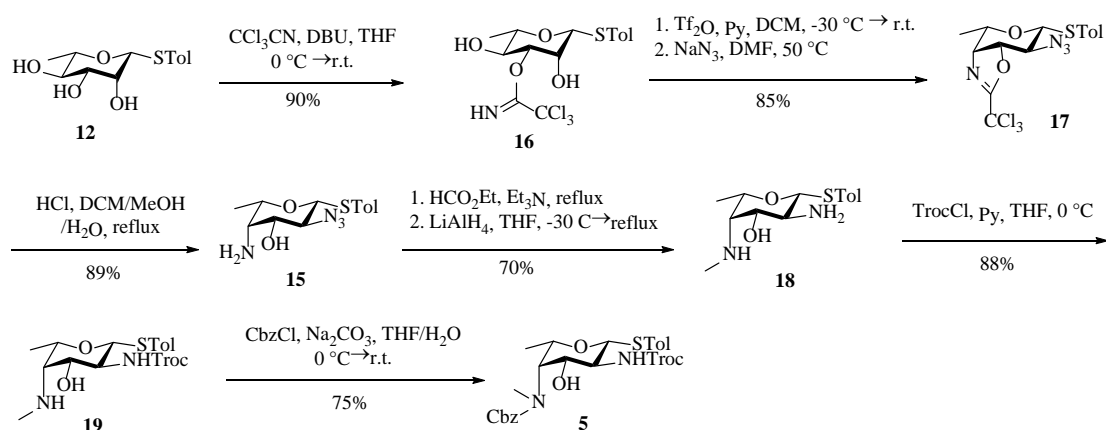
Scheme 2.4. Preparation of building block **5**.

Preparation of the mannoheptose building block with the desired (L, D) configuration[9-13] started from Swern oxidation of the mannosyl thioglycoside **20** (**Scheme 2.5**). The resulting aldehyde was not stable, which was directly subjected to Wittig olefination to give the product **21** in 83% yield. Treatment of the olefin **21** with osmium tetraoxide (OsO$_4$) and 4-methylmorpholine *N*-oxide (NMO) at 0 °C furnished diols **22** and **23** in 2.4:1 ratio (**22**: H-6 3.93 ppm, C-7 63.1 ppm; **23**: H-6 3.98 ppm, C-7 65.0 ppm[12]), which were separated by column chromatography. The D, D diastereoisomer **22** was then epimerized to the desired L, D-isomer **23**. Acetylation of the diol afforded the desired mannoheptose building block **3** in 91% yield.
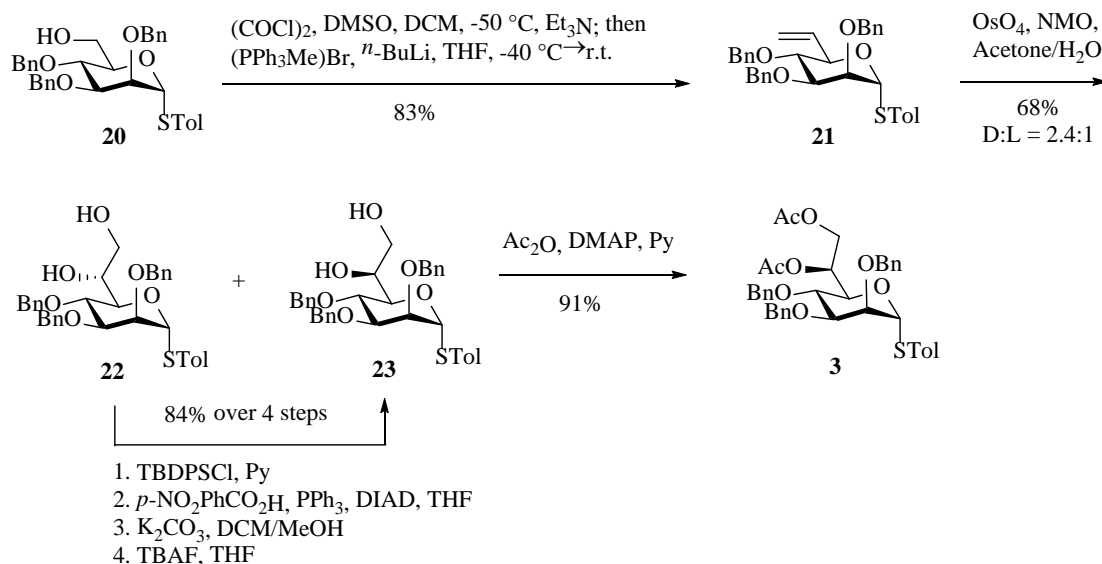
Scheme 2.5. Preparation of building block **3**.

2.2. Stereochemical Challenges in Formation of the C-D Linkage

With all monosaccharide building blocks in hand, we began the oligosaccharide assembly. Reaction of donor **3** with acceptor **4** proceeded smoothly promoted by *p*-TolSCl and AgOTf affording the DE disaccharide **24** in 80% yield (J_{H1-C1} = 171.0, 159.5 Hz). Removal of the *t*-butyldiphenylsilyl (TBDPS) of **24** exposed 6-OH on glucosamine, which was poised to be glycosylated by a fucosamine donor (**Scheme 2.6.1**).

To test the formation of BC disaccharide, glycosylation of acceptor **5** by donor **6** under the activation of *p*-TolSCl and AgOTf at -78 °C produced disaccharide **26** in 70% yield (J_{H1-C1} = 163.0, 161.0 Hz). Removal of 2-*O*-levulinoyl group exposed free hydroxyl in **27**, which was then triflated and substituted by azide to furnish the mannose configuration in BC disaccharide **28**. The glycosylation of **28** and disaccharide acceptor **25** was explored next. While tetrasaccharide

29 was formed in good yield (73%), surprisingly, the newly formed glycosyl linkage was α only ($J_{\text{H1-C1}}$ = 177.0, 171.0, 163.5, 166.0 Hz) despite the presence of the 2-*N*-Troc capable of neighboring group participation (**Scheme 2.6.2**).
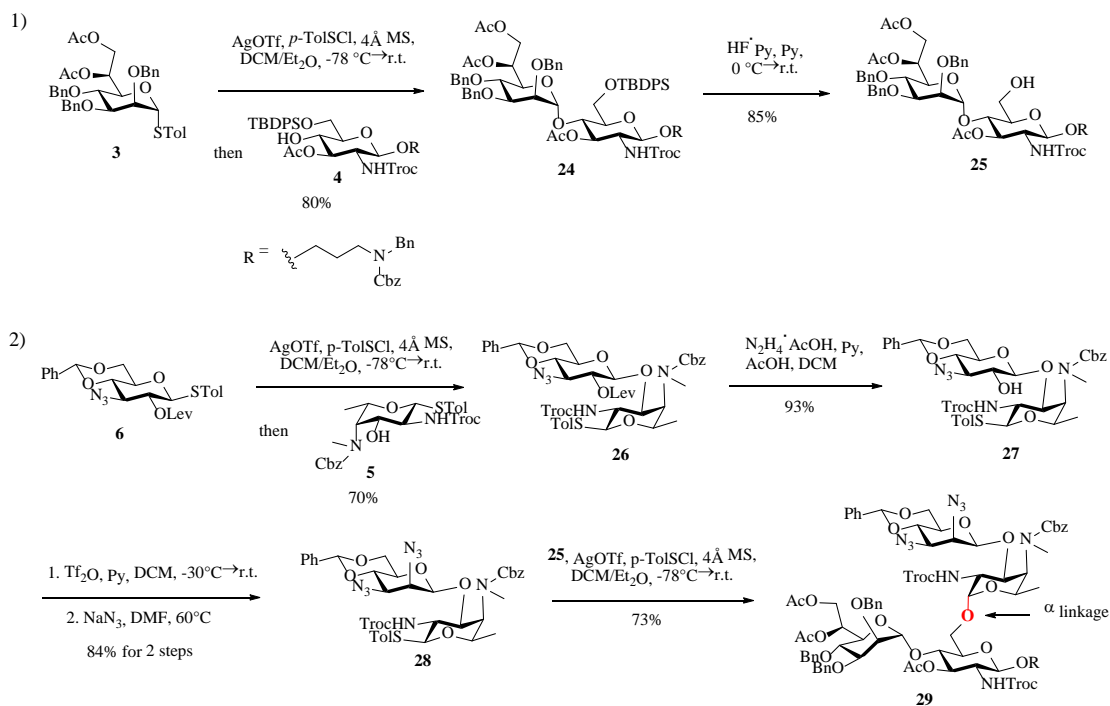
Scheme 2.6. Undesired α-isomer **29** isolated from glycosylation between **28** and 2**5**.

To form the desired β-isomer for CD linkage, we tested a series of reactions by varying protecting groups on the fucosamine donor with 3-azido propanol **30** as the model acceptor (**Table 2.1**). Glycosylation of donor **31** with acceptor **30** with *p*-TolSCl/AgOTf promoter gave a 3:2 α:β ratio using dichloromethane (DCM) as the reaction solvent (entry 1). Switching the promoter to NIS/TfOH gave a small improvement of the β selectivity (entry 2). Acetonitrile is well known to favor the formation of equatorial glycosides. However, 10% acetonitrile as the
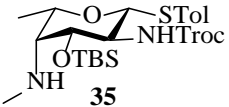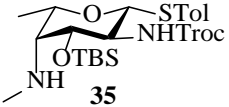
co-solvent did not impact stereoselectivity much (entry 3). Increasing the amount of acetonitrile to 50% gave very low yield of the glycoside product (entry 4). The 2-picoloyl was pioneered by the Demchenko group as a remote participating group, which can form a hydrogen bond with the acceptor and direct the addition of the acceptor to the activated glycosyl donor with high syn selectivity.[14] However, in our system, introduction of picoloyl onto the 3-OH of the fucosamine donor gave worse β selectivity (entry 5). Switching the 4-NCbz to 4-NPico or leaving the 3-OH unprotected in the fucosamine donor did not change the stereoselectivity much (entries 6, 7 and 8). The 3-Lev bearing donor **34** favored the formation of the β-isomer with 3-azidopropanol. Unfortunately, the α-glycoside became the major product (α:β = 2:1) when glycosylating disaccharide acceptor **25**.

One possible reason for the difficulty in forming β-glycoside is the epimerization of β-glycoside during the reaction as the α-glycoside should be more stable due to the anomeric effect. To test this, the β-glycoside product was subjected to the glycosylation condition with the addition of 1 eq of TfOH. No appreciable amounts of the α-glycoside were found suggesting the β-glycoside once formed was stable under the reaction condition.

Table 2.1. Investigation of protecting group schemes for β-selective fucosylation

Entry	Substrate	Reaction Condition	Yield	α : β
1	**31**	[*p*-TolSCl][a], DCM	89%	3 : 2
2	**31**	[NIS][b], DCM	92%	2 : 3
3	**31**	[NIS], DCM/MeCN = 9/1	90%	2 : 3
4	**31**	[NIS], DCM/MeCN = 1/1	25%	α only
5	**32**	[NIS], DCM	60%	5 : 1
6	**33**	[NIS], DCM	<5%	N/A
7	**33**	[*p*-TolSCl], DCM	30%	α only
8	**5**	[NIS], DCM	80%	3 : 1
9	**34**	[NIS], DCM	91%	1 : 2

Table 2.1. (cont'd)

10	(structure **35**)	[NIS], DCM	<5%	N/A
11	(structure **35**)	[*p*-TolSCl], DCM	60%	1 : 2.5[c]

a. [*p*-TolSCl]: *p*-TolSCl, AgOTf, 4Å MS, -78°C
b. [NIS]: NIS, TfOH, 4Å MS, -78°C
c. Ratio determined by crude NMR

To better understand the preference for α-glycoside formation using donors **31**-**34**, molecular modeling of the postulated oxocarbenium intermediate of donor **31** was performed. To obtain conformers covering a wide range of the configuration space, plain molecular dynamics (MD) simulations were performed at 900 K. From the resulting MD frames, 100 conformers with equal time intervals were extracted, and further optimized using the B3LYP/6-31G* method. Then, the optimized 100 conformers were sorted by their energies and the 20 most stable conformers were selected for geometrical comparison. Only 4 out of those 20 conformers exhibited the anticipated neighboring group participation by the carbonyl oxygen of 2-NHTroc with a distance of 1.58-1.59 Å between the carbonyl oxygen and C1 (d_2 in **Table 2.2**). Intriguingly, most of the stable conformers revealed an unexpected remote group participation by the carbonyl oxygen of 4-NMeCbz (d_3 = 1.51-1.55 Å in **Table 2.2**). This information provided a potential explanation why an α/β mixture was generated when the intermediate was reacted with a small aliphatic alcohol **30**. As a non-participating group in the subsequent S$_N$-2 like reaction, the Cbz carbonyl oxygen was closer to the anomeric carbon than Troc (2.74-2.76 Å vs 2.89-3.31 Å). Moreover, the

orientation of the Cbz group in conformer No. 9, 10, 12 and 13 blocked the S_N-2 like attack (**Figure 2.2B**), while the non-participating Troc group, such as in conformer No. 4, pointed away from the backside (**Figure 2.2A**). The difference in steric hindrance could explain why a larger amount of α stereoisomer was formed when the bulkier disaccharide acceptor **25** was used for glycosylation (**Scheme 2.7.1**).

Table 2.2. The relative energies and geometry of the most stable 20 conformers
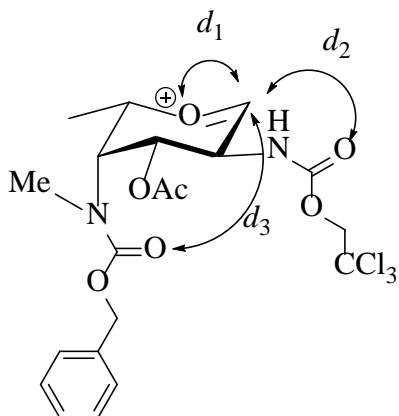
Conformer No.	Relative E (kcal/mol)	d_1 (Å)	d_2 (Å)	d_3 (Å)
1	0.000	1.3625	3.0308	1.5152
2	0.000	1.3626	3.0307	1.5152
3	1.373	1.3606	3.0075	1.5226
4	1.746	1.361	3.0115	1.522
5	1.788	1.3569	2.8922	1.5363
6	1.834	1.3564	2.9113	1.5343
7	2.045	1.3626	3.2624	1.5132
8	2.056	1.3618	3.2151	1.5138
9	2.153	1.3333	1.5893	2.7571
10	2.153	1.3333	1.5893	2.7574
11	2.268	1.3584	2.9889	1.5325
12	2.382	1.3349	1.5848	2.7395
13	2.382	1.335	1.5849	2.7393
14	2.404	1.359	2.9811	1.5304
15	2.412	1.3618	3.2133	1.5259
16	2.441	1.3483	3.3137	1.5491
17	2.504	1.3597	2.9887	1.5302
18	2.504	1.3597	2.9888	1.5302
19	2.504	1.3598	2.9886	1.5301
20	2.504	1.3597	2.9887	1.5302
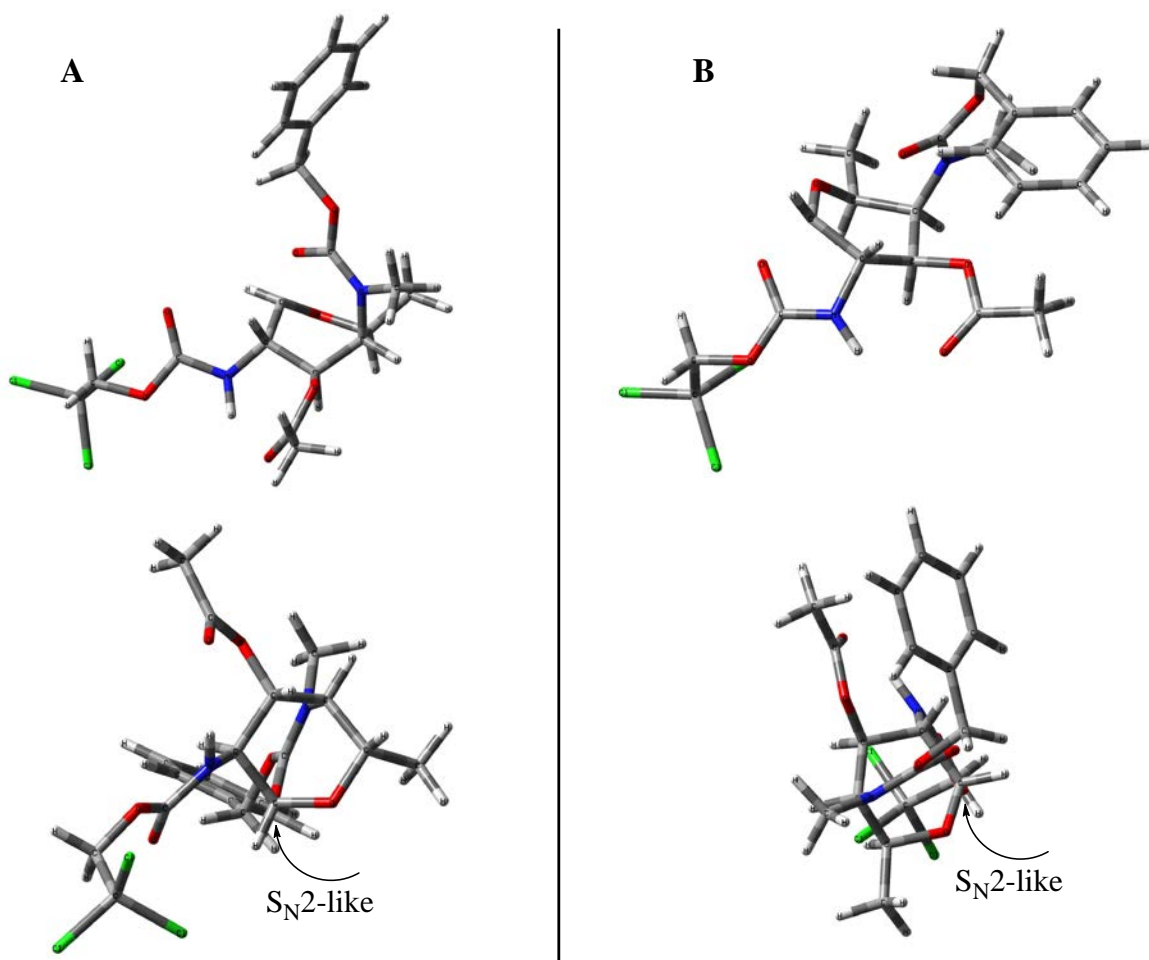
Figure 2.2. **Two stable conformers of the postulated oxocarbenium intermediate.** A) Remote group participation by the carbonyl oxygen of Cbz in conformer No. 4. B) Neighboring group participation by the carbonyl oxygen of Troc in conformer No. 9. S_N-2 like backside attack of conformer 9 by an acceptor is more sterically hindered than that of conformer 4 due to the existence of Cbz.

This information led us to design donor **35**, where the 4-methyl amino group was unprotected. Donor **35** failed to be activated by NIS/TfOH to glycosylate 3-azidopropanol presumably due to neutralization of TfOH by the free secondary amine in the donor. Changing the promoter to *p*-TolSCl/AgOTf gave the β anomer (β:α = 2.5:1) as the major product (entry 11). Interestingly, the reaction of **35** with acceptor **25** gave excellent β-selectivity. Following Cbz

protection, the two anomers were separated providing **37α** (10%) and **37β** (73%) for the 2 steps. Although selective β-glycosylation of 2,4-diamino fucose has been reported in the synthesis of O-specific polysaccharides of *Shigella sonnei*[15-17] and *Providencia alcalifaciens*[18], this is the first time that such a β-linked fucosamine glycoside bearing methyl amine has been produced to the best of our knowledge.
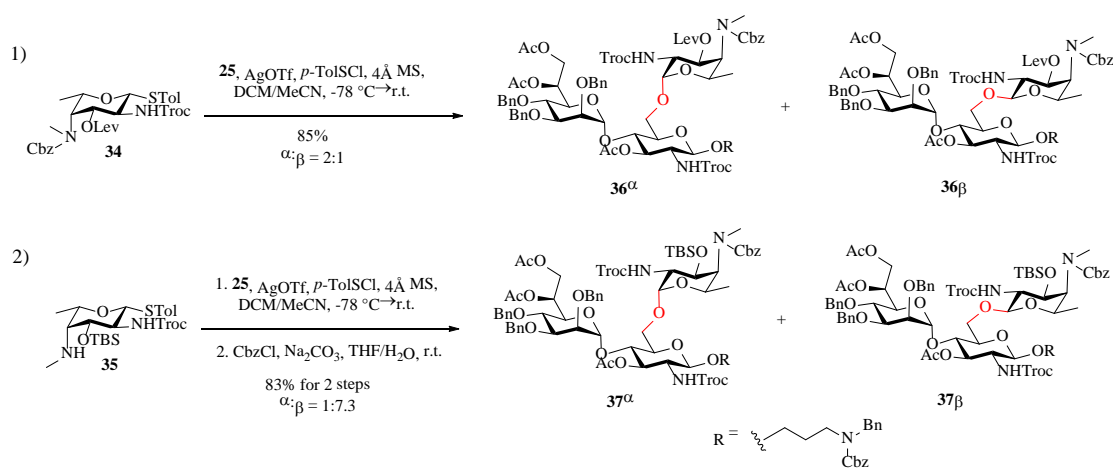
Scheme 2.7. Selective formation of β-fucoside.

2.3. Assembly of Pertussis Pentasaccharide and Deprotection

With the challenge of β-fucosamine formation overcome, we next focused on assembling the full pentasaccharide. After removal of TBS from **37β**, the acceptor **38** was glycosylated with donor **6** yielding tetrasaccharide **39**. The 2-*O*-Lev group was removed with hydrazine hydrate in 84% yield. The liberated 2-OH on **40** was then subjected to triflation, whereupon nucleophilic displacement of 2-*O*-triflate by NaN₃ afforded mannose configuration on **41** in 86% yield over 2 steps. The benzylidene group of **41** was cleaved with trifluoroacetic acid (TFA) in presence of

H₂O to give the diol **42** in 86% yield. Selective oxidation of the 6-OH followed by methylation

with methyl iodide (MeI) produced the tetrasaccharide acceptor **43** in 66% yield over 2 steps.

The last glycosylation with donor **7** completed the backbone construction and gave the fully

protected pentasaccharide **44** in 63% yield.

The deprotection of **44** was carried out by first converting all azido and NHTroc groups to

acetamido with zinc power, acetic acid and acetic anhydride in THF in 65% yield. The major

side product isolated was found to carry one dichloroethyloxycarbonyl group due to partial

reduction by zinc. Saponification of **45** with lithium hydroxide (LiOH) followed by

hydrogenolysis over palladium hydroxide (Pd(OH)₂) gave the deprotected **2**, completing the first

synthesis of pertussis like pentasaccharide.
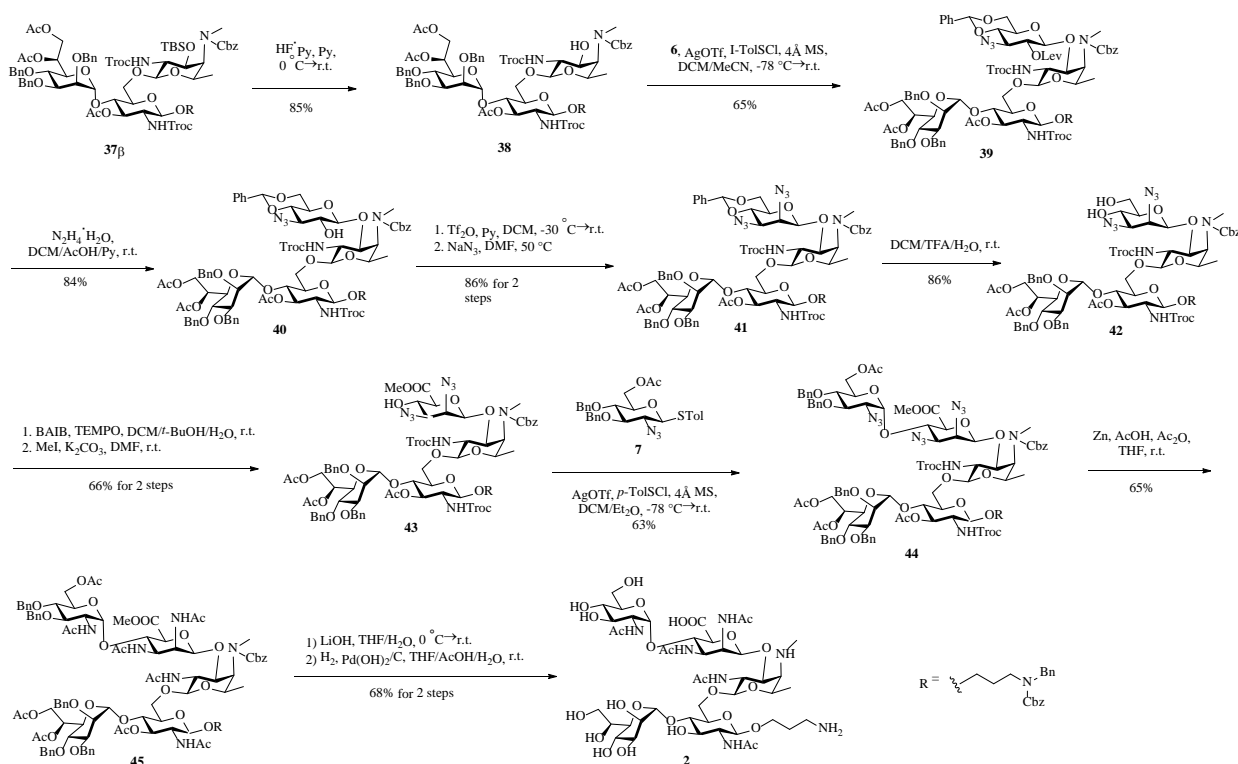
Scheme 2.8. Complete synthesis of the target pentasaccharide **2**.

2.4. Bioconjugation of Pertussis-like Pentasaccharide with Bacteriophage Qβ Carrier

As carbohydrates are typically T cell independent B cell antigens, to generate high titers of anti-glycan IgG antibodies, it is important to link the carbohydrates to an immunogenic carrier capable of activating helper T cells. We have previously demonstrated that bacteriophage Qβ is a superior carrier to deliver tumor associated carbohydrate antigens. To elicit powerful anti-pertussis antibody responses, we investigated the conjugation of pertussis pentasaccharide **2** with Qβ.

For bioconjugation, pertussis pentasaccharide **2** was first treated with $CSCl_2$ to convert the free amine to a thiocyanate moiety. However, the highly reactive $CSCl_2$ also reacted with the secondary amine on Unit C, resulting in split methyl peaks on Unit C in NMR and higher molecular weight in ESI-MS. We next investigated NHS activated ester chemistry by treating **2** with adipic acid di-NHS ester **46** to produce pertussis pentasaccharide activated ester **47**. The doublet for 6-methyl on Unit C of **47** remained unchanged in ^{1}H-NMR compared to **2**. **47** was then incubated with bacteriophage Qβ in PBS buffer at pH 7.4, which successfully introduced pertussis pentasaccharide onto Qβ (Scheme **2.9.1**). On average, there were 235 copies of the glycan per Qβ particle according to the analysis via electrospray-ionization mass spectrometry (ESI-MS). To compare the effect of carrier protein in eliciting anti-glycan antibodies, we adopted the commonly used keyhole limpet hemocyanin (KLH). Similar conjugation reaction with **47** resulted in 1180 copies of the glycan per KLH (Scheme **2.9.2**), as determined by the anthrone-sulfuric acid assay.[19] For the enzyme-linked immunosorbent assay (ELISA) analysis of

serum antibodies, a bovine serum albumin (BSA)-glycan conjugate with 14 copies of glycan was

prepared (Scheme **2.9.3**).
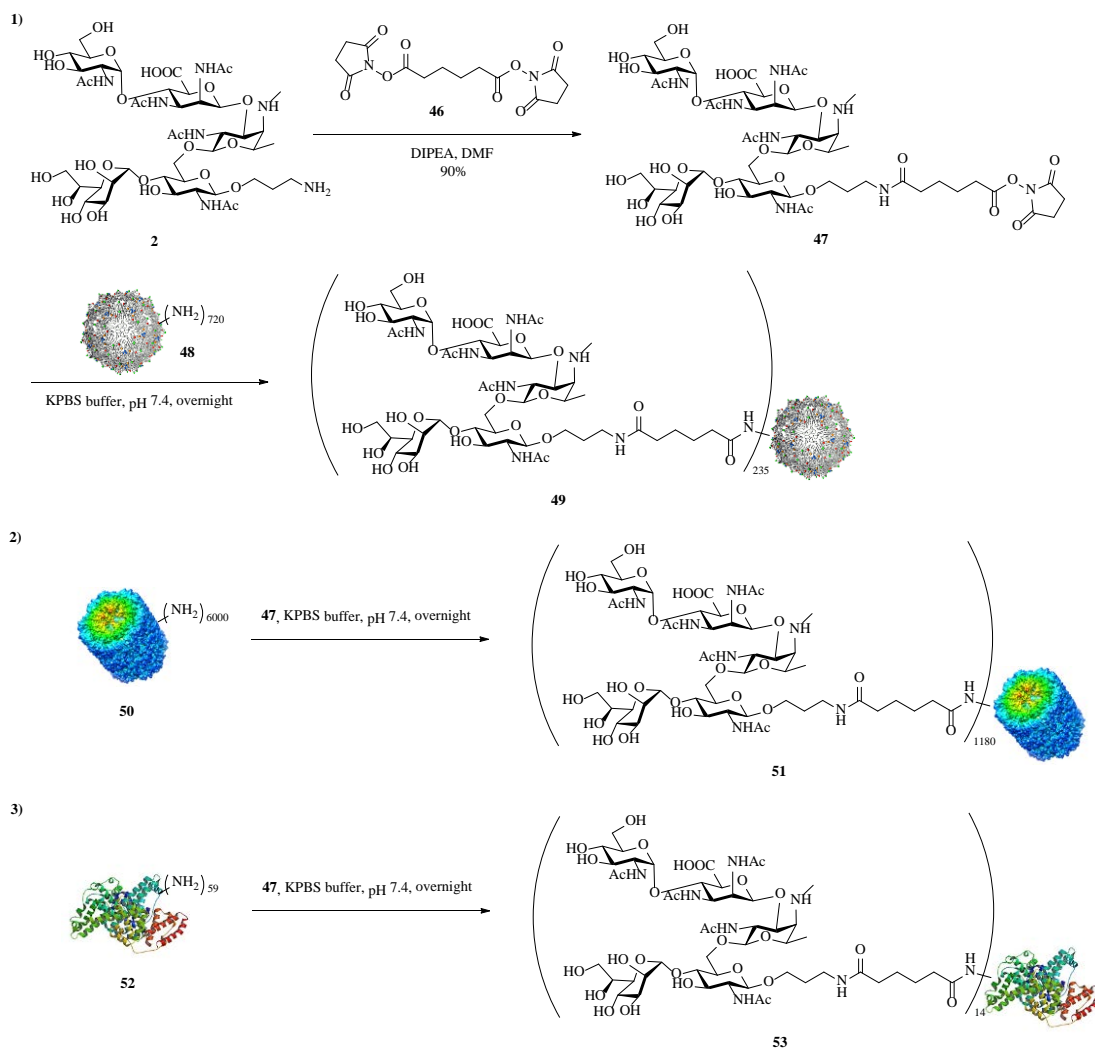
Scheme 2.9. Preparation of protein-glycan conjugates by reaction of activated NHS ester compound **47** with 1) Qβ, 2) KLH and 3) BSA.

2.5. Immunization Study

With the Qβ-glycan conjugate **49** in hand, we then investigated its ability to generate

anti-glycan antibodies. C57BL/6 mice were immunized subcutaneously with three biweekly injections of **49** containing 2 μg or 8 μg glycan or **51** containing 2 μg glycan, along with MPLA as the adjuvant. Sera were collected from the mice one week after each injection. Unconjugated Qβ was used for immunization for the control group of mice. ELISA analysis of post-immunization mouse sera showed good titers for anti-glycan antibodies, compared to those of the control group of mice immunized by unconjugated Qβ. Although immunization with **49** at different doses did not lead to much difference in antibody level, the carrier protein Qβ elicited much higher IgG antibody response than did KLH (**Figure 2.3A**). The IgG antibody level reached maximum on day 35 and remained at a high level over 250 days (**Figure 2.3B**). A study on the subclasses of IgG antibodies indicated a higher level for IgG2 compared with IgG1 and IgG3, which suggested a more Th1-weighted immune response (**Figure 2.3C**). Booster injection on day 261 was able to raise the antibody level (**Figure 2.3D**). Since aP vaccines mainly elicited a Th2-skewed immune response,[20-23] our synthetic glycoconjugate vaccine might be a good complement to the current treatment schemes.
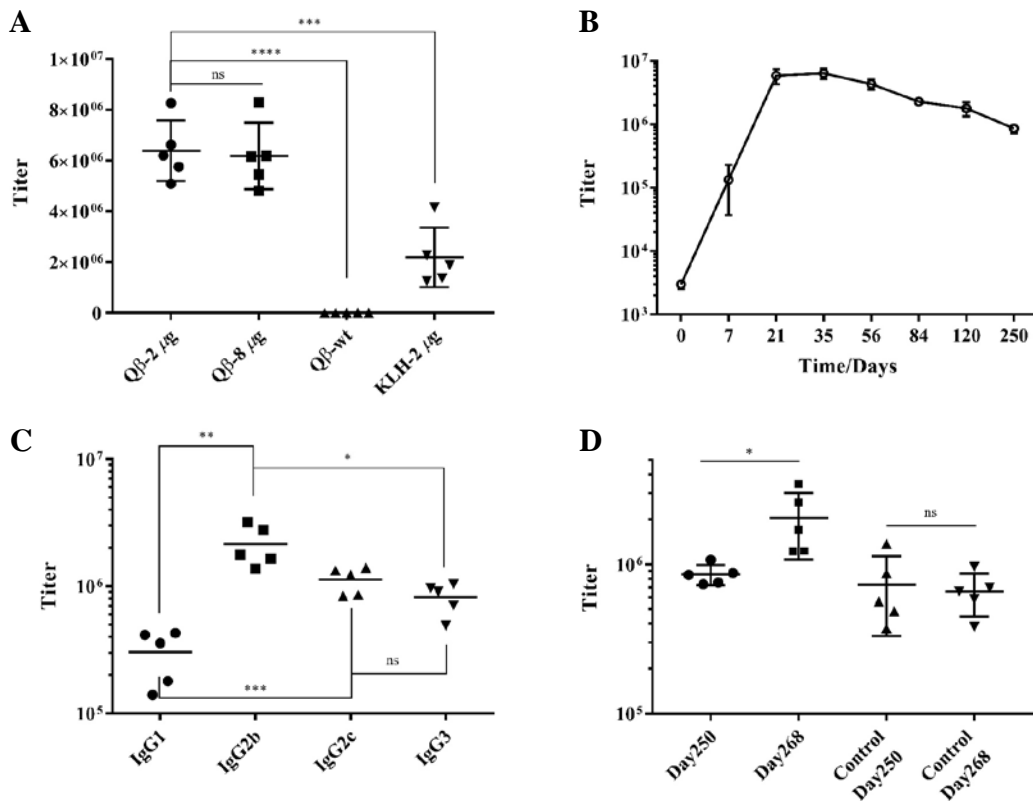
Figure 2.3. **Immunological evaluation of Qβ-glycan conjugate vaccine.** A) Comparison of serum IgG titers from mice immunized at difference doses or with different carrier proteins. Qβ-2/8 μg: **49** containing 2/8 μg glycan. Qβ-wt: **48** only. KLH-2 μg: **51** containing 2 μg glycan. B) Serum IgG titer profile over 250 days. Mice were immunized at the dose of 2 μg with **49** on day 0, 14 and 28. C) The level of anti-glycan IgG subclasses measured by ELISA. D) The level of IgG titers as determined by ELISA after another booster injection on day 261. Sera from mice which received the first three injections but not the fourth booster were tested as a control. * p $\leq$ 0.05; ** p $\leq$ 0.01; *** p $\leq$ 0.001; ns: not significant.

To test the binding of our mouse antisera against *B. pertussis*, the strain Tohama I was used in the flow cytometry experiments (This part was done by the Dr. Jennifer Maynard lab). However, only slightly better binding was observed for the antisera than the negative control despite the high titers against the synthetic glycan, while a much stronger binding was observed for the sera from whole cell vaccine (**Figure 2.4**, the blue area centered $\sim 10^3$).

Complement-dependent cytotoxicity was observed for mouse 1, 7 and 9 (**Figure 2.5**) but overall

it was much weaker compared to the sera from whole cell vaccine (data not shown).

	Sample Name	Geometric Mean : APC-A
	Michigan Samples_2nd Only.fcs	25.2
	Michigan Samples_CSM3.fcs	82.5
	Michigan Samples_CSM5.fcs	75.7
	Michigan Samples_M1.fcs	49.5
	Michigan Samples_M2.fcs	24.4
	Michigan Samples_M3.fcs	69.3
	Michigan Samples_M4.fcs	127
	Michigan Samples_M5.fcs	54.0
	Michigan Samples_M6.fcs	87.1
	Michigan Samples_M7.fcs	25.8
	Michigan Samples_M8.fcs	47.7
	Michigan Samples_M9.fcs	73.7
	Michigan Samples_M10.fcs	78.5
	Michigan Samples_QbM1.fcs	108
	Michigan Samples_QbM2.fcs	155
	Michigan Samples_QbM3.fcs	129
	Michigan Samples_Unstained.fcs	4.01
	Michigan Samples_WCV Sera.fcs	1443
	Michigan Samples_D26E.fcs	143

Figure 2.4. Flow cytometry indicated that the mouse antisera had no significant binding with the bacteria. Only whole-cell vaccine control sera had strong binding against *B. pertussis*. M1-5 were immunized at the dose of 2 μg, and M6-10 were immunized at the dose of 8 μg.
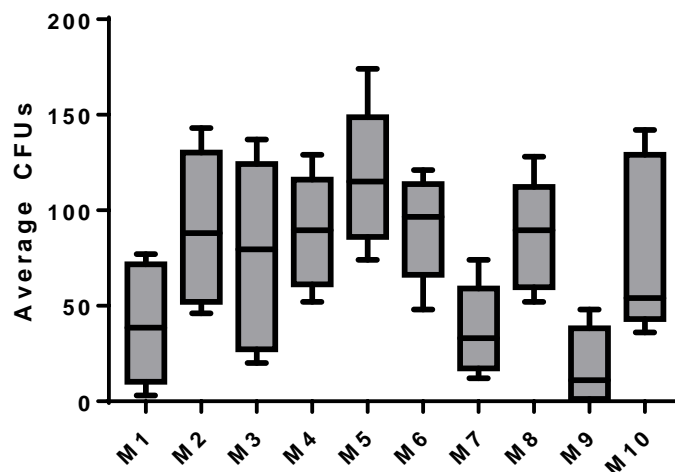
Figure 2.5. Complement-dependent cytotoxic assay of mouse antisera. The bactericidal activity of mouse antisera was assessed by counting the colony-forming units of *B. pertussis*.

2.6. Conclusions and Future Plans

In this study, we successfully synthesized the pentasaccharide from *B. pertussis* in a linear synthetic route. The key challenge in selective β-fucosylation was solved and well explained by molecular modeling. Conjugation of the pentasaccharide to the carrier protein Qβ elicited a Th1-weighted immune response as well as high titers of anti-glycan antibodies. However, the mouse antisera showed little binding affinity against *B. pertussis* strain Tohama I and low complement-dependent cytotoxicity.

The main difficulty in designing a more convergent synthetic route resides in the choice of protecting groups on the fucose. The remote group participation hampers selective β-fucosylation and therefore any carbamate protection groups have to be ruled out. The current protection group-free protocol helped formation of the β-isomer when the fucose building block was used as the donor in glycosylation reactions. However, previous trials using the same fucose building block as acceptor gave no desired product. Novel protecting schemes for the methylamino group remain to be developed to facilitate the design of a convergent synthetic route for the pentasaccharide or the whole dodecasaccharide.

It was considered that the reducing-end glucosamine was not important in immune reactions since conversion to anhydromannose by treatment with nitrous acid still led to antibodies that bound to *B. pertussis*. However, our synthetic glycan failed to elicit strong-binding antibodies or high bactericidal activity. A previous study on the LOS monoclonal antibodies[24] also indicated that the glucosamine played a role in the epitope recognition. Since the activity of antibodies relies on the recognition of epitopes, it is necessary to analyze the epitopes on the synthetic

glycan recognized by mouse antisera. Redesigning the carbohydrate antigen accordingly may help the development of a better vaccine against *B. pertussis*.

2.7. Experimental Section

2.7.1. Synthesis of the Glycan-Carrier Protein Conjugates

To the carrier protein (Qβ/BSA/KLH) suspended in potassium phosphate buffer (KPB, 0.1 M, pH 7.0, 1mL) was added compound **47** (4 eq per NH_2) in DMSO (0.1 mL). The reaction mixture was rotated on a rotating mixer at room temperature overnight. The solution was then subjected to ultracentrifugation in Millipore 100k MWCO centrifugal filter tube to remove excess glycan. The conjugates were purified by size exclusion chromatography (SEC) on an AKTApure 25L system equipped with Superose 6 Increase 10/300 GL column.

2.7.2. Quantification of Glycan Number on the Carrier Protein

For Qβ conjugate, the particle was treated with dithiothreitol (DTT) at 90 °C for 30 min. The average number of conjugated glycan on each viral capsid subunit was estimated from the intensity of peaks in the deconvoluted mass spectra from LC-MS analysis. Results are shown in **Figure 2.6**.

For BSA conjugate, the number of conjugated glycan was calculated from the mass obtained from MALDI-TOF MS analysis. Results are shown in **Figure 2.7**.

For KLH conjugate, the number of conjugated glycan was measured with a previously reported anthrone-sulfuric acid assay.[19]
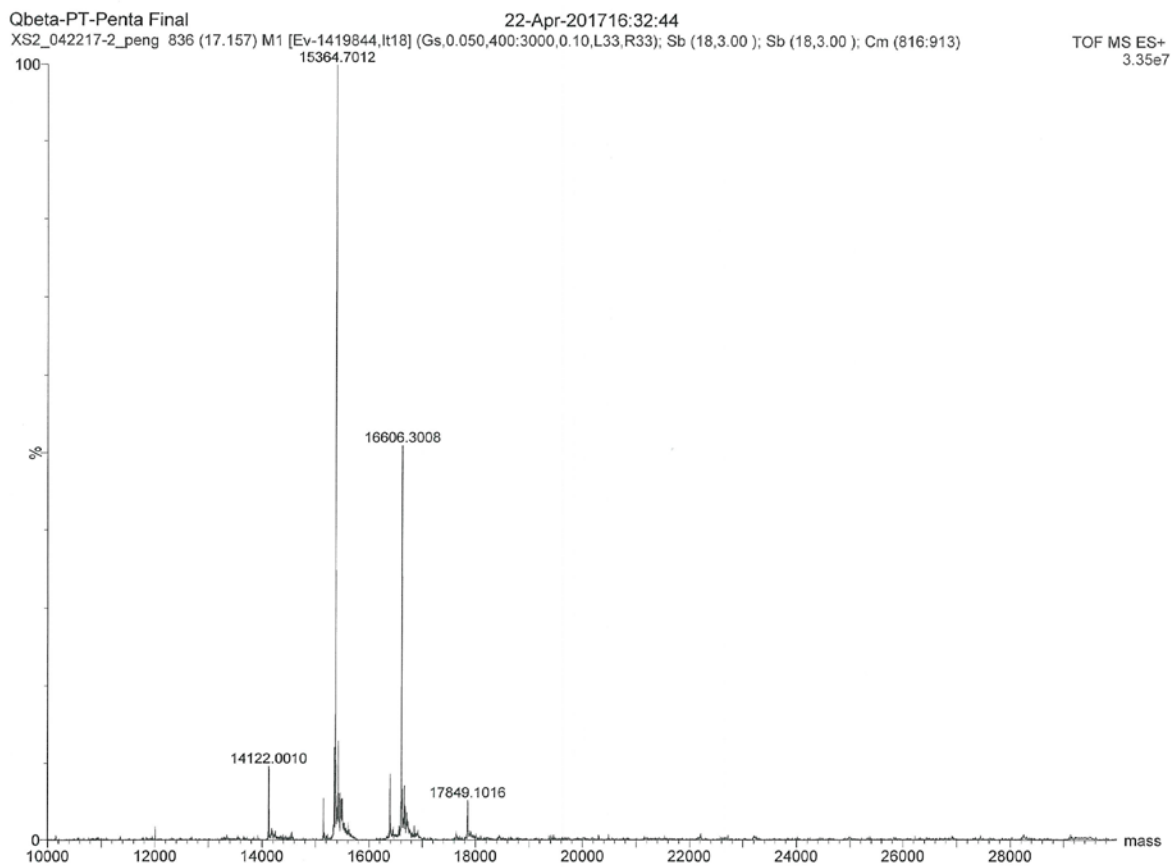
Figure 2.6. ESI-MS analysis of the Qβ-glycan conjugate **49**.

:Untitled> 28 Apr 2017 18:02 Cal: 9 Jul 2007 10:16
dzu Biotech Axima CFR 2.9.3.20110624: Mode Linear, Power: 93, Blanked, P.Ext. @ 67000 (bin 313)
t.   0.5 mV[sum= 77 mV] Profiles 1-140 Smooth Av 20000 -Baseline 60000
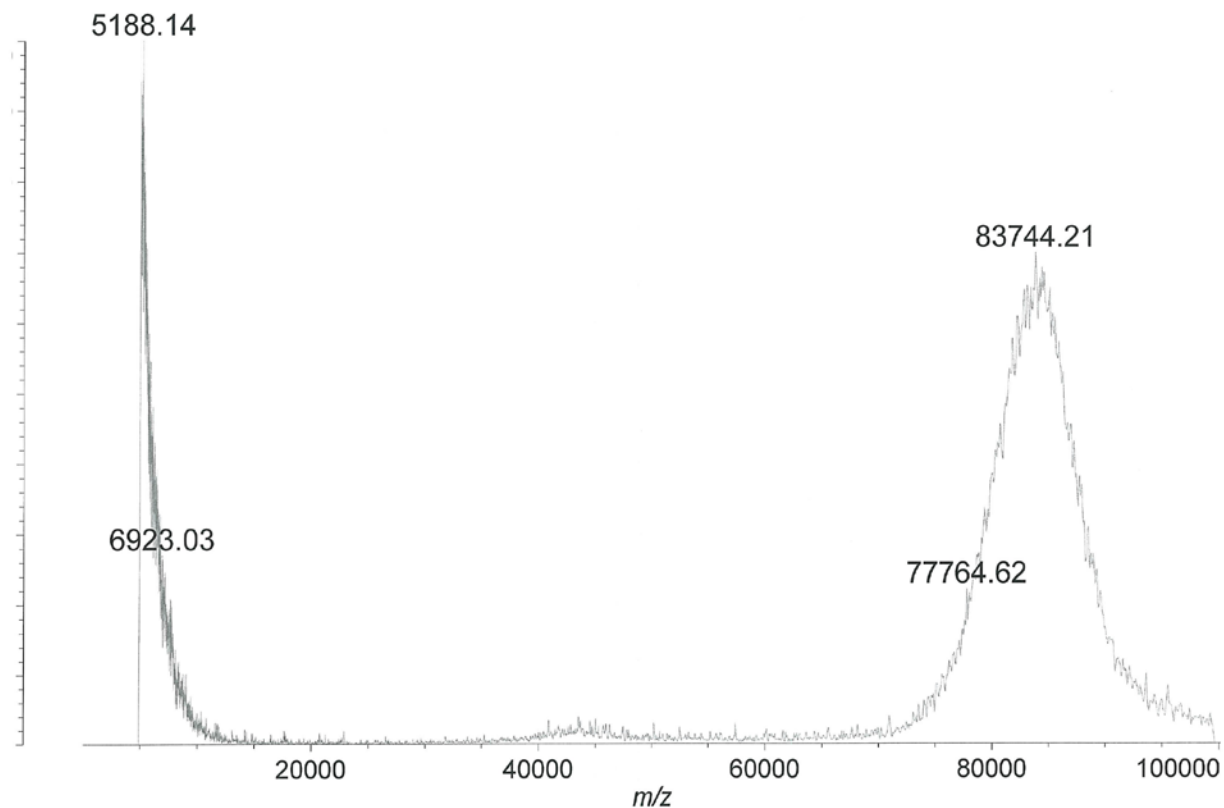
Figure 2.7. MALDI-TOF MS analysis of the BSA-glycan conjugate **53**.

2.7.3. Immunization Studies

Pathogen-free C57BL/6 female mice age 6-10 weeks were obtained from Jackson Laboratory and maintained in the University Laboratory Animal Resources facility of Michigan State University. All animal care procedures and experimental protocols have been approved by the Institutional Animal Care and Use Committee (IACUC) of Michigan State University. Groups of 5 mice were injected subcutaneously under the scruff on day 0 with 0.2 mL of Qβ conjugate (contain 2 μg or 8 μg glycan) or KLH conjugate (contain 2 μg glycan) with lipid A

monophosphoryl (MPLA, from *Salmonella enterica* serotype minnesota Re 595, Sigma-Aldrich, 20 μg) as the adjuvant. Boosters at the same dose were given subcutaneously under the scruff on day 14 and 28. Serum samples were collected on day 0 (before immunization), 7, 21 and 35.

2.7.4. Enzyme-linked Immunosorbent Assay (ELISA)

A Nunc MaxiSorp® flat-bottom 96 well plate was first coated with BSA-glycan (10 μg/mL) in $NaHCO_3$/Na_2CO_3 buffer (0.05 M, pH = 9.6) overnight at 4 °C. The coated plate was then washed 4 times with PBS/0.5% Tween-20 (PBST), followed by the addition of 1% (w/v) BSA in PBS to each well and incubation at room temperature for one hour. The plate was washed again 4 times with PBST. 100 μl of the dilution of mouse sera in 0.1% BSA/PBS were added to each well. The plate was incubated for two hours at 37 °C and washed. A 1:2000 diluted horseradish peroxidase (HRP)-conjugated goat anti-mouse IgG, IgG1, IgG2b, IgG2c, or IgG3 antibody (Jackson ImmunoResearch Laborator) in 0.1% BSA/PBS was added to each well, respectively. The plate was incubated for one hour at 37 °C, washed, and a solution of 3,3',5,5'-tetramethylbenzidine (TMB) was added (200 μL). The color was allowed to develop for 15 min, and then a solution of 0.5 M H_2SO_4 (50 μL) was added to stop the reaction. The optical density was measured at 450 nm using a microplate autoreader (BioRad). Each experiment was repeated at least four times, and the average of the quadruplicate was used to calculate the titer. The titer was determined by linear regression analysis with reciprocal of dilution plotted with optical density (background subtracted). The titer was calculated as the highest dilution that gave OD = 0.1.

2.7.5. Cell Culture of *B. pertussis*

B. pertussis strain Tohama I was grown on 15% BG blood agar plates (Bordet-Gengou agar supplemented with 15% defibrinated sheep's blood). The plates were placed at the top of 37 °C incubator for 3 days.

2.7.6. Flow Cytometry Experiment

B. pertussis was scraped from blood plates into FACS buffer in 1.5 mL tubes. They were centrifuged, washed 3 times and adjusted with FACS buffer to O.D. ~1.0 at 600 nm. Primary antibodies or mouse antisera were diluted to proper concentration in 100 μL FACS buffer and 10 μL of *B. pertussis* was added. The mixture was incubated on ice for 30 min and washed twice. The residue was resuspended in 100 μL 1:50 secondary antibodies (AF647 anti-human Fc or AF647 anti-mouse Fc) and incubated on ice for 30 min. After washing twice, the residue was resuspended in 700 μL FACS buffer and measured by flow cytometry (Thresholds: FSC-500, SSC-200; Voltages: FSC-595, SSC-160).

2.7.7. Complement Assay

The entire plate was inoculated in 25mL Stainer-Scholte media (SSM) in a 125mL polycarbonate filter-top Erlenmeyer flask. The culture was then put in a 37 °C incubator, shaking at 210rpm until the O.D. reached 0.22 (~3-4 hours). Note: the culture was not allowed to grow past 5 hours regardless of the optical density to avoid Brk- mutations and complement resistance. In this time, the reaction plate was set up. Duplicate wells were established in a non-treated 96-well assay plate with lid (Costar, 3370) for all of the antibodies to be tested and the controls. A total volume of 40uL of SSM or SSM + 1.25 μg antibody was added to the duplicate wells.

Once at the proper O.D., the culture was serially diluted ten-fold twice to get a working stock solution. 5uL of this bacterial working stock was added to all wells and mixed thoroughly. The plate was covered and allowed to equilibrate at 37 °C for 30 min. 5 μL was then added to each of the wells: naïve sera to all of the antibody samples and the duplicate naïve control wells, infected sera to those controls, and 5uL of SSM to the media only control. This reaction was covered and allowed to incubate 1 hour at 37 °C. Blood plates were brought to room temperature at this time. After the hour, 15 μL from each well was diluted into 135 μL of PBS and then 50 μL was taken from this first tube into a second tube of 450 μL PBS to achieve two ten-fold dilutions. 7.5 μL was then taken three times from the plate to create three spaced out drops across the top of a blood plate, forming row one. Three drops were then added below this from the first tube and then below that from the second tube. This was repeated for all the wells and the plates were allowed to dry thoroughly. The plates were then covered, inverted, and placed on the top rack of a 37 °C incubator for 3 days. After 3 days, the number of colonies per drip was counted, and the colony number from the second row (first dilution tube) was reported as an average of the three drops over the two duplicate sample plates.

2.7.8. Product Preparation and Characterization Data
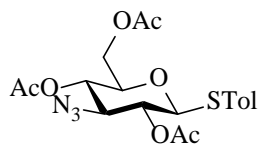
p-Tolyl 2, 4, 6-tri-*O*-acetyl-3-azido-3-deoxy-1-thio-*β*-D-glucopyranoside (**9**)

10% HCl (25 mL) was added to 3-azido-1,2:5,6-di-*O*-isopropylidene-3-deoxy-*α*-D-allofuranose[2]

(1.52 g, 5.3 mmol) and the mixture was stirred at r.t. for 16 hours. The solution was then concentrated, diluted with pyridine (10 mL) and cooled to 0°C. Acetic anhydride (Ac$_2$O, 12 mL) and DMAP (100 mg, 0.8 mmol) were added. The solution was allowed to warm up slowly to r.t. and stirred overnight. Upon completion, excess Ac$_2$O was quenched by the slow addition of MeOH. The reaction mixture was concentrated under vacuum, diluted with EtOAc and washed successively with 1M HCl, saturated Na$_2$CO$_3$ solution and saturated brine. The organic layer was then dried over anhydrous Na$_2$SO$_4$, filtered and concentrated. The product was mixed with p-toluenethiol (1.02 g, 8.2 mmol), dissolved in DCM and cooed to 0°C. Then BF$_3$ •Et$_2$O (3.0 mL, 24.6 mmol) was added and the reaction was stirred for 6 hours. The mixture was washed with saturated NaHCO$_3$ solution, dried and concentrated. Compound **9** was purified from column chromatography (Hexanes/EtOAc = 3/1) as a white powder in 54% yield.

^{1}HNMR (500 MHz, CDCl$_3$): δ = 2.08 (s, 3H), 2.11 (s, 3H), 2.18 (s, 3H), 2.35 (s, 3H), 3.62-3.66 (m, 2H), 4.16-4.17 (m, 2H), 4.58 (d, 1H, J = 10 Hz), 4.87 (t, 1H, J = 10 Hz), 4.92 (t, 1H, J = 10 Hz), 7.11-7.13 (m, 2H), 7.38-7.40 (m, 2H). ^{13}CNMR (125 MHz, CDCl$_3$): δ = 20.85, 20.96, 21.06, 21.38, 62.37, 65.99, 68.44, 70.19, 76.52, 86.59, 128.02, 129.86, 133.79, 138.93, 169.25, 169.37, 170.81. HRMS: m/z calc. for C$_{19}$H$_{27}$N$_4$O$_7$S: 455.1600; found: 455.1614 [M + NH$_4$]$^+$.
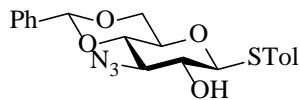
p-Tolyl 3-azido-4, 6-O-benzylidene-3-deoxy-1-thio-β-D-glucopyranoside (**10**)

Compound **9** (1.5 g, 3.4 mmol) was dissolved in a mixture of DCM/MeOH (7/7 mL) and the pH

was adjusted to 11 with 30% NaOMe. The reaction was stirred for 1 h and then neutralized with H$^+$ resin. The mixture was then filtered through celite and concentrated. The residue was diluted with MeCN (40 mL) and then benzaldehyde dimethyl acetal (0.77 mL, 5.1 mmol) and (1S)-(+)-10-camphorsulfonic acid (CSA, 230 mg, 1.0 mmol) was added to the solution, which was allowed to stir at r.t. overnight. Upon completion as judged by TLC, the reaction was quenched with Et$_3$N and concentrated. The residue was diluted with DCM and washed with brine. Compound **10** was obtained through recrystallization in Hexanes/EtOAc (4/1) as a white powder in 81% yield.

^{1}HNMR (500 MHz, CDCl$_3$): δ = 2.37 (s, 3H), 2.62 (d, 1H, J = 2.5 Hz), 3.35 (dt, 1H, J = 2.5, 9.5 Hz), 3.47 (t, 1H, J = 9.5 Hz), 3.54 (dt, 1H, J = 5, 9.5 Hz), 3.72 (t, 1H, J = 9.5 Hz), 3.76 (t, 1H, J = 9.5 Hz), 4.39 (dd, 1H, J = 5, 10.5 Hz), 4.56 (d, 1H, J = 10 Hz), 5.55 (s, 1H), 7.15-7.17 (m, 2H), 7.35-7.39 (m, 3H), 7.41-7.43 (m, 2H), 7.46-7.49 (m, 2H). ^{13}CNMR (125 MHz, CDCl$_3$): δ = 21.41, 65.97, 68.74, 71.64, 71.7, 79.33, 89.34, 101.71, 126.17, 126.71, 128.52, 129.37, 130.2, 134.12, 136.78, 139.41. HRMS: m/z calc. for C$_{20}$H$_{22}$N$_3$O$_4$S: 400.1331; found: 400.1323 [M + H]$^+$.
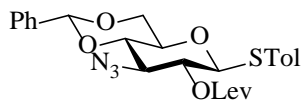
p-Tolyl 3-azido-4, 6-*O*-benzylidene-3-deoxy-2-levulinoyl-1-thio-β-D-glucopyranoside (**6**)

Compound **10** (1.0 g, 2.5 mmol) was dissolved in DCM (40 mL) followed by the addition of levulinic acid (0.77 mL, 7.5 mmol), EDC·HCl (1.58 g, 8.3 mmol) and DMAP (31 mg, 0.25

mmol). The reaction was stirred at r.t. overnight and then washed with saturated $NaHCO_3$ solution. Compound **6** was obtained through column chromatography (Hexanes/EtOAc = 2/1) as a white solid in 91% yield.

^{1}HNMR (500 MHz, CDCl$_3$): δ = 2.23 (s, 3H), 2.35 (s, 3H), 2.67-2.74 (m, 2H), 2.80-2.90 (m, 2H), 3.52 (dt, 1H, J = 5.0, 9.5 Hz), 3.57 (t, 1H, J = 9.5 Hz), 3.76-3.81(m, 2H), 4.39 (dd, 1H, J = 4.5, 10.5 Hz), 4.66 (d, 1H, J = 9.5 Hz), 4.85 (t, 1H, J = 9.5 Hz), 5.57 (s, 1H), 7.12-7.16 (m, 2H), 7.34-7.41 (m, 5H), 7.45-7.49 (m, 2H). ^{13}CNMR (125 MHz, CDCl$_3$): δ = 21.33, 28.09, 30.0, 37.94, 64.74, 68.58, 70.69, 71.34, 79.17, 87.3, 101.54, 126.07, 127.91, 128.44, 129.3, 129.9, 133.79, 136.63, 138.92, 171.3, 206.12. HRMS: m/z calc. for $C_{25}H_{27}N_3NaO_6S$: 520.1518; found: 520.1517 [M + Na]$^+$.
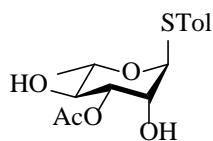
p-Tolyl 3-*O*-acetyl-1-thio-*α*-L-rhamnopyranoside (**11**)

Compound **11** was prepared by following the previously reported protocol.[25]

^{1}HNMR (500 MHz, CDCl$_3$): δ = 1.35 (d, 3H, J = 6.0 Hz), 2.18 (s, 3H), 2.33 (s, 3H), 2.42 (br, 2H), 3.71 (t, 1H, J = 9.5 Hz), 4.23 (dq, 1H, J = 6.5, 9.5 Hz), 4.29 (dd, 1H, J = 1.5, 3.0 Hz), 5.05 (dd, 1H, J = 3.0, 9.5 Hz), 5.38 (d, 1H, J = 1.5 Hz), 7.12 (d, 2H, J = 8.0 Hz), 7.35 (d, 2H, J = 8.5 Hz). ^{13}CNMR (125 MHz, CDCl$_3$): δ = 17.58, 21.25, 21.27, 70.0, 71.21, 71.69, 75.02, 88.11, 129.94, 130.04, 132.33, 138.04, 171.6. HRMS: m/z calc. for $C_{15}H_{20}NaO_5S$: 335.0929; found 335.0937 [M + Na]$^+$.
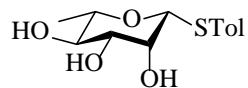
p-Tolyl 1-thio-α-L-rhamnopyranoside (**12**)

Compound **12** was prepared by following the previously reported protocol.[26]

^{1}HNMR (500 MHz, CD$_3$OD): δ = 1.31 (d, 3H, *J* = 6.0 Hz), 2.31 (s, 3H), 3.25 (dq, 1H, *J* = 6.0, 9.0 Hz), 3.37 (t, 1H, *J* = 9.0 Hz), 3.44 (dd, 1H, *J* = 3.5, 9.5 Hz), 4.04 (dd, 1H, *J* = 1.0, 3.5 Hz), 4.86 (d, 1H, *J* = 1.0 Hz), 7.12 (d, 2H, *J* = 7.5 Hz), 7.36 (d, 2H, *J* = 8.0 Hz). ^{13}CNMR (125 MHz, CD$_3$OD): δ = 18.24, 21.05, 73.64, 74.19, 75.91, 77.88, 89.04, 130.62, 131.87, 133.3, 138.2. HRMS: m/z calc. for C$_{13}$H$_{18}$NaO$_4$S: 293.0823; found 293.0833 [M + Na]$^+$.
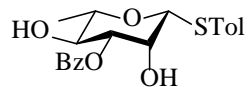
p-Tolyl 3-*O*-benzoyl-1-thio-β-L-rhamnopyranoside (**13**)

Compound **13** was prepared by following the previously reported protocol.[25]

^{1}HNMR (500 MHz, CDCl$_3$): δ = 1.44 (d, 3H, *J* = 6.0 Hz), 2.28 (br, 1H), 2.35 (s, 3H), 2.43 (br, 1H), 3.46 (dq, 1H, *J* = 6.0, 9.0 Hz), 3.89 (t, 1H, *J* = 9.5 Hz), 4.39 (s, 1H), 4.89 (d, 1H, *J* = 1.0 Hz), 4.98 (dd, 1H, *J* = 3.0, 10.0 Hz), 7.12-7.16 (m, 2H), 7.40-7.49 (m, 4H), 7.56-7.62 (m, 1H), 8.06-8.11 (m, 2H). ^{13}CNMR (125 MHz, CDCl$_3$): δ = 18.08, 21.29, 70.83, 70.98, 77.13, 77.8, 87.46, 128.69, 129.44, 129.84, 130.02, 130.04, 132.6, 133.77, 138.3, 166.83. HRMS: m/z calc. for C$_{20}$H$_{22}$NaO$_5$S: 397.1086; found 397.1089 [M + Na]$^+$.
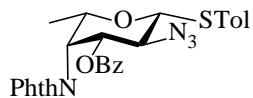
p-Tolyl 2-azido-3-*O*-benzoyl-2, 4-dideoxy-4-phthalimido-1-thio-*β*-L-rhamnopyranoside (**14**)

Compound **14** was prepared by following the previously reported protocol.[6]

^{1}HNMR (500 MHz, CDCl$_3$): δ = 1.18 (d, 3H, *J* = 6.5 Hz), 2.37 (s, 3H), 3.94-4.00 (m, 1H), 4.65 (d, 1H, *J* = 10.5 Hz), 4.89 (t, 1H, *J* = 10.0 Hz), 5.02 (dd, 1H, *J* = 3.0, 7.0 Hz), 5.36 (dd, 1H, *J* = 7.0, 9.5 Hz), 7.14-7.19 (m, 2H), 7.27-7.33 (m, 2H), 7.43-7.51 (m, 2H), 7.52-7.57 (m, 2H), 7.66-7.79 (m, 3H), 7.82-7.87 (m, 2H). ^{13}CNMR (125 MHz, CDCl$_3$): δ = 17.07, 21.37, 51.7, 62.15, 73.19, 73.59, 89.45, 123.78, 128.58, 128.72, 128.8, 129.77, 129.84, 129.91, 130.03, 130.07, 133.12, 133.66, 134.24, 138.4, 165.19. HRMS: m/z calc. for C$_{28}$H$_{25}$N$_4$O$_5$S: 529.1546; found: 529.1548 [M + H]$^+$.
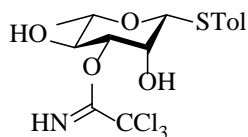
p-Tolyl 1-thio-3-trichloroacetimidate-*β*-L-rhamnopyranoside (**16**)

p-Tolyl 1-thio-*β*-L-rhamnopyranoside **12** (11.5 g, 42.7 mmol) was dissolved in THF (150 mL) followed by the addition of 1,8-diazabicyclo[5.4.0]undec-7-ene (DBU, 1.3 mL, 8.5 mmol). To this mixture, trichloroacetonitrile (5.1 mL, 51 mmol) in THF (30 mL) was added over a period of 1 h at 0 °C. The reaction was allowed to warm up and stirred at r.t. overnight. It was concentrated and purified through column (DCM/EtOAc = 3/1). The impurities (not characterized, might be from extra side reactions on 2- and 4-OH) were dissolved in DCM/MeOH/AcOH (40/40/5 mL)

and purified with the same condition, which gave compound **16** as a white solid in a combined

yield of 90%.

^{1}HNMR (500 MHz, CDCl$_3$): δ = 1.43 (d, 3H, J = 6.5 Hz), 2.34 (s, 3H), 2.81 (br, 3H), 3.46 (dq,

1H, J = 1.0, 6.5 Hz), 4.18 (dd, 1H, J = 1.0, 6.5 Hz), 4.54 (t, 1H, J = 6.5 Hz), 4.90-4.94 (m, 2H),

7.13 (d, 2H, J = 7.5 Hz), 7.44 (m, 2H). ^{13}CNMR (125 MHz, CDCl$_3$): δ = 18.89, 21.28, 71.91,

76.28, 80.19, 82.7, 84.66, 103.51, 117.13, 129.92, 130.95, 131.91, 138.01. HRMS: m/z calc. for

C$_{15}$H$_{18}$Cl$_3$NNaO$_4$S: 435.9920; found: 435.9928 [M + Na]$^+$.
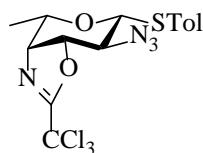
p-Tolyl 2-azido-2, 4-dideoxy-1-thio-3, 4-trichlorooxazoline-*β*-L-fucopyranoside (**17**)

Compound **16** (16.0 g, 38.5 mmol) was dissolved in anhydrous DCM (200 mL) and cooled to

-30 °C. Pyridine (31.0 mL, 0.38 mol) and trifluoromethanesulfonic anhydride (19.4 mL, 0.12

mol) were added and the solution was allowed to warm up to r.t. over 3 h. Upon completion by

TLC, the reaction was quenched and washed with saturated NaHCO$_3$ solution. The organic layer

was dried with Na$_2$SO$_4$, concentrated and redissolved in DMF (60 mL). NaN$_3$ (7.5 g, 0.12 mol)

was added and the reaction was stirred at 50 °C overnight. The mixture was diluted with EtOAc,

washed with brine, dried and concentrated. Compound **17** was obtained through column

chromatography (Hexanes/DCM/EtOAc = 3/1/1) as a colorless solid in a yield of 85%.

^{1}HNMR (500 MHz, CDCl$_3$): δ = 1.58 (d, 3H, J = 6.0 Hz), 2.33 (s, 3H), 3.29 (dd, 1H, J = 7.0,

10.0 Hz), 3.89 (dq, 1H, J = 3.0, 6.5 Hz), 4.10 (dd, 1H, J = 3.0, 8.0 Hz), 4.34 (d, 1H, J = 10.5 Hz),

4.88 (dd, 1H, J = 6.5, 8.0 Hz), 7.14 (m, 2H), 7.46 (m, 2H). ^{13}CNMR (125 MHz, CDCl$_3$): δ =

18.16, 21.16, 62.31, 68.78, 73.03, 84.86, 85.37, 86.31, 126.71, 129.83, 134.12, 138.9, 162.64.

HRMS: m/z calc. for C$_{15}$H$_{16}$Cl$_3$N$_4$O$_2$S: 421.0060; found: 421.0072 [M + H]$^+$.
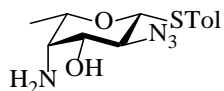
p-Tolyl 4-amino-2-azido-2, 4-dideoxy-1-thio-*β*-L-fucopyranoside (**15**)

Compound **17** (13.9 g, 33.0 mmol) was dissolved in DCM/MeOH/H$_2$O/conc. HCl (40/50/20/30

mL) and the mixture was refluxed at 90 °C overnight. The reaction was then concentrated,

diluted with DCM and washed with saturated NaHCO$_3$ solution. The organic layer was collected

and dried with Na$_2$SO$_4$. Compound **15** was obtained through column chromatography

(DCM/MeOH = 10/1) as a colorless syrup in a yield of 89%.

^{1}HNMR (500 MHz, CDCl$_3$): δ = 1.28 (d, 3H, J = 6.5 Hz), 2.35 (s, 3H), 2.82 (d, 1H, J = 4.0 Hz),

3.04 (t, 1H, J = 10.0 Hz), 3.51 (dd, 1H, J = 4.5, 9.5 Hz), 3.61 (q, 1H, J = 6.5 Hz), 4.28 (d, 1H, J

= 10.5 Hz), 7.15 (d, 2H, J = 8.5 Hz), 7.48 (d, 2H, J = 8.0 Hz). ^{13}CNMR (125 MHz, CDCl$_3$): δ =

17.16, 21.21, 54.31, 63.35, 73.61, 75.07, 86.04, 127.56, 129.77, 133.98, 138.72. HRMS: m/z calc.

for C$_{13}$H$_{19}$N$_4$O$_2$S: 295.1229; found: 295.1242 [M + H]$^+$.
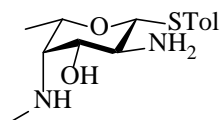
p-Tolyl 2-amino-2, 4-dideoxy-4-methylamino-1-thio-*β*-L-fucopyranoside (**18**)

Compound **15** (6.1 g, 20.7 mmol) was dissolved in ethyl formate (50 mL) and Et$_3$N (3 mL) was

added. The mixture was refluxed overnight and concentrated. The obtained syrup was diluted in anhydrous THF (60 mL) and cooled to -30 °C. To the solution was added LiAlH$_4$ in THF (37.2 mL, 2M). The mixture was refluxed overnight and quenched with 15% NaOH, followed by filtration through celite and concentration. Compound **18** was obtained through column chromatography (DCM/MeOH = 8/1 with 1% Et$_3$N) as a colorless oil in a yield of 70%.

^{1}HNMR (500 MHz, CD$_3$OD): δ = 1.31 (d, 3H, J = 6.5 Hz), 2.32 (s, 3H), 2.51 (s, 3H), 2.54 (dd, 1H, J = 1.0, 4.0 Hz), 2.61 (t, 1H, J = 10.0 Hz), 3.43 (dd, 1H, J = 4.5, 9.5 Hz), 3.68 (dq, 1H, J = 1.0, 6.5 Hz), 4.37 (d, 1H, J = 10.0 Hz), 7.14 (d, 2H, J = 8.0 Hz), 7.43 (d, 2H, J = 8.5 Hz).

^{13}CNMR (125 MHz, CD$_3$OD): δ = 16.85, 19.73, 37.59, 52.36, 63.5, 74.1, 75.2, 89.15, 129.26, 129.45, 132.15, 137.68. HRMS: m/z calc. for C$_{28}$H$_{44}$N$_4$NaO$_4$S$_2$: 587.2702; found: 587.2707 [2M + Na]$^+$.
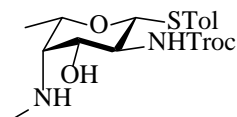
p-Tolyl   2,4-dideoxy-4-methylamino-1-thio-2-(2,2,2-trichloroethyloxycarbonylamino)-β-L-fucopyranoside (**19**)

Compound **18** (3.7 g, 13.1 mmol) was dissolved in THF (100 mL) and pyridine (3.2 mL, 39.2 mmol) was added. The mixture was cooled in ice bath and trichloroethyl chloroformate (1.7 mL, 12.4 mmol) in THF (50 mL) was added slowly over 1 h. The reaction was concentrated, diluted with DCM and washed with saturated NaHCO$_3$ solution. Compound **19** was obtained through column chromatography (DCM/MeOH = 6/1 with 1% Et$_3$N) as a white solid in a yield of 88%.

^{1}HNMR (500 MHz, CDCl$_3$): δ = 1.37 (d, 3H, J = 6.5 Hz), 2.32 (s, 3H), 2.60 (s, 3H), 2.64 (dd, 1H, J = 1.5, 4.5 Hz), 3.20 (q, 1H, J = 10.0 Hz), 3.57 (dd, 1H, J = 4.0, 9.5 Hz), 3.70 (q, 1H, J = 6.5 Hz), 4.61 (d, 1H, J = 10.5 Hz), 4.68 (d, 1H, J = 12.0 Hz), 4.81 (d, 1H, J = 12.0 Hz), 5.29 (br, 1H), 7.10 (d, 2H, J = 8.0 Hz), 7.37 (d, 2H, J = 7.5 Hz). ^{13}CNMR (125 MHz, CDCl$_3$): δ = 17.93, 21.13, 38.39, 55.43, 63.07, 71.52, 74.55, 75.68, 87.3, 95.54, 129.63, 129.67, 132.55, 137.95, 154.51. HRMS: m/z calc. for C$_{17}$H$_{24}$Cl$_3$N$_2$O$_4$S: 457.0522; found: 457.0523 [M + H]$^+$.

p-Tolyl 4-[*N*-(methyl)-benzyloxycarbonylamino]-2,4-dideoxy-1-thio-2-(2,2,2-trichloroethyloxycarbonylamino)-β-L-fucopyranoside (**5**)

Compound **19** (3.0 g, 6.55 mmol) was dissolved in THF/H$_2$O (40/10 mL) and cooled to 0°C. To the solution was added benzyl chloroformate (1.1 mL, 7.86 mmol) and sodium carbonate (1.39 g, 13.1 mmol). The reaction was allowed to warm up to room temperature and stirred overnight. The reaction was concentrated, diluted with DCM and washed with saturated NaHCO$_3$ solution. Compound **5** was obtained through column chromatography (Hexanes/EtOAc = 1/1) as a white solid in a yield of 75%.

^{1}HNMR (500 MHz, d^6-DMSO): δ = 1.05&1.07 (d, 3H, J = 6.0 Hz, H-6), 2.27&2.28 (s, 3H, STol-Me), 2.82&2.88 (s, 3H, *N*-Me), 3.64-3.73 (m, 1H, H-2), 3.75-3.88 (m, 2H, H-3, H-5), 4.27&4.35 (dd, 1H, J = 2.5, 6.0 Hz, H-4), 4.66&4.69 (d, 1H, J = 10.0 Hz, H-1), 4.76 (d, 1H, J = 12.5 Hz, Troc-CH$_2$), 4.91&4.92 (d, 1H, J = 12.5 Hz, Troc-CH$_2$), 4.98&5.10 (d, 1H, J = 13.0 Hz,

Cbz-CH$_2$), 5.08 (s, 1H, Cbz-CH$_2$), 5.45&5.53 (d, 1H, J = 6.0 Hz, OH), 7.12-7.17 (m, 2H), 7.27-7.39 (m, 7H), 7.73 (d, 1H, J = 9.5 Hz, Troc-NH). ^{13}CNMR (125 MHz, d^6-DMSO): δ = 16.8, 16.95, 20.64, 32.56, 32.98, 54.01, 54.11, 56.87, 56.92, 66.17, 66.29, 69.66, 69.74, 73.49, 73.51, 73.9, 74.04, 86.32, 96.26, 127.16, 127.27, 127.61, 127.68, 128.31, 128.4, 129.46, 129.49, 129.52, 129.59, 131.63, 131.8, 136.9, 136.99, 137.13, 137.2, 154.46, 156.97, 157.19. HRMS: m/z calc. for C$_{25}$H$_{30}$Cl$_3$N$_2$O$_6$S: 591.0890; found: 591.0878 [M + H]$^+$.
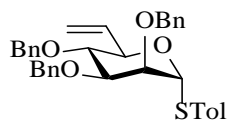

p-Tolyl 2, 3, 4-tri-*O*-benzyl-6,7-dideoxy-1-thio-α-D-mannohept-6-enopyranoside (**21**)

To a solution of oxalyl chloride (202 μL, 2.36 mmol) in DCM (4 mL) was added a solution of DMSO (200 μL, 2.83 mmol) in DCM (6 mL) at -65°C. After 15 min, a solution of *p*-Tolyl 2, 3, 4-tri-*O*-benzyl-1-thio-α-D-mannopyranoside **20** (875 mg, 1.57 mmol) in DCM (5 mL) was added to the above solution via syringe. The reaction was allowed to stir at -50 °C for 2 h. Et$_3$N was added and the above mixture was warmed up to r.t. over a period of 4 h before it was quenched with water and extracted with DCM. The organic layer was washed with brine, dried and concentrated to give the crude aldehyde which was used without further purification. To a suspension of methyl triphenylphosphonium bromide (843 mg, 2.36 mmol) in THF (6 mL) at -40 °C was added n-BuLi (0.94 mL, 2.36 mmol, 2.5 M solution in hexane) and after 0.5 h, the above aldehyde in THF (5 mL) was added and the mixture was stirred at the same temperature for 1 h. The reaction was slowly warmed up to r.t. over 4 h before quenched with saturated

NH$_4$Cl solution and extracted with EtOAc. The organic layer was washed with brine, dried and concentrated. Compound **21** was obtained through column chromatography (Hexanes/EtOAc = 10/1) as a yellow syrup in a yield of 83%.

^{1}HNMR (500 MHz, CDCl$_3$): δ = 2.33 (s, 3H), 3.81 (t, 1H, J = 9.5 Hz), 3.88 (dd, 1H, J = 3.0, 9.5 Hz), 4.00 (dd, 1H, J = 1.5, 3.0 Hz), 4.56 (dd, 1H, J = 6.5, 9.5 Hz), 4.60-4.68 (m, 4H), 4.73 (d, 1H, J = 12.5 Hz), 4.88 (d, 1H, J = 11.0 Hz), 5.28-5.31 (m, 1H), 5.43-5.49 (m, 2H), 6.04 (ddd, 1H, J = 6.0, 10.5, 17.0 Hz), 7.10 (d, 2H, J = 8.0 Hz), 7.26-7.38 (m, 17H). ^{13}CNMR (125 MHz, CDCl$_3$): δ = 21.25, 72.19, 72.47, 73.87, 75.4, 76.57, 78.97, 79.86, 86.26, 118.43, 127.8, 127.81, 127.87, 127.94, 128.11, 128.19, 128.46, 128.51, 128.53, 129.93, 130.72, 132.29, 135.13, 137.77, 138.04, 138.38, 138.54. HRMS: m/z calc. for C$_{35}$H$_{40}$NO$_4$S: 570.2678; found: 570.2681 [M + NH$_4$]$^+$.
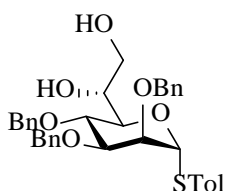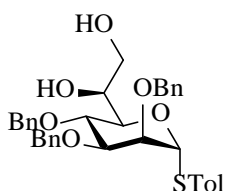

p-Tolyl 2, 3, 4-tri-*O*-benzyl-D-glycero-1-thio-α-D-mannoheptopyranoside (**22**)

To a solution of compound **21** (2.57 g, 4.65 mmol) in Acetone/water (27/3 mL) at 0 °C were added 4-methylmorpholine *N*-oxide (NMO, 1.09 g, 9.3 mmol) and OsO$_4$ (2.3 mL, 0.18 mmol, 2.5%wt in *t*-BuOH). The reaction was allowed to stir at r.t. for 6 h before it was quenched with saturated NaHSO$_3$ solution. After 15 min, the mixture was concentrated and extracted with EtOAc. The organic layer was washed with brine, dried and concentrated. Column chromatography (Hexanes/EtOAc = 2/1) afforded compound **22** (1.3 g, 48%) and compound **23**

(0.52 g, 20 %).

^{1}HNMR (500 MHz, CDCl$_3$): δ = 2.04 (br, 1H), 2.33 (s, 3H), 3.06 (br, 1H), 3.57 (dd, 1H, J = 4.0, 11.5 Hz), 3.65 (dd, 1H, J = 5.0, 12.0 Hz), 3.90 (dd, 1H, J = 3.0, 9.0 Hz), 3.93 (q, 1H, J = 4.5 Hz), 3.99 (dd, 1H, J = 2.0, 3.0 Hz), 4.05 (t, 1H, J = 9.5 Hz), 4.22 (dd, 1H, J = 5.0, 9.5 Hz), 4.58 (d, 1H, J = 11.5 Hz), 4.61 (d, 1H, J = 11.5 Hz), 4.63-4.69 (m, 3H), 5.04 (d, 1H, J = 11.0 Hz), 5.39 (d, 1H, J = 1.5 Hz), 7.12 (d, 2H, J = 8.0 Hz), 7.27-7.38 (m, 17H). ^{13}CNMR (125 MHz, CDCl$_3$): δ = 21.14, 63.09, 71.93, 72.24, 72.3, 72.66, 75.08, 75.87, 76.63, 80.25, 86.25, 127.86, 127.9, 127.93, 128.05, 128.18, 128.47, 128.52, 128.57, 129.57, 129.96, 132.75, 137.57, 137.68, 137.72, 138.25. HRMS: m/z calc. for C$_{35}$H$_{38}$NaO$_6$S: 609.2287; found: 609.2278 [M + Na]$^+$.
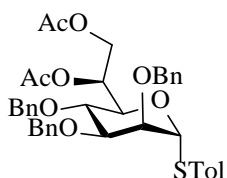

p-Tolyl 2, 3, 4-tri-*O*-benzyl-L-glycero-1-thio-*α*-D-mannoheptopyranoside (**23**)

Compound **22** (1.28 g, 2.18 mmol) was dissolved in pyridine (8 mL) and *t*-butyldiphenylsilyl chloride (TBDPSCl, 1.13 mL, 4.26 mmol) was added. The reaction was stirred at r.t. overnight before it was diluted with DCM and washed with brine. The organic layer was dried and concentrated to give the crude silyl ether which was taken forward without purification. A solution of the silyl ether, PPh$_3$ (1.14 g, 4.26 mmol) and *p*-nitrobenzoic acid (0.73 g, 4.36 mmol) in THF (30 mL) was treated with DIAD (858 µL, 4.36 mmol) at r.t. and stirred for 5 h. The reaction was the concentrated, diluted with DCM and washed with brine. The organic layer was

concentrated and diluted with DCM/MeOH (10/30 mL) and K_2CO_3 (0.5 g, 3.57 mmol) was added. The reaction was stirred at r.t. for 3 h before concentrated, diluted with EtOAc and washed with brine. The organic layer was concentrated, dissolved in THF (30 mL) and treated with TBAF (3.5 mL, 3.5 mmol, 1 M in THF) overnight. The mixture was then concentrated, diluted with EtOAc and washed with brine. Column chromatography (Hexanes/EtOAc = 2/1) gave compound **23** in an 84% yield over 4 steps.

^{1}HNMR (500 MHz, CDCl$_3$): δ = 2.33 (s, 3H), 3.56 (m, 2H), 3.88 (dd, 1H, J = 3.0, 9.0 Hz), 3.97 (m, 2H), 4.05 (dd, 1H, J = 1.0, 9.5 Hz), 4.20 (t, 1H, J = 9.5 Hz), 4.62 (d, 1H, J = 12.0 Hz), 4.65 (d, 1H, J = 12.0 Hz), 4.69 (s, 2H), 4.71 (d, 1H, J = 10.5 Hz), 4.98 (d, 1H, J = 10.5 Hz), 5.47 (d, 1H, J = 1.5 Hz), 7.12 (d, 2H, J = 8.5 Hz), 7.24 (d, 2H, J = 8.0 Hz), 7.27-7.37 (m, 15H). ^{13}CNMR (125 MHz, CDCl$_3$): δ = 21.29, 65.21, 69.25, 72.37, 72.52, 74.0, 74.51, 75.56, 76.05, 80.08, 86.36, 127.93, 127.97, 127.99, 128.0, 128.05, 128.26, 128.61, 129.54, 130.21, 132.47, 137.96, 138.18, 138.37, 138.41. HRMS: m/z calc. for $C_{35}H_{42}NO_6S$: 604.2733; found: 604.2745 $[M + NH_4]^+$.


p-Tolyl 6, 7-di-*O*-acetyl-2, 3, 4-tri-*O*-benzyl-L-glycero-1-thio-α-D-mannoheptopyranoside (**3**)

Compound **23** (1.64 g, 2.80 mmol) was dissolved in pyridine (10 mL) and treated with Ac$_2$O (1.1 mL, 11.2 mmol) and DMAP (17 mg, 0.14 mmol) at 0 °C. The reaction was allowed to warm up to r.t. and stirred overnight. It was then concentrated, diluted with EtOAc and washed with 1 M

HCl, brine, saturated NaHCO$_3$ and brine in order. The organic layer was dried and concentrated. Column chromatography (Hexanes/EtOAc = 3/1) gave compound **3** as a colorless syrup in a yield of 91%.

^{1}HNMR (500 MHz, CDCl$_3$): δ = 1.92 (s, 3H), 2.12 (s, 3H), 2.32 (s, 3H), 3.86-3.92 (m, 2H), 3.99 (dd, 1H, J = 1.5, 3.0 Hz), 4.04-4.13 (m, 2H), 4.24 (d, 1H, J = 13.0 Hz), 4.47 (d, 1H, J = 9.5 Hz), 4.58 (s, 2H), 4.64 (d, 1H, J = 12.5 Hz), 4.76 (d, 1H, J = 12.5 Hz), 4.90 (d, 1H, J = 10.0 Hz), 5.63 (d, 1H, J = 1.5 Hz), 5.66 (ddd, 1H, J = 1.5, 6.0, 7.5 Hz), 7.09 (d, 2H, J = 8.5 Hz), 7.23 (d, 2H, J = 8.5 Hz), 7.27-7.39 (m, 15H). ^{13}CNMR (125 MHz, CDCl$_3$): δ = 20.65, 20.95, 21.07, 62.29, 68.24, 70.77, 71.77, 72.0, 73.67, 75.36, 75.47, 80.36, 85.54, 127.8, 127.85, 127.91, 127.96, 128.38, 128.45, 128.48, 128.57, 129.91, 130.0, 131.25, 137.72, 137.79, 137.88, 170.31, 170.41. HRMS: m/z calc. for C$_{39}$H$_{46}$NO$_8$S: 688.2944; found: 688.2937 [M + NH$_4$]$^+$.
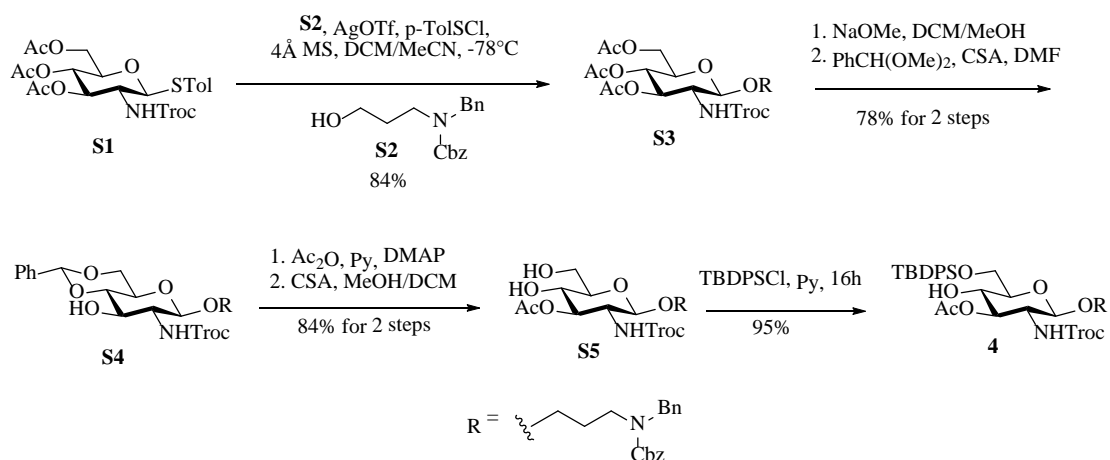
Scheme **2.10**. Preparation of building block **4**.
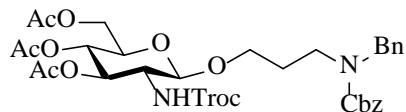
N-(Benzyl)-benzyloxycarbonyl-3-aminopropyl   3,4,6-tri-*O*-acetyl-2-deoxy-2-

(2,2,2-trichloroethyloxycarbonylamino)-*β*-D-glucopyranoside (**S3**)

A solution of *p*-tolyl 3,4,6-tri-*O*-acetyl-2-deoxy-2- (2,2,2-trichloroethyloxycarbonylamino)

-1-thio-β-D-glucopyranoside **S1** (2.12 g, 3.61 mmol), *N*-(benzyl)-benzyloxycarbonyl-

3-aminopropanol **S2** (1.0 g, 3.33 mmol) and freshly activated 4 Å molecular sieves (1.5 g) in

DCM (50 mL) was stirred at r.t. for 20 min and then cooled to -78 °C. To the above solution was

added silver trifluoromethanesulfonate (AgOTf, 2.23 g, 8.68 mmol) in MeCN (2.5 mL). The

mixture was stirred for 10 min and *p*-TolSCl (480 μL, 3.61 mmol) was added directly into it via

microsyringe. The reaction was allowed to stir at the same temperature for 2 h before quenched

with Et_3N (0.5 mL). The mixture was then filtered through celite and concentrated. Column

chromatography gave compound **S3** in a yield of 84%.

^{1}HNMR (500 MHz, $CDCl_3$): δ = 1.73 (m, 2H), 2.04 (s, 3H), 2.05 (s, 3H), 2.08 (s, 3H), 2.98 (m,

1H), 3.20-3.50 (m, 2H), 3.56 (m, 1H), 3.75 (q, 1H, *J* = 9.5 Hz), 3.83 (m, 1H), 3.92 (m, 1H), 4.10

(d, 1H, *J* = 12.0 Hz), 4.24 (d, 0.5H, *J* = 4.5 Hz), 4.27 (d, 0.5H, *J* = 5.0 Hz), 4.34 (d, 1H, *J* = 9.0

Hz), 4.52-4.78 (m, 3H), 5.07 (m, 1H), 5.13-5.22 (m, 3H), 6.29 (d, 1H, *J* = 9.0 Hz), 7.17 (d, 1H, *J*

= 7.0 Hz), 7.27-7.44 (m, 9H). ^{13}CNMR (125 MHz, $CDCl_3$): δ = 20.66, 20.75, 20.77, 27.31, 43.03,

50.08, 56.13, 61.99, 67.07, 67.49, 68.64, 71.74, 73.09, 74.31, 101.19, 127.2, 127.47, 127.95,

128.03, 128.53, 128.64, 136.76, 137.45, 154.79, 156.5, 169.46, 170.64, 170.75. HRMS: m/z calc.

for $C_{33}H_{39}Cl_3N_2NaO_{12}$: 783.1466; found: 783.1440 [M + Na]$^+$.
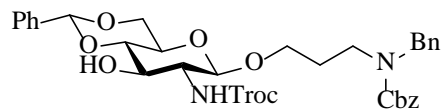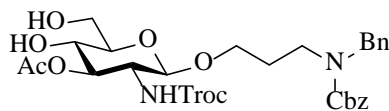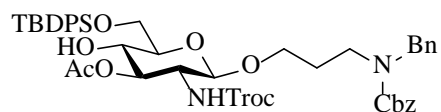
N-(Benzyl)-benzyloxycarbonyl-3-aminopropyl 4,6-*O*-benzylidene-2-deoxy-2-(2,2,2-trichloroethyloxycarbonylamino)-*β*-D-glucopyranoside (**S4**)

Compoud **S3** (2.13 g, 2.80 mmol) was dissolved in DCM/MeOH (10/10 mL) and the solution was cooled to -10 ℃. NaOMe was added to adjust the pH to 11 and the solution was stirred at the same temperature for 2 h. After neutralizing with H$^+$ resin, the solution was filtered, concentrated and diluted in DMF (10 mL). Benzaldehyde dimethyl acetal (611 μL, 4.07 mmol) and CSA (166 mg, 0.72 mmol) were added and the mixture was heated at 50 ℃ overnight. Upon completion by TLC the reaction was quenched with Et$_3$N, diluted with EtOAc and washed with brine. The organic layer was dried and concentrated. Column chromatography (Hexanes/EtOAc = 1/1) gave compound **S4** in a 78% yield over 2 steps.

^{1}HNMR (500 MHz, CDCl$_3$): δ = 1.69-1.77 (m, 2H), 2.94 (d, 1H, *J* = 14.0 Hz), 3.27-3.39 (m, 2H), 3.46-3.61 (m, 2H), 3.69-3.82 (m, 2H), 3.83-3.94 (m, 2H), 4.21-4.32 (m, 2H), 4.34 (d, 1H, *J* = 8.5 Hz), 4.42-4.66 (m, 2H), 4.70 (d, 1H, *J* = 16.0 Hz), 4.81 (d, 1H, *J* = 12.0 Hz), 5.13-5.27 (m, 2H), 5.54 (s, 1H), 6.93 (br, 1H), 7.17 (d, 2H, *J* = 7.5 Hz), 7.26-7.43 (m, 11H), 7.46-7.54 (m, 2H).

^{13}CNMR (125 MHz, CDCl$_3$): δ = 27.45, 42.92, 43.34, 50.05, 50.76, 59.02, 59.04, 66.03, 66.13, 66.91, 67.38, 67.56, 68.6, 72.98, 74.61, 81.43, 95.6, 101.32, 101.89, 126.38, 127.2, 127.5, 127.89, 128.15, 128.23, 128.34, 128.37, 128.53, 128.62, 128.67, 129.25, 136.65, 137.1, 137.37, 156.38, 156.65. HRMS: m/z calc. for C$_{34}$H$_{38}$Cl$_3$N$_2$O$_9$: 723.1643; found: 723.1631 [M + H]$^+$.

N-(Benzyl)-benzyloxycarbonyl-3-aminopropyl   3-*O*-acetyl-2-deoxy-2-

(2,2,2-trichloroethyloxycarbonylamino)-*β*-D-glucopyranoside (**S5**)

To a solution of **S4** (1.66 g, 2.30 mmol) in pyridine (6 mL) was added acetic anhydride (1 mL,

10 mmol)) and DMAP (20 mg, 0.16 mmol) at 0 °C. The solution was stirred at r.t. overnight

before it was quenched with MeOH, concentrated, diluted with EtOAc and washed with brine.

The organic layer was dried, concentrated and dissolved in DCM/MeOH (8/8 mL). CSA (150 mg,

0.65 mmol) was added and the solution was stirred at r.t. overnight, followed by quenching with

Et$_3$N. The mixture was concentrated, diluted with EtOAc, washed with brine, dried and

concentrated again. Column chromatography (DCM/EtOAc = 1/2) gave compound **S5** in an 84%

yield over 2 steps.

^{1}HNMR (500 MHz, CDCl$_3$): δ =1.71-1.77 (m, 2H), 2.10 (s, 3H), 2.64 (br, 1H), 3.05-3.16 (m, 2H),

3.21-3.37 (m, 2H), 3.39-3.45 (m, 1H), 3.60-3.74 (m, 2H), 3.76-3.93 (m, 3H), 4.27-4.35 (m, 1H),

4.37 (d, 1H, *J* = 8.5 Hz), 4.48-4.63 (m, 2H), 4.64-4.68 (m, 1H), 4.95-4.99 (m, 1H), 5.13-5.22 (m,

2H), 6.18 (d, 1H, *J* = 8.5 Hz), 7.11-7.20 (m, 2H), 7.25-7.42 (m, 8H). ^{13}CNMR (125 MHz,

CDCl$_3$): δ = 21.14, 27.65, 28.16, 43.38, 43.63, 50.31, 56.12, 62.26, 67.42, 67.65, 69.71, 74.44,

75.73, 76.27, 95.83, 101.41, 127.34, 127.60, 128.04, 128.21, 128.66, 128.78, 136.70, 137.59,

154.99, 156.65, 172.24. HRMS: m/z calc. for C$_{29}$H$_{35}$Cl$_3$N$_2$NaO$_{10}$: 699.1255; found: 699.1227 [M

+ Na]$^+$.

N-(Benzyl)-benzyloxycarbonyl-3-aminopropyl 3-*O*-acetyl-6-*tert*-butyldiphenylsilyl-2-deoxy-2-(2,2,2-trichloroethyloxycarbonylamino)-*β*-D-glucopyranoside (**4**)

To a solution of **S5** (0.86 g, 1.27 mmol) in pyridine (6 mL) was added TBDPSCl (0.65 mL, 2.5 mmol) and the mixture was allowed to stir at r.t. overnight. Then it was concentrated, diluted with EtOAc and washed with brine. The organic layer was dried, concentrated and purified through column chromatography to afford compound **4** in a 95% yield.

^{1}HNMR (500 MHz, CDCl$_3$): δ = 1.07 (s, 9H), 1.70-1.75 (m, 2H), 2.12 (s, 3H), 2.97-3.05 (m, 1H), 3.09-3.16 (m, 1H), 3.18-3.41 (m, 3H), 3.65-3.85 (m, 4H), 3.86-3.95 (m, 2H), 4.22-4.33 (m, 1H), 4.40-4.57 (m, 1H), 4.59-4.72 (m, 2H), 4.91-5.02 (m, 1H), 5.10-5.24 (m, 2H), 6.14 (d, 1H, *J* = 9.0 Hz), 7.12-7.19 (m, 2H), 7.26-7.48 (m, 14H), 7.63-7.73 (m, 4H). ^{13}CNMR (125 MHz, CDCl$_3$): δ = 19.32, 21.16, 22.78, 25.4, 26.91, 27.03, 27.49, 28.33, 31.71, 34.79, 43.46, 50.32, 50.97, 55.99, 64.79, 66.66, 67.4, 67.54, 71.28, 74.4, 74.61, 74.86, 74.98, 76.08, 95.87, 100.64, 101.14, 127.33, 127.53, 127.91, 127.95, 128.0, 128.06, 128.16, 128.63, 128.73, 130.04, 132.74, 132.93, 135.67, 135.76, 136.83, 137.7, 137.91, 154.28, 155.01, 156.51, 156.82, 171.92. HRMS: m/z calc. for C$_{45}$H$_{57}$Cl$_3$N$_3$O$_{10}$Si: 932.2879; found: 932.2835 [M + NH$_4$]$^+$.
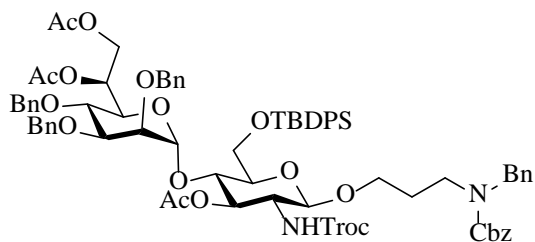
*N*-(Benzyl)-benzyloxycarbonyl-3-aminopropyl 6, 7-di-*O*-acetyl-2, 3, 4-tri-*O*-benzyl-L-glycero

-α-D-mannoheptopyranosyl-(1→4)-3-*O*-acetyl-6-*tert*-butyldiphenylsilyl-2-deoxy-2-

(2,2,2-trichloroethyloxycarbonylamino)-β-D-glucopyranoside (**24**)

A solution of compound **3** (160 mg, 0.24 mmol), **4** (197 mg, 0.21 mmol) and freshly activated 4

Å molecular sieves (300 mg) in DCM (5 mL) was stirred at r.t. for 20 min and then cooled to

-78 ℃. To the above solution was added AgOTf (153 mg, 0.60 mmol) in Et$_2$O/DCM (6/1 mL).

The mixture was stirred for 10 min and *p*-TolSCl (31.5 μL, 0.24 mmol) was added directly into it

via microsyringe. The reaction was allowed to warm up to r.t. over a period of 2 h before

quenched with Et$_3$N. The mixture was then filtered through celite and concentrated. Column

chromatography gave compound **24** in a yield of 80%.

^{1}HNMR (500 MHz, CDCl$_3$): δ = 1.03 (s, 9H), 1.71-1.76 (m, 2H), 1.88 (s, 3H), 1.92 (s, 3H), 2.07

(s, 3H), 2.95-3.00 (m, 1H), 3.24-3.36 (m, 3H), 3.55-3.68 (m, 3H), 3.72-3.80 (m, 4H), 3.82-3.92

(m, 3H), 4.06 (dd, 1H, *J* = 7.5, 11.5 Hz), 4.23 (d, 1H, *J* = 8.0 Hz), 4.28 (d, 1H, *J* = 15.0 Hz), 4.43

(d, 1H, *J* = 10.5 Hz), 4.46-4.54 (m, 1H), 4.55-4.58 (m, 2H), 4.62-4.69 (m, 4H), 4.77-4.84 (m,

1H), 5.04-5.10 (m, 1H), 5.14-5.22 (m, 3H), 5.43-5.46 (m, 1H), 6.16 (d, 1H, *J* = 8.5 Hz),

7.14-7.19 (m, 2H), 7.22-7.41 (m, 29H), 7.62-7.71 (m, 4H). ^{13}CNMR (125 MHz, CDCl$_3$): δ =

19.42, 20.86, 21.07, 26.93, 27.04, 27.46, 43.34, 50.31, 50.99, 56.68, 63.11, 63.29, 66.53, 67.62,

68.7, 72.02, 72.29, 72.43, 73.82, 74.42, 74.72, 75.19, 75.50, 75.58, 75.86, 79.8, 99.21, 100.75,

127.34, 127.58, 127.64, 127.79, 127.85, 127.87, 127.98, 128.14, 128.44, 128.51, 128.57, 128.61, 128.65, 128.77, 129.8, 129.91, 133.02, 133.42, 135.68, 135.89, 136.85, 137.71, 138.13, 138.22, 155.06, 156.55, 170.28, 170.48, 170.54. Two C1-H1 coupling constants (171.0, 159.5 Hz) confirmed the stereochemistry.

HRMS: m/z calc. for $C_{77}H_{91}Cl_3N_3O_{18}Si$: 1478.5132; found: 1478.5088 $[M + NH_4]^+$.
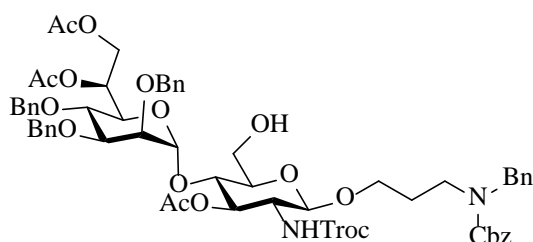
N-(Benzyl)-benzyloxycarbonyl-3-aminopropyl 6, 7-di-*O*-acetyl-2, 3, 4-tri-*O*-benzyl-L-glycero -α-D-mannoheptopyranosyl-(1→4)-3-*O*-acetyl-2-deoxy-2-(2,2,2-trichloroethyloxycarbonylamin o)-β-D-glucopyranoside (**25**)

To a solution of **24** (190 mg, 0.13 mmol) in pyridine (4 mL) in a plastic centrifuge tube, HF pyridine complex (2 mL) was added at 0 °C. The mixture was allowed to warm up to r.t. and stirred overnight. It was then diluted with DCM, washed with saturated $CuSO_4$ solution, 1M HCl and brine. The organic layer was dried and concentrated. Column chromatography (Hexanes/EtOAc = 1/1) gave **25** in a yield of 85%.

^{1}HNMR (500 MHz, CDCl₃): δ = 1.72-1.76 (m, 2H), 1.94 (s, 3H), 2.05 (s, 3H), 2.11 (s, 3H), 2.44 (br, 1H), 3.06-3.14 (m, 1H), 3.23-3.31 (m, 2H), 3.35-3.42 (m, 1H), 3.60-3.77 (m, 4H), 3.77-3.90 (m, 6H), 4.26-4.36 (m, 3H), 4.37-4.43 (dd, 1H, *J* = 4.5, 11.5 Hz), 4.47 (d, 1H, *J* = 11.5 Hz), 4.57-4.72 (m, 6H), 4.77-4.84 (m, 1H), 5.14-5.23 (m, 4H), 5.60-5.65 (m, 1H), 6.12 (m, 1H),

7.14-7.18 (m, 2H), 7.24-7.44 (m, 23H). ^{13}CNMR (125 MHz, CDCl$_3$): δ = 20.92, 21.02, 21.15, 27.58, 29.77, 43.41, 50.21, 56.59, 61.33, 63.06, 67.32, 67.58, 68.85, 72.0, 72.2, 72.78, 73.75, 74.09, 74.36, 74.88, 74.99, 75.11, 75.64, 79.56, 95.73, 99.22, 101.17, 127.26, 127.52, 127.57, 127.64, 127.79, 127.95, 128.09, 128.45, 128.49, 128.52, 128.57, 128.71, 136.73, 137.57, 137.91, 138.09, 138.14, 154.87, 156.56, 170.49, 170.59, 170.76. HRMS: m/z calc. for C$_{61}$H$_{70}$Cl$_3$N$_2$O$_{18}$: 1223.3689; found: 1223.3668 [M + H]$^+$.
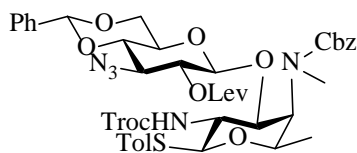
p-Tolyl

3-azido-4,6-*O*-benzylidene-3-deoxy-2-levulinoyl-β-D-glucopyranosyl-(1→3)-4-[*N*-(methyl)-benzyloxycarbonylamino]-2,4-dideoxy-2-(2,2,2-trichloroethyloxycarbonylamino)-β-L-fucopyranoside (**26**)

A solution of compound **6** (788 mg, 1.58 mmol) and freshly activated 4 Å molecular sieves (1.6 g) in DCM (20 mL) was stirred at r.t. for 20 min and then cooled to -78 °C. To the above solution was added AgOTf (1.02 g, 3.96 mmol) in Et$_2$O/DCM (20/2 mL). The mixture was stirred for 10 min and *p*-TolSCl (209 μL, 1.58 mmol) was added directly into it via microsyringe. After activation completed as indicated by disappearance of orange color and by TLC, acceptor **4** (797 mg, 1.35 mmol) in DCM (5 mL) was added slowly along the wall of the flask. Another 3 mL of DCM was used to rinse once. The reaction was allowed to warm up to r.t. over a period of 2 h before quenched with Et$_3$N. The mixture was then filtered through celite and concentrated.

Column chromatography gave compound **26** in a yield of 70%.

^{1}HNMR (500 MHz, CDCl$_3$): δ = 1.20-1.28 (m, 3H), 2.13&2.21 (s, 3H), 2.33&2.34 (s, 3H), 2.40-2.82 (m, 4H), 2.86&2.94 (s, 3H), 3.03 (t, 1H, J = 10.0 Hz), 3.37-3.73 (m, 5H), 3.77-3.88 (m, 1.5H), 4.22 (dd, 0.5H, J = 5.0, 10.5 Hz), 4.32 (d, 1H, J = 8.0 Hz), 4.37-4.47 (m, 1H), 4.53 (0.5H, dd, J = 2.5, 7.0 Hz), 4.59 (d, 0.5H, J = 12.0 Hz), 4.64&4.66 (d, 0.5H, J = 10.0 Hz), 4.68 (d, 0.5H, J = 7.5 Hz), 4.71-4.84 (m, 3H), 5.01 (d, 1H, J = 12.0 Hz), 5.14 (d, 0.5 H, J = 12.0 Hz), 5.23 (d, 1H, J = 12.5 Hz), 5.35 (d, 0.5H, J = 12.0 Hz), 5.49&5.54 (s, 1H), 7.07-7.13 (m, 2H), 7.28-7.44 (m, 10H), 7.45-7.52 (m, 2H). ^{13}CNMR (125 MHz, CDCl$_3$): δ = 21.1, 27.61, 29.82, 32.73, 37.59, 37.82, 51.55, 53.18, 62.78, 63.06, 67.22, 67.68, 71.25, 71.56, 85.48, 96.84, 99.94, 101.57, 125.95, 126.01, 127.92, 128.19, 128.38, 128.55, 128.9, 128.95, 129.23, 129.26, 129.67, 129.7, 133.85, 134.16, 136.44, 138.49, 138.69, 156.49, 157.6. Two C1-H1 coupling constants (163.0, 161.0 Hz) confirmed the stereochemistry. Most peaks were split due to the secondary amides on the fucose.

HRMS: m/z calc. for C$_{43}$H$_{49}$Cl$_3$N$_5$O$_{12}$S: 964.2164; found: 964.2117 [M + H]$^+$.
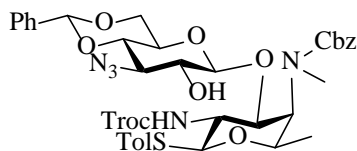
p-Tolyl

3-azido-4,6-*O*-benzylidene-3-deoxy-β-D-glucopyranosyl-(1→3)-4-[*N*-(methyl)-benzyloxycarbon ylamino]-2,4-dideoxy-2-(2,2,2-trichloroethyloxycarbonylamino)-β-L-fucopyranoside (**27**)

Compound **26** (366 mg, 0.379 mmol) was dissolved in DCM/Pyridine (10/0.05 mL) followed by addition of N$_2$H$_4$ • AcOH (50 mg, 0.543 mmol). The mixture was stirred at r.t. for 4 h before it

was diluted with DCM and washed with brine. The organic layer was dried and concentrated. Column chromatography (Hexanes/DCM/EtOAc = 1/1/1) gave **27** as white solid in a yield of 93%.

^{1}HNMR (500 MHz, CDCl$_3$): δ = 1.31 (d, 3H, J = 6.5 Hz), 2.33 (s, 3H), 2.98 (s, 3H), 3.40 (t, 1H, J = 9.5 Hz), 3.42-3.52 (m, 2H), 3.61 (t, 1H, J = 9.5 Hz), 3.76 (t, 1H, J = 9.5 Hz), 3.88 (dd, 1H, J = 3.0, 6.5 Hz), 4.14 (dd, 1H, J = 5.5, 11.5 Hz), 4.32 (dd, 1H, J = 5.0, 10.5 Hz), 4.40 (d, 1H, J = 7.5 Hz), 4.59 (dd, 1H, J = 3.0, 5.5 Hz), 4.76 (d, 1H, J = 12.5 Hz), 4.81 (d, 1H, J = 12.0 Hz), 4.86 (d, 1H, J = 2.0 Hz), 4.91 (d, 1H, J = 10.5 Hz), 5.09 (d, 1H, J = 12.5 Hz), 5.20 (d, 1H, J = 12.5 Hz), 5.34 (d, 1H, J = 7.5 Hz), 5.52 (s, 1H), 7.08-7.13 (m, 2H), 7.32-7.45 (m, 10H), 7.46-7.52 (m, 2H). ^{13}CNMR (125 MHz, CDCl$_3$): δ = 17.3, 21.33, 33.2, 53.4, 56.21, 64.49, 67.58, 68.27, 68.58, 73.32, 74.35, 74.63, 79.02, 81.7, 86.27, 95.62, 101.73, 106.53, 125.42, 126.18, 127.75, 128.15, 128.35, 128.46, 128.49, 128.78, 129.16, 129.37, 129.8, 134.42, 136.23, 136.67, 138.92, 154.22, 159.87. Two C1-H1 coupling constants (161.0, 156.5 Hz) confirmed the stereochemistry.

HRMS: m/z calc. for C$_{38}$H$_{43}$Cl$_3$N$_5$O$_{10}$S: 866.1796; found: 866.1745 [M + H]$^+$.
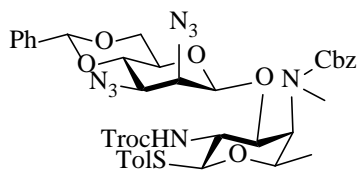
p-Tolyl

2,3-diazido-4,6-*O*-benzylidene-2,3-dideoxy-β-D-mannopyranosyl-(1→3)-4-[*N*-(methyl)-benzylo xycarbonylamino]-2,4-dideoxy-2-(2,2,2-trichloroethyloxycarbonylamino)-β-L-fucopyranoside

(**28**)

Compound **27** (307 mg, 0.35 mmol) was dissolved in anhydrous DCM (10 mL) and cooled to -30 °C. Pyridine (285 μL, 3.54 mmol) and Tf_2O (179 μL, 1.06 mmol) were added and the mixture was allowed to warm up to r.t. over a period over 4 h. It was then quenched with MeOH, diluted with DCM and washed with brine. The organic layer was dried, concentrated and dissolved with DMF (10 mL). NaN_3 (140 mg, 2.17 mmol) was added and the mixture was heated at 50 °C overnight. After diluting with EtOAc and washing with brine, compound **28** was purified through column chromatography (Hexanes/DCM/EtOAc = 3/2/1) in a yield of 84% over 2 steps.

^{1}HNMR (500 MHz, $CDCl_3$): δ = 1.31 (d, 3H, J = 6.5 Hz), 2.33 (s, 3H), 2.96 (s, 3H), 3.26 (d, 1H, J = 3.5 Hz), 3.32 (dt, 1H, J = 5.0, 9.5 Hz), 3.46 (dd, 1H, J = 4.0, 10.0 Hz), 3.60-3.69 (m, 1H), 3.74-3.89 (m, 3H), 4.12-4.20 (m, 1H), 4.26 (dd, 1H, J = 4.5, 10.5 Hz), 4.56-4.62 (m, 2H), 4.72 (d, 1H, J = 1.5 Hz), 4.80 (d, 1H, J = 10.5 Hz), 4.95 (d, 1H, J = 12.0 Hz), 5.06 (d, 1H, J = 12.5 Hz), 5.14 (d, 1H, J = 6.5 Hz), 5.20 (d, 1H, J = 12.5 Hz), 5.56 (s, 1H), 7.08-7.14 (m, 2H), 7.32-7.51 (m, 12H). ^{13}CNMR (125 MHz, $CDCl_3$): δ = 17.3, 21.32, 32.88, 52.83, 54.13, 59.96, 62.38, 67.74, 67.94, 68.37, 74.39, 74.64, 76.07, 76.73, 86.75, 95.69, 98.6, 101.61, 101.76, 125.92, 125.99, 128.05, 128.43, 128.61, 128.72, 128.98, 129.26, 129.3, 129.74, 129.77, 134.19, 134.53, 136.63, 136.67, 138.74, 154.22, 158.48. Two C1-H1 coupling constants (163.5, 163.0 Hz) confirmed the stereochemistry. Most peaks were split due to the secondary amides on the fucose.

HRMS: m/z calc. for $C_{38}H_{42}Cl_3N_8O_9S$: 891.1861; found: 891.1813 $[M + H]^+$.
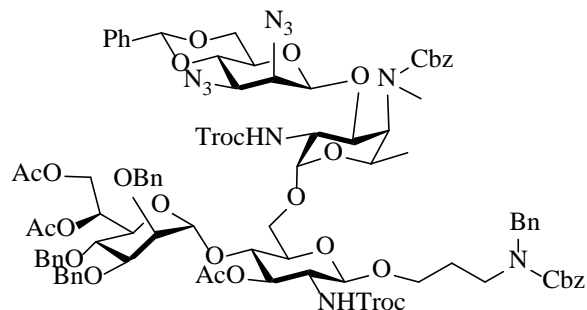
N-(Benzyl)-benzyloxycarbonyl-3-aminopropyl 2,3-diazido-4,6-*O*-benzylidene-2,3-dideoxy -*β*-D-mannopyranosyl-(1→3)-4-[*N*-(methyl)-benzyloxycarbonylamino]-2,4-dideoxy-2-(2,2,2-trichloroethyloxycarbonylamino)-*α*-L-fucopyranosyl-(1→6)-[6,7-di-*O*-acetyl-2,3,4-tri-*O*-benzyl-L-glycero-*α*-D-mannoheptopyranosyl-(1→4)]-3-*O*-acetyl-2-deoxy-2-(2,2,2-trichloroethyloxycarbonylamino)-*β*-D-glucopyranoside (**29**)

A solution of compound **28** (50 mg, 0.0561 mmol), **25** (55 mg, 0.0449 mmol) and freshly activated 4 Å molecular sieves (100 mg) in DCM (5 mL) was stirred at r.t. for 20 min and then cooled to -78 °C. To the above solution was added AgOTf (36 mg, 0.14 mmol) in Et$_2$O/DCM (3/0.5 mL). The mixture was stirred for 10 min and *p*-TolSCl (7.4 μL, 0.0561 mmol) was added directly into it via microsyringe. The reaction was allowed to warm up to r.t. over a period of 2 h before quenched with Et$_3$N. The mixture was then filtered through celite and concentrated. Column chromatography (Hexanes/DCM/EtOAc = 2/2/1) gave compound **29** in a yield of 73%.

^{1}HNMR (500 MHz, CDCl$_3$): δ = 1.20 (d, 3H, *J* = 7.0 Hz), 1.65-1.77 (m, 2H), 1.86 (s, 3H), 2.06 (s, 3H), 2.12 (s, 3H), 2.85-2.94 (m, 1H), 3.19 (s, 3H), 3.25-3.31 (m, 1H), 3.34-3.49 (m, 4H), 3.53 (dd, 1H, *J* = 4.0, 10.0 Hz), 3.60-3.72 (m, 3H), 3.73-3.91 (m, 8H), 4.00-4.08 (m, 1H), 4.12 (dd, 1H, *J* = 4.0, 11.0 Hz), 4.15-4.32 (m, 5H), 4.33-4.41 (m, 1H), 4.47 (d, 2H, *J* = 10.0 Hz), 4.55-4.65 (m, 5H), 4.67-4.77 (m, 4H), 4.77-4.88 (m, 3H), 5.01-5.09 (m, 2H), 5.11 (d, 1H, *J* = 12.5 Hz),

5.14-5.23 (m, 3H), 5.35 (d, 1H, J = 4.0 Hz), 5.40 (d, 1H, J = 7.5 Hz), 5.58 (s, 1H), 5.60-5.65 (m, 1H), 6.46 (d, 1H, J = 8.5 Hz), 7.12-7.19 (m, 2H), 7.26-7.52 (m, 33H). ^{13}CNMR (125 MHz, CDCl$_3$): δ = 16.69, 16.74, 20.95, 21.0, 21.06, 27.37, 29.81, 33.21, 42.84, 50.05, 51.12, 54.54, 56.33, 59.92, 62.56, 63.17, 65.0, 65.82, 66.86, 67.69, 67.88, 68.25, 68.42, 68.64, 72.08, 72.23, 72.67, 73.78, 74.02, 74.39, 74.44, 74.6, 75.27, 75.42, 75.52, 76.69, 77.36, 77.63, 79.58, 95.92, 97.66, 99.08, 100.75, 101.75, 125.95, 126.03, 127.26, 127.58, 127.61, 127.66, 127.89, 127.96, 128.02, 128.1, 128.12, 128.39, 128.47, 128.58, 128.6, 128.68, 128.76, 129.1, 129.16, 129.21, 136.62, 136.76, 137.38, 137.76, 137.98, 138.04, 154.41, 155.17, 156.65, 158.49, 170.37, 170.42, 170.55. Four C1-H1 coupling constants (177.0, 171.0, 166.0, 163.5 Hz) confirmed the stereochemistry. Most peaks were split due to the secondary amides on the fucose and the linker.

HRMS: m/z calc. for C$_{92}$H$_{106}$Cl$_6$N$_{11}$O$_{27}$: 2006.5391; found: 2006.5326 [M + NH$_4$]$^+$.
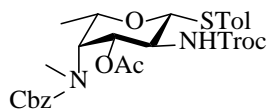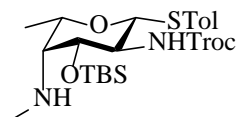

p-Tolyl

3-*O*-acetyl-4-[*N*-(methyl)-benzyloxycarbonylamino]-2,4-dideoxy-1-thio-2-(2,2,2-trichloroethyloxycarbonylamino)-β-L-fucopyranoside (**31**)

Compound **5** (102 mg, 0.172 mmol) was dissolved in pyridine (3 mL) followed by addition of DMAP (10 mg) and acetic anhydride (200 μL) at 0 °C. The reaction was stirred at room temperature overnight. Upon completion by TLC, the reaction was diluted with EtOAc, washed with 1 M HCl, sat. NaHCO$_3$ solution and brine. Column chromatography (Hexanes/DCM/EtOAc

= 1/1/1) gave compound **31** in a yield of 85%.

^{1}HNMR (500 MHz, CDCl$_3$): δ = 1.22&1.27 (d, 3H, J = 6.5 Hz, H-6), 1.76 (s, 3H, Ac), 2.32 (s, 3H, STol-Me), 2.87&2.92 (s, 3H, N-Me), 3.83-3.92 (m, 1H, H-5), 3.92-4.01 (m, 1H, H-2), 4.48-4.52&4.56-4.60 (m, 1H, H-4), 4.59&4.64 (d, 1H, J = 10.5 Hz, H-1), 4.73 (d, 1H, J = 11.5 Hz, Troc-CH$_2$), 4.80 (d, 1H, J = 12.0 Hz Troc-CH$_2$), 5.02&5.04 (d, 1H, J = 12.5 Hz, Cbz-CH$_2$), 5.08&5.17 (d, 1H, J = 12.5 Hz, Cbz-CH$_2$), 5.12 (dd, 1H, J = 5.5, 11.0 Hz, H-3), 5.20-5.30 (m, 1H, Troc-NH), 7.08-7.14 (m, 2H), 7.27-7.38 (m, 5H), 7.41-7.47 (m, 2H). ^{13}CNMR (125 MHz, CDCl$_3$): δ = 17.07, 17.08, 20.45, 20.55, 21.3, 32.78, 33.17, 51.74, 51.86, 54.64, 54.78, 67.47, 67.73, 71.71, 71.83, 74.59, 74.64, 86.48, 86.95, 95.65, 127.55, 127.9, 128.13, 128.33, 128.35, 128.6, 128.64, 129.7, 129.74, 134.4, 134.74, 136.37, 136.82, 138.81, 154.14, 154.35, 157.31, 158.07, 170.51. HRMS: m/z calc. for C$_{27}$H$_{32}$Cl$_3$N$_2$O$_7$S: 633.0996; found: 633.1012 [M + H]$^+$.
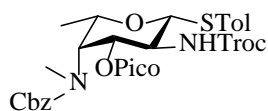
p-Tolyl

4-[*N*-(methyl)-benzyloxycarbonylamino]-2,4-dideoxy-3-*O*-picoloyl-1-thio-2-(2,2,2-trichloroethy loxycarbonylamino)-*β*-L-fucopyranoside (**32**)

Compound **5** (134 mg, 0.226 mmol) was dissolved in DCM (5 mL), followed by addition of picolinic acid (84 mg, 0.678 mmol), EDC·HCl (143 mg, 0.747 mmol) and DMAP (5.5 mg, 0.045 mmol). The reaction was stirred at room temperature overnight before concentrated and washed with sat. NaHCO$_3$ solution. The organic phase was dried over Na$_2$SO$_4$, concentrated and purified

through column (Hexanes/DCM/EtOAc = 2/2/3) to obtain compound **32** in a yield of 94%.

^{1}HNMR (500 MHz, CDCl$_3$): δ = 1.26&1.29 (d, 3H, J = 6.5 Hz, H-6), 2.30&2.33 (s, 3H, STol-Me), 2.96&3.00 (s, 3H, N-Me), 3.96-4.02&4.10-4.15 (m, 1H, H-5), 4.15-4.24 (m, 1H, H-2), 4.53&4.90 (d, 1H, J = 12.5 Hz, Cbz-CH$_2$), 4.58&4.69 (d, 1H, J = 12.0 Hz, Troc-CH$_2$), 4.62 (s, 1H, Troc-CH$_2$), 4.65&4.84 (dd, 1H, J = 3.0, 6.5 Hz, H-4), 4.80&4.93 (d, 1H, J = 10.5 Hz, H-1), 4.82&4.86 (d, 1H, J = 12.5 Hz, Cbz-CH$_2$), 5.56&5.77 (dd, 1H, J = 6.0, 11.0 Hz, H-3), 5.96&4.82 (d, 1H, J = 9.0 Hz, Troc-NH), 7.03-7.30 (m, 6H), 7.35-7.90 (m, 5H), 8.69-8.79 (m, 1H).

^{13}CNMR (125 MHz, CDCl$_3$): δ = 17.12, 17.15, 21.3, 32.94, 33.28, 51.67, 51.74, 54.97, 55.02, 67.28, 67.72, 73.44, 73.8, 74.34, 74.51, 74.54, 86.0, 86.14, 95.54, 95.65, 125.17, 125.46, 126.91, 126.99, 127.21, 127.32, 127.7, 127.96, 128.09, 128.13, 128.39, 128.49, 129.6, 129.71, 134.83, 135.0, 135.96, 136.65, 137.14, 137.51, 138.77, 139.07, 146.81, 147.11, 150.17, 150.36, 154.49, 154.68, 157.39, 157.98, 163.63, 163.85. HRMS: m/z calc. for C$_{31}$H$_{33}$Cl$_3$N$_3$O$_7$S: 696.1105; found: 696.1123 [M + H]$^+$.
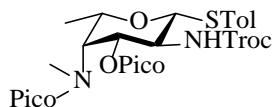
p-Tolyl

4-[*N*-(methyl)-*N*-(picoloyl)-amino]-2,4-dideoxy-3-*O*-picoloyl-1-thio-2-(2,2,2-trichloroethyloxyc arbonylamino)-β-L-fucopyranoside (**33**)

Compound **19** (157 mg, 0.343 mmol) was dissolved in DCM (5 mL), followed by addition of picolinic acid (127 mg, 1.03 mmol), EDC·HCl (237 mg, 1.24 mmol) and DMAP (8.4 mg, 0.069

mmol). The reaction was stirred at room temperature overnight before concentrated and washed with sat. NaHCO$_3$ solution. The organic phase was dried over Na$_2$SO$_4$, concentrated and purified through column (DCM/MeOH = 8/1) to obtain compound **33** in a yield of 99%.

^{1}HNMR (500 MHz, CDCl$_3$): δ = 1.21&1.39&1.43 (d, 3H, J = 6.5 Hz, H-6), 2.29&2.32&2.35 (s, 3H, STol-Me), 3.08&3.12 (s, 3H, N-Me), 3.73-3.79&3.92-3.96&4.07-4.14 (m, 1H, H-5), 4.18-4.31&5.33-5.38 (m, 1H, H-2), 4.62&4.74&4.80 (d, 1H, J = 12.0 Hz, Troc-CH$_2$), 4.61-4.67 (m, 1H, Troc-CH$_2$), 4.68&3.91 (dd, 1H, J = 3.0, 6.5 Hz, H-4), 4.73&4.85 (d, 1H, J = 10.0 Hz, H-1), 5.42&5.75 (dd, 1H, J = 6.5, 11.0 Hz, H-3), 5.58-5.67&5.91-6.01 (m, 1H, Troc-NH), 7.04-7.19 (m, 3H), 7.26-7.53 (m, 4H), 7.65-8.01 (m, 2H), 8.20-8.77 (m, 2H). ^{13}CNMR (125 MHz, CDCl$_3$): δ = 16.99, 17.13, 17.41, 21.29, 21.35, 32.47, 36.32, 51.94, 52.41, 52.57, 57.4, 60.24, 72.59, 72.62, 74.07, 74.39, 74.93, 86.09, 86.8, 95.47, 95.56, 123.16, 123.84, 124.33, 124.43, 125.07, 125.32, 125.68, 126.13, 126.62, 127.19, 127.28, 127.44, 129.69, 129.74, 129.77, 134.56, 134.73, 135.25, 136.92, 137.06, 137.12, 137.44, 138.71, 138.8, 139.29, 147.09, 147.14, 147.16, 148.1, 148.61, 150.03, 150.27, 153.8, 153.94, 154.37, 154.59, 163.73, 164.12, 169.94, 171.18, 171.33. HRMS: m/z calc. for C$_{29}$H$_{30}$Cl$_3$N$_4$O$_6$S: 667.0952; found: 667.0966 [M + H]$^+$.
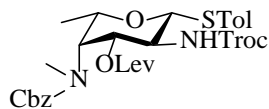
p-Tolyl

4-[*N*-(methyl)-benzyloxycarbonylamino]-2,4-dideoxy-3-*O*-levuniloyl-1-thio-2-(2,2,2-trichloroethyloxycarbonylamino)-β-L-fucopyranoside (**34**)

Compound **5** (1.81 g, 3.06 mmol) was dissolved in DCM (40 mL), followed by addition of levulinic acid (626 μL, 6.12 mmol), EDC·HCl (1.46 g, 7.64 mmol) and DMAP (38 mg, 0.31 mmol). The reaction was stirred at room temperature overnight before concentrated and washed with sat. $NaHCO_3$ solution. The organic phase was dried over Na_2SO_4, concentrated and purified through column (Hexanes/DCM/EtOAc =1/1/1) to obtain compound **34** in a yield of 93%.

^{1}HNMR (500 MHz, CDCl$_3$): δ = 1.21&1.25 (d, 3H, J = 6.5 Hz, H-6), 2.06&2.08 (s, 3H, Lev-Me), 2.10-2.60 (m, 4H, Lev-CH$_2$), 2.31 (s, 3H, STol-Me), 2.87&2.92 (s, 3H, *N*-Me), 3.87-3.99 (m, 2H, H-2, H-5), 4.50&4.57 (dd, 1H, J = 3.0, 6.0 Hz, H-4), 4.64&4.69 (d, 1H, J = 10.5 Hz, H-1), 4.68&4.87&4.90 (d, 2H, J = 12.0 Hz, Troc-CH$_2$), 5.02&5.05&5.16 (d, 2H, J = 12.5 Hz, Cbz-CH$_2$), 5.11 (dd, 1H, J = 6.0, 10.0 Hz, H-3), 5.51&5.61 (d, 1H, J = 9.5 Hz, Troc-NH), 7.07-7.12 (m, 2H), 7.27-7.37 (m, 5H), 7.38-7.45 (m, 2H). ^{13}CNMR (125 MHz, CDCl$_3$): δ = 17.04, 17.09, 21.27, 27.83, 29.75, 29.76, 32.81, 33.19, 37.76, 37.84, 51.63, 51.89, 54.61, 54.78, 67.44, 67.68, 71.88, 72.15, 74.43, 74.56, 86.27, 86.79, 95.73, 127.87, 128.09, 128.19, 128.23, 128.56, 128.58, 129.66, 129.69, 134.13, 134.53, 136.51, 136.87, 138.62, 138.87, 154.43, 157.27, 158.01, 171.86, 172.15, 206.52. HRMS: m/z calc. for $C_{30}H_{36}Cl_3N_2O_8S$: 689.1258; found: 689.1236 $[M + H]^+$.

p-Tolyl

3-*O*-*tert*-butyldimethylsilyl-2,4-dideoxy-4-methylamino-1-thio-2-(2,2,2-trichloroethyloxycarbon

ylamino)-β-L-fucopyranoside (**35**)

Compound **19** (1.2 g, 2.62 mmol) was dissolved in DCM (50 mL) followed by the addition of

t-butyldimethylsilyl trifluoromethanesulfonate (TBSOTf, 0.9 mL, 3.93 mmol) and 2, 6-lutidine

(0.61 mL, 5.24 mmol) at -40°C. The mixture was allowed to warm up to r.t. and stirred overnight.

Compound **35** was obtained through column chromatography (DCM/EtOAc = 3/1) as a white

solid in a yield of 87%.

^{1}HNMR (500 MHz, CDCl$_3$): δ = 0.06 (s, 3H), 0.08 (s, 3H), 0.88 (s, 9H), 1.33 (d, 3H, J = 6.5 Hz),

2.31 (s, 3H), 2.51 (dd, 1H, J = 1.5, 4.5 Hz), 2.53 (s, 3H), 3.46 (q, 1H, J = 9.5 Hz), 3.59 (q, 1H, J

= 6.5 Hz), 3.94 (dd, 1H, J = 3.5, 10.0 Hz), 4.64 (d, 1H, J = 11.5 Hz), 4.70 (d, 1H, J = 12.0 Hz),

4.82 (d, 1H, J = 10.5 Hz), 4.99 (d, 1H, J = 8.5 Hz), 7.07 (d, 2H, J = 8.0 Hz), 7.39 (d, 2H, J = 8.0

Hz). ^{13}CNMR (125 MHz, CDCl$_3$): δ = -4.83, -4.31, 18.01, 18.23, 21.19, 25.75, 39.01, 54.54,

64.93, 73.81, 74.75, 75.68, 86.87, 95.34, 129.62, 130.2, 132.48, 137.57, 153.78. HRMS: m/z calc.

for C$_{23}$H$_{38}$Cl$_3$N$_2$O$_4$SSi: 571.1387; found: 571.1378 [M + H]$^+$.
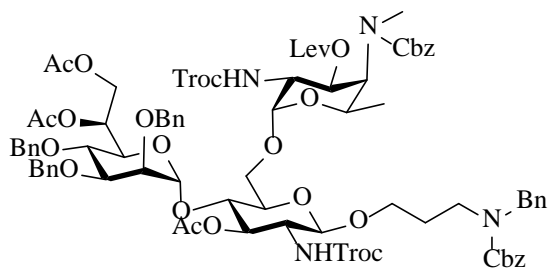
N-(Benzyl)-benzyloxycarbonyl-3-aminopropyl

4-[*N*-(methyl)-benzyloxycarbonylamino]-2,4-dideoxy-3-*O*-levuniloyl-2-(2,2,2-trichloroethyloxy

carbonylamino)-α-L-fucopyranosyl-(1→6)-[6,7-di-*O*-acetyl-2,3,4-tri-*O*-benzyl-L-glycero-α-D-m

annoheptopyranosyl-(1→4)]-3-*O*-acetyl-2-deoxy-2-(2,2,2-trichloroethyloxycarbonylamino)-*β*-D-glucopyranoside (**36α**)

A solution of compound **34** (51 mg, 0.0735 mmol), **25** (72 mg, 0.0588 mmol) and freshly activated 4 Å molecular sieves (100 mg) in DCM (3 mL) was stirred at r.t. for 20 min and then cooled to -78 °C. To the above solution was added AgOTf (47 mg, 0.184 mmol) in Et_2O/DCM (3/0.5 mL). The mixture was stirred for 10 min and *p*-TolSCl (9.7 μL, 0.0735 mmol) was added directly into it via microsyringe. The reaction was allowed to warm up to r.t. over a period of 2 h before quenched with Et_3N. The mixture was then filtered through celite and concentrated. Column chromatography (Hexanes/DCM/EtOAc = 1/1/1) gave compound **36α** (60 mg, 57%) and **36β** (30 mg, 28%).

^{1}HNMR (500 MHz, CDCl$_3$): δ = 1.05&1.11 (d, 3H, *J* = 6.5 Hz), 1.64-1.78 (m, 2H), 1.90&1.91 (s, 3H), 2.02&2.04 (s, 3H), 2.09 (s, 3H), 2.10&2.11 (s, 3H), 2.11-2.49 (m, 4H), 2.59-2.68 (m, 1H), 2.84-2.91 (m, 1H), 3.22 (s, 3H), 3.25-3.45 (m, 3H), 3.50-3.98 (m, 9H), 4.14-4.37 (m, 5H), 4.39-4.88 (m, 12H), 5.00-5.30 (m, 8H), 5.38 (d, 1H, *J* = 9.5 Hz), 5.55-5.64 (m, 1H), 6.47-6.57 (m, 1H), 7.10-7.20 (m, 2H), 7.22-7.50 (m, 28H). ^{13}CNMR (125 MHz, CDCl$_3$): δ = 16.36, 16.45, 20.86, 20.89, 21.0, 21.03, 27.4, 27.82, 27.84, 29.78, 29.81, 29.87, 33.27, 33.66, 37.61, 37.78, 42.76, 50.0, 50.2, 50.33, 50.82, 54.8, 54.9, 56.37, 56.43, 63.4, 65.42, 65.55, 67.02, 67.37, 67.66, 68.75, 69.22, 72.14, 72.37, 72.71, 72.75, 73.78, 74.22, 74.35, 74.61, 74.77, 75.0, 79.34, 95.68, 95.78, 98.08, 98.28, 100.12, 100.2, 100.98, 127.27, 127.55, 127.57, 127.7, 127.78, 127.87, 128.08, 128.11, 128.25, 128.37, 128.42, 128.52, 128.55, 128.59, 128.73, 136.55, 136.76, 136.92, 137.44, 137.94, 138.01, 154.38, 154.45, 155.13, 156.68, 157.32, 157.99, 170.44, 170.46, 170.62,

170.65, 172.02, 172.22, 205.95, 206.32. Three C1-H1 coupling constants (175.0, 173.0, 162.0 Hz) confirmed the stereochemistry. Most peaks were split due to the secondary amides on the fucose and the linker.

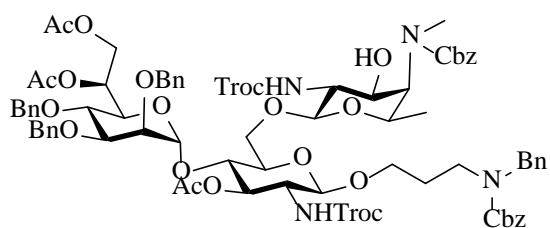HRMS: m/z calc. for $C_{84}H_{97}Cl_6N_4O_{26}$: 1787.4522; found: 1787.4478 $[M + H]^+$.
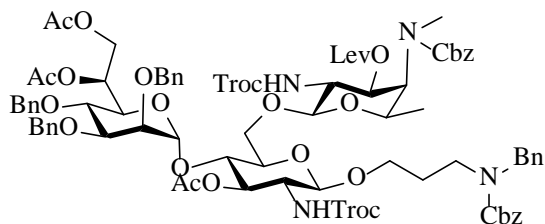
N-(Benzyl)-benzyloxycarbonyl-3-aminopropyl

4-[*N*-(methyl)-benzyloxycarbonylamino]-2,4-dideoxy-3-*O*-levuniloyl-2-(2,2,2-trichloroethyloxy carbonylamino)-*β*-L-fucopyranosyl-(1→6)-[6,7-di-*O*-acetyl-2,3,4-tri-*O*-benzyl-L-glycero-*α*-D-m annoheptopyranosyl-(1→4)]-3-*O*-acetyl-2-deoxy-2-(2,2,2-trichloroethyloxycarbonylamino)-*β*-D-glucopyranoside (**36β**)

^{1}HNMR (500 MHz, CDCl$_3$): δ = 1.14&1.20 (d, 3H, *J* = 6.5 Hz), 1.67-1.75 (m, 2H), 1.76&1.81 (s, 3H), 2.03&2.05 (s, 3H), 2.10 (s, 6H), 2.27-2.54 (m, 4H), 2.57-2.67 (m, 1H), 3.00-3.10 (m, 1H), 3.17&3.18 (s, 3H), 3.25-3.46 (m, 3H), 3.52-3.96 (m, 11H), 4.20-4.36 (m, 4H), 4.41-4.87 (m, 13H), 5.02-5.23 (m, 6H), 5.57-5.66 (m, 1H), 5.70-5.84 (m, 1H), 5.97-6.12 (m, 1H), 7.11-7.19 (m, 2H), 7.23-7.44 (m, 28H). ^{13}CNMR obtained from HSQC: δ = 16.4, 16.5, 18.22, 19.32, 20.79, 20.87, 20.97, 21.27, 22.67, 27.58, 29.57, 29.71, 29.81, 31.42, 31.52, 33.2, 33.29, 37.67, 37.7, 49.99, 52.23, 54.1, 54.3, 63.47, 63.54, 65.72, 67.25, 67.46, 67.65, 68.58, 68.62, 70.16, 70.29, 71.11, 71.67, 71.99, 72.02, 72.09, 72.17, 72.52, 72.8, 73.65, 73.73, 73.76, 74.13, 74.27, 74.5,

74.55, 74.64, 75.18, 75.27, 75.31, 75.89, 77.94, 79.48, 99.93, 100.84, 102.61, 124.67, 125.58, 125.64, 125.66, 126.07, 126.3, 126.55, 127.13, 127.29, 127.48, 128.05, 128.33, 128.41, 130.07, 130.13, 131.08. Three C1-H1 coupling constants (172.0, 162.0, 160.0 Hz) confirmed the stereochemistry. Most peaks were split due to the secondary amides on the fucose and the linker.

HRMS: m/z calc. for $C_{84}H_{97}Cl_6N_4O_{26}$: 1787.4522; found: 1787.4562 $[M + H]^+$.
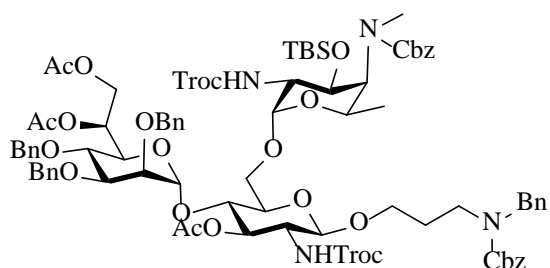
N-(Benzyl)-benzyloxycarbonyl-3-aminopropyl

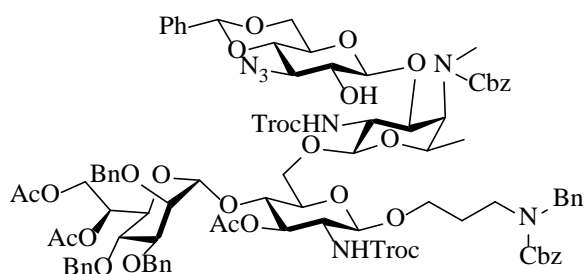4-[*N*-(methyl)-benzyloxycarbonylamino]-3-*O*-*tert*-butyldimethylsilyl-2,4-dideoxy-2-(2,2,2-trichloroethyloxycarbonylamino)-*α*-L-fucopyranosyl-(1→6)-[6,7-di-*O*-acetyl-2,3,4-tri-*O*-benzyl-L-glycero-*α*-D-mannoheptopyranosyl-(1→4)]-3-*O*-acetyl-2-deoxy-2-(2,2,2-trichloroethyloxycarbonylamino)-*β*-D-glucopyranoside (**37α**)

A solution of compound **35** (0.89 g, 1.56 mmol), compound **25** (1.53 g, 1.25 mmol) and freshly activated 4 Å molecular sieves (1.6 g) in DCM (35 mL) was stirred at r.t. for 20 min and then cooled to -78 °C. To the above solution was added AgOTf (1.0 g, 3.91 mmol) in DCM/MeCN (5/1 mL). The mixture was stirred for 10 min and *p*-TolSCl (207 μL, 1.56 mmol) was added directly into it via microsyringe. The reaction was allowed to warm up to r.t. over a period of 2 h. TLC indicated that acceptor was not completely consumed yet. The reaction was cooled to -78 °C

followed by addition of **35** (0.53 g, 0.94 mmol), AgOTf (0.60 g, 2.35 mmol) and *p*-TolSCl (124 µL, 0.94 mmol) in order. After warming up over another period of 2 h, the mixture was quenched with Et₃N, filtered through celite and concentrated. Column chromatography gave inseparable *α* and *β* mixtures, which was dissolved in THF/water (40/10 mL) and treated with benzyl chloroformate (535 µL, 3.75 mmol) and sodium carbonate (0.66 g, 6.25 mmol). The reaction was stirred at r.t. for 4 h followed by concentration, dilution with EtOAc and wash with saturated NaHCO₃ and brine. The organic layer was dried, concentrated and purified through column chromatography (Hexanses/DCM/EtOAc = 3/2/2) to give compound **37α** (225 mg, 10%) and **37β** (1.46 g, 73%) over 2 steps.

¹HNMR (500 MHz, CDCl₃): δ = -0.07-0.14 (m, 6H, TBS), 0.83 (s, 9H), 1.06&1.13 (d, 3H, *J* = 6.5Hz, Fuc-6-Me), 1.66-1.74 (m, 2H), 1.89 (s, 3H), 1.98 (s, 1H) + 2.05 (s, 2H, Ac), 2.10 (s, 3H), 2.85-2.91 (m, 1H), 3.15-3.29 (m, 5H), 3.40-3.57 (m, 2H), 3.62-3.74 (m, 3H), 3.76-3.92 (m, 6H), 4.00 (dd, 1H, *J* = 6.5, 11.0 Hz), 4.14-4.22 (m, 2H), 4.22-4.32 (m, 3H), 4.40-4.50 (m, 2H), 4.51-4.56 (m, 1H), 4.57-4.66 (m, 4H), 4.66-4.84 (m, 6H), 5.01-5.12 (m, 4H), 5.13-5.23 (m, 3H), 5.58-5.64 (m, 1H), 6.45-6.57 (m, 1H), 7.13-7.17 (m, 2H), 7.24-7.45 (m, 28H).. ¹³CNMR (125 MHz, CDCl₃): δ = -4.93, -4.85, -4.83, -4.73, 16.5, 16.55, 17.77, 17.78, 17.8, 20.81, 20.91, 20.98, 21.05, 25.59, 25.6, 27.41, 33.1, 33.31, 33.71, 42.75, 50.02, 52.99, 53.04, 53.56, 56.25, 56.32, 57.44, 57.54, 63.34, 65.92, 66.78, 66.83, 67.42, 67.64, 67.68, 68.17, 68.28, 68.66, 68.75, 72.17, 72.21, 72.75, 73.86, 74.37, 74.75, 74.9, 75.02, 75.09, 75.19, 75.52, 95.47, 95.77, 98.63, 100.62, 100.91, 127.27, 127.58, 127.68, 127.87, 127.9, 127.92, 127.98, 128.01, 128.15, 128.42, 128.49, 128.54, 128.55, 128.58, 128.75, 136.53, 136.77, 136.87, 137.38, 137.83, 138.01, 138.05, 154.23,

154.27, 155.16, 156.67, 157.21, 157.72, 170.42, 170.57. Three C1-H1 coupling constants (175.5, 172.0, 160.0 Hz) confirmed the stereochemistry. Most peaks were split due to the secondary amides on the fucose and the linker.

HRMS: m/z calc. for $C_{85}H_{105}Cl_6N_4O_{24}Si$: 1803.5019; found: 1803.5009 $[M + H]^+$.
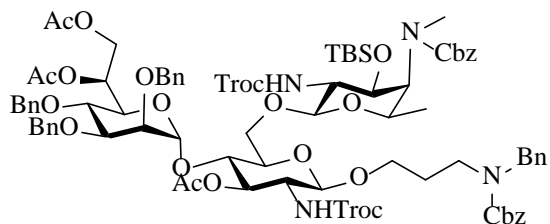
N-(Benzyl)-benzyloxycarbonyl-3-aminopropyl

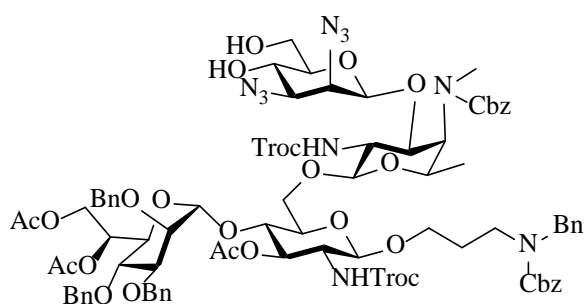4-[*N*-(methyl)-benzyloxycarbonylamino]-3-*O*-*tert*-butyldimethylsilyl-2,4-dideoxy-2-(2,2,2-trichloroethyloxycarbonylamino)-*β*-L-fucopyranosyl-(1→6)-[6,7-di-*O*-acetyl-2,3,4-tri-*O*-benzyl-L-glycero-*α*-D-mannoheptopyranosyl-(1→4)]-3-*O*-acetyl-2-deoxy-2-(2,2,2-trichloroethyloxycarbonylamino)-*β*-D-glucopyranoside (**37β**)

^{1}HNMR (500 MHz, CDCl$_3$): $δ$ = -0.09-0.12 (m, 6H), 0.83 (s, 9H), 1.09-1.22 (m, 3H), 1.67-1.77 (m, 2H), 1.84 (s, 3H), 2.04 (s, 3H), 2.10-2.12(m, 3H), 2.97-3.07 (m, 1H), 3.14-3.18 (m, 3H), 3.24-3.42 (m, 3H), 3.56-3.77 (m, 5H), 3.77-3.90 (m, 5H), 3.92-4.05 (m, 2H), 4.16-4.25 (m, 1H), 4.26-4.40 (m, 3H), 4.42-4.51 (m, 2H), 4.53-4.80 (m, 10H), 4.91 (d, 1H, J = 12.0 Hz), 4.96-5.08 (m, 2H), 5.10-5.21 (m, 3H), 5.64-5.85 (m, 3H), 6.11-6.18 (m, 1H), 7.10-7.19 (m, 2H), 7.23-7.47 (m, 28H). ^{13}CNMR (125 MHz, CDCl$_3$): $δ$ = -4.99, -4.93, -4.81, -4.77, 16.58, 17.8, 17.83, 20.94, 21.04, 25.62, 27.51, 29.79, 33.29, 33.72, 43.28, 50.15, 56.2, 56.92, 57.23, 57.39, 64.06, 65.31, 66.94, 67.41, 67.57, 67.63, 68.47, 68.54, 70.15, 70.42, 70.96, 71.93, 72.02, 72.12, 73.65, 74.34,

74.68, 74.89, 75.31, 76.17, 79.74, 95.76, 99.82, 100.9, 102.16, 127.07, 127.27, 127.56, 127.61, 127.66, 127.78, 127.93, 127.97, 128.1, 128.21, 128.47, 128.51, 128.53, 128.57, 128.61, 128.74, 136.53, 136.75, 136.87, 137.59, 138.02, 138.13, 141.07, 154.14, 154.25, 154.84, 156.54, 157.16, 157.78, 170.38, 170.52, 171.25, 171.39. Three C1-H1 coupling constants (173.0, 160.5, 160.5 Hz) confirmed the stereochemistry. Most peaks were split due to the secondary amides on the fucose and the linker.

HRMS: m/z calc. for $C_{85}H_{105}Cl_6N_4O_{24}Si$: 1803.5019; found: 1803.4955 $[M + H]^+$.

N-(Benzyl)-benzyloxycarbonyl-3-aminopropyl 4-[*N*-(methyl)-benzyloxycarbonylamino]-2,4-dideoxy-2-(2,2,2-trichloroethyloxycarbonylamino)-*β*-L-fucopyranosyl-(1→6)-[6,7-di-*O*-acetyl-2,3,4-tri-*O*-benzyl-L-glycero-*α*-D-mannoheptopyranosyl-(1→4)]-3-*O*-acetyl-2-deoxy-2-(2,2,2-trichloroethyloxycarbonylamino)-*β*-D-glucopyranoside (**38**)

Compound **37β** (1.80 g, 1.0 mmol) was dissolved with pyridine (10 mL) in a plastic centrifuge tube. After cooling to 0 °C, HF pyridine complex (5 mL) was added and the reaction was allowed to warm up to r.t. and continued to stir for 3 days. The reaction was then diluted with DCM, washed with saturated $CuSO_4$ solution, 1 M HCl and saturated $NaHCO_3$ solution successively. The organic layer was dried, concentrated and purified through column chromatography (Hexanes/DCM/EtOAc = 1/1/2) to give **38** as white foam in a yield of 85%.

^{1}HNMR (500 MHz, CDCl$_3$): δ = 1.19&1.24 (d, 3H, J = 6.5 Hz, Fuc-6-Me), 1.70-1.76 (m, 2H), 1.85 (s, 3H), 2.03&2.05 (s, 3H), 2.10&2.11 (s, 3H), 3.00-3.09 (m, 1H), 3.16 (s, 3H), 3.29 (d, 1H, J = 9.5 Hz), 3.34-3.48 (m, 2H), 3.57-3.93 (m, 11 Hz), 3.94-4.13 (m, 2H), 4.29-4.37 (m, 4H), 4.40-4.53 (m, 3H), 4.56-4.75 (m, 7H), 4.76-4.88 (m, 3H), 5.06-5.27 (m, 6H), 5.60-5.69 (m, 1H), 5.93-6.04 (m, 1H), 6.06-6.20 (m, 1H), 7.13-7.20 (m, 2H), 7.24-7.44 (m, 28H). ^{13}CNMR (125 MHz, CDCl$_3$): δ = 16.75, 16.76, 20.95, 21.02, 27.63, 29.78, 33.27, 33.7, 43.31, 50.15, 56.26, 56.44, 56.55, 56.81, 63.51, 67.06, 67.4, 67.58, 68.64, 70.58, 70.81, 71.87, 71.95, 72.07, 72.25, 72.42, 73.69, 74.32, 74.45, 74.59, 75.21, 75.35, 75.6, 79.66, 95.72, 95.82, 99.78, 100.94, 102.84, 127.23, 127.57, 127.68, 127.78, 127.86, 127.95, 128.0, 128.08, 128.48, 128.52, 128.56, 128.59, 128.76, 136.73, 136.87, 137.49, 137.9, 138.07, 138.13, 154.7, 156.58, 157.85, 158.97, 170.35, 170.57, 170.84, 170.94. Most peaks were split due to the secondary amides on the fucose and the linker.

HRMS: m/z calc. for C$_{79}$H$_{90}$Cl$_6$FeN$_4$O$_{24}$: 872.1713; found: 872.1685 [M + Fe]$^{2+}$.
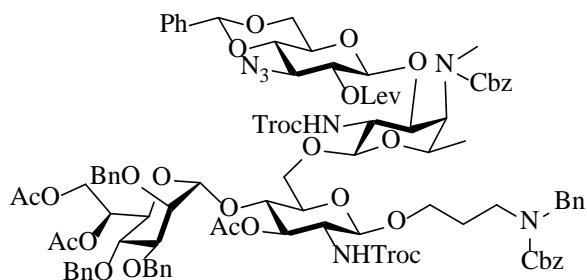
N-(Benzyl)-benzyloxycarbonyl-3-aminopropyl 3-azido-4, 6-*O*-benzylidene-3-deoxy-2-levulinoyl-β-D-glucopyranosyl-(1→3)-4-[*N*-(methyl)-benzyloxycarbonylamino]-2,4-dideoxy-2-(2,2,2-trichloroethyloxycarbonylamino)-β-L-fucopyranosyl-(1→6)-[

6,7-di-*O*-acetyl-2,3,4-tri-*O*-benzyl-L-glycero-*α*-D-mannoheptopyranosyl-(1→4)]-3-*O*-acetyl-2-d

eoxy-2-(2,2,2-trichloroethyloxycarbonylamino)-*β*-D-glucopyranoside (**39**)

A solution of compound **6** (756 mg, 1.52 mmol), **38** (1.54 g, 0.91 mmol) and freshly activated 4

Å molecular sieves (1.2 g) in DCM (20 mL) was stirred at r.t. for 20 min and then cooled to

-78 °C. To the above solution was added AgOTf (974 mg, 3.79 mmol) in DCM/MeCN (5/0.5

mL). The mixture was stirred for 10 min and *p*-TolSCl (201 μL, 1.52 mmol) was added directly

into it via microsyringe. The reaction was allowed to warm up to r.t. over a period of 2 h before

quenched with Et$_3$N. The mixture was then filtered through celite and concentrated. Column

chromatography (Hexanes/DCM/EtOAc = 2/2/3) gave compound **39** in a yield of 65%.

^{1}HNMR (500 MHz, CDCl$_3$): δ = 1.18 (d, 3H, J = 6.0 Hz), 1.68-1.75 (m, 2H), 1.86 (s, 3H),

2.04&2.05 (s, 3H), 2.09-2.13 (m, 4H), 2.17-2.22 (m, 2H), 2.40-2.58 (m, 2H), 2.58-2.76 (3H),

2.76-2.87 (m, 1H), 2.95-3.05 (m, 1H), 3.08 + 3.11 (s, 3H), 3.21-3.44 (m, 4H), 3.47-3.58 (m, 2H),

3.58-3.73 (m, 5H), 3.74-3.90 (m, 6H), 3.92-4.03 (m, 1H), 4.16-4.23 (m, 1H), 4.24-4.39 (m, 4H),

4.40-4.52 (m, 2H), 4.53-4.63 (m, 3H), 4.63-4.90 (m, 9H), 5.01 (d, 1H, J = 11.5 Hz), 5.12-5.30 (m,

4H), 5.38 (d, 1H, J = 12.0 Hz), 5.45-5.57 (m, 1H), 5.58-5.73 (m, 2H), 6.08-6.19 (m, 1H),

7.12-7.20 (m, 2H), 7.22-7.55 (m, 33H).. ^{13}CNMR (125 MHz, CDCl$_3$): δ = 16.33, 16.58, 20.9,

20.95, 20.99, 21.02, 27.48, 27.69, 29.74, 29.83, 29.89, 33.02, 33.32, 37.73, 37.91, 43.21, 50.09,

50.87, 52.86, 53.02, 54.71, 54.91, 56.06, 62.91, 63.16, 63.39, 63.56, 66.7, 67.03, 67.14, 67.35,

67.54, 67.63, 67.71, 68.49, 68.56, 70.48, 70.63, 70.7, 71.35, 71.72, 71.8, 71.85, 72.07, 72.22,

73.64, 74.25, 74.31, 74.79, 75.31, 77.36, 79.12, 79.33, 79.72, 89.09, 95.79, 96.08, 96.9, 97.2,

99.53, 100.28, 100.9, 101.41, 101.51, 126.01, 126.08, 127.24, 127.53, 127.58, 127.74, 127.89,

128.02, 128.07, 128.21, 128.36, 128.4, 128.44, 128.45, 128.49, 128.53, 128.59, 128.65, 128.7, 128.71, 128.99, 129.22, 129.26, 136.55, 136.59, 136.67, 136.7, 136.76, 137.52, 137.95, 138.11, 153.93, 154.79, 156.52, 157.68, 170.39, 170.45, 170.48, 170.8, 170.92, 171.24, 171.55, 205.95, 206.37. Most peaks were split due to the secondary amides on the fucose and the linker.

HRMS: m/z calc. for $C_{97}H_{117}Cl_6N_9O_{30}$: 1048.8018; found: 1048.7975 $[M + Na + NH_4]^{2+}$.

N-(Benzyl)-benzyloxycarbonyl-3-aminopropyl 3-azido-4,6-*O*-benzylidene-3-deoxy -*β*-D-glucopyranosyl-(1→3)-4-[*N*-(methyl)-benzyloxycarbonylamino]-2,4-dideoxy-2-(2,2,2-trich loroethyloxycarbonylamino)-*β*-L-fucopyranosyl-(1→6)-[6,7-di-*O*-acetyl-2,3,4-tri-*O*-benzyl-L-gl ycero-*α*-D-mannoheptopyranosyl-(1→4)]-3-*O*-acetyl-2-deoxy-2-(2,2,2-trichloroethyloxycarbony lamino)-*β*-D-glucopyranoside (**40**)

Compound **39** (1.22 g, 0.59 mmol) was dissolved in DCM/AcOH/Pyridine (15/1/1.5 mL) followed by addition of $N_2H_4 \cdot H_2O$ (200 μL, 64%). The mixture was stirred at r.t. for 4 h before it was diluted with DCM and washed with brine. The organic layer was dried and concentrated. Column chromatography (Hexanes/DCM/EtOAc = 2/2/3) gave **40** as white foam in a yield of 84%.

^{1}HNMR (500 MHz, CDCl₃): *δ* = 1.26 (d, 3H, *J* = 5.5 Hz), 1.68-1.76 (m, 2H), 1.84 (s, 3H), 2.05

(s, 3H), 2.11 (s, 3H), 3.00-3.14 (m, 2H), 3.20 (s, 3H), 3.24-3.32 (d, 1H, $J = 9.5$ Hz), 3.34-3.51 (m, 4H), 3.53-3.72 (m, 5H), 3.72-3.91 (m, 8H), 3.94-4.09 (m, 2H), 4.18-4.26 (m, 1H), 4.26-4.44 (m, 5H), 4.44-4.50 (d, 1H, $J = 10.0$ Hz), 4.50-4.80 (m, 10H), 4.95-5.08 (m, 2H), 5.10-5.28 (m, 6H), 5.53 (s, 1H), 5.65 (t, 1H, $J = 6.5$ Hz), 5.79 (d, 1H, $J = 8.5$ Hz), 6.10 (d, 1H, $J = 8.5$ Hz), 7.14-7.21 (m, 2H), 7.23-7.47 (m, 31 H), 7.48-7.54 (m, 2H). ^{13}CNMR (125 MHz, CDCl$_3$): $\delta =$ 16.85, 20.93, 21.01, 21.03, 27.58, 29.78, 33.45, 43.36, 50.22, 54.78, 55.9, 56.16, 60.49, 63.65, 64.52, 66.83, 67.26, 67.47, 67.56, 68.14, 68.56, 68.65, 69.83, 71.84, 72.1, 73.28, 73.65, 74.18, 74.32, 74.44, 74.75, 75.12, 75.3, 76.01, 77.36, 79.04, 79.71, 95.77, 95.95, 99.8, 100.88, 101.6, 102.24, 106.29, 126.15, 127.28, 127.58, 127.77, 127.81, 127.92, 128.05, 128.1, 128.35, 128.39, 128.47, 128.49, 128.52, 128.53, 128.62, 128.7, 128.75, 129.24, 136.25, 136.71, 136.77, 137.56, 137.97, 138.06, 138.12, 154.44, 154.81, 156.54, 159.85, 170.36, 170.46, 170.99. Four C1-H1 coupling constants (174.5, 163.0, 163.0, 160.0 Hz) confirmed the stereochemistry. Most peaks were split due to the secondary amides on the fucose and the linker.

HRMS: m/z calc. for C$_{92}$H$_{103}$Cl$_6$FeN$_7$O$_{28}$: 1009.7166; found: 1009.7142 [M + Fe]$^{2+}$.
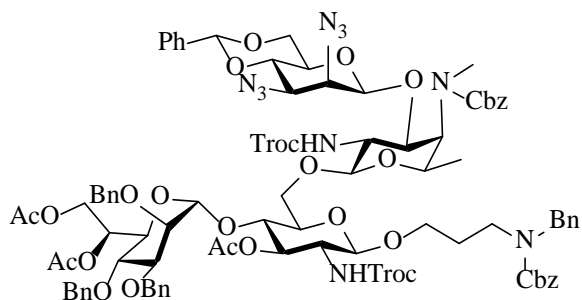
N-(Benzyl)-benzyloxycarbonyl-3-aminopropyl

2,3-diazido-4,6-*O*-benzylidene-2,3-dideoxy-*β*-D-mannopyranosyl-(1→3)-4-[*N*-(methyl)-benzylo

xycarbonylamino]-2,4-dideoxy-2-(2,2,2-trichloroethyloxycarbonylamino)-*β*-L-fucopyranosyl-(1

→6)-[6,7-di-*O*-acetyl-2,3,4-tri-*O*-benzyl-L-glycero-*α*-D-mannoheptopyranosyl-(1→4)]-3-*O*-acet

yl-2-deoxy-2-(2,2,2-trichloroethyloxycarbonylamino)-*β*-D-glucopyranoside (**41**)

Compound **40** (974 mg, 0.50 mmol) was dissolved in anhydrous DCM (10 mL) and cooled to

-30 °C. Pyridine (400 μL, 4.95 mmol) and Tf_2O (333 μL, 1.98 mmol) were added and the

mixture was allowed to warm up to r.t. over a period over 4 h. It was then quenched with MeOH,

diluted with DCM and washed with brine. The organic layer was dried, concentrated and

dissolved with DMF (10 mL). NaN_3 (200 mg, 3.1 mmol) was added and the mixture was heated

at 50 °C overnight. After diluting with EtOAc and washing with brine, compound **41** was

purified through column chromatography in a yield of 86% over 2 steps.

^{1}HNMR (500 MHz, $CDCl_3$): δ = 1.25 (d, 3H, J = 6.5 Hz), 1.68-1.77 (m, 2H), 1.82 (s, 3H), 2.04

(s, 3H), 2.11 (s, 3H), 2.98-3.08 (m, 1H), 3,19 (s, 3H), 3.24-3.48 (m 6H), 3.57-3.89 (m, 12H),

3.98-4.08 (m, 1H), 4.20 (d, 1H, J = 8.0 Hz), 4.27 (dd, 1H, J = 5.5, 10.5 Hz), 4.29-4.37 (m, 3H),

4.46 (d, 1H, J = 9.5 Hz), 4.51 (dd, 1H, J = 3.0, 6.0 Hz), 4.53-4.78 (m, 10H), 4.80-4.92 (m, 2H),

4.95 (d, 1H, J = 12.0 Hz), 5.00-5.07 (m, 1H), 5.08 (d, 1H, J = 12.5 Hz), 5.14-5.21 (m, 3H), 5.23

(d, 1H, J = 12.5 Hz), 5.44-5.52 (m, 1H), 5.55 (s, 1H), 5.64 (t, 1H, J = 6.5 Hz), 6.09 (d, 1H, J =

9.0 Hz), 7.17 (d, 2H, J = 7.5 Hz), 7.25-7.46 (m, 31H), 7.46-7.50 (m, 2H). ^{13}CNMR (125 MHz,

$CDCl_3$): δ = 16.79, 16.84, 20.94, 20.99, 21.06, 21.08, 27.54, 29.8, 33.19, 43.36, 50.22, 53.86,

54.29, 56.13, 59.89, 60.51, 62.36, 63.58, 66.89, 67.11, 67.57, 67.62, 67.9, 68.46, 68.63, 69.98,

71.83, 72.0, 72.1, 73.68, 74.21, 74.34, 74.47, 74.92, 75.2, 75.35, 76.1, 76.57, 76.69, 77.36, 79.75,

95.81, 96.07, 98.45, 99.78, 100.97, 101.67, 102.28, 125.92, 125.98, 127.29, 127.58, 127.61,

127.67, 127.77, 127.97, 128.12, 128.39, 128.49, 128.53, 128.59, 128.63, 128.69, 128.76, 128.98, 129.19, 129.23, 136.51, 136.7, 136.77, 137.59, 138.01, 138.15, 138.18, 154.4, 154.81, 156.55, 156.84, 158.46, 170.43, 170.53, 170.88. Most peaks were split due to the secondary amides on the fucose and the linker.

HRMS: m/z calc. for $C_{92}H_{102}Cl_6FeN_{10}O_{27}$: 1022.2198; found: 1022.2167 $[M + Fe]^{2+}$.

N-(Benzyl)-benzyloxycarbonyl-3-aminopropyl 2,3-diazido-2,3-dideoxy -*β*-D-mannopyranosyl-(1→3)-4-[*N*-(methyl)-benzyloxycarbonylamino]-2,4-dideoxy-2-(2,2,2-tric hloroethyloxycarbonylamino)-*β*-L-fucopyranosyl-(1→6)-[6,7-di-*O*-acetyl-2,3,4-tri-*O*-benzyl-L-g lycero-*α*-D-mannoheptopyranosyl-(1→4)]-3-*O*-acetyl-2-deoxy-2-(2,2,2-trichloroethyloxycarbon ylamino)-*β*-D-glucopyranoside (**42**)

Compound **41** (850 mg, 0.43 mmol) was dissolved in DCM/TFA/water (15/1.5/0.5 mL) and stirred at r.t. for 30 min. The reaction was then washed with brine, dried and concentrated. Column chromatography gave compound **42** as white foam in a yield of 86%.

^{1}HNMR (500 MHz, CDCl$_3$): δ = 1.24 (d, 3H, *J* = 6.5 Hz), 1.70-1.77 (m, 2H), 1.79-1.93 (m, 3H, Ac), 2.05 (s, 3H), 2.10 (s, 3H), 3.00-3.50 (m, 11H), 3.51-3.93 (m, 14H), 3.93-4.09 (m, 2H), 4.17-4.37 (m, 4H), 4.43-4.52 (m, 2H), 4.54-4.71 (m, 7H), 4.71-4.77 (m, 2H), 4.79-4.93 (m, 2H),

4.93-5.30 (m, 7H), 5.64 (t, 1H, J = 6.5 Hz), 6.01-6.27 (m, 2H), 7.13-7.22 (m, 2H), 7.24-7.47 (m, 28H). ^{13}CNMR (125 MHz, CDCl$_3$): δ = 16.78, 20.93, 21.0, 27.44, 33.26, 43.38, 50.17, 50.86, 54.14, 54.38, 56.05, 62.04, 62.23, 63.23, 63.69, 66.92, 67.55, 68.57, 70.02, 71.82, 72.06, 73.64, 74.32, 74.97, 75.34, 77.36, 79.71, 95.74, 95.92, 97.9, 99.61, 100.95, 102.12, 127.26, 127.56, 127.58, 127.73, 127.91, 128.09, 128.46, 128.5, 128.58, 128.65, 128.73, 136.5, 136.7, 137.53, 137.96, 138.12, 138.15, 154.63, 154.84, 156.58, 158.58, 170.41, 170.52, 171.17. Most peaks were split due to the secondary amides on the fucose and the linker.

HRMS: m/z calc. for C$_{85}$H$_{98}$Cl$_6$FeN$_{10}$O$_{27}$: 978.2041; found: 978.2010 [M + Fe]$^{2+}$.
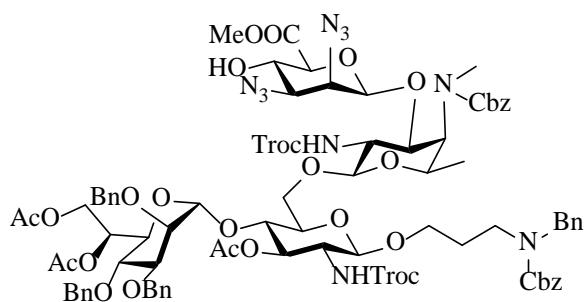
N-(Benzyl)-benzyloxycarbonyl-3-aminopropyl methyl 2,3-diazido-2,3-dideoxy -β-D-mannopyranosyluronate-(1→3)-4-[*N*-(methyl)-benzyloxycarbonylamino]-2,4-dideoxy-2-(2, 2,2-trichloroethyloxycarbonylamino)-β-L-fucopyranosyl-(1→6)-[6,7-di-*O*-acetyl-2,3,4-tri-*O*-ben zyl-L-glycero-α-D-mannoheptopyranosyl-(1→4)]-3-*O*-acetyl-2-deoxy-2-(2,2,2-trichloroethyloxy carbonylamino)-β-D-glucopyranoside (**43**)

Compound **42** (700 mg, 0.37 mmol) was dissolved in DCM/t-BuOH/water (4/4/1 mL) followed by addition of BAIB (473 mg, 1.47 mmol) and TEMPO (23 mg, 0.15 mmol). The reaction was stirred at r.t. overnight. It was then diluted with DCM, washed with brine, dried and concentrated.

The crude product was dissolved in DMF (10 mL) and treated with MeI (228 μL, 3.67 mmol) and K_2CO_3 (507 mg, 3.67 mmol). Upon completion by TLC, the mixture was diluted with EtOAc and washed with brine. The organic layer was dried, concentrated and purified through column chromatography to afford compound **43** in a yield of 66% over 2 steps.

^{1}HNMR (500 MHz, $CDCl_3$): δ = 1.27 (d, 3H, J = 6.5 Hz), 1.62-1.78 (m, 2H), 1.71&1.91 (s, 3H, Ac), 2.04 (s, 3H), 2.12 (s, 3H), 2.93-3.04 (m, 1H), 3.10-3.17 (m, 1H), 3.20 (s, 3H), 3.23-3.27 (dd, 1H, J = 3.5, 9.5 Hz), 3.28-3.48 (m, 3H), 3.52-3.68 (m, 3H), 3.68-3.78 (m, 4H), 3.81 (s, 3H), 3.83-3.88 (m, 3H), 3.89-4.07 (m, 3H), 4.07-4.19 (m, 2H), 4.21-4.42 (m, 4H), 4.42-4.58 (m, 6H), 4.60-4.80 (m, 6H), 4.86 (d, 1H, J = 10.0 Hz), 4.92-5.02 (m, 1H), 5.05 (d, 1H, J = 12.0 Hz), 5.17 (d, 1H, J = 7.0 Hz), 5.22 (d, 1H, J = 12.0 Hz), 5.24-5.30 (m, 1H), 5.59-5.75 (m, 2H), 6.16 (d, 1H, J = 7.5 Hz), 7.10-7.20 (m, 2H), 7.22-7.51 (m, 28H), . ^{13}CNMR (125 MHz, $CDCl_3$): δ = 16.84, 20.76, 20.99, 21.11, 27.59, 29.81, 33.25, 43.29, 50.24, 53.41, 54.1, 56.14, 60.98, 62.1, 63.31, 66.99, 67.13, 67.61, 67.64, 68.67, 69.90, 71.49, 71.7, 72.11, 73.63, 74.22, 75.13, 75.38, 76.11, 77.36, 79.80, 95.92, 96.27, 98.32, 99.59, 101.17, 103.82, 127.25, 127.61, 127.63, 127.71, 127.91, 128.02, 128.05, 128.15, 128.48, 128.50, 128.57, 128.63, 128.68, 128.78, 136.74, 137.57, 138.06, 138.21, 138.26, 154.75, 154.95, 156.58, 158.67, 169.83, 170.32, 170.58, 170.70. Most peaks were split due to the secondary amides on the fucose and the linker.

HRMS: m/z calc. for $C_{86}H_{98}Cl_6FeN_{10}O_{28}$: 992.2016; found: 992.1984 $[M + Fe]^{2+}$.
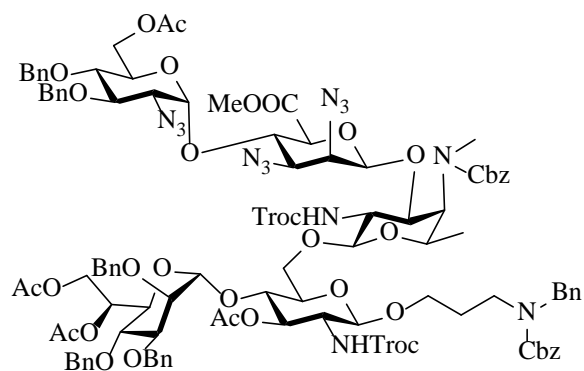
N-(Benzyl)-benzyloxycarbonyl-3-aminopropyl

6-*O*-acetyl-2-azido-3,4-di-*O*-benzyl-2-deoxy-α-D-glucopyranosyl-(1→4)-methyl

2,3-diazido-2,3-dideoxy-β-D-mannopyranosyluronate-(1→3)-4-[*N*-(methyl)-benzyloxycarbonyla

mino]-2,4-dideoxy-2-(2,2,2-trichloroethyloxycarbonylamino)-β-L-fucopyranosyl-(1→6)-[6,7-di-

O-acetyl-2,3,4-tri-*O*-benzyl-L-glycero-α-D-mannoheptopyranosyl-(1→4)]-3-*O*-acetyl-2-deoxy-2

-(2,2,2-trichloroethyloxycarbonylamino)-β-D-glucopyranoside (**44**)

A solution of compound **7** (258 mg, 0.48 mmol), **43** (467 mg, 0.24 mmol) and freshly activated 4

Å molecular sieves (400 mg) in DCM (5 mL) was stirred at r.t. for 20 min and then cooled to

-78 °C. To the above solution was added AgOTf (310 mg, 1.21 mmol) in Et$_2$O/DCM (6/1 mL).

The mixture was stirred for 10 min and *p*-TolSCl (64 μL, 0.48 mmol) was added directly into it

via microsyringe. The reaction was allowed to warm up to r.t. over a period of 3 h before

quenched with Et$_3$N. The mixture was then filtered through celite and concentrated. Column

chromatography (Hexanes/DCM/EtOAc = 2/2/3) gave compound **44** in a yield of 63%.

^{1}HNMR (500 MHz, CDCl$_3$): δ = 1.26 (d, 3H, *J* = 6.5 Hz), 1.69-1.77 (m, 2H), 1.82 (s, 3H), 2.04

(s, 3H), 2.05 (s, 3H), 2.11 (s, 3H), 2.98-3.08 (m, 1H), 3.22 (s, 3H), 3.26-3.44 (m, 4 H), 3.44-3.50

(m, 1H), 3.53-3.62 (m, 2H), 3.63-3.93 (m, 15H), 3.95-4.10 (m, 3H), 4.18-4.25 (m, 2H), 4.25-4.38

(m, 4H), 4.40-4.52 (m, 3H), 4.52-4.65 (m, 5H), 4.65-4.81 (m, 7H), 4.82-4.89 (m, 3H), 4.90-4.94 (m, 1H), 4.99-5.06 (m, 1H), 5.09 (d, 1H, J = 13.0 Hz), 5.14-5.23 (m, 3H), 5.26 (d, 1H, J = 12.5 Hz), 5.36-5.52 (m, 2H), 5.60-5.68 (m, 1H), 6.06-6.16 (m, 1H), 7.15-7.22 (m, 2H), 7.26-7.48 (m, 38H). ^{13}CNMR (125 MHz, CDCl$_3$): δ = 16.75, 20.86, 20.95, 20.99, 27.47, 29.71, 33.2, 43.27, 50.16, 53.03, 53.65, 54.04, 56.14, 61.41, 62.06, 62.71, 63.32, 63.82, 66.85, 67.09, 67.42, 67.47, 68.57, 69.89, 70.26, 71.67, 71.81, 72.0, 73.59, 74.04, 74.22, 74.28, 74.39, 74.77, 75.08, 75.16, 75.22, 75.65, 75.68, 75.76, 75.93, 76.05, 77.19, 77.3, 79.63, 80.19, 80.23, 95.75, 95.98, 97.67, 98.89, 99.59, 100.91, 102.18, 127.22, 127.47, 127.53, 127.63, 127.68, 127.82, 127.9, 127.98, 128.05, 128.08, 128.19, 128.4, 128.43, 128.5, 128.52, 128.56, 128.62, 128.66, 129.17, 136.73, 136.76, 137.48, 137.56, 137.97, 138.07, 138.13, 154.35, 154.65, 156.46, 156.68, 158.33, 167.28, 170.3, 170.44, 170.58, 170.74. Most peaks were split due to the secondary amides on the fucose and the linker.

HRMS: m/z calc. for C$_{108}$H$_{129}$Cl$_6$N$_{15}$O$_{33}$: 1186.8504; found: 1186.8445 [M + 2NH$_4$]$^{2+}$.
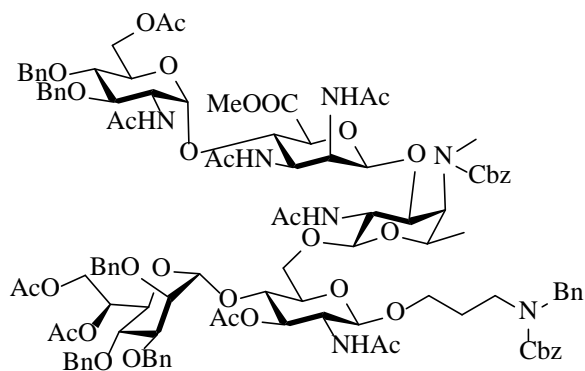
N-(Benzyl)-benzyloxycarbonyl-3-aminopropyl 2-acetamido-6-*O*-acetyl-3, 4-di-*O*-benzyl-2-deoxy-*α*-D-glucopyranosyl-(1→4)-methyl 2,3-diacetamido-2,3-dideoxy

-β-D-mannopyranosyluronate-(1→3)-2-acetamido-4-[N-(methyl)-benzyloxycarbonylamino]-2,4-dideoxy-β-L-fucopyranosyl-(1→6)-[6,7-di-O-acetyl-2,3,4-tri-O-benzyl-L-glycero-α-D-mannoheptopyranosyl-(1→4)]-2-acetamido-3-O-acetyl-2-deoxy-β-D-glucopyranoside (**45**)

Compound **44** (357 mg, 0.15 mmol) was dissolved in THF (10 mL) followed by addition of Ac$_2$O (1.73 mL, 18.3 mmol), AcOH (1.04 mL, 18.3 mmol) and Zn (1.48 g, 22.9 mmol). The reaction was stirred at r.t. overnight before it was quenched with MeOH and filtered through celite to remove the insoluble impurities. The filtrate was concentrated, diluted with EtOAc and washed with saturated NaHCO$_3$ solution. The organic layer was dried, concentrated and purified through column chromatography (DCM/MeOH = 10/1) to give compound **45** in a yield of 65%.

^{1}HNMR (500 MHz, CDCl$_3$): δ = 1.08&1.16 (d, 2H, J = 6.5 Hz, Fuc-6-Me), 1.64-1.72 (m, 2H), 1.81 (s, 3H), 1.89 (s, 3H), 1.98-2.01 (m, 6H), 2.03 (s, 9H), 2.04 (s, 3H), 2.08 (s, 3H), 2.90-2.98 (m, 1H), 3.03-3.10 (m, 1H), 3.15 + 3.18 (s, 3H, Fuc-4-N-Me), 3.19-3.33 (m, 3H), 3.60-3.73 (m, 6H), 3.76-3.92 (m, 8H), 4.01-4.12 (m, 2H), 4.20-4.35 (m, 6H), 4.38 (dd, 1H, J = 5.5, 12.0 Hz), 4.40-4.47 (m, 3H), 4.47-4.60 (m, 5H), 4.60-4.65 (m, 1H), 4.65-4.74 (m, 4H), 4.75-4.80 (m, 1H), 4.80-4.88 (m, 4H), 4.94 (d, 1H, J = 12.0 Hz), 4.97 (dd, 1H, J = 3.5, 7.0 Hz), 5.01 (d, 1H, J = 3.5 Hz), 5.04 (d, 1H, J = 3.5 Hz), 5.10-5.22 (m, 4H), 5.29 (d, 1H, J = 12.5 Hz), 5.57-5.63 (m, 1H), 6.42 (d, 1H, J = 9.5 Hz), 6.85 (m, 2H), 7.13-7.21 (m, 2H), 7.21-7.42 (m, 38H) . ^{13}CNMR (125 MHz, CDCl$_3$): δ = 16.36, 16.43, 20.81, 20.88, 20.91, 20.94, 20.97, 22.73, 22.8, 22.86, 22.92, 23.0, 23.06, 23.17, 24.03, 24.06, 26.97, 33.0, 33.42, 42.66, 49.74, 52.49, 52.71, 52.8, 53.81, 54.1, 62.14, 62.42, 62.66, 63.4, 63.67, 64.35, 66.37, 67.43, 67.62, 68.09, 68.29, 68.68, 69.98, 70.17, 71.67, 71.9, 71.97, 72.16, 73.54, 73.73, 74.24, 74.42, 75.1, 75.3, 75.33, 75.38, 75.49, 75.98,

76.35, 77.36, 79.72, 80.49, 99.55, 99.76, 99.85, 100.8, 102.39, 103.05, 127.3, 127.47, 127.51, 127.54, 127.57, 127.61, 127.65, 127.69, 127.71, 127.74, 127.78, 127.8, 127.85, 127.88, 127.92, 127.98, 128.01, 128.09, 128.15, 128.26, 128.37, 128.41, 128.46, 128.48, 128.5, 128.57, 128.62, 128.72, 136.0, 136.08, 136.7, 137.28, 137.67, 137.72, 137.91, 138.04, 138.1, 138.18, 138.28, 156.59, 158.27, 170.45, 170.59, 170.69, 170.79, 170.8, 170.82, 170.84, 171.02, 171.22, 171.44, 171.53, 171.61, 171.67, 172.0, 172.24, 175.36. Five C1-H1 coupling constants (174.5, 171.0, 163.0, 164.0, 160.5 Hz) confirmed the stereochemistry. Most peaks were split due to the secondary amides on the fucose and the linker.

HRMS: m/z calc. for $C_{112}H_{137}N_7O_{34}$: 1061.9603; found: 1061.9554 $[M + 2H]^{2+}$.
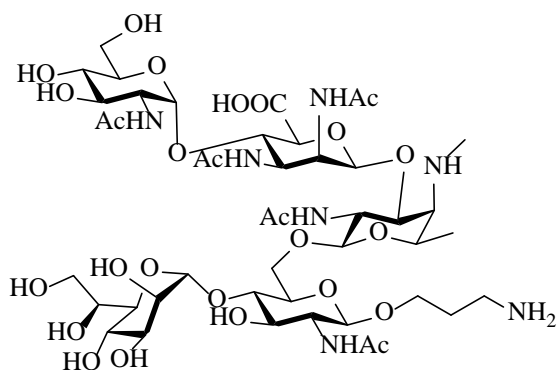
3-Aminopropyl 2-acetamido-2-deoxy-*α*-D-glucopyranosyl-(1→4)-2,3-diacetamido-2,3-dideoxy -*β*-D-mannopyranosyluronate-(1→3)-2-acetamido-2,4-dideoxy-4-methylamino-*β*-L-fucopyranos yl-(1→6)-[L-glycero-*α*-D-mannoheptopyranosyl-(1→4)]-2-acetamido-2-deoxy-*β*-D-glucopyrano side (**2**)

Compound **45** (210 mg, 0.099 mmol) was dissolved in THF/water (20/5 mL) followed by addition of 1M LiOH solution (2.5 mL) at 0 °C. The reaction was allowed to warm up to r.t. and

stirred overnight. H$^+$ resin was added to neutralize the solution and filtered off through sintered glass funnel. The filtrate was concentrated and purified through column chromatography (DCM/MeOH = 4/1). To a solution of the product in THF/water/AcOH (2/2/2 mL) was added Pd(OH)$_2$/C (100 mg) and it was stirred at r.t. overnight under H$_2$ atmosphere. Pd(OH)$_2$/C was filtered off and the filtrate was concentrated and purified through a G10 column followed by Na$^+$ ion exchange column. The final aqueous solution was lyophilized to afford compound **2** in a yield of 68%.

^{1}HNMR (500 MHz, D$_2$O): δ = 1.25 (d, 3H, J = 6.5 Hz), 1.74 (s, 3H), 1.75 (s, 3H), 1.76-1.80 (m, 2H), 1.83 (s, 3H), 1.88 (s, 3H), 1.89 (s, 3H), 1.92 (s, 3H), 2.61 (s, 3H), 2.90 (t, 2H, J = 7.5 Hz), 3.32 (t, 1H, J = 10.0 Hz), 3.36-3.43 (m, 4H), 3.45-3.60 (m, 8H), 3.60-3.69 (m, 5H), 3.69-3.75 (m, 2H), 3.76-3.92 (m, 6H), 4.06 (dd, 1H, J = 4.0, 11.0 Hz), 4.11 (dd, 1H, J = 4.0, 10.5 Hz), 4.18 (d, 1H, J = 4.0 Hz), 4.26 (m, 1H), 4.43 (d, 1H, J = 8.0 Hz), 4.82 (s, 1H), 4.95 (d, 1H, J = 4.0 Hz), 5.11 (s, 1H). ^{13}CNMR (125 MHz, D$_2$O): δ = 15.98, 21.65, 21.73, 21.81, 21.97, 22.42, 23.19, 26.57, 36.21, 37.3, 50.89, 51.47, 53.22, 53.37, 55.66, 59.67, 60.97, 63.05, 65.75, 67.67, 68.29, 68.46, 68.89, 69.28, 70.06, 70.19, 70.24, 71.57, 72.48, 73.48, 73.78, 75.15, 75.75, 78.71, 96.5, 96.66, 101.07, 101.1, 101.88, 173.62, 173.93, 174.17, 174.63, 174.81, 175.07, 181.34. HRMS: m/z calc. for C$_{45}$H$_{79}$N$_7$O$_{26}$: 566.7537; found: 566.7537 [M + 2H]$^{2+}$.
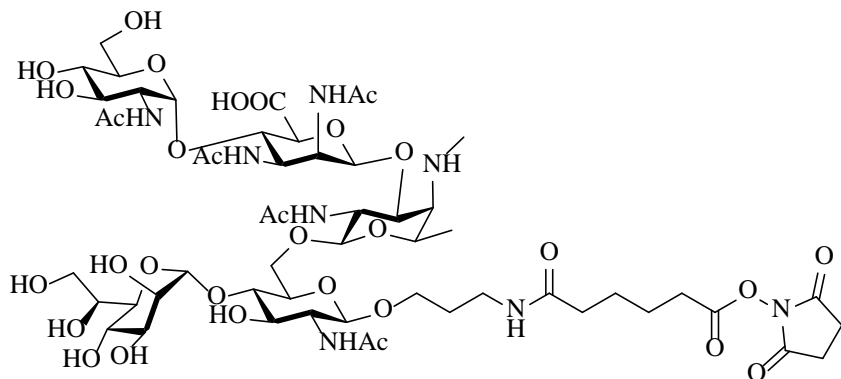
N-(5-(succinimidyloxycarbonyl)pentanoyl)-3-aminopropyl

2-acetamido-2-deoxy-α-D-glucopyranosyl-(1→4)-2,3-diacetamido-2,3-dideoxy-β-D-mannopyra

nosyluronate-(1→3)-2-acetamido-2,4-dideoxy-4-methylamino-β-L-fucopyranosyl-(1→6)-[L-gly

cero-α-D-mannoheptopyranosyl-(1→4)]-2-acetamido-2-deoxy-β-D-glucopyranoside (**47**)

Compound **2** (15 mg, 0.01324 mmol) together with compound **46** (22.5 mg, 0.066 mmol) was

dissolved in dry DMF (2.5 mL) followed by addition of DIPEA (2 µL). The reaction was stirred

at r.t. for 3 h and then DMF was removed by vacuum. The residue was washed with DCM and **47**

was used for Qβ coupling without further purification.

^{1}HNMR (500 MHz, CD$_3$OD): δ = 1.35 (d, 3H, J = 6.5 Hz), 1.63-1.79 (m, 5H), 1.89 (s, 3H), 1.97

(s, 3H), 1.98 (s, 3H), 2.03 (s, 3H), 2.09 (s, 3H), 2.20-2.29 (m, 2H), 2.50-2.72 (m, 6H), 2.84 (s,

3H), 3.02-3.22 (m, 3H), 3.35 (s, 4H), 3.45-4.10 (m, 24H), 4.27 (dd, 1H, J = 4.0, 9.5 Hz),

4.32-4.38 (m, 2H), 4.40 (d, 1H, J = 8.0 Hz), 5.11 (d, 1H, J = 3.5 Hz), 5.41 (s, 1H). HRMS: m/z

calc. for C$_{55}$H$_{89}$N$_8$O$_{31}$: 1357.5633; found: 1357.5582 [M + H]$^+$.

APPENDIX

Product Characterization Spectra
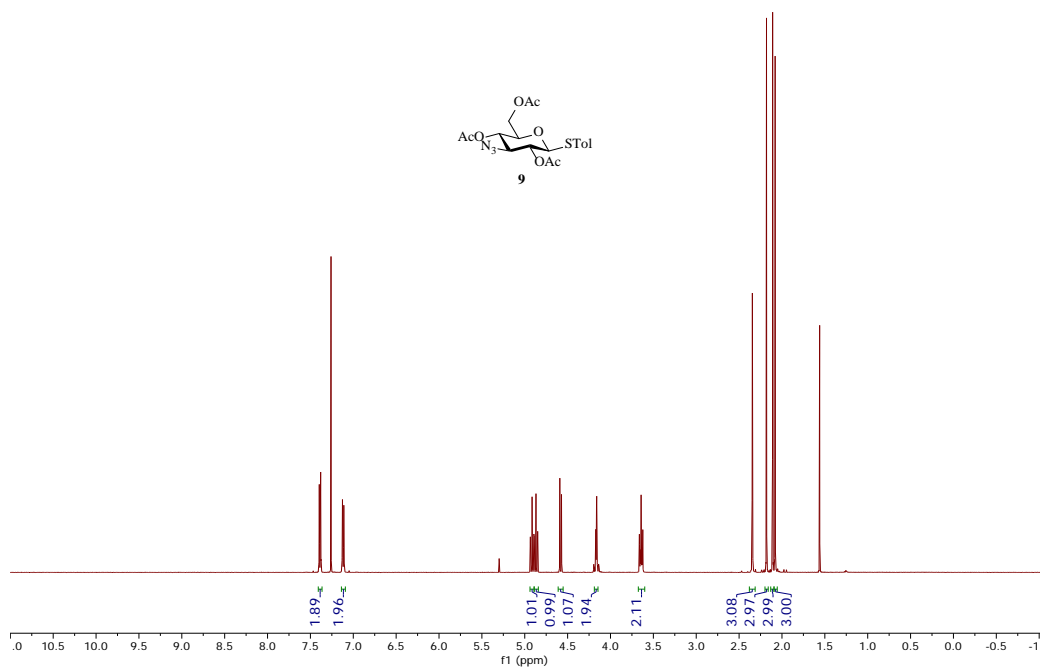
Figure 2.8. ^{1}H-NMR of **9** (500 MHz CDCl$_3$)
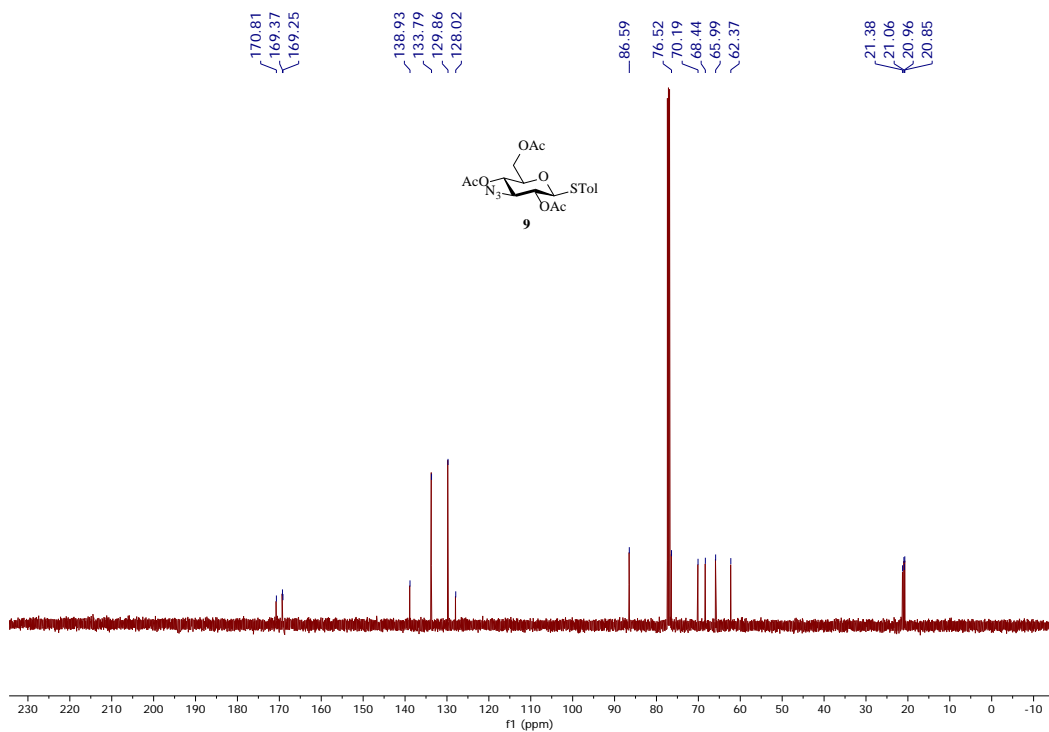
Figure 2.9. ^{13}C-NMR of **9** (125 MHz CDCl$_3$)
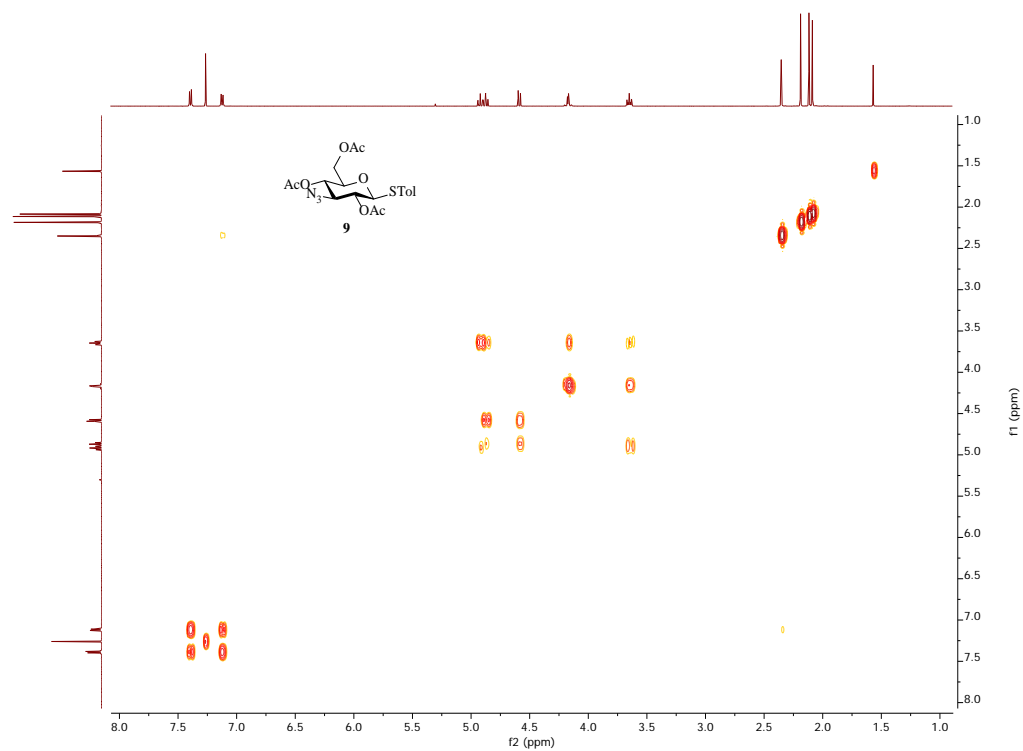
Figure 2.10. ^1H-^1H gCOSY of **9** (500 MHz CDCl$_3$)
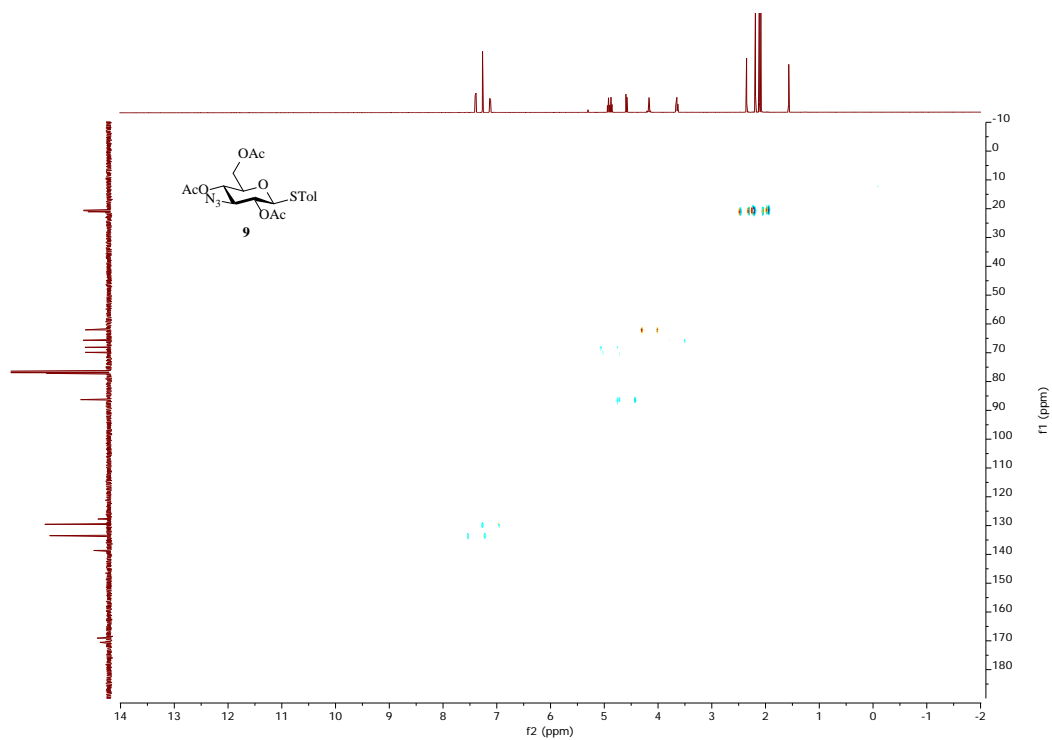
Figure 2.11. ^1H-^{13}C gHSQCAD of **9** (500 MHz CDCl$_3$)
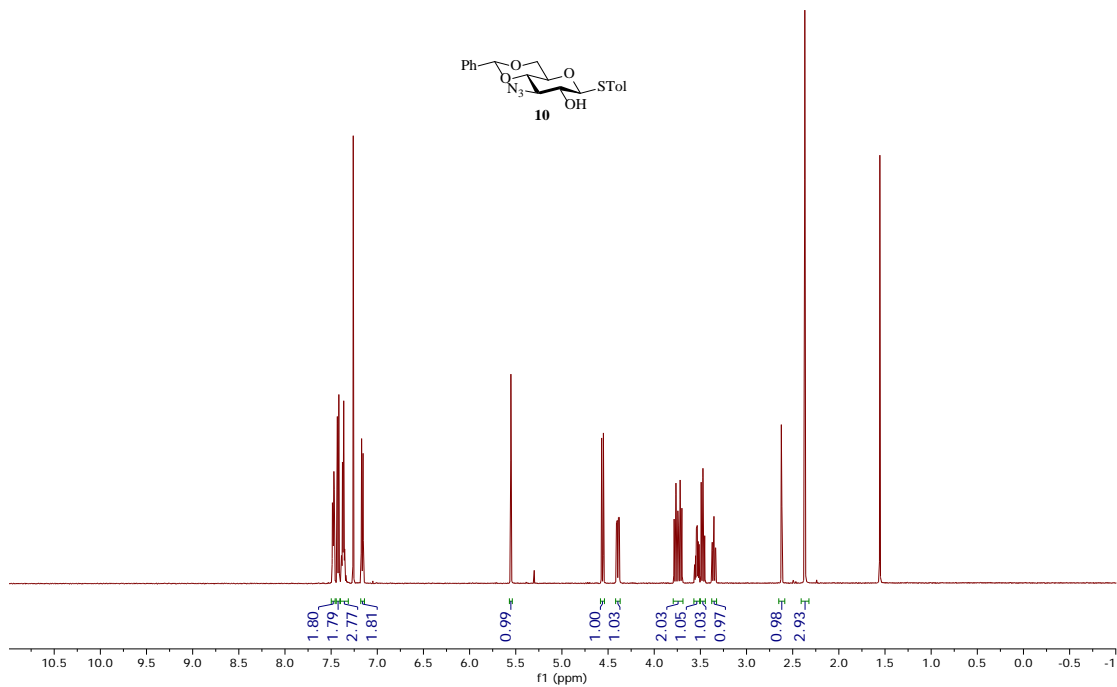
Figure 2.12. ^{1}H-NMR of **10** (500 MHz CDCl$_3$)
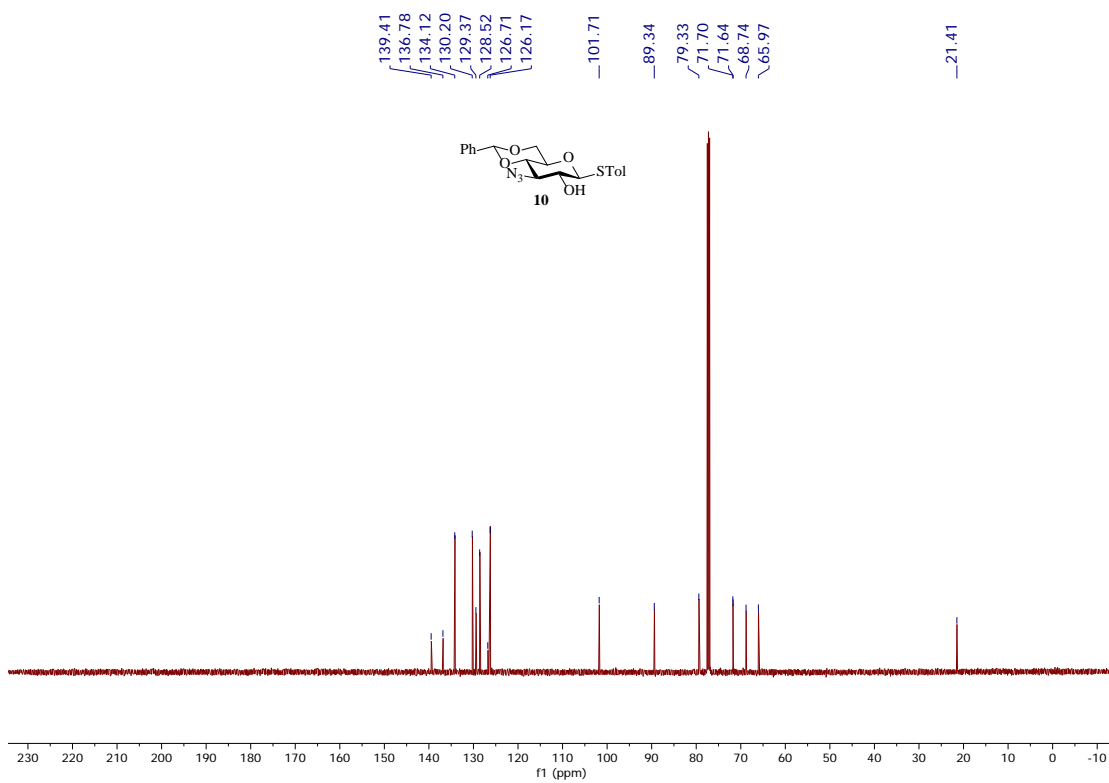
Figure 2.13. ^{13}C-NMR of **10** (125 MHz CDCl$_3$)

112
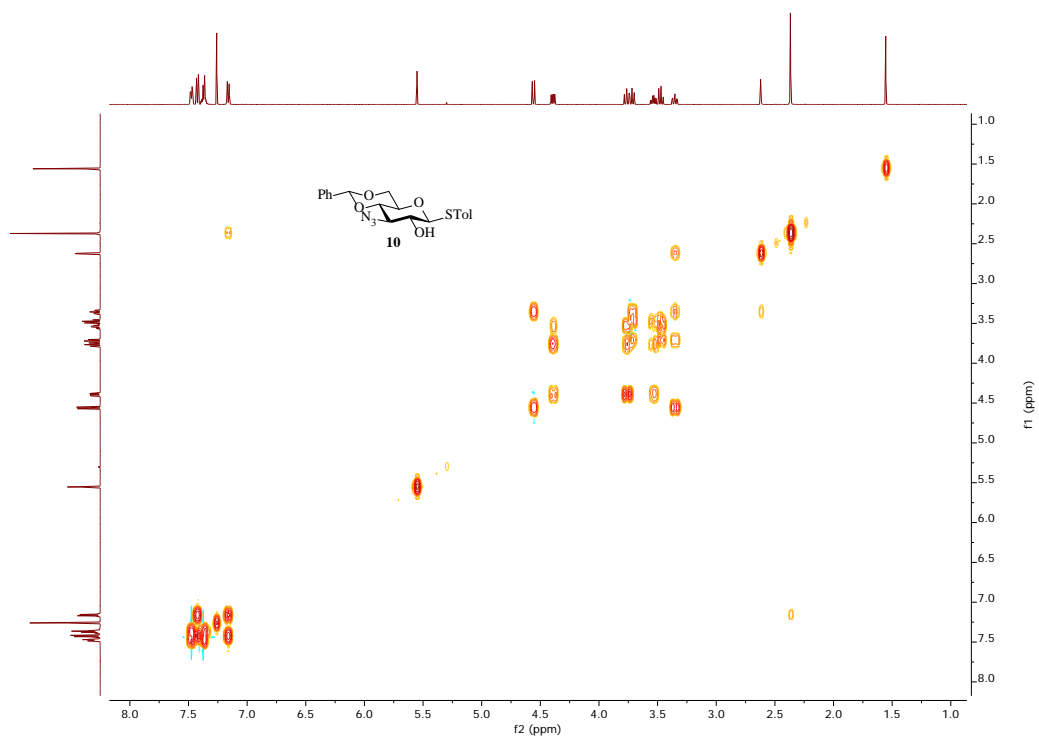
Figure 2.14. ^{1}H-^{1}H gCOSY of **10** (500 MHz CDCl$_3$)
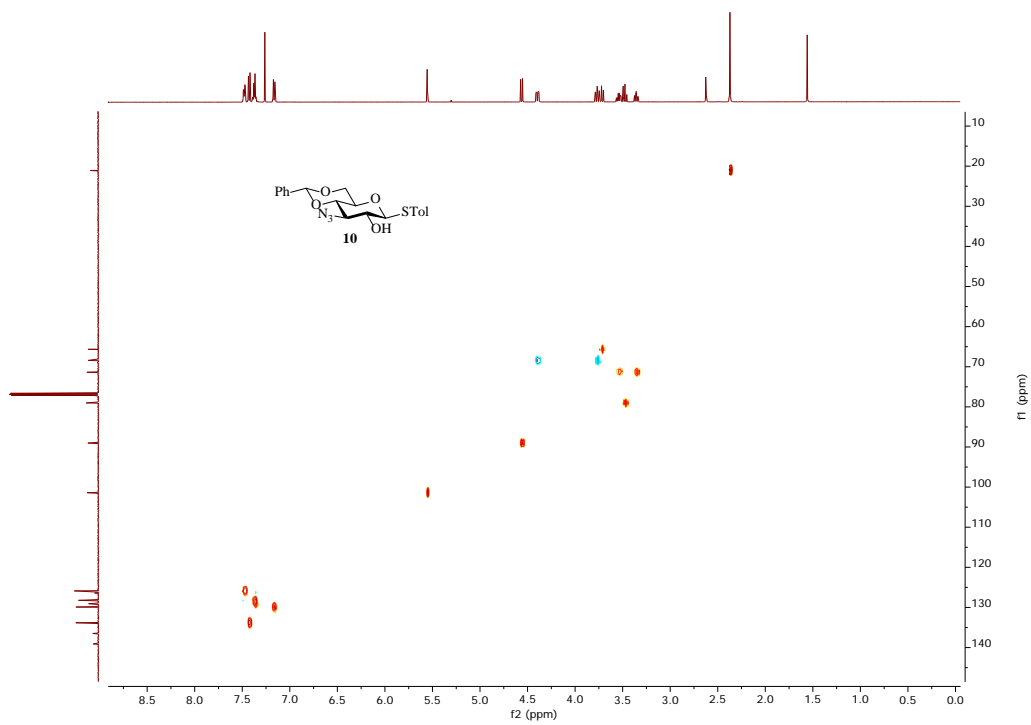
Figure 2.15. ^{1}H-^{13}C gHSQCAD of **10** (500 MHz CDCl$_3$)
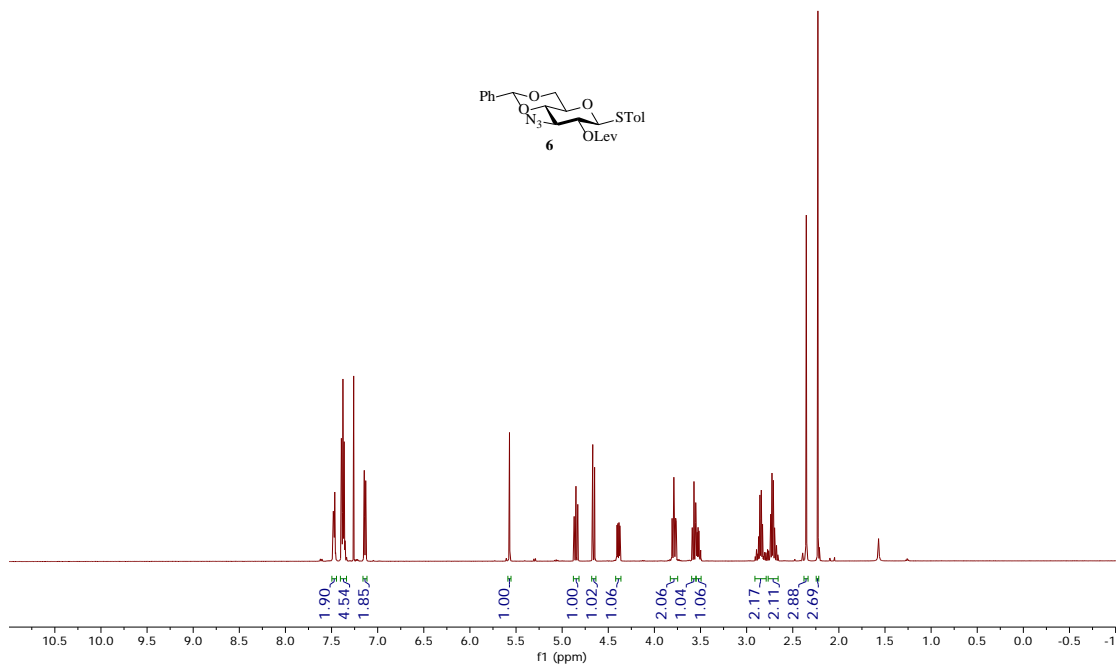
Figure 2.16. ^{1}H-NMR of **6** (500 MHz CDCl$_3$)
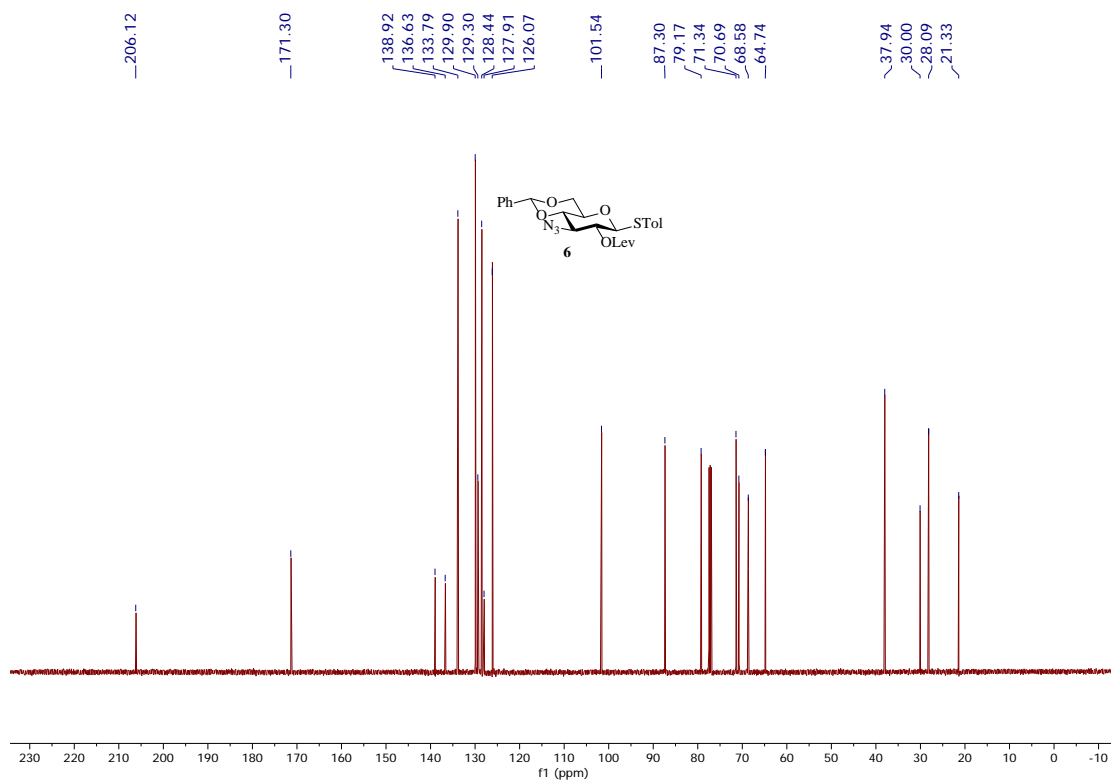
Figure 2.17. ^{13}C-NMR of **6** (125 MHz CDCl$_3$)

114
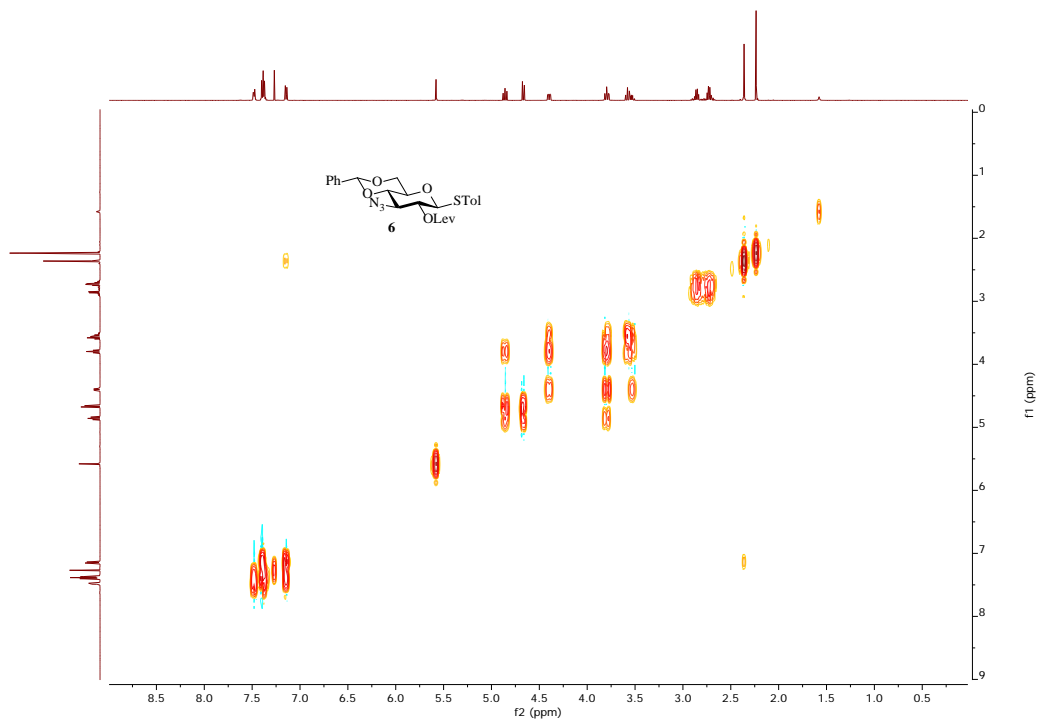
Figure 2.18. ^{1}H-^{1}H gCOSY of **6** (500 MHz CDCl$_3$)
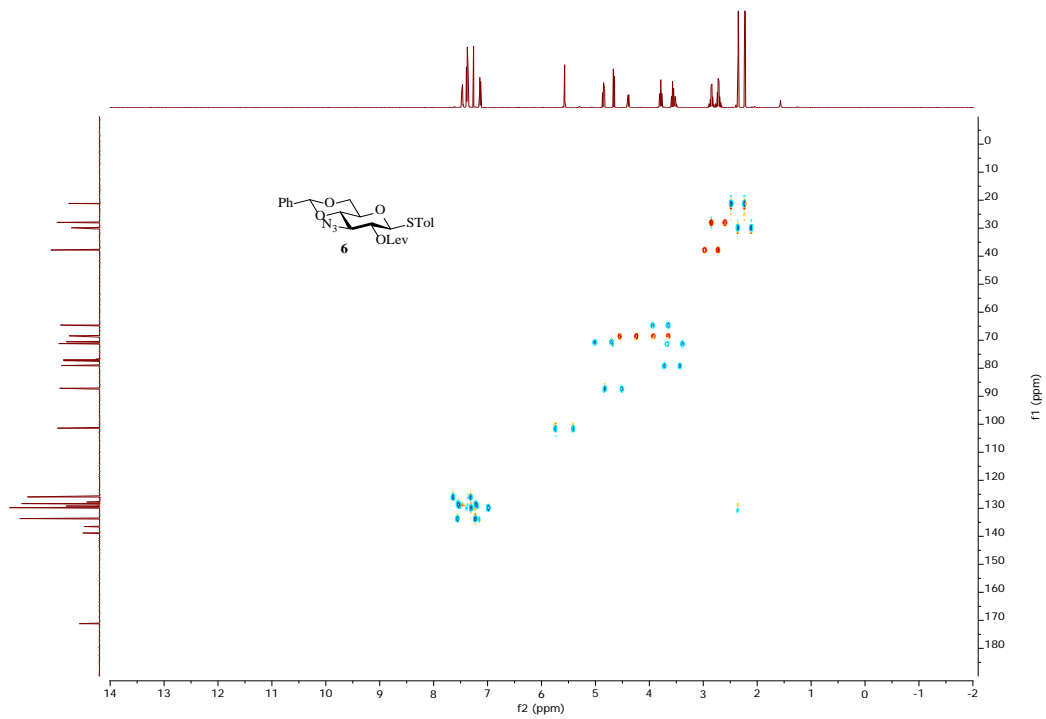
Figure 2.19. ^{1}H-^{13}C gHSQCAD of **6** (500 MHz CDCl$_3$)
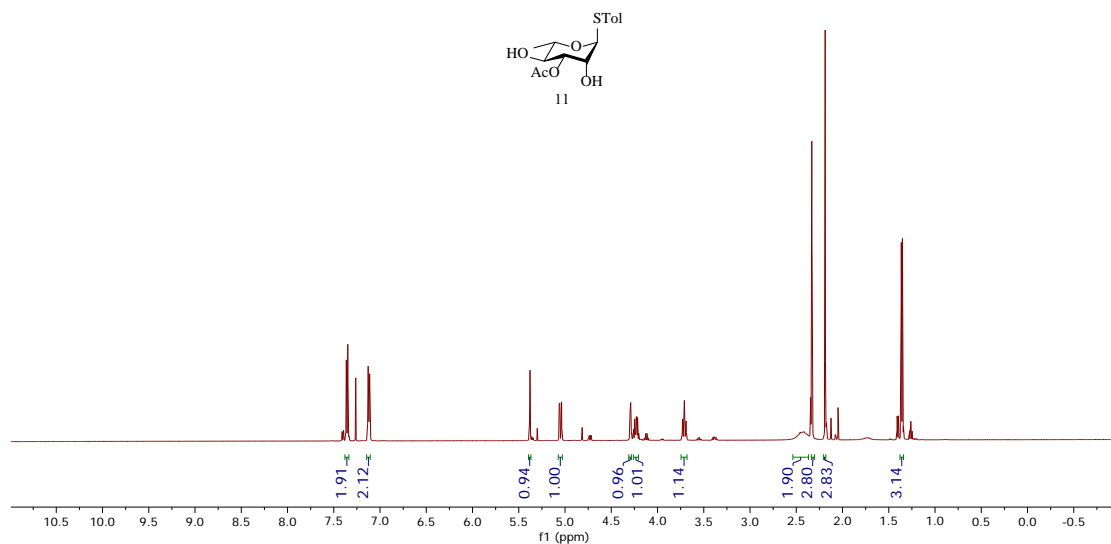
Figure 2.20. ^{1}H-NMR of **11** (500 MHz CDCl$_3$)
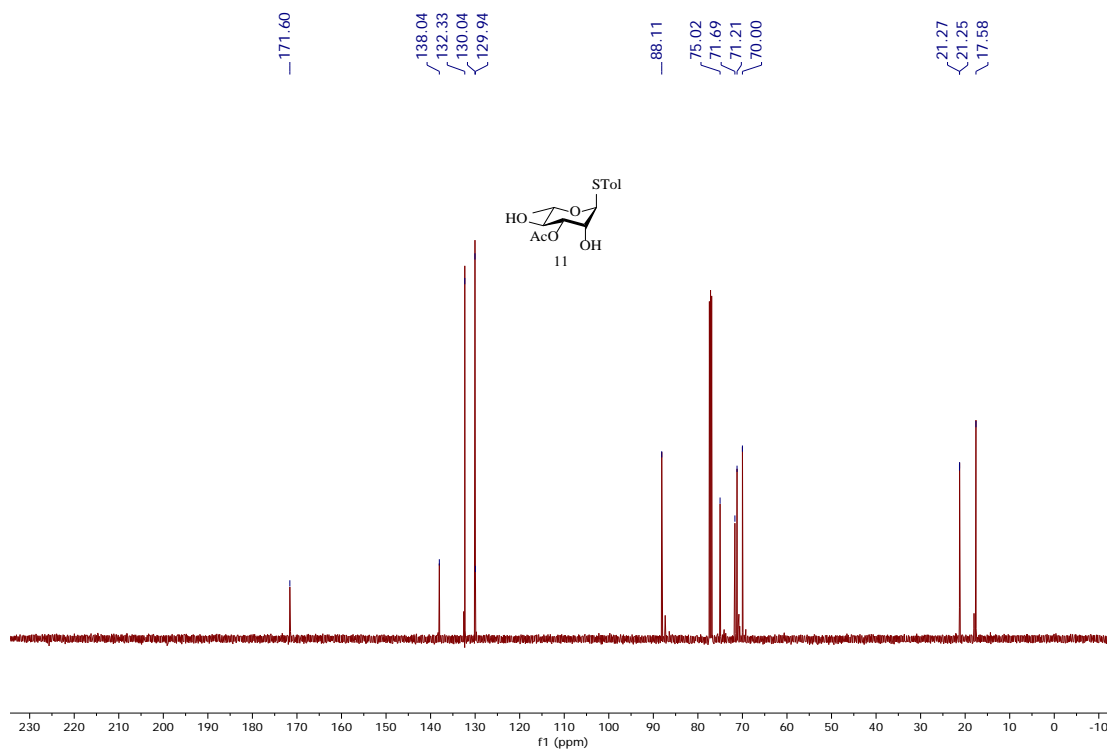
Figure 2.21. ^{13}C-NMR of **11** (125 MHz CDCl$_3$)
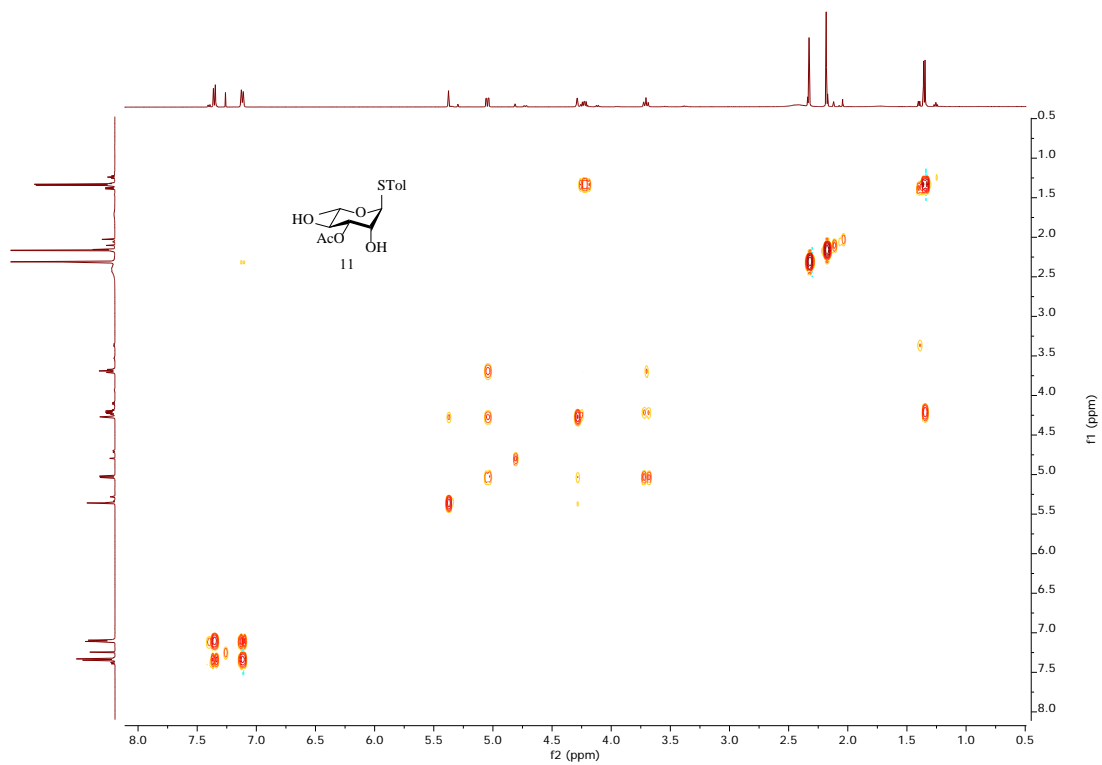
Figure 2.22. ^{1}H-^{1}H gCOSY of **11** (500 MHz CDCl$_3$)
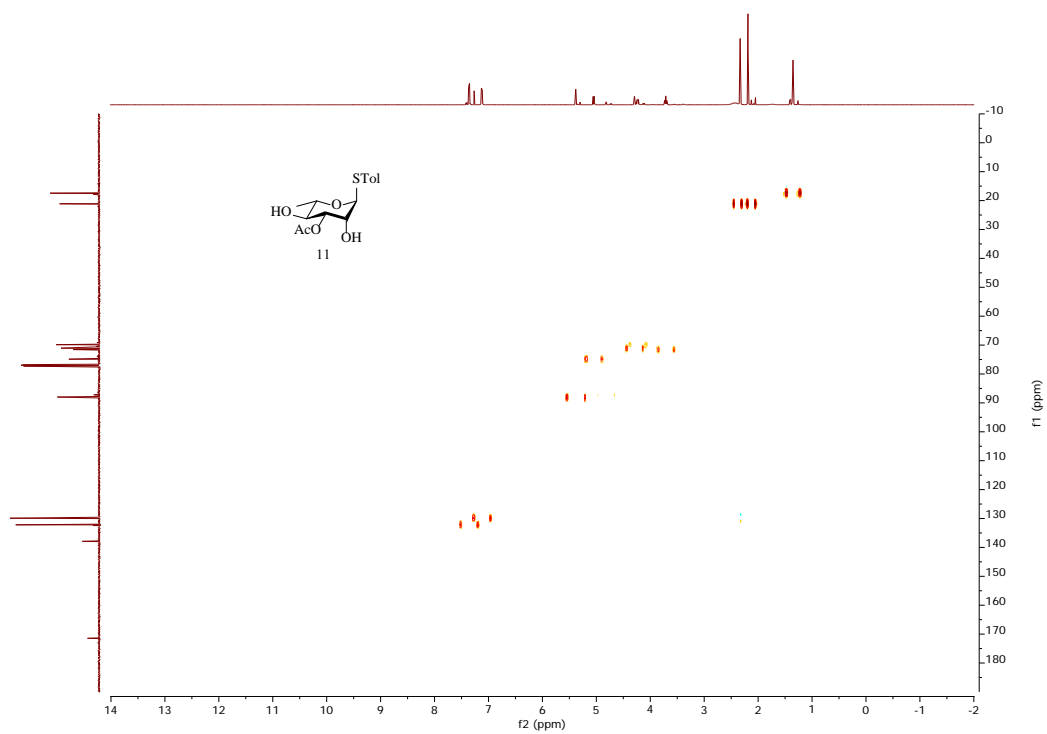
Figure 2.23. ^{1}H-^{13}C gHSQCAD of **11** (500 MHz CDCl$_3$)

117
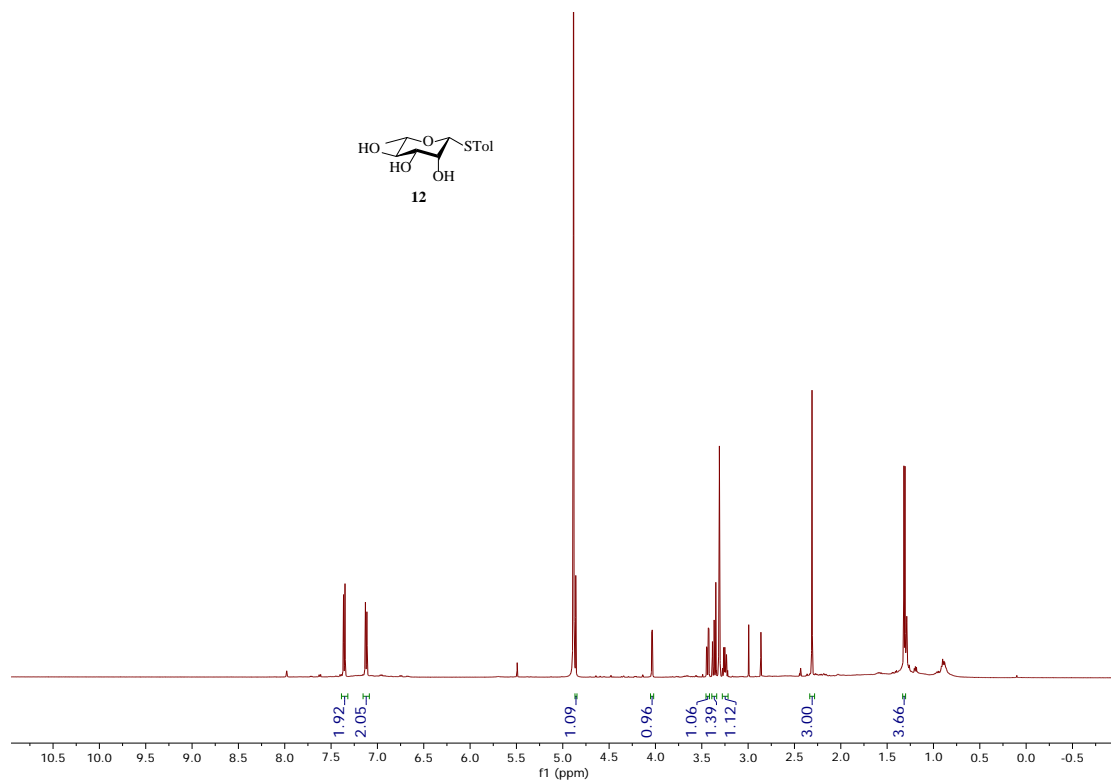
Figure 2.24. ^{1}H-NMR of **12** (500 MHz CD$_3$OD)
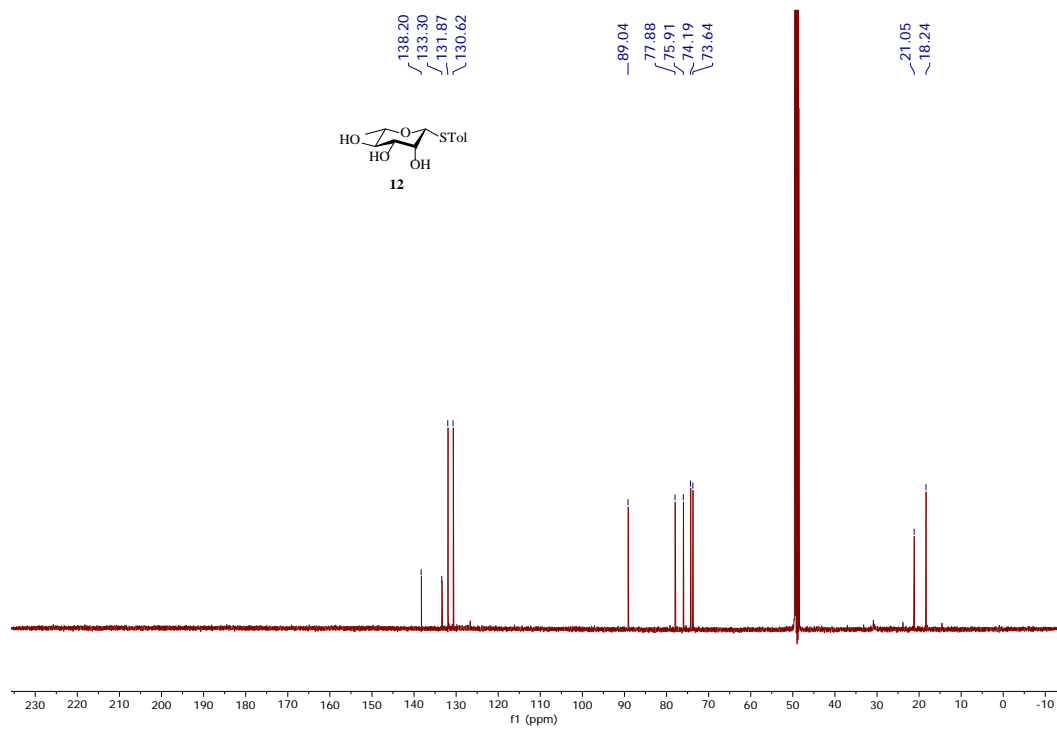
Figure 2.25. ^{13}C-NMR of **12** (125 MHz CD$_3$OD)
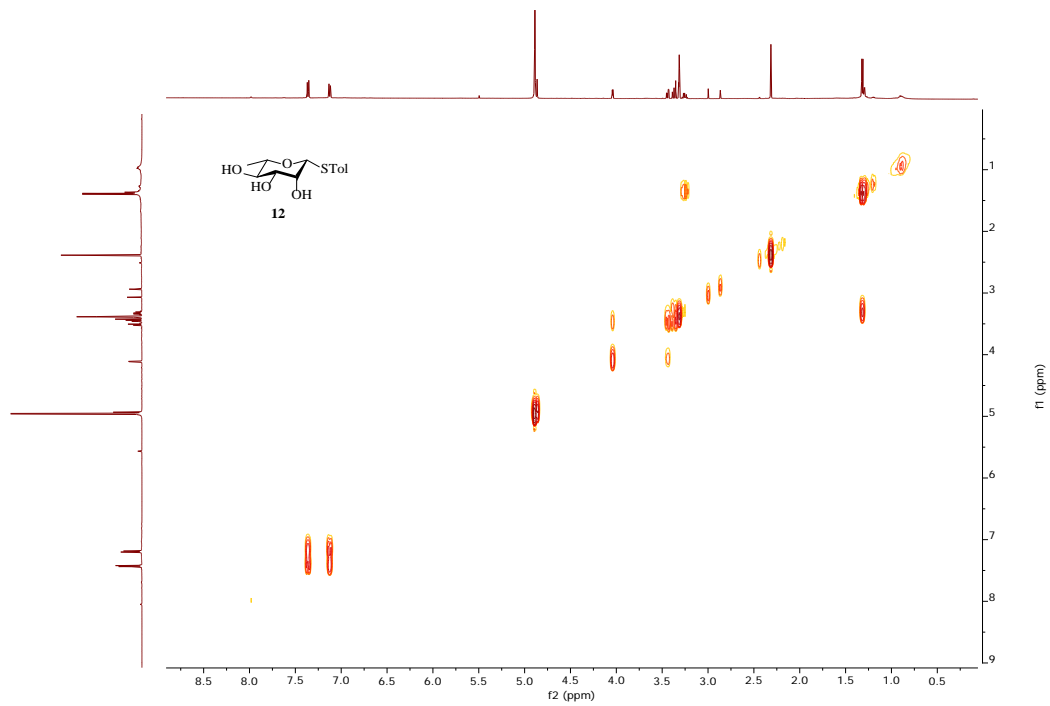
Figure 2.26. ^{1}H-^{1}H gCOSY of **12** (500 MHz CD$_3$OD)
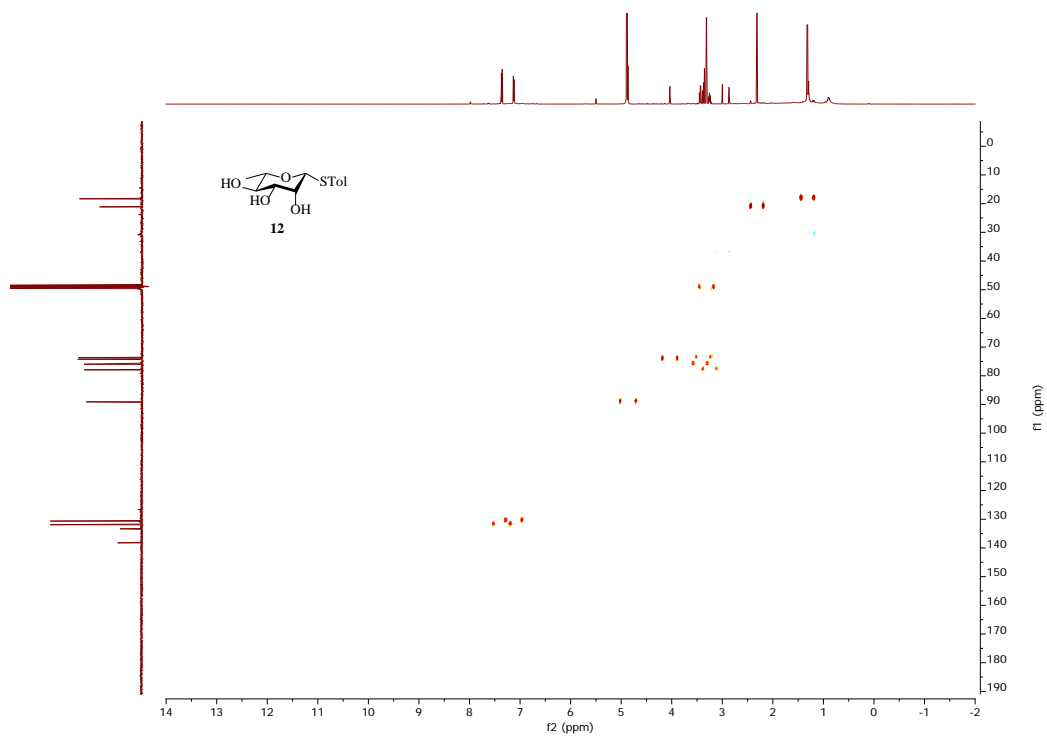
Figure 2.27. ^{1}H-^{13}C gHSQCAD of **12** (500 MHz CD$_3$OD)
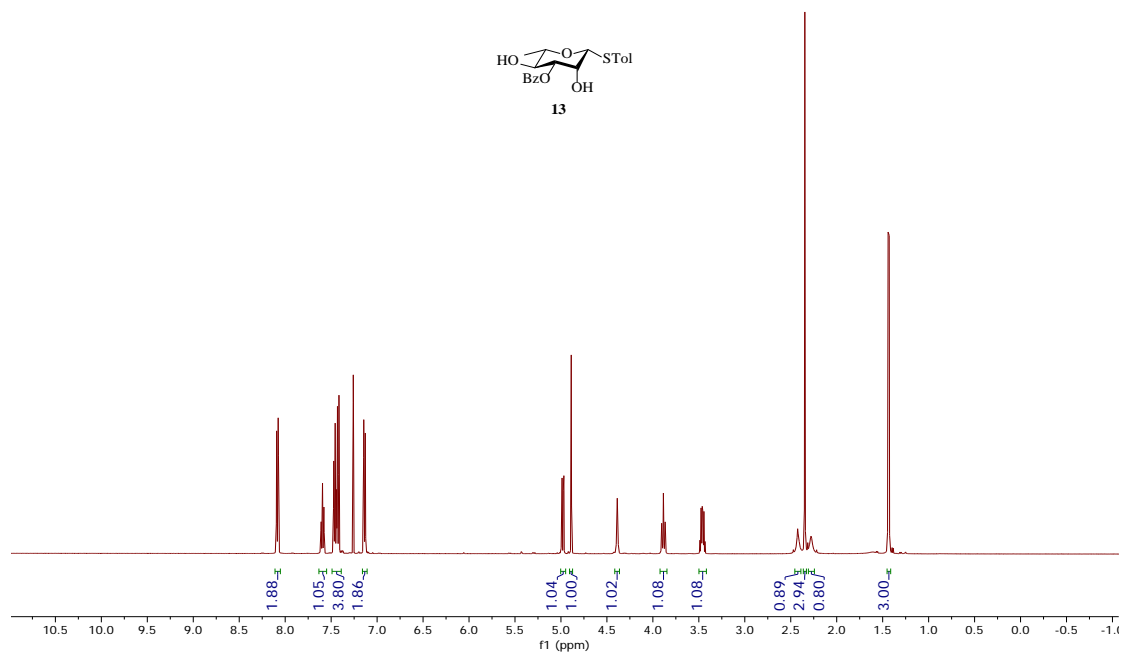
Figure 2.28. ^{1}H-NMR of **13** (500 MHz CDCl$_3$)
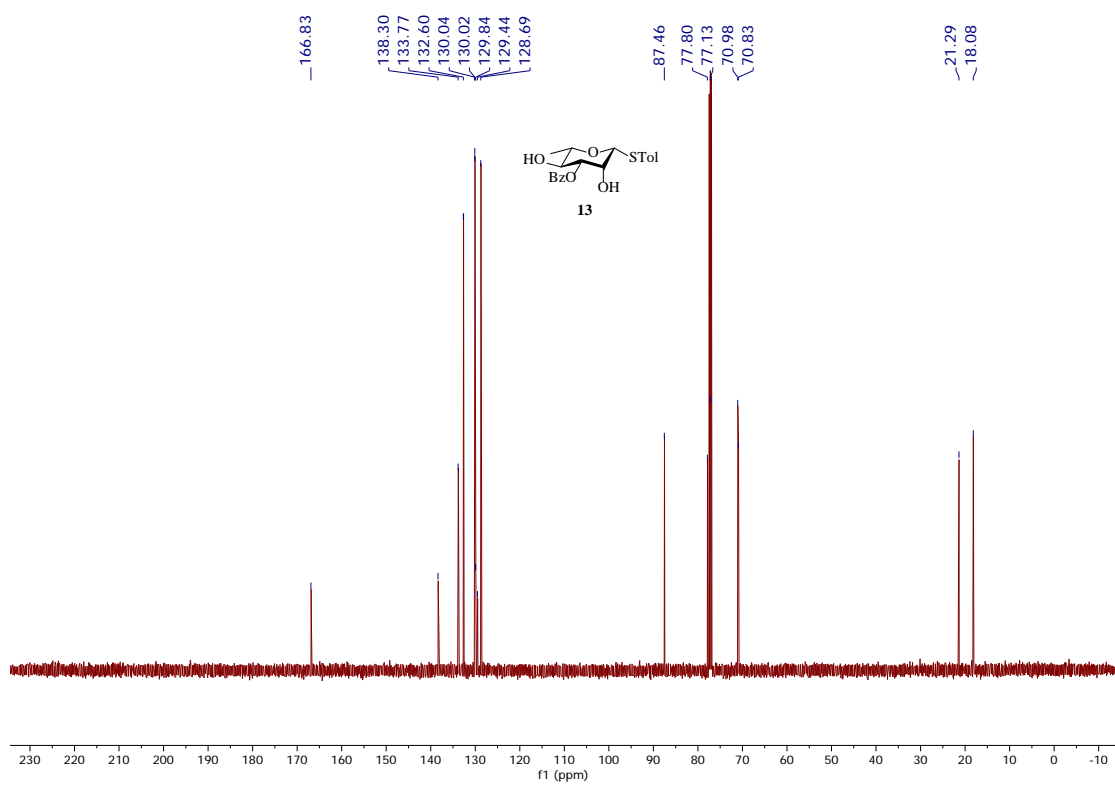
Figure 2.29. ^{13}C-NMR of **13** (125 MHz CDCl$_3$)

120
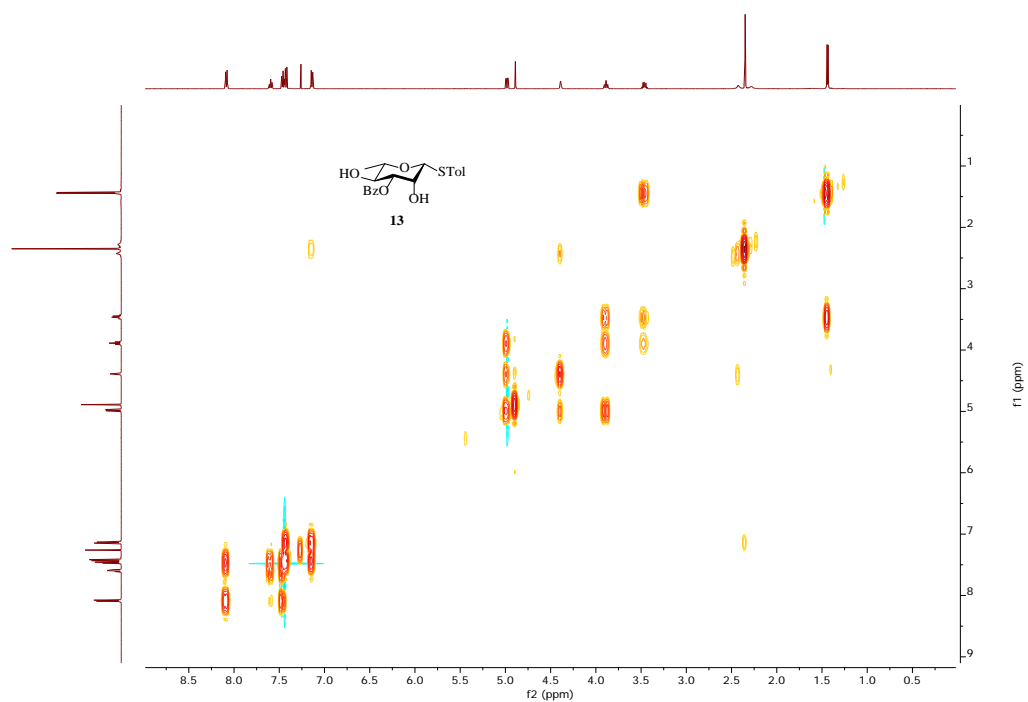
Figure 2.30. ^{1}H-^{1}H gCOSY of **13** (500 MHz CDCl$_3$)
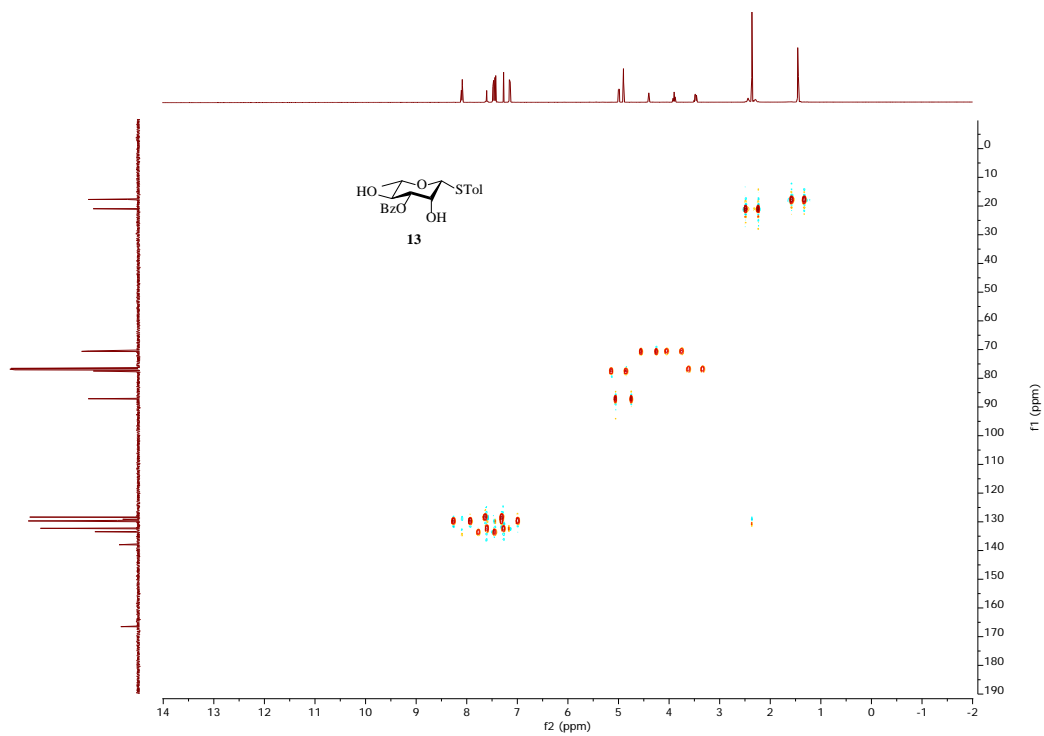
Figure 2.31. ^{1}H-^{13}C gHSQCAD of **13** (500 MHz CDCl$_3$)
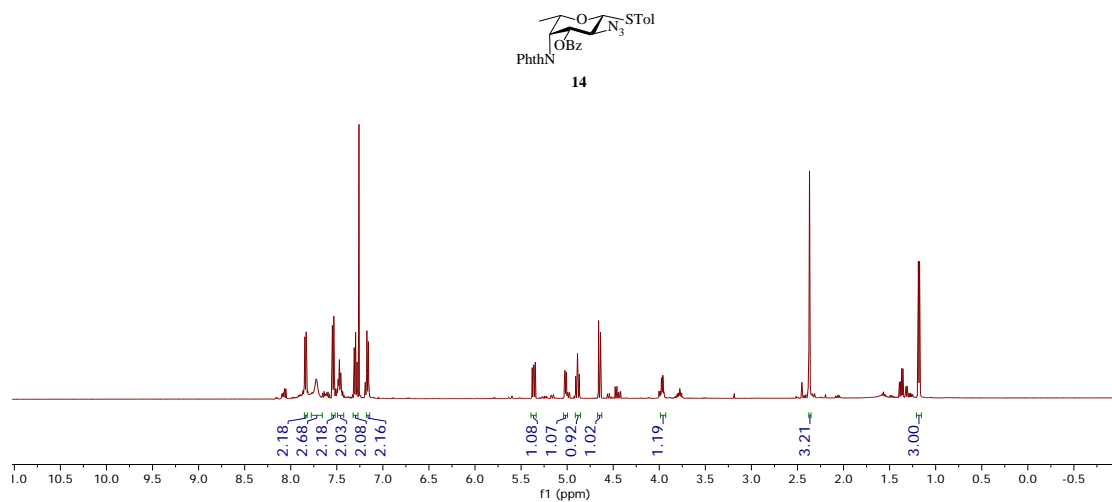
Figure 2.32. ^{1}H-NMR of **14** (500 MHz CDCl$_3$)
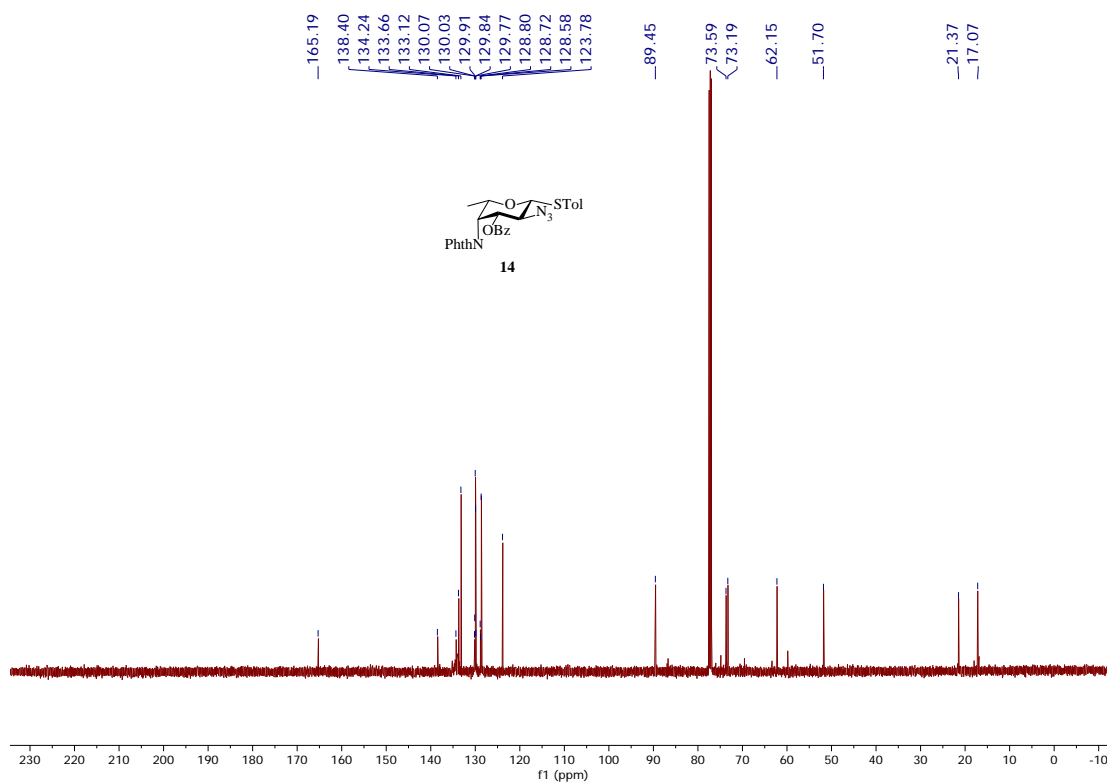
Figure 2.33. ^{13}C-NMR of **14** (125 MHz CDCl$_3$)
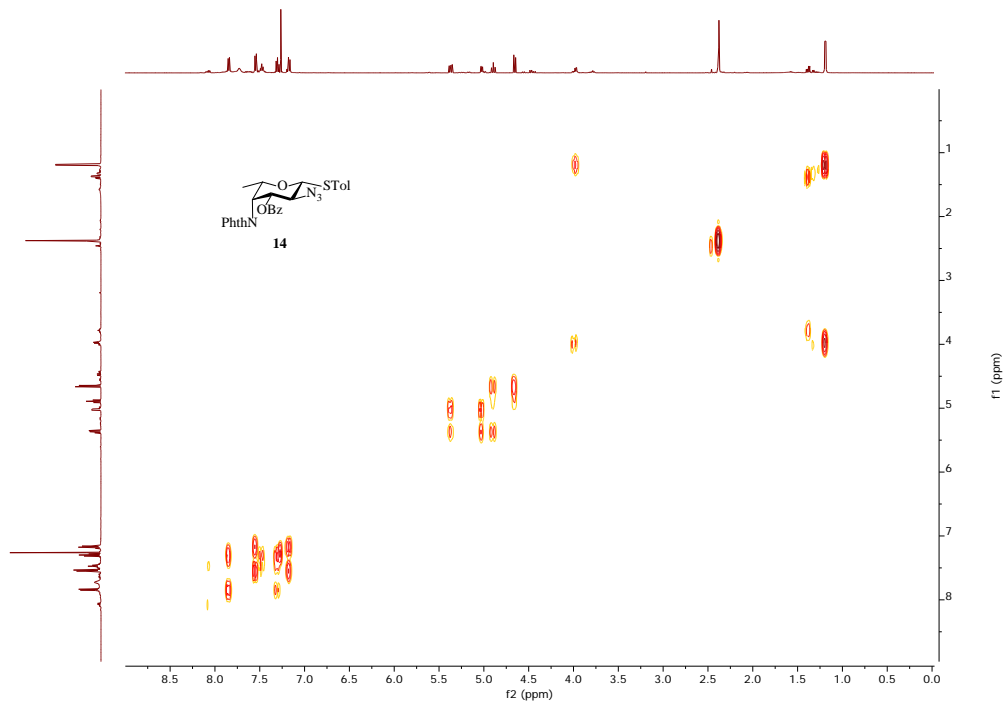
Figure 2.34. ^{1}H-^{1}H gCOSY of **14** (500 MHz CDCl$_3$)
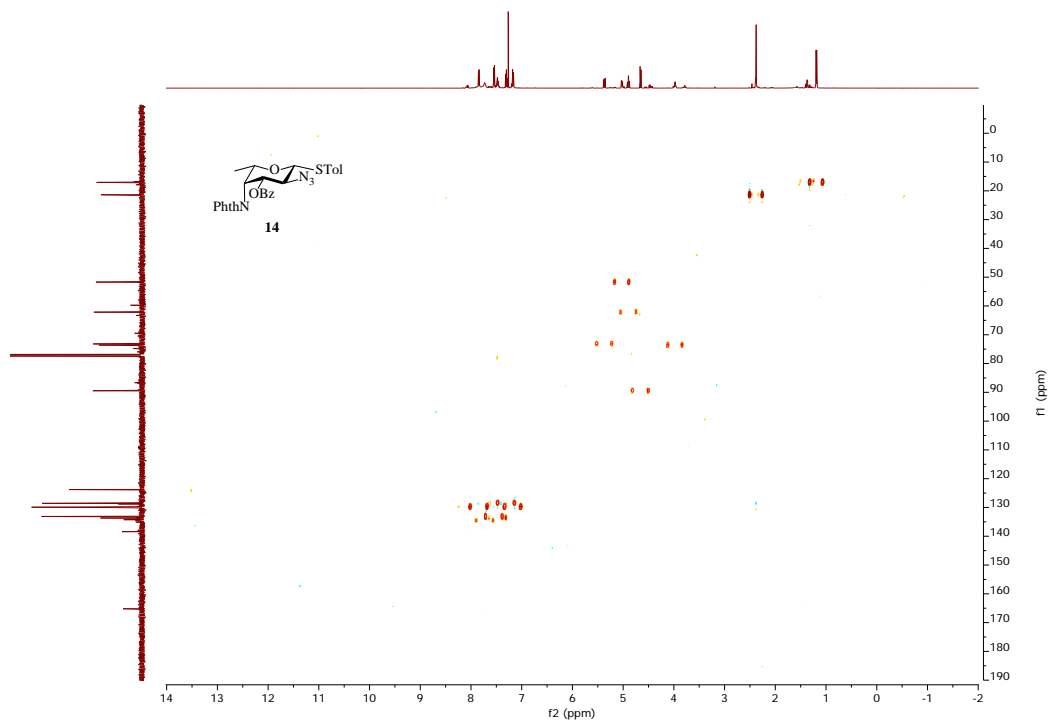
Figure 2.35. ^{1}H-^{13}C gHSQCAD of **14** (500 MHz CDCl$_3$)
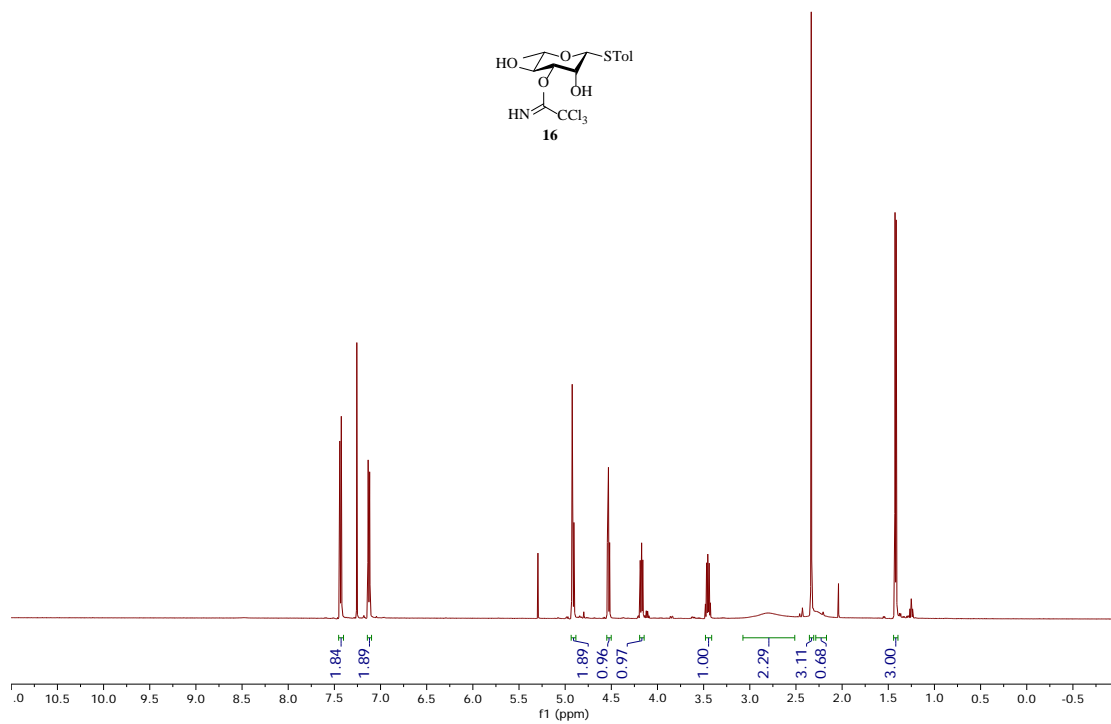
Figure 2.36. ^{1}H-NMR of **16** (500 MHz CDCl$_3$)
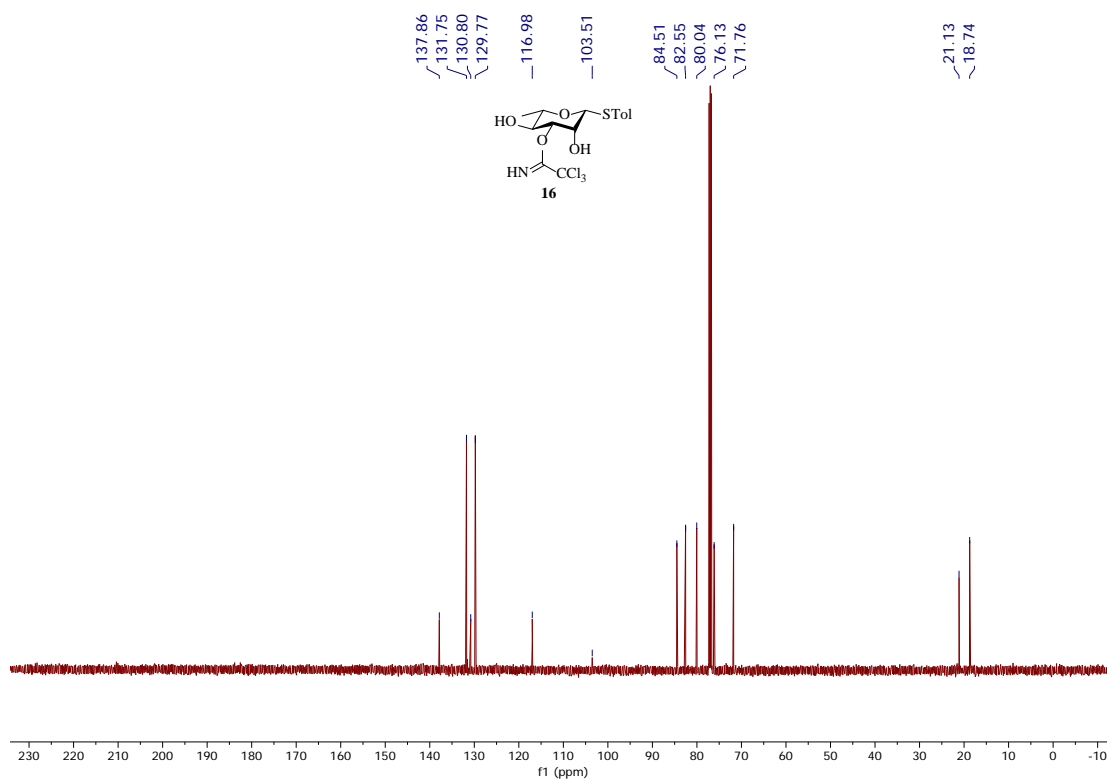
Figure 2.37. ^{13}C-NMR of **16** (125 MHz CDCl$_3$)
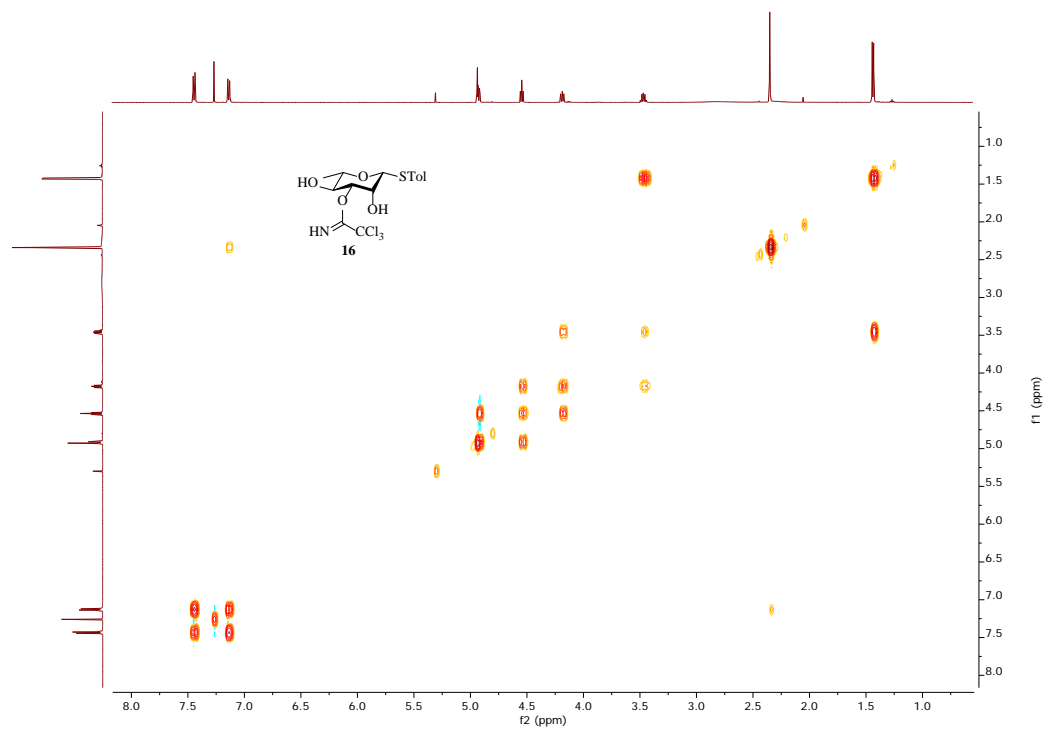
Figure 2.38. ^{1}H-^{1}H gCOSY of **16** (500 MHz CDCl$_3$)
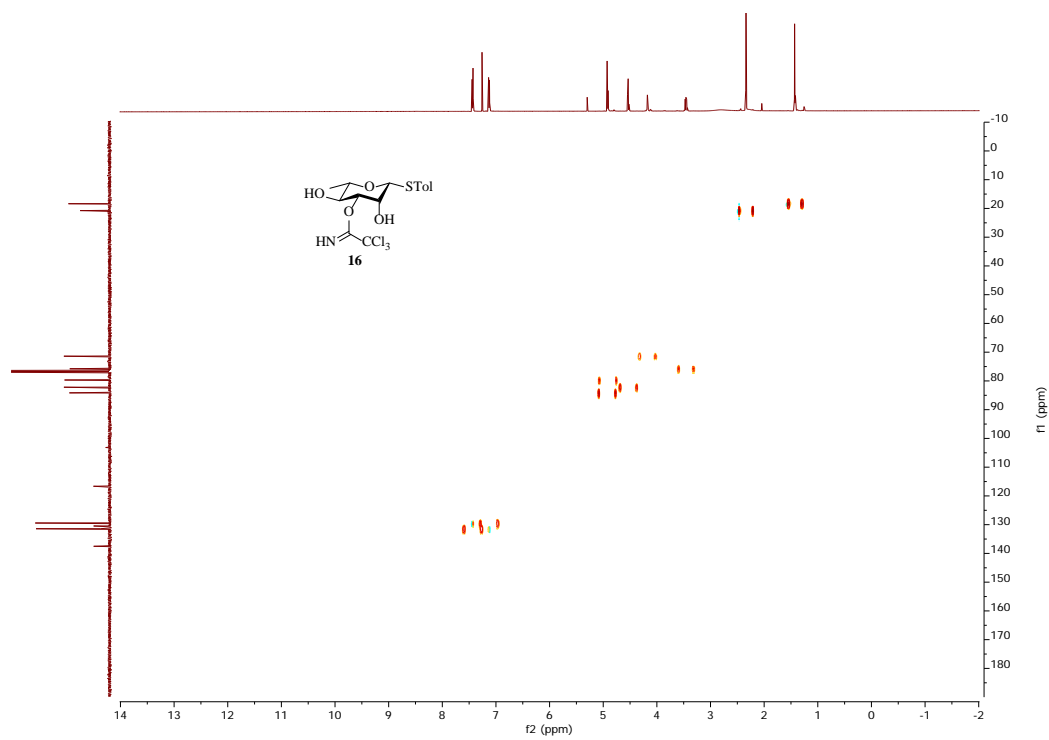
Figure 2.39. ^{1}H-^{13}C gHSQCAD of **16** (500 MHz CDCl$_3$)

125

Figure 2.40. ^{1}H-NMR of **17** (500 MHz CDCl$_3$)

Figure 2.41. ^{13}C-NMR of **17** (125 MHz CDCl$_3$)
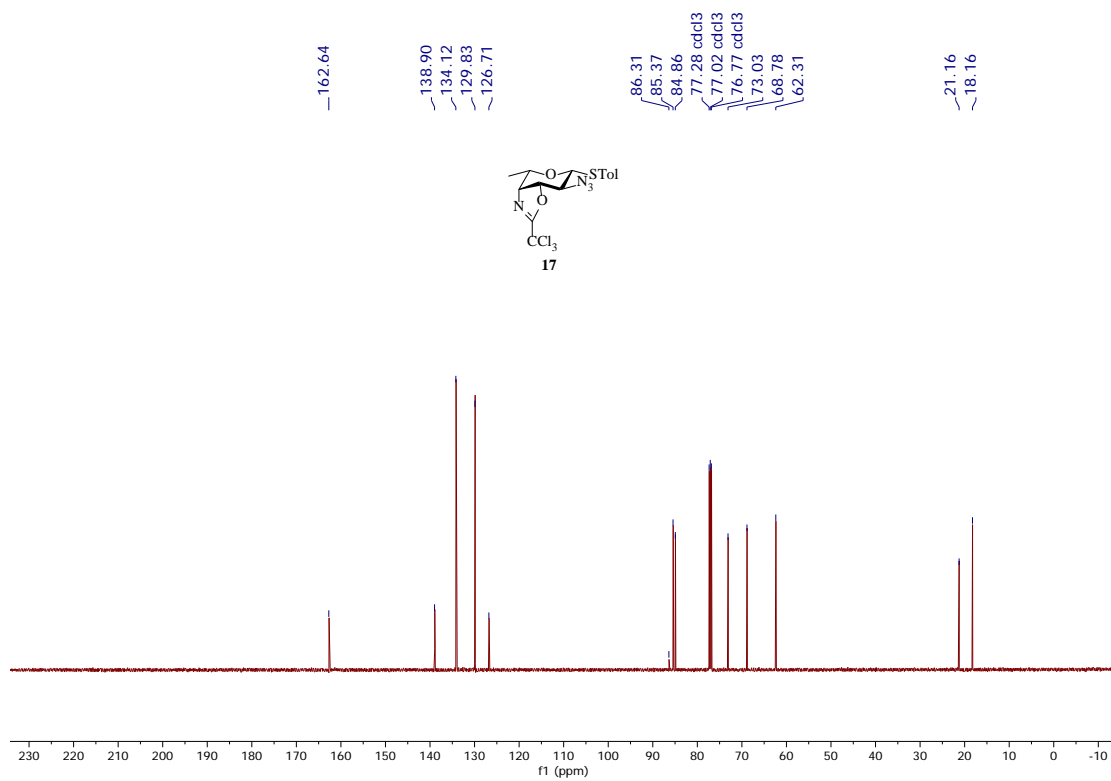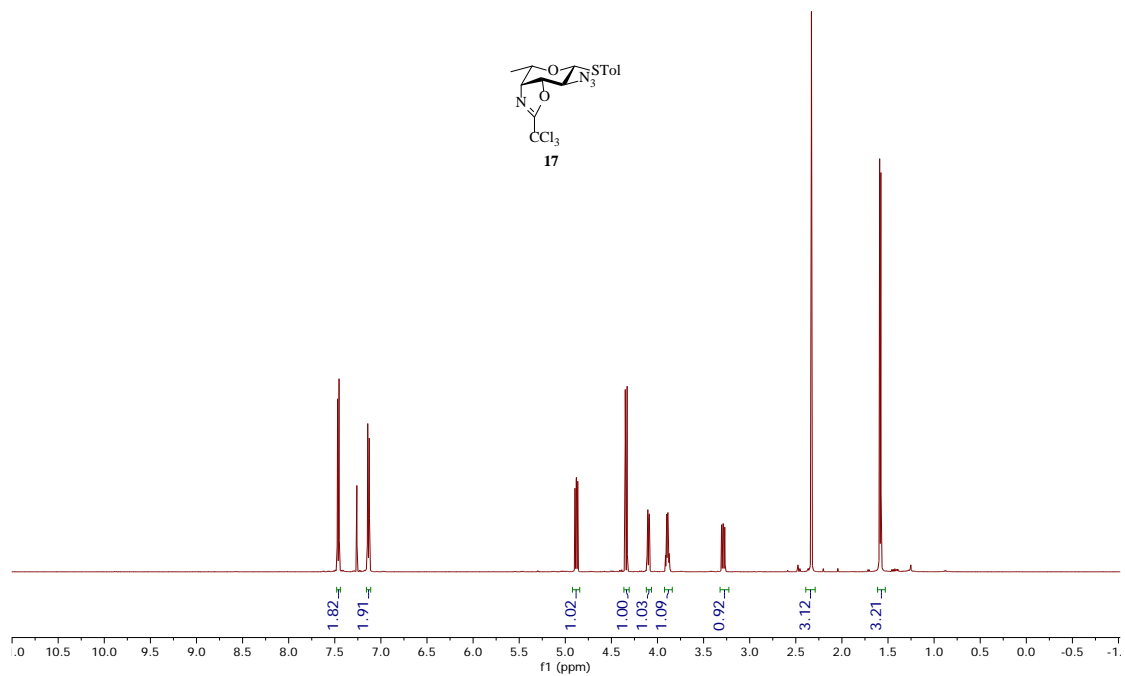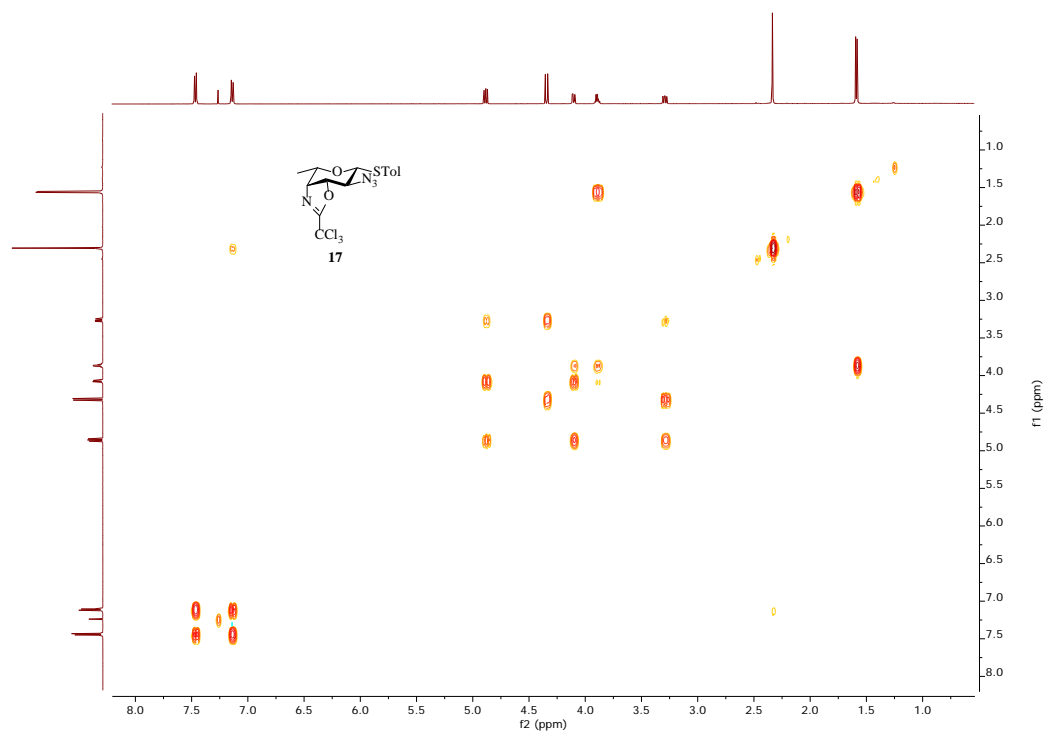
Figure 2.42. ^{1}H-^{1}H gCOSY of **17** (500 MHz CDCl$_3$)
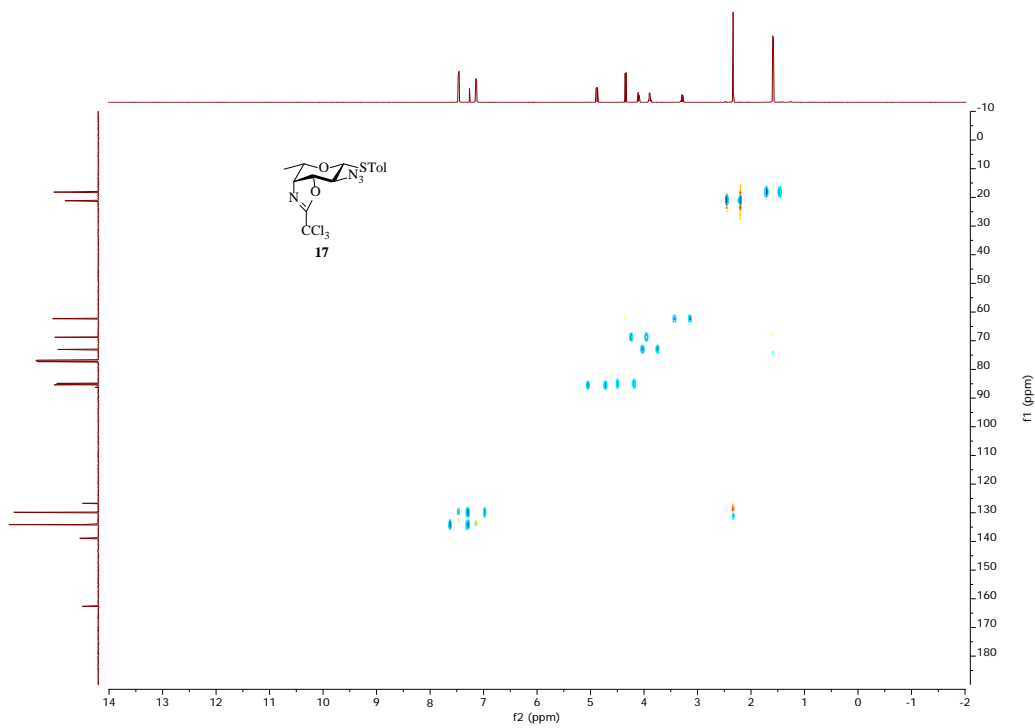
Figure 2.43. ^{1}H-^{13}C gHSQCAD of **17** (500 MHz CDCl$_3$)

Figure 2.44. ^{1}H-NMR of **15** (500 MHz CDCl$_3$)

Figure 2.45. ^{13}C-NMR of **15** (125 MHz CDCl$_3$)
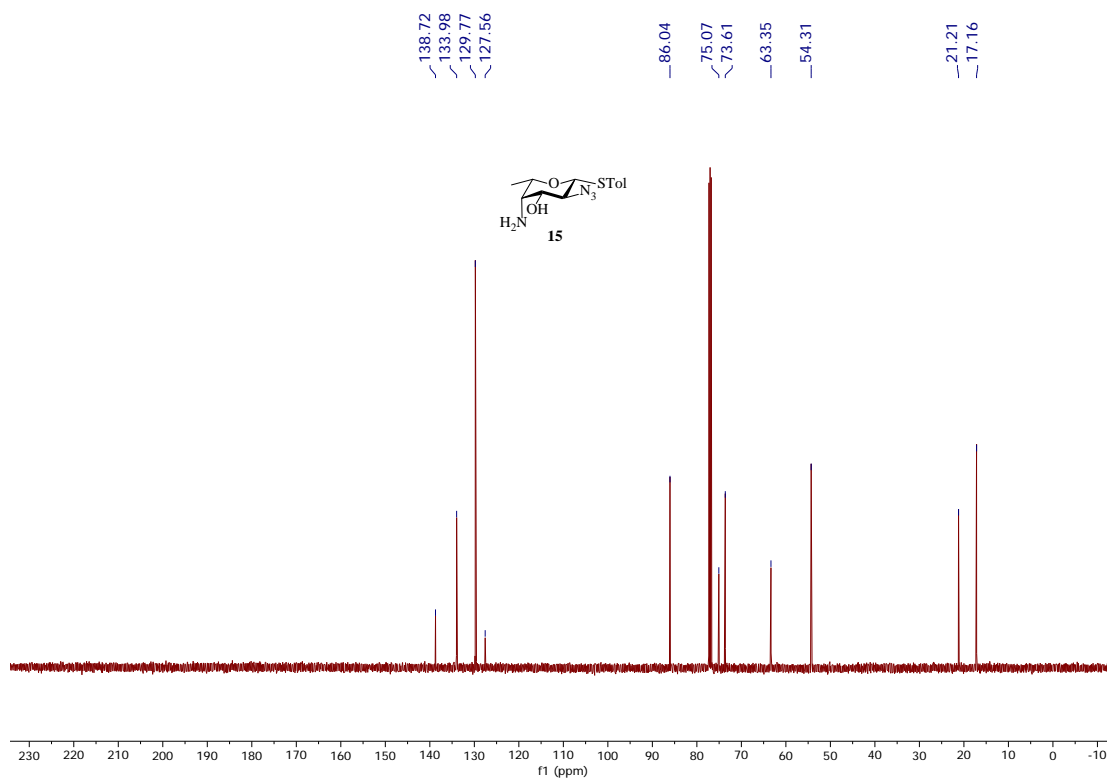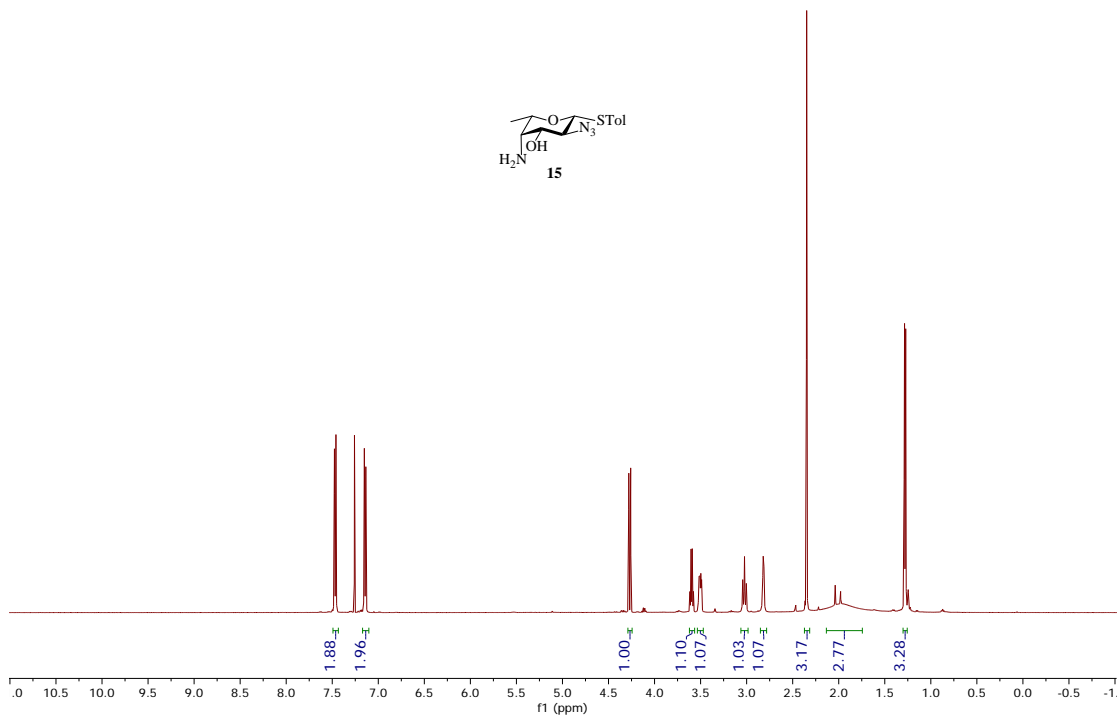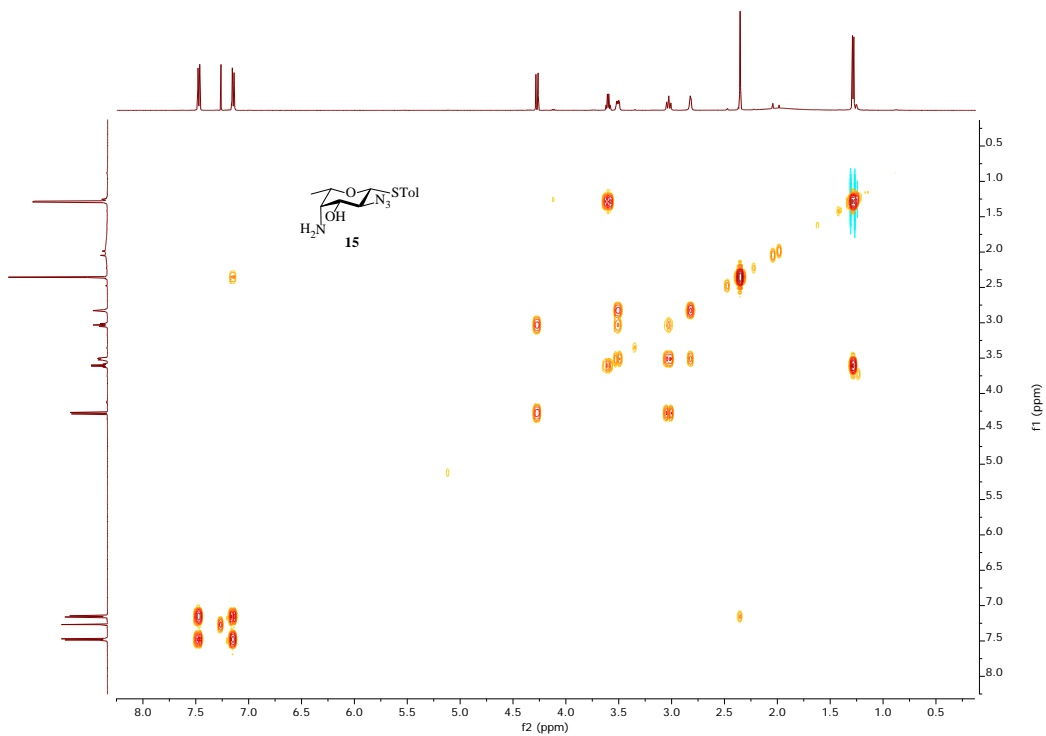
Figure 2.46. ^{1}H-^{1}H gCOSY of **15** (500 MHz CDCl$_3$)
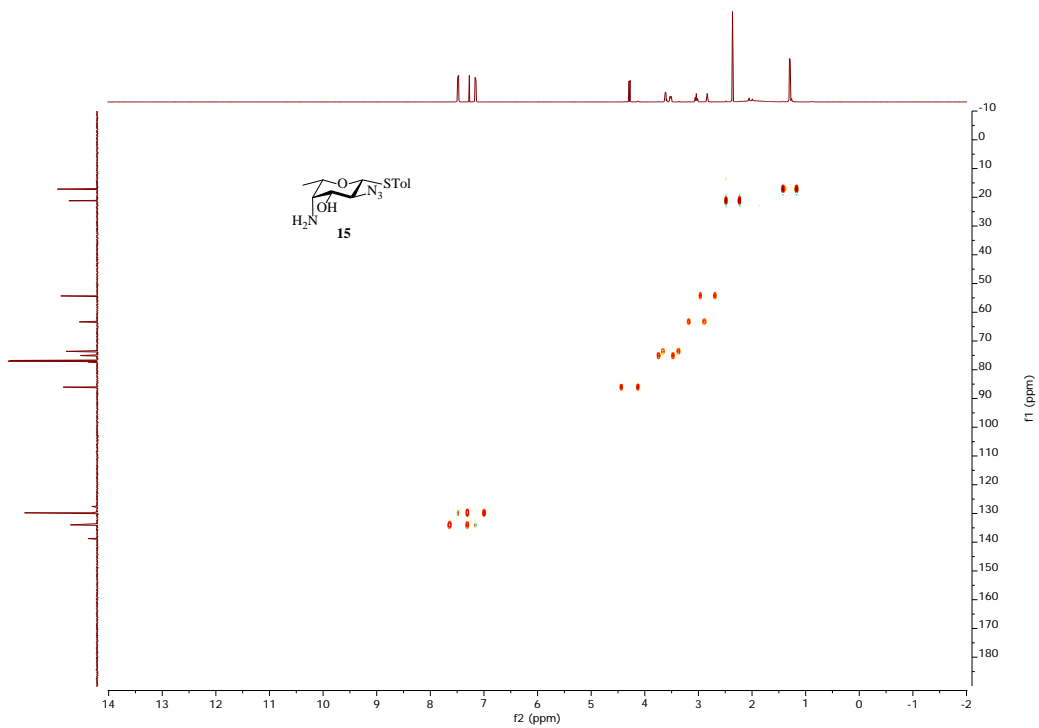
Figure 2.47. ^{1}H-^{13}C gHSQCAD of **15** (500 MHz CDCl$_3$)

Figure 2.48. ^{1}H-NMR of **18** (500 MHz CD$_3$OD)

Figure 2.49. ^{13}C-NMR of **18** (125 MHz CD$_3$OD)
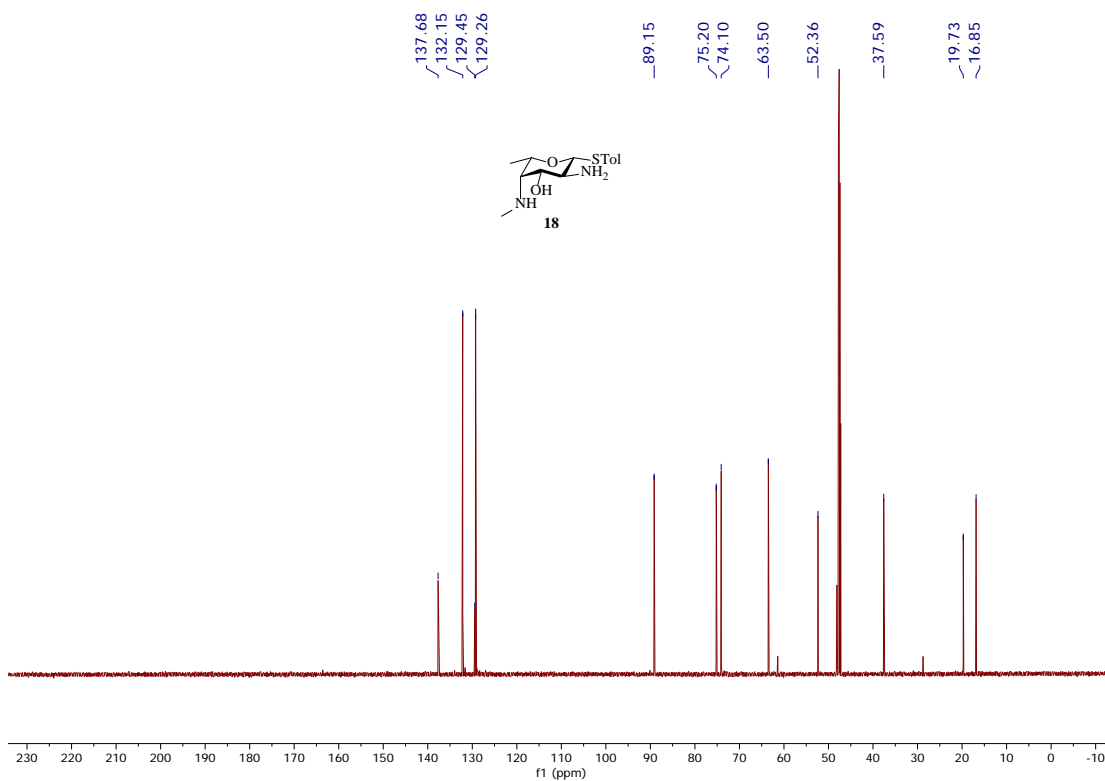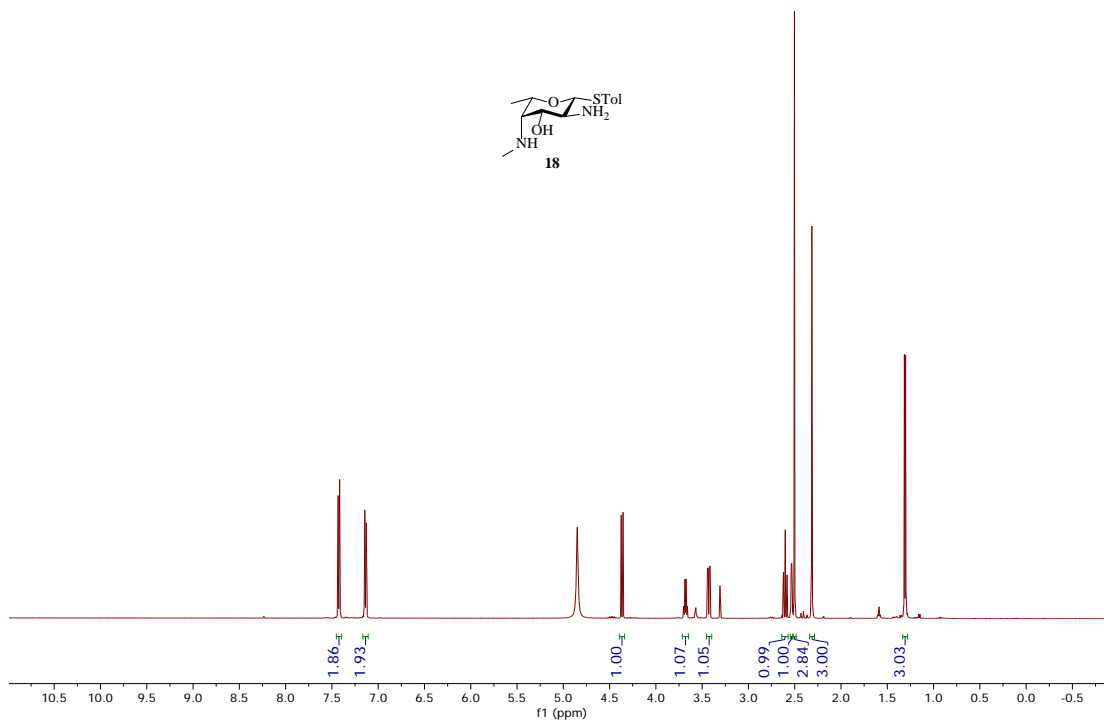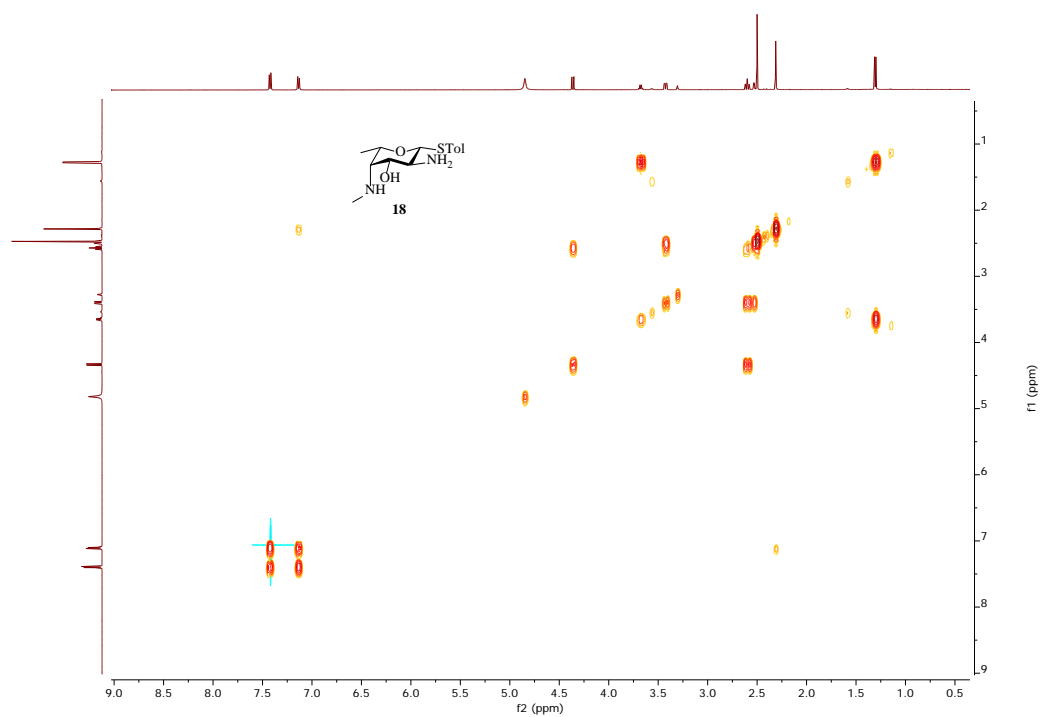
Figure 2.50. ^{1}H-^{1}H gCOSY of **18** (500 MHz CD$_3$OD)
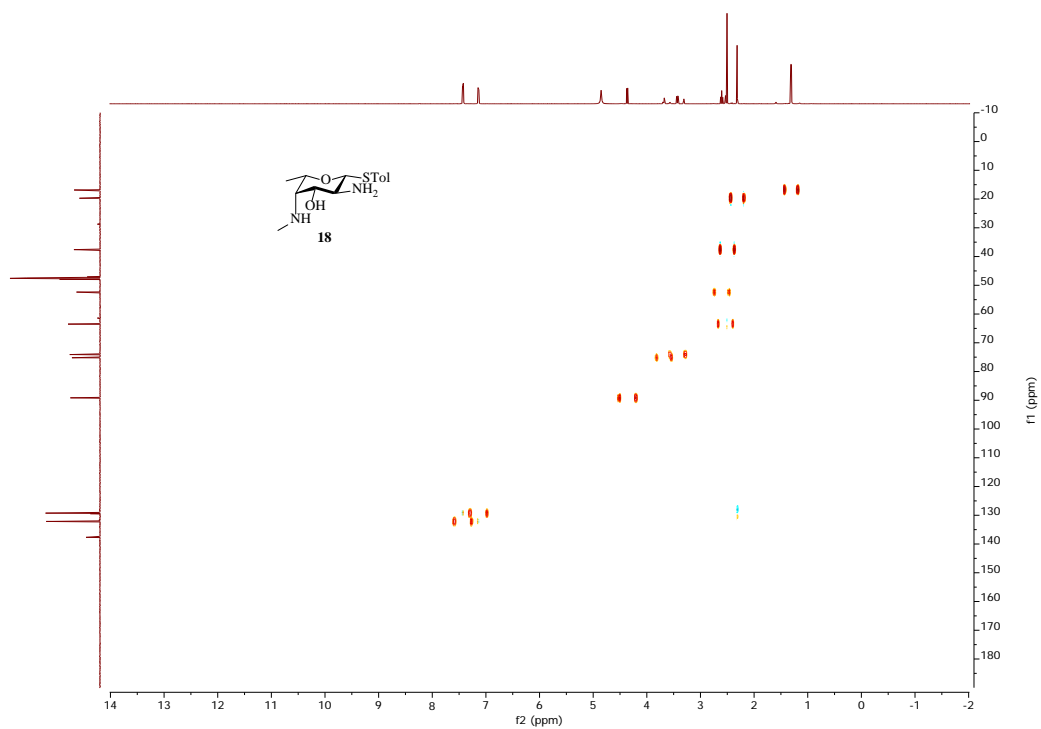
Figure 2.51. ^{1}H-^{13}C gHSQCAD of **18** (500 MHz CD$_3$OD)

Figure 2.52. ^{1}H-NMR of **19** (500 MHz CDCl$_3$)

Figure 2.53. ^{13}C-NMR of **19** (125 MHz CDCl$_3$)

132
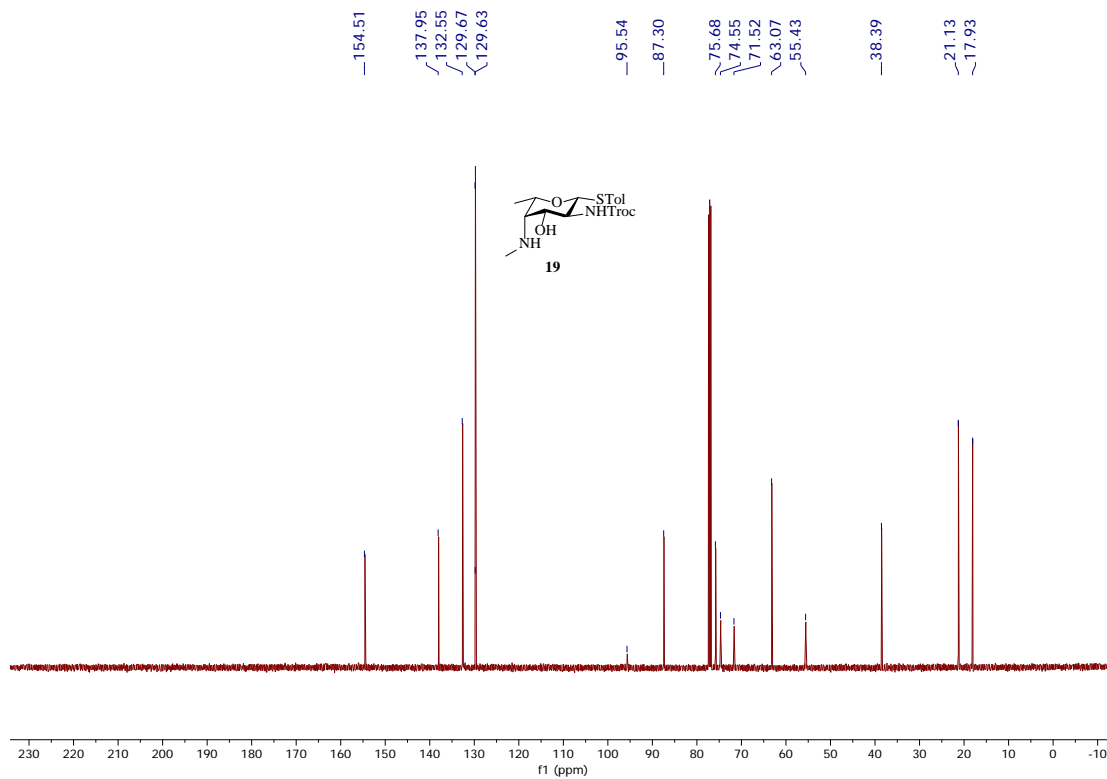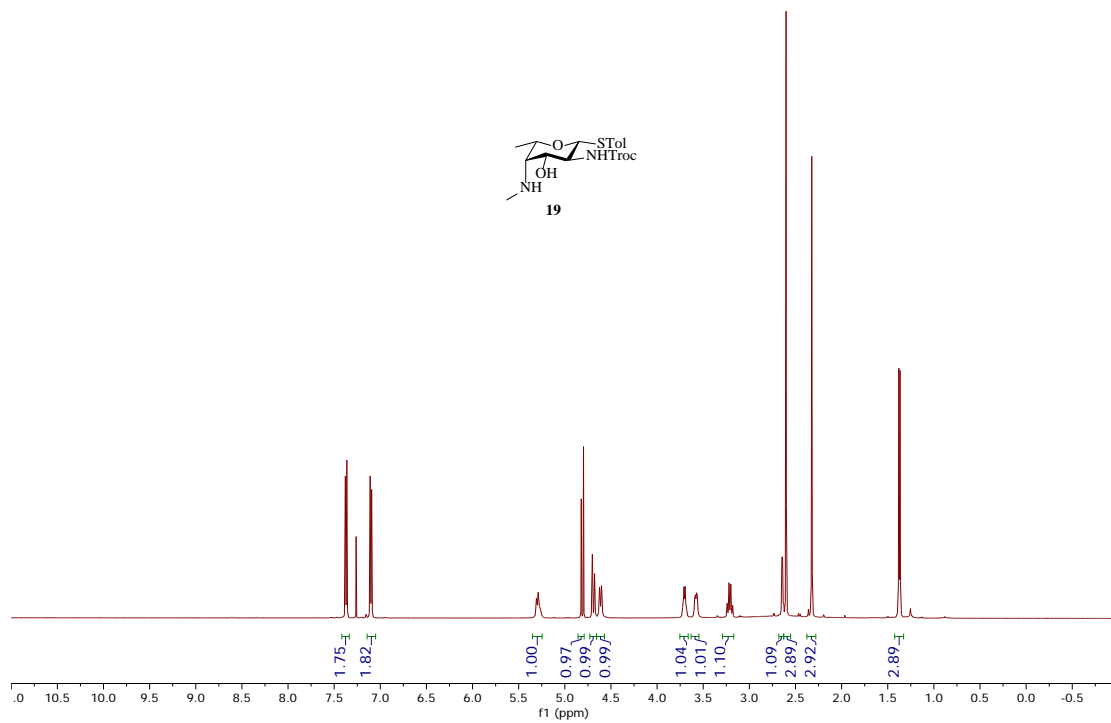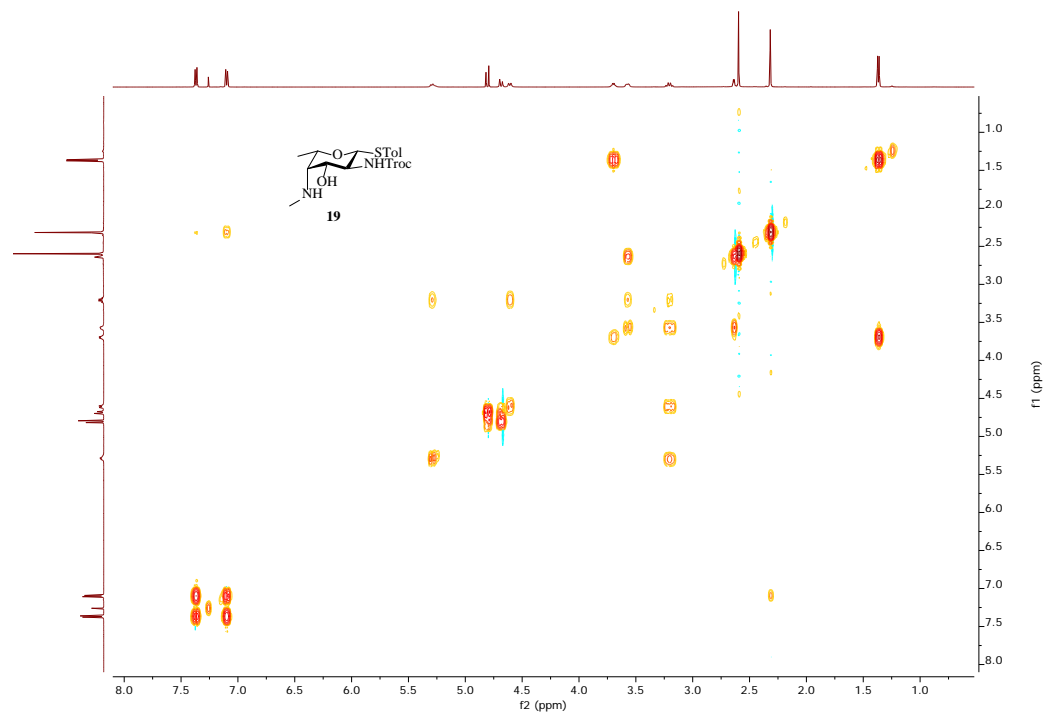
Figure 2.54. ^{1}H-^{1}H gCOSY of **19** (500 MHz CDCl$_3$)
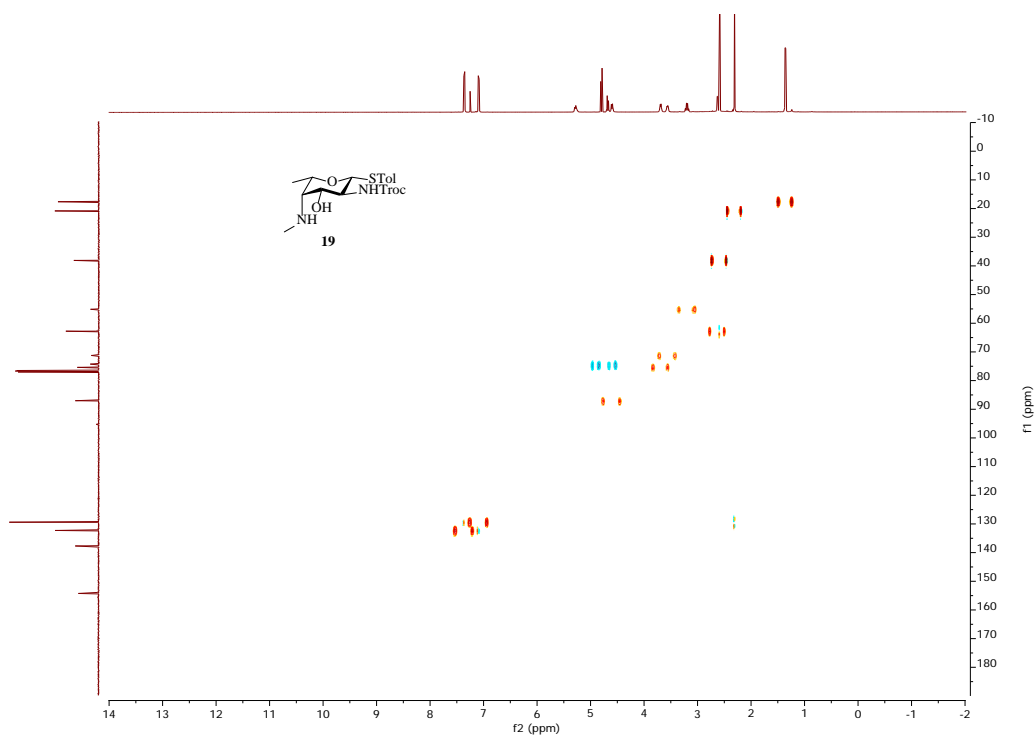
Figure 2.55. ^{1}H-^{13}C gHSQCAD of **19** (500 MHz CDCl$_3$)
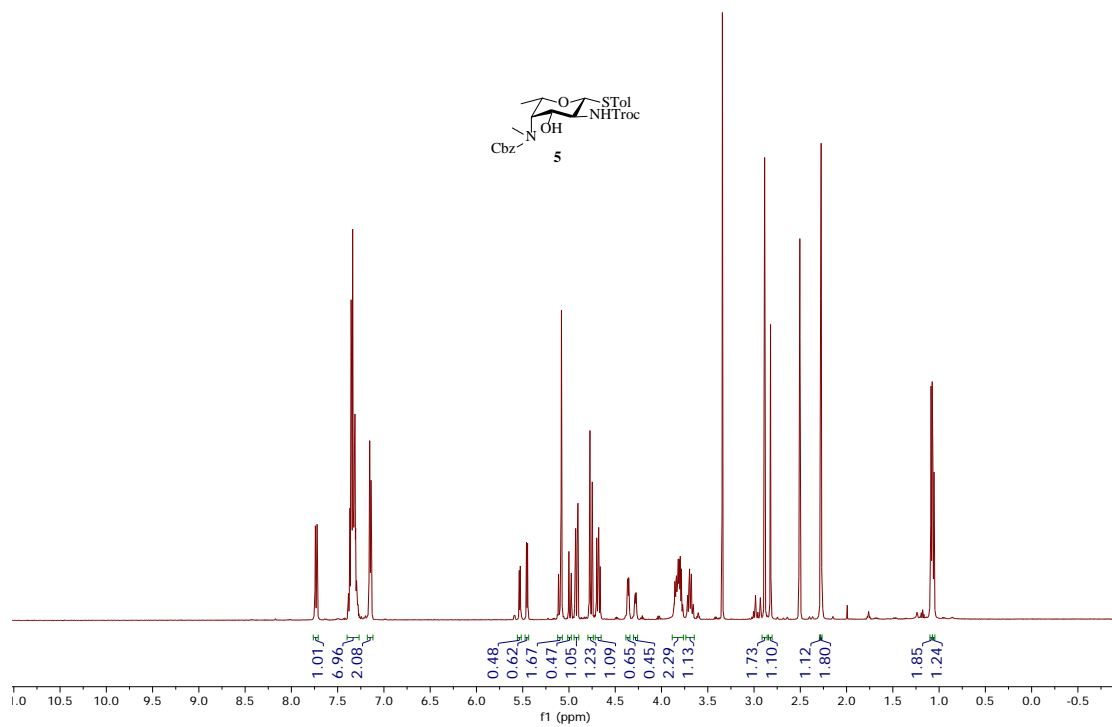
Figure 2.56. ^{1}H-NMR of **5** (500 MHz d^6-DMSO)
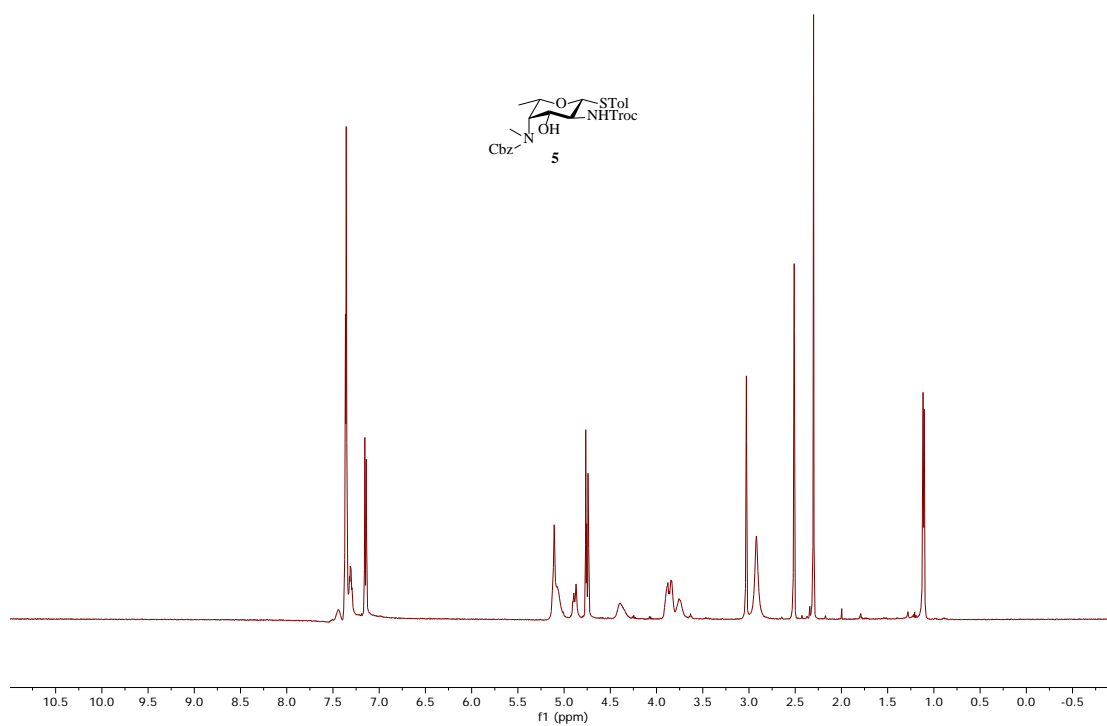
Figure 2.57. ^{1}H-NMR of **5** (500 MHz d^6-DMSO, VT at 90 °C)
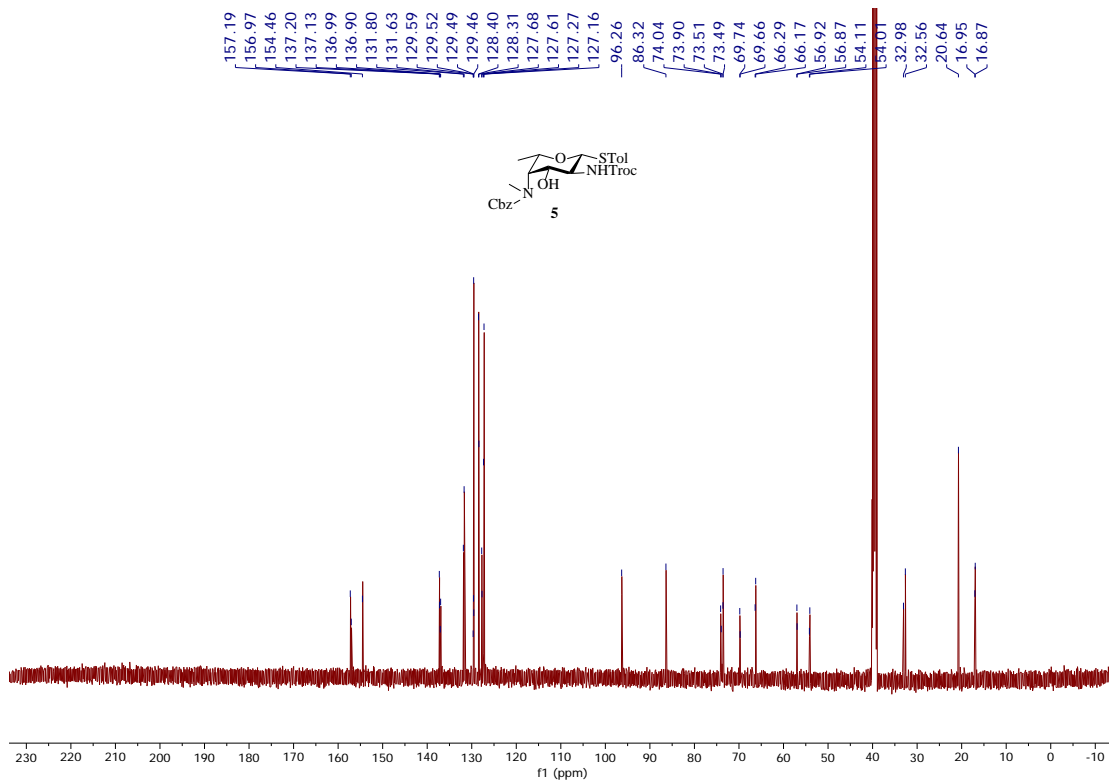
Figure 2.58. ^{13}C-NMR of **5** (125 MHz d^6-DMSO)
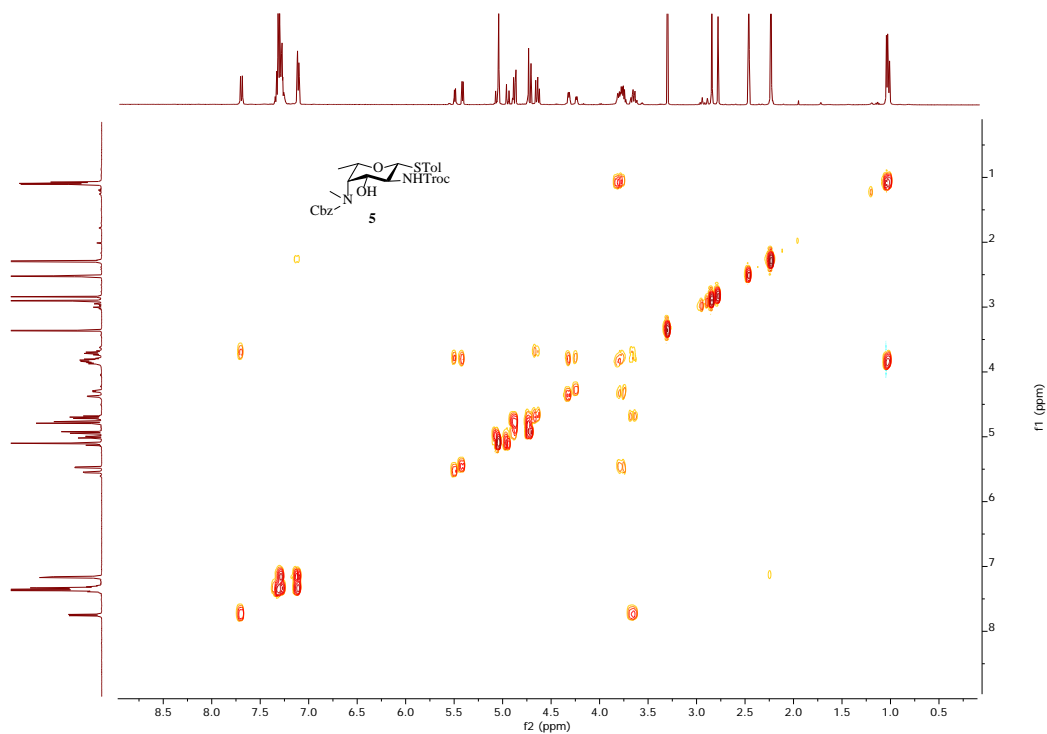
Figure 2.59. ^{1}H-^{1}H gCOSY of **5** (500 MHz d^6-DMSO)
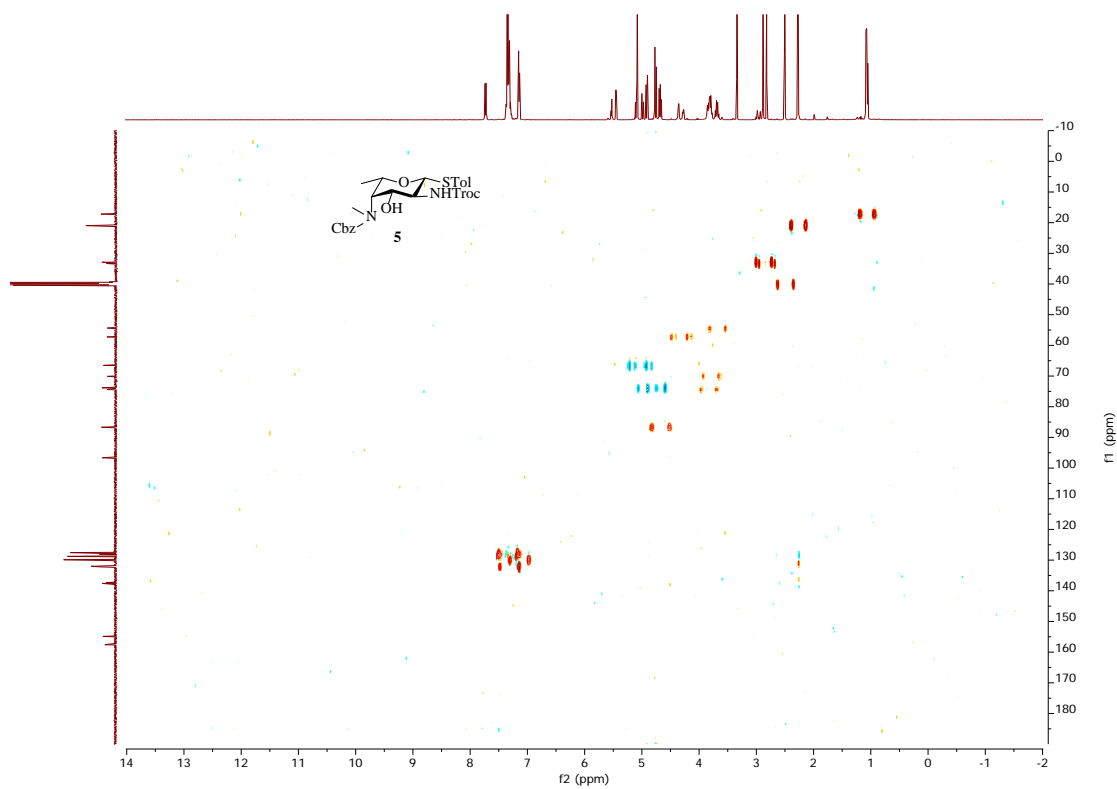
Figure 2.60. ^{1}H-^{13}C gHSQCAD of **5** (500 MHz d^{6}-DMSO)
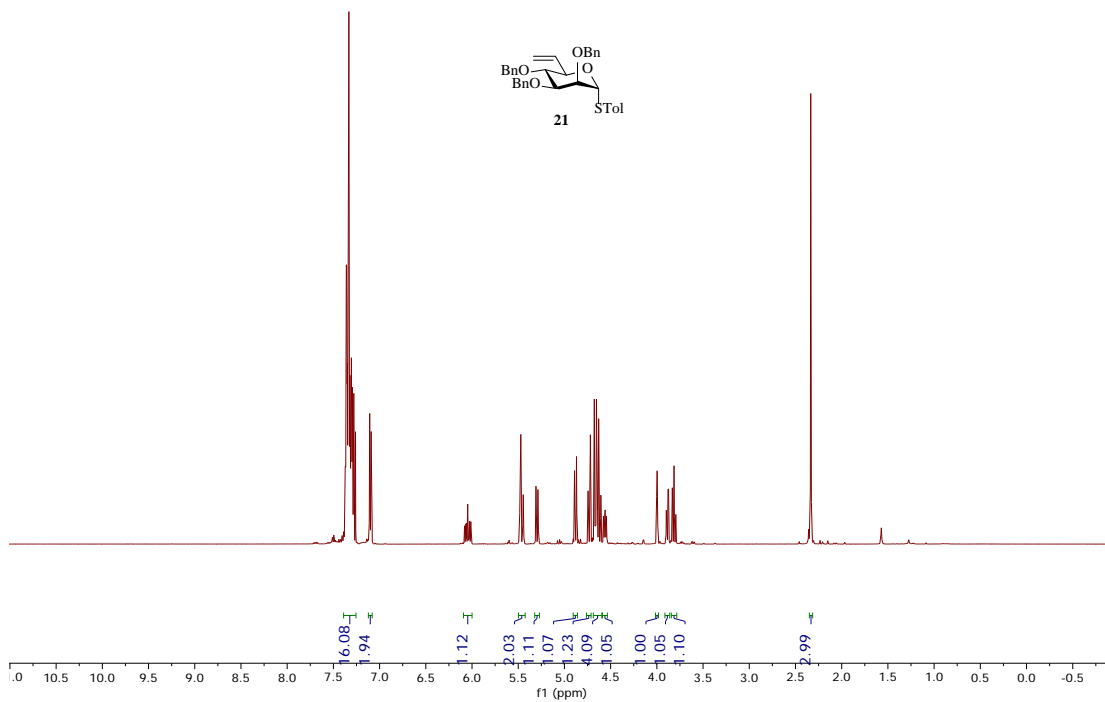
Figure 2.61. ^{1}H-NMR of **21** (500 MHz CDCl$_3$)
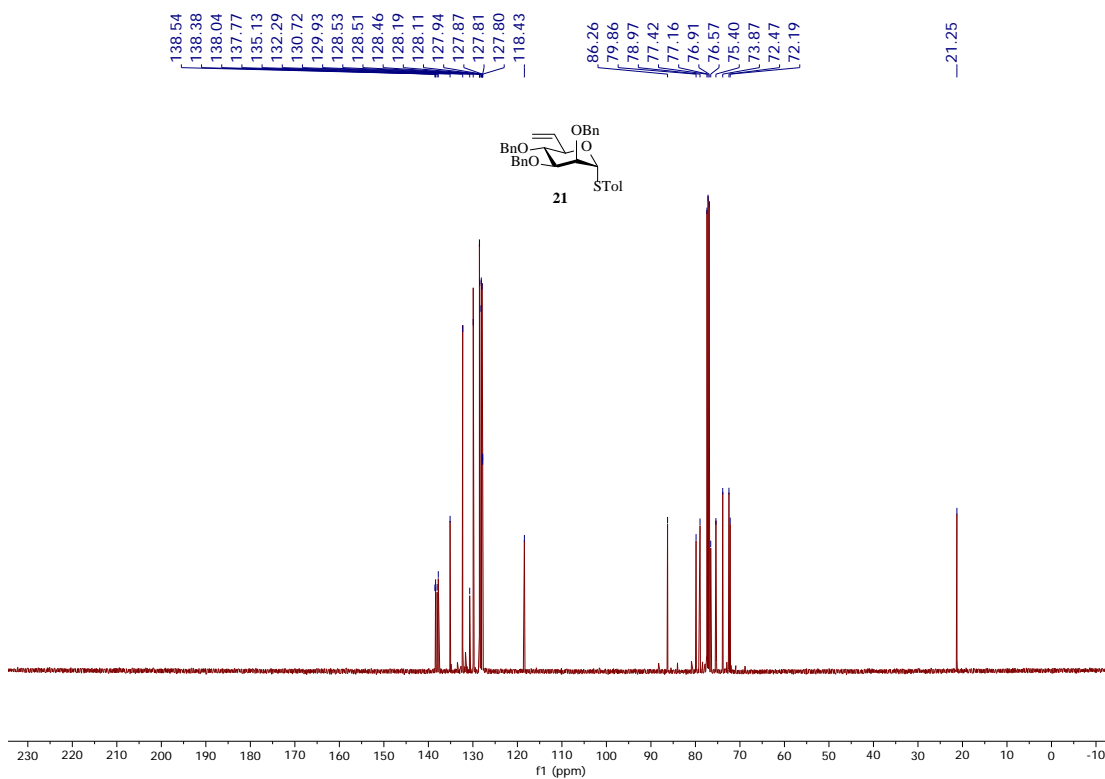
Figure 2.62. ^{13}C-NMR of **21** (125 MHz CDCl$_3$)
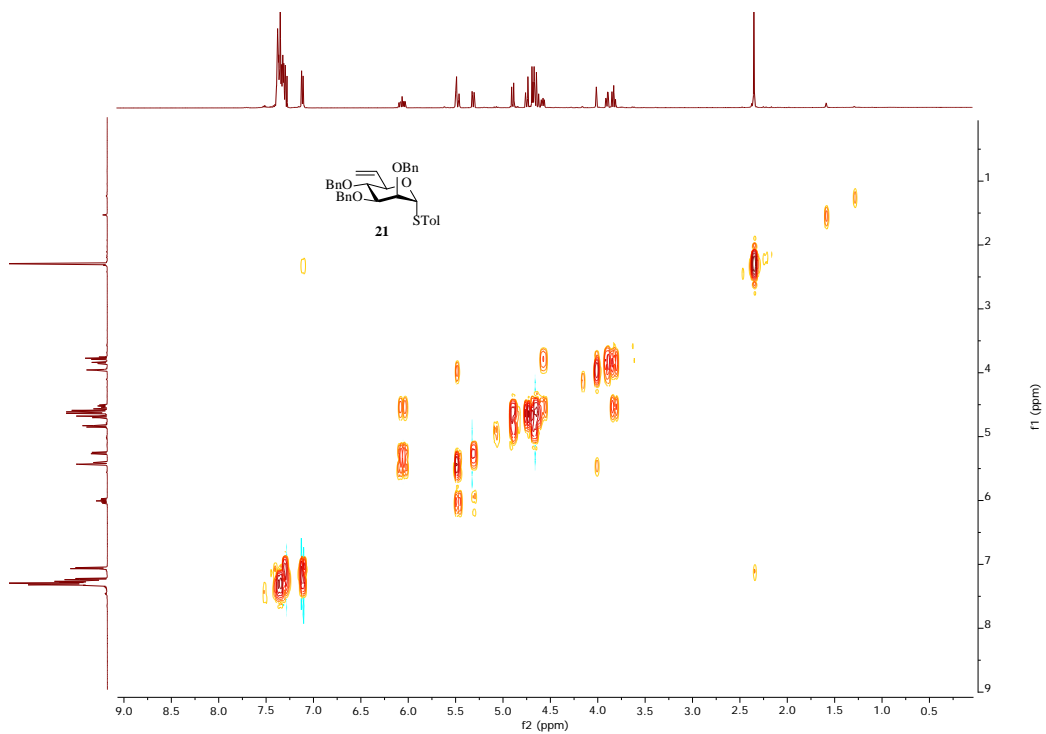
Figure 2.63. ^{1}H-^{1}H gCOSY of **21** (500 MHz CDCl$_3$)
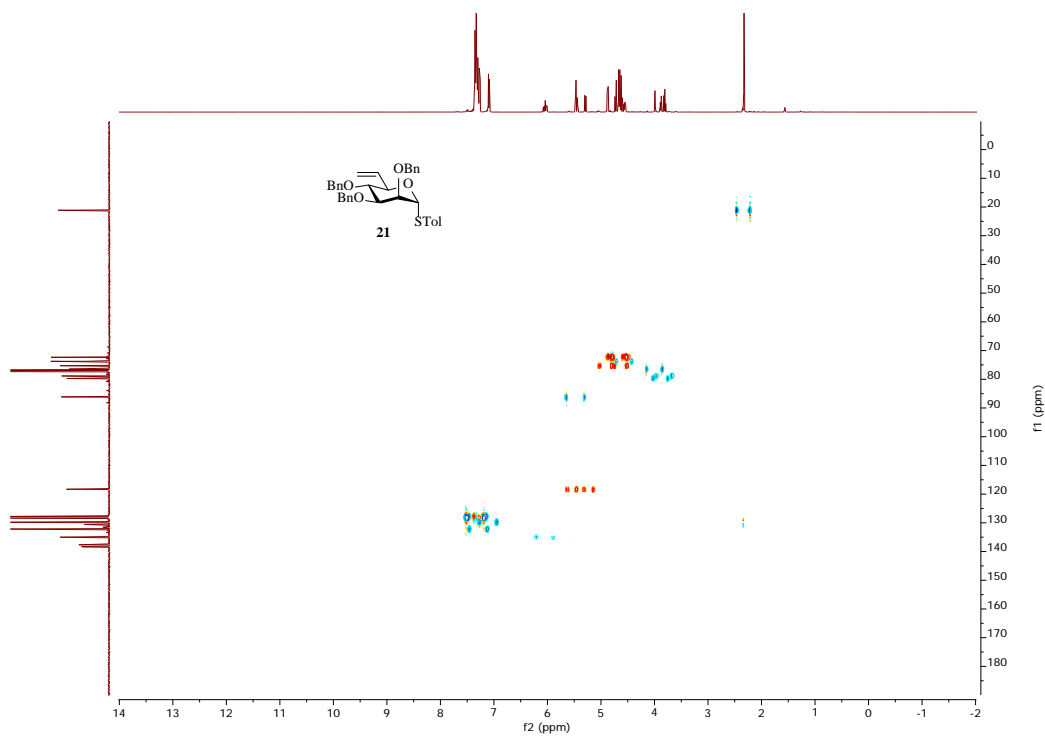
Figure 2.64. ^{1}H-^{13}C gHSQCAD of **21** (500 MHz CDCl$_3$)
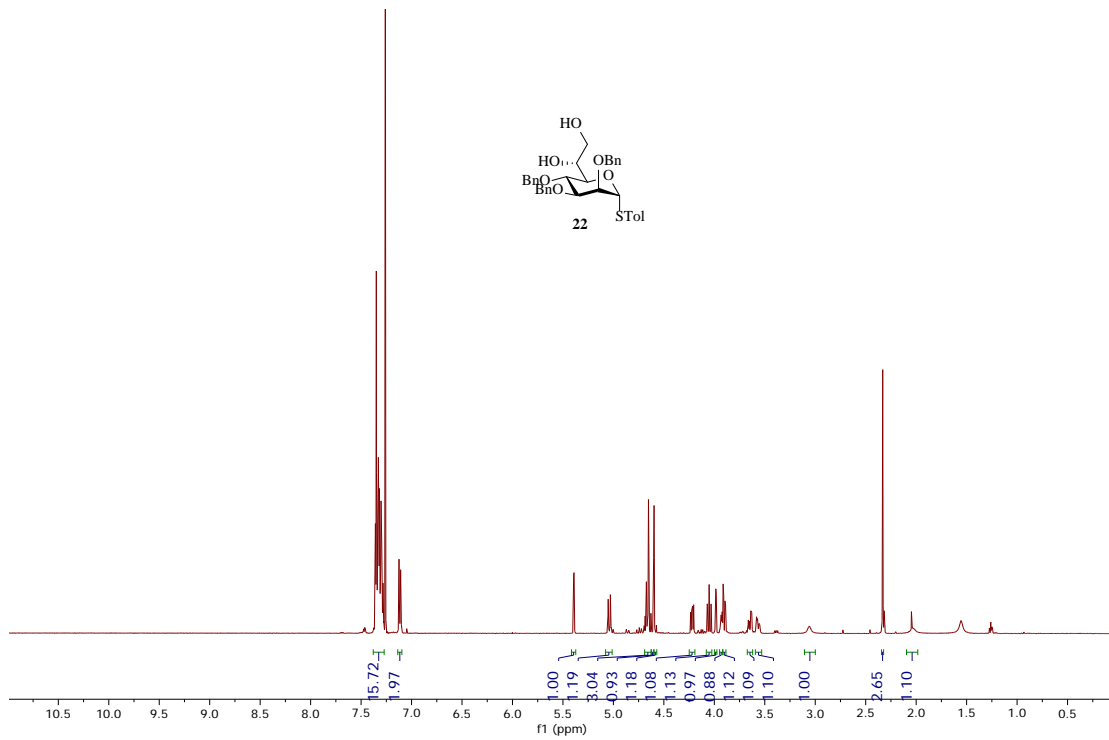
Figure 2.65. ^{1}H-NMR of **22** (500 MHz CDCl$_3$)
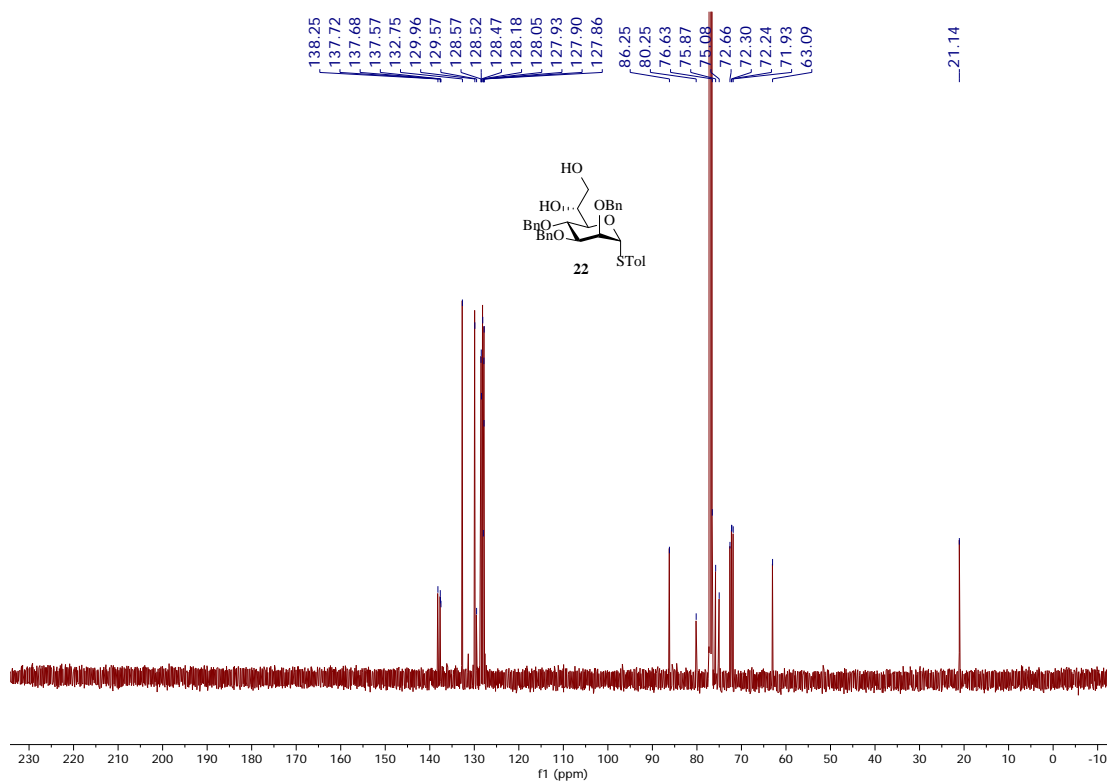
Figure 2.66. ^{13}C-NMR of **22** (125 MHz CDCl$_3$)
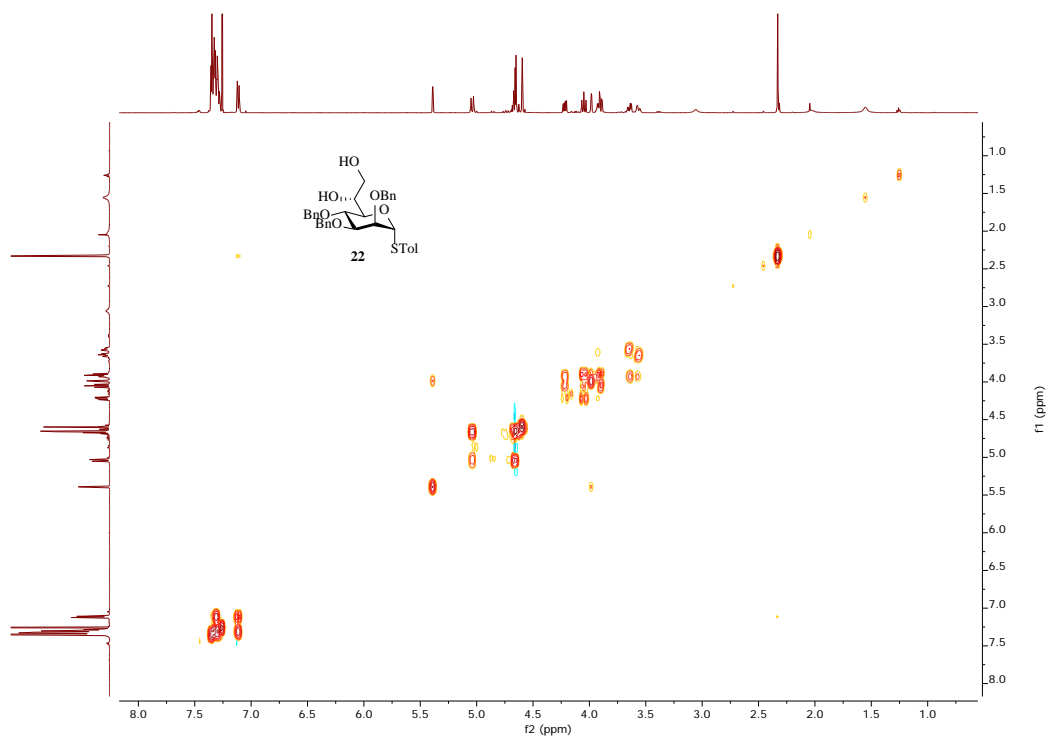
Figure 2.67. ^{1}H-^{1}H gCOSY of **22** (500 MHz CDCl$_3$)
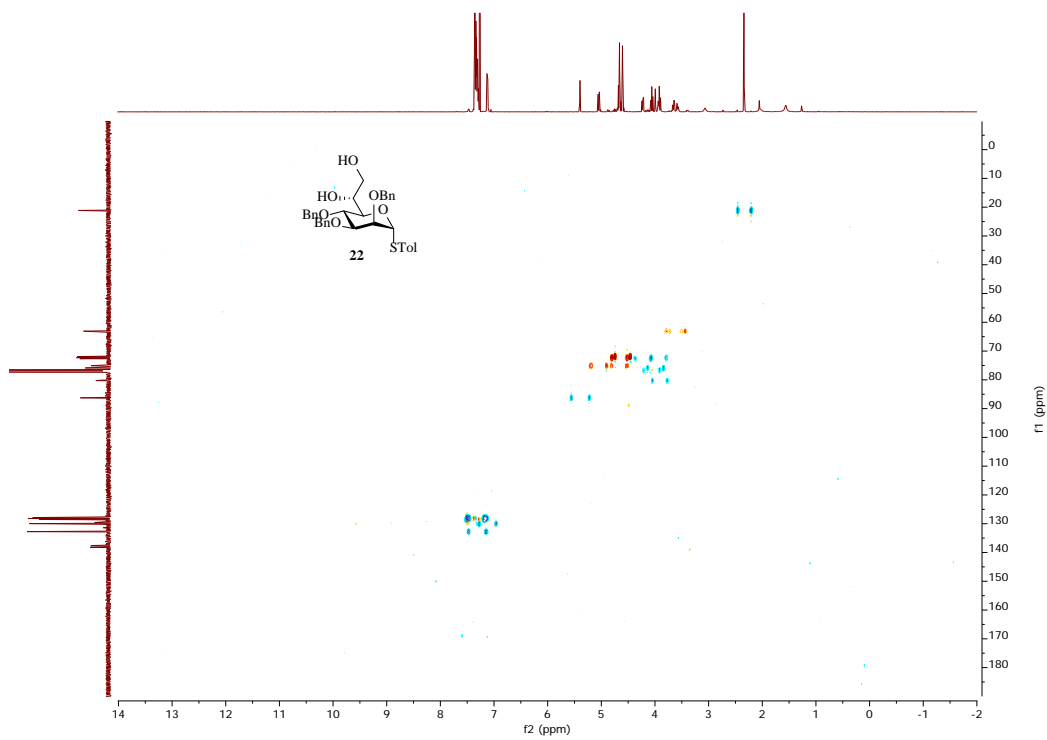
Figure 2.68. ^{1}H-^{13}C gHSQCAD of **22** (500 MHz CDCl$_3$)
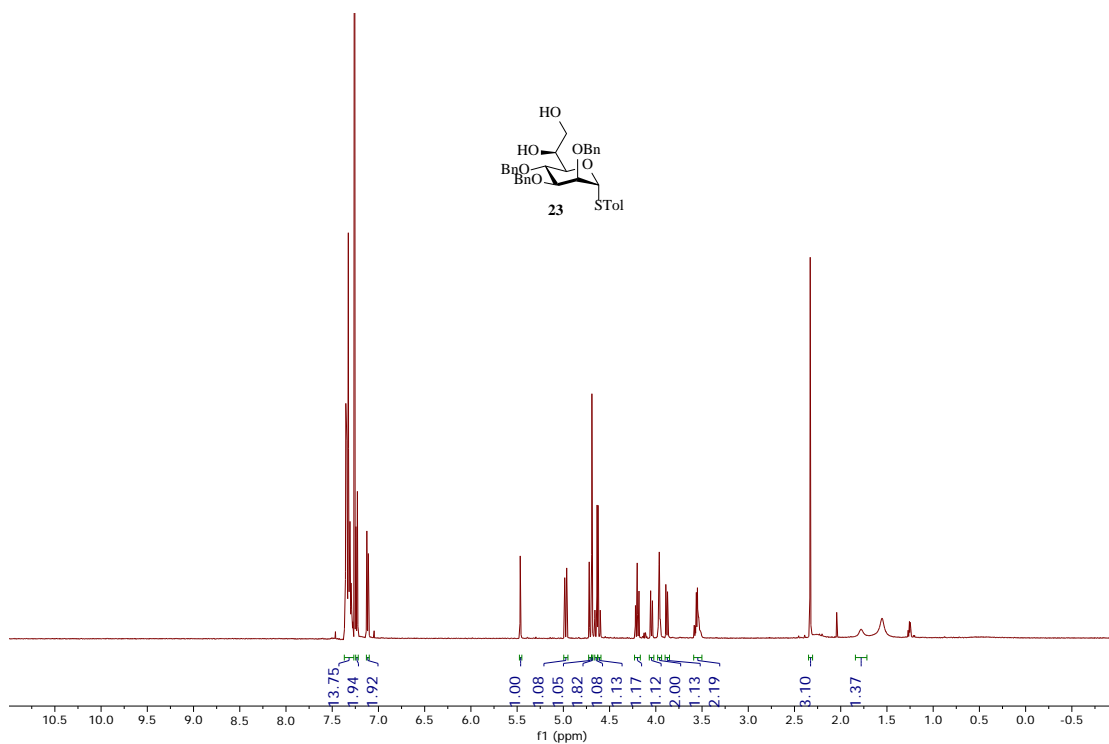
Figure 2.69. ^{1}H-NMR of **23** (500 MHz CDCl$_3$)
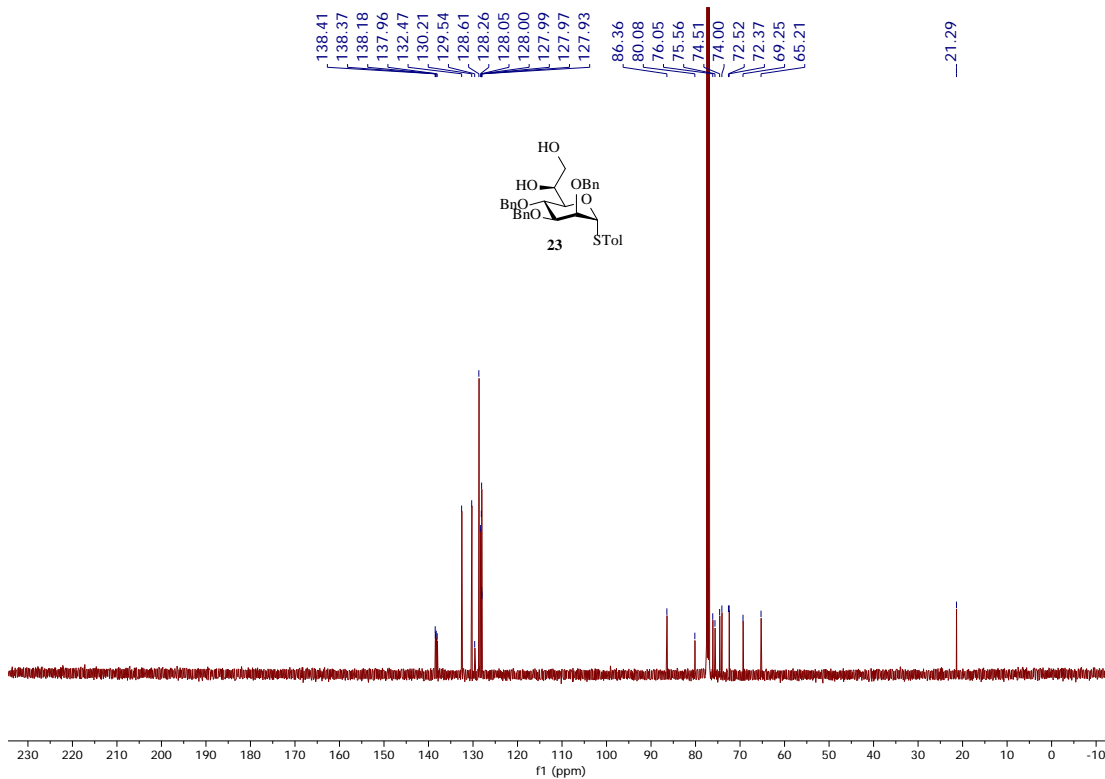
Figure 2.70. ^{13}C-NMR of **23** (125 MHz CDCl$_3$)

141
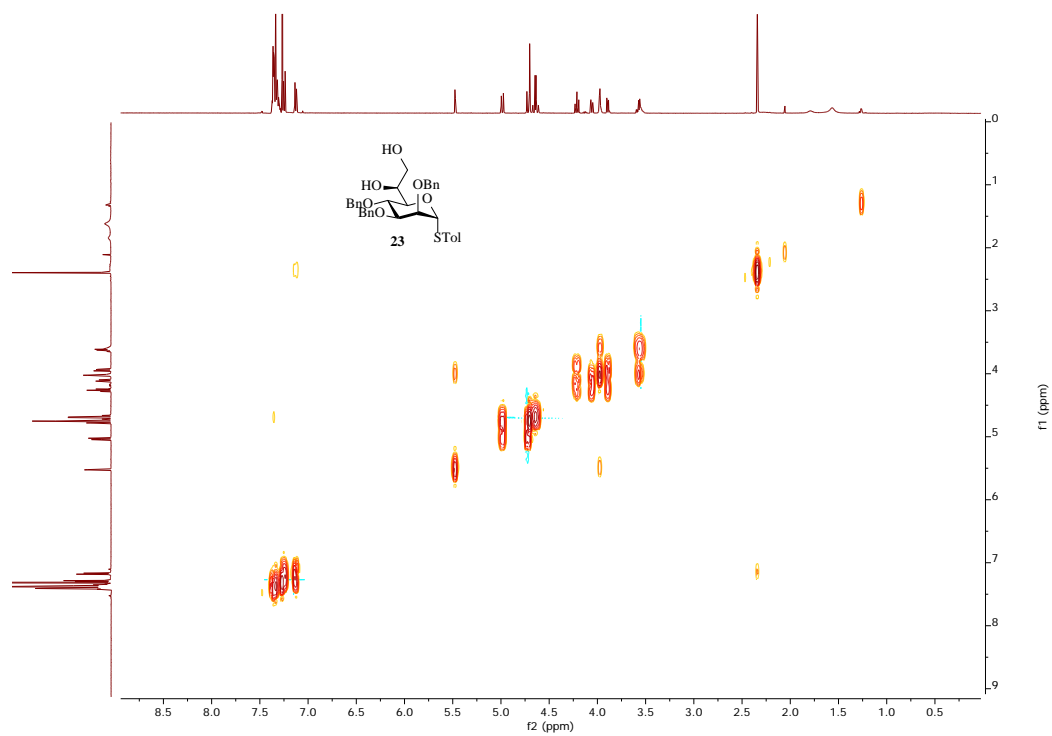
Figure 2.71. ^{1}H-^{1}H gCOSY of **23** (500 MHz CDCl$_3$)
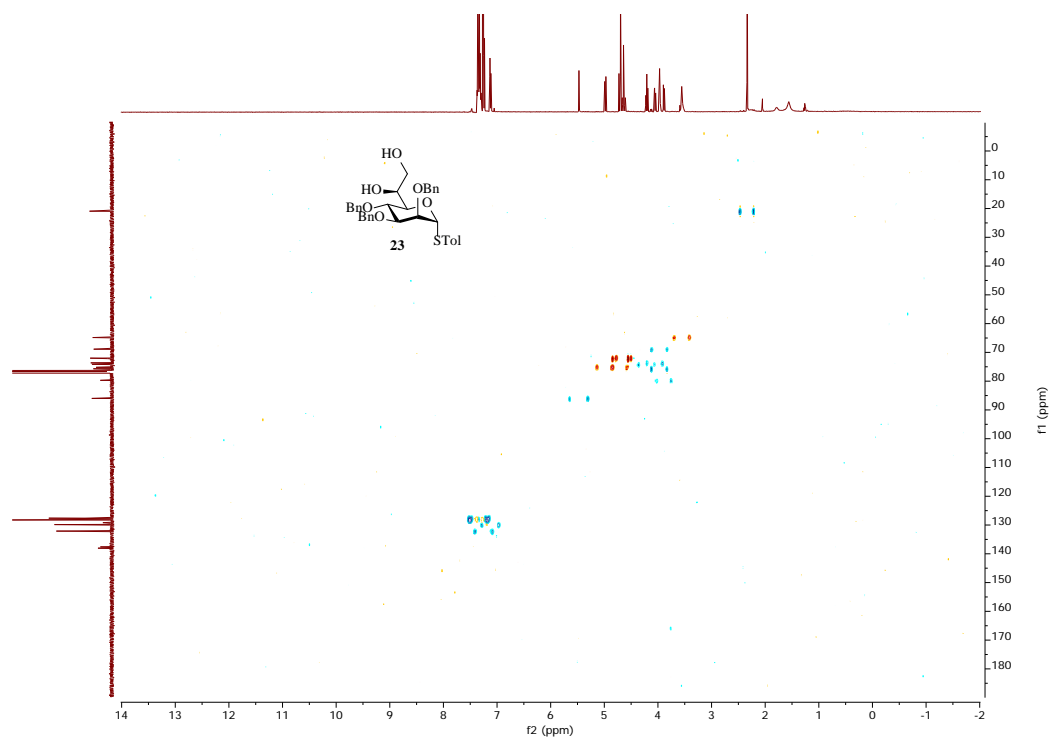
Figure 2.72. ^{1}H-^{13}C gHSQCAD of **23** (500 MHz CDCl$_3$)
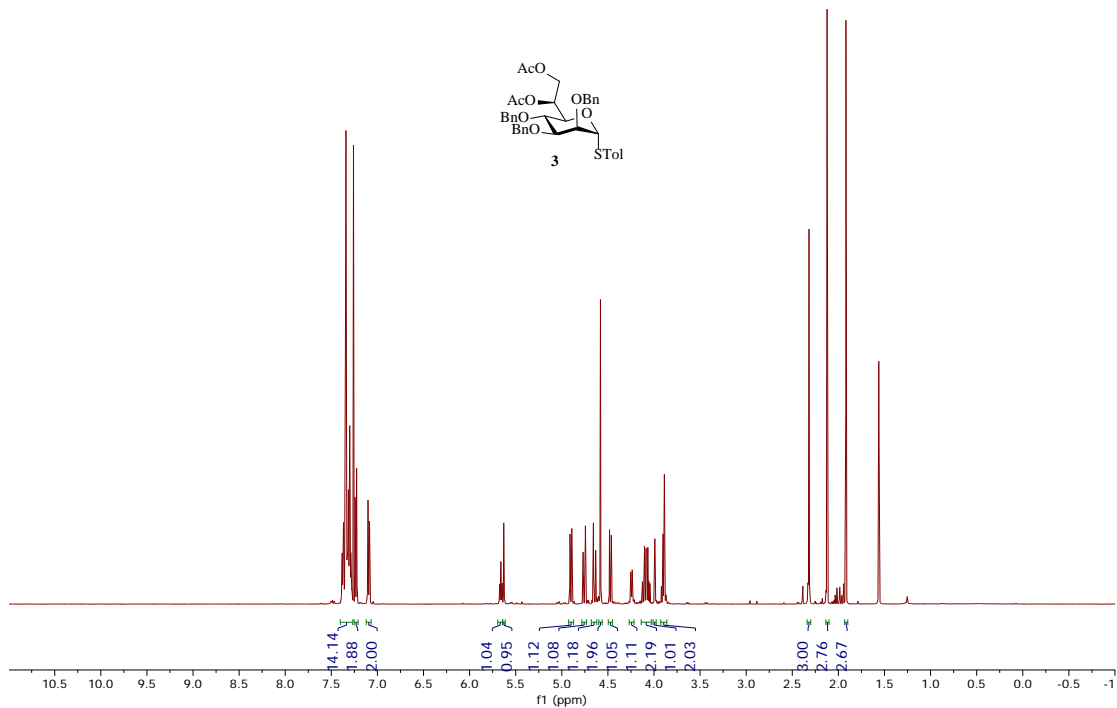
Figure 2.73. ^{1}H-NMR of **3** (500 MHz CDCl$_3$)
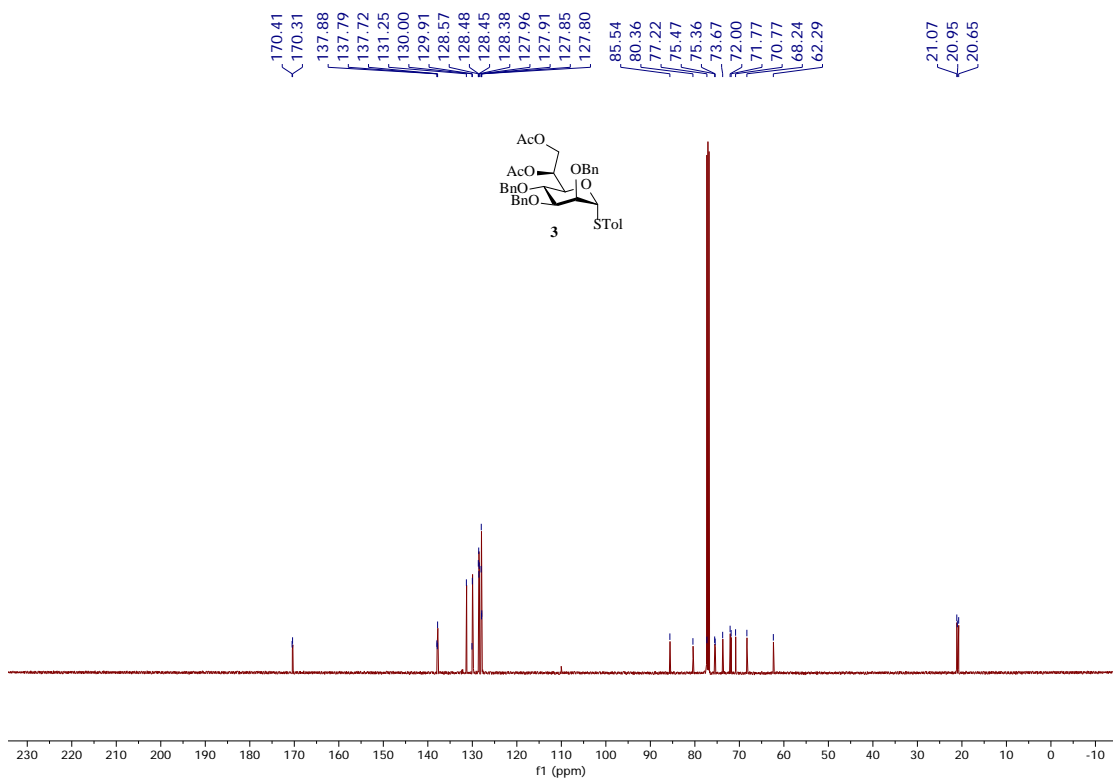
Figure 2.74. ^{13}C-NMR of **3** (125 MHz CDCl$_3$)

143
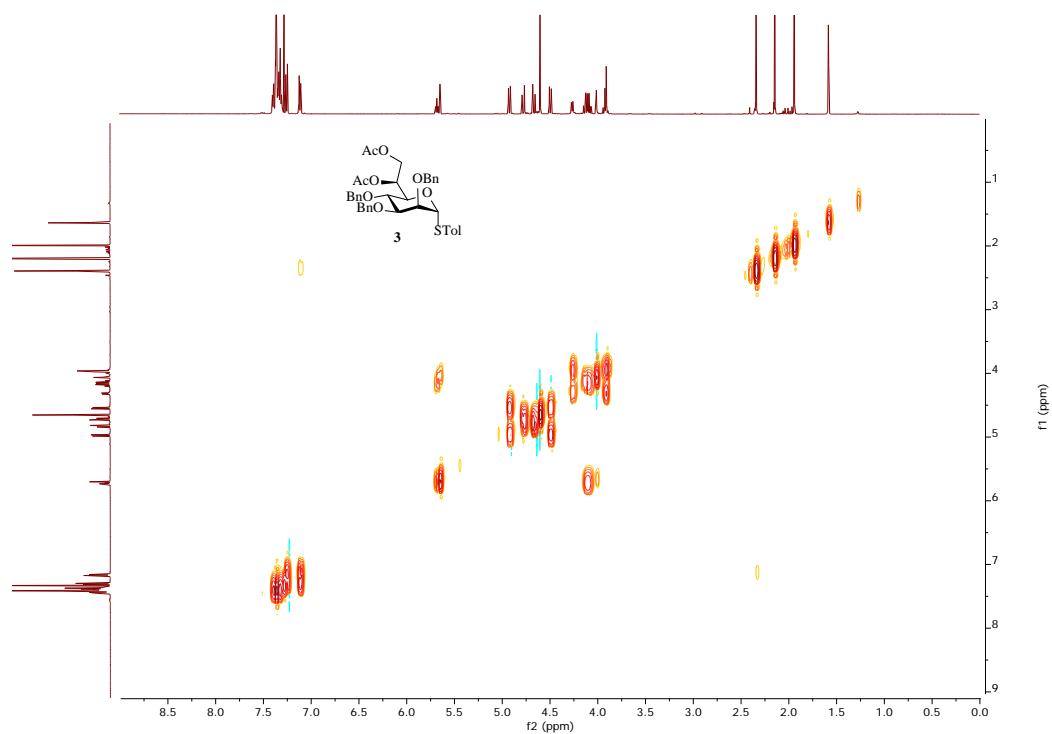
Figure 2.75. ^{1}H-^{1}H gCOSY of **3** (500 MHz CDCl$_3$)
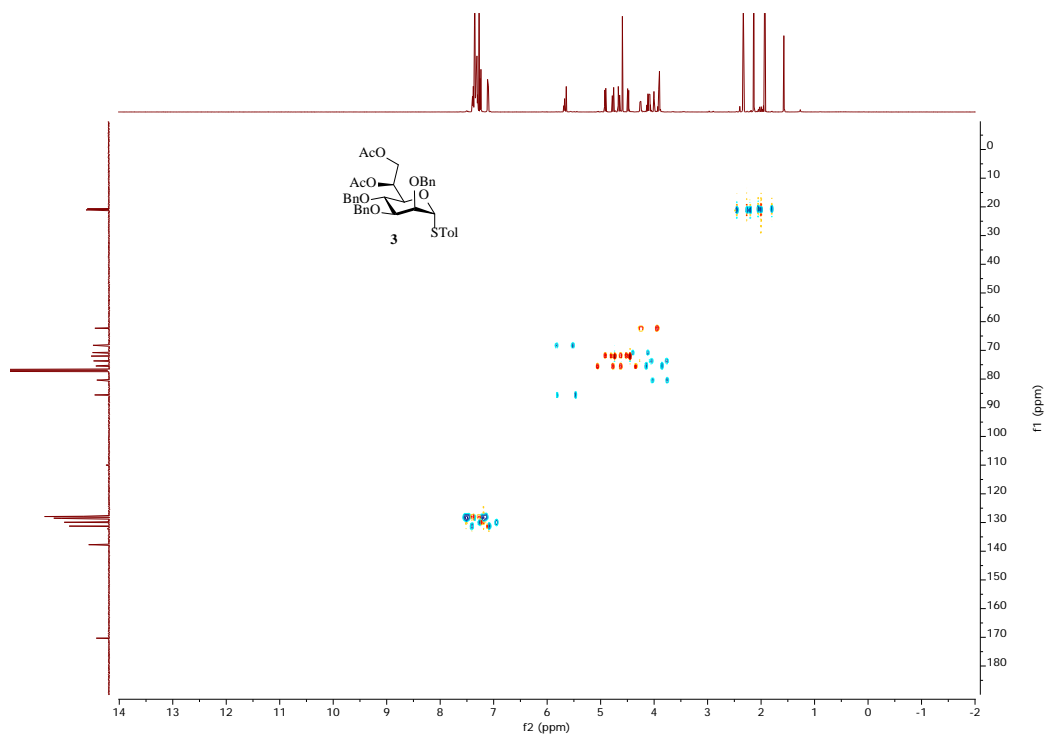
Figure 2.76. ^{1}H-^{13}C gHSQCAD of **3** (500 MHz CDCl$_3$)
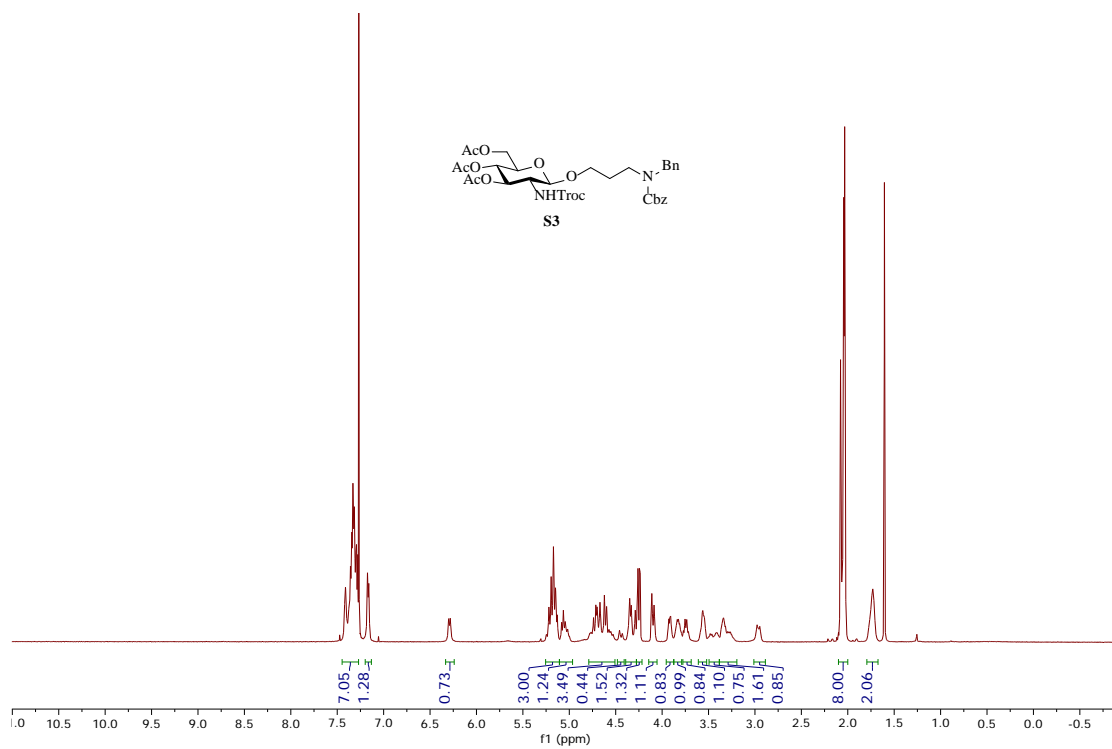
Figure 2.77. ^{1}H-NMR of **S3** (500 MHz CDCl$_3$)
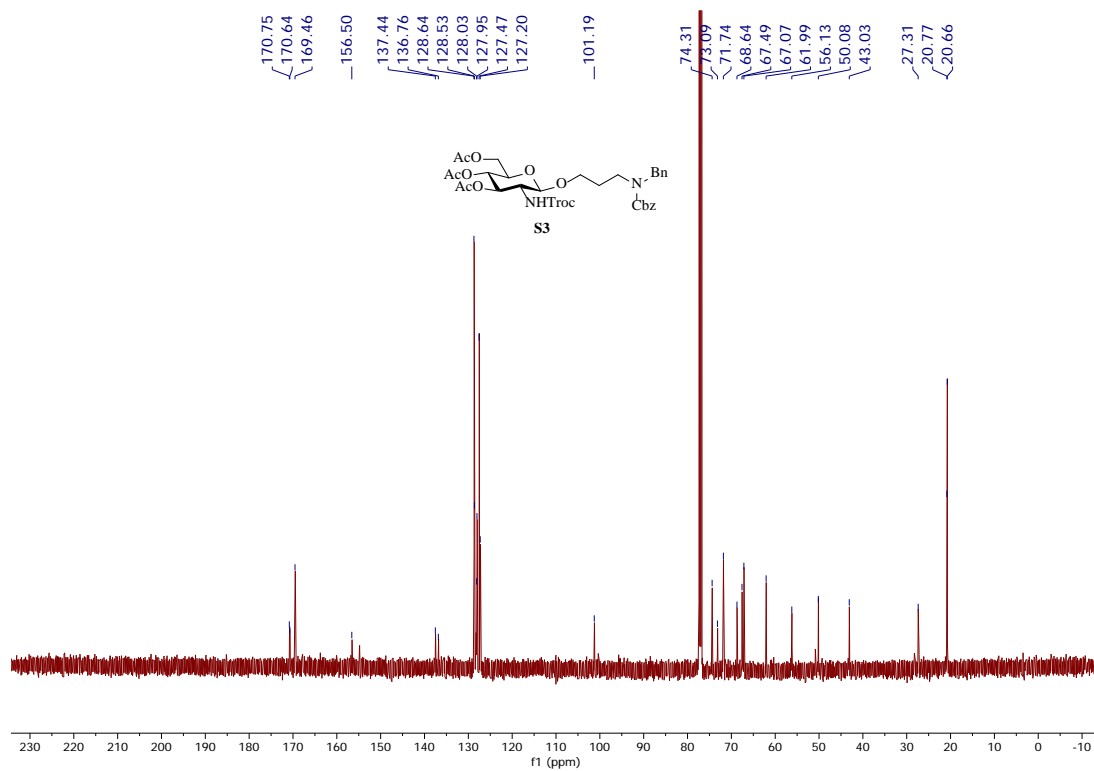
Figure 2.78. ^{13}C-NMR of **S3** (125 MHz CDCl$_3$)
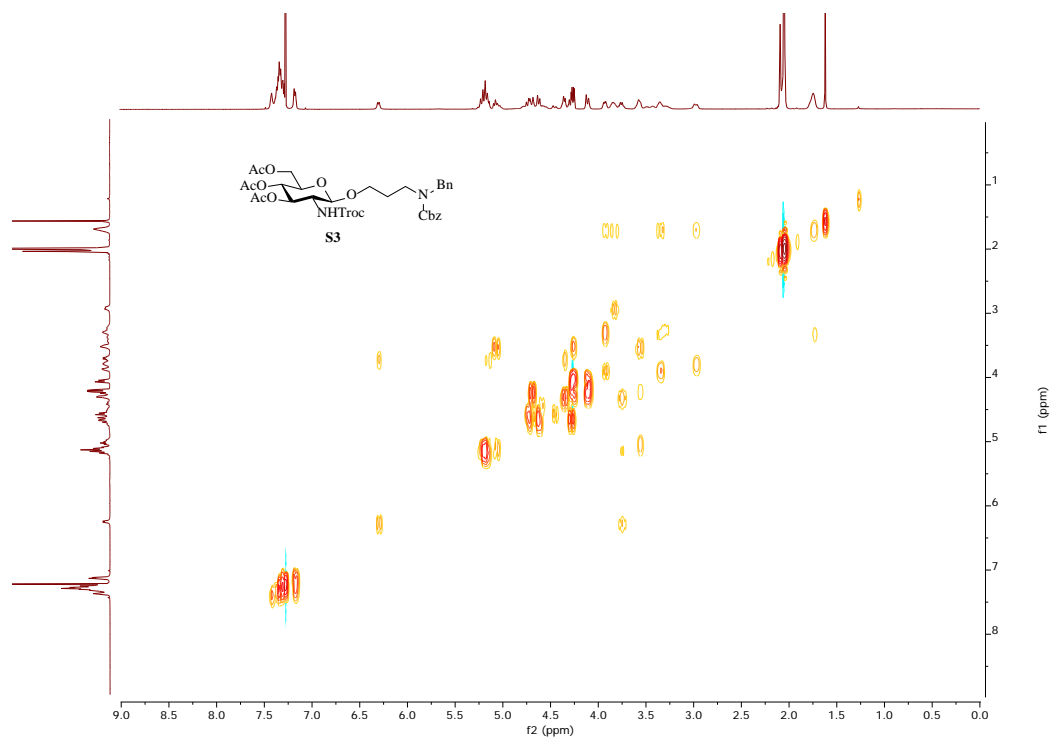
Figure 2.79. ^{1}H-^{1}H gCOSY of **S3** (500 MHz CDCl$_3$)
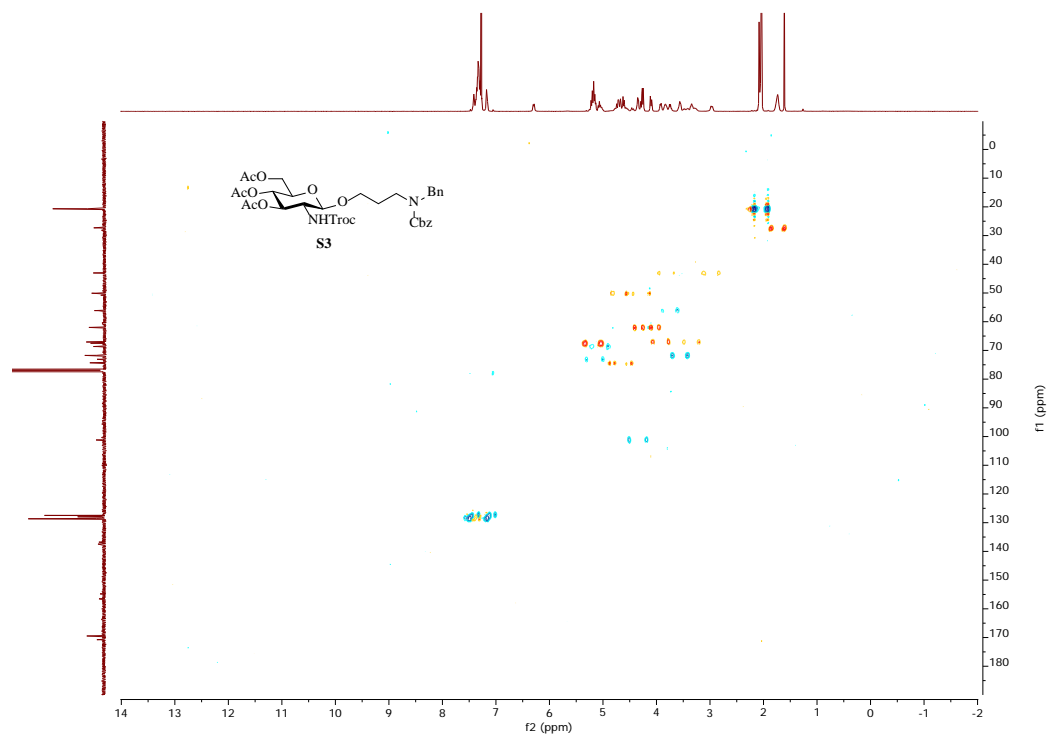
Figure 2.80. ^{1}H-^{13}C gHSQCAD of **S3** (500 MHz CDCl$_3$)

Figure 2.81. ^{1}H-NMR of **S4** (500 MHz CDCl$_3$)
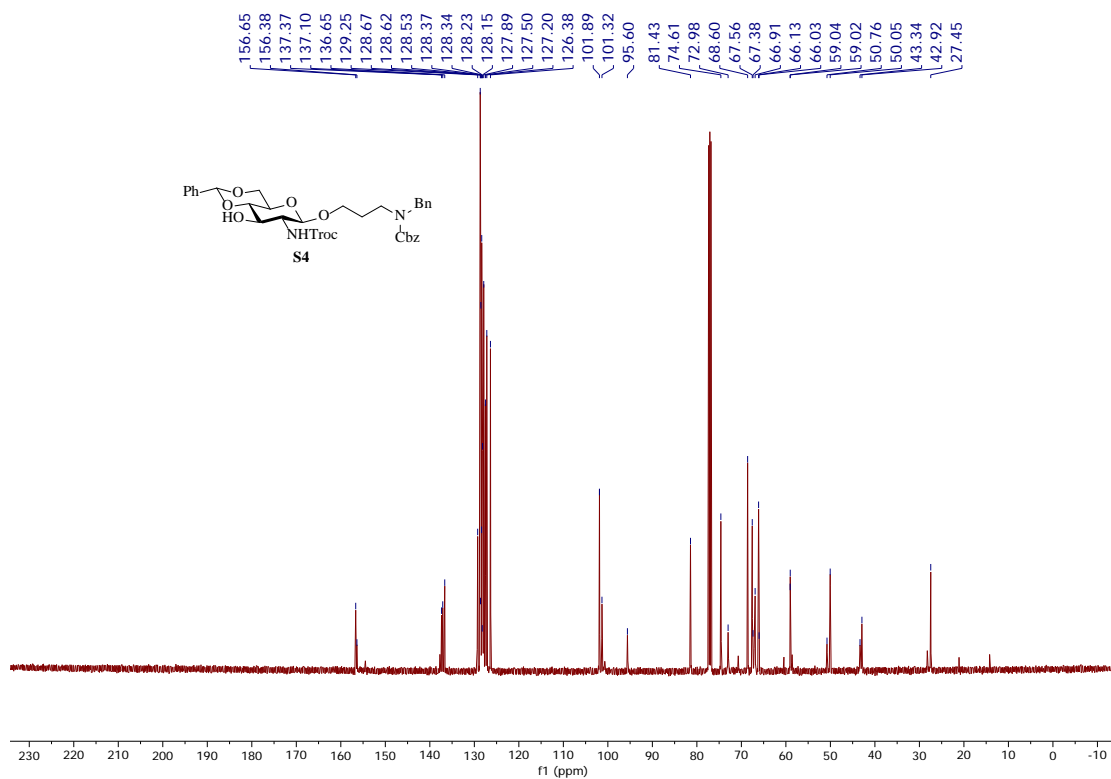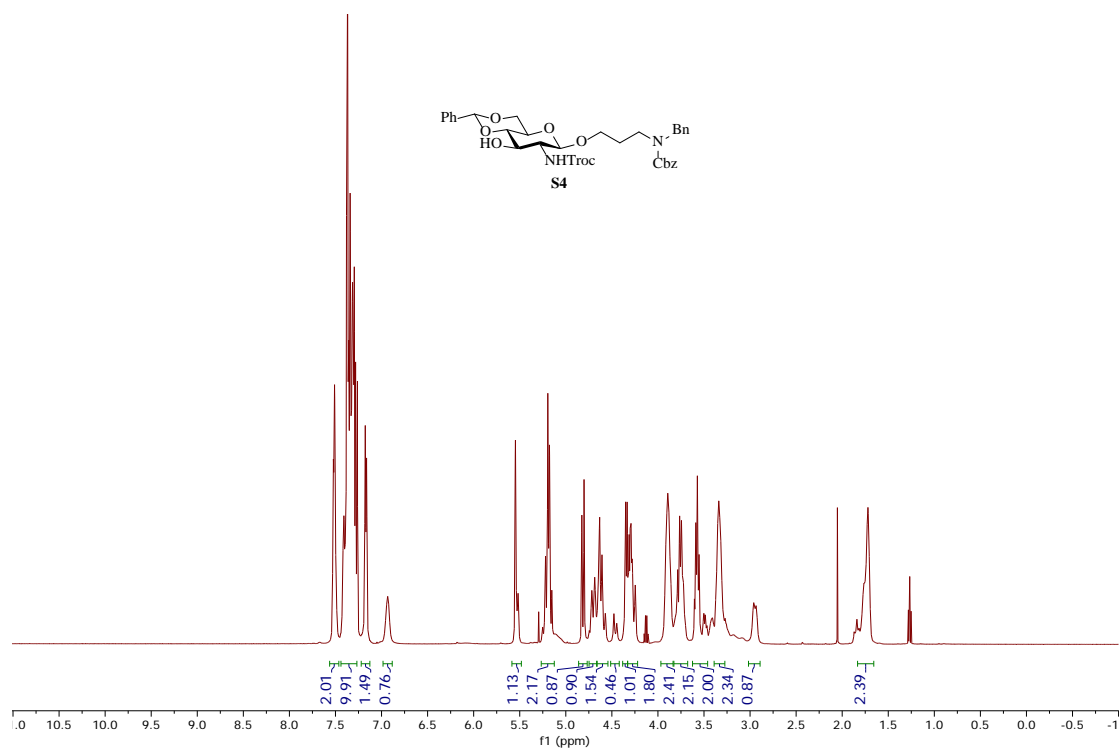
Figure 2.82. ^{13}C-NMR of **S4** (125 MHz CDCl$_3$)
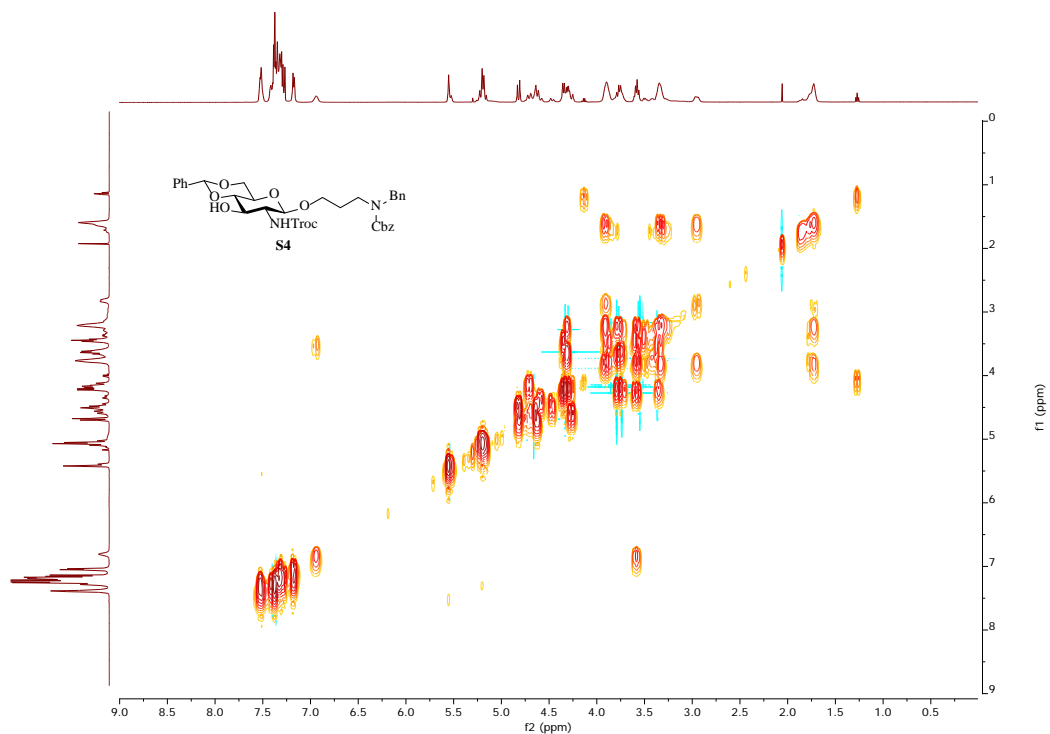
Figure 2.83. ^{1}H-^{1}H gCOSY of **S4** (500 MHz CDCl$_3$)
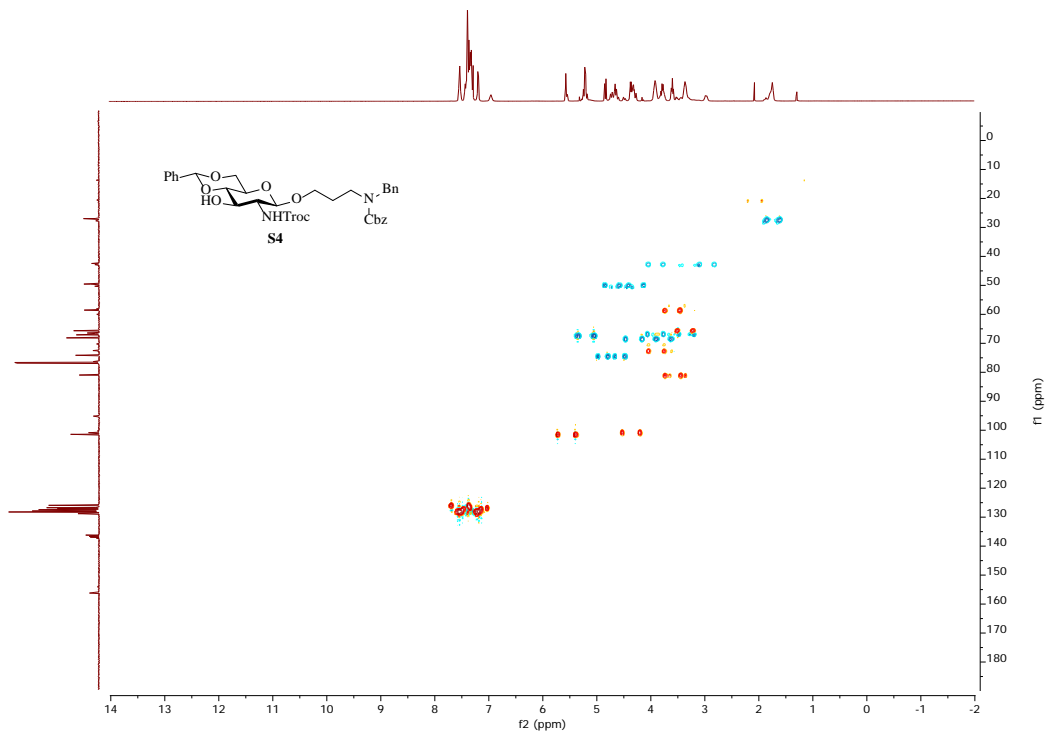
Figure 2.84. ^{1}H-^{13}C gHSQCAD of **S4** (500 MHz CDCl$_3$)
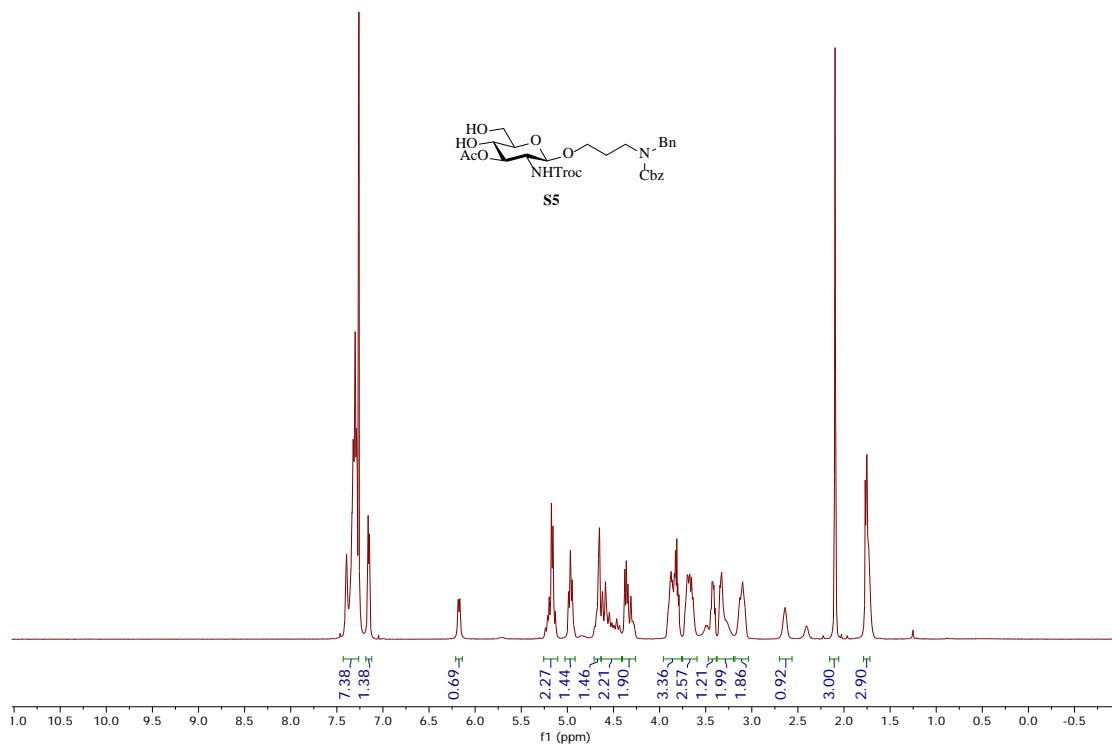
Figure 2.85. ^{1}H-NMR of **S5** (500 MHz CDCl$_3$)
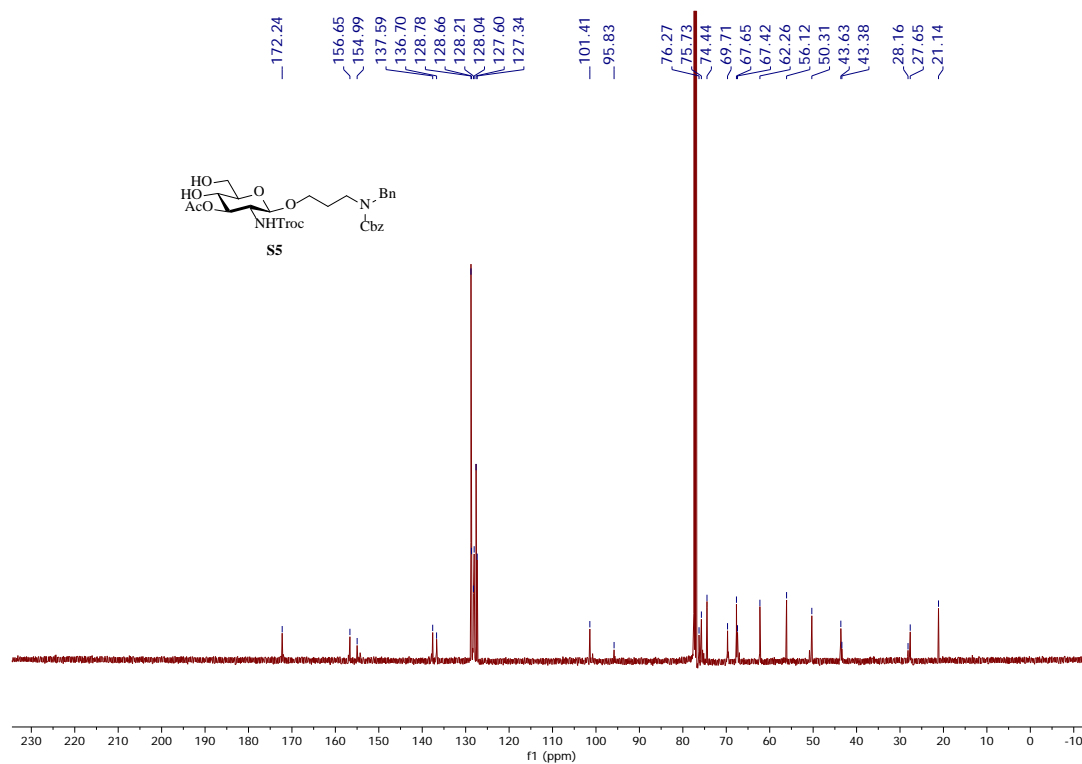
Figure 2.86. ^{13}C-NMR of **S5** (125 MHz CDCl$_3$)
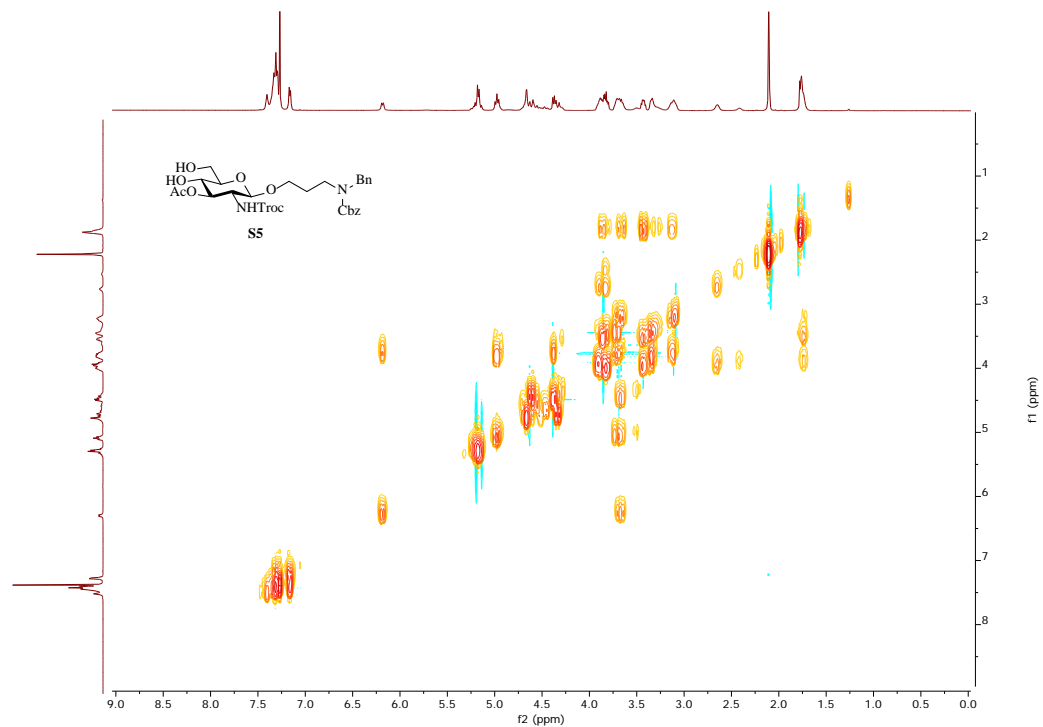
Figure 2.87. ^{1}H-^{1}H gCOSY of **S5** (500 MHz CDCl$_3$)
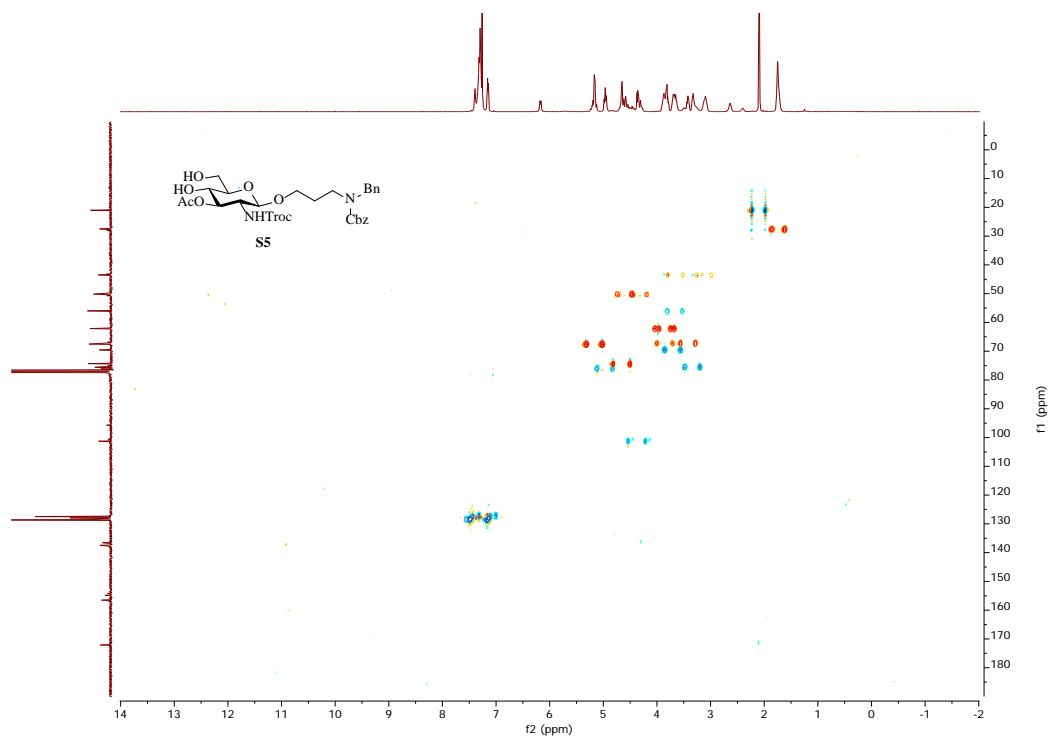
Figure 2.88. ^{1}H-^{13}C gHSQCAD of **S5** (500 MHz CDCl$_3$)
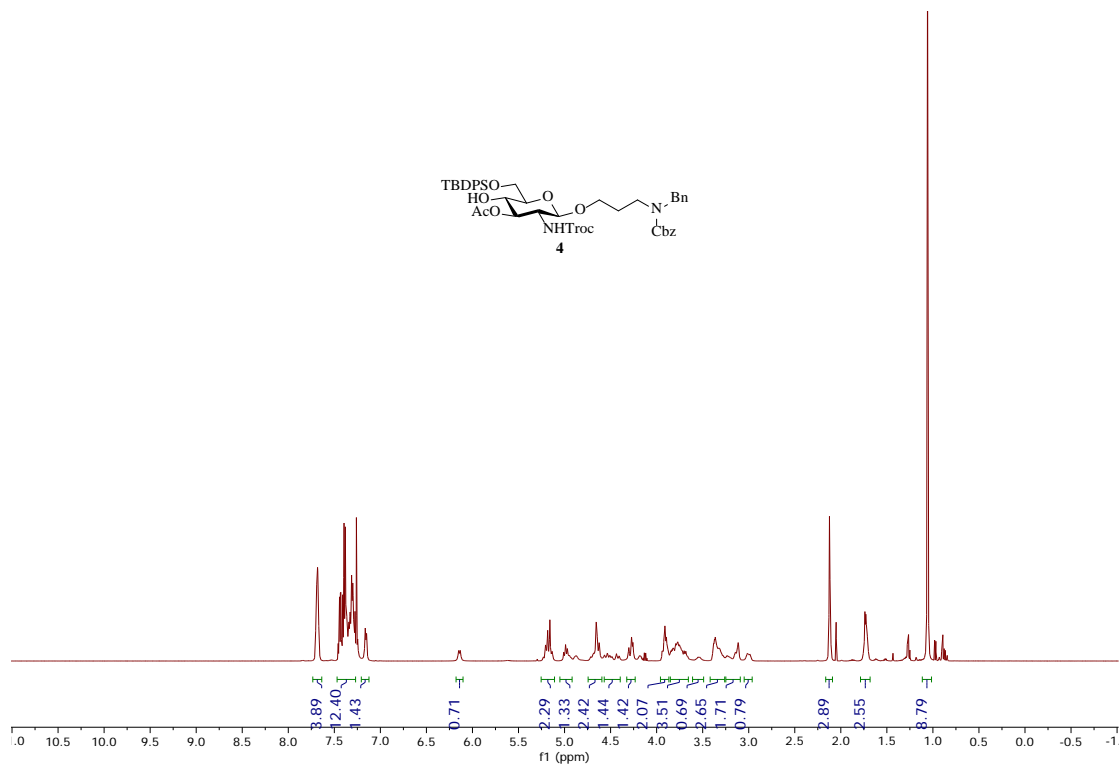
Figure 2.89. ^{1}H-NMR of **4** (500 MHz CDCl$_3$)
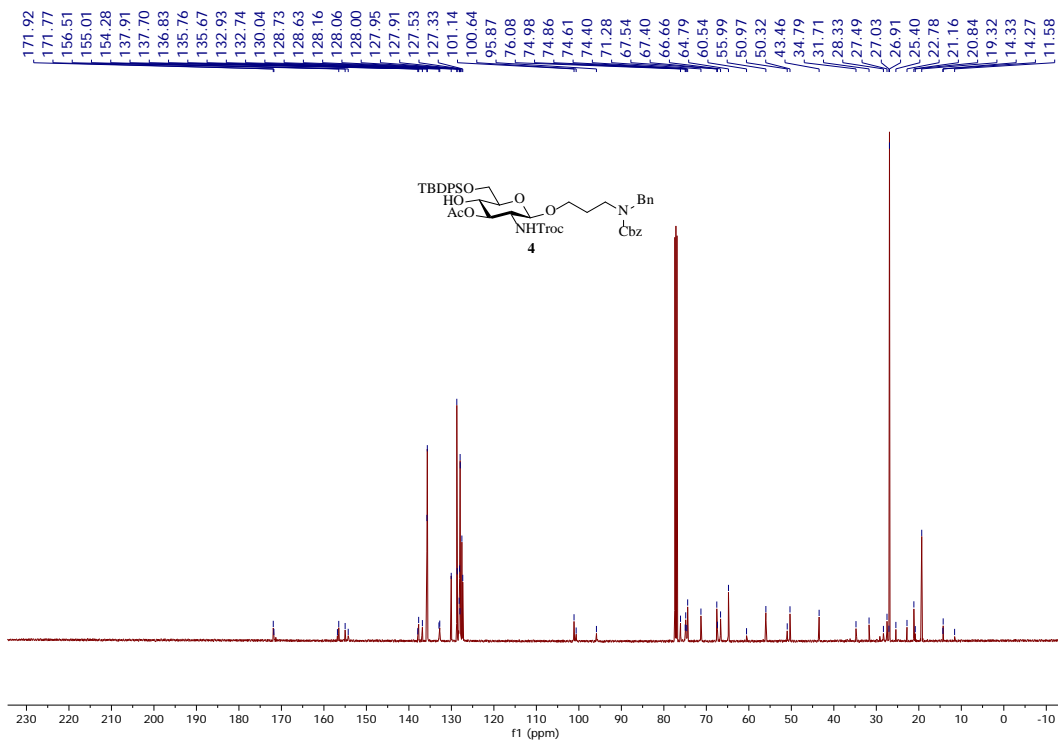
Figure 2.90. ^{13}C-NMR of **4** (125 MHz CDCl$_3$)
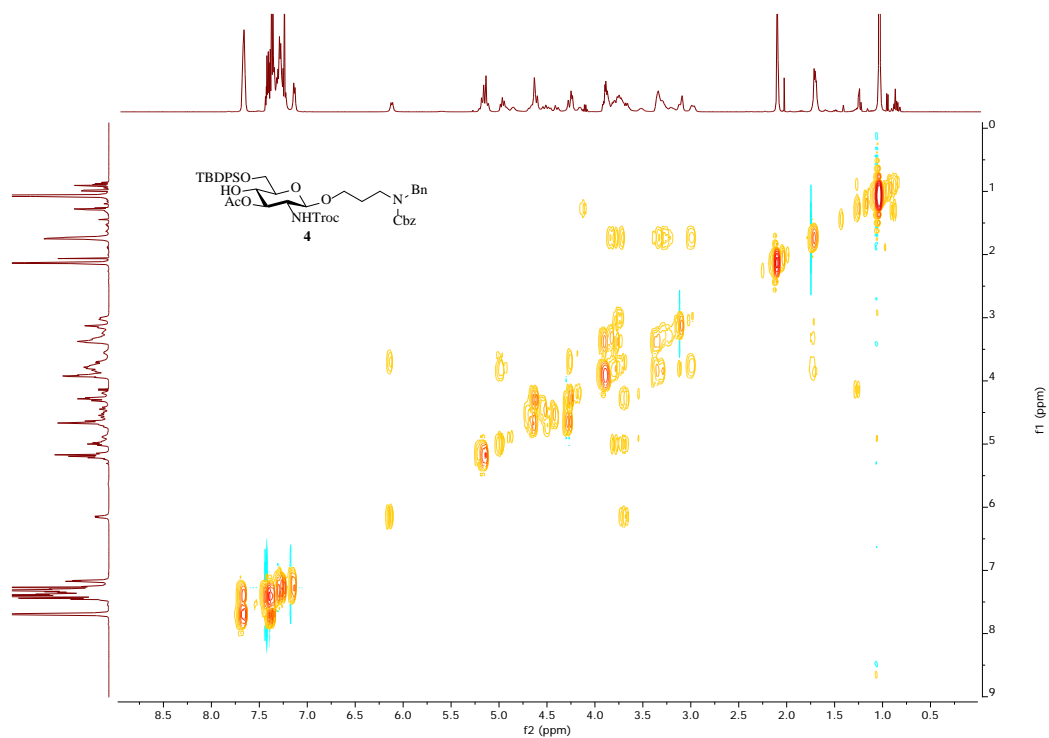
Figure 2.91. ^{1}H-^{1}H gCOSY of **4** (500 MHz CDCl$_3$)
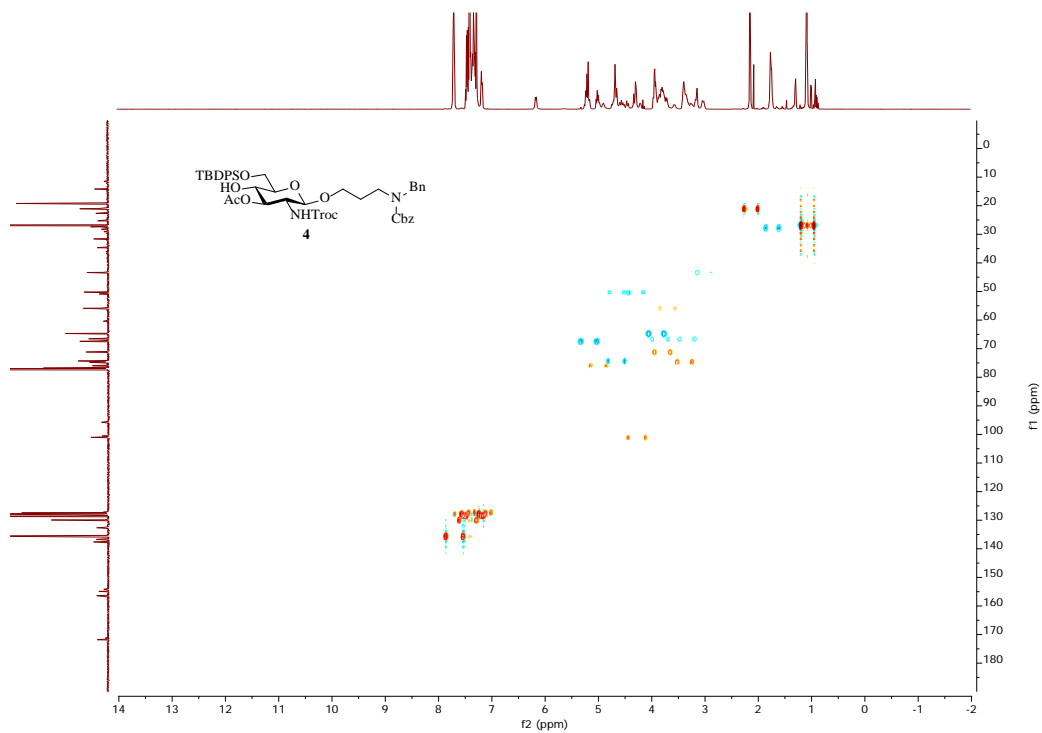
Figure 2.92. ^{1}H-^{13}C gHSQCAD of **4** (500 MHz CDCl$_3$)
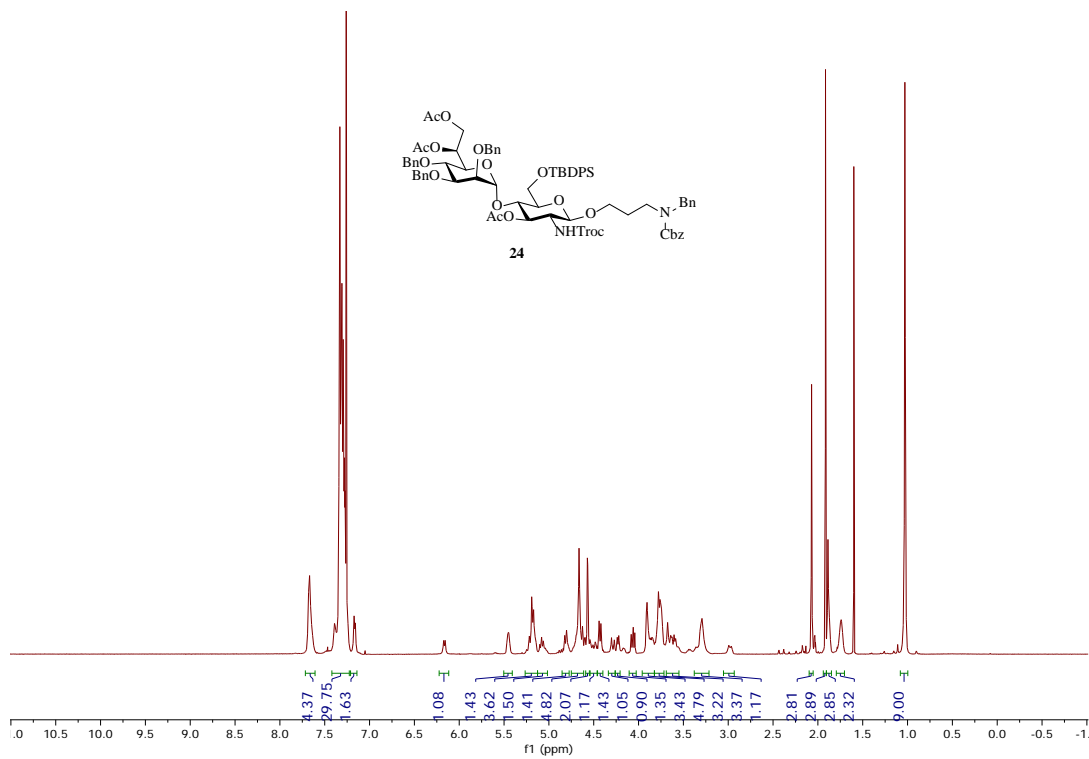
Figure 2.93. ^{1}H-NMR of **24** (500 MHz CDCl$_3$)
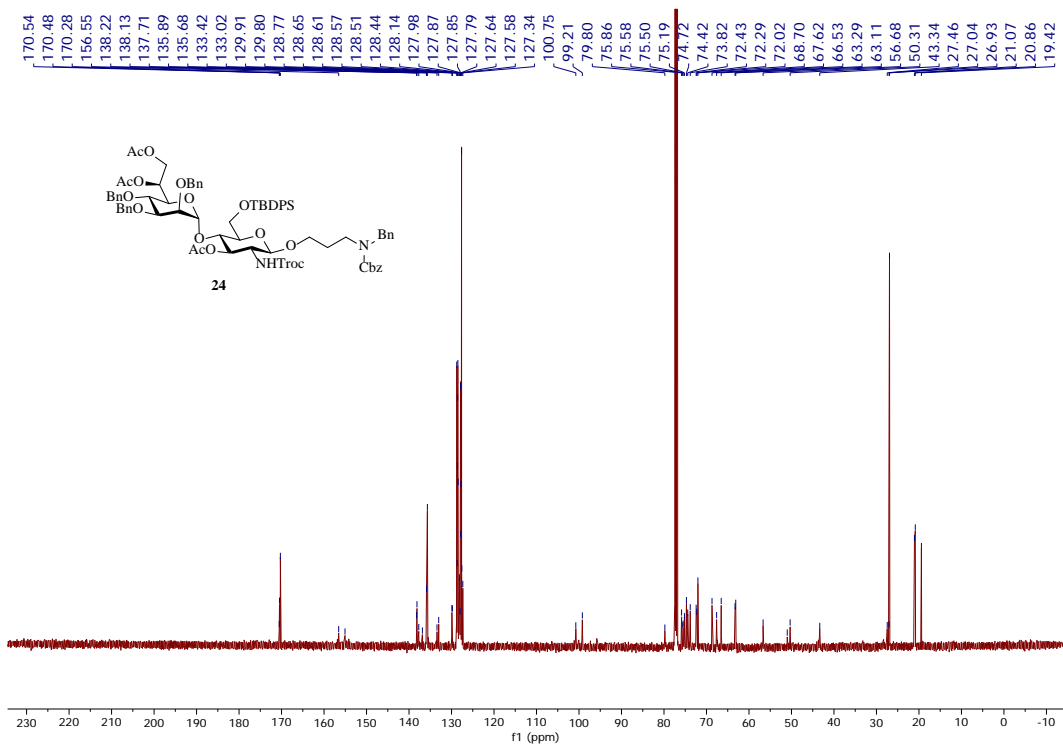
Figure 2.94. ^{13}C-NMR of **24** (125 MHz CDCl$_3$)
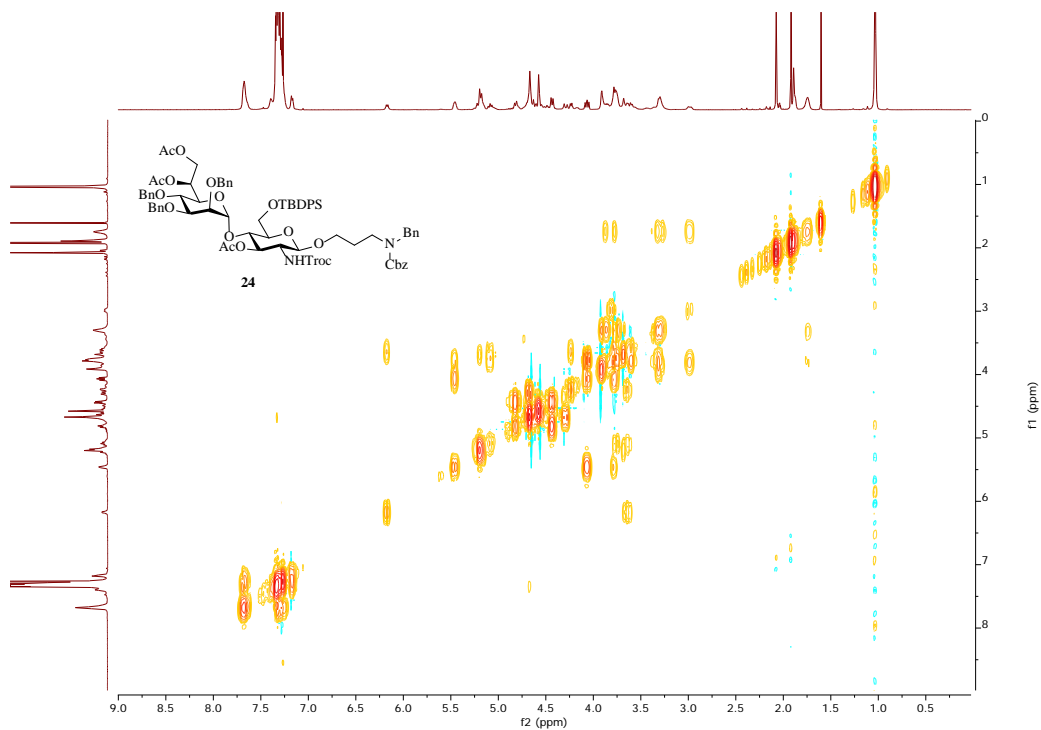
Figure 2.95. ^{1}H-^{1}H gCOSY of **24** (500 MHz CDCl$_3$)
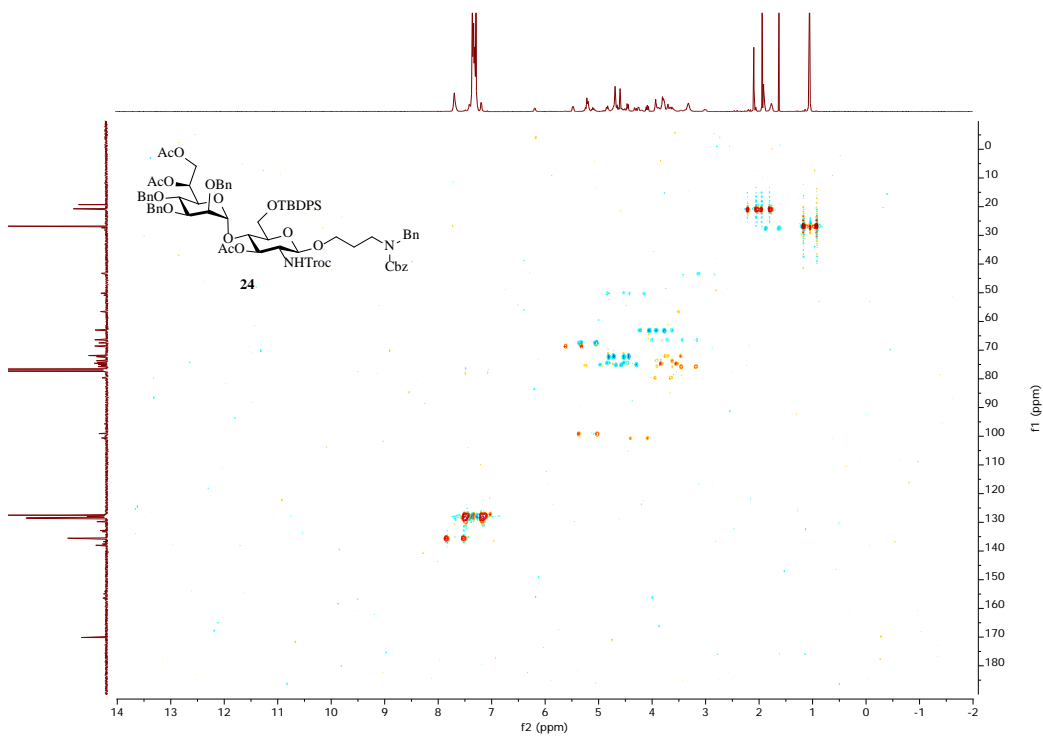
Figure 2.96. ^{1}H-^{13}C gHSQCAD of **24** (500 MHz CDCl$_3$)
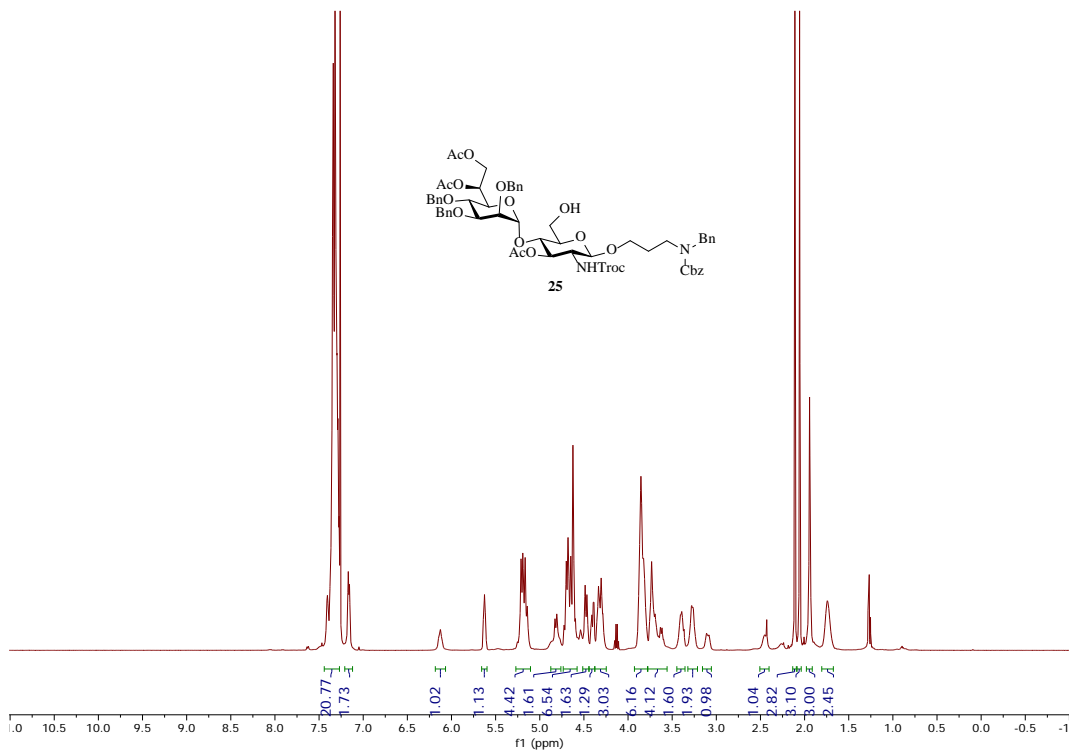
Figure 2.97. ^{1}H-NMR of **25** (500 MHz CDCl$_3$)
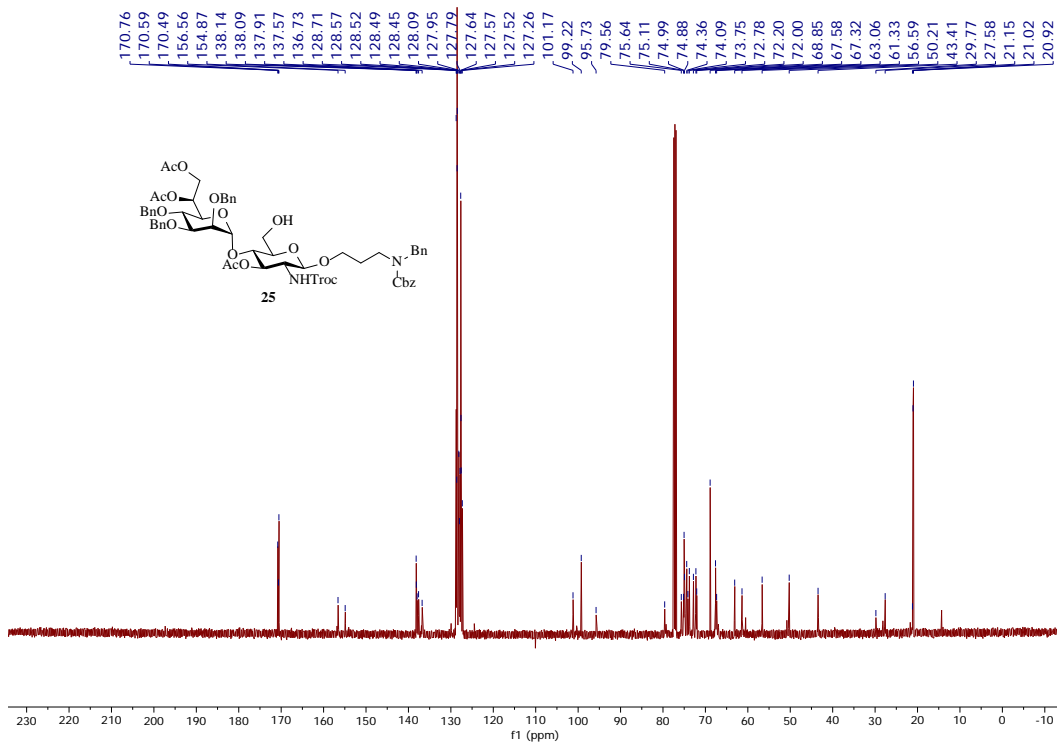
Figure 2.98. ^{13}C-NMR of **25** (125 MHz CDCl$_3$)

155
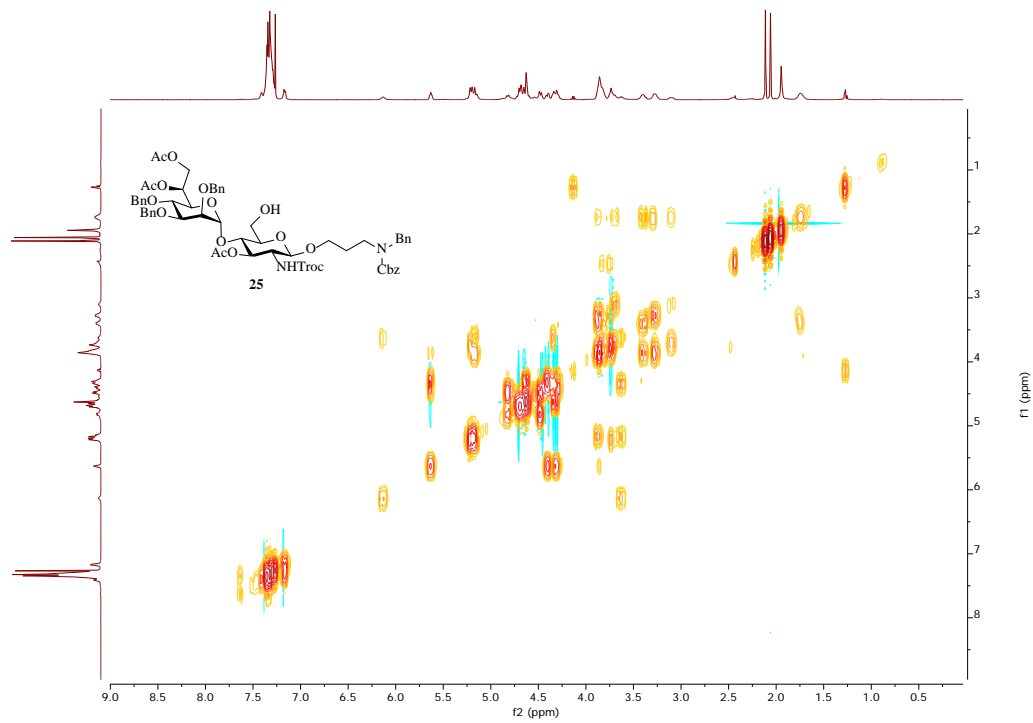
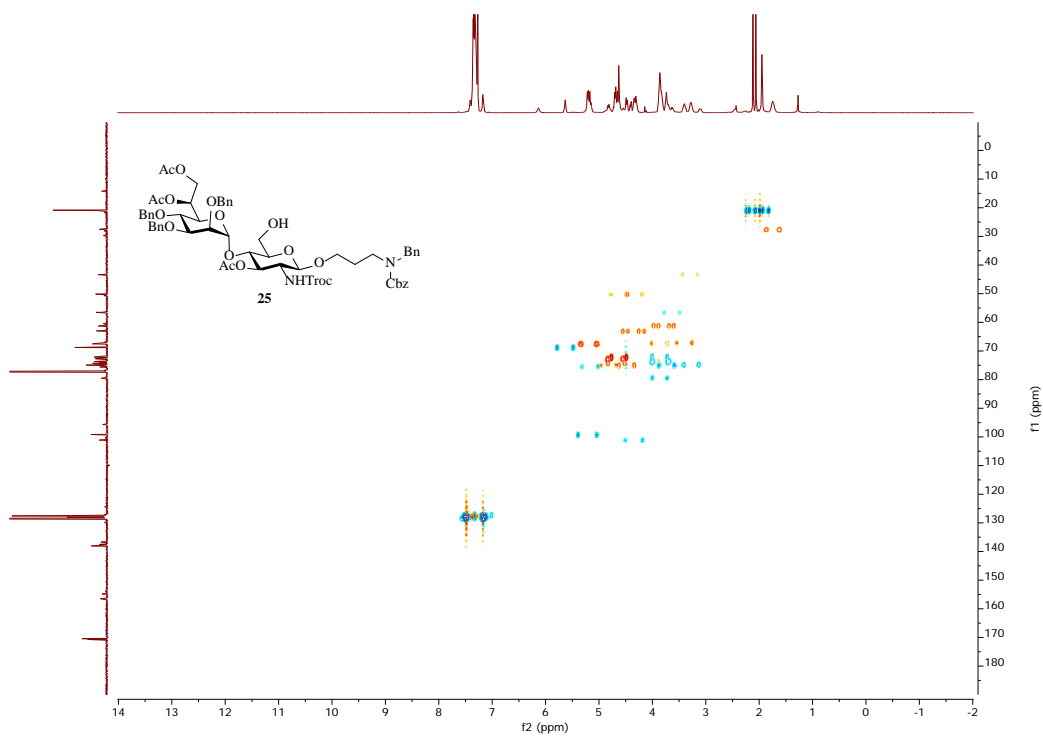**Figure 2.99.** ^{1}H-^{1}H gCOSY of **25** (500 MHz CDCl$_3$)

Figure 2.100. ^{1}H-^{13}C gHSQCAD of **25** (500 MHz CDCl$_3$)

Figure 2.101. ^{1}H-NMR of **26** (500 MHz CDCl$_3$)

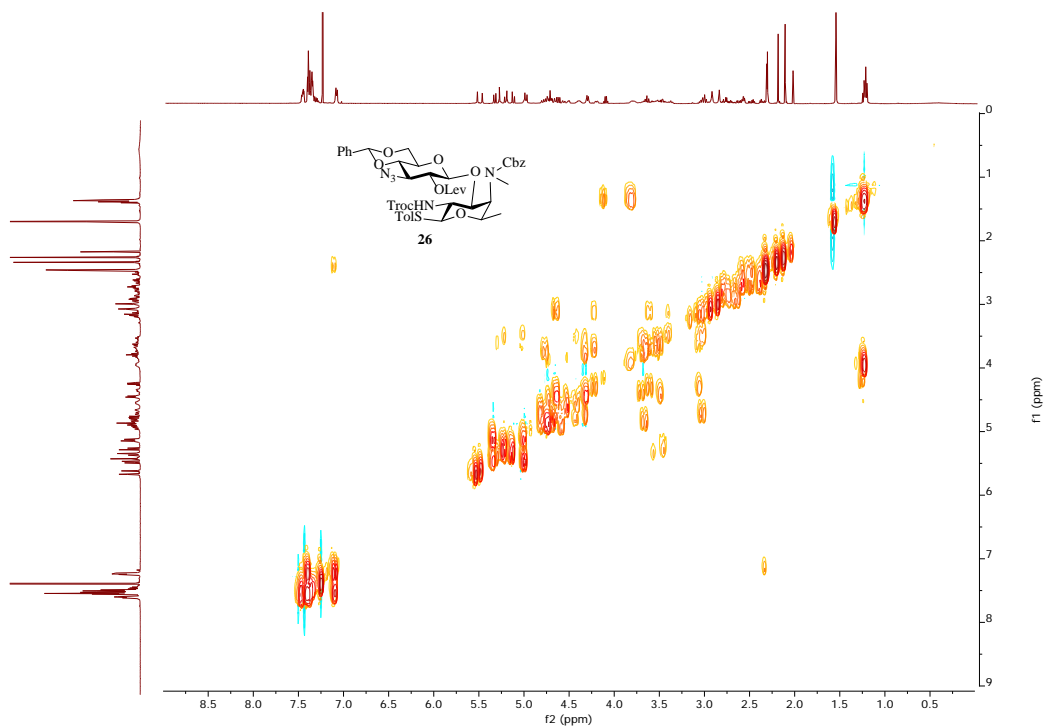**Figure 2.102.** ^{13}C-NMR of **26** (125 MHz CDCl$_3$)
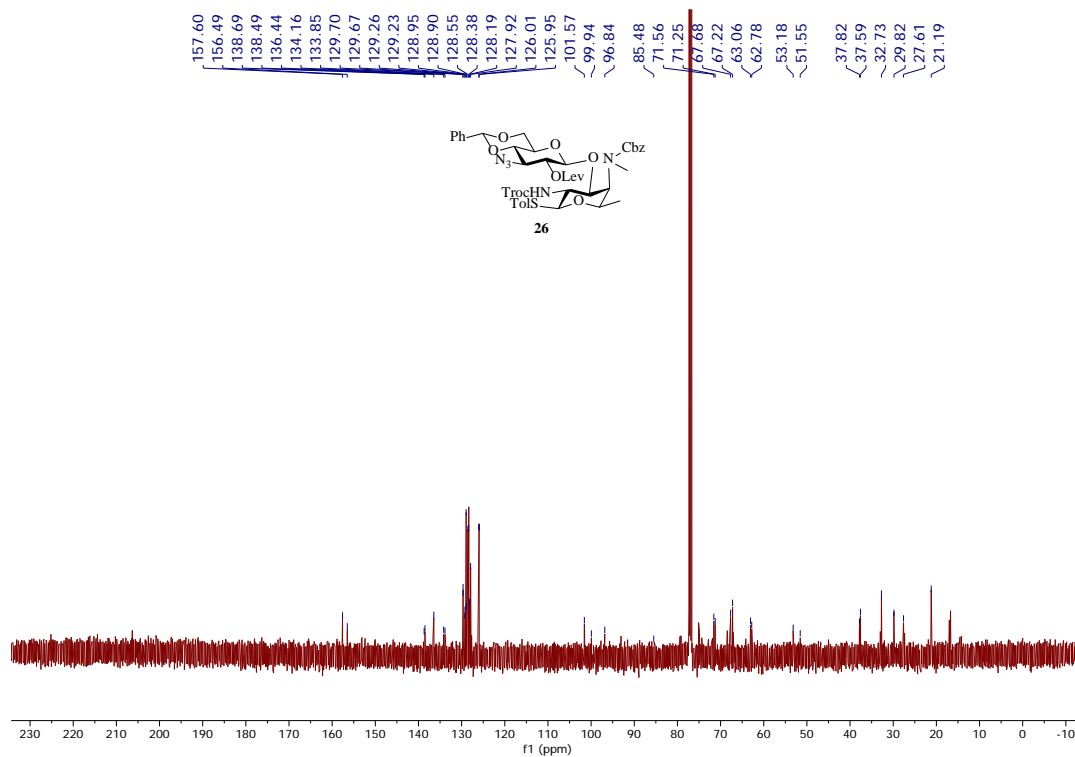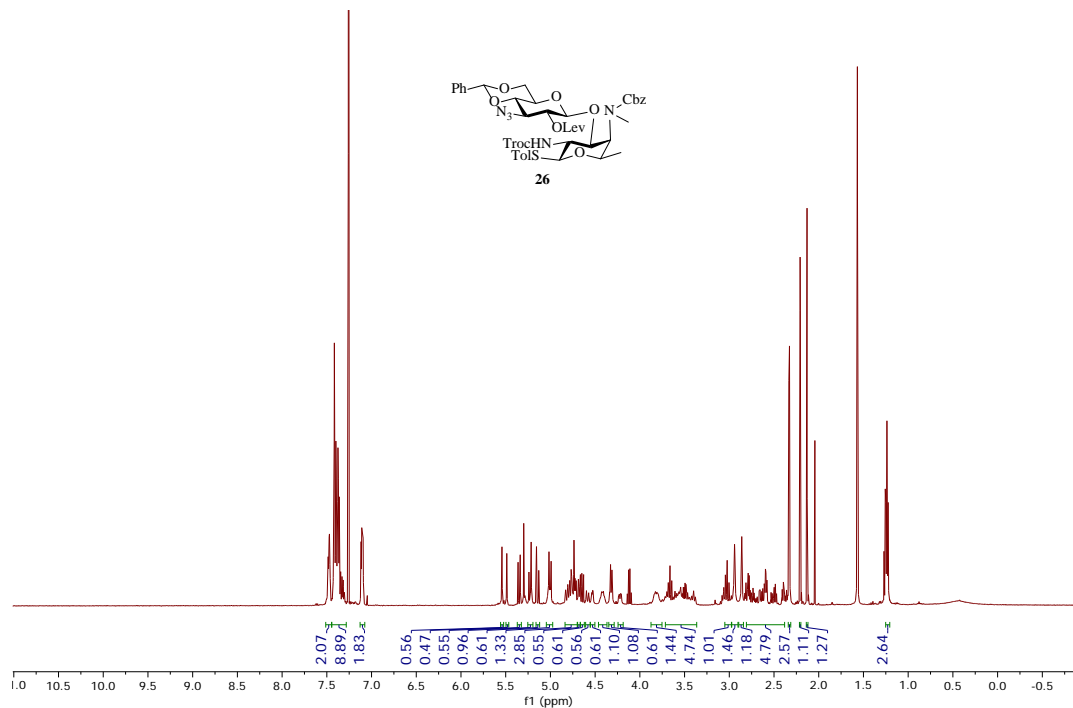
Figure 2.103. ^{1}H-^{1}H gCOSY of **26** (500 MHz CDCl$_3$)
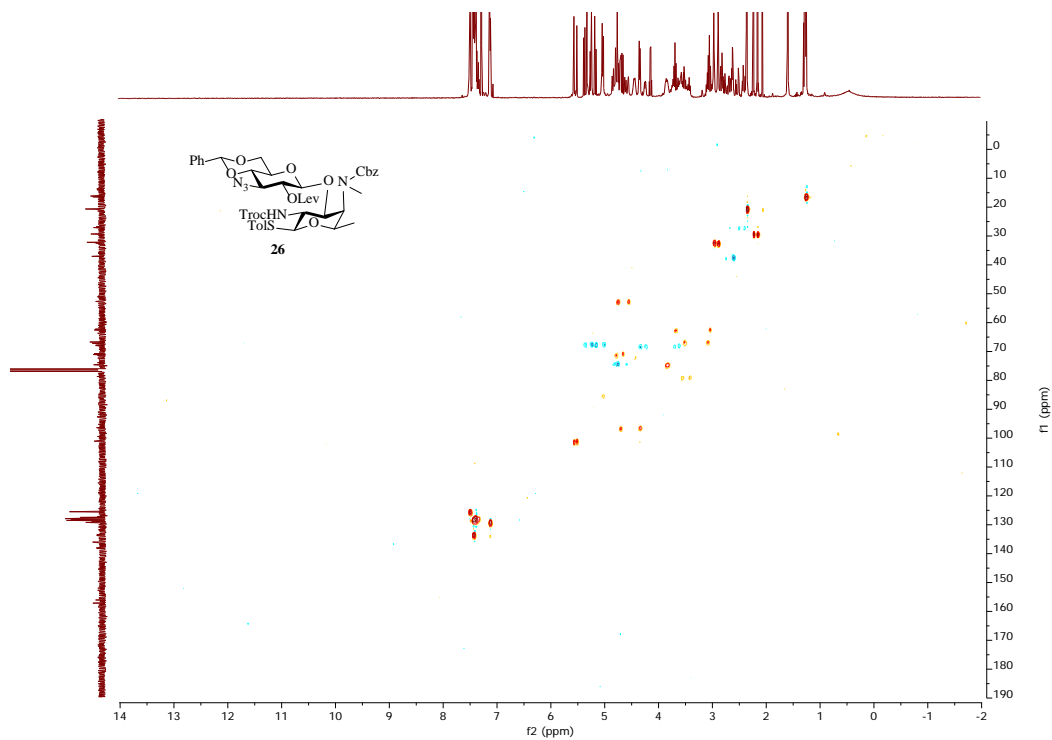
Figure 2.104. ^{1}H-^{13}C gHSQCAD of **26** (500 MHz CDCl$_3$)
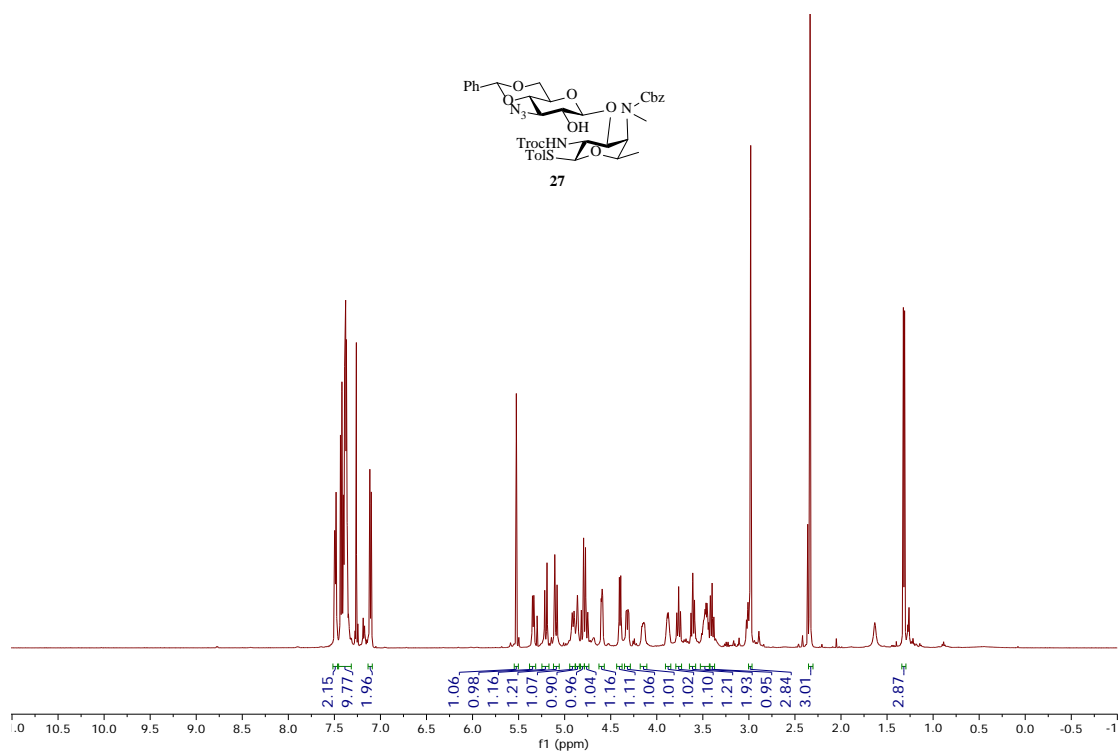
Figure 2.105. ^{1}H-NMR of **27** (500 MHz CDCl$_3$)

Figure 2.106. ^{13}C-NMR of **27** (125 MHz CDCl$_3$)

Figure 2.107. ^{1}H-^{1}H gCOSY of **27** (500 MHz CDCl$_3$)
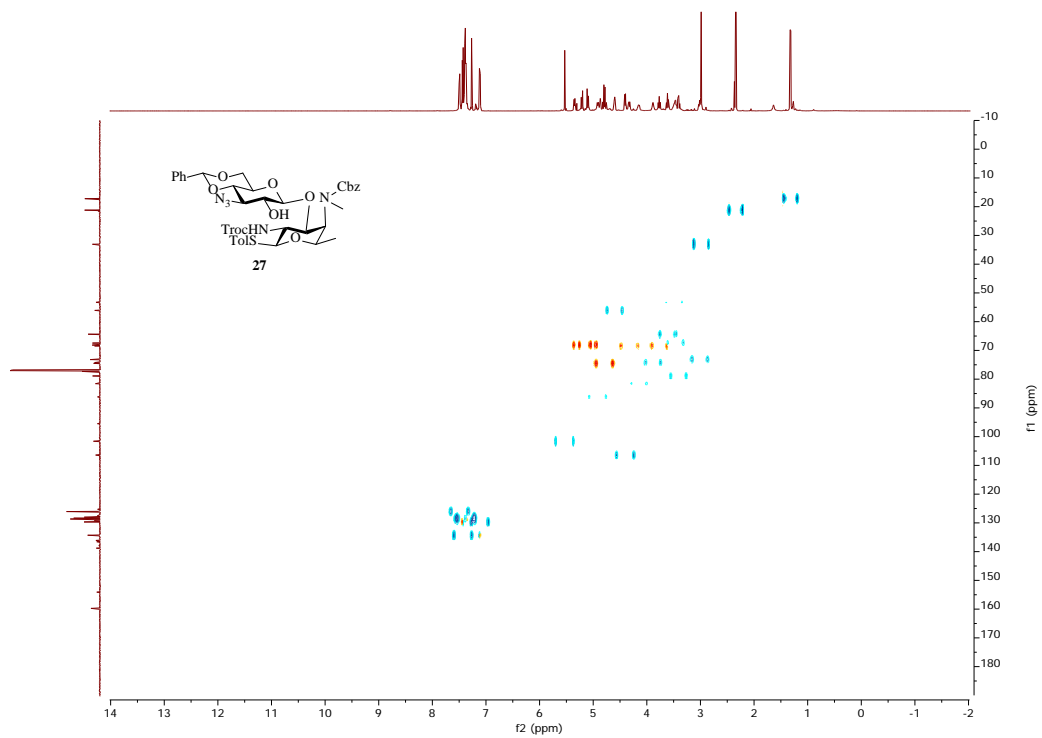
Figure 2.108. ^{1}H-^{13}C gHSQCAD of **27** (500 MHz CDCl$_3$)
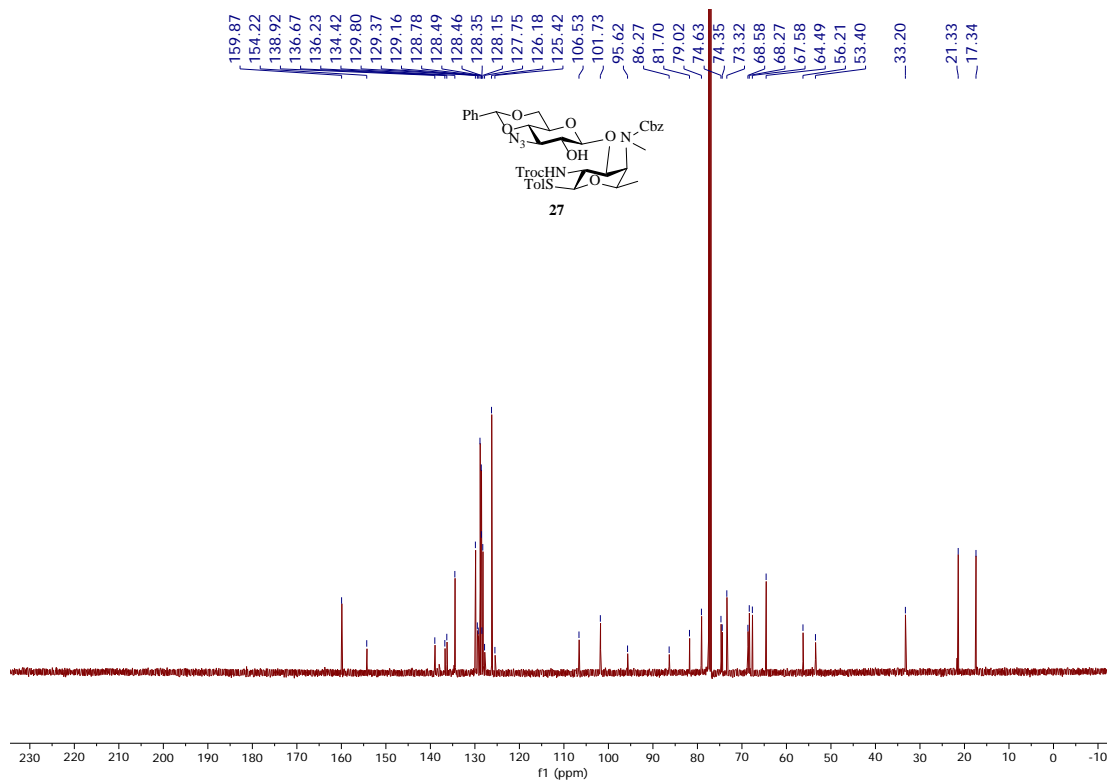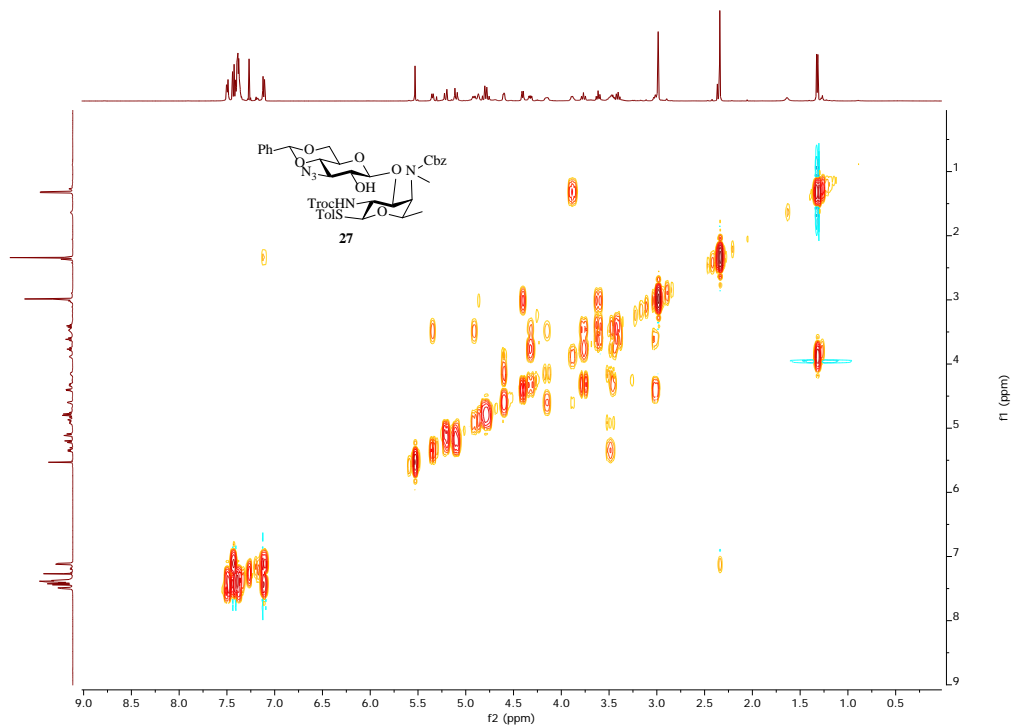
Figure 2.109. ^{1}H-NMR of **28** (500 MHz CDCl$_3$)

Figure 2.110. ^{13}C-NMR of **28** (125 MHz CDCl$_3$)
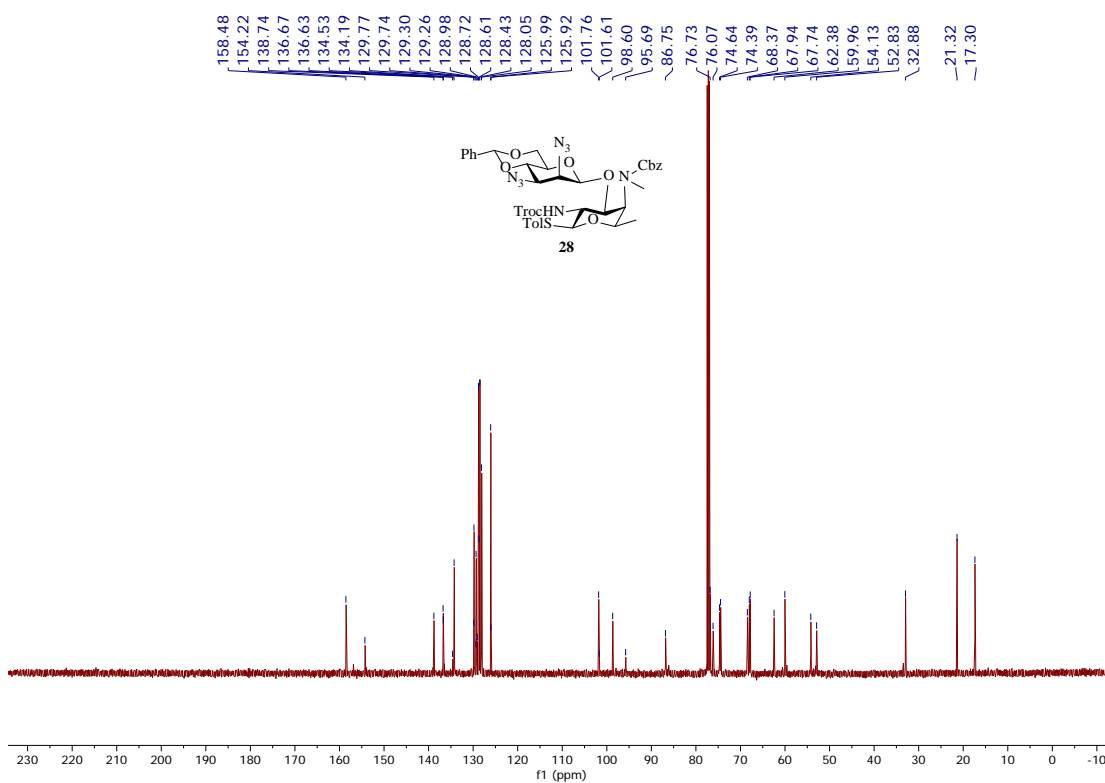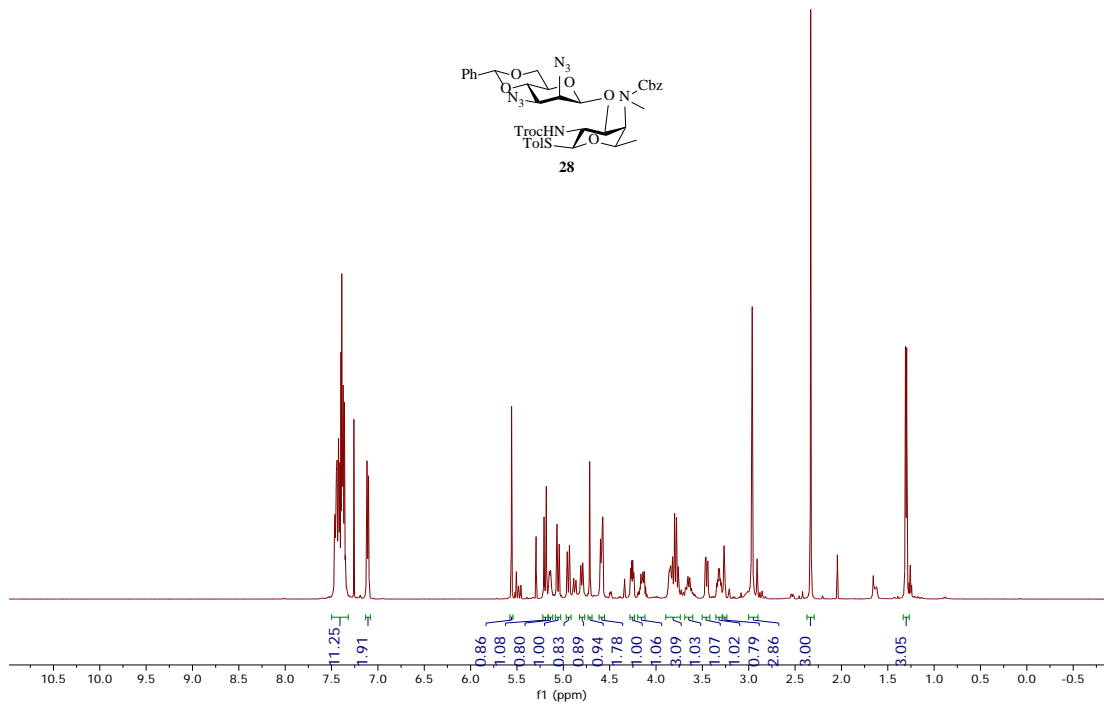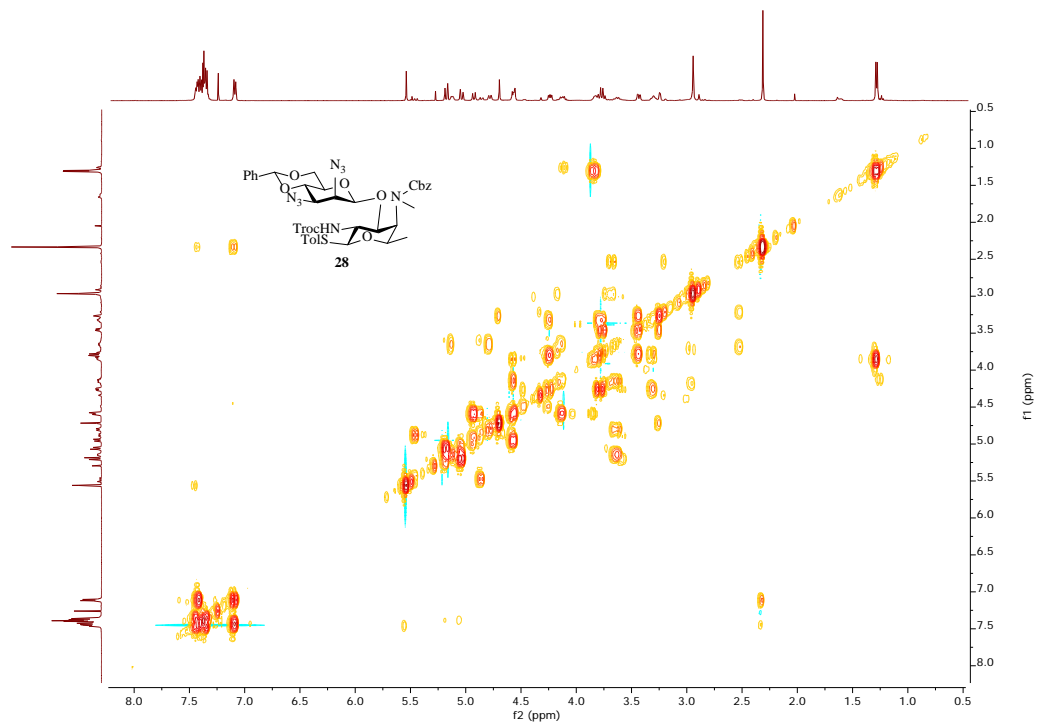
Figure 2.111. ^{1}H-^{1}H gCOSY of **28** (500 MHz CDCl$_3$)
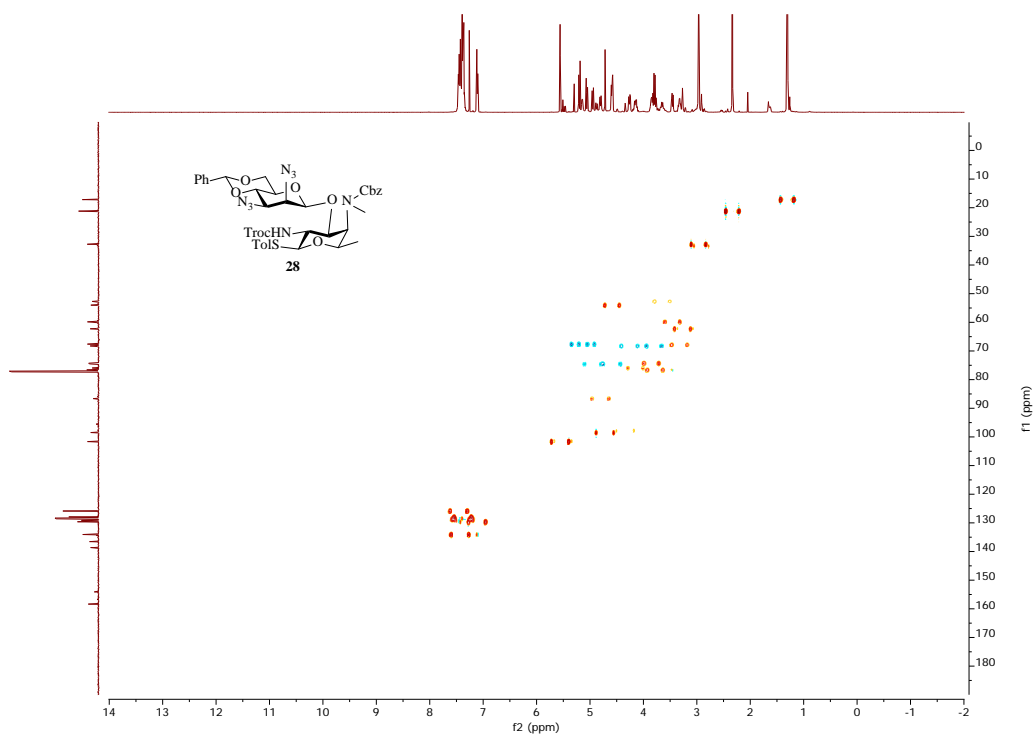
Figure 2.112. ^{1}H-^{13}C gHSQCAD of **28** (500 MHz CDCl$_3$)
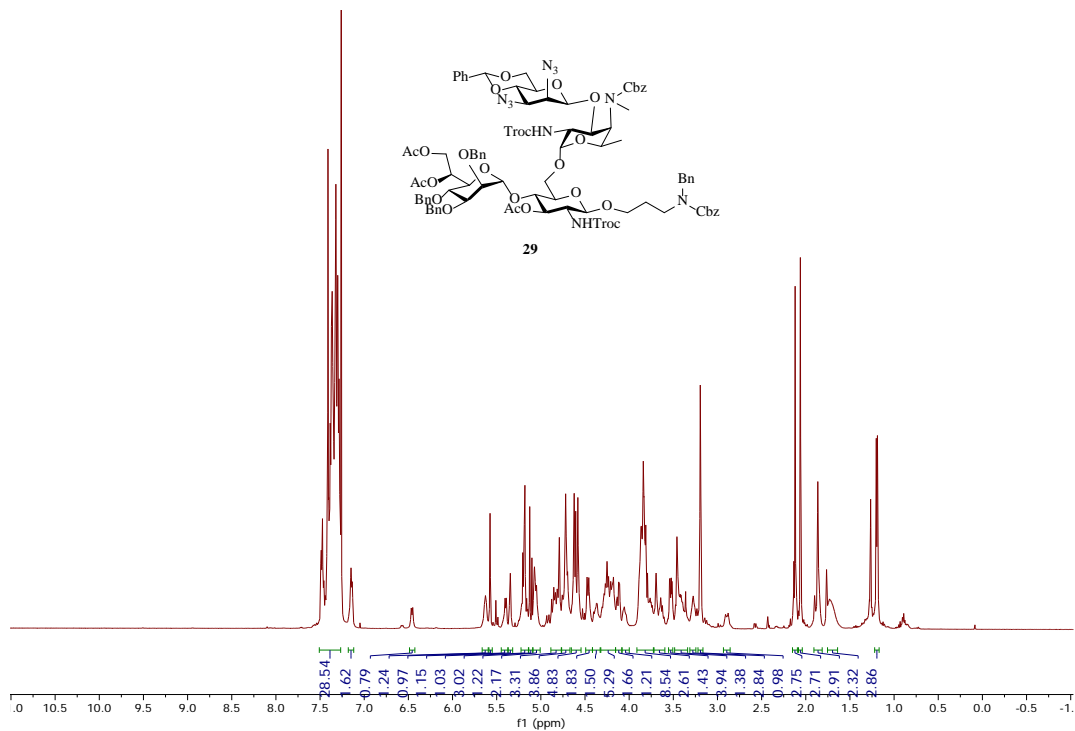
Figure 2.113. ^{1}H-NMR of **29** (500 MHz CDCl$_3$)
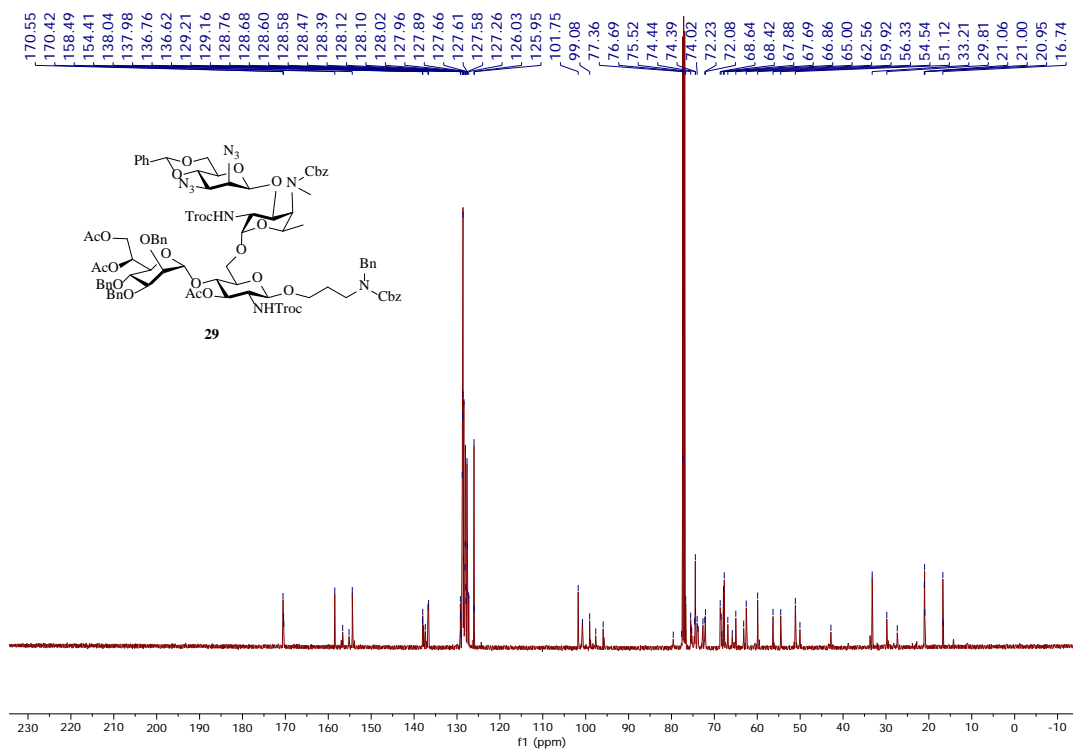
Figure 2.114. ^{13}C-NMR of **29** (125 MHz CDCl$_3$)
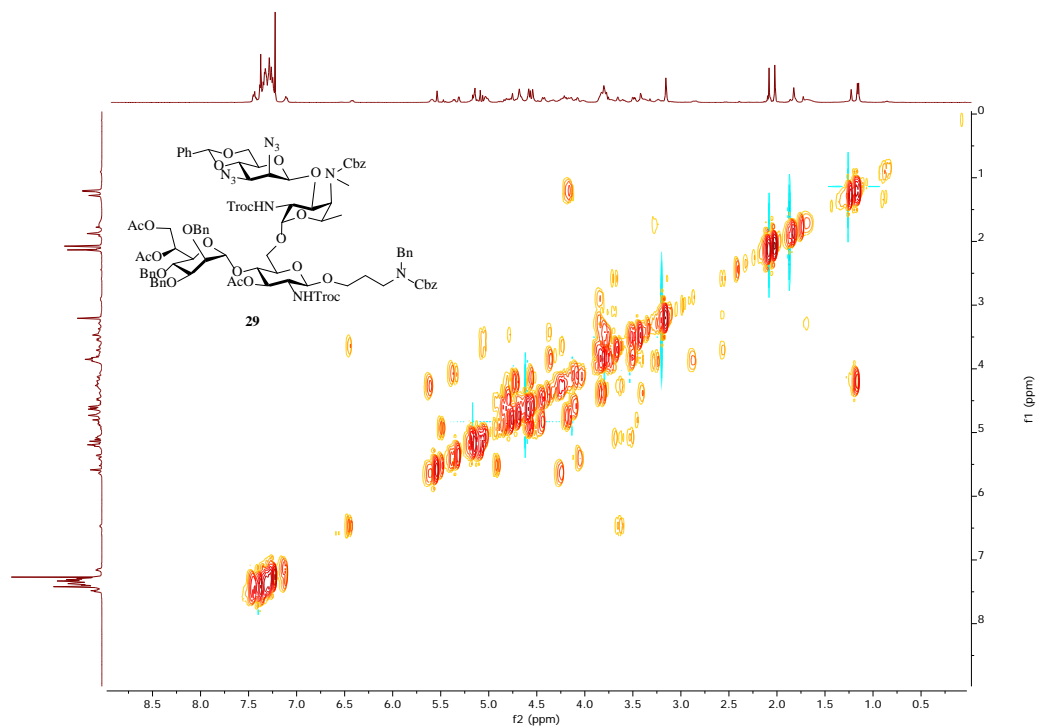
Figure 2.115. ^{1}H-^{1}H gCOSY of **29** (500 MHz CDCl$_3$)
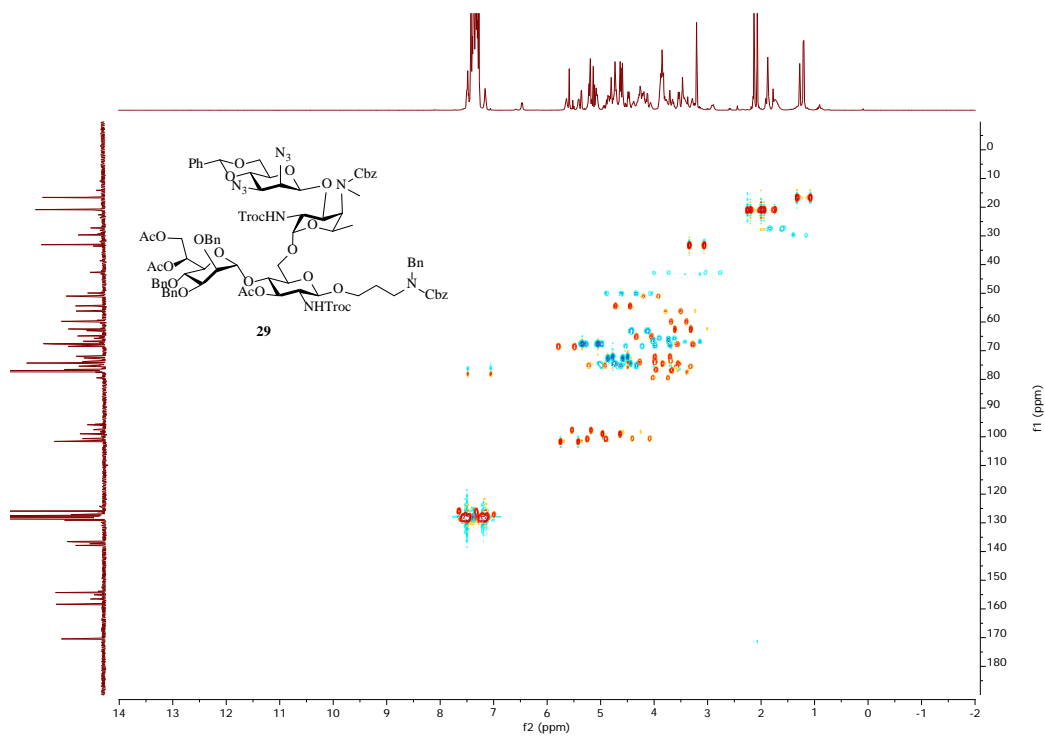
Figure 2.116. ^{1}H-^{13}C gHSQCAD of **29** (500 MHz CDCl$_3$)
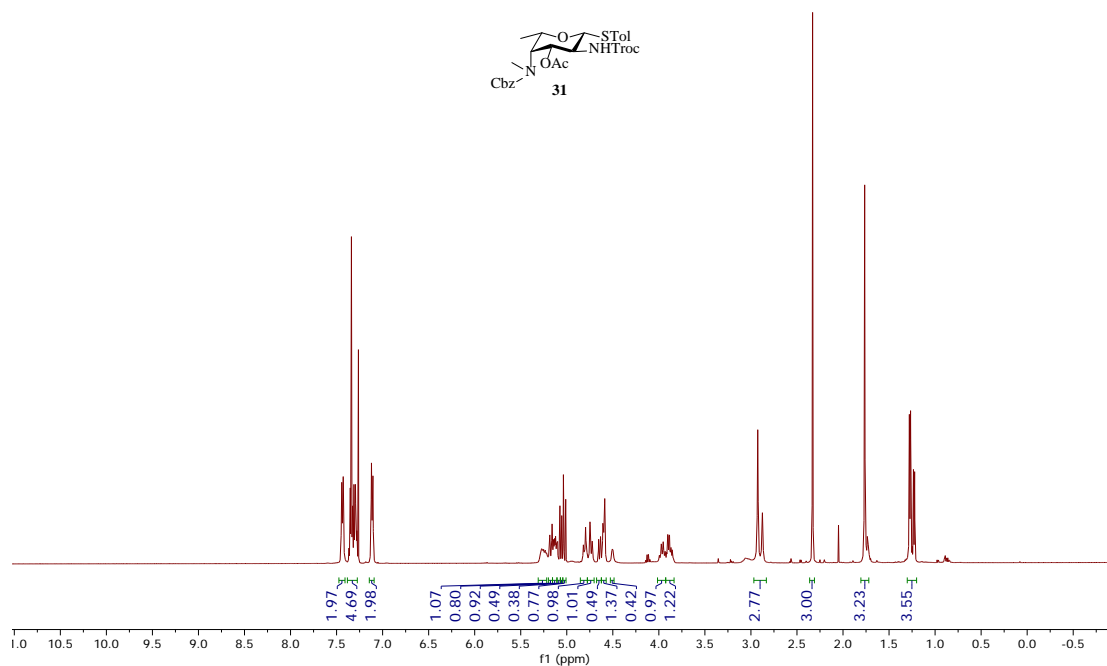
Figure 2.117. ^{1}H-NMR of **31** (500 MHz CDCl$_3$)
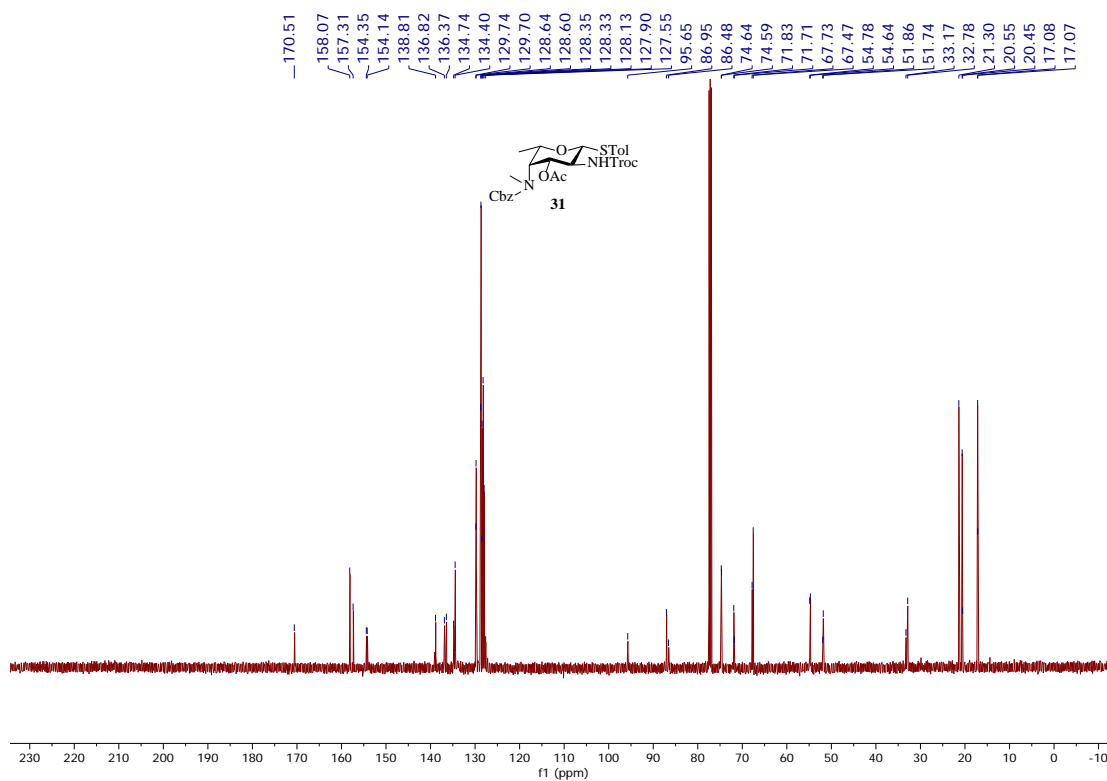
Figure 2.118. ^{13}C-NMR of **31** (125 MHz CDCl$_3$)

165
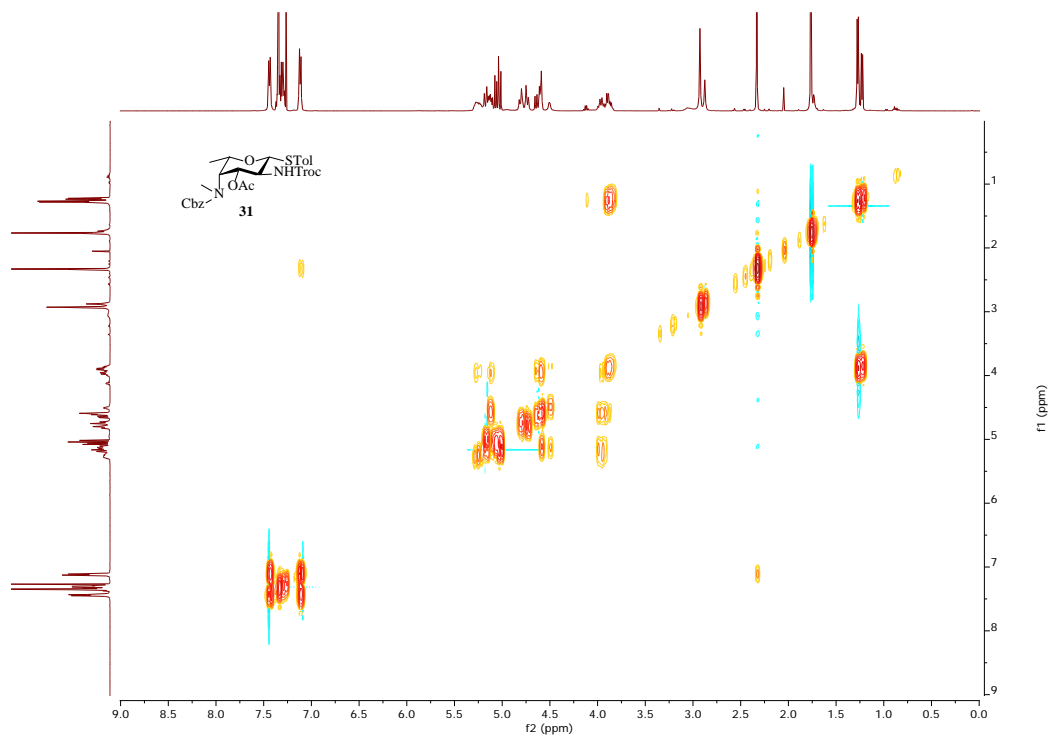
Figure 2.119. ^{1}H-^{1}H gCOSY of **31** (500 MHz CDCl$_3$)
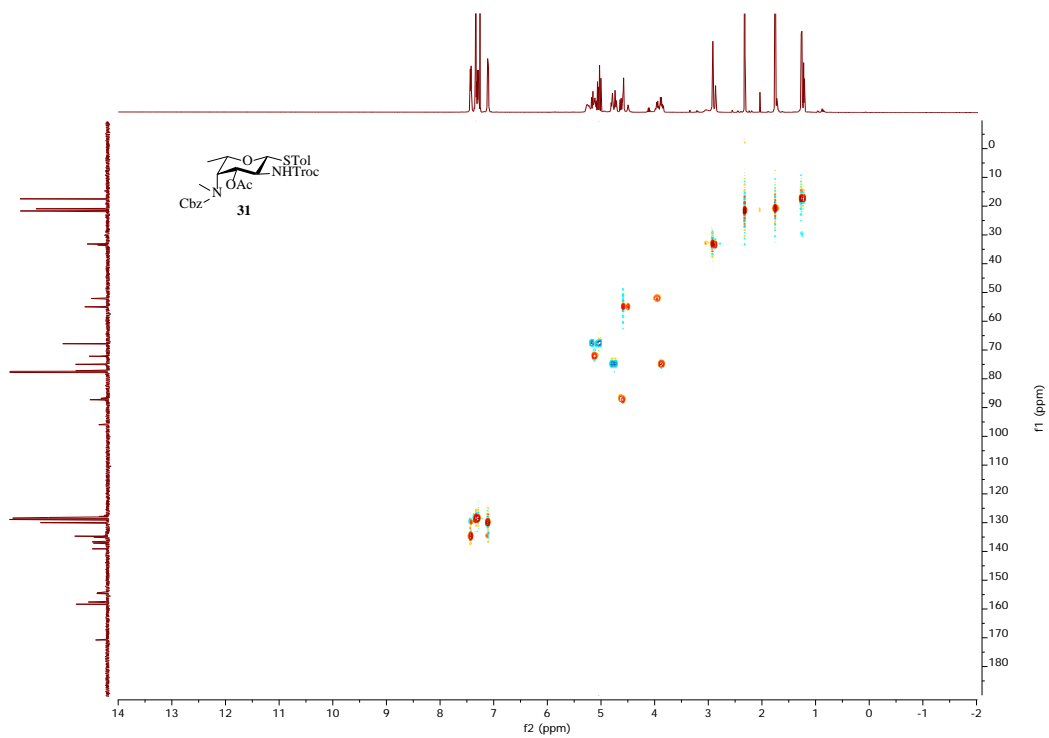
Figure 2.120. ^{1}H-^{13}C gHSQCAD of **31** (500 MHz CDCl$_3$)
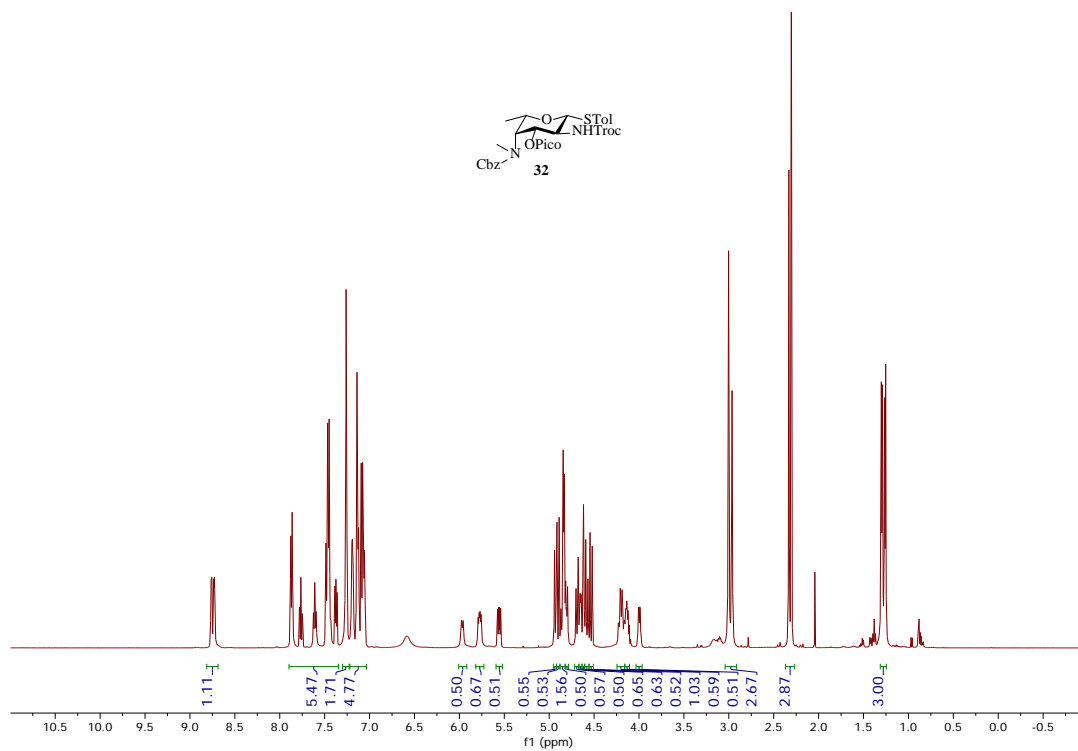
Figure 2.121. ^{1}H-NMR of **32** (500 MHz CDCl$_3$)
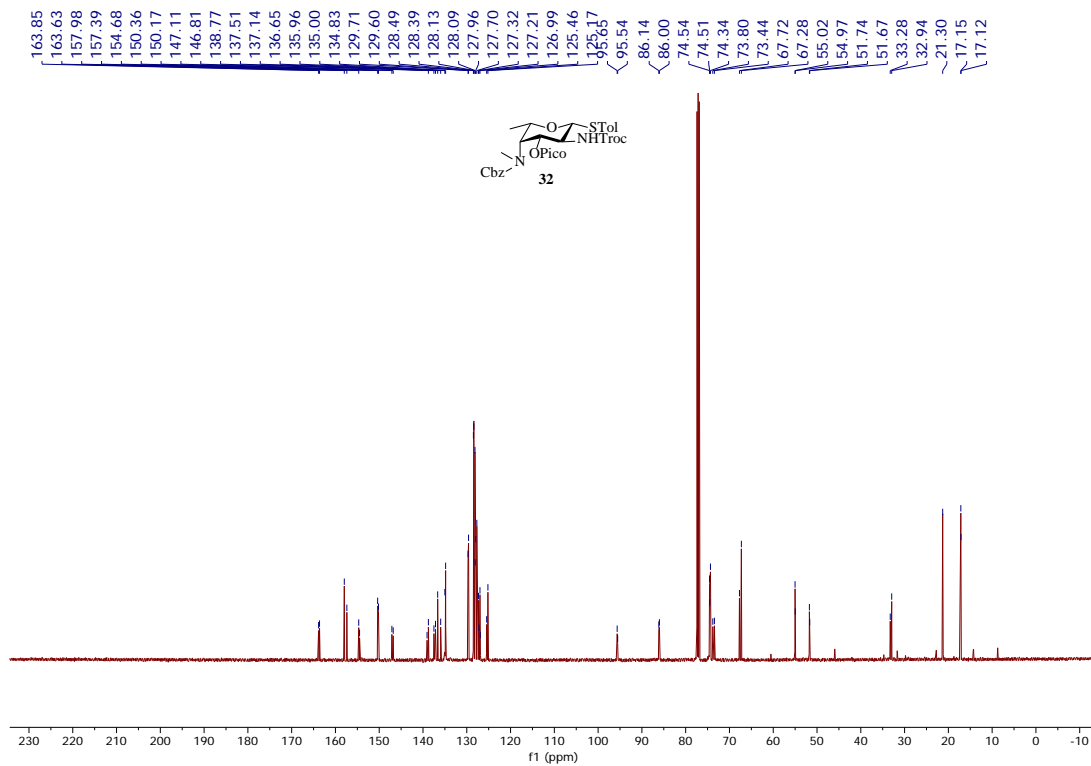
Figure 2.122. ^{13}C-NMR of **32** (125 MHz CDCl$_3$)
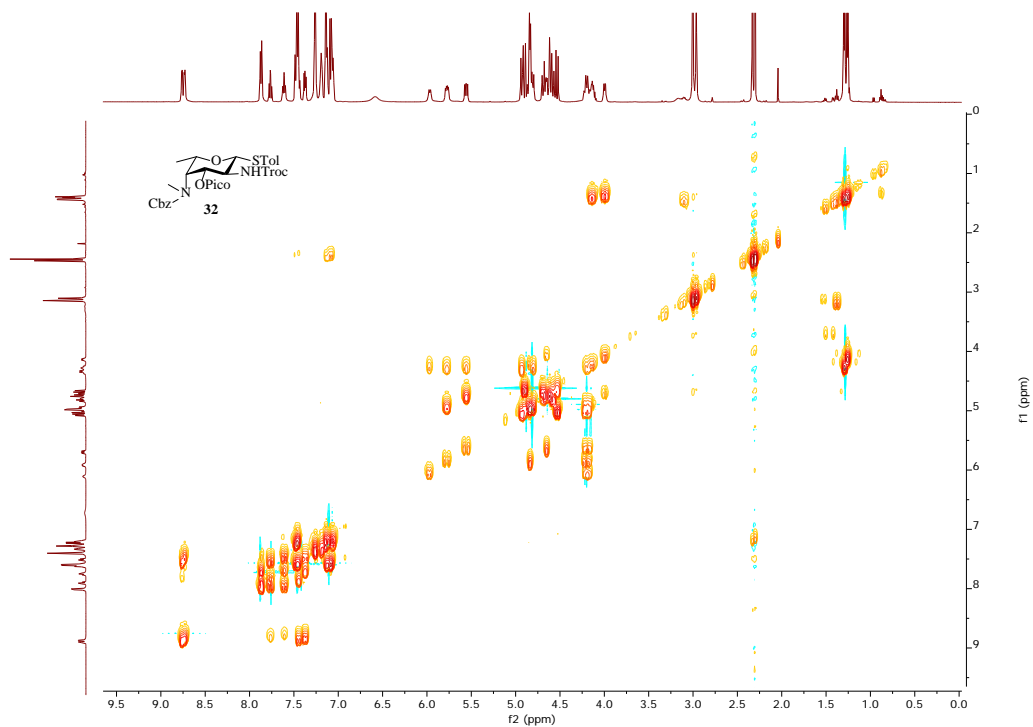
Figure 2.123. ^{1}H-^{1}H gCOSY of **32** (500 MHz CDCl$_3$)
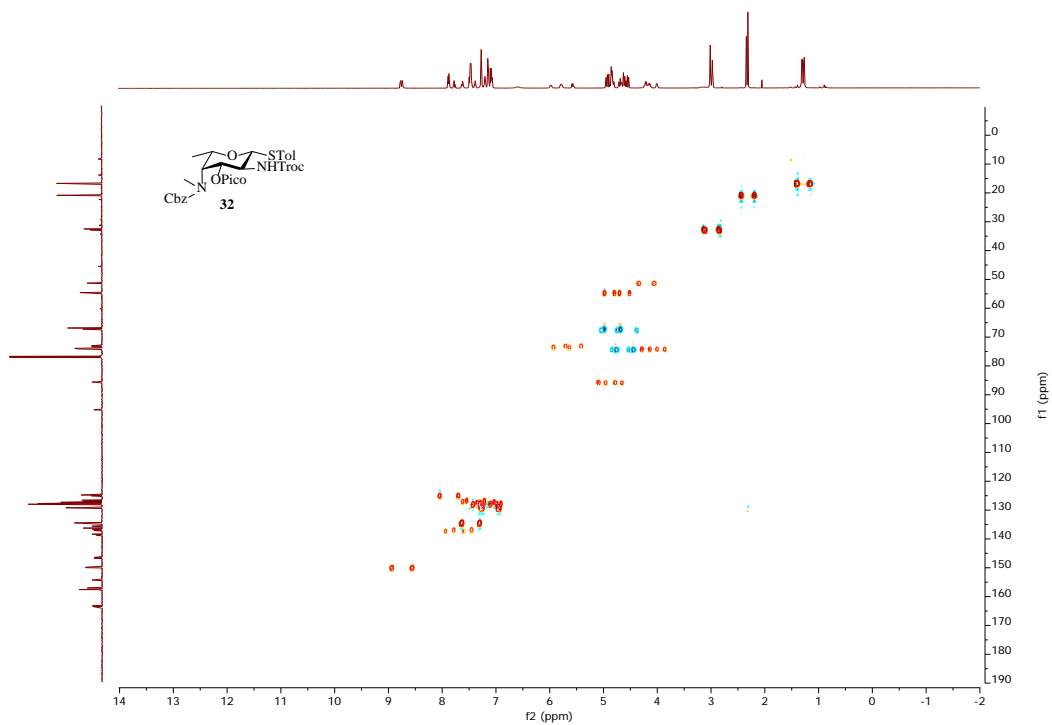
Figure 2.124. ^{1}H-^{13}C gHSQCAD of **32** (500 MHz CDCl$_3$)
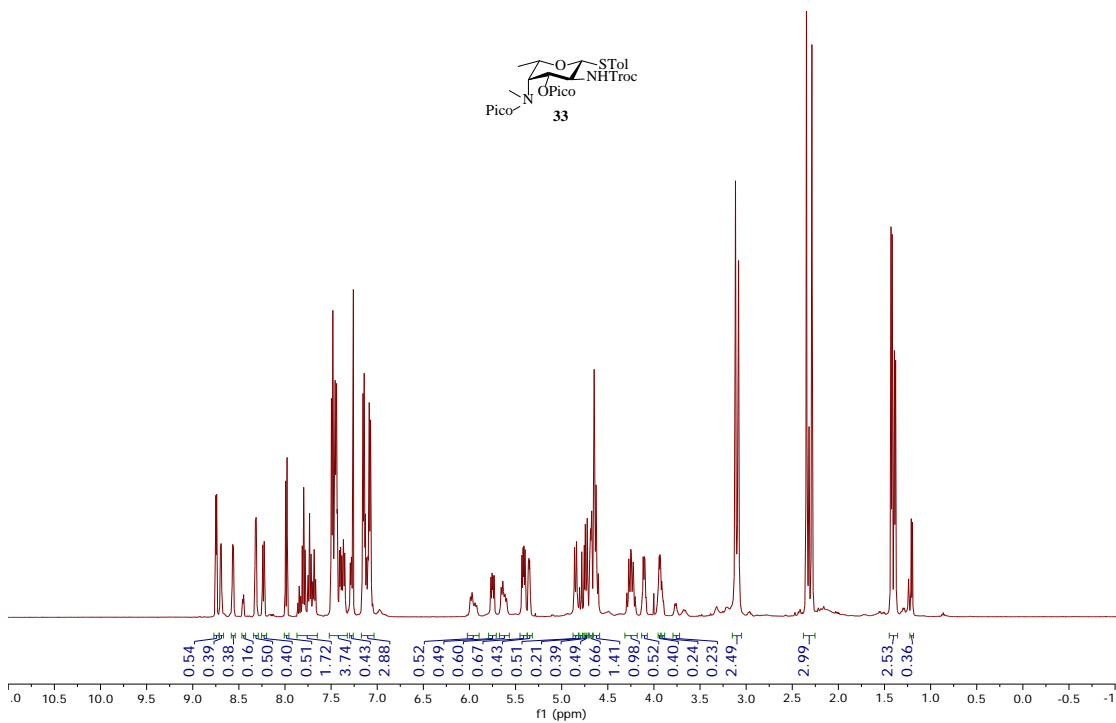
Figure 2.125. ^{1}H-NMR of **33** (500 MHz CDCl$_3$)
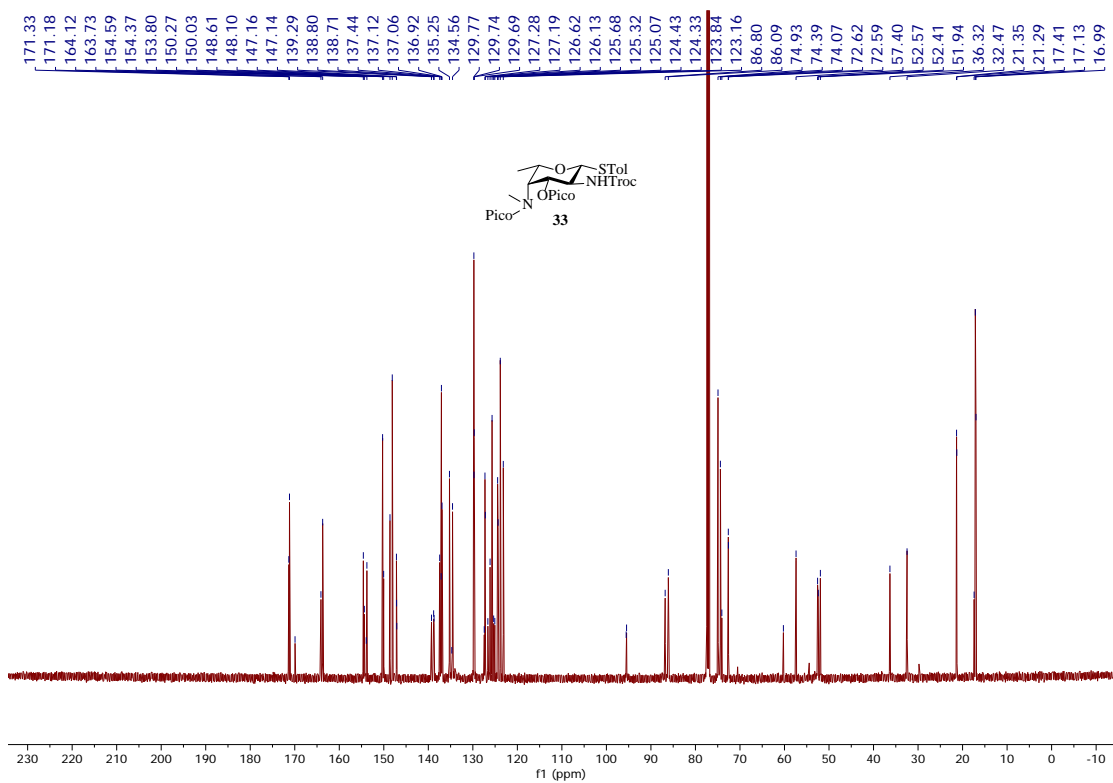
Figure 2.126. ^{13}C-NMR of **33** (125 MHz CDCl$_3$)

169
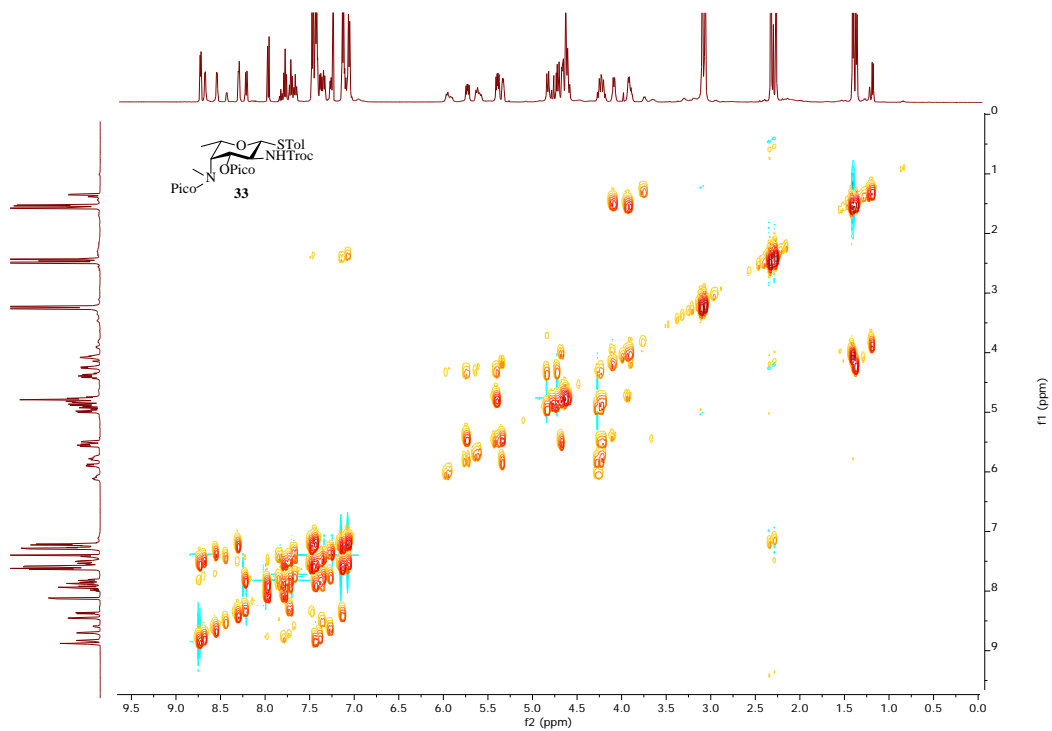
Figure 2.127. ^{1}H-^{1}H gCOSY of **33** (500 MHz CDCl$_3$)
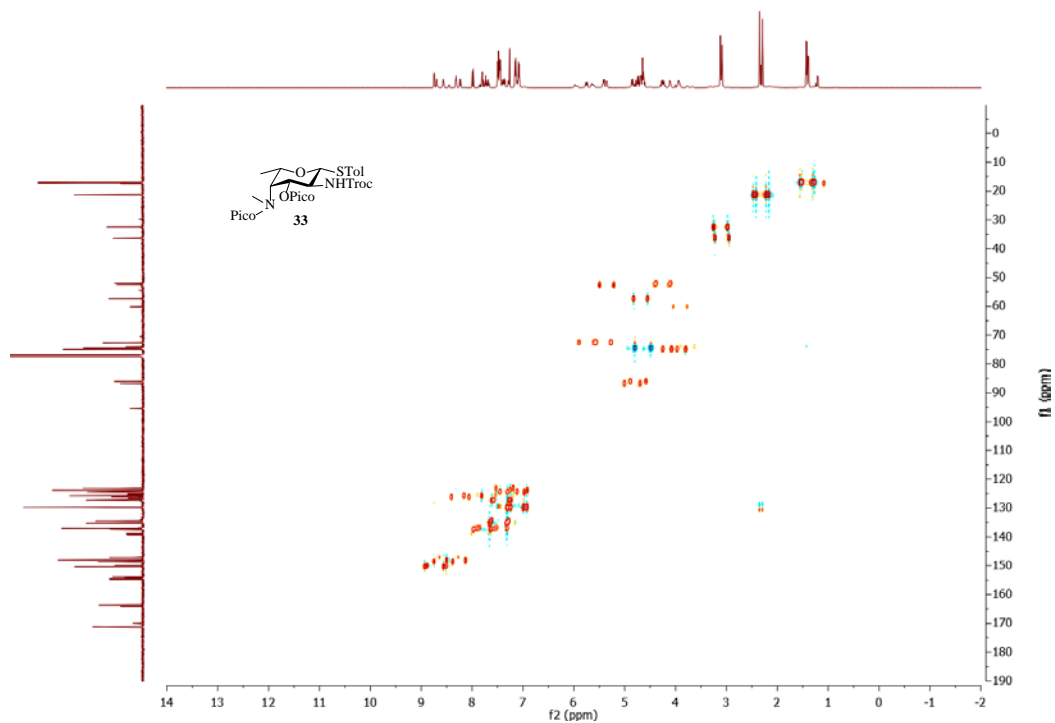
Figure 2.128. ^{1}H-^{13}C gHSQCAD of **33** (500 MHz CDCl$_3$)
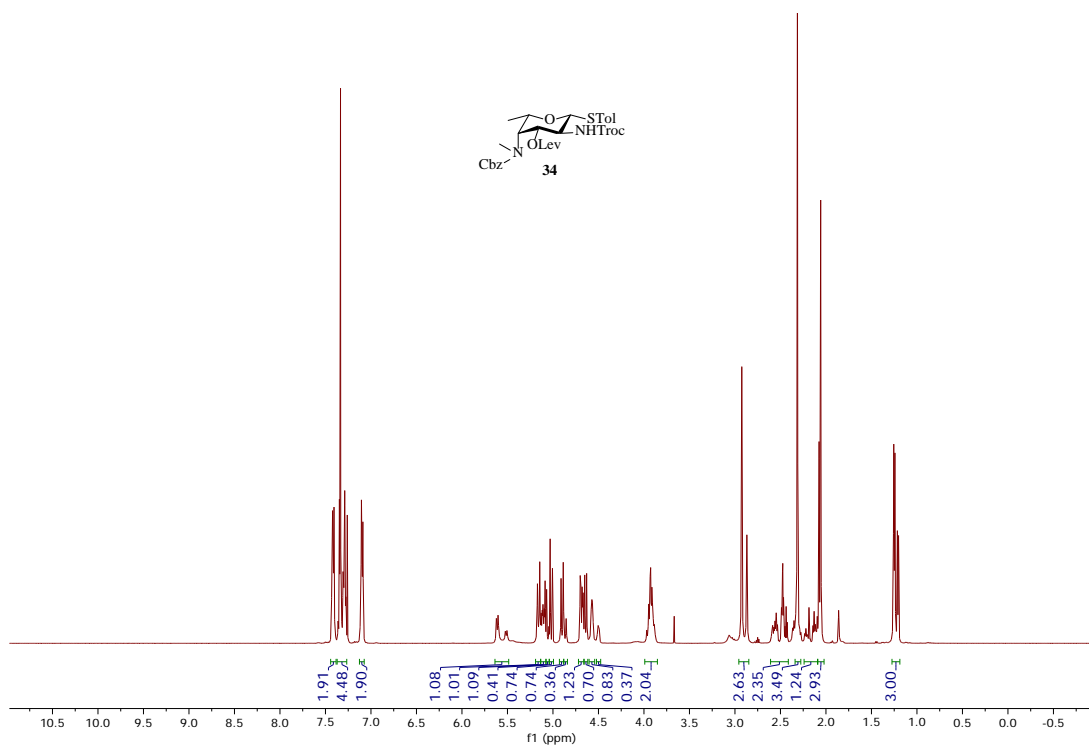
Figure 2.129. ^{1}H-NMR of **34** (500 MHz CDCl$_3$)
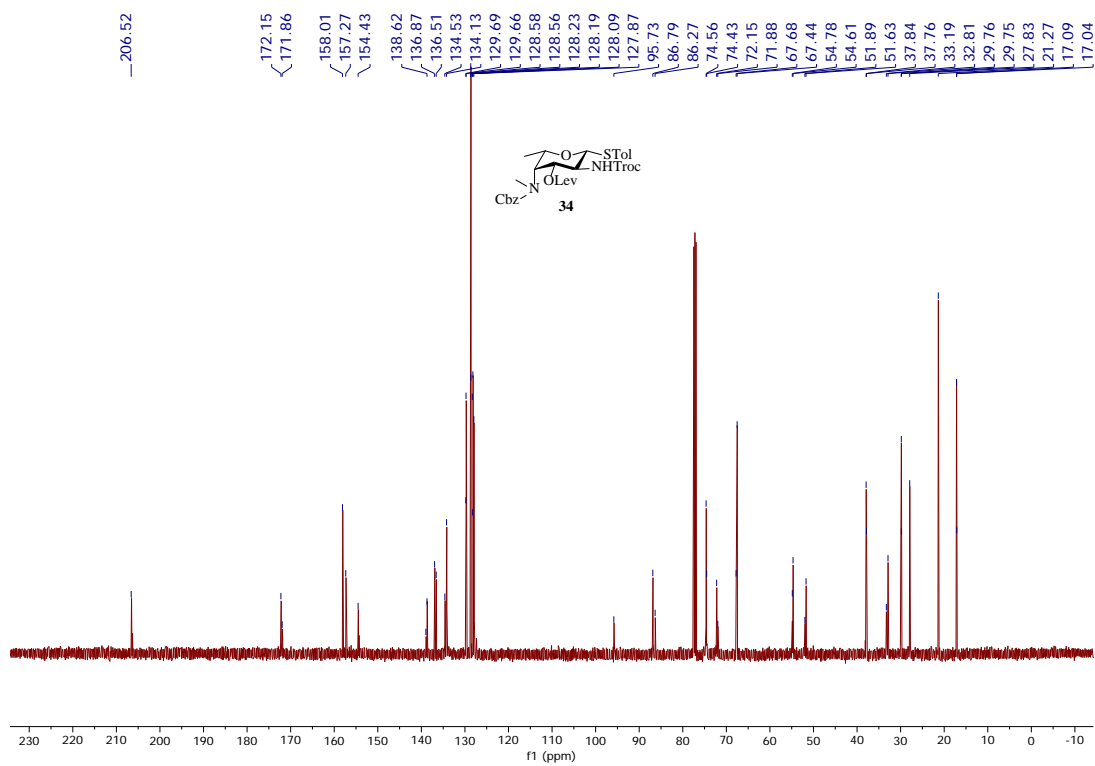
Figure 2.130. ^{13}C-NMR of **34** (125 MHz CDCl$_3$)

171

Figure 2.131. ^{1}H-^{1}H gCOSY of **34** (500 MHz CDCl$_3$)
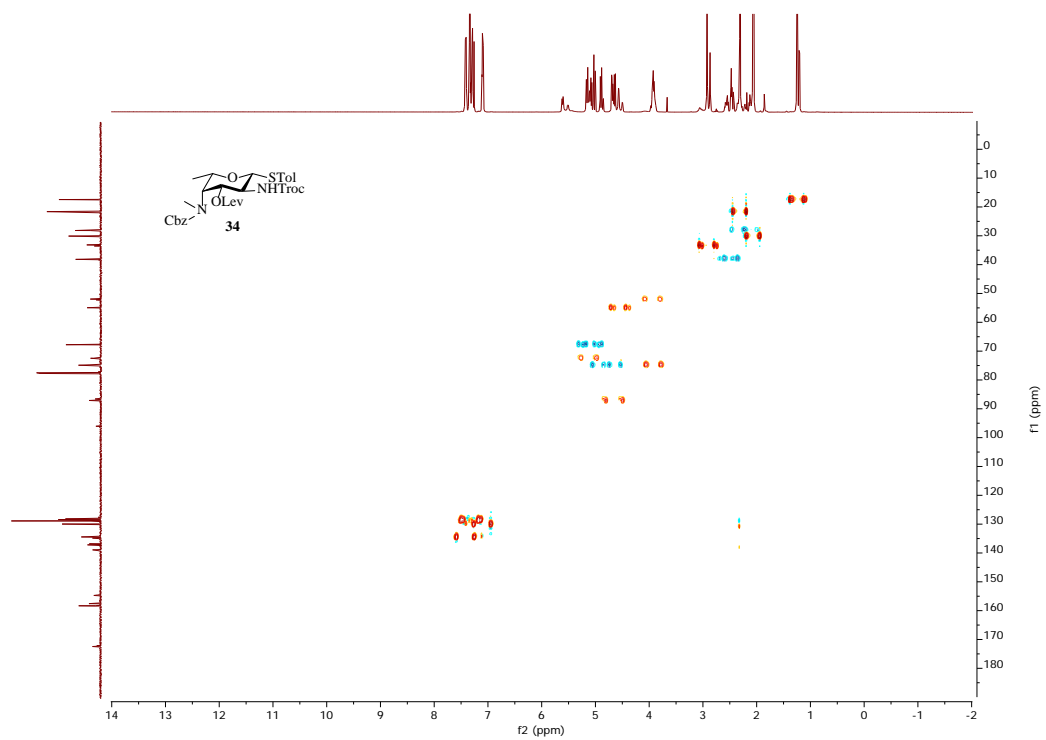
Figure 2.132. ^{1}H-^{13}C gHSQCAD of **34** (500 MHz CDCl$_3$)
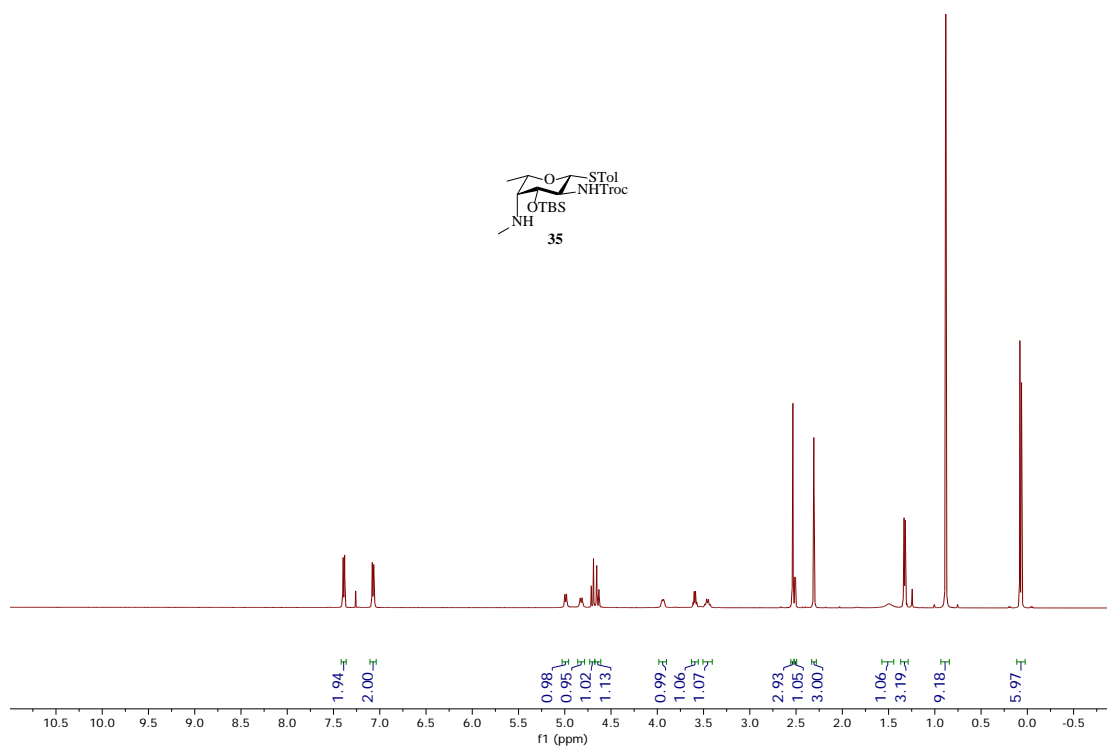
Figure 2.133. ^{1}H-NMR of **35** (500 MHz CDCl$_3$)
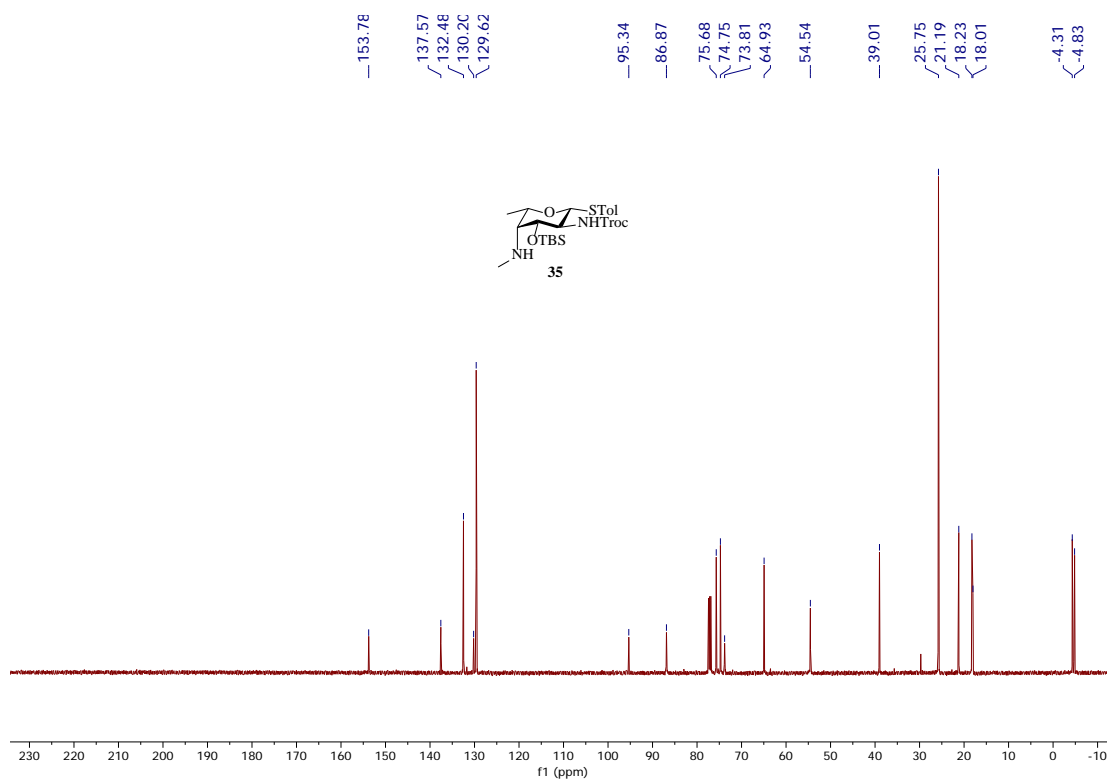
Figure 2.134. ^{13}C-NMR of **35** (125 MHz CDCl$_3$)
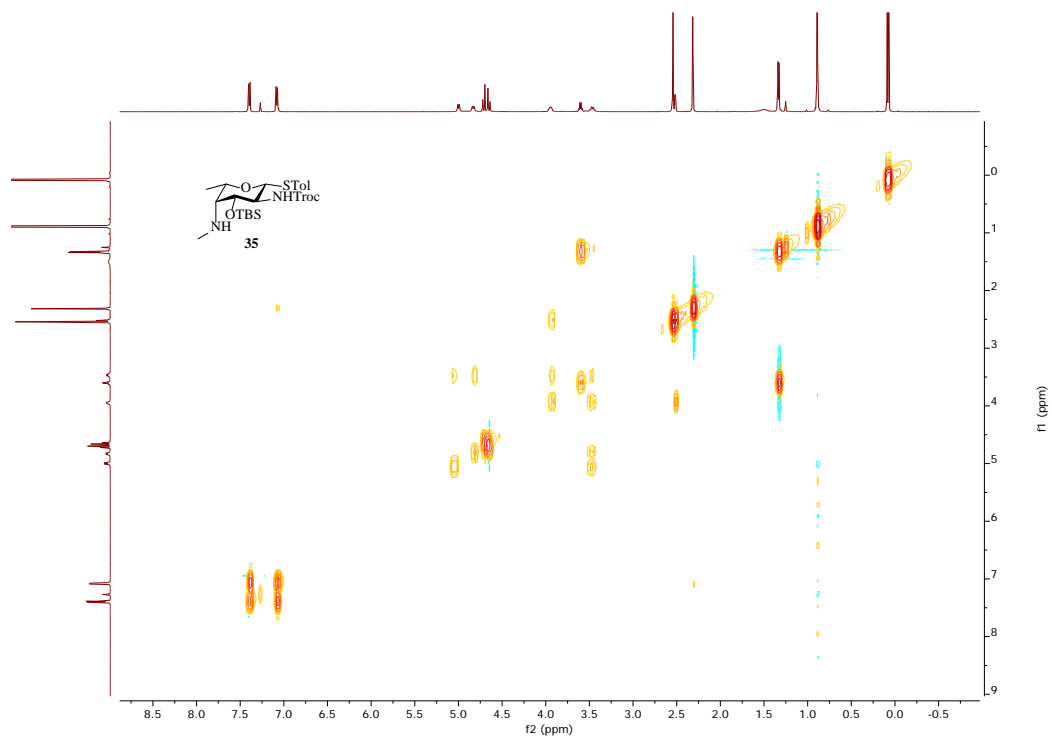
Figure 2.135. ^{1}H-^{1}H gCOSY of **35** (500 MHz CDCl$_3$)
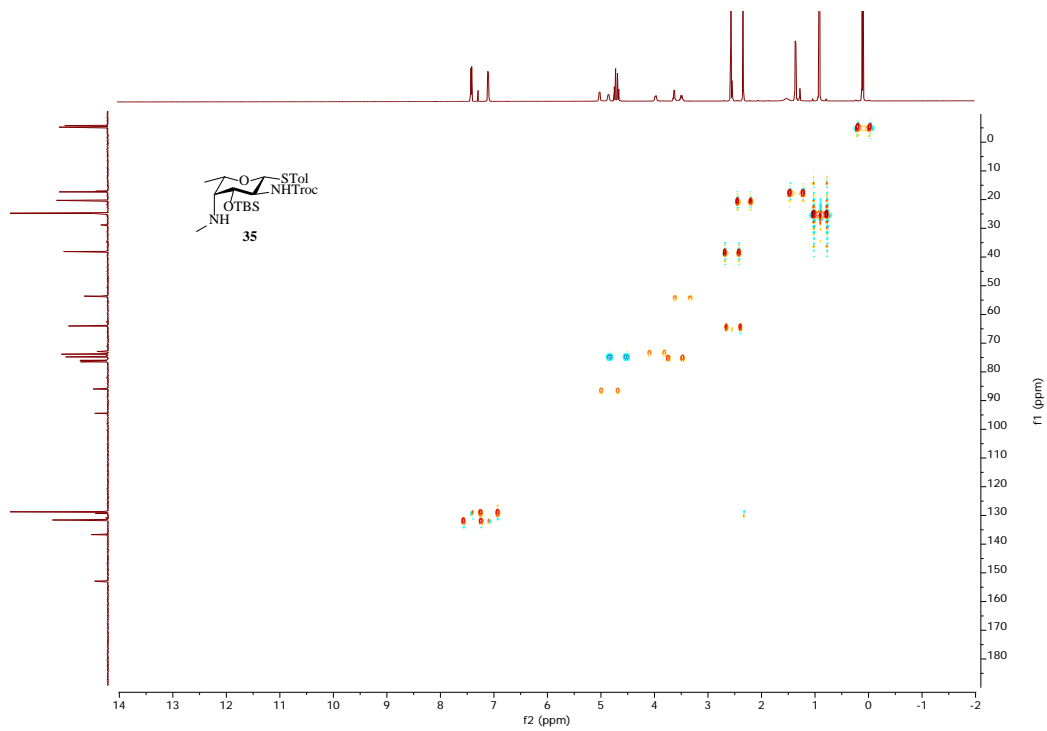
Figure 2.136. ^{1}H-^{13}C gHSQCAD of **35** (500 MHz CDCl$_3$)
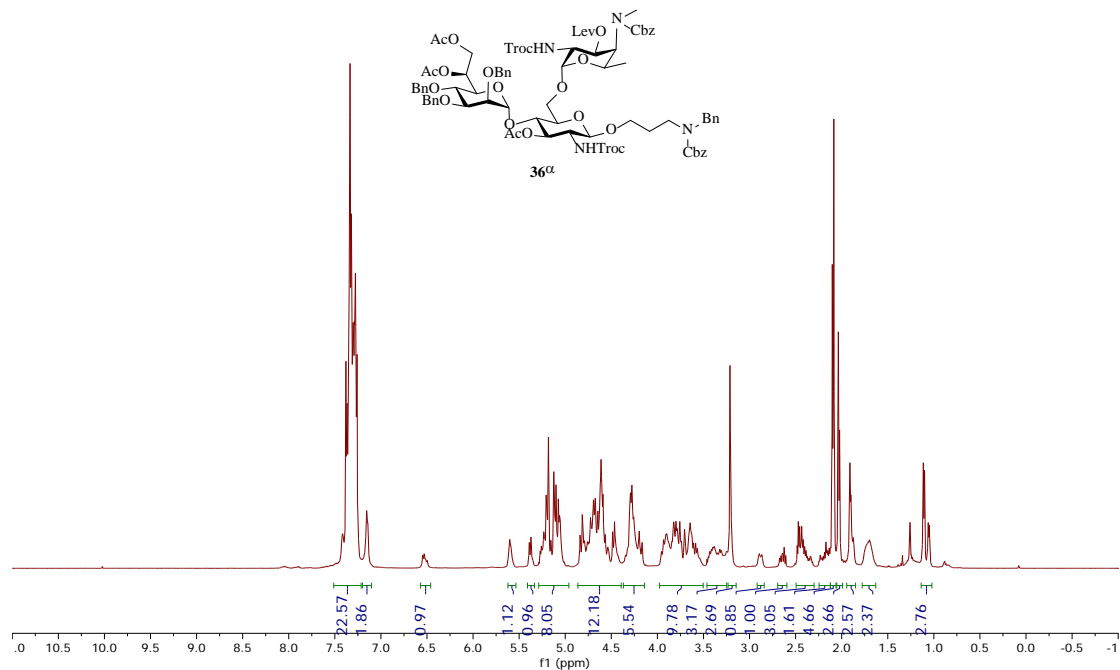
Figure 2.137. ^{1}H-NMR of **36α** (500 MHz CDCl$_3$)
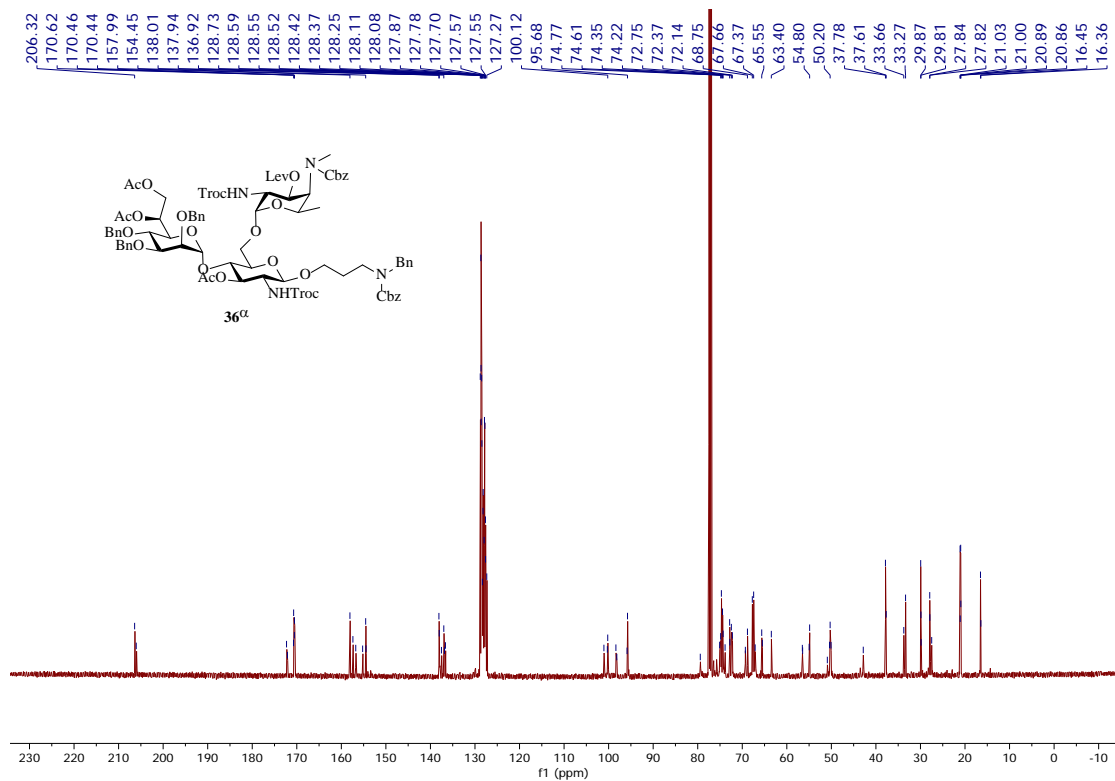
Figure 2.138. ^{13}C-NMR of **36α** (125 MHz CDCl$_3$)

175
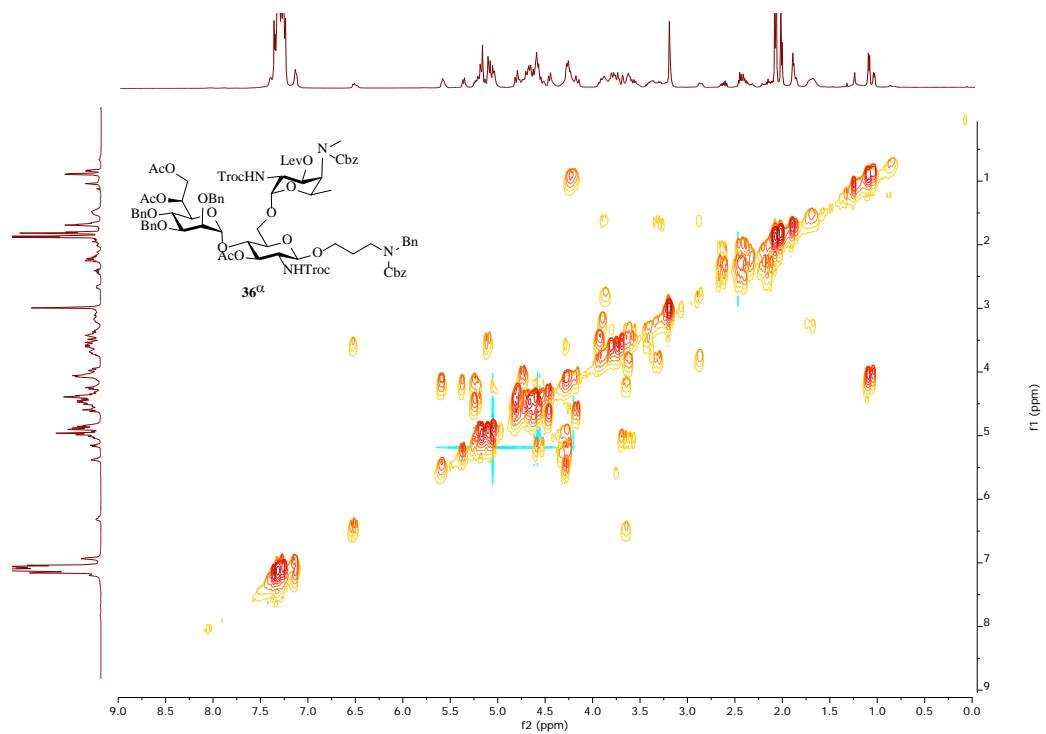
Figure 2.139. ^{1}H-^{1}H gCOSY of **36α** (500 MHz CDCl$_3$)
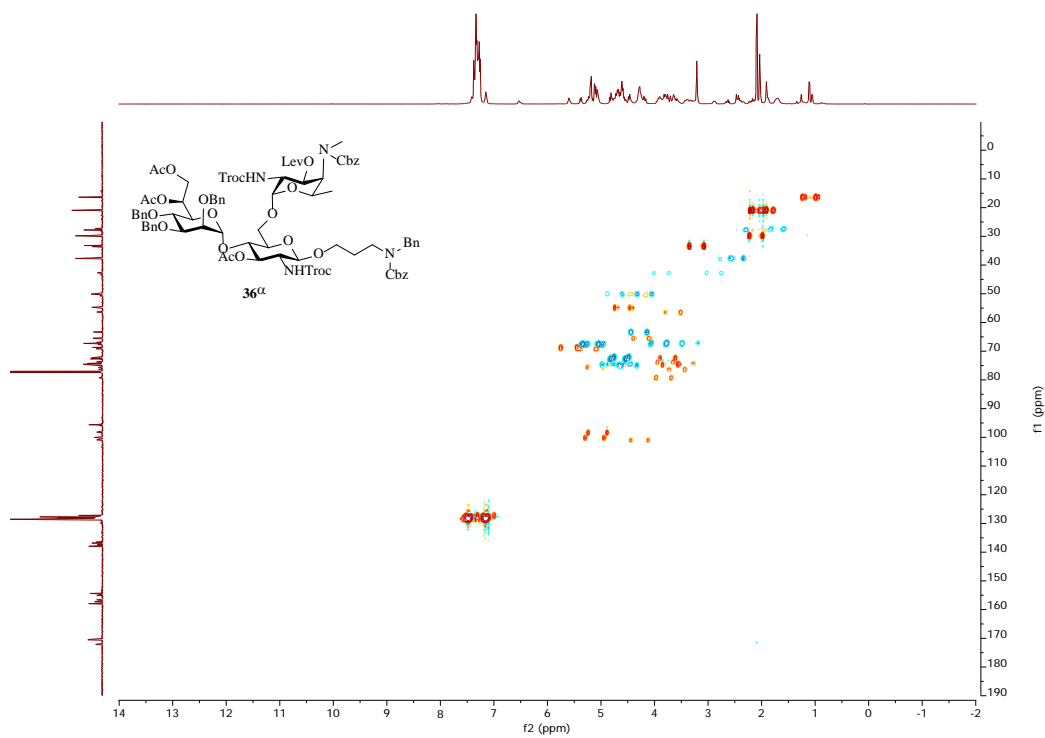
Figure 2.140. ^{1}H-^{13}C gHSQCAD of **36α** (500 MHz CDCl$_3$)
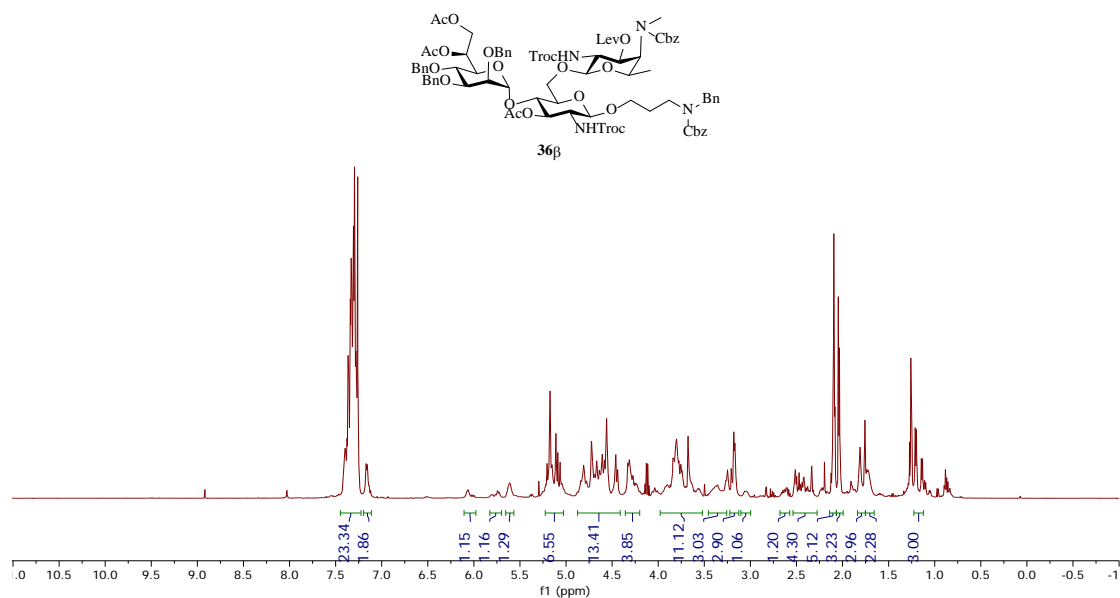
Figure 2.141. ^{1}H-NMR of **36β** (500 MHz CDCl$_3$)
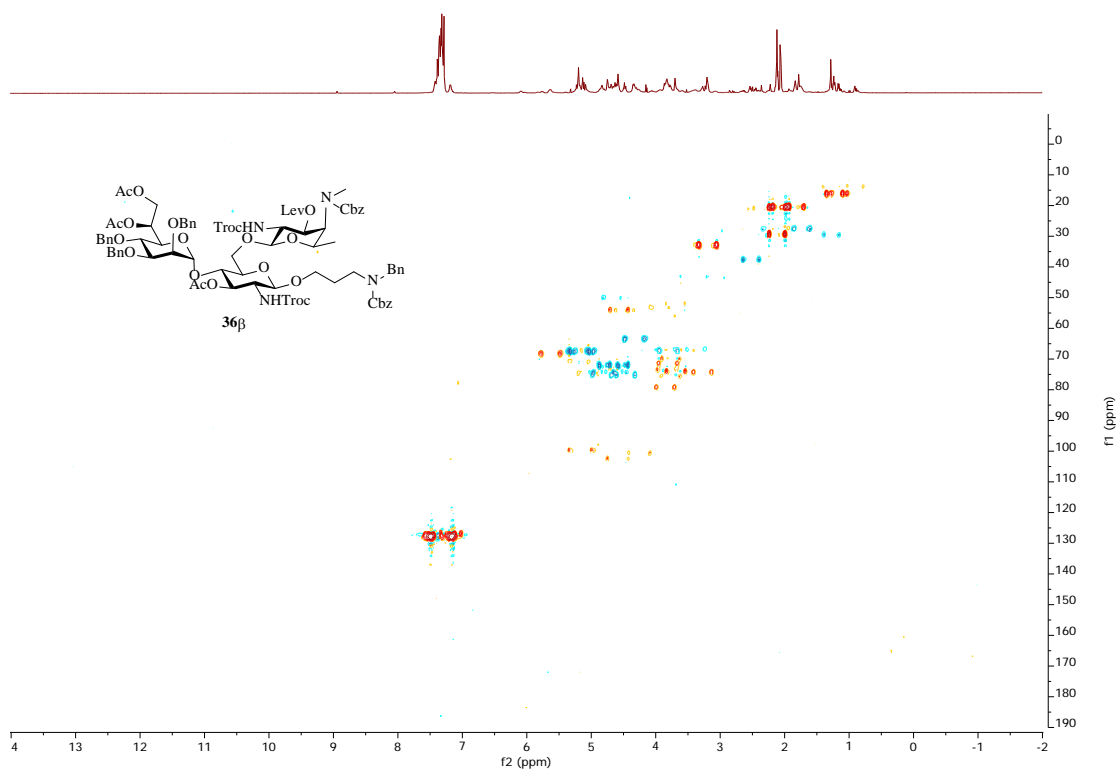
Figure 2.142. ^{1}H-^{13}C gHSQCAD of **36β** (500 MHz CDCl$_3$)
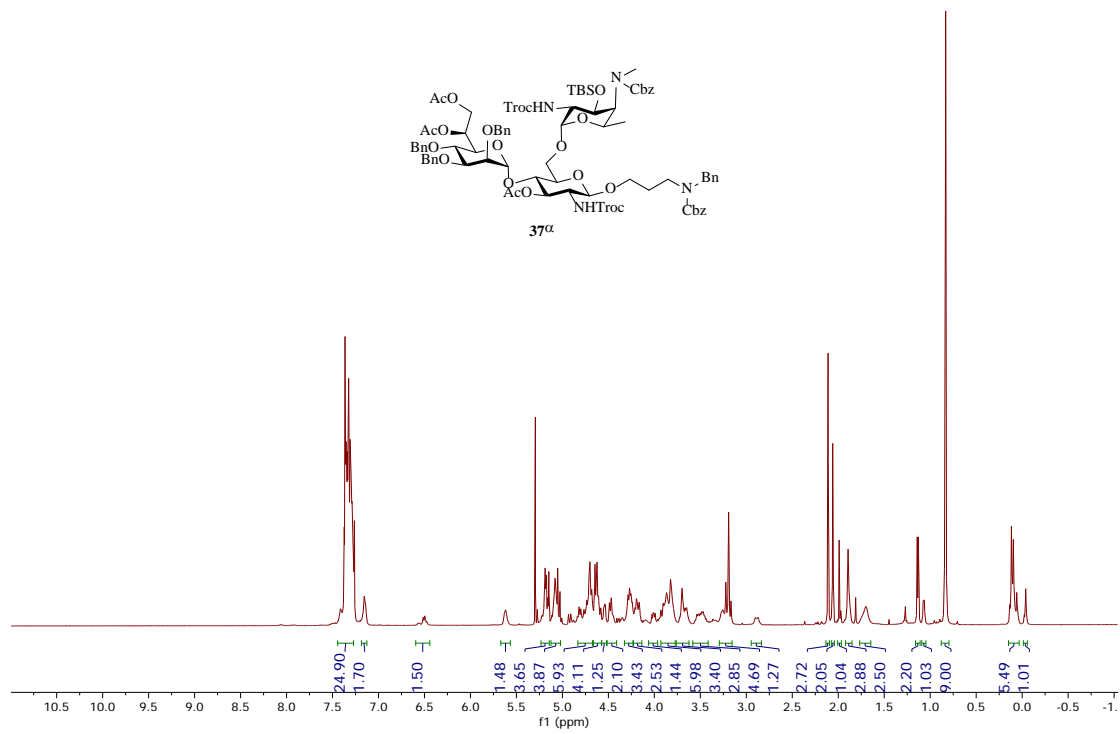
Figure 2.143. ^{1}H-NMR of **37α** (500 MHz CDCl$_3$)
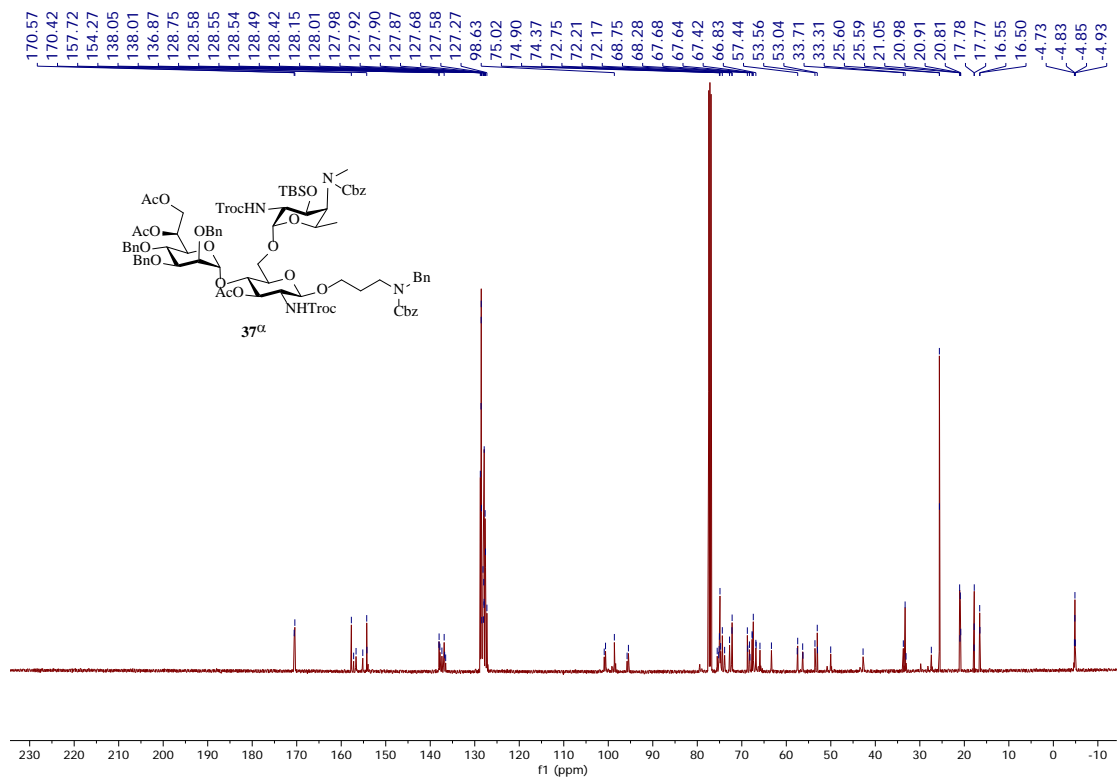
Figure 2.144. ^{13}C-NMR of **37α** (125 MHz CDCl$_3$)

178
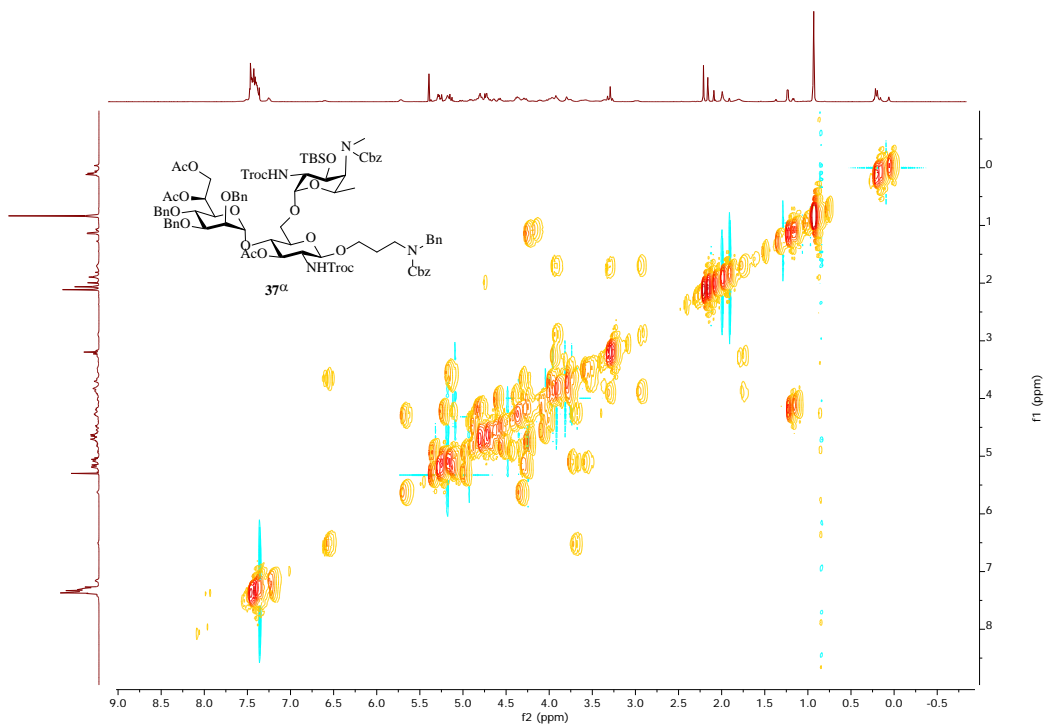
Figure 2.145. ^{1}H-^{1}H gCOSY of **37α** (500 MHz CDCl$_3$)
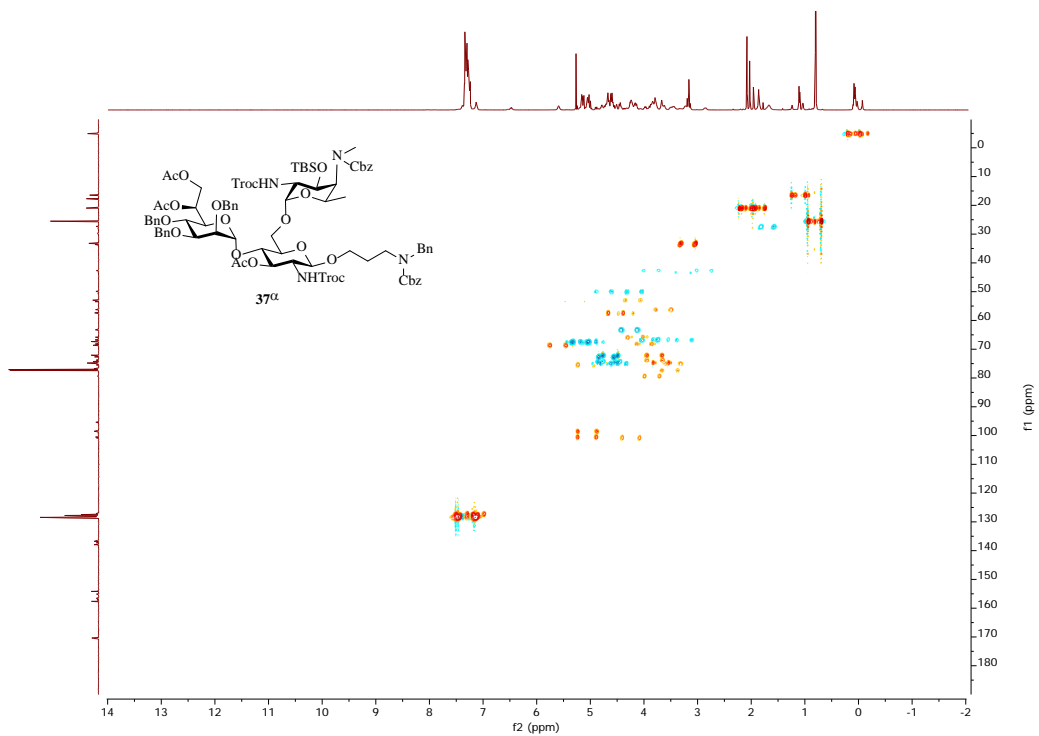
Figure 2.146. ^{1}H-^{13}C gHSQCAD of **37α** (500 MHz CDCl$_3$)
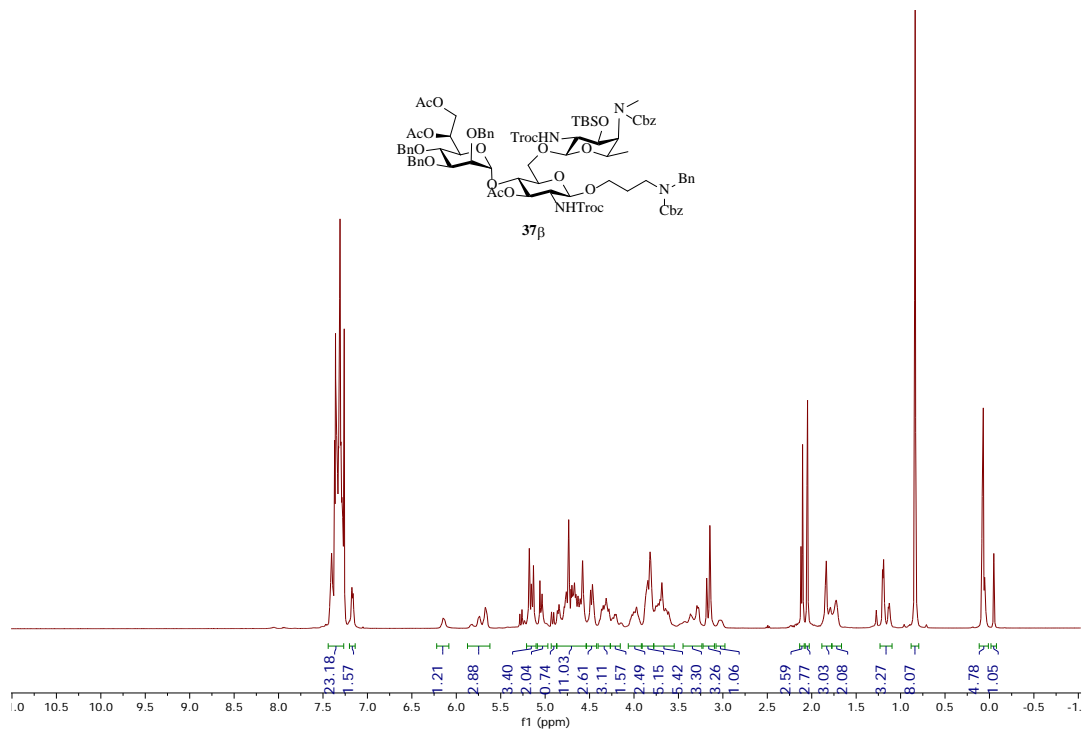
Figure 2.147. ^{1}H-NMR of **37β** (500 MHz CDCl$_3$)
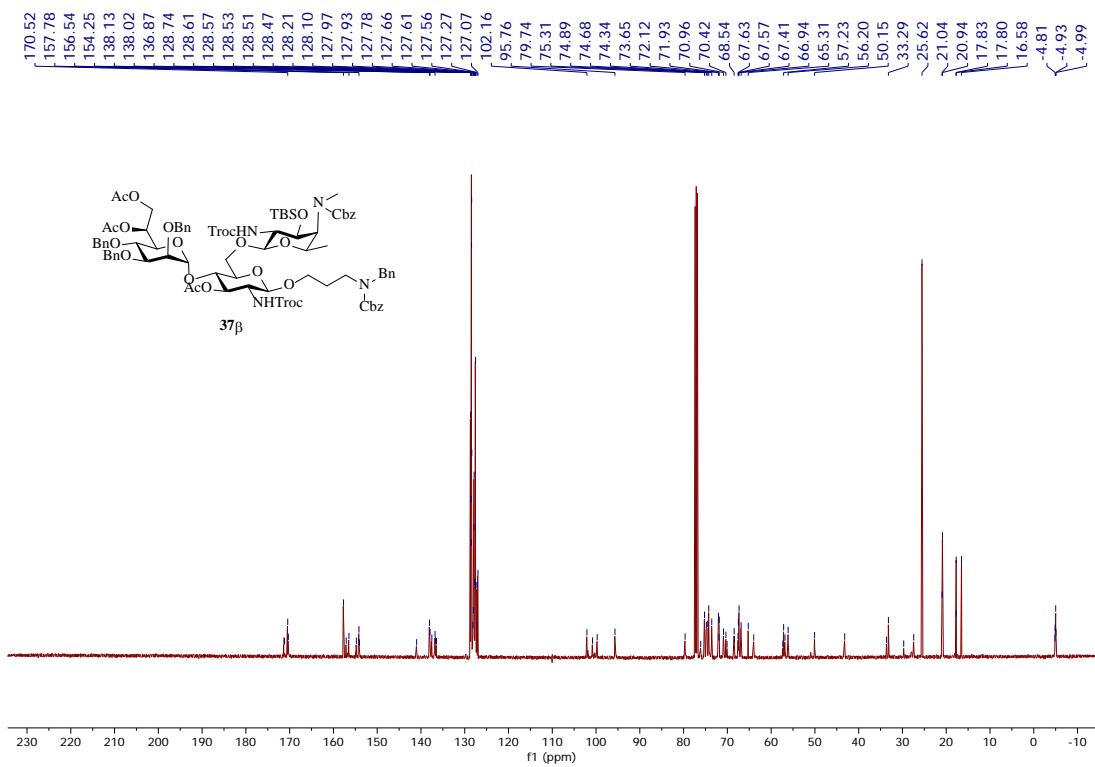
Figure 2.148. ^{13}C-NMR of **37β** (125 MHz CDCl$_3$)
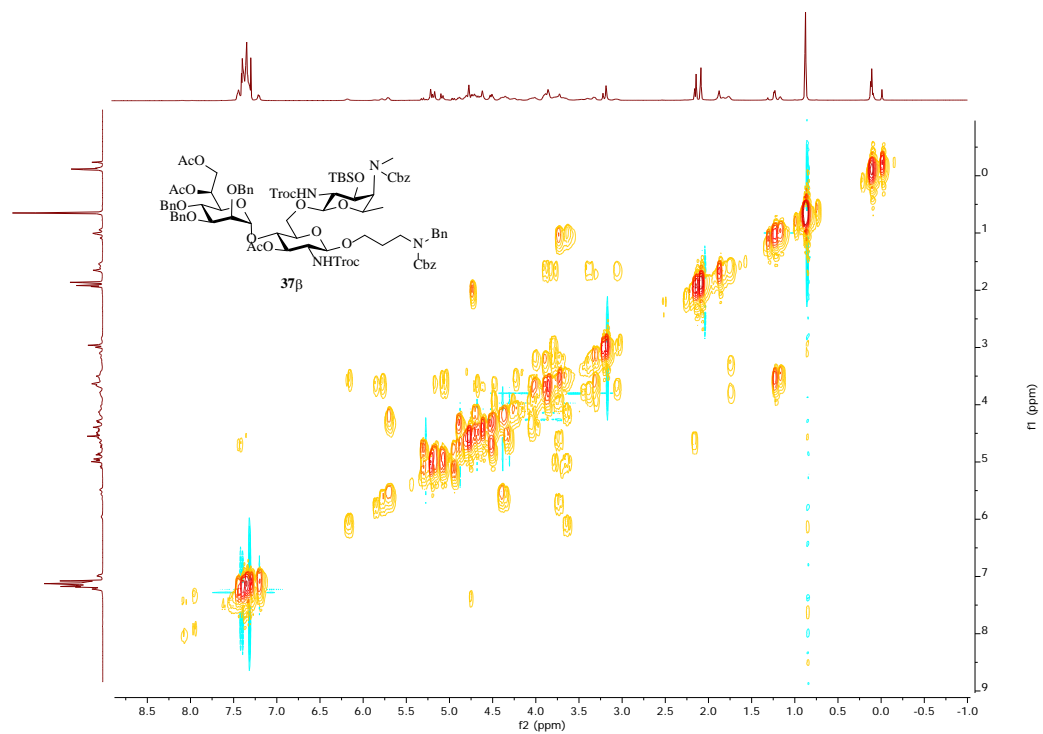
Figure 2.149. ^{1}H-^{1}H gCOSY of **37β** (500 MHz CDCl$_3$)
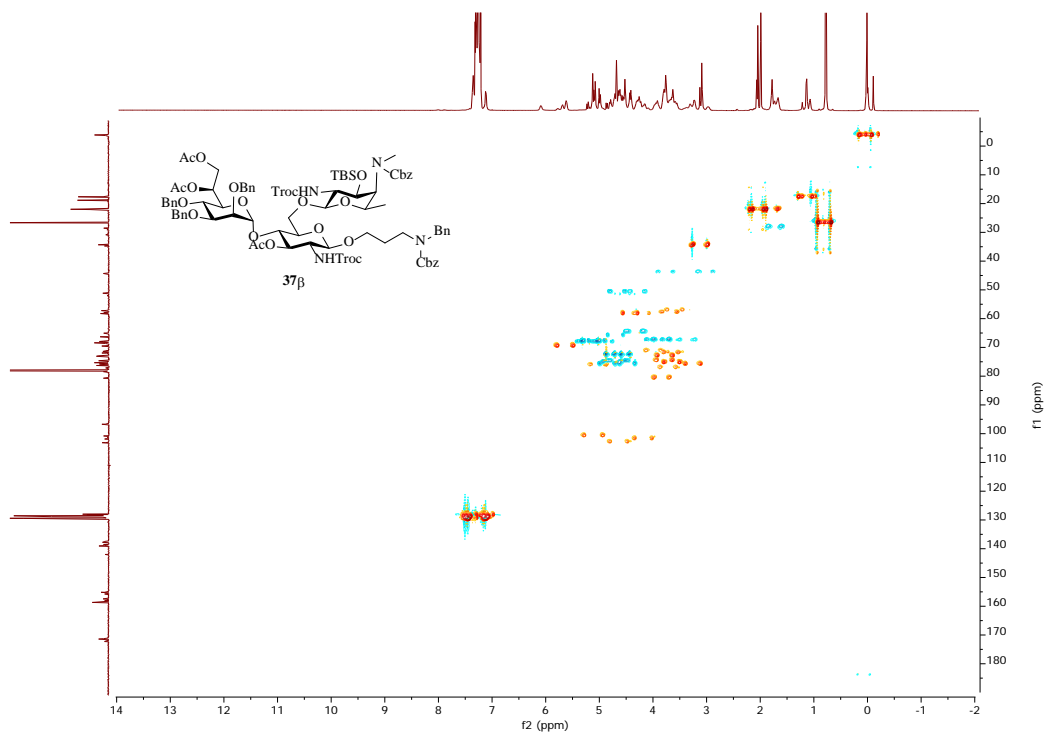
Figure 2.150. ^{1}H-^{13}C gHSQCAD of **37β** (500 MHz CDCl$_3$)
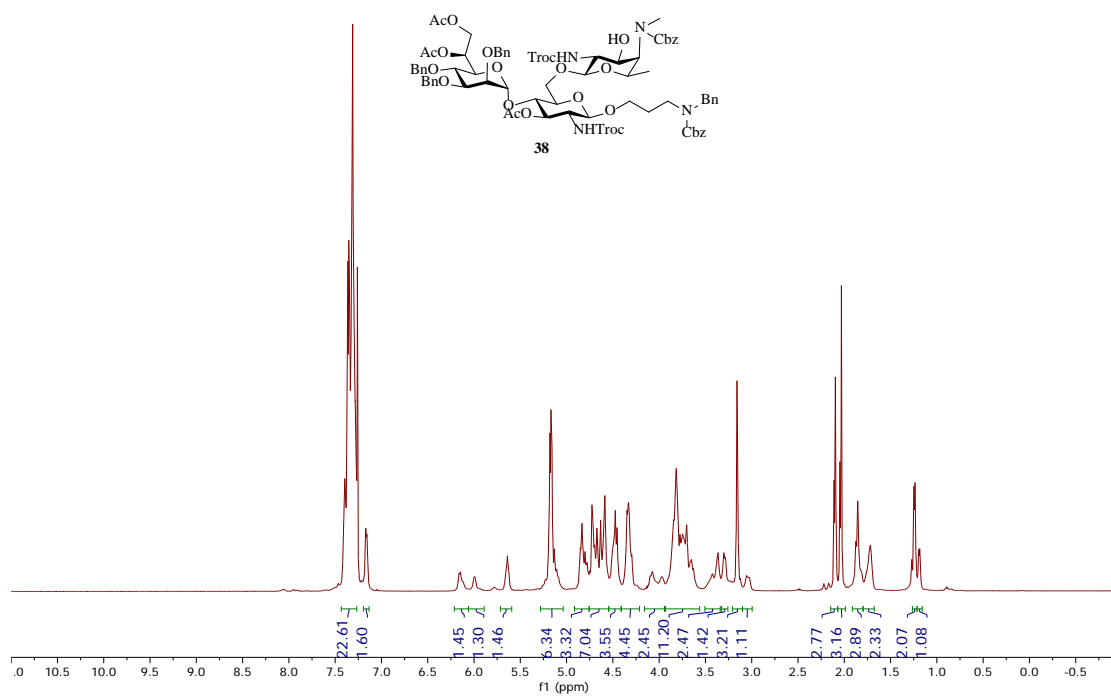
Figure 2.151. ^{1}H-NMR of **38** (500 MHz CDCl$_3$)
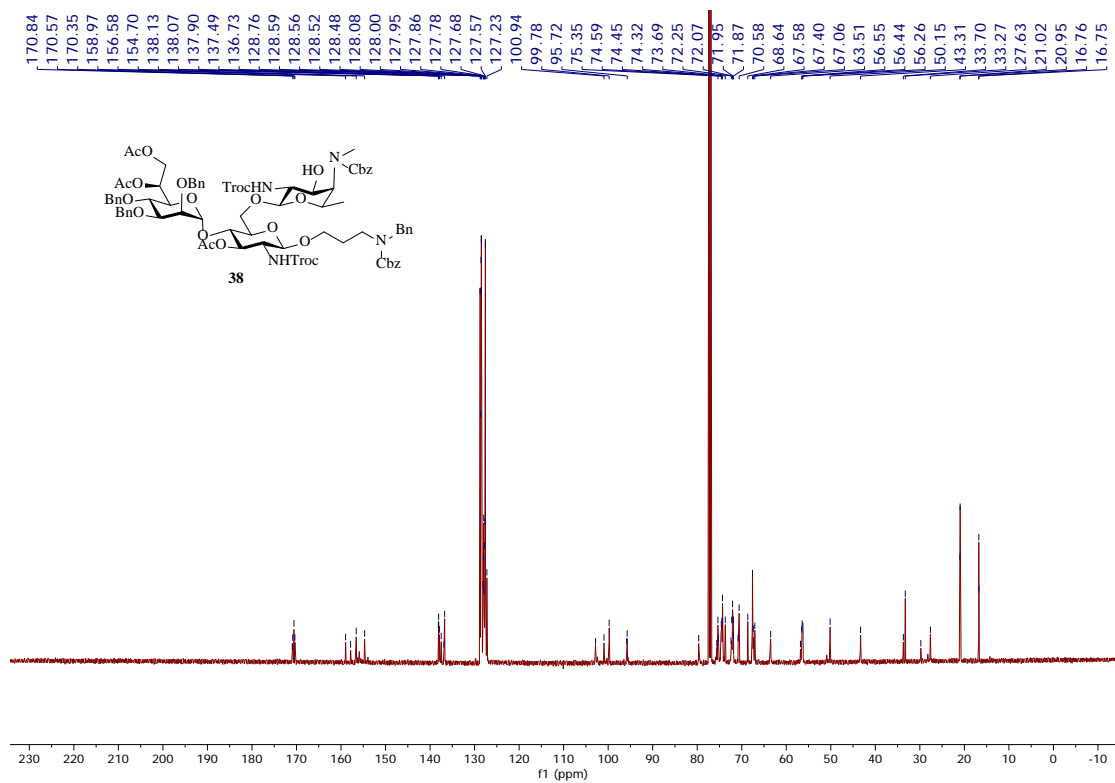
Figure 2.152. ^{13}C-NMR of **38** (125 MHz CDCl$_3$)
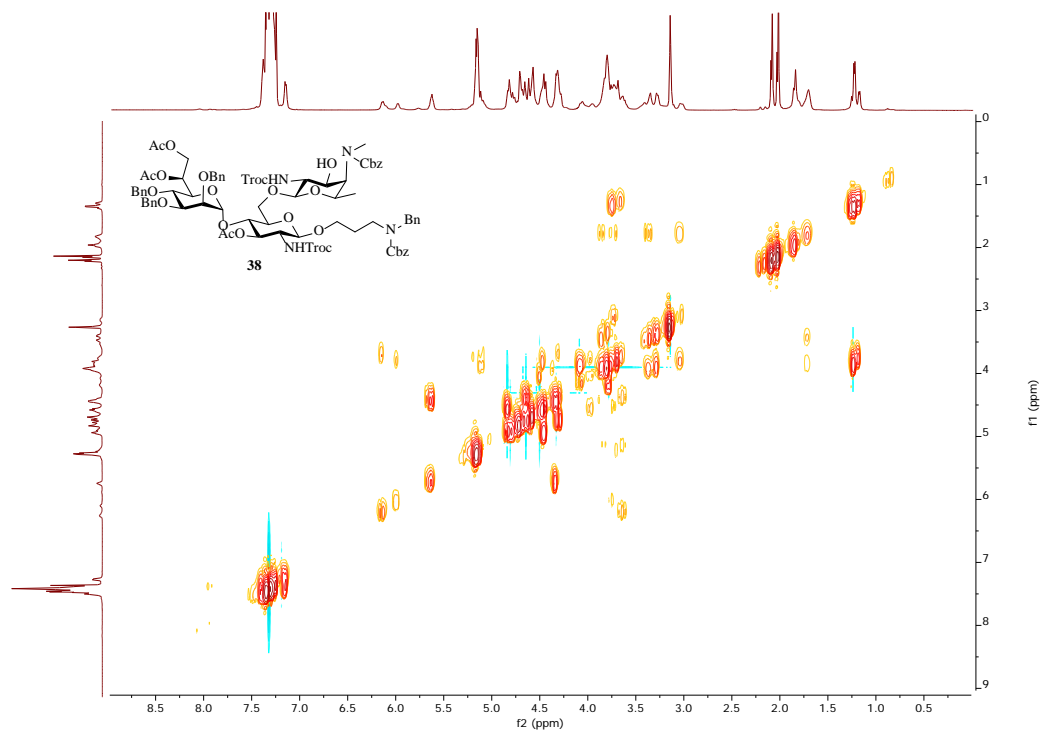
Figure 2.153. ^{1}H-^{1}H gCOSY of **38** (500 MHz CDCl$_3$)
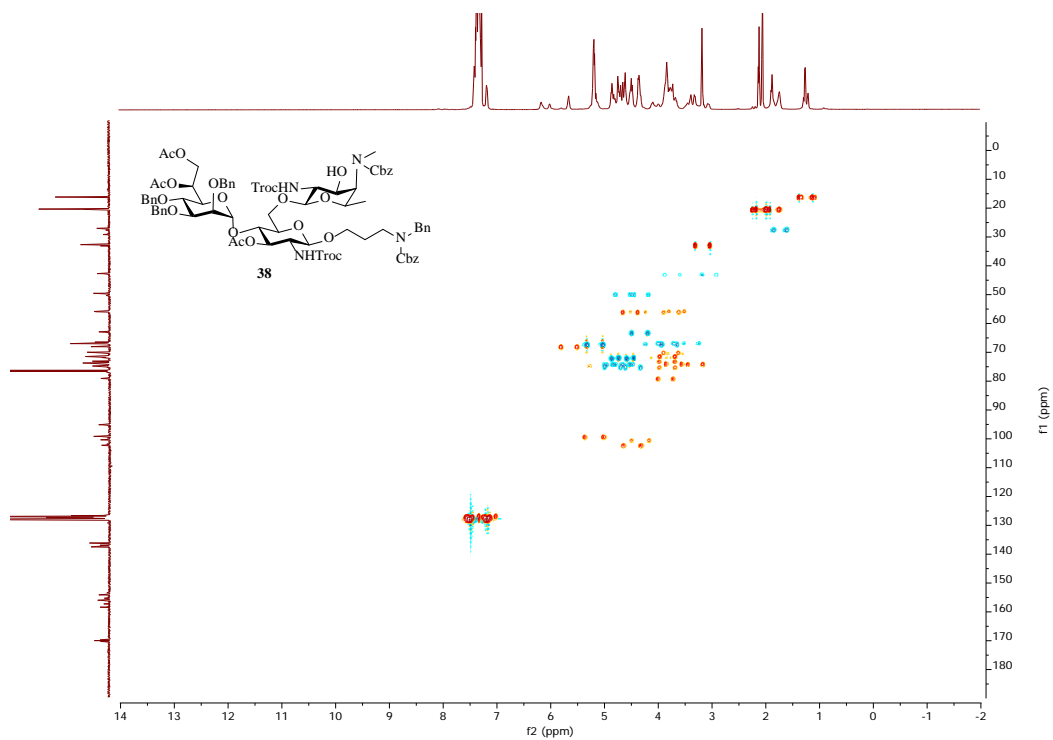
Figure 2.154. ^{1}H-^{13}C gHSQCAD of **38** (500 MHz CDCl$_3$)
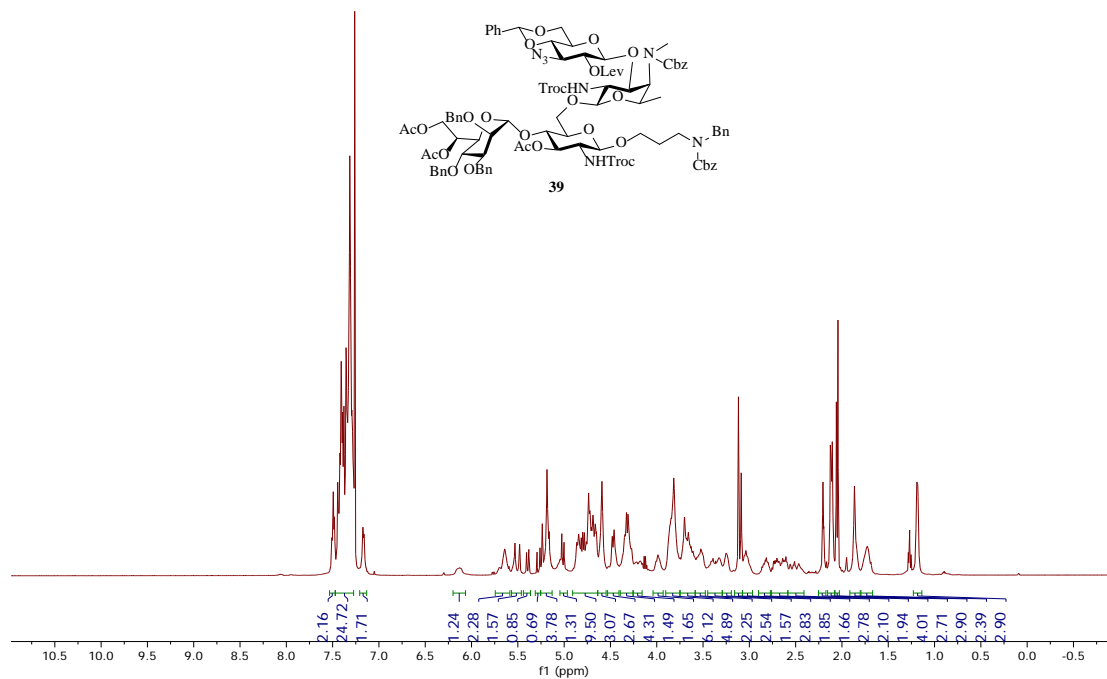
Figure 2.155. ^{1}H-NMR of **39** (500 MHz CDCl$_3$)
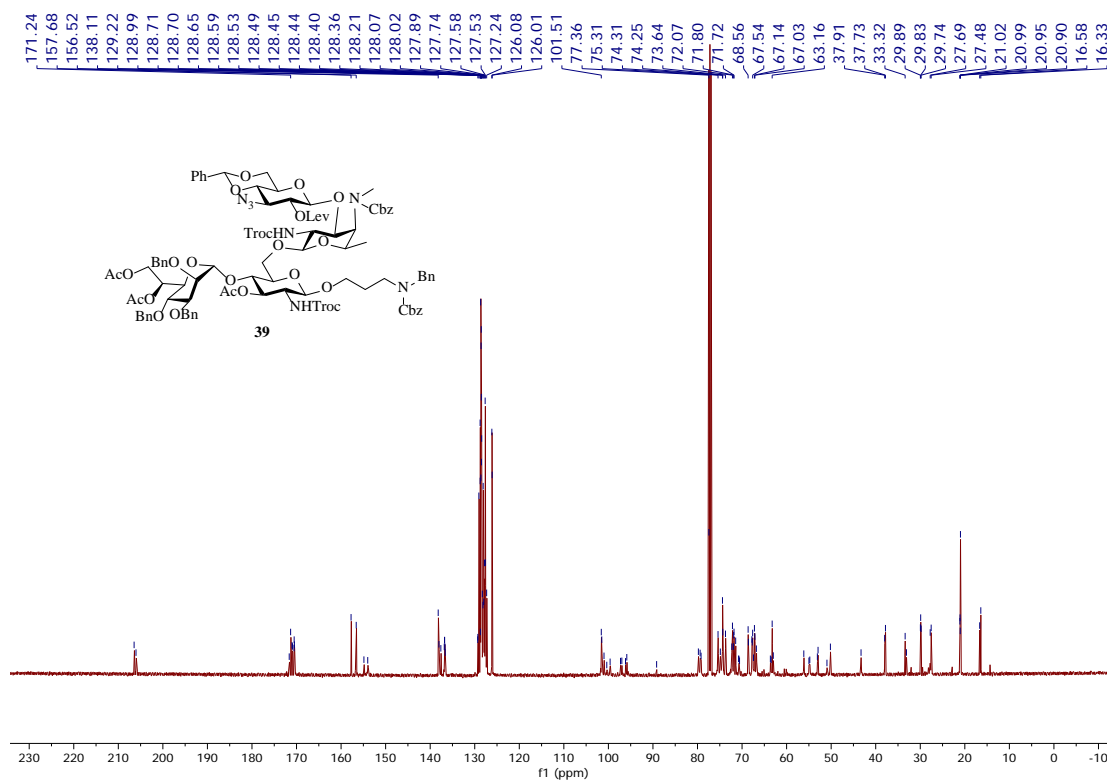
Figure 2.156. ^{13}C-NMR of **39** (125 MHz CDCl$_3$)
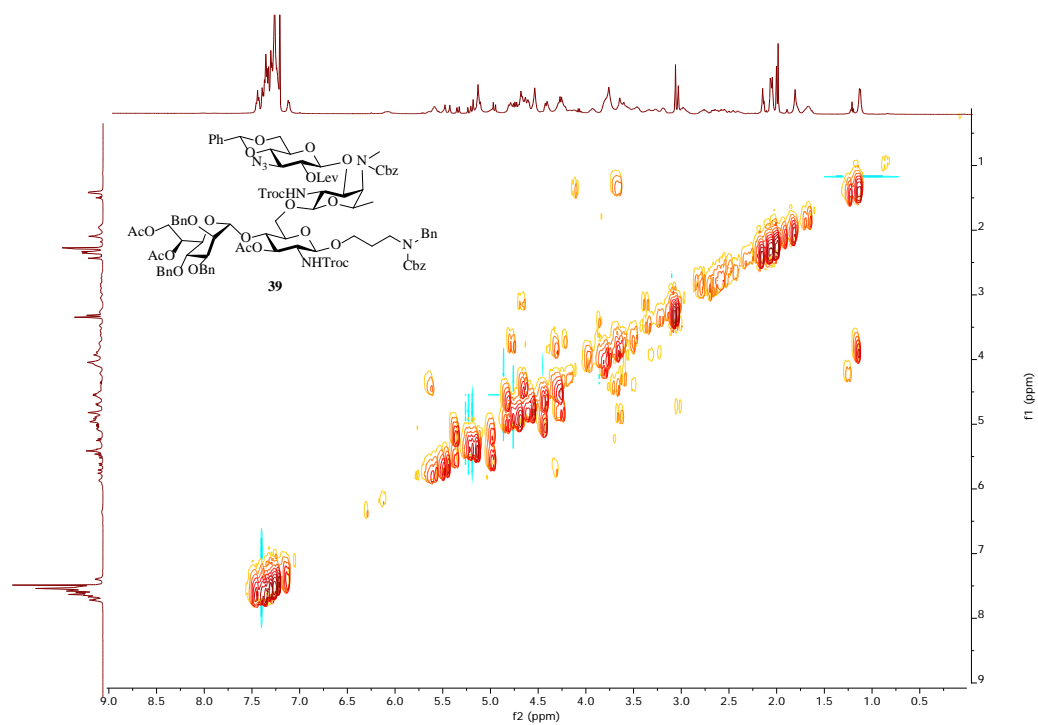
Figure 2.157. ^{1}H-^{1}H gCOSY of **39** (500 MHz CDCl$_3$)
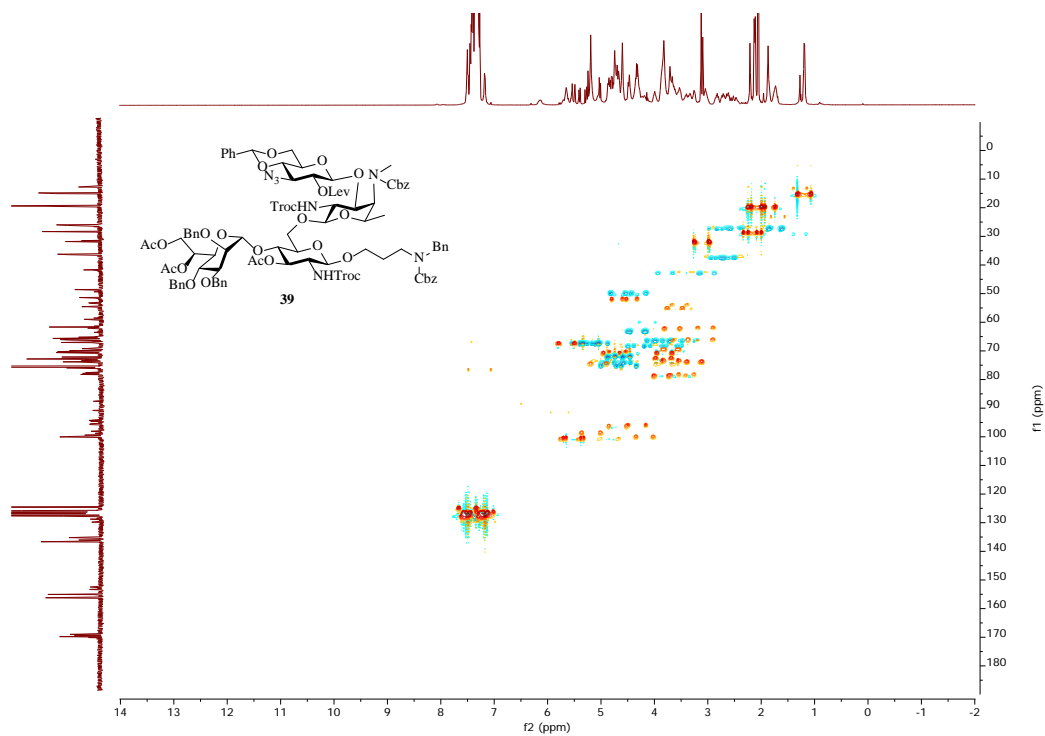
Figure 2.158. ^{1}H-^{13}C gHSQCAD of **39** (500 MHz CDCl$_3$)
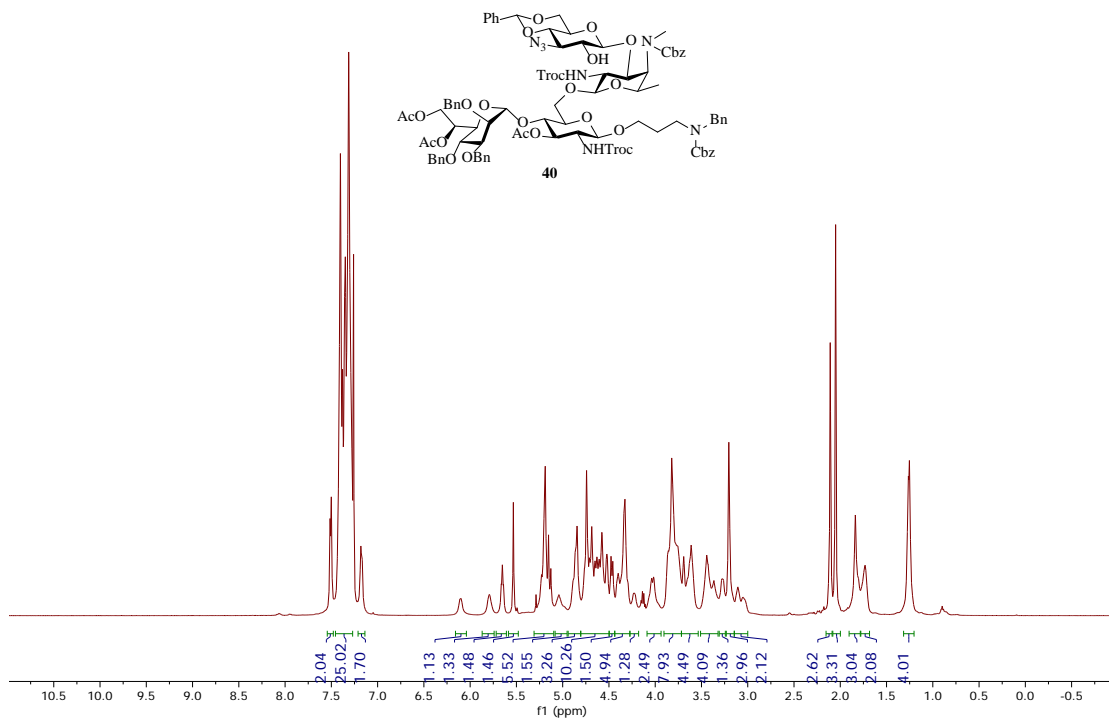
Figure 2.159. ^{1}H-NMR of **40** (500 MHz CDCl$_3$)
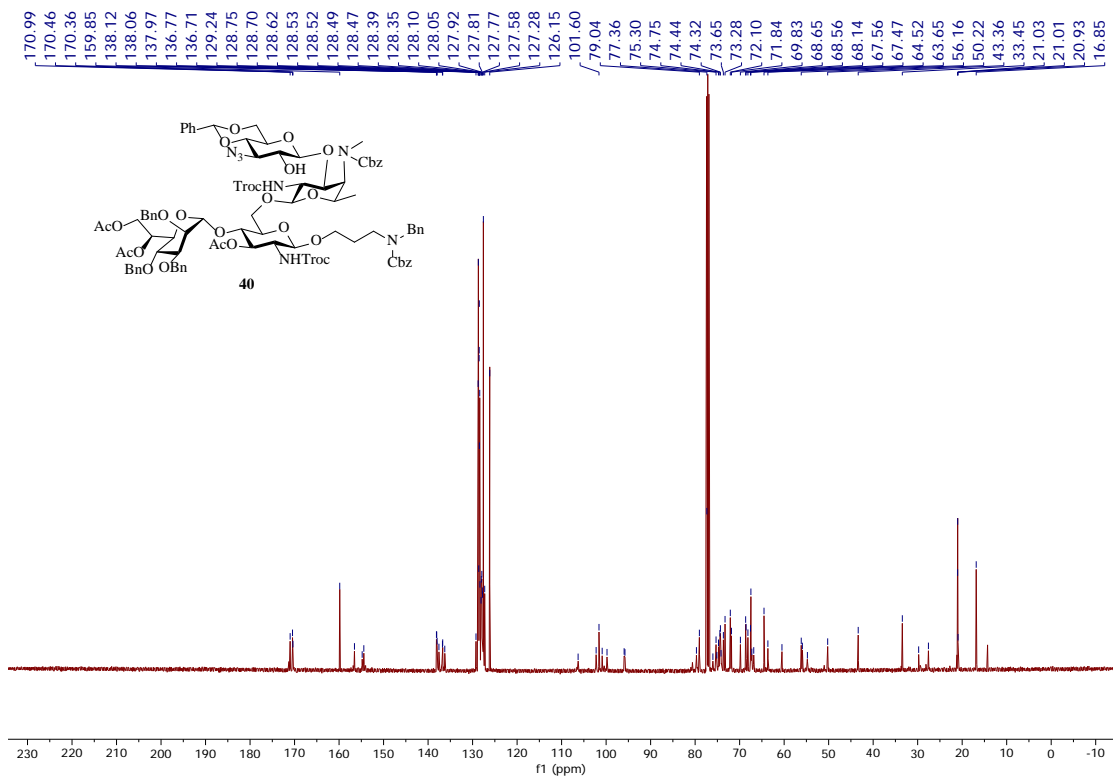
Figure 2.160. ^{13}C-NMR of **40** (125 MHz CDCl$_3$)
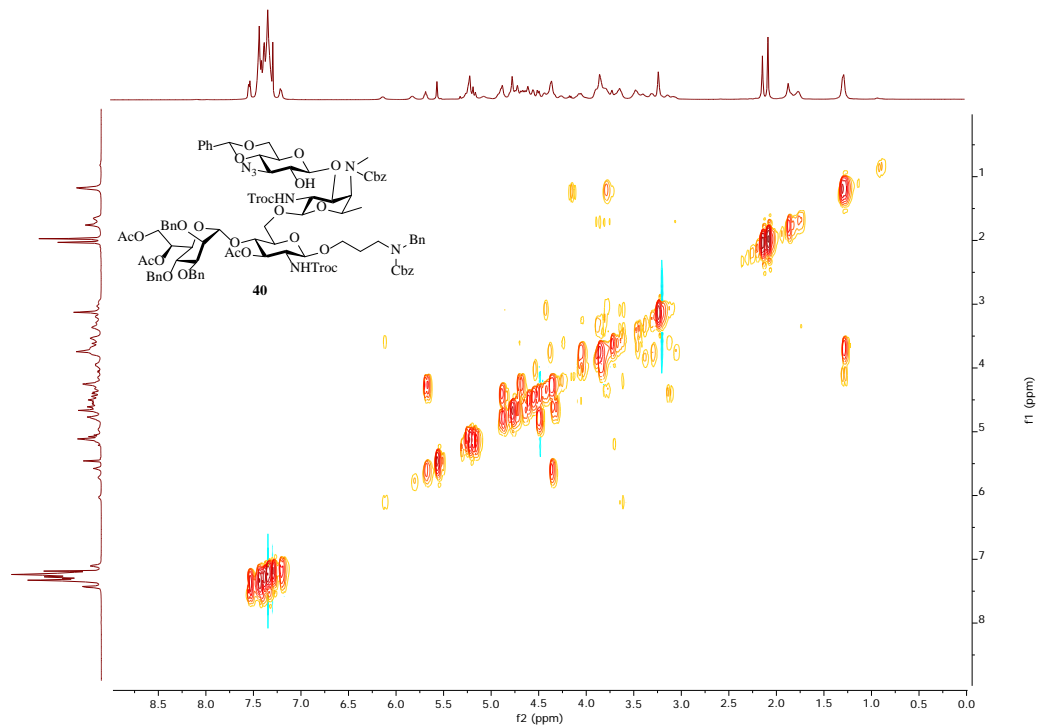
Figure 2.161. ^{1}H-^{1}H gCOSY of **40** (500 MHz CDCl$_3$)
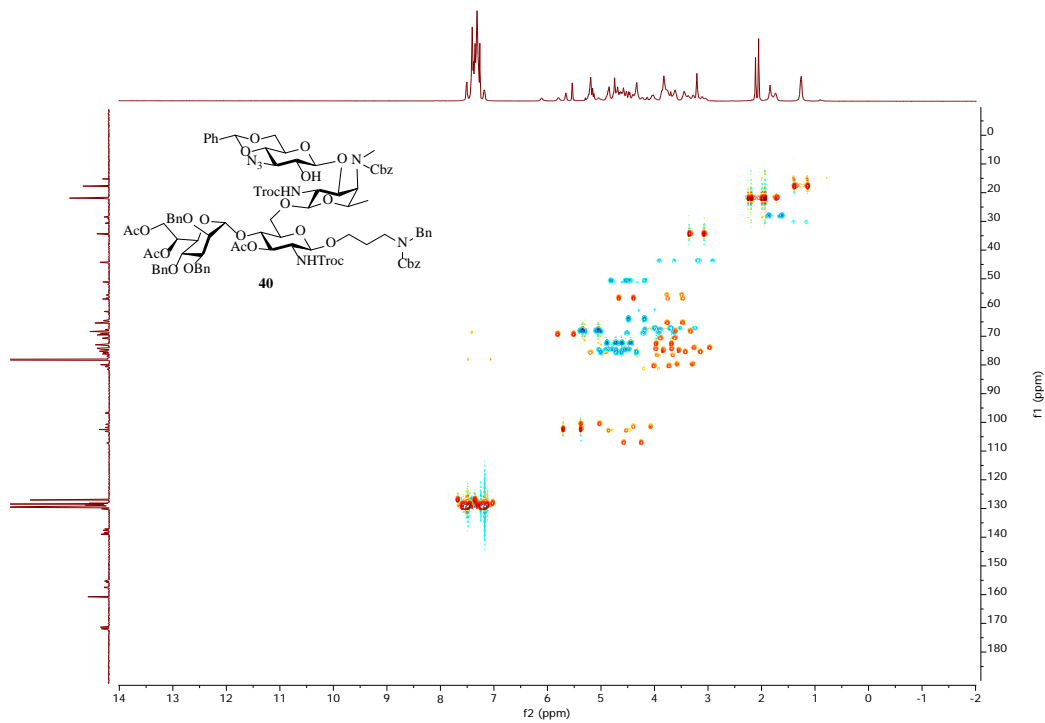
Figure 2.162. ^{1}H-^{13}C gHSQCAD of **40** (500 MHz CDCl$_3$)
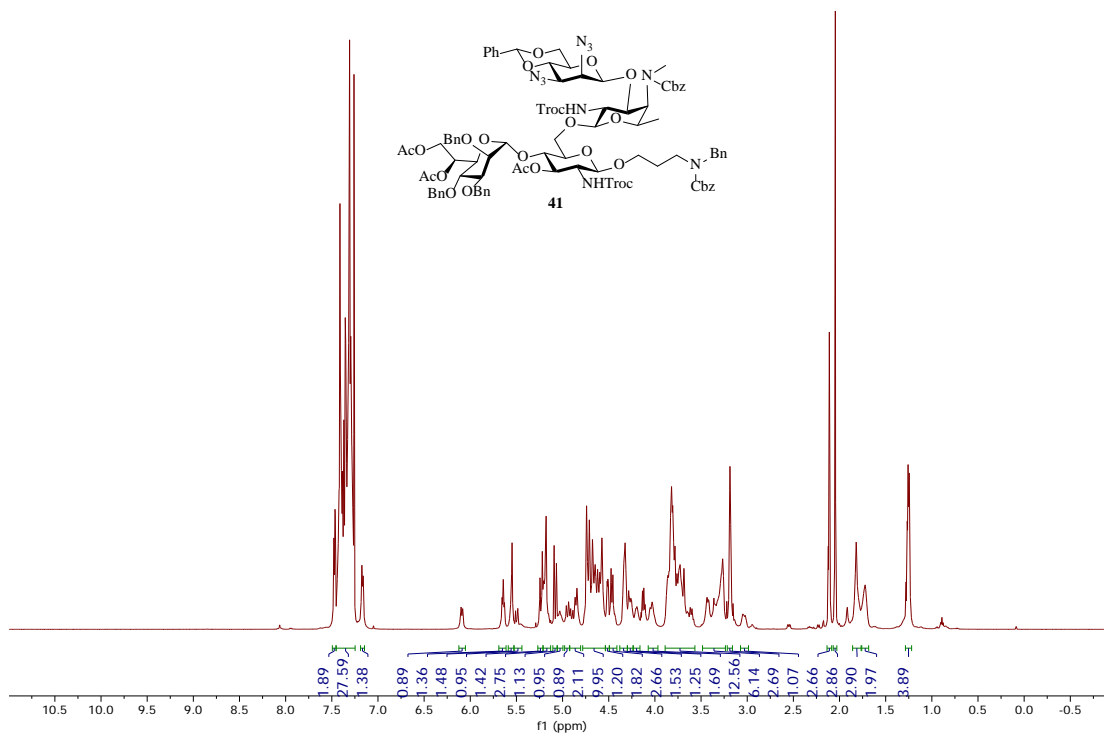
Figure 2.163. ^{1}H-NMR of **41** (500 MHz CDCl$_3$)
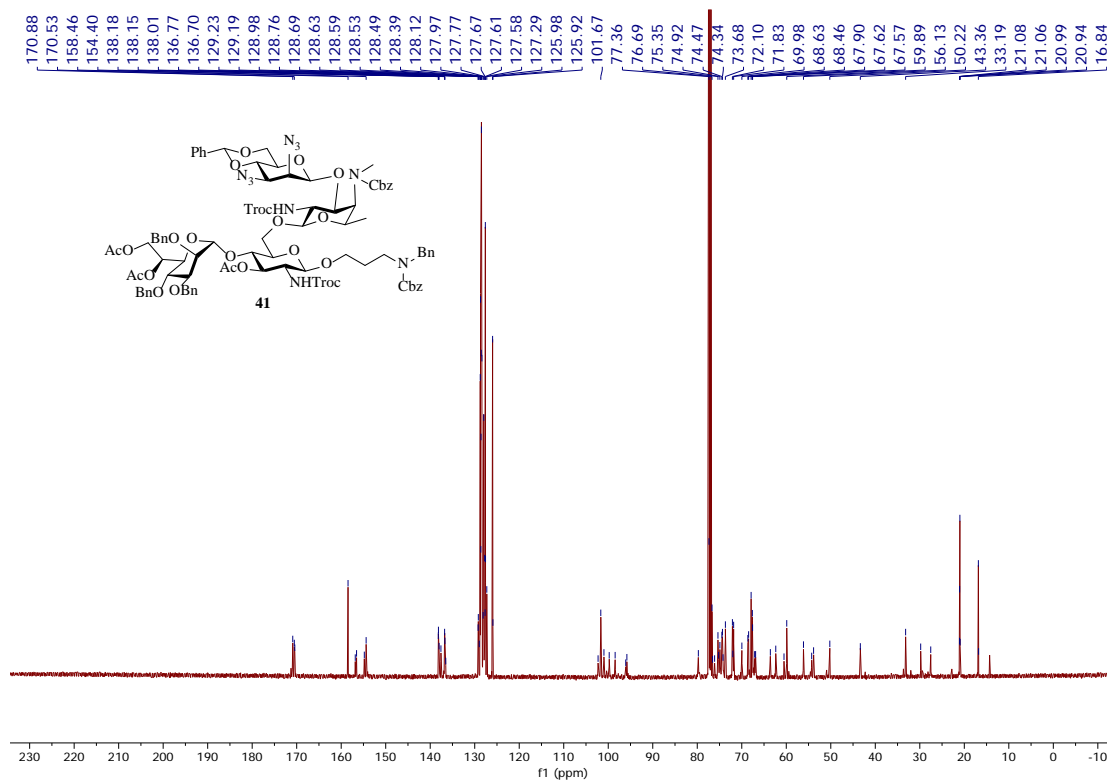
Figure 2.164. ^{13}C-NMR of **41** (125 MHz CDCl$_3$)
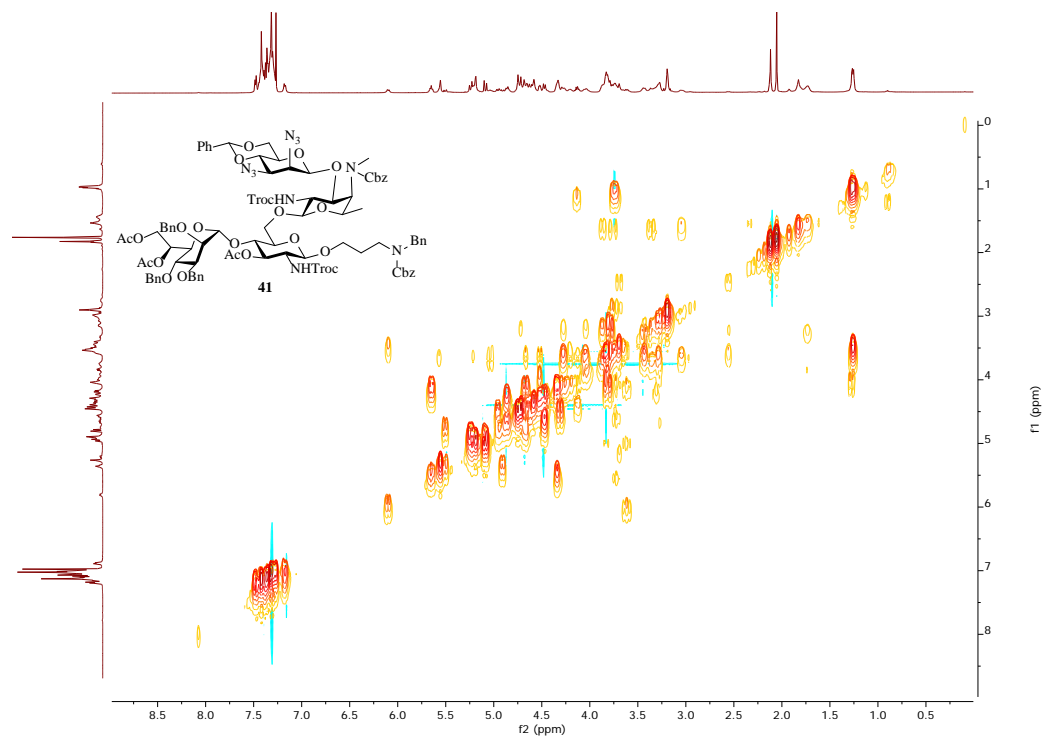
Figure 2.165. ^{1}H-^{1}H gCOSY of **41** (500 MHz CDCl$_3$)
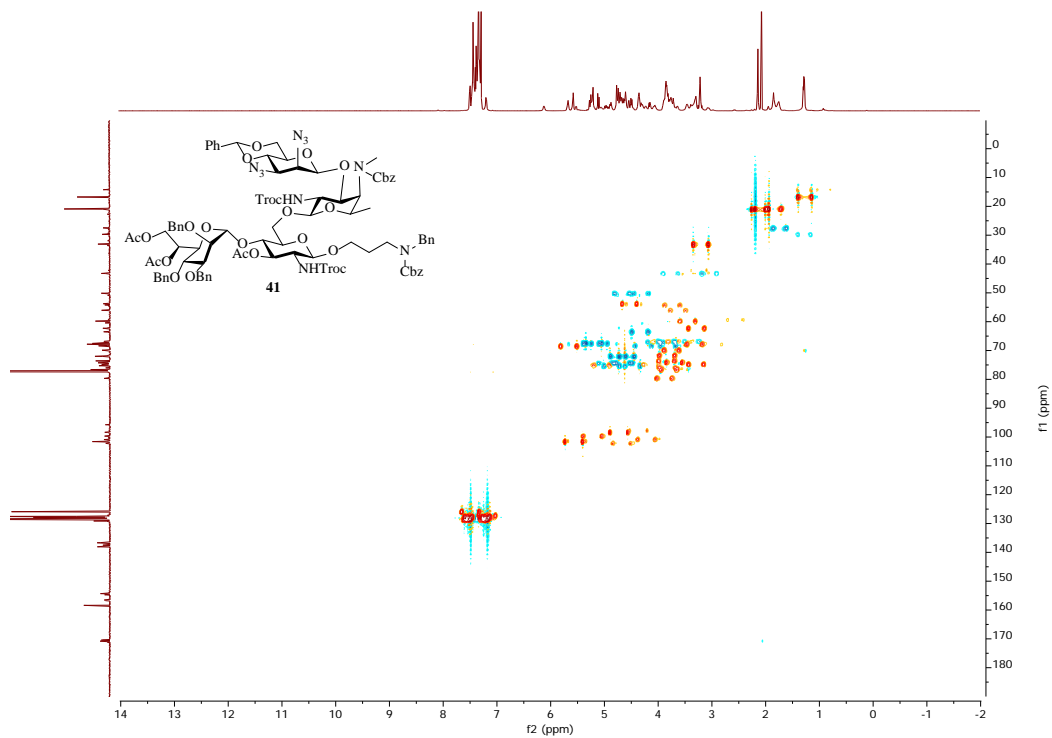
Figure 2.166. ^{1}H-^{13}C gHSQCAD of **41** (500 MHz CDCl$_3$)
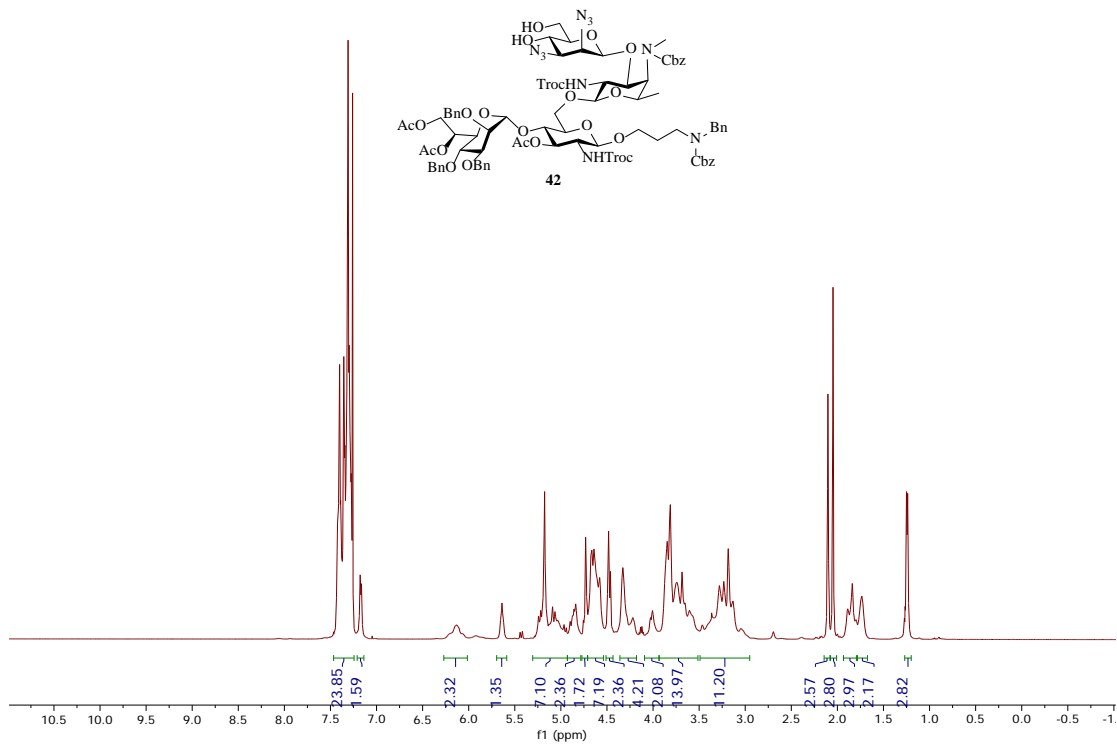
Figure 2.167. ^{1}H-NMR of **42** (500 MHz CDCl$_3$)
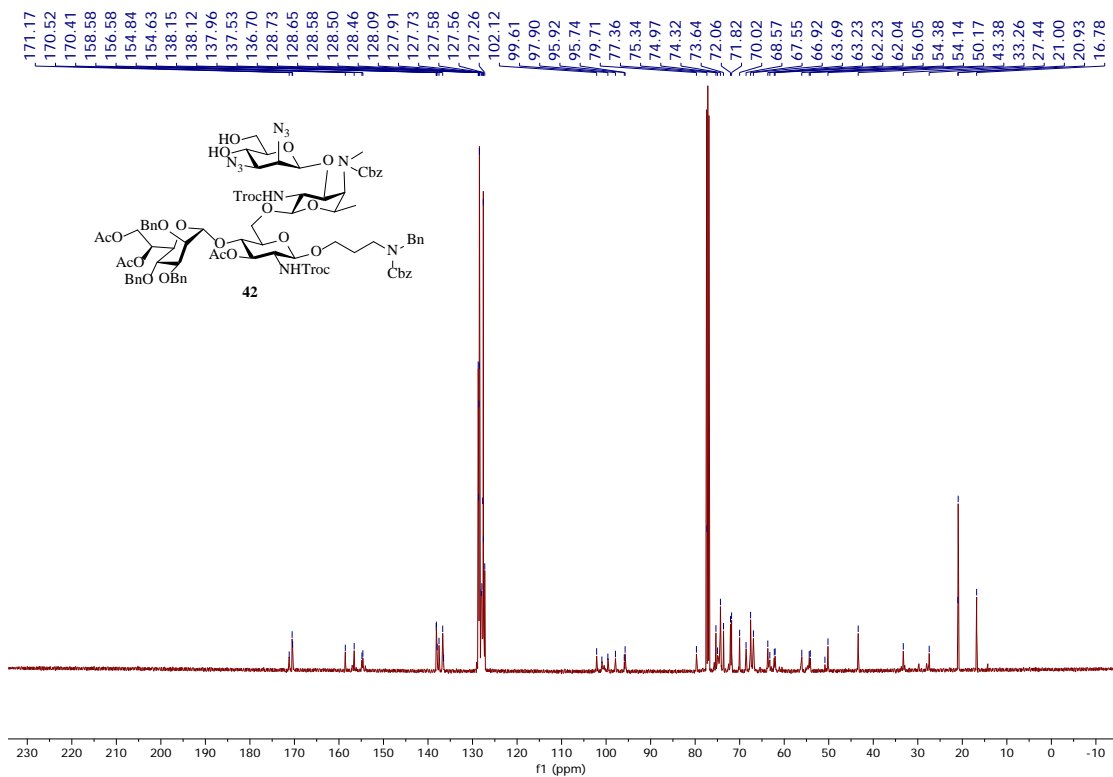
Figure 2.168. ^{13}C-NMR of **42** (125 MHz CDCl$_3$)
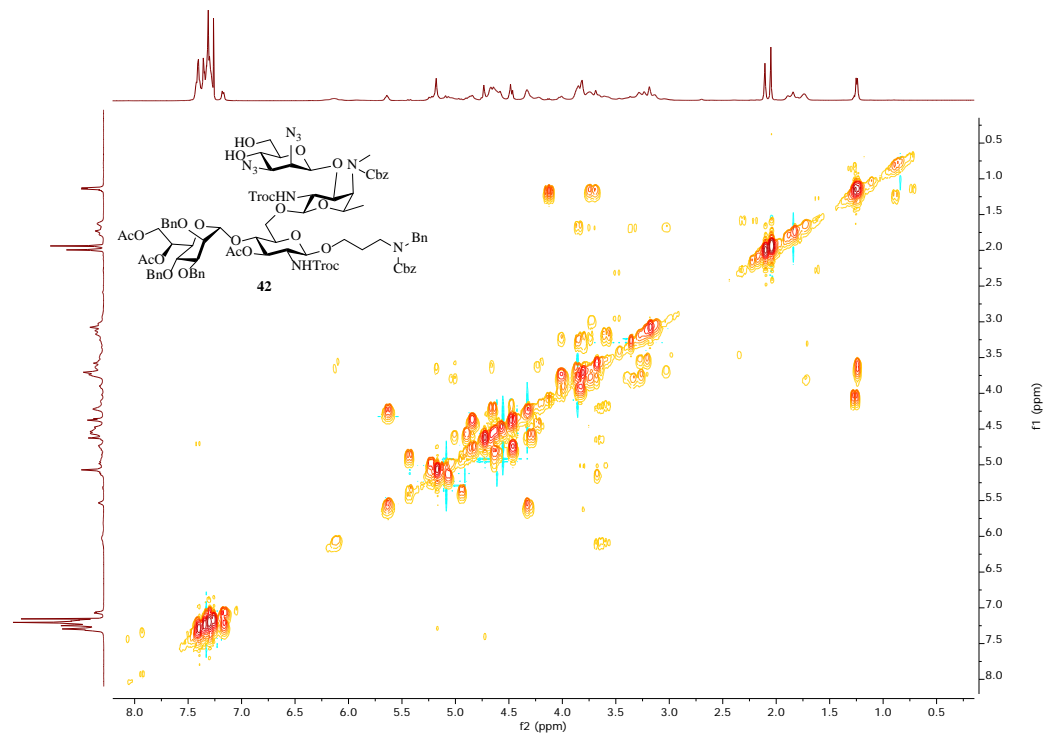
Figure 2.169. ^{1}H-^{1}H gCOSY of **42** (500 MHz CDCl$_3$)
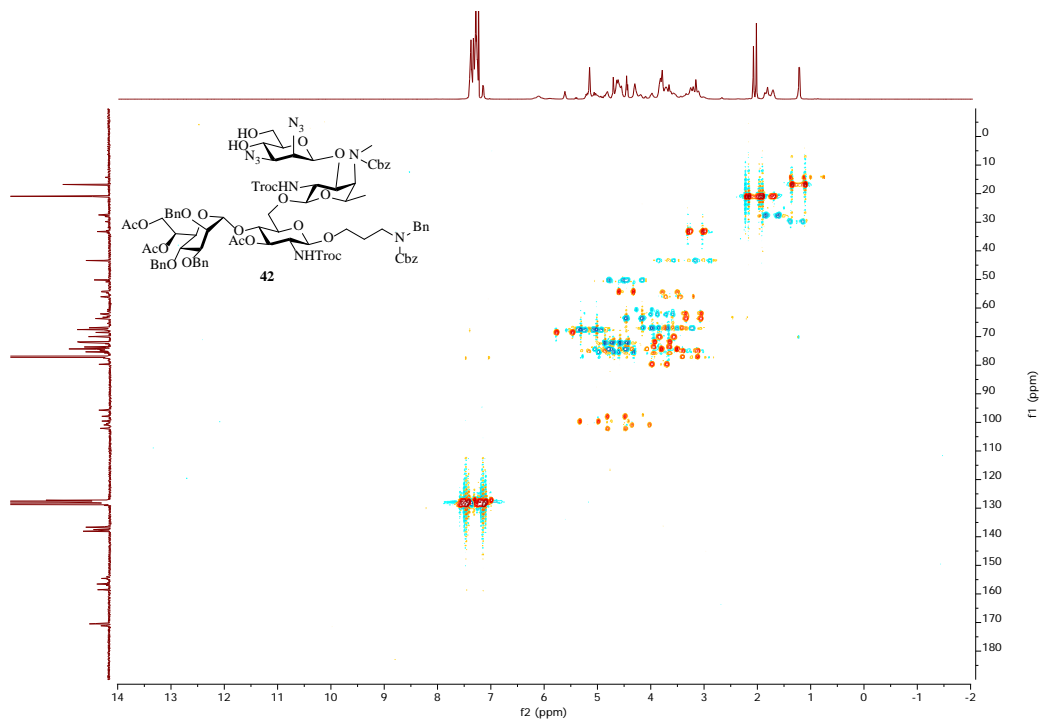
Figure 2.170. ^{1}H-^{13}C gHSQCAD of **42** (500 MHz CDCl$_3$)
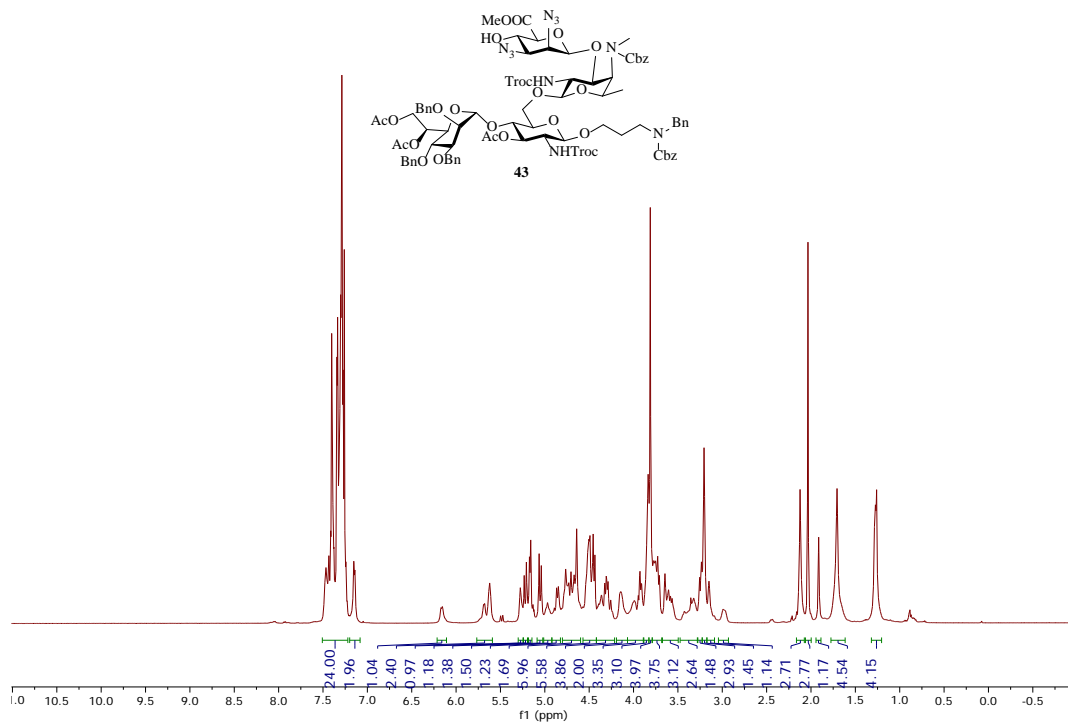
Figure 2.171. ^{1}H-NMR of **43** (500 MHz CDCl$_3$)
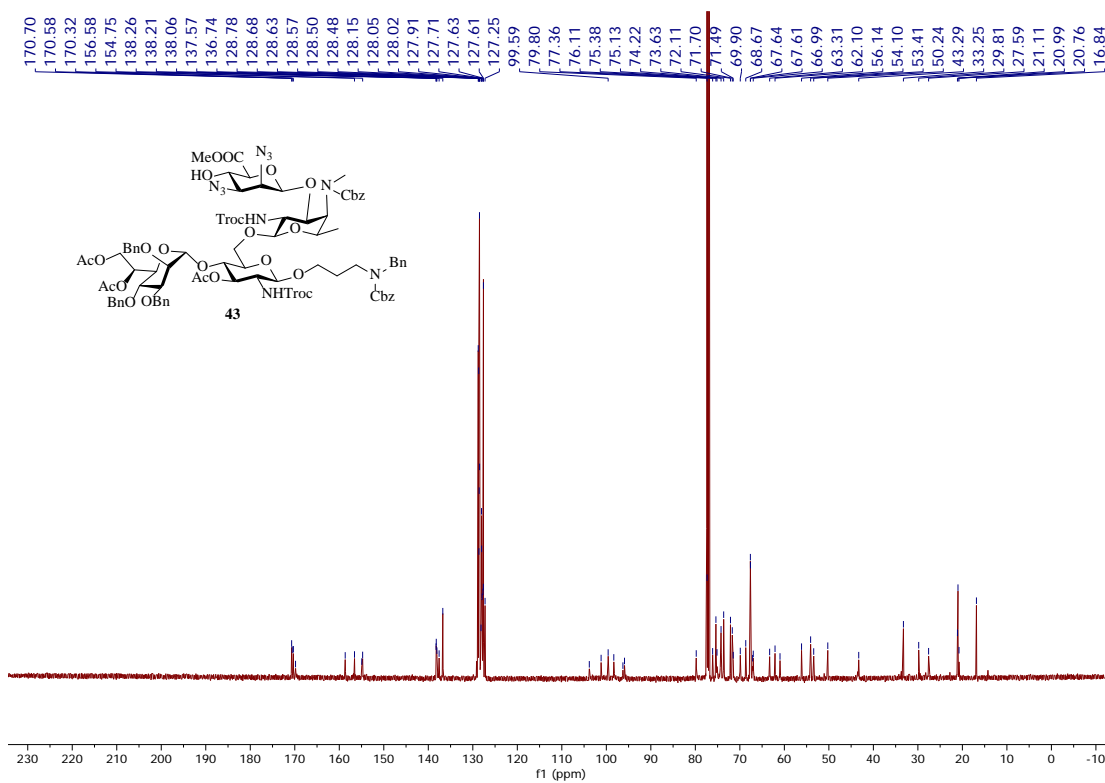
Figure 2.172. ^{13}C-NMR of **43** (125 MHz CDCl$_3$)
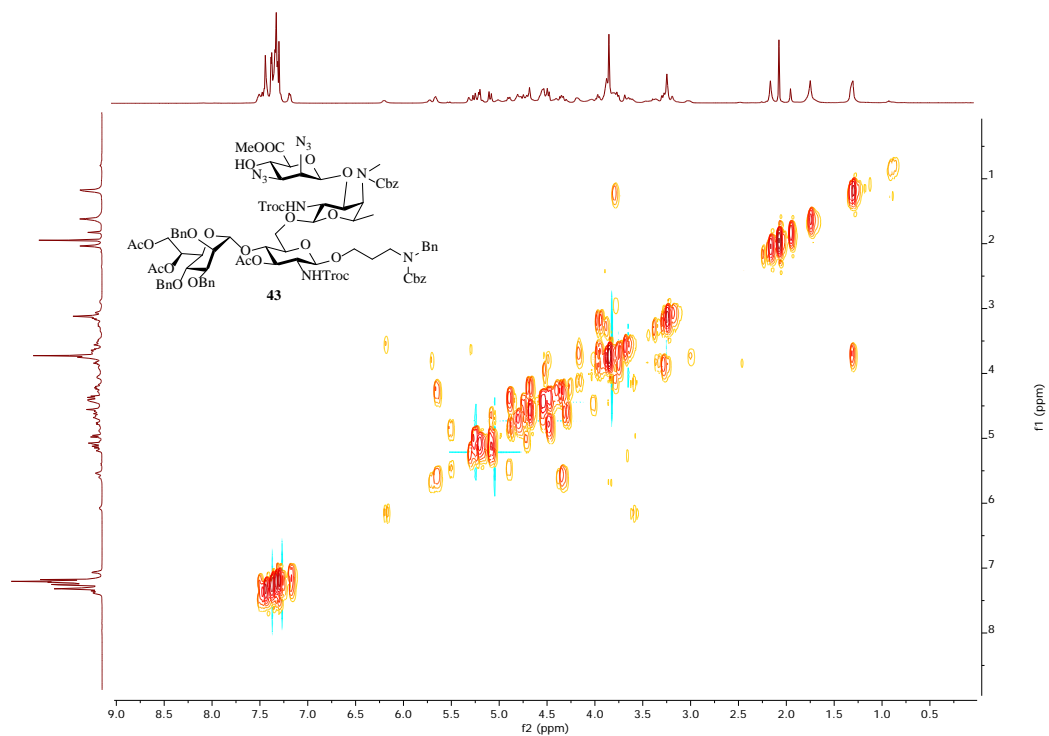
Figure 2.173. ^{1}H-^{1}H gCOSY of **43** (500 MHz CDCl$_3$)
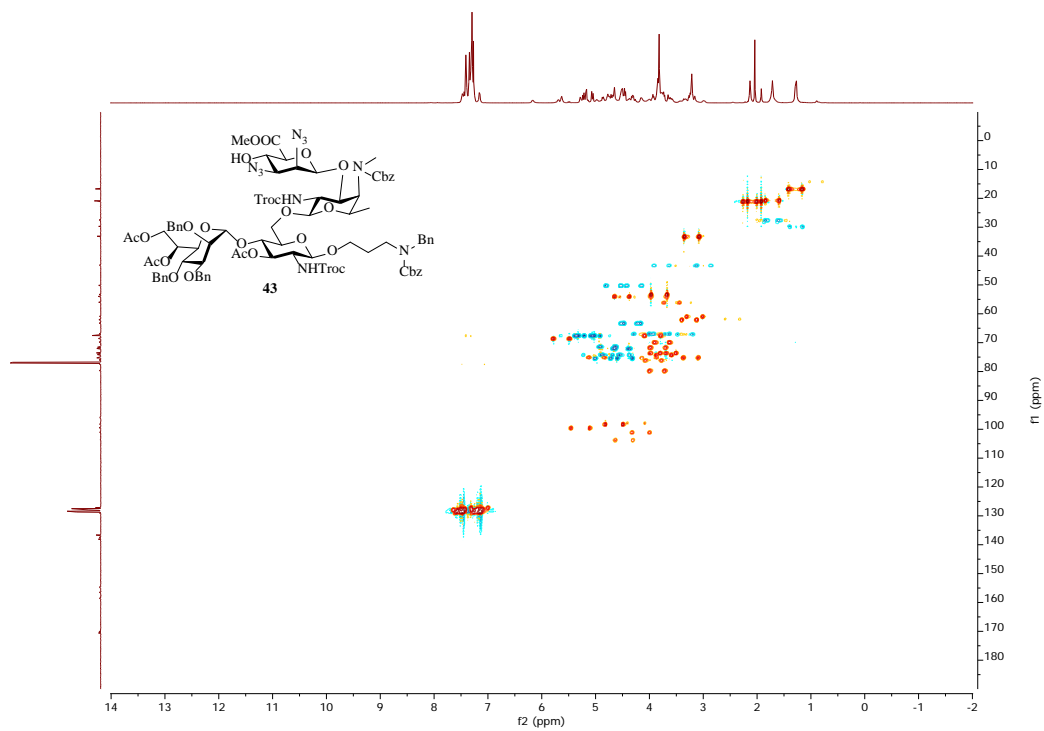
Figure 2.174. ^{1}H-^{13}C gHSQCAD of **43** (500 MHz CDCl$_3$)
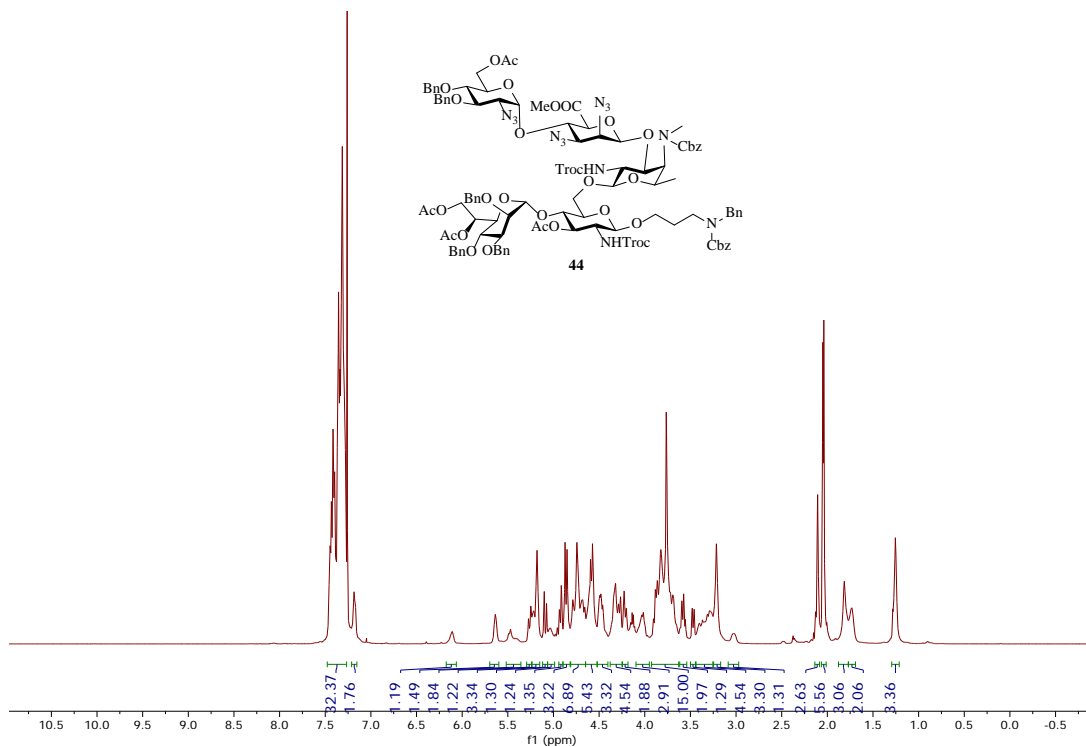
Figure 2.175. ^{1}H-NMR of **44** (500 MHz CDCl$_3$)
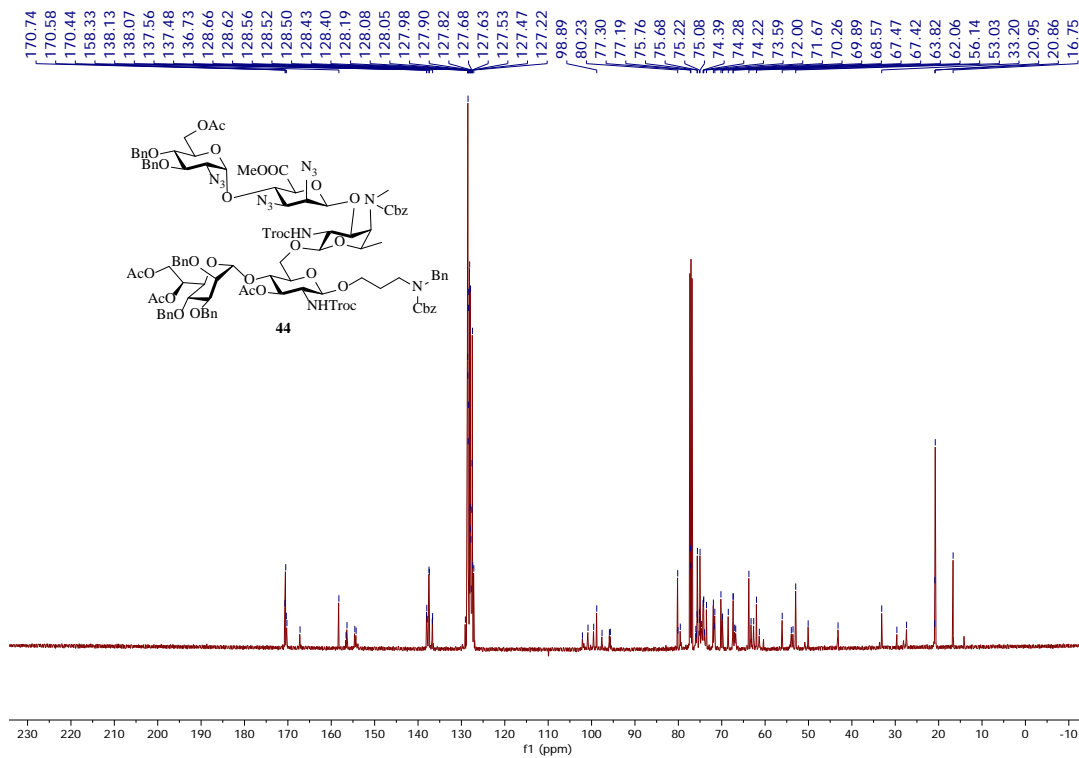
Figure 2.176. ^{13}C-NMR of **44** (125 MHz CDCl$_3$)
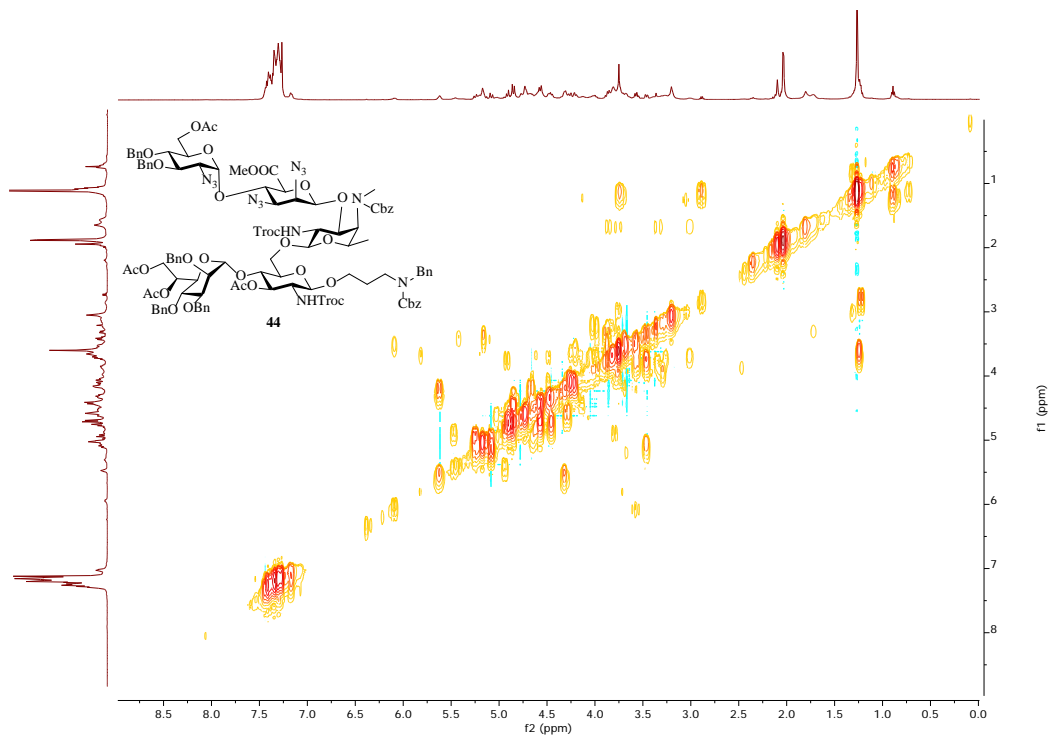
Figure 2.177. ^{1}H-^{1}H gCOSY of **44** (500 MHz CDCl$_3$)
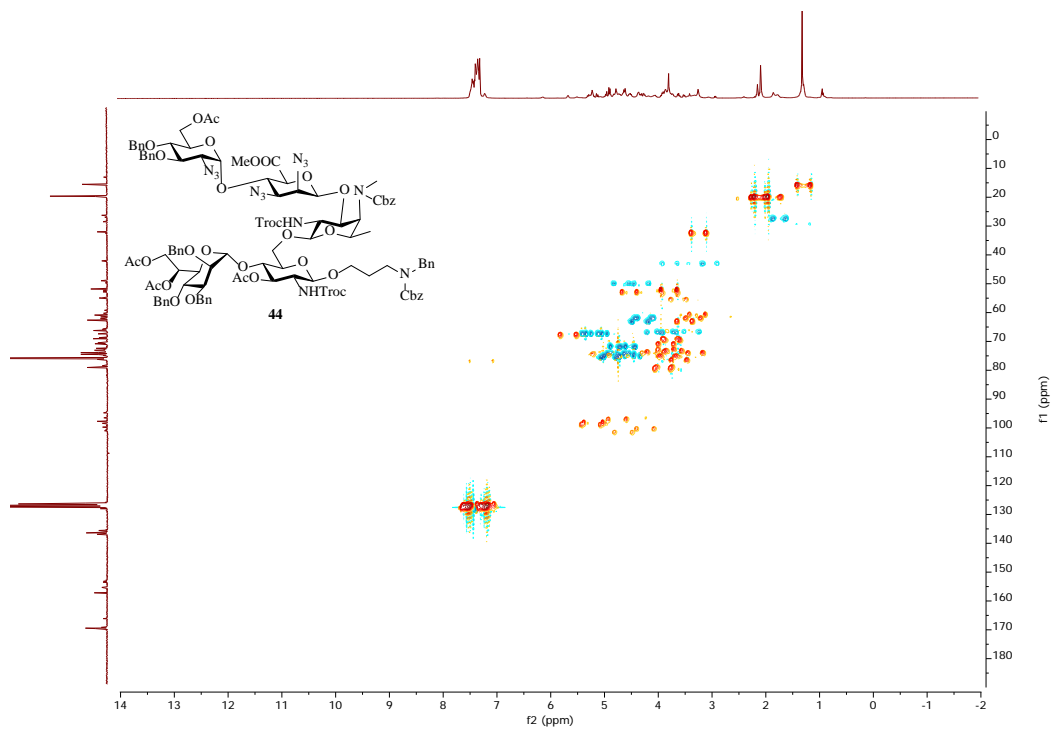
Figure 2.178. ^{1}H-^{13}C gHSQCAD of **44** (500 MHz CDCl$_3$)
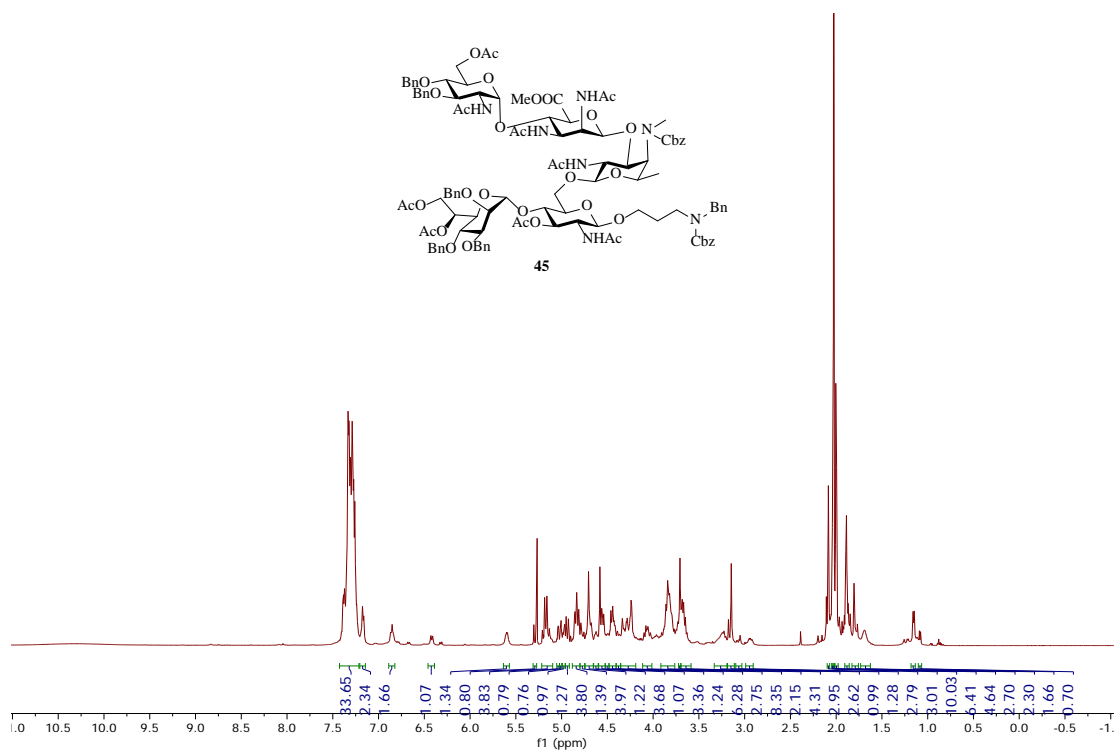
Figure 2.179. ^{1}H-NMR of **45** (500 MHz CDCl$_3$)
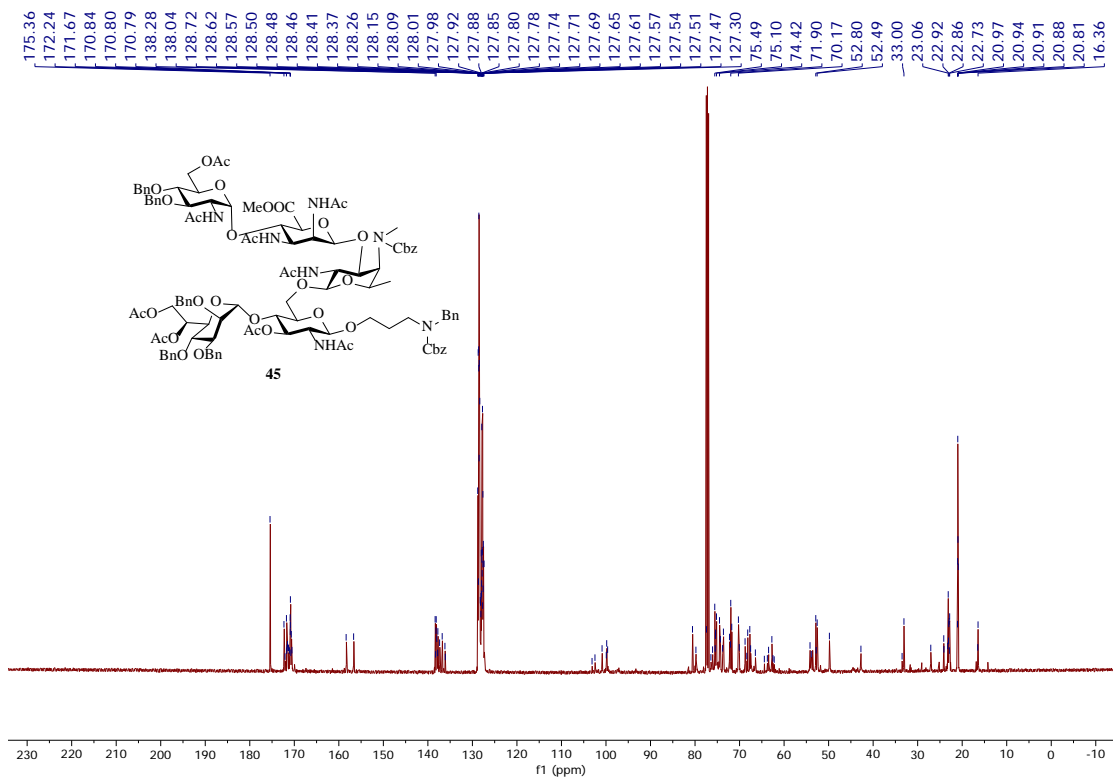
Figure 2.180. ^{13}C-NMR of **45** (125 MHz CDCl$_3$)
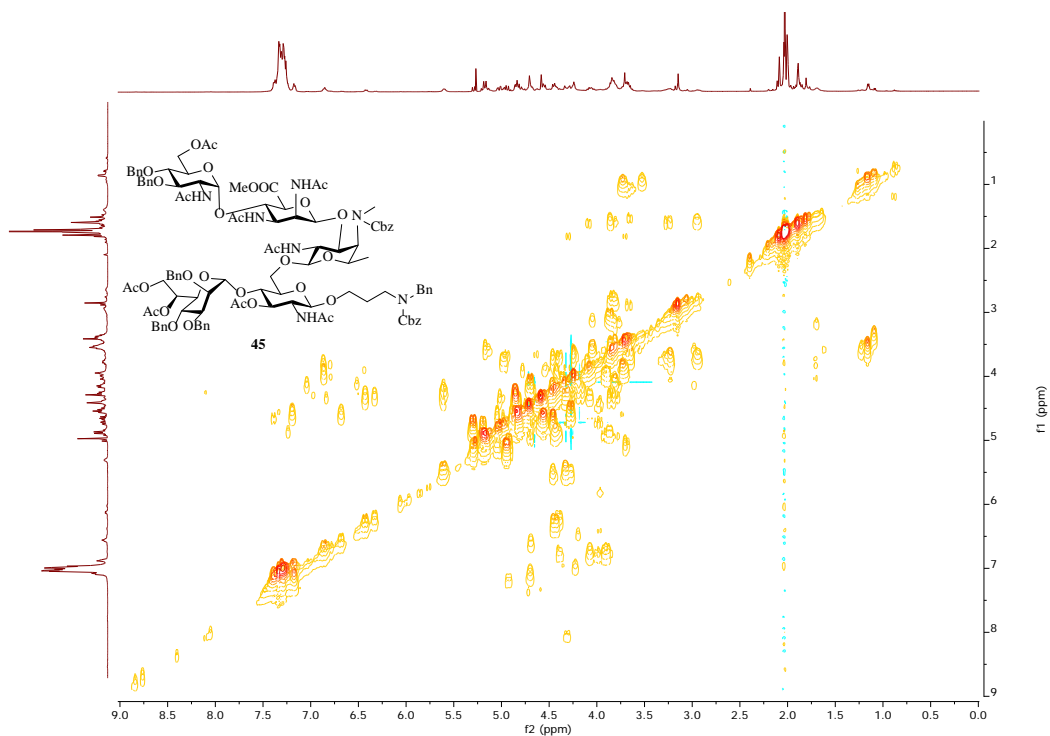
Figure 2.181. ^{1}H-^{1}H gCOSY of **45** (500 MHz CDCl$_3$)
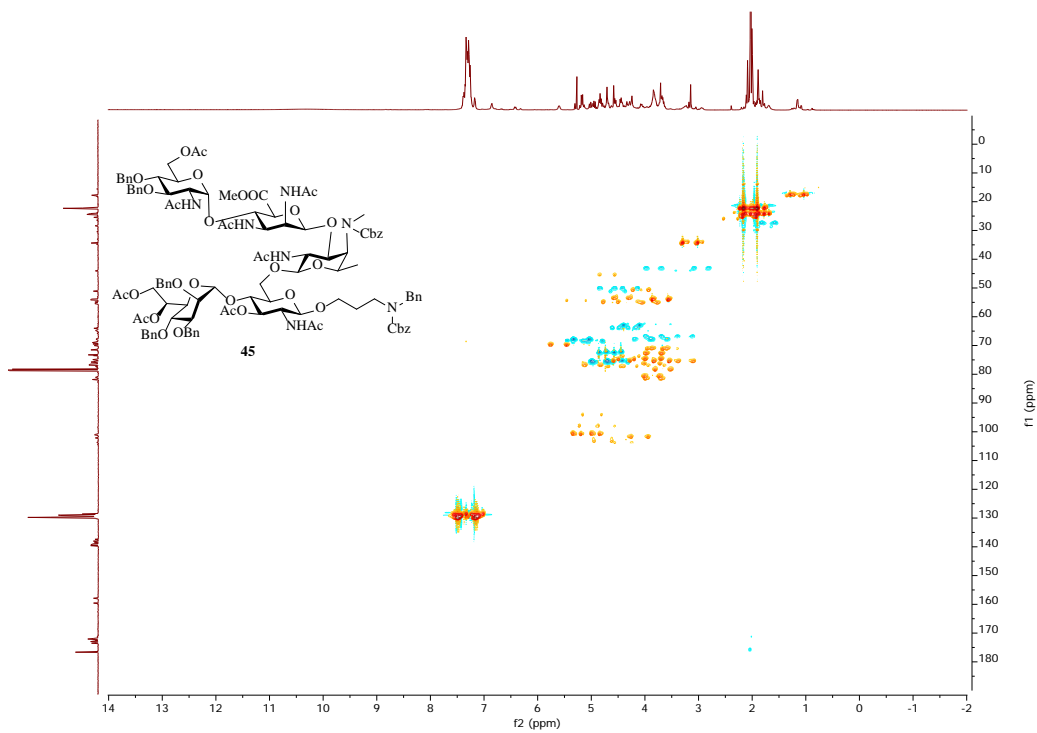
Figure 2.182. ^{1}H-^{13}C gHSQCAD of **45** (500 MHz CDCl$_3$)
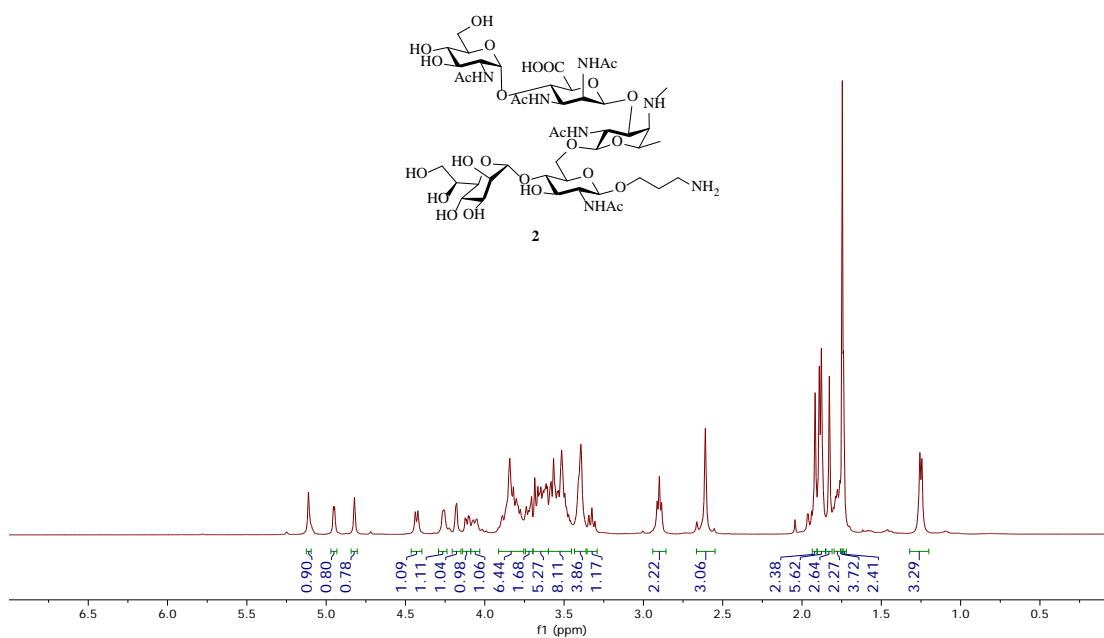
Figure 2.183. ^{1}H-NMR of **2** (500 MHz D$_2$O, PRESAT)
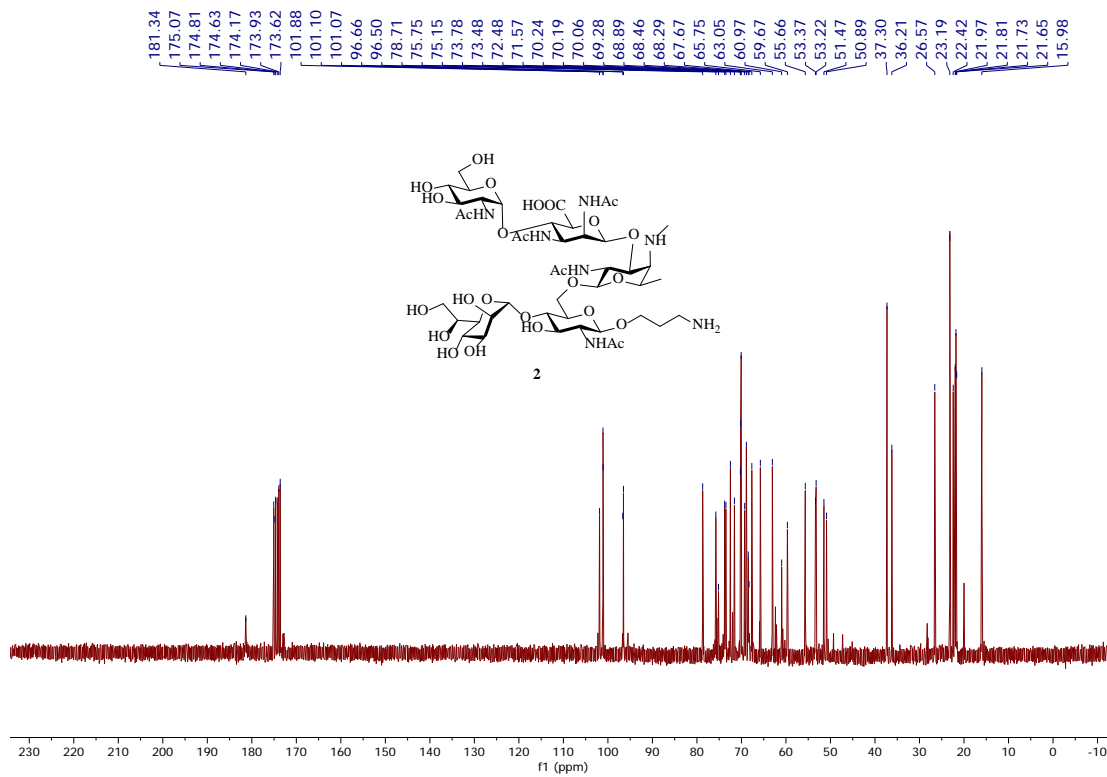
Figure 2.184. ^{13}C-NMR of **2** (125 MHz D$_2$O)
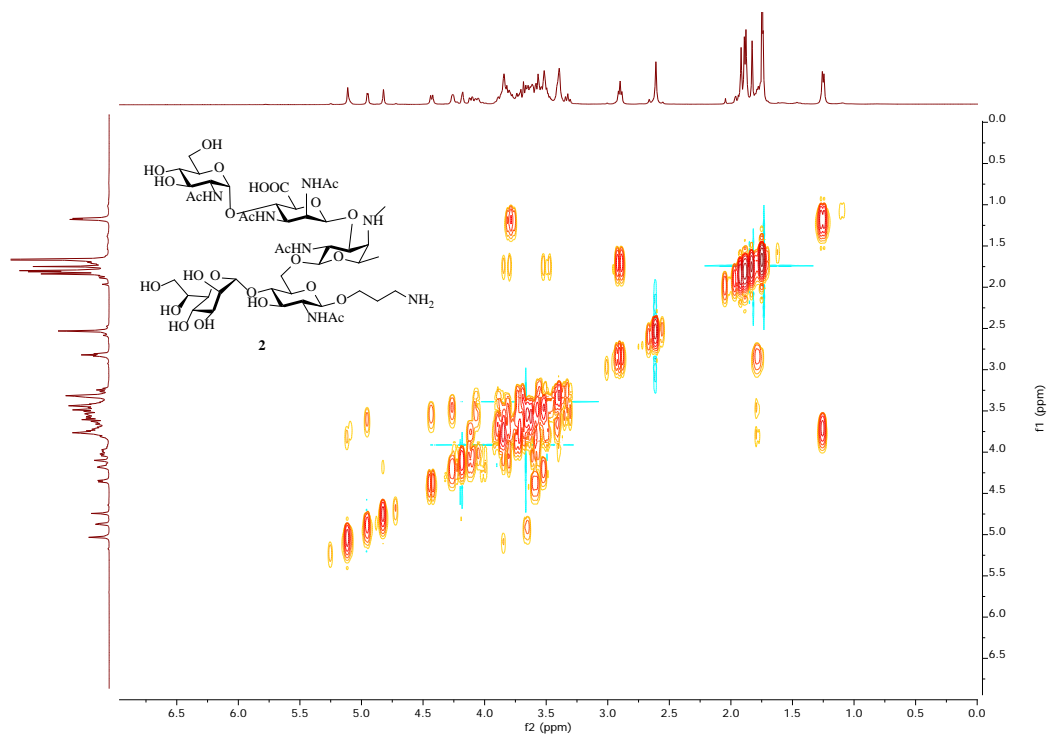
Figure 2.185. ^{1}H-^{1}H gCOSY of **2** (500 MHz D$_2$O)
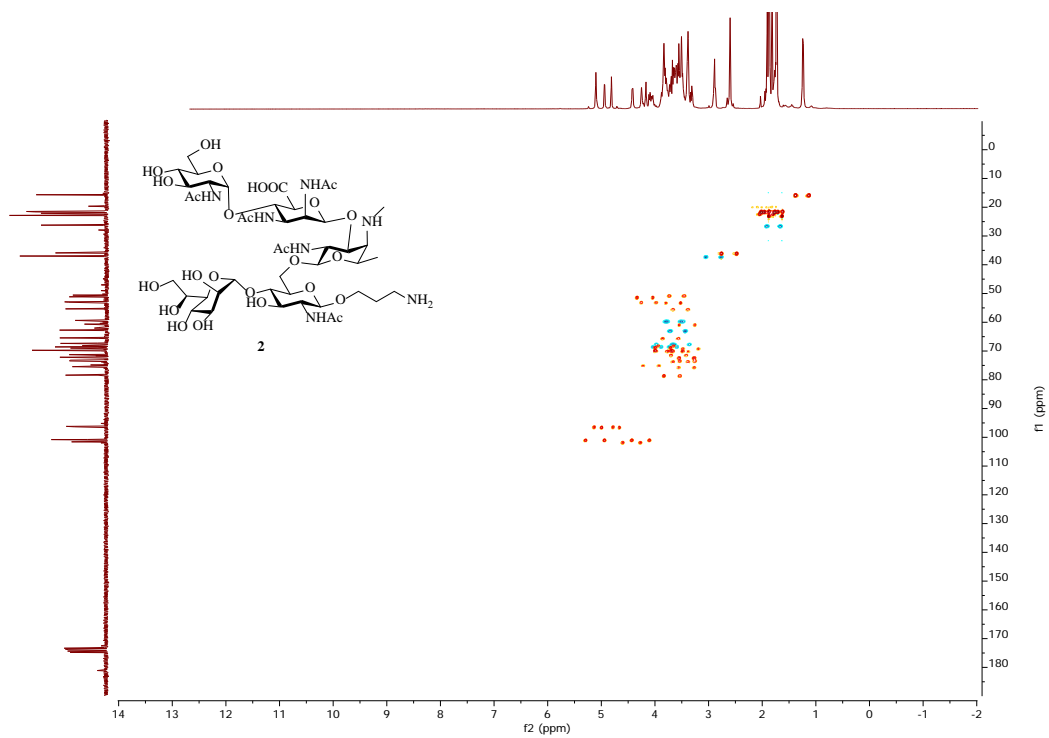
Figure 2.186. ^{1}H-^{13}C gHSQCAD of **2** (500 MHz D$_2$O)
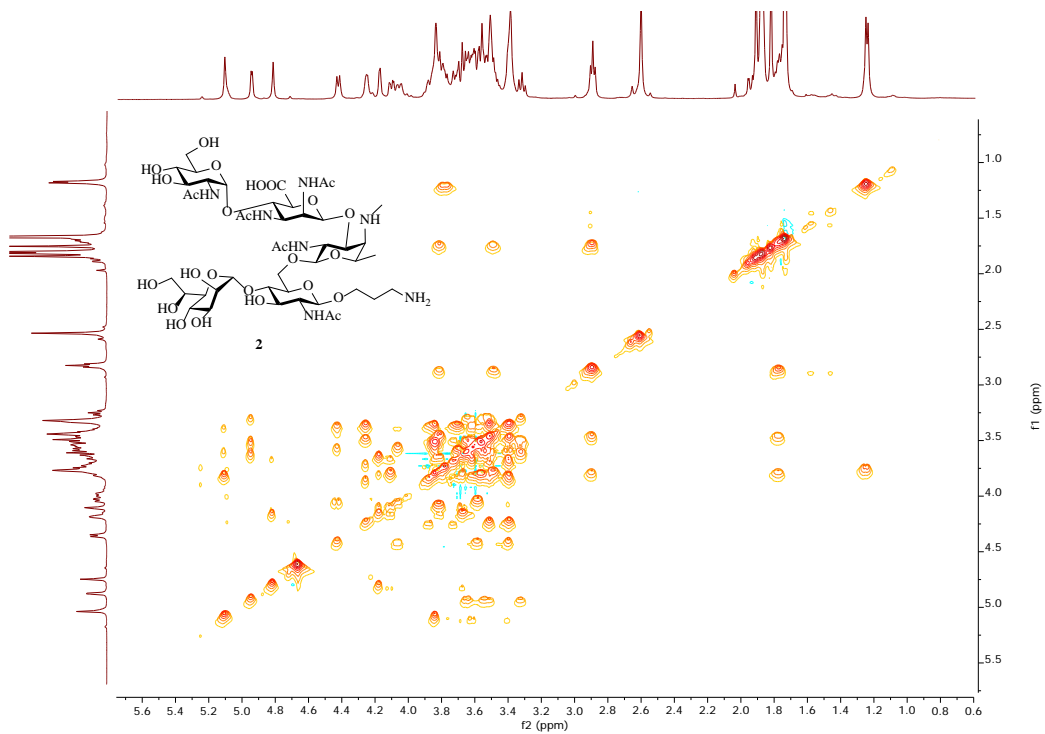
Figure 2.187. ^{1}H-^{1}H TOCSY of **2** (500 MHz D$_2$O)
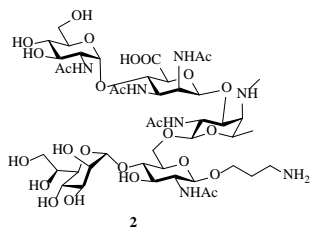
Figure 2.188. ESI-MS of **2**
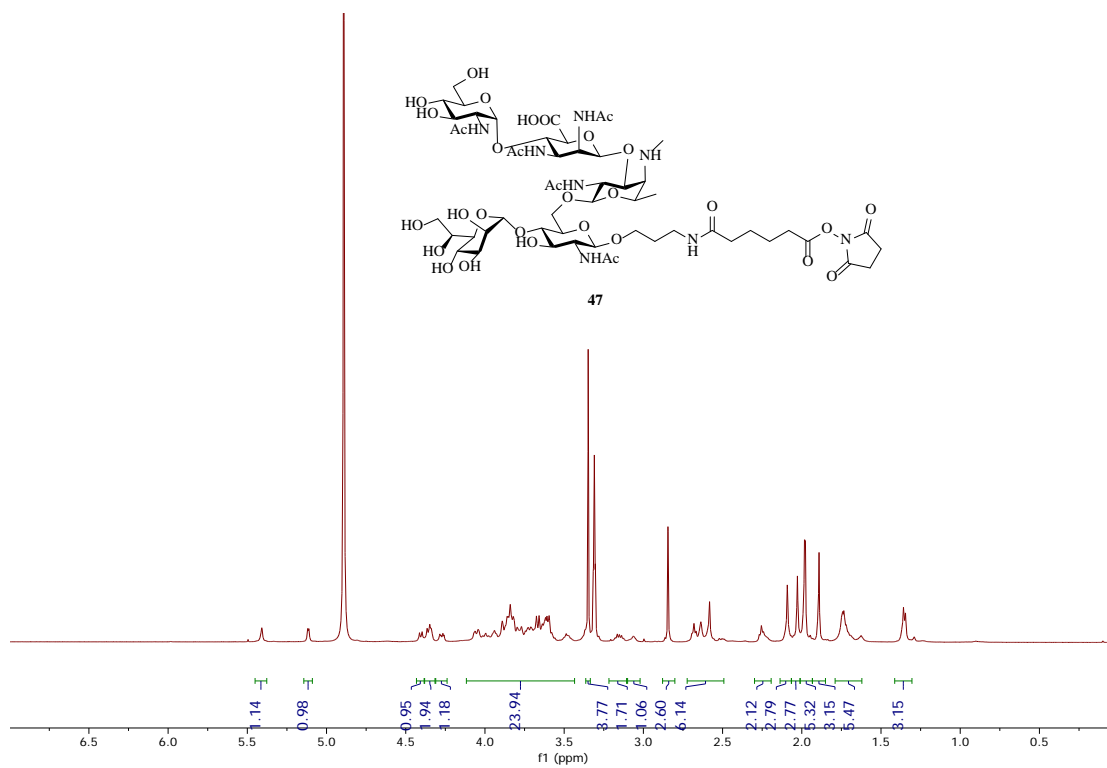
Figure 2.189. ^{1}H-NMR of **47** (500 MHz CD₃OD)
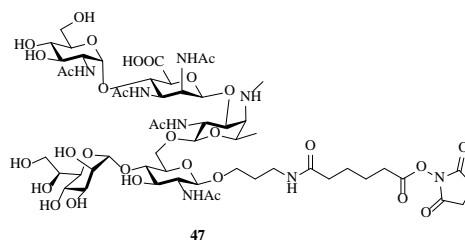
Figure 2.190. ESI-MS of **47**

REFERENCES

REFERENCES

1. Niedziela, T.; Letowska, I.; Lukasiewicz, J.; Kaszowska, M.; Czarnecka, A.; Kenne, L.; Lugowski, C., Epitope of the vaccine-type *Bordetella pertussis* strain 186 lipooligosaccharide and antiendotoxin activity of antibodies directed against the terminal pentasaccharide-tetanus toxoid conjugate. *Infect. Immun.* **2005,** *73* (11), 7381-7389.

2. Guo, J.; Frost, J. W., Kanosamine biosynthesis: a likely source of the aminoshikimate pathway's nitrogen atom. *J. Am. Chem. Soc.* **2002,** *124* (36), 10642-10643.

3. Mo, K.-F.; Li, X.; Li, H.; Low, L. Y.; Quinn, C. P.; Boons, G.-J., Endolysins of *Bacillus anthracis* bacteriophages recognize unique carbohydrate epitopes of vegetative cell wall polysaccharides with high affinity and selectivity. *J. Am. Chem. Soc.* **2012,** *134* (37), 15556-15562.

4. Visansirikul, S.; Yasomanee, J. P.; Pornsuriyasak, P.; Kamat, M. N.; Podvalnyy, N. M.; Gobble, C. P.; Thompson, M.; Kolodziej, S. A.; Demchenko, A. V., A concise synthesis of the repeating unit of capsular polysaccharide *Staphylococcus aureus* type 8. *Org. Lett.* **2015,** *17* (10), 2382-2384.

5. Emmadi, M.; Kulkarni, S. S., Expeditious synthesis of bacterial, rare sugar building blocks to access the prokaryotic glycome. *Org. Biomol. Chem.* **2013,** *11* (19), 3098-3102.

6. Emmadi, M.; Kulkarni, S. S., Synthesis of orthogonally protected bacterial, rare-sugar and D-glycosamine building blocks. *Nat. Protoc.* **2013,** *8* (10), 1870-1889.

7. Van den Bos, L. J.; Codée, J. D.; Van Boom, J. H.; Overkleeft, H. S.; Van der Marel, G. A., A novel strategy towards the synthesis of orthogonally functionalised 4-aminoglycosides. *Org. Biomol. Chem.* **2003,** *1* (23), 4160-4165.

8. Van den Bos, L. J.; Boltje, T. J.; Provoost, T.; Mazurek, J.; Overkleeft, H. S.; Van der Marel, G. A., A synthetic study towards the PSA1 tetrasaccharide repeating unit. *Tetrahedron Lett.* **2007,** *48* (15), 2697-2700.

9. Crich, D.; Banerjee, A., Synthesis and stereoselective glycosylation of D- and L-glycero-β-D-manno-heptopyranoses. *Org. Lett.* **2005,** *7* (7), 1395-1398.

10. Ohara, T.; Adibekian, A.; Esposito, D.; Stallforth, P.; Seeberger, P. H., Towards the synthesis of a *Yersinia pestis* cell wall polysaccharide: enantioselective synthesis of an L-glycero-D-manno-heptose building block. *Chem. Commun.* **2010,** *46* (23), 4106-4108.

11. Durka, M.; Tikad, A.; Périon, R.; Bosco, M.; Andaloussi, M.; Floquet, S.; Malacain, E.; Moreau, F.; Oxoby, M.; Gerusz, V.; Vincent, S. P., Systematic synthesis of inhibitors of the two

first enzymes of the bacterial heptose biosynthetic pathway: Towards antivirulence molecules targeting lipopolysaccharide biosynthesis. *Chem. Eur. J.* **2011,** *17* (40), 11305-11313.

12. Mulani, S. K.; Cheng, K.-C.; Mong, K.-K. T., General homologation strategy for synthesis of L-glycero-and D-glycero-heptopyranoses. *Org. Lett.* **2015,** *17* (22), 5536-5539.

13. Stanetty, C.; Baxendale, I. R., Large-Scale synthesis of crystalline 1,2,3,4,6,7-hexa-*O*-acetyl-L-glycero-α-D-manno-heptopyranose. *Eur. J. Org. Chem.* **2015,** 2718-2726.

14. Yasomanee, J. P.; Demchenko, A. V., Effect of remote picolinyl and picoloyl substituents on the stereoselectivity of chemical glycosylation. *J. Am. Chem. Soc.* **2012,** *134* (49), 20097-20102.

15. Medgyes, A.; Farkas, E.; Lipták, A.; Pozsgay, V., Synthesis of the monosaccharide units of the O-specific polysaccharide of *Shigella sonnei*. *Tetrahedron* **1997,** *53* (12), 4159-4178.

16. Medgyes, A.; Bajza, I.; Farkas, E.; Pozsgay, V.; Lipták, A., Synthetic studies towards the O-specific polysaccharide of *Shigella Sonnei*. *J. Carbohydr. Chem.* **2000,** *19* (3), 285-310.

17. Pfister, H. B.; Mulard, L. A., Synthesis of the zwitterionic repeating unit of the O-antigen from *Shigella sonnei* and chain elongation at both ends. *Org. Lett.* **2014,** *16* (18), 4892-4895.

18. Podilapu, A. R.; Kulkarni, S. S., Total synthesis of repeating unit of O-polysaccharide of *Providencia alcalifaciens* O22 via one-pot glycosylation. *Org. Lett.* **2017,** *19* (19), 5466-5469.

19. Leyva, A.; Quintana, A.; Sánchez, M.; Rodríguez, E. N.; Cremata, J.; Sánchez, J. C., Rapid and sensitive anthrone–sulfuric acid assay in microplate format to quantify carbohydrate in biopharmaceutical products: method development and validation. *Biologicals* **2008,** *36* (2), 134-141.

20. Zlamy, M., Rediscovering pertussis. *Front. Pediatr.* **2016,** *4*:52.

21. Marzouqi, I.; Richmond, P.; Fry, S.; Wetherall, J.; Mukkur, T., Development of improved vaccines against whooping cough: current status. *Hum. Vaccin.* **2010,** *6* (7), 543-553.

22. Friedman, R. L.; Nordensson, K.; Wilson, L.; Akporiaye, E.; Yocum, D., Uptake and intracellular survival of *Bordetella pertussis* in human macrophages. *Infect. Immun.* **1992,** *60* (11), 4578-4585.

23. Lamberti, Y.; Perez Vidakovics, M. L.; van der Pol, L.-W.; Rodríguez, M. E., Cholesterol-rich domains are involved in *Bordetella pertussis* phagocytosis and intracellular survival in neutrophils. *Microb. Pathog.* **2008,** *44* (6), 501-511.

24. Le Blay, K.; Caroff, M.; Blanchard, F.; Perry, M. B.; Chaby, R., Epitopes of *Bordetella*

pertussis lipopolysaccharides as potential markers for typing of isolates with monoclonal antibodies. *Microbiology* **1996,** *142* (4), 971-978.

25. Demizu, Y.; Kubo, Y.; Miyoshi, H.; Maki, T.; Matsumura, Y.; Moriyama, N.; Onomura, O., Regioselective protection of sugars catalyzed by dimethyltin dichloride. *Org. Lett.* **2008,** *10* (21), 5075-5077.

26. Crich, D.; Picione, J., Direct synthesis of the β-l-rhamnopyranosides. *Org. Lett.* **2003,** *5* (5), 781-784.

Chapter 3. Heparin Nanoparticles for β Amyloid Binding and Mitigation of β Amyloid Associated Cytotoxicity

3.1. Introduction

Alzheimer's disease (AD) has become the most common form of dementia, which is affecting about 5.2 million Americans.[1] The number of AD patients is predicted to increase significantly and expected to triple by 2050.[2] One of the main pathological hallmarks of AD is the senile plaques formed by Aβ. Aβ is derived from amyloid precursor protein processing by β- and γ-secretases and proposed to be a causative agent of AD.[3] Aβ can aggregate into highly toxic oligomers and deposit as plaques on the cerebral cortex damaging the nervous system.[4-6] Glycosaminoglycans (GAGs) are believed to play a central role in the amyloidosis pathway with many GAG bearing proteoglycans (PGs) found in both diffuse and neuritic amyloid plaques.[7-8] GAGs on surface of neuronal cells can serve as nucleating sites for Aβ aggregation, contribute to the formation of neurotoxic Aβ deposits on cells.[9-14]

Heparin is a member of the GAG family, which is known to be able to bind with Aβ [12, 15-16]. We envision that nanoparticles coated with heparin can be utilized to mimic PG bearing neuronal cells and potentially compete for their interactions with Aβ. Although heparin nanoparticles have been utilized for cancer targeting, anti-coagulation, tissue engineering and drug delivery,[17-22] their interactions with Aβ have not been studied before. Herein we report the synthesis of heparin-functionalized magnetic glyconanoparticles. These nanoparticles can bind with Aβ, induce the formation of fibril, and protect neuronal cells from Aβ induced cell death.

3.2. Results and Discussion

3.2.1. Preparation and Characterization of Hep-SPION.

We selected magnetic nanoparticles as the core of our heparin nanoparticles since magnetic nanoparticles are a powerful platform for biological applications due to their high surface area, biocompatibility and magnetic relaxivity.[23-25] Two methods were explored to immobilize heparin polysaccharides onto magnetic nanoparticles. In the first approach, we adapted our previous synthesis of colloidal hyaluronan nanoparticles.[26] Magnetite nanoparticles were first produced through the thermal decomposition method, resulting in hydrophobic magnetic nanoparticles mainly coated with oleic acid (**Scheme 3.1A**). Exchanging the oleic acid ligand with heparin was performed in a water/toluene biphasic system. However, although the resulting nanoparticles could be dispersed in water or phosphate buffered saline (PBS), they quickly precipitated out of aqueous solutions. This was most likely due to the lower efficiency of ligand displacement from the hydrophobic nanoparticles by heparin as compared to hyaluronan, as heparin is more charged and presumably less soluble in the organic solvent for ligand exchange.

An entirely aqueous solution based synthetic route was tested next. The magnetite core was constructed by the co-precipitation method by mixing ferric chloride and ferrous chloride with ammonium hydroxide in water (**Scheme 3.1B**).[22] The resulting superparamagnetic iron oxide nanoparticles (SPION) were collected with a magnet and resuspended in water. Heparin sodium salt was then added, which could chelate with the SPIONs to form a stable colloid suspension. Removal of excess heparin by ultrafiltration produced the heparin-coated SPIONs

(Hep-SPION).

A) Fe(acac)$_3$
+
Oleic acid
+
Oleylamine
+
1,2-hexadecanediol

Benzyl ether

200 °C 2h then
300 °C 1h

Fe$_3$O$_4$

Toluene : H$_2$O

Heparin
reflux

Fe$_3$O$_4$

B)

FeCl$_3$•6H$_2$O
+
FeCl$_2$•4H$_2$O

conc. NH$_3$•H$_2$O

H$_2$O, N$_2$

Fe$_3$O$_4$

SPION

Heparin

Fe$_3$O$_4$
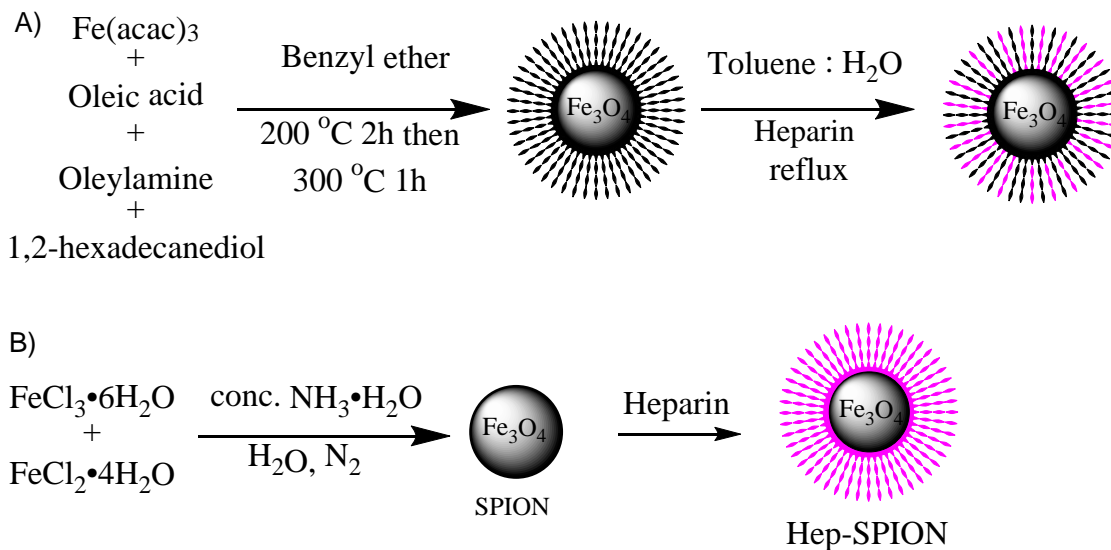
Hep-SPION

Scheme 3.1. Synthesis of heparin coated magnetic nanoparticles by A) the thermal decomposition and ligand exchange method, and B) the co-precipitation method.

Hep-SPION was characterized by a series of techniques including transmission electron microscopy (TEM), dynamic light scattering (DLS), zeta potential and thermogravimetric analysis (TGA). TEM images showed that the magnetite core had an average diameter around 10 nm (**Figure 3.1A**), with the hydrodynamic diameters of 68 nm in water and 59 nm in PBS buffer respectively. The successful attachment of heparin was supported by TGA analysis. While the amount of organic compounds only accounted for 3% of the gross weight of SPION by TGA analysis, heating the Hep-SPION to above 700 °C led to 63% weight loss suggesting that about 60% of the Hep-SPION mass was due to heparin attachment (**Figure 3.1B**). Furthermore, the zeta potential of the nanoparticles changed from +12.3 mV (SPION) to -53.3 mV (Hep-SPION), consistent with the high negative charge of heparin on Hep-SPION.
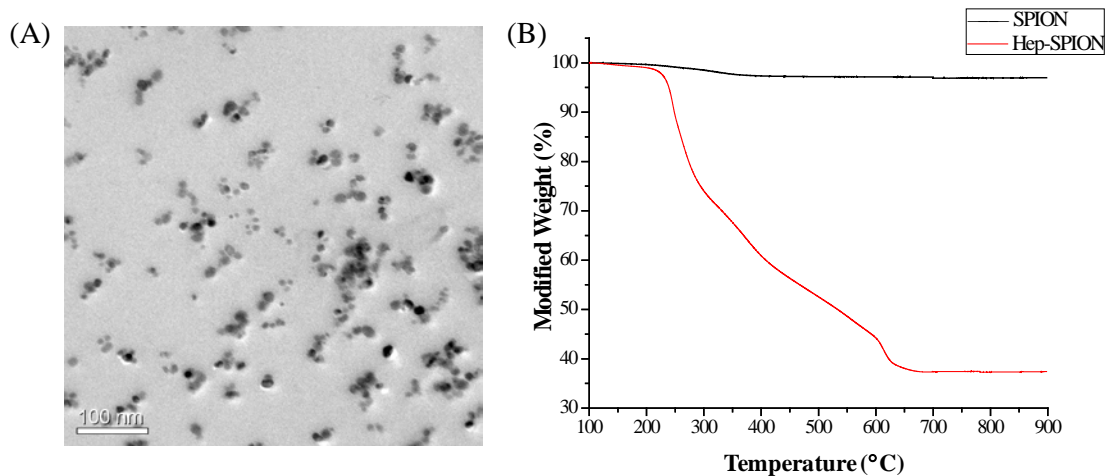
Figure 3.1. (A) TEM characterization of Hep-SPION; (B) TGA of SPION and Hep-SPION.

3.2.2. Assessment of Binding between Aβ and Hep-SPION by ELISA.

With the Hep-SPION in hand, its interaction with Aβ was investigated. Naturally isolated Aβ peptides exist in variable lengths ranging from 36 to 42 amino acid residues. We chose Aβ1-42 for our study, as it is the more amyloidogenic Aβ form.[27-28] Furthermore, it is prone to aggregation[6, 29] and is the major species found in the senile plaques of AD brains[30].

Aβ1-42 monomers were dissolved in 10 mM NaOH, neutralized with HCl and were incubated at 37℃ for 2 days. The resulting fibrils were added to a 96-well plate, which could adhere to the surface of the wells. Upon removal of the unbound peptide, the bound Aβ was detected by an anti-Aβ IgG monoclonal antibody 6E10 (mAb) through an enzyme linked immunosorbent assay (ELISA) using a horseradish peroxidase (HRP) conjugated anti-IgG secondary antibody and 3, 3', 5, 5'-tetramethylbenzidine (TMB) substrate. The relative amounts of Aβ bound could be determined from the absorbance at 450 nm. If heparin could bind with Aβ, the heparin should coat the surface of the fibril and shield the Aβ from adhesion to

the plate. To test heparin binding, Aβ fibrils were pre-mixed with varying concentrations of Hep-SPION and incubated in each well overnight. Upon washing off unbound material, the amounts of Aβ remaining in the well were semi-quantified by ELISA. A concentration dependent decrease in absorbance at 450 nm was observed with increasing amounts of Hep-SPION (**Figure 3.2A**). Incubation of Aβ with uncoated SPION showed no effect on the absorbance, which revealed the crucial role of heparin on the surface of nanoparticles (**Figure 3.2B**). Hep-SPION did not bind to the surface of wells (data not shown), thus precluding the possibility that the decrease in absorbance was due to Hep-SPION passivating the wells.
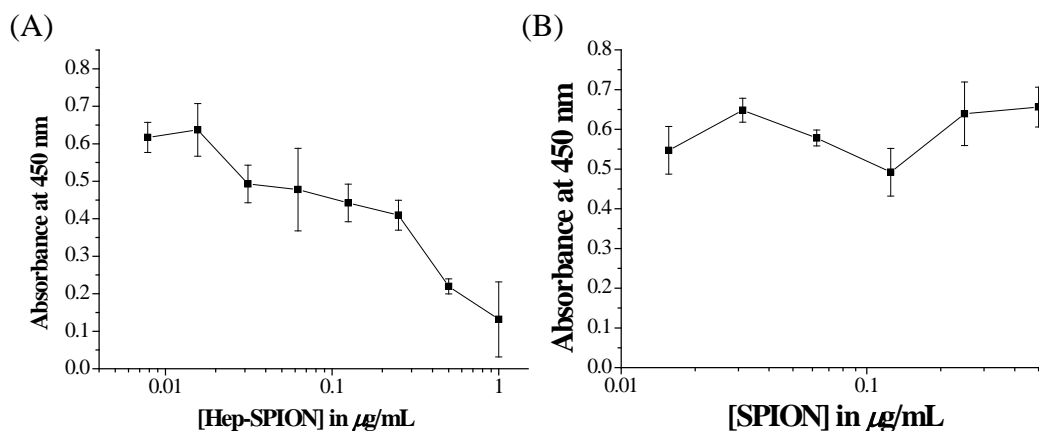
Figure 3.2. (A) Aβ binding to plate decreased with increasing concentrations of Hep-SPION. The bound Aβ was detected by an anti-Aβ IgG mAb 6E10, followed by addition of HRP-conjugated anti-IgG secondary antibody and the TMB substrate. (B) ELISA curve for Aβ incubated with increasing concentrations of SPION. SPIONs without heparin coating showed little effect on Aβ binding to the plate.

3.2.3. Effect of Hep-SPION on Aβ Aggregation.

As Hep-SPION can bind with Aβ, we analyzed its effects on Aβ aggregation by native polyacrylamide gel electrophoresis (PAGE). Aβ monomers (25 μM) were incubated with

Hep-SPION at 37℃ for 2 days followed by analysis via native PAGE. Without any Hep-SPION, Aβ existed as a mixture of low molecular weight oligomers and high molecular weight fibril (**Figure 3.3A**). With increasing concentrations of Hep-SPION (0.0078, 0.0156, 0.0312, 0.125 mg/mL), the relative amounts of the low-molecular-weight Aβ oligomers decreased (**Figure 3.3A**). At the concentration of 0.125 mg/mL Hep-SPION, almost all Aβ (>90%) had formed large fibrils appearing at higher molecular weight region on the gel (**Figure 3.3A, B**). This suggested that Hep-SPION can eliminate low-molecular-weight oligomers by direct binding or facilitating the conversion of Aβ oligomers to fibrils.
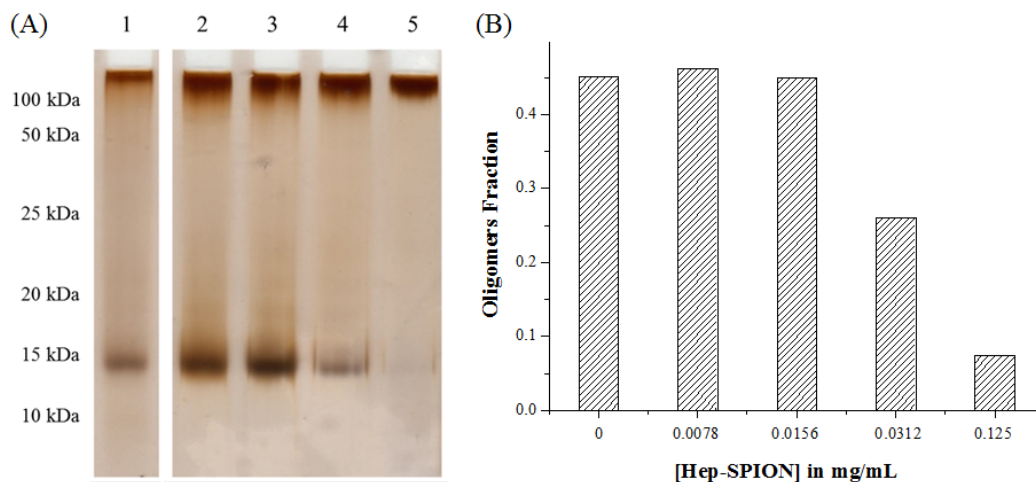
Figure 3.3. (A) PAGE gel of Aβ only (lane 1) or Aβ (25 μM) incubated with 0.0078 mg/mL (lane 2), 0.0156 mg/mL (lane 3), 0.0312mg/mL (lane 4) and 0.125 mg/mL (lane 5) of Hep-SPION. (B) Percentage of low-molecular-weight Aβ oligomer in total Aβ in presence of various concentrations of Hep-SPION. The percentage was calculated by dividing the intensity of the low molecular weight oligomer band by the sum of the intensities of all bands in the specific lane.

To further confirm the effect of Hep-SPION on Aβ aggregation, a thioflavin T (ThT) binding

assay was performed. ThT is a cationic benzothiazole dye[31] that displays enhanced fluorescence when interacting with β-sheet structures (**Figure 3.4A**, 1st vs 2nd column). When incubated with Aβ, Hep-SPION accelerated β-sheet formation and gave rise to markedly enhanced ThT fluorescence (**Figure 3.4A**, 3rd – 5th column). Hep-SPION itself did not result in any fluorescence enhancement of ThT even at the highest nanoparticle concentration tested (**Figure 3.4A**, 6th column), which excluded the direct effect of Hep-SPION on ThT fluorescence. Uncoated SPION without any heparin did not impact the fluorescence of ThT (Figure **3.4B**, 2nd column), which further confirmed the imperative role of heparin.

It has been proposed that heparin can function as a structural template and facilitate the nucleation step of Aβ aggregation.[13] Our results that Hep-SPION induced extensive aggregation of Aβ were consistent with the reported effects of heparin on Aβ1-40.[11]
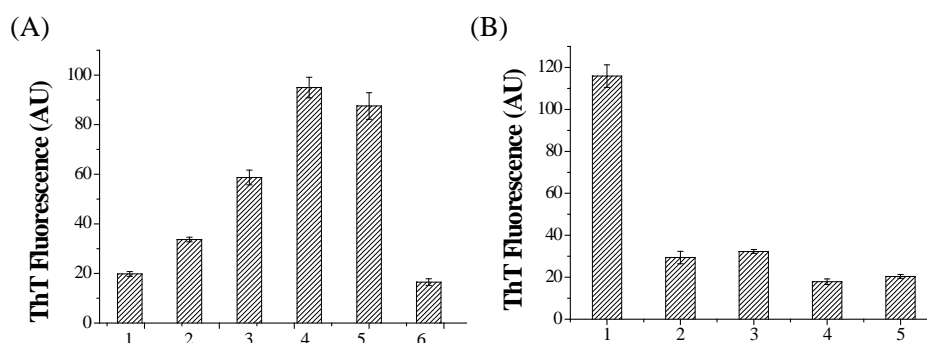
Figure 3.4. The intensities of ThT fluorescence at 489 nm (λ_{ex} = 440 nm). (A) Incubation of Aβ in the presence of Hep-SPION significantly enhanced ThT fluorescence. From left to right: ThT fluorescence in the presence of 1) H_2O; 2) Aβ (25 μM); 3) Aβ (25 μM) + Hep-SPION (0.0020 mg/mL); 4) Aβ (25 μM) + Hep-SPION (0.0078 mg/mL); 5) Aβ (25 μM) + Hep-SPION (0.0312 mg/mL); 6) Hep-SPION (0.0312 mg/mL). (B) ThT fluorescence in the presence of 1) Aβ (25 μM) + Hep-SPION (0.0625 mg/mL); 2) Aβ (25 μM) + SPION (0.0625 mg/mL); 3) Aβ (25 μM); 4) SPION (0.0625 mg/mL); and 5) H_2O.

3.2.4. Effect of Hep-SPION on Aβ-Induced Cytotoxicity

Although it remains debatable whether Aβ peptides cause AD, the toxicity of Aβ on neuronal cells is an important contributing factor to the pathology of the disease. While Aβ can exist in monomer, oligomer and fibril forms, the soluble Aβ oligomers have been proven to be the most toxic among all Aβ species.[4] Shifting the equilibrium between the oligomers and fibril towards the more benign fibrils can potentially reduce the adverse effects of Aβ.[32-33] As Hep-SPION can convert Aβ oligomers into the fibrillar forms (**Figure 3.3A**), we hypothesized that Hep-SPION could protect neuronal cells from Aβ induced toxicity.

To test the effects of Aβ and Hep-SPION on cells, cell viability assays were performed with SH-SY5Y neuroblastoma cells, a common model utilized in Aβ toxicity studies.[33-34] Various concentrations of Aβ were incubated with SH-SY5Y cells in a 96-well cell culture plate. Cells in each well were collected and then mixed with 7-aminoactinomycin D (7-AAD), a fluorescent stain specific to dead cells. The numbers of live and dead cells were counted via fluorescence-activated cell sorting (FACS), with the percentage of live cells without any treatment set as 100%. Aβ peptide exhibited dose dependent cytotoxicities (**Figure 3.5A**) with about 75% cell viability when treated with 5 μM Aβ. The SH-SY5Y cells were then incubated with Aβ (5 μM) in the presence of increasing concentrations of Hep-SPION. As shown in **Figure 3.5B**, Hep-SPION could protect the cells from Aβ induced toxicity with 0.01 mg/mL of Hep-SPION enough to fully mitigate the effect of Aβ on the cells. Hep-SPION by itself did not have a significant impact on the viability of the cells, demonstrating the biocompatibility of the nanoparticles. The protective effect of Hep-SPION can potentially be due to two factors: 1) the

nanoparticles can induce the transformation of Aβ into the more benign fibril form; and 2) by

binding with Aβ, the Hep-SPION can serve as a sink to reduce the Aβ available for interactions

with the neuronal cells.
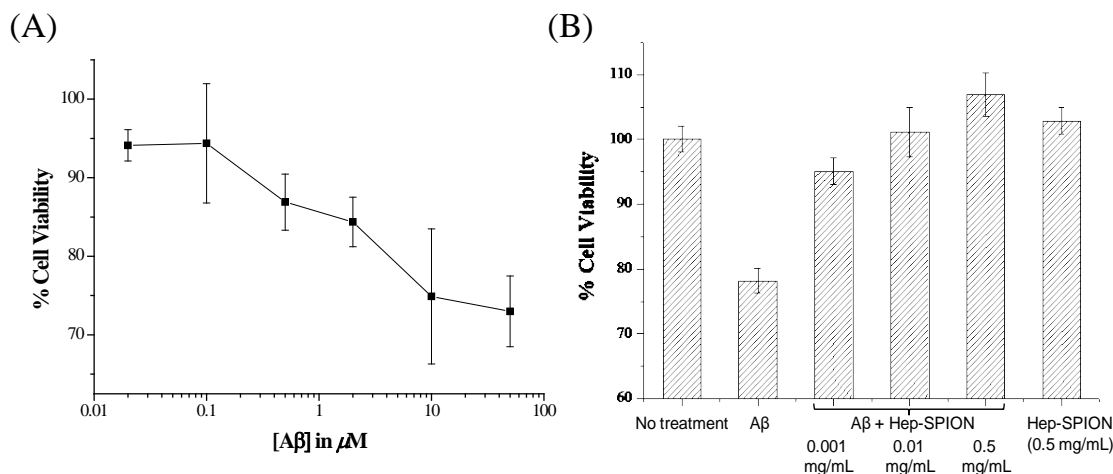
Figure 3.5. Cell viability assay of SH-SY5Y cells. (A) Increasing concentrations of Aβ induced higher cytotoxicity against SH-SY5Y cells. (B) Addition of Hep-SPION protected SH-SY5Y cells from Aβ induced cytotoxicity. Incubation of cells with Hep-SPION (0.5 mg/mL) did not exhibit any cytotoxicity indicating the high biocompatibility of the nanoparticles.

Aβ peptides exist in a dynamic equilibrium among monomers, oligomers and fibrils, while

heparin can perturb the equilibrium and therefore affect the aggregation process. It has been

reported that heparin bind to fibrillar Aβ in an analysis via affinity co-electrophoresis,[15] which is

also proved in our study.   Hep-SPION could eliminate the most toxic oligomer form and protect

SH-SY5Y cells. However, more details about how heparin is involved in the process remain

concealed. Further study on the effect of Hep-SPION on different forms of Aβ will help with

better understanding of the role of heparin in the aggregation of Aβ.

3.3. Conclusions

We demonstrated that Hep-SPION could bind Aβ and heparin was essential for the interaction. Furthermore, Hep-SPION promoted the transition of Aβ into the more benign fibrils. This in turn could protect neuronal cells from Aβ induced cytotoxicity. As iron oxide nanoparticles have been widely applied as MRI contrast agents and drug carriers,[23-25] Hep-SPION can potentially be a useful platform for future imaging and drug delivery studies targeting Aβ.

3.4. Experimental Section

3.4.1. Materials and Instrumentation

Unless otherwise indicated, all starting materials, reagents and solvents were obtained from commercial suppliers and used as supplied without further purifications. Ferric chloride hexahydrate ($FeCl_3 \cdot 6H_2O$) was purchased from Honeywell Riedel-de Haen. Ferrous chloride tetrahydrate ($FeCl_2 \cdot 4H_2O$), ferric acetylacetonate [$Fe(acac)_3$], oleic acid, 1, 2-hexadecanediol, 1, 1, 1, 3, 3, 3-hexafluoro-2-propanol, Cameo syringe filter (0.22 micron) and 7-aminoactinomycin D (7-AAD) were purchased from Sigma-Aldrich. Ammonium hydroxide (NH_4OH, 28−30%) and hydrogen peroxide (H_2O_2, 30%) were purchased from CCI. Benzyl ether and 3, 3', 5, 5'-tetramethylbenzidine were purchased from Acros Organics. Oleyl amine was purchased from Fluka. Heparin sodium was purchased from Celsus Laboratories, Inc. Thioflavin T (ThT), UltraPure Grade was purchased from AnaSpec. Aβ1-42 was purchased from GL Biochem. (Shanghai) Ltd. (No. 52487). Anti Aβ1-16 IgG (6E10) monoclonal antibody was purchased

from Covance. Goat anti-mouse HRP-conjugated secondary antibody was purchased from Jackson ImmunoResearch Laboratory. SH-SY5Y cells were purchased from American Type Culture Collection (ATCC). Ultrathin-carbon type A, 400 mesh copper grids for TEM were purchased form Ted Pella, Inc. Ultrafiltration membranes and centrifugal filters were purchased from Millipore.

All cell culture media was supplemented with 10% heat inactivated FBS, 1% Pen-Strep mixture, glutamine (2 mM), and sodium pyruvate (1 mM). Dynamic light scattering (DLS) and zeta potential measurements were performed on a Zetasizer Nano zs apparatus (Malvern, U.K.). Transmission electron microscopy (TEM) images were collected on a JEM-2200FS operating at 200 kV using Gatan multiscan CCD camera with Digital Micrograph imaging software. Thermogravimetric analysis (TGA) was carried on a Thermal Advantage (TA-Instruments-Waters LLC) TGA-Q500 series and the samples were burned under nitrogen. Native-PAGE gel analysis was performed via ImageJ 1.42q (NIH). FACS experiments were conducted on a BD Vantage SE flow cytometer.

3.4.2. Synthesis of Hep-SPION

A. Thermal decomposition approach

Fe(acac)$_3$ (0.71 g, 2 mmol), 1, 2-hexadecanediol (2.58 g, 10 mmol), oleic acid (1.69 g, 6 mmol), oleyl amine (1.61 g, 6 mmol), and benzyl ether (40 mL) were mixed and stirred under a nitrogen atmosphere. The mixture was heated to 200 ℃ for 2 h followed by refluxing for 1 h. The black mixture was cooled down to room temperature and ethanol (50 mL) was added. The iron oxide nanoparticles were collected by an external magnet and washed three times with

ethanol to remove excess starting materials. The nanoparticles were then dispersed in hexane (50 mL) and the mixture was placed on an external magnet to remove undispersed magnetic material. The supernatant containing nanoparticles was centrifuged to remove large particulates and give the OA-SPION (6 mg/mL). OA-SPION (25 mg) was dried from hexane and re-dissolved in toluene (15 mL). Heparin sodium salt (50 mg) was dissolved in MilliQ water (30 mL) and pH of the solution was adjusted to 8.5 with NaOH solution. The heparin solution was mixed with OA-SPION in toluene and the two phase system was refluxed for 24 h under rapid stirring. The aqueous layer containing the Hep-SPION was collected using a separatory funnel, centrifuged to remove large particulates and purified by ultrafiltration (MWCO 100,000) to remove excess heparin and NaOH. The purified Hep-SPION was diluted with MillQ water to a final volume of 30 mL (0.8 mg/mL).

B. Co-precipitation approach

$FeCl_3 \cdot 6H_2O$ (500 mg, 1.85 mmol) and $FeCl_2 \cdot 4H_2O$ (185 mg, 0.93 mmol) were dissolved in MilliQ water (30 mL) that had been deoxygenated by bubbling with nitrogen for 20 min. The solution was filtered through 0.22 μm syringe filter to remove any undissolved solid. To this solution, NH_4OH (30%, 2 mL) was added under a nitrogen atmosphere while stirring vigorously for 1 h at room temperature. An external magnet was used to collect iron oxide nanoparticles and the supernatant solution was discarded. The nanoparticles were washed three times and re-suspended in MilliQ water (30 mL). Heparin sodium salt (0.5 g) in 10 mL MilliQ water was added and the mixture was stirred for 2 h followed by sonication for 1 h. The solution was centrifuged to remove any aggregation and then heated at 80 ℃ for 1 h to achieve stabilization.

217

Excess heparin was removed by ultrafiltration and the final Hep-SPION solution (2.5 mg/mL) was kept at 4 °C for further use.

3.4.3. Transmission Electron Microscopy (TEM) Procedure

10 μL of the Hep-SPION solution was deposited on ultrathin-carbon type A, 400 mesh copper grids and let to evaporate under the hood. Once dry, 1% solution of uranyl acetate was added for 10 seconds and the solution was wicked away with filter paper. The grids were then washed with water and dried for 15 min at room temperature.

3.4.4. Preparation of Aβ

Aβ peptide (0.5 mg) was dissolved in spectroscopy grade 99.9% 1, 1, 1, 3, 3, 3-hexafluoro-2-propanol (1.5 mL), sonicated for 15 min, and lyophilized for 72 h. The thin film was then dissolved in 0.22 μm filtered solution of 10 mM NaOH solution (0.25 mL). The pH of the solution was adjusted to 6 with 10 mM HCl solution and diluted with deionized water to a total volume of 1.0 mL (the concentration of Aβ stock solution was 100 μM). For experiments that needed Aβ fibrils, the stock solution was incubated at 37°C for 48 h.

3.4.5. Native-PAGE Gel Electrophoresis

Aβ monomers (25 μM) were incubated either without Hep-SPION or with different concentration of Hep-SPION (0.125, 0.0312, 0.0156, 0.0078 mg/mL) at 37℃ for 2 days. After incubation, 20 μL of the mixture was added to 5 μL of non-SDS sample buffer and was subjected to electrophoresis (200 V) on a 15% native-PAGE gel. The gels were then stained with silver staining.

3.4.6. Thioflavin T Assay

ThT fluorescence measurements were performed in a clear bottom black 96-well fluorescence plate (COSTAR 3695-96) on a FLUOstar OPTIMA (BMG Labtechnologies). The control solution was 220 μL water and 200 μL ThT (25 μM) + 20 μL water. 20 μL Aβ (25 μM) solutions incubated with different concentration of Hep-SPION were added to 200 μL ThT (25 μM) solutions. ThT fluorescence measurements were performed with λ_{ex} = 440 nm and λ_{em} = 489 nm.

3.4.7. ELISA Assay

Aβ fibrils (100 nM) along with Hep-SPION at different concentrations (0.008, 0.016, 0.031, 0.062, 0.125, 0.25, 0.50, 1.0 μg/mL) were added into a 96-well plate (100 μL/well) and incubated at 22℃ overnight. All wells were washed with 300 μL PBST three times and blocked with 1% BSA (300 μL/well) at 22℃ for 1 h. After washing with 300 μL PBST three times, anti Aβ1-16 IgG (6E10) monoclonal antibody (100 μL/well, 0.82 nM, 1 : 4000 in 1% BSA containing PBS) was added and then incubated at 37℃ for 1 h. The solutions were then discarded and washed again with 300 μL PBST three times. The goat anti-mouse HRP-conjugated secondary antibody (100 μL/well, 5.1 nM, 1: 6000 in 1% BSA containing PBS) was added into each well and incubated at 37℃ for 1 h followed by washing with 300 μL PBST three times. To a freshly prepared 3, 3', 5, 5'-tetramethylbenzidine (TMB) solution (5 mg of TMB was dissolved in 2 mL of DMSO and then diluted to 20 mL with citrate phosphate buffer), 20 μL of H_2O_2 was added. This mixture (150 μL/well) was immediately added to the plate and a blue color was allowed to develop for 20 min. The reaction was then quenched by 0.5 M H_2SO_4 (50 μL/well) and the

absorbance was measured at 450 nm on an iMark microplate reader.

3.4.8. Cell Viability Assay.

Different concentrations of Hep-SPION solutions (0.002, 0.02, 0.2, 1 mg/mL) were pre-incubated with or without Aβ fibrils for 24h and then added into 96-well plate (50 μL/well). In each well, $2*10^4$ cells were added in 4% serum solution. The final solutions in those wells are Aβ (5 μM), Hep-SPION (0.001, 0.01, 0.1, 0.5 mg/mL) in 2% serum (100 μL/well). The plate was incubated for 24 h at 37℃. All media were collected in separate eppendorf tubes. Trypsin (50 μL) was then added into each well to digest cells and 4% culture media (200 μL*2) was used to wash wells and combined with original media in the eppendorf tubes. Cells were pelleted by centrifugation and resuspended in FACS buffer (300 μL) in FACS tubes. 7-AAD (3 μL) was added into each tube, followed by incubation at 0℃ for 10 min. All solutions were then analyzed by a flow cytometer to evaluate the cell viability.

REFERENCES

REFERENCES

1.   Alzhermer's disease facts and figures. http://www.alz.org/downloads/facts_figures_2013.pdf, 2013.

2.   Hebert, L. E.; Scherr, P. A.; Bienias, J. L.; Bennett, D. A.; Evans, D. A., Alzheimer disease in the US population: prevalence estimates using the 2000 census. *Arch. Neurol.* **2003,** *60* (8), 1119-1122.

3.   Hardy, J. A.; Higgins, G. A., Alzheimer's disease: the amyloid cascade hypothesis. *Science* **1992,** *256*, 184-185.

4.   Dahlgren, K. N.; Manelli, A. M.; Stine, W. B.; Baker, L. K.; Krafft, G. A.; LaDu, M. J., Oligomeric and fibrillar species of amyloid-β peptides differentially affect neuronal viability. *J. Biol. Chem.* **2002,** *277* (35), 32046-32053.

5.   Bieschke, J.; Herbst, M.; Wiglenda, T.; Friedrich, R. P.; Boeddrich, A.; Schiele, F.; Kleckers, D.; del Amo, J. M. L.; Grüning, B. A.; Wang, Q.; Schmidt, M. R.; Lurz, R.; Anwyl, R.; Schnoegl, S.; Fändrich, M.; Frank, R. F.; Reif, B.; Günther, S.; Walsh, D. M.; Wanker, E. E., Small-molecule conversion of toxic oligomers to nontoxic β-sheet–rich amyloid fibrils. *Nat. Chem. Biol.* **2012,** *8* (1), 93-101.

6.   Masters, C. L.; Selkoe, D. J., *Biochemistry of amyloid β-protein and amyloid deposit in Alzheimer disease*. Cold Spring Harbor Laboratory Press: Cold Spring Harbor, New York, 2012.

7.   Snow, A. D.; Mar, H.; Nochlin, D.; Kimata, K.; Kato, M.; Suzuki, S.; Hassell, J.; Wight, T., The presence of heparan sulfate proteoglycans in the neuritic plaques and congophilic angiopathy in Alzheimer's disease. *Am. J. Pathol.* **1988,** *133* (3), 456-463.

8.   Snow, A. D.; Sekiguchi, R. T.; Nochlin, D.; Fraser, P.; Kimata, K.; Mizutani, A.; Arai, M.; Schreier, W. A.; Morgan, D. G., An imporant role of heparan sulfate proteoglycan (perlecan) in a model system for the deposition and persistence of fibrillar Aβ-amyloid in rat brain. *Neuron* **1994,** *12*, 219-234.

9.   Gupta-Bansal, R.; Frederickson, R. C.; Brunden, K. R., Proteoglycan-mediated inhibition of Aβ proteolysis. A potential cause of senile plaque accumulation. *J. Biol. Chem.* **1995,** *270* (31), 18666-18671.

10. Bame, K. J.; Danda, J.; Hassall, A.; Tumova, S., Aβ (1–40) Prevents heparanase-catalyzed degradation of heparan sulfate glycosaminoglycans and proteoglycans *in vitro*. A role for heparan sulfate proteoglycan turnover in Alzheimer's disease. *J. Biol. Chem.* **1997,** *272* (27), 17005-17011.

11. Castillo, G. M.; Lukito, W.; Wight, T. N.; Snow, A. D., The sulfate moieties of glycosaminoglycans are critical for the enhancement of β-Amyloid protein fibril formation. *J. Neurochem.* **1999,** *72* (4), 1681-1687.

12. Walzer, M.; Lorens, S.; Hejna, M.; Fareed, J.; Hanin, I.; Cornelli, U.; Lee, J. M., Low molecular weight glycosaminoglycan blockade of β-amyloid induced neuropathology. *Eur. J. Pharmacol.* **2002,** *445,* 211-220.

13. McLaurin, J.; Franklin, T.; Zhang, X.; Deng, J.; Fraser, P. E., Interactions of Alzheimer amyloid-β peptides with glycosaminoglycans. *Eur. J. Biochem.* **1999,** *266* (3), 1101-1110.

14. Fraser, P. E.; Darabie, A. A.; McLaurin, J., Amyloid-β interactions with chondroitin sulfate-derived monosaccharides and disaccharides: implications for drug development. *J. Biol. Chem.* **2001,** *276* (9), 6412-6419.

15. Watson, D. J.; Lander, A. D.; Selkoe, D. J., Heparin-binding properties of the amyloidogenic peptides Aβ and amylin dependence on aggregation state and inhibition by congo red. *J. Biol. Chem.* **1997,** *272* (50), 31617-31624.

16. Lindahl, B.; Westling, C.; Giménez-Gallego, G.; Lindahl, U.; Salmivirta, M., Common binding sites for β-amyloid fibrils and fibroblast growth factor-2 in heparan sulfate from human cerebral cortex. *J. Biol. Chem.* **1999,** *274,* 30631–30635.

17. Kemp, M. M.; Linhardt, R. J., Heparin-based nanoparticles. *WIREs Nanomed. Nanobiotechnol.* **2010,** *2,* 77-87 and references cited therein.

18. Tan, Q.; Tang, H.; Hu, J.; Hu, Y.; Zhou, X.; Tao, Y.; Wu, Z., Controlled release of chitosan/heparin nanoparticledelivered VEGF enhances regeneration of decellularized tissue-engineered scaffolds. *Int. J. Nanomed.* **2011,** *6,* 929-942.

19. Nurunnabi, M.; Khatun, Z.; Moon, W.-C.; Lee, G.; Lee, Y.-K., Heparin based nanoparticles for cancer targeting and noninvasive imaging. *Quant. Imaging Med. Surg.* **2012,** *2,* 219-226.

20. Shahbazi, M.-A.; Hamidi, M.; Mohammadi-Samani, S., Preparation, optimization, and in-vitro/in-vivo/ex-vivo characterization of chitosan-heparin nanoparticles: drug-induced gelation. *J. Pharm. Pharmacol.* **2013,** *65,* 1118-1133.

21. Zhang, J.; Shin, M. C.; David, A. E.; Zhou, J.; Lee, K.; He, H.; Yang, V. C., Long-circulating heparin-functionalized magnetic nanoparticles for potential application as a protein drug delivery platform. *Mol. Pharm.* **2013,** *10,* 3892-3902.

22. Lee, J.-h.; Jung, M. J.; Hwang, Y. H.; Lee, Y. J.; Lee, S.; Lee, D. Y.; Shin, H., Heparin-coated superparamagnetic iron oxide for *in vivo* MR imaging of human MSCs. *Biomaterials* **2012,** *33* (19), 4861-4871.

23. Corot, C.; Robert, P.; Idée, J.-M.; Port, M., Recent advances in iron oxide nanocrystal technology for medical imaging. *Adv. Drug Del. Rev.* **2006,** *58*, 1471-1504.

24. Colombo, M.; Carregal-Romero, S.; Casula, M. F.; Gutiérrez, L.; Morales, M. P.; Böhm, I. B.; Heverhagen, J. T.; Prosperi, D.; Parak, W. J., Biological applications of magnetic nanoparticles. *Chem. Soc. Rev.* **2012,** *41*, 4306-4334.

25. He, H.; David, A.; Chertok, B.; Cole, A.; Lee, K.; Zhang, J.; Wang, J.; Huang, Y.; Yang, V. C., Magnetic nanoparticles for tumor imaging and therapy: a so-called theranostic system. *Pharm. Res.* **2013,** *30*, 2445-2458.

26. El-Dakdouki, M. H.; El-Boubbou, K.; Zhu, D. C.; Huang, X., A simple method for the synthesis of hyaluronic acid coated magnetic nanoparticles for highly efficient cell labelling and *in vivo* imaging. *RSC Adv.* **2011,** *1*, 1449-1452.

27. García-Matas, S.; de Vera, N.; Aznar, A. O.; Marimon, J. M.; Adell, A.; Planas, A. M.; Cristòfol, R.; Sanfeliu, C., In vitro and in vivo activation of astrocytes by amyloid-beta is potentiated by pro-oxidant agents. *J. Alzheimers Dis.* **2010,** *20*, 229-245.

28. Allaman, I.; Gavillet, M.; Bélanger, M.; Laroche, T.; Viertl, D.; Lashuel, H. A.; Magistretti, P. J., Amyloid-beta aggregates cause alterations of astrocytic metabolic phenotype: impact on neuronal viability. *J. Neurosci.* **2010,** *30*, 3326-3338.

29. Bitan, G.; Vollers, S. S.; Teplow, D. B., Elucidation of primary structure elements controlling early amyloid β-protein oligomerization. *J. Biol. Chem.* **2003,** *278* (37), 34882-34889.

30. Roher, A. E.; Lowenson, J. D.; Clarke, S.; Woods, A. S.; Cotter, R. J.; Gowing, E.; Ball, M. J., Beta-amyloid-(1−42) is a major component of cerebrovascular amyloid deposits: Implications for the pathology of Alzheimer disease. *Proc. Natl. Acad. Sci., U.S.A.* **1993,** *90*, 10836−10840.

31. LeVine, H., Quantification of β-sheet amyloid fibril structures with Thioflavin T. *Meth. Enzymol.* **1999,** *309*, 274-284.

32. Vilasi, S.; Sarcina, R.; Maritato, R.; De Simone, A.; Irace, G.; Sirangelo, I., Heparin induces harmless fibril formation in amyloidogenic W7FW14F apomyoglobin and amyloid aggregation in wild-type protein in vitro. *PloS One* **2011,** *6* (7), e22076.

33. Kouyoumdjian, H.; Zhu, D. C.; El-Dakdouki, M. H.; Lorenz, K.; Chen, J.; Li, W.; Huang, X., Glyconanoparticle Aided detection of β-amyloid by magnetic resonance imaging and attenuation of β-amyloid induced cytotoxicity. *ACS Chem. Neurosci.* **2013,** *4*, 575-584.

34. Luo, J.; Mohammed, I.; Wärmländer, S. K. T. S.; Hiruma, Y.; Gräslund, A.; Abrahams, J. P., Endogenous polyamines reduce the toxicity of soluble Aβ peptide aggregates associated with Alzheimer's disease. *Biomacromolecules* **2014,** *15* (6), 1985-1991.

Chapter 4. Mitigation of Neurotoxicities of Toxic Tau Oligomers by Heparin Like Oligosaccharides

4.1. Introduction

Alzheimer's disease (AD) is a progressive degenerative brain disease, which is estimated to affect 5.5 million Americans in 2017.[1] Although the causes for most AD cases have not been firmly established, the pathology of tau protein is believed to play important roles.[2] Tau protein in its native state exists as a soluble monomer, which is critical in stabilizing microtubules. However, tau can misfold and aggregate leading to the formation of oligomers and hyperphosphorilated tau aggregates known as neurofibrillary tangles (NFTs), a hallmark of AD.[3] While NFTs are abundant in the brains of late stage AD patients, some patients show neuronal loss and cognitive deficits prior to the formation of histologically identifiable NFTs.[4] In animal studies, NFTs have been found not to be associated with neuronal death, suggesting that these large insoluble aggregates may not be the key toxic species in AD.[5-7]

In order to explain tau pathology, tau oligomer hypothesis has been proposed recently with strong evidence supporting that the soluble, oligomeric tau rather than the NFTs are likely the most toxic species producing disease pathology.[8-9] Tau oligomers (TauO) are found in human AD patients and are able to propagate extracellularly through different brain regions, contributing to neuronal cell death in addition to learning and memory deficits.[10-12] Injection of tau oligomers isolated from the cerebral cortex of AD brains initiated tau pathology in cognitively normal mice, and cause synaptic and mitochondrial dysfunction associated with memory loss in their brains.[11-13] Even brief exposure to human tau oligomers could produce an immediate impairment

of long-term potentiation and memory.[14] The tau oligomer hypothesis was further strengthened by the observations that lowering tau oligomer levels protected against behavioral deficits and tau pathology in multiple mouse models without affecting NFTs levels.[13, 15] Therefore, strategies that can reduce the oligomer associated neurotoxicity are highly desirable.

Heparan sulfate (HS) and its more sulfated analog heparin are a class of highly negatively charged polysaccharides present on mammalian cells including neuronal cells.[16-17] HS and heparin are composed of repeating disaccharide subunits with D-glucosamine (GlcN) α-1,4 linked with a uronic acid (either L-iduronic acid (IdoA) or D-glucuronic acid (GlcA)).[18-19] The amine moiety, 3-OH and 6-OH of GlcN and 2-OH of the uronic acid of heparin can be sulfated. Heparin is known to bind with tau.[20-24] Yi Liang and coworkers characterized a tight 1:1 complex between tau fragment $Tau_{244-372}$ and heparin (average molecular mass = 7 kDa).[20] They also proposed a model for tau filament formation where the formation of the complex with heparin initiated nucleation and promoted elongation of tau fibrils. NMR analysis mapped the binding region to the paired helical filament (PHF) core region, which was rich in positive charges.[22] A study using enzyme-cleaved fragments of heparin with different sulfation patterns and lengths revealed a key 6-*O*-sulfate residue in the tau-binding affinity, as reported by Fuming Zhang and coworkers.[24] Although HSPG on cell surface has been found important in the uptake of tau aggregates,[21] it is not known whether heparin can interact with tau oligomers. Herein, using structurally well-defined synthetic oligosaccharides, we report for the first time that heparin-like oligosaccharides as small as tetrasaccharides can bind and interact with the toxic tau oligomers. Furthermore, treatment of human neuroblastoma cell line with heparin like oligosaccharides can

protect the cells from tau oligomers-induced toxicity providing an exciting new direction in addressing tauopathy.

4.2. Results and Discussion

4.2.1. Preparation of Heparin Oligosaccharide Backbones

In order to obtain heparin like oligosaccharides, we based our synthetic design on disaccharide modules **1**, **2** and **3**. Disaccharides **1** and **2** were synthesized starting from disaccharide **4** following literature procedures.[25] For the non-reducing end disaccharide module, while TBS bearing disaccharide **4** could be used, we found it was impossible to remove the TBS group from sulfated oligosaccharides during late stage deprotection of sulfated glycans.[25] This consideration prompted us to prepare the 4'-*O*-Bn protected disaccharide **3**. Pre-activation of benzyl (Bn) protected glucosamine donor **5** with *p*-TolSCl and AgOTf[26] followed by the addition of acceptor **6**, gave the α-linked disaccharide **7** in 87% yield (J_{H1-C1} = 166.5, 171.0 Hz) (**Scheme 4.1**). Protective group manipulation of **7** yielded disaccharide module **3**.
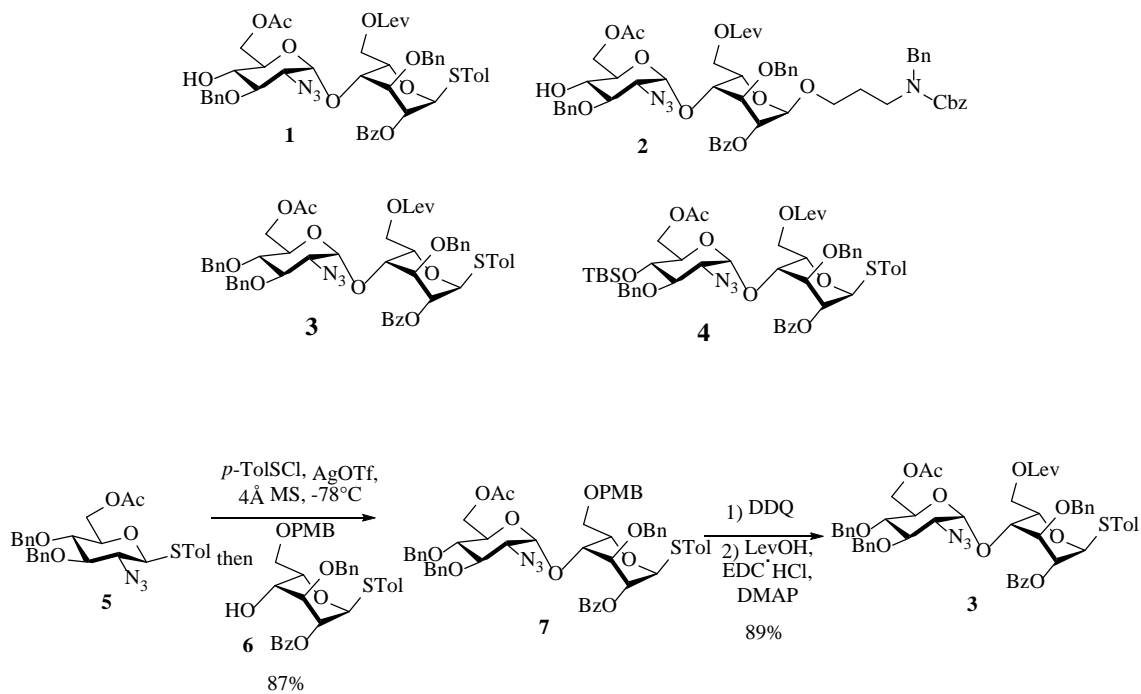
Scheme 4.1. Synthesis of non-reducing end disaccharide module **3**.

With the necessary disaccharide building blocks in hand, we performed glycosylation to elongate the backbones. Reaction of the donor **3** with acceptor **1** generated tetrasaccharide **8** in 85% yield (**Scheme 4.2**). Alternatively, **3** glycosylated the reducing end disaccharide module **2** giving tetrasaccharide **9** (**Scheme 4.2b**). In a similar manner, TBS bearing tetrasaccharide donor **10** was formed (**Scheme 4.2c**).
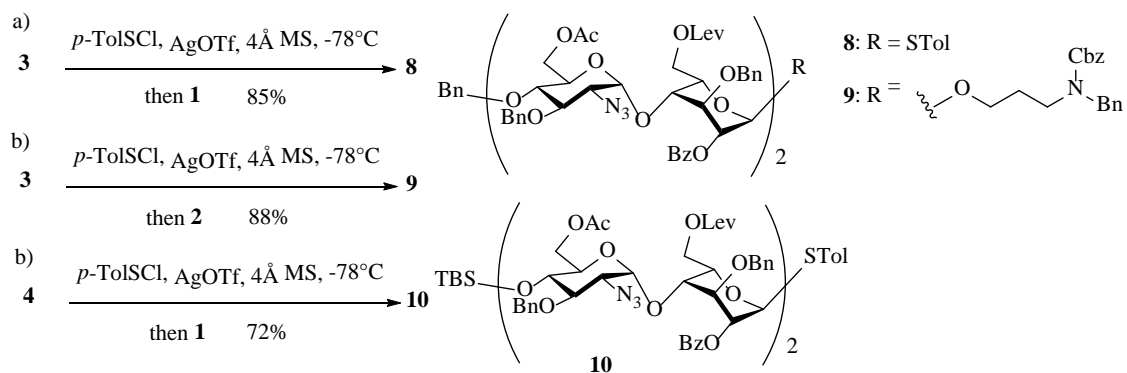
Scheme 4.2. Construction of heparin tetrasaccharide backbones.

To produce the hexasaccharide backbone, a 4+2 glycosylation was carried out between the tetrasaccharide donor **8** and acceptor **2** producing hexasaccharide **11** (**Scheme 4.3a**). The 4-*O*-TBS protected tetrasaccharide donor **10** also reacted well with disaccharide **2**. Removal of the TBS group from the glycosylation product led to the hexasaccharide acceptor **12** (**Scheme 4.3b**), which was subsequently glycosylated by tetrasaccharide donor **8**, forming decasaccharide **13** in 84% yield (**Scheme 4.3c**).

a)

8 → *p*-TolSCl, AgOTf, 4Å MS, -78°C; then **2**; 58% → **11**

b)

10 → 1) *p*-TolSCl, AgOTf, 4Å MS, -78°C; then **2**; 2) HF·pyridine, pyridine; 81% → **12**

c)

8 → *p*-TolSCl, AgOTf, 4Å MS, -78°C; then **12**; 84% → **13**
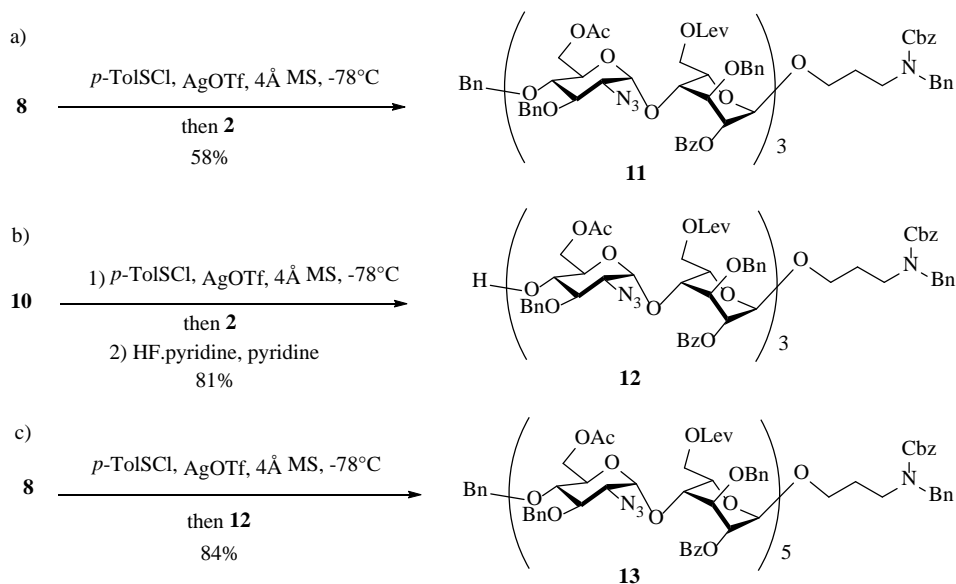
Scheme 4.3. Constructions of heparin hexa- and deca-saccharide backbones.

4.2.2. Deprotection and Sulfation

The deprotections and modifications of the backbones were carried out first by removal of 6-*O*-Lev from fully protected tetra-, hexa- and decasaccharide **9**, **11** and **13** respectively with hydrazine exposing the 6-OH (**Scheme 4.4**). The conversion of these primary hydroxyl groups to carboxylic acids was mediated by bis(acetoxy)iodobenzene (BAIB) assisted 2, 2, 6, 6-tetramethyl-1-piperidinyloxyl (TEMPO) oxidation.[27] Since free carboxylic acids were found to lead to low yields in subsequent sulfation reactions,[25] they were protected as either methyl (83% for tetrasaccharide **17** in 2 steps) or benzyl (77% for hexasaccharide **18** and 81% for decasaccharide **19** in 2 steps) esters. Removal of the acyl protecting groups was accomplished by treating oligosaccharides **17**-**19** with sodium methoxide, which gave **20**, **21** and **22** respectively.
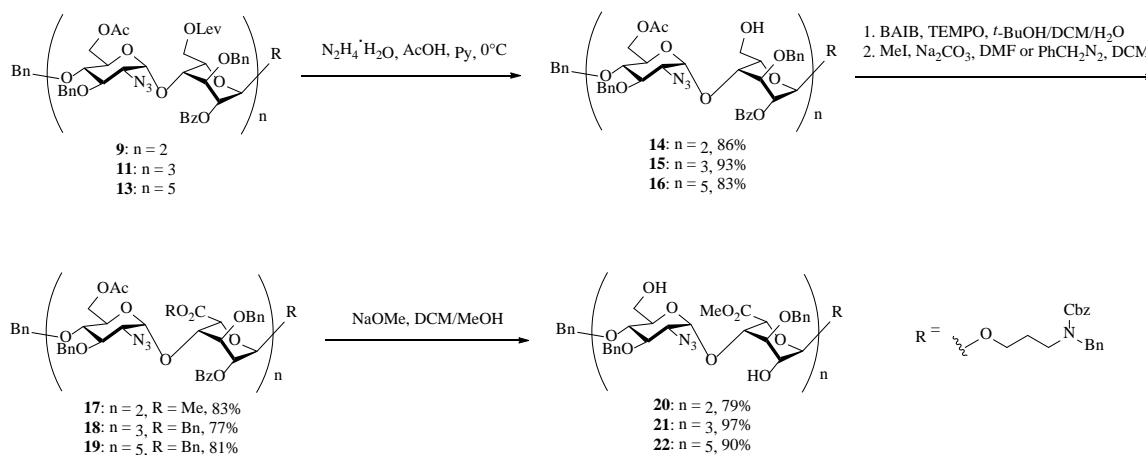
Scheme 4.4. Deprotection of heparin oligosaccharides.

The two azido groups in tetrasaccharide **20** were reduced by zinc powder in acetic acid and acetic anhydride leading to *N*-acetylated tetrasaccharide **23** in 99% yield, while performing the reaction in the absence of acetic anhydride provided **24** with two free amine groups (**Scheme 4.5**). Sulfations of free hydroxyls and amines of the tetrasaccharide **24** were performed stepwise. Firstly, **24** was dissolved in methanol with aqueous NaOH solution adjusting the pH to 9.5 in order to deprotonate amine groups and *N*-sulfation was performed by adding excess $SO_3 \cdot Et_3N$ complex to the mixture to give **25** in 78% yield. Hydrogenolysis and saponification of **25** gave the *N*-sulfated heparin like tetrasaccharide **27**. Alternatively, **25** was subjected to *O*-sulfation with $SO_3 \cdot$pyridine complex in pyridine overnight at 55 °C. Subsequent hydrogenolysis and saponification produced *N*, *O*-sulfated tetrasaccharide **29**. In a similar manner, from the *N*-acetylated tetrasaccharide **23**, tetrasaccharides **26** and **28** were generated.
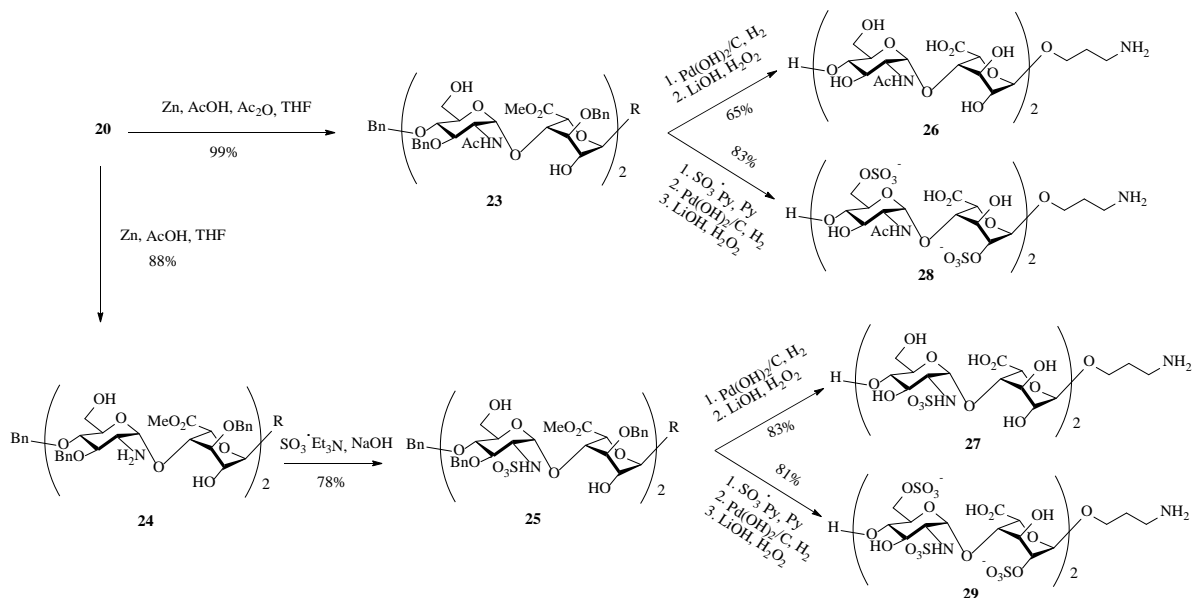
Scheme 4.5. Sulfation and deprotection of tetrasaccharides.

For the heparin hexasaccharide **21**, the reduction was performed with 1, 3-propanedithiol and triethylamine over 3 days[25] in a yield of 76% (**Scheme 4.6a**). Similar stepwise sulfation as in synthesis of tetrasaccharide **25** was attempted on hexasaccharide **30**, which only led to decomposition of the starting materials. Analysis of the reaction mixture showed the formation of side products due to β-elimination with the oligosaccharide backbone cleaved. Instead, treatment of the hexasaccharide **30** with 600 mM $SO_3 \cdot py$ complex in pyridine at 55 °C successfully installed both *N*- and *O*-sulfation in one step, which was followed by catalytic hydrogenation and methyl ester hydrolysis, giving the final heparin like hexasaccharide **31** at 64% yield over 3 steps (**Scheme 4.6a**). Analogously, the heparin like decasaccharide **32** was synthesized with an overall yield of 42% from **22** (**Scheme 4.6b**).
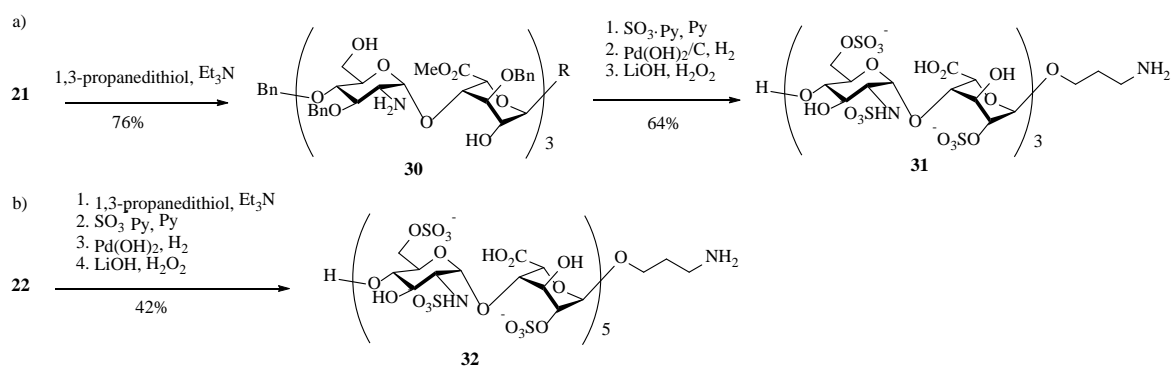
Scheme 4.6. Sulfation and deprotection of hexa- and deca-saccharide.

4.2.3. Binding Assay with Tau Oligomers

The majority of heparin – tau studies to date have been performed using polysaccharides isolated from nature, which are heterogeneous mixtures of many sequences with various backbone length and sulfation patterns. Structurally well-defined heparin oligosaccharides can provide useful information on structure-activity relationship. With the synthetic oligosaccharides **26-29**, **31**, **32** in hand, their binding with tau oligomers were analyzed. The sensorgrams showed that oligosaccharide as short as a tetrasaccharide (**29**) could exhibit significant binding to Tau oligomers with a K_D value of 2.79×10^{-7} M. Comparison within the tetrasaccharide series **26**-**29** indicated that tetrasaccharides with higher degree of sulfation are associated with stronger binding to tau oligomers (**Figure 4.1a-d**). Increasing the backbone length of the oligosaccharide to hexa- and deca-saccharides led to enhancement in tau oligomer binding, with K_D values of 1.41×10^{-7} M and 3.49×10^{-8} M for oligosaccharides **31** and **32** respectively. These results suggest that electrostatic interactions may play an important role in heparin – tau oligomer binding.
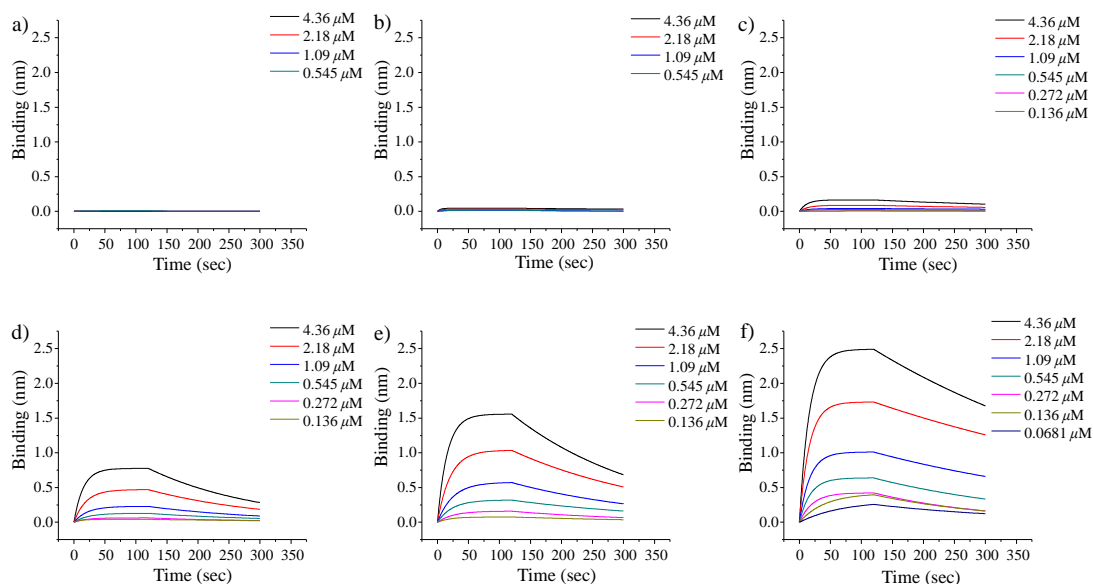
Figure 4.1. Sensograms of heparin like oligosaccharide binding with tau oligomers. Fit curves of interactions between BLI sensors loaded with a)**26**, b)**27**, c)**28**, d)**29**, e)**31** and f)**32** and tau oligomers at various concentrations were obtained using models from Octet Data Analysis 9.0.0.12. Higher sulfation degree or longer backbone length led to stronger binding with Tau oligomers.

4.2.4. Heparin Oligosaccharides Mitigates Cytotoxicity of Tau Oligomers (Done by Dr. Rakez Kayed lab)

In this study, we pursued an alternative approach to evaluate heparin like oligosaccharides' ability to modulate the aggregation state and toxicity of preformed tau oligomers.[28] Therefore, highly purified oligomeric tau species were incubated with and without oligosaccharides (5X) at room temperature on an orbital shaker, without stirring, for 16 hours under oligomerization conditions.[28] Atomic force microscopy (AFM) was performed to visualize and characterize the morphology and aggregation state of the end product of each reaction. AFM images of TauO displayed a homogeneous spherical morphology (**Figure 4.2a**) while, in the presence of

heparin-like oligosaccharides (**Figure 4.2b-e**), we observed the tendency of tau oligomers to aggregate leading to the formation of fibrils and protofibrils (**26-28**) and compound with higher sulfatation degree (**29**) or longer backbone length (**31-32**) convert them into larger non-toxic tau aggregates.
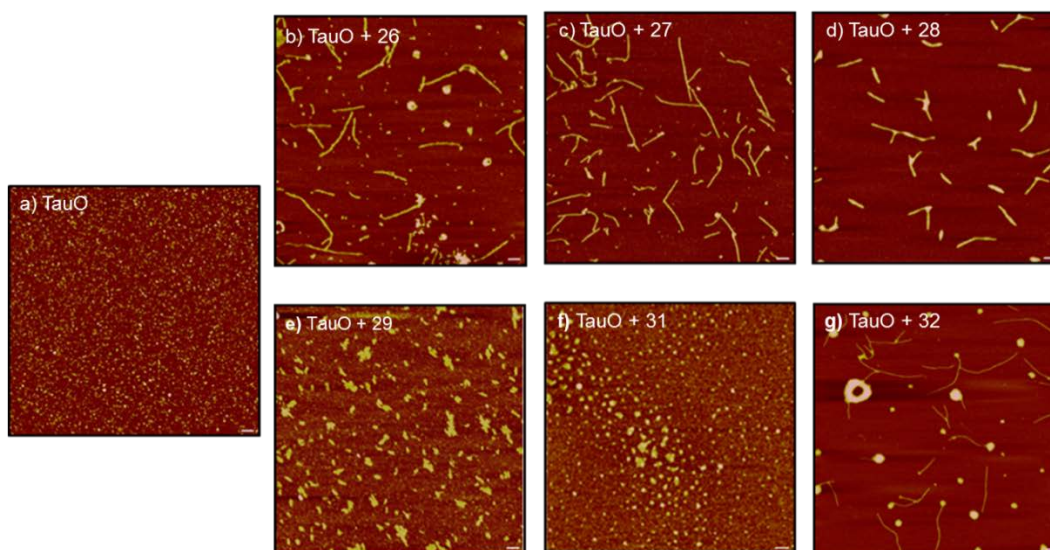

Figure 4.2. Biophysical characterization of Tau oligomers alone and in the presence of heparin-like oligosaccharides. Atomic Force Microscopy images of TauO without (a) and after incubation with heparin-like oligosaccharides (5X) b)**26**, c)**27**, d)**28**, e)**29**, f)**31** and g)**32**. AFM images show the ability of the compounds to modulate tau aggregation state forming larger tau aggregates. Scale bars = 100 nm.

Next, we evaluated the toxicity of tau aggregated species, resulting from the co-incubation of TauO alone and with heparin-like oligosaccharides, on human neuroblastoma cell line SH-SY5Y. Therefore, cells were treated with tau oligomers alone and in the presence of the compounds (**Figure 4.3**). SH-SY5Y cytotoxicity significantly increased after treatment with TauO alone while, in the presence of oligosaccharides (final concentration 10 μM), we observed

decreased LDH release as compared to TauO (**Figure 4.3a**). Furthermore, SH-SY5Y viability

significantly decreased after treatment with TauO alone while cells exposed to TauO in the

presence of heparin-like oligosaccharides reduced TauO-induced toxicity as shown by the higher

level of cell viability using a resazurin based assay (**Figure 4.3b**). Moreover, cells exposed to

each condition were evaluated for morphological differences, showing cells shrinkage and loss of

their processes once they were exposed to TauO as compared to either the untreated control or to

cells treated with tau oligomers in the presence of heparin-like oligosaccharides (**Figure 4.3c**).

Taken together these results suggest that heparin-like oligosaccharides interact and remodel toxic

tau oligomers converting them into less toxic high molecular weight aggregates.
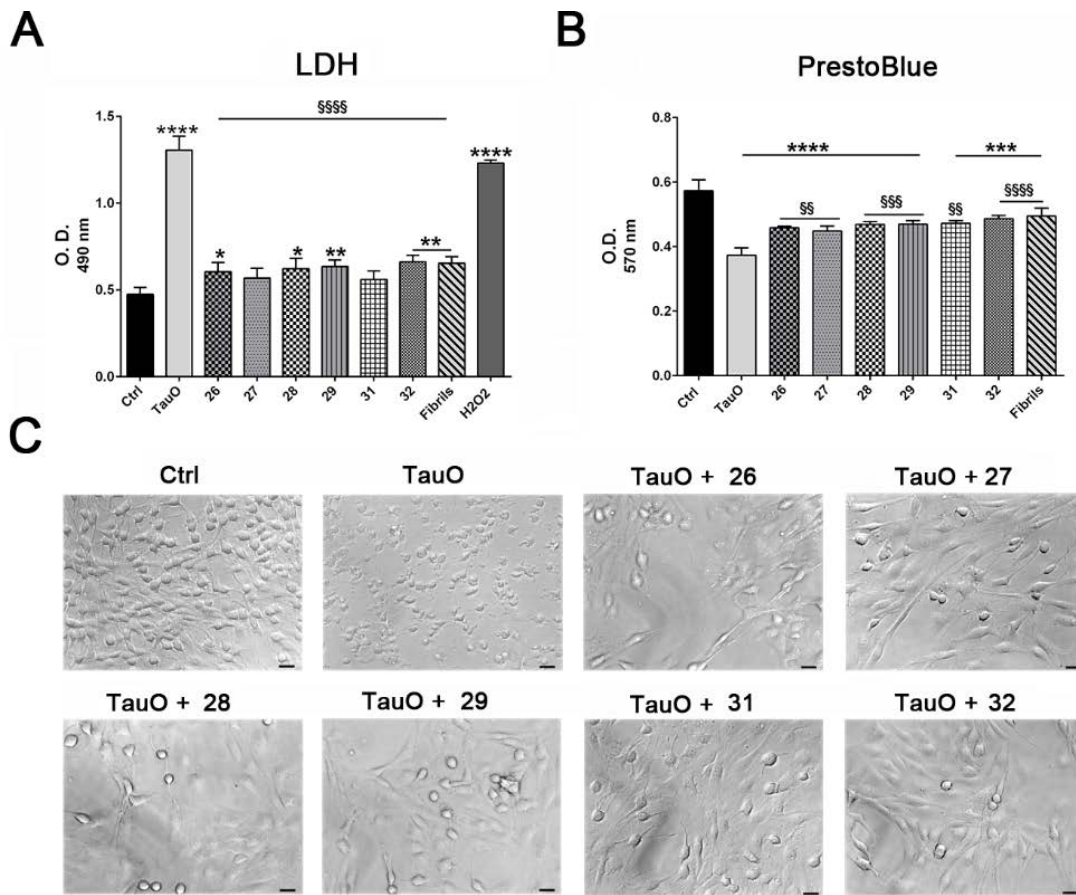
Figure 4.3. Viability and Cytotoxicity assays of Tau oligomers alone and in the presence of heparin-like oligosaccharides on human SH-SY5Y neuroblastoma cell line.
(A) SH-SY5Y cells cytotoxicity after exposure to 2μM tau oligomers, or 2μM tau oligomers with 10μM of each heparin-like oligosaccharide (**26-29, 31, 32**) and untreated control (**Ctrl**). Treatment of SH-SY5Y cells with TauO had significantly higher LDH release compared to untreated control and cells exposed to TauO in the presence of heparin-like oligosaccharides. (B) SH-SY5Y cells cytotoxicity after exposure to 2μM tau oligomers, or 2μM tau oligomers with 10μM of each heparin-like oligosaccharide (**26-29, 31, 32**) and **Ctrl**. Cells treated with TauO had significantly lower viability compared to untreated control while cells exposed to TauO in the presence of heparin-like oligosaccharides show to rescue TauO-induced toxicity. Each experiment was performed in triplicate (n = 3). Data were compared by one-way analysis of variance (ANOVA) followed by Dunnett's multiple comparison test: Ctrl vs TauO, 26-29, 31, 32, Fibrils: ****$p < 0.0001$, ***$p < 0.001$, **$p < 0.01$, *$p < 0.05$; TauO vs 26-29, 31, 32: §§§§$p < 0.0001$, §§§$p < 0.001$, §§$p < 0.01$. Bars and error bars represent means and standard deviations performed. (C) Untreated SH-SY5Y cells were compared to cells treated for 24 hours with TauO alone or TauO in the presence of heparin-like oligosaccharides (**26-29, 31, 32**) and evaluated for morphological changes. Scale bar =20 µm.

4.3. Conclusions

The binding of heparin with tau aggregates and HSPG mediated endocytosis suggested that heparin may play an important role in the propagation of tau pathology. However, the structural heterogeneity of naturally extracted heparin has been the obstacle in the study of the interactions. Also, no prior research has been performed on the interaction between heparin and tau oligomers, which is considered as the main culprit in tau pathology. We synthesized a series of heparin oligosaccharides, including different sulfation patterns and backbone lengths up to fully-sulfated decasaccharide. Direct binding between heparin oligosaccharides and tau oligomers were observed through BLI study, in which higher sulfation degree or longer backbone length both contributed to stronger binding the tau oligomers. AFM images displayed two different ways of heparin oligosaccharide promoting the aggregation of tau oligomers. Partially sulfated tetrasaccharides led to the formation of fibrils and protofibrils, while longer backbone length of heparin resulted in the formation of amorphous larger aggregates. Both effects of heparin binding were proven to be protective in the SH-SY5Y cytotoxicity or viability assay. This study may help understanding the structural-activity relationship of heparin in the binding the tau oligomers for the first time and elucidating the role of heparin in tauopathy.

4.4. Experimental Section

4.4.1. General Procedure for Preactivation Based Glycosylation.

A solution of donor (1.0 equiv) and freshly activated 4 Å molecular sieves (1 g per 20 mL of final solvent) in CH_2Cl_2 was stirred at room temperature for 10 min and then cooled to -78 °C.

AgOTf (2.5 equiv) dissolved in Et$_2$O/CH$_2$Cl$_2$ (10/1) was added directly to the solution. After 10 min, the orange-colored promoter *p*-TolSCl (1.0 equiv) was added with a microsyringe directly to the flask to avoid freezing the promoter on the walls of the flask. The color of *p*-TolSCl disappeared rapidly, indicating the consumption of *p*-TolSCl. After TLC indicated that the donor was fully activated (about 5 min at −78 °C), a solution of acceptor (0.8-1.0 equiv) in CH$_2$Cl$_2$ along with TTBP (1.0 equiv) was slowly added along the walls of the flask. This was done to allow the acceptor solution to cool before mixing with the activated donor. The final ratio of Et$_2$O/CH$_2$Cl$_2$ was 1/1 after all reagents were added. The reaction mixture was slowly warmed to 0 °C over 2 h. The mixture was quenched with Et$_3$N, diluted with CH$_2$Cl$_2$ and filtered through Celite. After washing the Celite with CH$_2$Cl$_2$ until all organic compounds were removed, as verified by TLC, the CH$_2$Cl$_2$ fractions were combined and washed with sat. NaHCO$_3$ solution and brine. The organic layer was collected and dried over Na$_2$SO$_4$. After removal of the solvent, the product was purified by silica gel chromatography unless noted.

4.4.2. General Procedure for TBS Removal

The TBS-containing oligosaccharide was dissolved in pyridine (5 mL per 1 g oligosaccharide) and transferred to a 50 mL plastic centrifuge tube. The pyridine solution was cooled to 0 °C, followed by dropwise addition of HF·pyridine (2.5 mL per 1 g oligosaccharide) while stirring. The reaction was then allowed to warm to room temperature and kept overnight or 3 days. The reaction was diluted with CH$_2$Cl$_2$ and washed sequentially with sat. CuSO$_4$, sat. NaHCO$_3$, and 1M HCl. The organic layer was dried over Na$_2$SO$_4$, concentrated, and purified by silica gel chromatography.

4.4.3. General Procedure for Removal of Levulinoyl Esters

A solution of the oligosaccharide containing Lev esters (1 equiv) in pyridine/AcOH (3/2) was cooled to 0 °C. To this was added hydrazine hydrate (5 equiv per Lev ester). The reaction was stirred at 0 °C for 3 h or until TLC showed that the reaction was complete. To quench the reaction, excess acetone was added and the reaction was stirred at room temperature for 30 min. The reaction mixture was then diluted with ethyl acetate and washed with 1 M HCl, sat. $NaHCO_3$ and brine. The resulting organic layer was then dried over Na_2SO_4, concentrated, and purified by silica gel chromatography.

4.4.4. General Procedure for Oxidation of 6-OH

The desired compound to be oxidized (1 equiv) was dissolved in a solution of DCM/t-BuOH/H_2O (4/4/1). To this solution was added TEMPO (0.3 equiv per 6-OH), followed by BAIB (3 equiv per 6-OH). The reaction was then stirred at room temperature overnight. After ensuring that the reaction was complete by TLC, the reaction was quenched by addition of excess $Na_2S_2O_3$ solution and allowed to stir at room temperature for 15 min. The mixture was then diluted with DCM and washed with brine. The organic layers were combined, dried over Na_2SO_4, and concentrated. The crude product could then be protected as a methyl or benzyl ester.

4.4.5. General Procedure for Methyl Ester Formation after Oxidation

The crude product from oxidation was dissolved in DMF. To this solution was added K_2CO_3 (5 equiv per COOH), followed by CH_3I (2.5 equiv per COOH), and the reaction was allowed to stir overnight at room temperature. After verifying that the reaction was complete by TLC, the reaction was diluted with ethyl acetate and water. The mixture was then washed with 1 M HCl

and sat. NaHCO$_3$, dried over Na$_2$SO$_4$, concentrated, and purified by silica gel chromatography.

4.4.6. General Procedure for Benzyl Ester Formation after Oxidation

The crude product from oxidation was dissolved in DCM. To this was added phenyl diazomethane until a deep red color persisted. The reaction was allowed to stir overnight. After TLC indicated that the reaction was complete, the mixture was concentrated and purified by silica gel chromatography.

4.4.7. General Procedure for Transesterification

The ester containing oligosaccharide was dissolved in a mixture of DC/MeOH (1/1). NaOMe solution was added to the oligosaccharide solution until the pH reached 10. The reaction was maintained at pH 10 and stirred at room temperature. After the reaction was confirmed complete by TLC, it was quenched by adding H$^+$ resin. The quenched reaction was filtered, concentrated and purified by silica gel chromatography.

4.4.8. General Procedure for 1, 3-Propanedithiol Mediated Azide Reduction

The starting oligosaccharide was dissolved in anhydrous MeOH (dried over 4 Å molecular sieves) and protected from light. To this solution were added triethylamine (30 equiv per N$_3$) and 1, 3-propanedithiol (30 equiv per N$_3$), and the reaction was stirred at room temperature for 72 h. The reaction was concentrated and purified by silica gel chromatography.

4.4.9. General Procedure for Selective *N*-Sulfation

To a solution of NH$_2$-containing compound (1 equiv) in MeOH was added 1 M aqueous NaOH solution at 0 °C until the pH reaches 10. SO$_3$·pyridine (10 equiv) was added to the solution at the same temperature followed by NaOH to adjust the pH back to 10. The solution

was allowed to warm up to room temperature and stirred overnight. The reaction was concentrated and purified by silica gel chromatography.

4.4.10. General Procedure for Simultaneous *O*, *N*-Sulfation

A compound (1 equiv) containing both free OH and NH_2 groups was dissolved in dry pyridine (1 mL per 5 mg compound, dried over 4 Å molecular sieves). To this mixture was added SO_3·pyridine (100 mg per 1mL pyridine), which had been previously washed with H_2O, MeOH, and DCM and dried under vacuum. The reaction was protected from light and stirred for 24 h at 55 °C. The reaction was diluted with 1:1 DCM:MeOH and eluted from a Sephadex LH-20 column, ensuring that all pyridine was removed. The fractions containing sugar were concentrated and further purified by prep TLC (EtOAc/MeOH/H_2O = 3/1/1).

4.4.11. General Procedure for Global Debenzylation

A mixture of the Bn-containing compound (for 6 mg of compound, 1 equiv), MeOH/H_2O (4 mL/2 mL), and Pd(OH)$_2$/C (100 mg) was stirred under H_2 at room temperature overnight and then filtered. The filtrate was concentrated to dryness under vacuum and then diluted with H_2O (15 mL). The aqueous phase was further washed with CH_2Cl_2 (3 × 5 mL) and EtOAc (3 × 5 mL), and then the aqueous phase was dried under vacuum. The crude product was further purified by a Sephadex G-15 column.

4.4.12. General Procedure for Methyl Ester Saponification

The solution of compound (1 equiv) in THF was cooled to 0 °C and 1 M LiOH (15 equiv per COOMe) was added dropwise, followed by addition of H_2O_2 (150 equiv per COOMe, 30%). Additional LiOH was added to adjust the pH to 9. The reaction was warmed up to room

temperature and stirred overnight. Then the mixture was eluted from a Sephadex G-15 column with H_2O. To simplify mass spectrometry analysis, the product was then eluted from a column of Dowex 50WX4-Na$^+$ to convert the compound into the sodium salt form.

4.4.13. Preparation of Tau Oligomers

Recombinant tau protein (tau-441 (2N4R) MW 45.9 kDa) was expressed and purified as described.[29-30] Tau pellet was treated with 8M urea followed by overnight dialysis against 1X phosphate-buffered saline (PBS), pH 7.4. Tau concentration was measured using bicinchoninic acid protein assay (Micro BCA kit, Pierce) and diluted to 1 mg/ml using 1X PBS. Aliquots of tau monomer in PBS were stored at -20°C. Each 300 µl of tau stock (0.3 mg) was added to 700 µl of 1X PBS and incubated for 1 hour on an orbital shaker at room temperature. After shaking, the resulting tau oligomers were purified by fast protein liquid chromatography (FPLC, Superdex 200HR 10/30 column, Amersham Biosciences).

4.4.14. BLI Binding Assay of Heparin and Tau Oligomers

The heparin oligosaccharides were biotinylated by reaction with sulfo-*N*-hydroxysuccinimide long-chain biotin (ApexBio Tech LLC) following a previously reported method.[31] The binding assay was performed on the Octet K2 System (Pall ForteBio). The biotinylated heparin oligosaccharides were absorbed to streptavidin (SA) sensor at a concentration of 50 μM for 2 min. The sensor was then balanced in the assay buffer (PBS containing 0.005% P20) and dipped into tau oligomer solution in assay buffer at different concentration (4.36, 2.18, 1.09, 0.545, 0.272, 0.136, 0.0681 μM). After 2 min of association, the

sensor was brought back to the previous assay buffer for a 3-min dissociation step. At the end of the assay, the sensor was regenerated in 1 M NaCl to remove the bound tau oligomers. Each measurement was repeated 3 times on the same sensor. The control assay was done with another sensor loaded with saturated biotin solution.

4.4.15. Preparation of Tau Oligomers in the Presence of Heparin-like Oligosaccharides

100 μl of tau oligomers (1μg/μl) were incubated with heparin-like oligosaccharides (1:5). Oligosaccharides were dissolved in ddH$_2$O at a final concentration of 50 mM and diluted in 1X PBS or cells medium for incubation or toxicity assays. Tau oligomers in the presence of oligosaccharides and controls were incubated on an orbital shaker, without stirring, for 16 hours under oligomerization conditions.

4.4.16. Atomic Force Microscopy (AFM)

Tau oligomers were characterized by AFM as previously described.[28] Briefly, samples were prepared by adding 10 µl tau oligomers in the absence or presence of AC on freshly-cleaved mica and were allowed to adsorb to the surface. Mica were then washed three times with distilled water to remove unbound protein and impurities followed by air-drying. Samples were then imaged with Multimode 8 AFM machine (Veeco, CA) using a non-contact tapping method (ScanAsyst-Air).

4.4.17. Cell Toxicity Assays

Human neuroblastoma SH-SY5Y cells were cultured and treated for measuring cytotoxicity using either lactate dehydrogenase (LDH) release assay (Cytotoxicity Detection KitPLUS -LDH,

Roche) or a resazurin-based assay (PrestoBlueTM, Invitrogen) following manufacturers'

instructions as previously described.[28, 32] Briefly, cells were maintained in Dulbecco`s modified

Eagle's medium (DMEM) and grown to confluency in 96-well plates. Cells ($\approx$10,000 cells /well)

were treated for 24 hours with 2.0 µM tau oligomers and 2.0 µM tau oligomers incubated with

10 µM of heparin-like oligosaccharides (**26**-**29**, **31**, **32**) followed by assaying with LDH or

PrestoBlue. Optical density (OD) was measured at 490 nm and 570 nm, for LDH and PrestoBlue,

respectively, with POLARstar OMEGA microplate reader (BMG Labtech). All measurements

were performed in triplicate and corrected by the vehicle background. Statistical analysis was

based on one-way analysis of variance (ANOVA), followed by Dunnett's multiple comparison

test performed using GraphPad Prism 6.01.

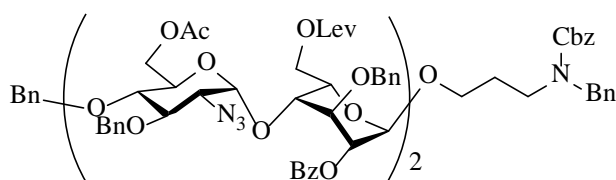### 4.4.18. Product Preparation and Characterization Data
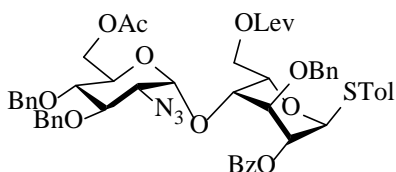
p-Tolyl 6-*O*-acetyl-2-azido-3, 4-di-*O*-benzyl-2-deoxy-*α*-D-glucopyranosyl-(1→4)-2-*O*-benzoyl-

3-*O*-benzyl-6-*O*-levulinoyl-1-thio-*α*-L-idopyranoside (**3**)

Compound **3** was prepared from compound **7** in 2 steps. Firstly, compound **7** (1.04 g, 1.03 mmol)

was dissolved in DCM/H_2O (45/5 mL), cooled to 0 °C and DDQ (467 mg, 2.06 mmol) was

added. The reaction was allowed to warm up to room temperature and stirred overnight. Upon

completion, the reaction was quenched with sat. $NaHCO_3$, diluted with DCM and washed

sequentially with water and sat. $NaHCO_3$. The organic phase was dried over Na_2SO_4,

concentrated, and purified through silica gel (Hexanes/EtOAc = 2/1). The product was then

diluted in DCM (25 mL). To this solution was added EDC·HCl (522 mg, 2.77 mmol), DMAP (10

mg, 0.08 mmol) and levulinic acid (257 μL, 2.52 mmol), and the reaction was stirred at room

temperature overnight. The mixture was then diluted with DCM, washed with sat. NaHCO$_3$,

dried over Na$_2$SO$_4$, concentrated, and purified by silica gel column to afford compound **3** in 89%

yield over 2 steps.

^{1}HNMR (500 MHz, CDCl$_3$): δ = 2.02 (s, 3H), 2.16 (s, 3H), 2.35 (s, 3H), 2.56-2.62 (m, 2H),

2.69-2.75 (m, 2H), 3.29 (dd, 1H, J = 3.5, 10.0 Hz), 3.38 (t, 1H, J = 9.5 Hz), 3.56 (t, 1H, J = 9.5

Hz), 3.64 (s, 1H), 3.91 (d, 1H, J = 10.5 Hz), 3.93-3.97 (m, 1H), 4.17 (s, 1H), 4.20-4.26 (m, 2H),

4.26-4.31 (m, 1H), 4.33 (dd, 1H, J = 4.0, 11.5 Hz), 4.42 (dd, 1H, J = 8.0, 12.0 Hz), 4.50 (d, 1H, J

= 10.5 Hz), 4.56 (d, 1H, J = 4.0 Hz), 4.73 (d, 1H, J = 10.5 Hz), 4.78 (d, 1H, J = 11.5 Hz),

4.94-4.98 (m, 1H), 5.00 (d, 1H, J = 12.0 Hz), 5.39 (s, 1H), 5.58 (s, 1H), 7.10-7.18 (m, 4H),

7.21-7.44 (m, 14H), 7.46-7.53 (m, 4H), 8.13-8.18 (m, 2H). ^{13}CNMR (125 MHz, CDCl$_3$): δ =

20.85, 21.22, 27.86, 29.91, 37.93, 62.79, 63.88, 63.94, 66.06, 69.55, 70.41, 71.34, 72.64, 75.04,

75.13, 76.08, 77.64, 80.82, 86.5, 99.26, 127.95, 128.06, 128.14, 128.16, 128.38, 128.46, 128.54,

128.58, 128.71, 129.8, 129.89, 130.05, 131.97, 132.23, 133.29, 137.29, 137.45, 137.47, 137.8,

165.73, 170.74, 172.4, 206.45. HRMS: m/z calc. for C$_{54}$H$_{61}$N$_4$O$_{13}$S: 1005.3956; found:

1005.3941 [M + NH$_4$]$^+$.
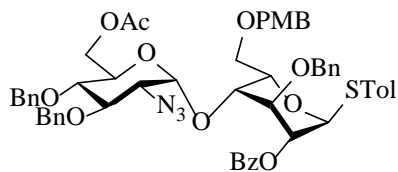
p-Tolyl 6-*O*-acetyl-2-azido-3, 4-di-*O*-benzyl-2-deoxy-*α*-D-glucopyranosyl-(1→4)-2-*O*-benzoyl-3-*O*-benzyl-6-*O*-*p*-methoxybenzyl-1-thio-*α*-L-idopyranoside (**7**)

Compound **7** was prepared from compound **5** (533 mg, 1.0 mmol) and **6** (600 mg, 1.0 mmol) by following the general procedure for preactivation based glycosylation. The reaction was performed at -78 °C until quenched by Et₃N at the same temperature to avoid decomposition under acidic conditions. Purification through silica gel column (Hexanes/EtOAc = 3/1) provided compound **7** in 87% yield.

^{1}HNMR (500 MHz, CDCl₃): δ = 2.02(s, 3H), 2.34 (s, 3H), 3.31 (dd, 1H, J = 3.5, 10.0 Hz), 3.43 (dd, 1H, J = 8.5, 10.0 Hz), 3.64 (dd, 1H, J = 9.0, 10.5 Hz), 3.74 (t, 1H, J = 3.0 Hz), 3.79 (d, 2H, J = 6.0 Hz), 3.82 (s, 3H), 3.98 (dt, 1H, J = 3.5, 10.0 Hz), 4.14 (d, 1H, J = 10.5 Hz), 4.17-4.21 (m, 3H), 4.32 (d, 1H, J = 10.5 Hz), 4.50-4.55 (m, 3H), 4.72 (d, 1H, J = 3.5 Hz), 4.76 (d, 1H, J = 3.5 Hz), 4.78 (d, 1H, J = 5.0 Hz), 4.94 (dd. 1H, J = 2.5, 6.5 Hz), 4.97 (d, 1H, J = 12.0 Hz), 5.42 (s, 1H), 5.57 (s, 1H), 6.88 (d, 2H, J = 9.0 Hz), 7.07 (d, 2H, J = 7.5 Hz), 7.17-7.21 (m, 2H), 7.25-7.43 (m, 16H), 7.48 (d, 4H, J = 8.0 Hz), 8.13-8.16 (m, 2H). ^{13}CNMR (125 MHz, CDCl₃): δ = 20.9, 21.24, 55.35, 62.82, 64.06, 67.18, 69.13, 70.06, 70.12, 72.08, 72.67, 73.08, 75.12, 75.17, 77.72, 80.8, 86.52, 98.64, 113.84, 127.99, 128.02, 128.08, 128.17, 128.21, 128.5, 128.52, 128.52, 128.62, 128.69, 129.44, 129.74, 129.95, 130.01, 130.26, 131.92, 132.52, 133.27, 137.52, 137.56, 137.59, 137.66, 159.28, 165.76, 170.65. HRMS: m/z calc. for C₅₇H₆₃N₄O₁₂S:1027.4163; found:

1027.4120 [M + NH$_4$]$^{+}$.
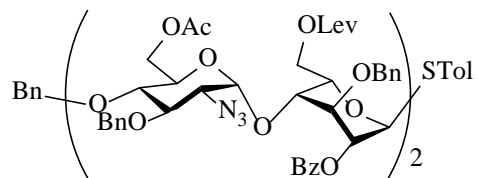
p-Tolyl 6-*O*-acetyl-2-azido-3, 4-di-*O*-benzyl-2-deoxy-*α*-D-glucopyranosyl-(1→4)-2-*O*-benzoyl

-3-*O*-benzyl-6-*O*-levulinoyl-*α*-L-idopyranosyl-(1→4)-6-*O*-acetyl-2-azido-3-*O*-benzyl-2-deoxy-*α*

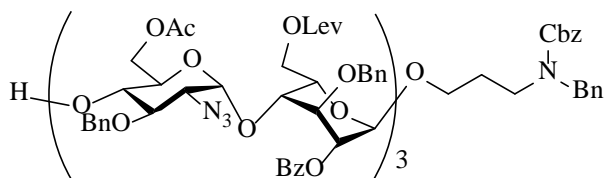-D-glucopyranosyl-(1→4)-2-*O*-benzoyl-3-*O*-benzyl-6-*O*-levulinoyl-1-thio-*α*-L-idopyranoside (**8**)

Compound **8** was prepared from compound **3** (412 mg, 0.42 mmol) and **1** (374 mg, 0.42 mmol)

by following the general procedure for preactivation based glycosylation. Purification through

silica gel column (Hexanes/EtOAc = 1/1) provided compound **8** in 85% yield.

^{1}HNMR (500 MHz, CDCl$_3$): δ = 1.99 (s, 3H), 2.04 (s, 3H), 2.10 (s, 3H), 2.15 (s, 3H), 2.35 (s,

3H), 2.43-2.51 (m, 2H), 2.51-2.58 (m, 2H), 2.58-2.63 (m, 2H), 2.65-2.75 (m, 2H), 3.27 (ddd, 2H,

J = 2.5, 4.0, 10.0 Hz), 3.45 (t, 1H, *J* = 9.5 Hz), 3.48 (t, 1H, *J* = 9.5 Hz), 3.62 (t, 1H, *J* = 2.5 Hz),

3.66-3.73 (m, 4H), 3.83-3.88 (m, 2H), 4.02-4.07 (m, 2H), 4.14-4.17 (m, 1H), 4.20-4.40 (m, 9H),

4.47-4.56 (m, 4H), 4.71 (d, 1H, *J* = 4.0 Hz), 4.74-4.80 (m, 3H), 4.83 (d, 1H, *J* = 11.5 Hz), 4.94

(ddd, 1H, *J* = 1.5, 4.0, 7.0 Hz), 4.98 (d, 1H, *J* = 12.0 Hz), 5.08 (d, 1H, *J* = 3.5 Hz), 5.12 (t, 1H, *J*

= 4.0 Hz), 5.38 (t, 1H, *J* = 2.0 Hz), 5.59 (s, 1H), 7.14 (d, 4H, *J* = 8.0 Hz), 7.20-7.53 (m, 31H),

8.10 (d, 2H, *J* = 7.0 Hz), 8.16 (d, 2H, *J* = 6.5 Hz). ^{13}CNMR (125 MHz, CDCl$_3$): δ = 20.7, 20.8,

21.18, 27.76, 27.79, 29.83, 29.84, 37.76, 37.89, 62.18, 62.34, 62.56, 63.6, 63.67, 63.9, 65.94,

67.61, 69.53, 70.11, 70.15, 70.23, 71.19, 72.6, 73.43, 74.14, 74.73, 74.88, 75.17, 75.22, 75.29,

75.76, 77.62, 79.17, 80.46, 86.42, 97.8, 98.81, 98.91, 127.61, 127.99, 128.03, 128.07, 128.11, 128.13, 128.16, 128.25, 128.28, 128.33, 128.44, 128.49, 128.5, 128.62, 128.68, 129.61, 129.76, 129.84, 129.86, 129.92, 131.92, 132.15, 133.35, 133.42, 137.24, 137.31, 137.34, 137.5, 137.72, 137.74, 165.44, 165.73, 170.62, 170.74, 172.25, 172.26, 206.36, 206.39. HRMS: m/z calc. for $C_{94}H_{104}N_7O_{26}S$:1778.6752; found:1778.6780 [M + NH$_4$]$^+$.
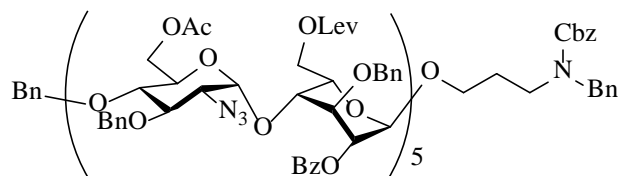

N-(Benzyl)-benzyloxycarbonyl-3-aminopropyl 6-*O*-acetyl-2-azido-3, 4-di-*O*-benzyl-2-deoxy-*α*-D-glucopyranosyl-(1→4)-2-*O*-benzoyl-3-*O*-benzyl-6-*O*-levulinoyl-*α*-L-idopyranosyl-(1→4)-6-*O*-acetyl-2-azido-3-*O*-benzyl-2-deoxy-*α*-D-glucopyranosyl-(1→4)-2-*O*-benzoyl-3-*O*-benzyl-6-*O*-levulinoyl-*α*-L-idopyranoside (**9**)

Compound **9** was prepared from compound **3** (153 mg, 0.16 mmol) and **2** (150 mg, 0.14 mmol) by following the general procedure for preactivation based glycosylation. Purification through silica gel column (Hexanes/EtOAc = 1/1) provided compound **9** in 88% yield.

^{1}HNMR (500 MHz, CDCl$_3$): δ = 1.80-1.91 (m, 2H), 1.98 (s, 3H), 2.04 (s, 3H), 2.10 (s, 3H), 2.14 (s, 3H), 2.41-2.51 (m, 4H), 2.60 (t, 2H, *J* = 7.0 Hz), 2.64-2.73 (m, 2H), 3.23-3.28 (m, 2H), 3.31-3.40 (m, 2H), 3.41-3.52 (m, 2H), 3.54-3.60 (m, 1H), 3.60-3.77 (m, 5H), 3.80-3.87 (m, 2H), 3.93 (d, 1H, *J* = 10.0 Hz), 4.00-4.07 (m, 3H), 4.15-4.22 (m, 1H), 4.22-4.30 (m, 4H), 4.30-4.40 (m, 5H), 4.43-4.54 (m, 4H), 4.59-4.66 (m, 2H), 4.68 (d, 1H, *J* = 3.5 Hz), 4.69-4.74 (m, 1H),

4.74-4.86 (m, 4H), 4.88-4.98 (m, 1H), 5.06-5.13 (m, 3H), 5.16 (d, 2H, J = 10.0 Hz), 7.10-7.20 (m, 3H), 7.20-7.50 (m, 38H), 8.07-8.11 (m, 2H), 8.12-8.15 (m, 2H). ^{13}CNMR (125 MHz, CDCl$_3$): δ = 20.85, 20.87, 27.82, 29.9, 37.83, 62.33, 62.62, 63.75, 63.9, 65.41, 67.24, 67.49, 68.75, 70.01, 70.19, 70.21, 72.31, 73.43, 73.96, 74.93, 74.95, 75.18, 75.26, 75.34, 77.68, 79.19, 80.54, 97.91, 98.39, 98.87, 127.36, 127.68, 127.94, 128.03, 128.08, 128.15, 128.22, 128.29, 128.33, 128.41, 128.48, 128.51, 128.55, 128.58, 128.6, 128.67, 128.72, 129.69, 129.87, 129.9, 133.4, 137.36, 137.38, 137.54, 137.79, 165.52, 165.76, 170.67, 170.77, 172.29, 172.35, 206.4. HRMS: m/z calc. for C$_{105}$H$_{117}$N$_8$O$_{29}$: 1953.7926; found: 1953.7886 [M + NH$_4$]$^+$.
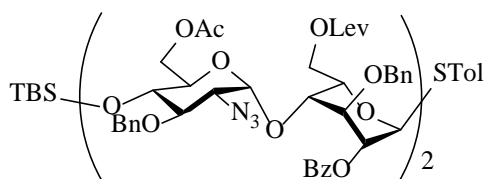
p-Tolyl

6-*O*-acetyl-2-azido-3-*O*-benzyl-4-*O*-tert-butyldimethylsilyl-2-deoxy-α-D-glucopyranosyl-(1→4) -2-*O*-benzoyl-3-*O*-benzyl-6-*O*-levulinoyl-α-L-idopyranosyl-(1→4)-6-*O*-acetyl-2-azido-3-*O*-benz yl-2-deoxy-α-D-glucopyranosyl-(1→4)-2-*O*-benzoyl-3-*O*-benzyl-6-*O*-levulinoyl-1-thio-α-L-idop yranoside (**10**)

Compound **10** was prepared from compound **4** (93 mg, 0.092 mmol) and **1** (83 mg, 0.092 mmol) by following the general procedure for preactivation based glycosylation. Purification through silica gel column (Hexanes/EtOAc = 2/1) provided compound **10** in 72% yield.

^{1}HNMR (500 MHz, CDCl$_3$): δ = -0.07 (s, 3H), 0.00 (s, 3H), 0.88 (s, 9H), 1.99 (s, 3H), 2.01 (s,

3H), 2.11 (s, 3H), 2.13 (s, 3H), 2.33 (s, 3H), 2.45-2.55 (m, 4H), 2.60-2.75 (m, 4H), 3.24 (ddd, 2H,

$J = 3.5, 9.0, 10.0$ Hz), 3.42-3.50 (m, 2H), 3.56 (dd, 1H, $J = 8.5, 9.5$ Hz), 3.60 (t, 1H, $J = 2.5$ Hz),

3.65 (dd, 1H, $J = 8.5, 10.0$ Hz), 3.69 – 3.76 (m, 3H), 3.82 (ddd, 1H, $J = 2.0, 4.5, 10.0$ Hz),

4.00-4.08 (m, 3H), 4.09-4.14 (m, 2H), 4.20 (dd, 1H, $J = 2.0, 12.0$ Hz), 4.24 (dd, 1H, $J = 5.0, 11.5$

Hz), 4.27-4.34 (m, 4H), 4.35-4.42 (m, 2H), 4.49 (t, 2H, $J = 10.5$ Hz), 4.54 (d, 1H, $J = 4.0$ Hz),

4.72 – 4.78 (m, 3H), 4.80 (d, 1H, $J = 3.5$ Hz), 4.90 (ddd, 1H, $J = 2.0, 4.5, 7.5$ Hz), 4.95 (d, 1H, J

$= 12.0$ Hz), 5.05 (d, 1H, $J = 4.0$ Hz), 5.12 (t, 1H, $J = 4.5$ Hz), 5.35-5.37 (m, 1H), 5.55 (s, 1H),

7.10-7.14 (m, 4H), 7.20-7.26 (m, 6H), 7.25-7.33 (m, 8H), 7.35-7.51 (m, 12H), 8.05-8.09 (m, 2H),

8.11-8.14 (m, 2H). Comparison with literature data confirmed its identity.[25]
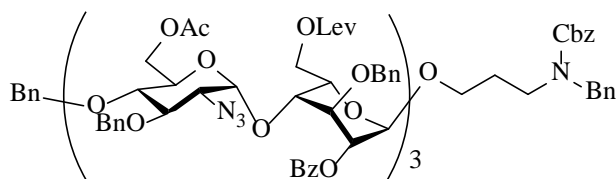
N-(Benzyl)-benzyloxycarbonyl-3-aminopropyl   6-*O*-acetyl-2-azido-3,

4-di-*O*-benzyl-2-deoxy-α-D-glucopyranosyl-(1→4)-2-*O*-benzoyl-3-*O*-benzyl-6-*O*-levulinoyl-α-L

-idopyranosyl-(1→4)-6-*O*-acetyl-2-azido-3-*O*-benzyl-2-deoxy-α-D-glucopyranosyl-(1→4)-2-*O*-

benzoyl-3-*O*-benzyl-6-*O*-levulinoyl-α-L-idopyranosyl-(1→4)-6-*O*-acetyl-2-azido-3-*O*-benzyl-2-

deoxy-α-D-glucopyranosyl-(1→4)   -2-*O*-benzoyl-3-*O*-benzyl-6-*O*-levulinoyl-α-L-idopyranoside

(**11**)

Compound **11** was prepared from compound **8** (110 mg, 0.062 mmol) and **2** (67 mg, 0.062 mmol)

by following the general procedure for preactivation based glycosylation. Purification through

silica gel column (Hexanes/DCM/EtOAc = 1/1/1) provided compound **11** in 58% yield.

^{1}HNMR (500 MHz, CDCl$_3$): δ = 1.78-1.92 (m, 2H), 1.98 (s, 3H), 2.02 (s, 6H), 2.10 (s, 6H), 2.14 (s, 3H), 2.39-2.74 (m, 12H), 3.21-3.28 (m, 3H), 3.29-3.40 (m, 3H), 3.43 (t, 2H, J = 9.5 Hz), 3.55 (t, 1H, J = 9.5 Hz), 3.58-3.72 (m, 6H), 3.73-3.78 (m, 2H), 3.91 (d, 1H, J = 10.5 Hz), 3.97-4.09 (m, 5H), 4.14-4.30 (m, 8H), 4.30-4.39 (m, 6H), 4.41-4.55 (m, 5H), 4.57-4.63 (m, 2H), 4.63-4.85 (m, 10H), 4.86-4.97 (m, 2H), 5.03-5.10 (m, 3H), 5.10-5.19 (m, 4H), 7.10-7.53 (m, 54H), 8.01-8.18 (m, 6H). ^{13}CNMR (125 MHz, CDCl$_3$): δ = 20.8, 20.85, 27.8, 27.82, 29.89, 37.8, 37.86, 43.93, 44.95, 50.83, 51.05, 62.04, 62.26, 62.32, 62.62, 62.96, 63.25, 63.43, 63.64, 63.74, 63.84, 65.4, 65.54, 65.74, 67.23, 67.44, 67.86, 68.73, 69.98, 70.15, 70.22, 70.43, 70.67, 71.31, 72.31, 72.37, 73.42, 73.58, 73.86, 74.36, 74.69, 74.9, 74.94, 75.11, 75.27, 75.35, 75.43, 77.67, 78.92, 79.07, 80.08, 80.56, 97.81, 97.97, 98.35, 98.47, 98.87, 127.36, 127.64, 127.73, 127.85, 127.9, 127.94, 127.96, 128.01, 128.04, 128.08, 128.11, 128.14, 128.19, 128.21, 128.26, 128.28, 128.3, 128.33, 128.41, 128.43, 128.46, 128.48, 128.53, 128.56, 128.58, 128.61, 128.68, 128.71, 128.75, 129.58, 129.68, 129.89, 129.92, 133.45, 133.5, 136.81, 136.91, 137.32, 137.35, 137.38, 137.53, 137.73, 137.78, 137.85, 137.98, 138.05, 156.22, 156.77, 165.52, 165.56, 165.75, 170.68, 170.72, 170.78, 171.95, 172.26, 172.31, 172.34, 206.42, 206.46. HRMS: m/z calc. for C$_{145}$H$_{164}$N$_{12}$O$_{42}$: 1372.5533; found: 1372.5518 [M + 2NH$_4$]$^{2+}$.

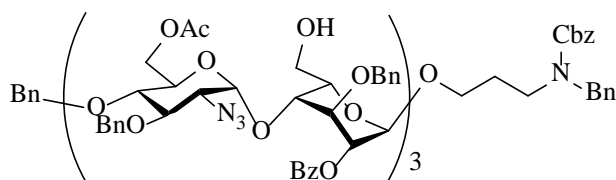*N*-(Benzyl)-benzyloxycarbonyl-3-aminopropyl

6-*O*-acetyl-2-azido-3-*O*-benzyl-2-deoxy-*α*-D-glucopyranosyl-(1→4)-2-*O*-benzoyl-3-*O*-benzyl-6-

O-levulinoyl-*α*-L-idopyranosyl-(1→4)-6-*O*-acetyl-2-azido-3-*O*-benzyl-2-deoxy-*α*-D-glucopyran

osyl-(1→4)-2-*O*-benzoyl-3-*O*-benzyl-6-*O*-levulinoyl-*α*-L-idopyranosyl-(1→4)-6-*O*-acetyl-2-azid

o-3-*O*-benzyl-2-deoxy-*α*-D-glucopyranosyl-(1→4)-2-*O*-benzoyl-3-*O*-benzyl-6-*O*-levulinoyl-*α*-L-

idopyranoside (**12**)

Compound **12** was prepared from compound **10** (200 mg, 0.11 mmol) and **2** (96 mg, 0.09 mmol)

by following the general procedure for preactivation based glycosylation and TBS removal.

Purification through silica gel column (Hexanes/DCM/EtOAc = 1/1/2) provided compound **12** in

84% yield over 2 steps.

^{1}HNMR (500 MHz, CDCl$_3$): δ = 1.80-1.90 (m, 2H), 2.01 (s, 3H), 2.02 (s, 3H), 2.04 (s, 3H), 2.10

(s, 3H), 2.12 (s, 3H), 2.13 (s, 3H), 2.36-2.56 (m, 6H), 2.57-2.73 (m, 6H), 3.21 (dd, 1H, *J* = 3.5,

10.0 Hz), 3.23-3.27 (m, 2H), 3.30-3.50 (m, 5H), 3.54 (t, 1H, *J* = 9.5 Hz), 3.57-3.65 (m, 3H),

3.65-3.71(m, 3H), 3.72-3.85 (m, 5H), 3.91 (d, 1H, *J* = 10.0 Hz), 3.98-4.07 (m, 5H), 4.10-4.24 (m,

5H), 4.25-4.39 (m, 8H), 4.41 (d, 1H, *J* = 11.0 Hz), 4.43-4.47 (m, 1H), 4.49 (d, 1H, *J* = 4.0 Hz),

4.51 (d, 1H, *J* = 4.0 Hz), 4.59 (d, 2H, *J* = 10.0 Hz), 4.61 (d, 1H, *J* = 7.5 Hz), 4.66-4.84 (m, 9H),

4.87-4.95 (m, 1H), 5.03-5.10 (m, 3H), 5.10-5.18 (m, 4H), 7.10-7.38 (m, 40H), 7.39-7.54 (m, 9H),

8.06-8.15 (m, 6H). ^{13}CNMR (125 MHz, CDCl$_3$): δ = 20.85, 20.86, 27.82, 28.41, 29.89, 29.92,

37.86, 37.9, 43.93, 44.95, 50.83, 51.05, 62.08, 62.21, 62.28, 62.4, 62.84, 63.1, 63.44, 63.72,

63.85, 65.41, 65.54, 65.75, 67.23, 67.63, 67.81, 68.73, 70.15, 70.21, 70.31, 70.38, 70.72, 71.26,

72.32, 72.45, 73.44, 73.56, 73.79, 74.16, 74.3, 74.7, 74.93, 75.07, 75.18, 75.3, 75.41, 78.84,

79.07, 79.81, 97.8, 97.86, 98.35, 98.44, 98.47, 98.52, 127.35, 127.63, 127.67, 127.84, 127.88, 127.93, 128.0, 128.1, 128.13, 128.16, 128.17, 128.24, 128.4, 128.46, 128.48, 128.6, 128.61, 128.68, 128.7, 128.73, 129.57, 129.88, 129.91, 133.42, 133.49, 133.54, 136.79, 136.89, 137.3, 137.37, 137.72, 137.78, 137.84, 137.89, 137.96, 137.98, 138.03, 156.2, 156.76, 165.51, 165.58, 165.75, 170.77, 170.8, 171.84, 172.25, 172.34, 172.43, 206.42, 206.48, 206.93. HRMS: m/z calc. for $C_{138}H_{154}N_{11}O_{42}$: 2637.0253; found: 2637.0212 $[M + NH_4]^+$.

N-(Benzyl)-benzyloxycarbonyl-3-aminopropyl 6-*O*-acetyl-2-azido-3, 4-di-*O*-benzyl-2-deoxy-α-D-glucopyranosyl-(1→4)-2-*O*-benzoyl-3-*O*-benzyl-6-*O*-levulinoyl-α-L -idopyranosyl-(1→4)-6-*O*-acetyl-2-azido-3-*O*-benzyl-2-deoxy-α-D-glucopyranosyl-(1→4)-2-*O*- benzoyl-3-*O*-benzyl-6-*O*-levulinoyl-α-L-idopyranosyl-(1→4)-6-*O*-acetyl-2-azido-3-*O*-benzyl-2- deoxy-α-D-glucopyranosyl-(1→4)-2-*O*-benzoyl-3-*O*-benzyl-6-*O*-levulinoyl-α-L-idopyranosyl-(1 →4)-6-*O*-acetyl-2-azido-3-*O*-benzyl-2-deoxy-α-D-glucopyranosyl-(1→4)-2-*O*-benzoyl-3-*O*-ben zyl-6-*O*-levulinoyl-α-L-idopyranosyl-(1→4)-6-*O*-acetyl-2-azido-3-*O*-benzyl-2-deoxy-α-D-gluco pyranosyl-(1→4) -2-*O*-benzoyl-3-*O*-benzyl-6-*O*-levulinoyl-α-L-idopyranoside (**13**)

Compound **13** was prepared from compound **8** (808 mg, 0.46 mmol) and **12** (841 mg, 0.32 mmol) by following the general procedure for preactivation based glycosylation. Purification through silica gel column (Hexanes/DCM/EtOAc = 1/1/1) provided compound **13** in 84% yield.

^{1}HNMR (500 MHz, CDCl$_3$): δ = 1.82-1.93 (m, 2H), 1.99 (s, 3H), 2.02 (s, 6H), 2.04 (s, 6H), 2.11 (s, 12H), 2.14 (s, 3H), 2.40-2.73 (m, 20H), 3.24-3.30 (m, 5H), 3.32-3.41 (m, 3H), 3.45 (t, 2H, J = 9.5 Hz), 3.56 (t, 1H, J = 9.5 Hz), 3.61-3.73 (m, 10H), 3.73-3.81 (m, 6H), 3.81-3.88 (m, 3H), 3.92 (d, 1H, J = 10.5 Hz), 3.99-4.09 (m, 9H), 4.14-4.26 (m, 10H), 4.26-4.39 (m, 14H), 4.43-4.49 (m, 2H), 4.49-4.55 (dd, 3H, J = 7.0, 10.5 Hz), 4.58-4.64 (m, 2H), 4.68 (d, 1H, J = 3.5 Hz), 4.71-4.85 (m, 15H), 4.88-4.97 (m, 2H), 5.05-5.12 (m, 5H), 5.12-5.20 (m, 6H), 7.11-7.55 (m, 80H), 8.07-8.17 (m, 10H). ^{13}CNMR (125 MHz, CDCl$_3$): δ = 20.7, 20.78, 27.74, 29.81, 37.72, 37.77, 37.79, 43.86, 44.88, 50.76, 50.98, 61.96, 62.18, 62.26, 62.31, 62.55, 63.36, 63.61, 63.68, 63.76, 65.31, 65.45, 65.67, 67.15, 67.39, 67.75, 68.64, 69.93, 70.09, 70.12, 70.15, 70.34, 72.23, 72.33, 73.35, 73.49, 73.52, 73.81, 74.18, 74.22, 74.34, 74.56, 74.61, 74.81, 74.85, 75.02, 75.06, 75.19, 75.28, 75.32, 75.38, 77.6, 78.72, 78.75, 78.87, 78.99, 80.48, 97.72, 97.8, 97.9, 98.29, 98.39, 98.79, 127.29, 127.57, 127.62, 127.67, 127.78, 127.82, 127.87, 127.94, 127.97, 128.0, 128.03, 128.07, 128.1, 128.12, 128.15, 128.24, 128.26, 128.34, 128.38, 128.41, 128.48, 128.51, 128.54, 128.61, 128.66, 128.68, 129.48, 129.49, 129.6, 129.82, 133.38, 133.43, 133.49, 136.75, 136.84, 137.25, 137.28, 137.32, 137.47, 137.67, 137.78, 137.83, 137.95, 156.14, 156.68, 165.43, 165.46, 165.48, 165.68, 170.59, 170.64, 170.7, 172.17, 172.2, 172.24, 172.27, 206.34, 206.38. HRMS: m/z calc. for C$_{225}$H$_{246}$N$_{17}$O$_{68}$: 4273.6314; found: 4273.6372 [M + NH$_4$]$^+$.
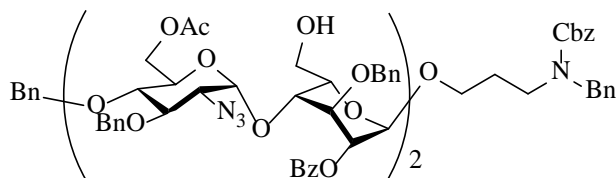
N-(Benzyl)-benzyloxycarbonyl-3-aminopropyl   6-*O*-acetyl-2-azido-3,
4-di-*O*-benzyl-2-deoxy-*α*-D-glucopyranosyl-(1→4)-2-*O*-benzoyl-3-*O*-benzyl-*α*-L-idopyranosyl-(1→4)-6-*O*-acetyl-2-azido-3-*O*-benzyl-2-deoxy-*α*-D-glucopyranosyl-(1→4)-2-*O*-benzoyl-3-*O*-benzyl-*α*-L-idopyranoside (**14**)

Compound **14** was prepared from compound **9** (1.0 g, 0.52 mmol) by following the general procedure for removal of levulinoyl esters. Purification through silica gel column (Hexanes/DCM/EtOAc = 1/1/1) provided compound **14** in 86% yield.

^{1}HNMR (500 MHz, CDCl$_3$): δ = 1.80-1.90 (m, 2H), 2.01 (s, 3H), 2.04 (s, 3H), 2.60 (br, 1H), 3.17-3.37 (m, 5H), 3.38-3.44 (m, 1H), 3.50-3.61 (m, 3H), 3.61-3.80 (m, 5H), 3.81-4.00 (m, 5H), 4.03-4.14 (m, 3H), 4.14-4.29 (m, 4H), 4.29-4.43 (m, 3H), 4.43-4.60 (m, 5H), 4.64-4.74 (m, 2H), 4.76 (d, 2H, *J* = 10.5 Hz), 4.81-4.97 (m, 3H), 4.98-5.05 (m, 1H), 5.05-5.21 (m, 4H), 7.10-7.50 (m, 41H), 8.08-8.17 (m, 4H). ^{13}CNMR (125 MHz, CDCl$_3$): δ = 20.89, 28.19, 28.35, 44.87, 50.61, 61.3, 62.72, 62.8, 63.79, 64.17, 66.33, 67.41, 68.9, 69.13, 70.01, 70.37, 72.14, 72.99, 74.03, 75.09, 75.24, 75.28, 77.74, 79.45, 80.7, 97.98, 98.22, 127.35, 127.42, 127.92, 127.95, 128.03, 128.07, 128.19, 128.22, 128.27, 128.39, 128.43, 128.5, 128.54, 128.57, 128.59, 128.65, 128.7, 129.73, 129.79, 129.92, 130.1, 133.26, 133.42, 137.4, 137.46, 137.52, 137.54, 137.87, 165.81, 170.58, 170.69. HRMS: m/z calc. for C$_{95}$H$_{102}$N$_7$O$_{25}$:1740.6925; found: 1740.6924 [M + H]$^+$.

N-(Benzyl)-benzyloxycarbonyl-3-aminopropyl 6-*O*-acetyl-2-azido-3, 4-di-*O*-benzyl-2-deoxy-α-D-glucopyranosyl-(1→4)-2-*O*-benzoyl-3-*O*-benzyl-α-L-idopyranosyl-(1→4)-6-*O*-acetyl-2-azido-3-*O*-benzyl-2-deoxy-α-D-glucopyranosyl-(1→4)-2-*O*-benzoyl-3-*O*-benzyl-α-L-idopyranosyl-(1→4)-6-*O*-acetyl-2-azido-3-*O*-benzyl-2-deoxy-α-D-glucopyranosyl-(1→4) -2-*O*-benzoyl-3-*O*-benzyl-α-L-idopyranoside (**15**)

Compound **15** was prepared from compound **11** (500 mg, 0.18 mmol) by following the general procedure for removal of levulinoyl esters. Purification through silica gel column (Hexanes/DCM/EtOAc = 1/1/1) provided compound **15** in 93% yield.

^{1}HNMR (500 MHz, CDCl$_3$): δ = 1.81-1.89 (m, 2H), 2.00 (s, 3H), 2.04 (s, 6H), 3.12-3.23 (m, 3H), 3.23-3.38 (m, 4H), 3.38-3.44 (m, 2H), 3.44-3.63 (m, 7H), 3.63-3.72 (m, 2H), 3.72-3.82 (m, 4H), 3.82-4.00 (m, 5H), 4.01-4.09 (m, 3H), 4.15-4.29 (m, 7H), 4.30-4.62 (m, 9H), 4.63-4.80 (m, 6H), 4.81-4.97 (m, 4H), 4.98-5.22 (m, 8H), 7.12-7.47 (m, 54H), 8.08-8.17 (m, 6H). ^{13}CNMR (125 MHz, CDCl$_3$): δ = 14.32, 20.88, 20.94, 21.18, 28.18, 50.59, 60.51, 61.24, 61.33, 62.41, 62.72, 62.79, 63.8, 64.02, 67.41, 67.67, 69.01, 70.0, 70.07, 70.42, 72.14, 72.91, 72.99, 73.14, 73.69, 74.03, 75.15, 75.18, 75.24, 75.27, 77.73, 79.35, 79.47, 80.73, 97.34, 97.89, 97.95, 98.22, 127.34, 127.43, 127.89, 127.93, 128.03, 128.07, 128.12, 128.23, 128.26, 128.29, 128.32, 128.4, 128.47, 128.54, 128.6, 128.66, 128.68, 129.66, 129.76, 129.88, 129.9, 130.1, 133.27, 133.41, 137.4, 137.48, 137.52, 137.86, 165.85, 165.91, 170.6, 170.7, 171.27. HRMS: m/z calc. for C$_{130}$H$_{139}$N$_{10}$O$_{36}$: 2415.9353; found: 2415.9319 [M + H]$^+$.
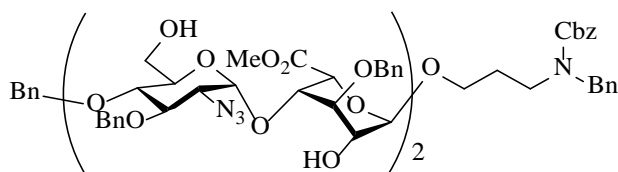
N-(Benzyl)-benzyloxycarbonyl-3-aminopropyl 6-*O*-acetyl-2-azido-3, 4-di-*O*-benzyl-2-deoxy-α-D-glucopyranosyl-(1→4)-2-*O*-benzoyl-3-*O*-benzyl-α-L-idopyranosyl-(1→4)-6-*O*-acetyl-2-azido-3-*O*-benzyl-2-deoxy-α-D-glucopyranosyl-(1→4)-2-*O*-benzoyl-3-*O*-benzyl-α-L-idopyranosyl-(1→4)-6-*O*-acetyl-2-azido-3-*O*-benzyl-2-deoxy-α-D-glucopyranosyl-(1→4)-2-*O*-benzoyl-3-*O*-benzyl-α-L-idopyranosyl-(1→4)-6-*O*-acetyl-2-azido-3-*O*-benzyl-2-deoxy-α-D-glucopyranosyl-(1→4)-2-*O*-benzoyl-3-*O*-benzyl-α-L-idopyranosyl-(1→4)-6-*O*-acetyl-2-azido-3-*O*-benzyl-2-deoxy-α-D-glucopyranosyl-(1→4)-2-*O*-benzoyl-3-*O*-benzyl-α-L-idopyranoside

(**16**)

Compound **16** was prepared from compound **13** (120 mg, 0.028 mmol) by following the general procedure for removal of levulinoyl esters. Purification through silica gel column (Hexanes/DCM/EtOAc = 1/1/1) provided compound **16** in 83% yield

^{1}HNMR (500 MHz, CDCl$_3$): δ = 1.80-1.89 (m, 2H), 1.99 (s, 3H), 2.01 (s, 3H), 2.02 (s, 6H), 2.03 (s, 3H), 3.07-3.24 (m, 5H), 3.28 (dd, 1H, J = 3.5, 10.0 Hz), 3.28-3.37 (m, 5H), 3.37-3.49 (m, 6H), 3.50-3.62 (m, 8H), 3.62-3.70 (m, 3H), 3.70-3.99 (m, 13H), 3.99-4.08 (m, 5H), 4.08-4.37 (m, 18H), 4.37-4.60 (m, 9H), 4.62-4.80 (m, 10H), 4.80-4.96 (m, 6H), 4.97-5.06 (m, 4H), 5.06-5.21 (m, 7H), 7.10-7.48 (m, 80H), 8.06-8.17 (m, 10H). ^{13}CNMR (125 MHz, CDCl$_3$): δ = 20.9, 20.96, 29.83, 61.31, 62.43, 62.74, 62.81, 63.82, 64.07, 67.45, 67.53, 67.7, 69.09, 70.01, 70.13, 70.45, 72.17, 72.8, 72.94, 73.03, 73.12, 73.17, 73.59, 73.7, 74.04, 75.2, 75.26, 75.3, 77.75, 79.4, 80.74,

97.34, 97.89, 97.98, 98.23, 127.44, 127.91, 127.94, 128.05, 128.09, 128.22, 128.24, 128.29, 128.31, 128.36, 128.42, 128.49, 128.53, 128.56, 128.59, 128.62, 128.68, 128.71, 128.74, 129.7, 129.77, 129.81, 129.88, 129.92, 133.47, 137.41, 137.43, 137.49, 137.53, 137.88, 165.87, 165.94, 165.97, 170.61, 170.72. HRMS: m/z calc. for $C_{200}H_{213}N_{16}O_{58}$: 3766.4209; found: 3766.4148 [M + H]$^+$.
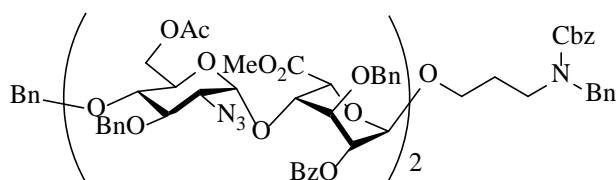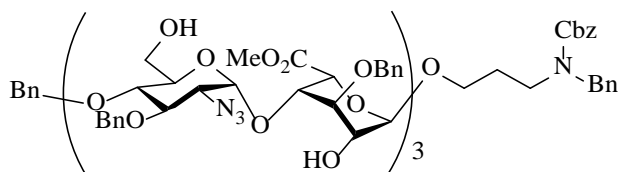

N-(Benzyl)-benzyloxycarbonyl-3-aminopropyl 6-O-acetyl-2-azido-3, 4-di-O-benzyl-2-deoxy-α-D-glucopyranosyl-(1→4)-methyl 2-O-benzoyl-3-O-benzyl-α-L-idopyranosyluronate-(1→4)-6-O-acetyl-2-azido-3-O-benzyl-2-deoxy-α-D-glucopyranosyl-(1→4)-methyl 2-O-benzoyl-3-O-benzyl-α-L-idopyranosyluronate (**17**)

Compound **17** was prepared from compound **14** (696 mg, 0.40 mmol) by following the general procedure for oxidation of 6-OH and formation of methyl esters after oxidation. Purification through silica gel column (Hexanes/DCM/EtOAc = 3/2/2) provided compound **14** in 83% yield over 2 steps.

^{1}HNMR (500 MHz, CDCl$_3$): δ = 1.77-1.88 (m, 2H), 1.99 (s, 3H), 2.11 (s, 3H), 3.18-3.26 (m, 2H), 3.27-3.46 (m, 3H), 3.47-3.57 (m, 3H), 3.60 (s, 3H), 3.65 (s, 3H), 3.73-3.84 (m, 3H), 3.87 (d, 1H, J = 10.0 Hz), 3.93-4.00 (m, 2H), 4.03-4.17 (m, 3H), 4.22-4.35 (m, 4H), 4.35-4.54 (m, 5H), 4.57 (d, 1H, J = 11.0 Hz), 4.65 (t, 2H, J = 3.5 Hz), 4.68-4.90 (m, 6H), 4.94 (d, 1H, J = 3.0 Hz),

5.02-5.20 (m, 5H), 5.48 (d, 1H, J = 4.0 Hz), 7.07-7.41 (m, 36H), 7.43-7.57 (m, 5H), 8.08-8.17

(m, 4H). ^{13}CNMR (125 MHz, CDCl$_3$): δ = 20.91, 20.95, 52.13, 52.27, 61.82, 62.29, 63.51, 63.61,

67.28, 67.45, 68.0, 69.71, 70.11, 70.25, 70.51, 72.28, 72.5, 74.09, 74.63, 74.86, 75.08, 75.11,

75.54, 75.71, 78.74, 80.03, 98.49, 99.1, 99.26, 127.69, 127.98, 128.03, 128.08, 128.1, 128.17,

128.19, 128.24, 128.43, 128.53, 128.57, 128.6, 128.62, 128.82, 128.85, 129.36, 129.98, 130.09,

133.53, 137.31, 137.57, 137.7, 137.78, 165.27, 169.51, 170.6, 170.79. HRMS: m/z calc. for

C$_{97}$H$_{105}$N$_8$O$_{27}$: 1813.7089; found: 1813.7002 [M + NH$_4$]$^+$.
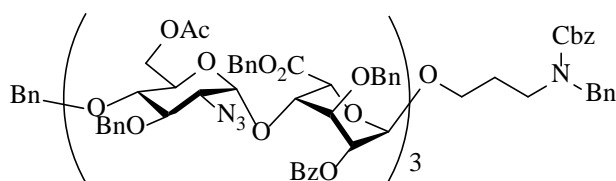
N-(Benzyl)-benzyloxycarbonyl-3-aminopropyl 6-*O*-acetyl-2-azido-3,

4-di-*O*-benzyl-2-deoxy-*α*-D-glucopyranosyl-(1→4)-benzyl

2-*O*-benzoyl-3-*O*-benzyl-*α*-L-idopyranosyluronate-(1→4)-6-*O*-acetyl-2-azido-3-*O*-benzyl-2-deo

xy-*α*-D-glucopyranosyl-(1→4)-benzyl

2-*O*-benzoyl-3-*O*-benzyl-*α*-L-idopyranosyluronate-(1→4)-6-*O*-acetyl-2-azido-3-*O*-benzyl-2-deo

xy-*α*-D-glucopyranosyl-(1→4)-benzyl 2-*O*-benzoyl-3-*O*-benzyl-*α*-L-idopyranosyluronate (**18**)

Compound **18** was prepared from compound **15** (290 mg, 0.18 mmol) by following the general

procedure for oxidation of 6-OH and formation of benzyl esters after oxidation. Purification

through silica gel column (Hexanes/DCM/EtOAc = 3/2/1) provided compound **18** in 77% yield

over 2 steps.

^{1}HNMR (500 MHz, CDCl$_3$): δ = 1.75-1.83 (m, 2H), 1.98 (s, 3H), 2.04 (s, 3H), 2.09 (s, 3H), 3.13 (dd, 1H, J = 3.5, 10.0 Hz), 3.19-3.24 (m, 2H), 3.25-3.35 (m, 2H), 3.40 (t, 2H, J = 9.5 Hz), 3.47-3.54 (m, 3H), 3.61 (dd, 1H, J = 9.0, 10.0 Hz), 3.65-3.79 (m, 4H), 3.85-3.98 (m, 6H), 4.03-4.18 (m, 6H), 4.20-4.27 (m, 2H), 4.28-4.37 (m, 6H), 4.40-4.46 (m, 2H), 4.48 (d, 1H, J = 5.0 Hz), 4.54 (d, 1H, J = 11.0 Hz), 4.62 (d, 1H, J = 3.5 Hz), 4.64 (d, 1H, J = 10.5 Hz), 4.68 (d, 1H, J = 4.5 Hz), 4.72-4.81 (m, 6H), 4.86 (d, 1H, J = 4.0 Hz), 4.93 (d, 1H, J = 3.5 Hz), 4.99 (s, 2H), 5.02-5.10 (m, 4H), 5.10-5.16 (m, 4H), 5.17-5.22 (m, 2H), 5.49 (d, 1H, J = 4.5 Hz), 5.54 (d, 1H, J = 5.0 Hz), 7.08-7.18 (m, 7H), 7.19-7.41 (m, 54H), 7.44-7.52 (m, 6H), 7.52-7.59 (m, 2H), 8.08-8.17 (m, 6H). ^{13}CNMR (125 MHz, CDCl$_3$): δ = 20.8, 20.91, 50.77, 51.06, 61.7, 61.84, 62.31, 63.24, 63.48, 63.6, 64.12, 67.12, 67.29, 67.64, 67.77, 69.31, 69.75, 70.02, 70.14, 70.86, 71.2, 71.51, 72.42, 73.17, 74.3, 74.39, 74.64, 74.8, 75.03, 75.23, 75.7, 75.96, 76.07, 76.91, 77.16, 77.36, 77.41, 77.53, 78.35, 78.41, 80.04, 98.36, 98.55, 99.14, 99.21, 100.18, 127.32, 127.52, 127.74, 127.91, 128.04, 128.07, 128.09, 128.12, 128.24, 128.27, 128.33, 128.36, 128.41, 128.49, 128.51, 128.56, 128.58, 128.61, 128.63, 128.68, 128.73, 128.77, 128.94, 128.97, 129.24, 129.31, 129.78, 130.01, 130.07, 130.12, 133.11, 133.68, 133.74, 134.89, 135.18, 137.23, 137.32, 137.65, 137.67, 137.84, 137.96, 165.25, 165.32, 169.0, 169.11, 170.58, 170.71, 170.75. HRMS: m/z calc. for C$_{151}$H$_{155}$N$_{11}$O$_{39}$: 1373.0242; found: 1373.0178 [M + H + NH$_4$]$^{2+}$.

N-(Benzyl)-benzyloxycarbonyl-3-aminopropyl 6-*O*-acetyl-2-azido-3, 4-di-*O*-benzyl-2-deoxy-*α*-D-glucopyranosyl-(1→4)-benzyl 2-*O*-benzoyl-3-*O*-benzyl-*α*-L-idopyranosyluronate-(1→4)-6-*O*-acetyl-2-azido-3-*O*-benzyl-2-deoxy-*α*-D-glucopyranosyl-(1→4)-benzyl 2-*O*-benzoyl-3-*O*-benzyl-*α*-L-idopyranosyluronate-(1→4)-6-*O*-acetyl-2-azido-3-*O*-benzyl-2-deoxy-*α*-D-glucopyranosyl-(1→4)-benzyl 2-*O*-benzoyl-3-*O*-benzyl-*α*-L-idopyranosyluronate-(1→4)-6-*O*-acetyl-2-azido-3-*O*-benzyl-2-deoxy-*α*-D-glucopyranosyl-(1→4)-benzyl 2-*O*-benzoyl-3-*O*-benzyl-*α*-L-idopyranosyluronate-(1→4)-6-*O*-acetyl-2-azido-3-*O*-benzyl-2-deoxy-*α*-D-glucopyranosyl-(1→4)-benzyl 2-*O*-benzoyl-3-*O*-benzyl-*α*-L-idopyranosyluronate (**19**)

Compound **19** was prepared from compound **16** (80 mg, 0.021 mmol) by following the general procedure for oxidation of 6-OH and formation of benzyl esters after oxidation. Purification through silica gel column (Hexanes/DCM/EtOAc = 3/2/1) provided compound **19** in 81% yield over 2 steps.

^{1}HNMR (500 MHz, CDCl$_3$): δ = 1.75-1.85 (m, 2H), 1.98 (s, 3H), 2.01 (s, 6H), 2.03 (s, 3H), 2.09 (s, 3H), 3.10-3.24 (m, 6H), 3.37-3.54 (m, 8H), 3.60 (d, 1H, *J* = 10.0 Hz), 3.65-3.72 (m, 2H), 3.72-3.90 (m, 9H), 3.91-3.99 (m, 5H), 4.05-4.47 (m, 24H), 4.47-4.63 (m, 7H), 4.63-4.80 (m, 13H), 4.80-4.88 (m, 4H), 4.92-5.01 (m, 7H), 5.01-5.10 (m, 4H), 5.10-5.22 (m, 8H), 5.45-5.49 (m, 3H), 5.54 (d, 1H, *J* = 10.0 Hz), 7.05-7.42 (m, 90H), 7.42-7.59 (m, 15H), 8.07-8.17 (m, 10H).

^{13}CNMR (125 MHz, CDCl$_3$): δ = 20.8, 20.89, 26.6, 50.79, 51.05, 53.56, 61.67, 61.75, 61.86, 62.31, 63.11, 63.24, 63.48, 63.58, 65.46, 66.42, 67.12, 67.16, 67.29, 67.64, 67.78, 69.8, 70.03,

70.15, 70.88, 71.24, 71.6, 72.42, 73.17, 74.28, 74.33, 74.43, 74.62, 74.83, 75.06, 75.23, 75.72, 75.99, 76.09, 76.25, 76.91, 77.16, 77.36, 77.42, 77.53, 78.07, 78.14, 78.3, 78.44, 80.04, 84.05, 98.31, 98.36, 98.55, 99.12, 99.2, 100.16, 127.08, 127.65, 127.7, 127.74, 127.77, 127.8, 127.91, 127.94, 128.02, 128.04, 128.07, 128.11, 128.18, 128.2, 128.22, 128.24, 128.25, 128.33, 128.36, 128.41, 128.45, 128.47, 128.49, 128.51, 128.56, 128.58, 128.61, 128.68, 128.73, 128.77, 128.88, 128.95, 129.18, 129.24, 130.02, 130.07, 130.13, 133.7, 133.84, 134.88, 135.13, 135.18, 137.23, 137.28, 137.3, 137.33, 137.65, 137.67, 137.83, 137.88, 137.95, 165.23, 165.26, 165.29, 165.53, 169.0, 169.09, 169.11, 169.13, 170.58, 170.69, 170.71, 170.74. HRMS: m/z calc. for $C_{235}H_{234}N_{16}O_{63}$: 2143.7799; found: 2143.7791 $[M + 2H]^{2+}$.

N-(Benzyl)-benzyloxycarbonyl-3-aminopropyl

2-azido-3,4-di-*O*-benzyl-2-deoxy-*α*-D-glucopyranosyl-(1→4)-methyl

3-*O*-benzyl-*α*-L-idopyranosyluronate-(1→4)-2-azido-3-*O*-benzyl-2-deoxy-*α*-D-glucopyranosyl-(1→4)-methyl 3-*O*-benzyl-*α*-L-idopyranosyluronate (**20**)

Compound **20** was prepared from compound **17** (400 mg, 0.22 mmol) by following the general procedure for transesterification. Purification through silica gel column (DCM/MeOH = 20/1) provided compound **20** in 79% yield.

^{1}HNMR (500 MHz, CDCl₃): *δ* = 1.67 (br, 1H), 1.78-1.91 (m, 2H), 2.22(br, 1H), 3.35-3.44 (m,

2H), 3.46(s, 3H), 3.47-3.65 (m, 7H), 3.65-3.72 (m, 3H), 3.76 (s, 3H), 3.77-3.84 (m, 4H), 3.84-3.90 (m, 3H), 3.94 (t, 1H, J = 9.5 Hz), 4.04 (t, 1H, J = 3.5 Hz), 4.13-4.18 (m, 1H), 4.43-4.54 (m, 3H), 4.58 (d, 1H, J = 11.5 Hz), 4.63 (d, 1H, J = 6.5 Hz), 4.65 (d, 1H, J = 6.5 Hz), 4.70 (d, 1H, J = 4.5 Hz), 4.75 (d, 2H, J = 11.0 Hz), 4.80-4.86 (m, 4H), 4.95-5.05 (m, 3H), 5.17 (s, 2H), 5.28-5.30 (m, 1H), 7.11-7.15 (m, 1H), 7.17-7.45 (m, 34H). ^{13}CNMR (125 MHz, CDCl$_3$): δ = 27.9, 28.36, 43.81, 44.53, 50.53, 50.86, 52.29, 52.52, 61.21, 61.26, 63.67, 64.16, 65.34, 65.36, 66.26, 66.62, 66.94, 67.34, 67.63, 68.05, 71.87, 71.95, 72.02, 72.22, 72.37, 72.64, 72.84, 73.06, 74.18, 74.81, 75.17, 75.86, 77.3, 79.35, 80.78, 95.55, 100.97, 101.84, 127.04, 127.23, 127.32, 127.39, 127.75, 127.94, 128.03, 128.06, 128.21, 128.24, 128.34, 128.46, 128.56, 128.57, 128.59, 128.64, 128.8, 136.71, 136.82, 137.14, 137.53, 137.69, 137.86, 141.04, 156.31, 156.78, 169.56, 170.24. HRMS: m/z calc. for C$_{79}$FeH$_{89}$N$_7$O$_{23}$: 779.7679; found: 779.7664 [M + Fe]$^{2+}$.

N-(Benzyl)-benzyloxycarbonyl-3-aminopropyl

2-azido-3,4-di-*O*-benzyl-2-deoxy-α-D-glucopyranosyl-(1→4)-methyl

3-*O*-benzyl-α-L-idopyranosyluronate-(1→4)-2-azido-3-*O*-benzyl-2-deoxy-α-D-glucopyranosyl-(1→4)-methyl

3-*O*-benzyl-α-L-idopyranosyluronate-(1→4)-2-azido-3-*O*-benzyl-2-deoxy-α-D-glucopyranosyl-(1→4)-methyl 3-*O*-benzyl-α-L-idopyranosyluronate (**21**)

Compound **21** was prepared from compound **18** (89 mg, 0.033 mmol) by following the general procedure for transesterification. Purification through silica gel column (DCM/MeOH = 20/1) provided compound **21** in 97% yield.

^{1}HNMR (500 MHz, CDCl$_3$): δ = 1.71-1.90 (m, 2H), 2.00-2.35 (br, 5H), 3.27-3.38 (m, 2H), 3.40 (s, 3H), 3.44 (s, 3H), 3.46-3.58 (m, 6H), 3.58-3.64 (m, 3H), 3.64-3.74 (m, 5H), 3.75 (s, 3H), 3.77-3.83 (m, 4H), 3.83-3.97 (m, 6H), 4.00-4.05 (m, 2H), 4.12-4.17 (m, 1H), 4.44-4.59 (m, 5H), 4.60-4.66 (m, 3H), 4.67-4.77 (m, 7H), 4.77-4.90 (m, 5H), 4.93-5.04 (m, 4H), 5.16 (s, 2H), 5.26 (s, 1H), 5.29 (s, 1H), 7.10-7.15 (m, 1H), 7.15-7.46 (m, 44H). ^{13}CNMR (125 MHz, CDCl$_3$): δ = 27.9, 28.36, 43.81, 44.54, 50.54, 50.86, 52.18, 52.29, 52.52, 61.21, 63.64, 64.05, 64.2, 65.35, 65.38, 66.26, 67.35, 67.64, 67.82, 68.08, 71.98, 72.15, 72.22, 72.39, 72.61, 72.67, 72.79, 72.87, 73.11, 73.94, 74.09, 74.82, 75.07, 75.85, 77.31, 79.16, 79.35, 80.75, 95.59, 100.89, 100.95, 101.84, 127.06, 127.28, 127.39, 127.7, 127.74, 127.76, 127.77, 127.94, 128.03, 128.07, 128.2, 128.21, 128.24, 128.32, 128.37, 128.39, 128.47, 128.5, 128.55, 128.57, 128.6, 128.63, 128.8, 128.82, 137.08, 137.12, 137.52, 137.7, 137.84, 140.99, 156.32, 169.55, 169.57. HRMS: m/z calc. for C$_{106}$H$_{120}$N$_{10}$Na$_2$O$_{33}$: 1053.3907; found: 1053.3929 [M + 2Na]$^{2+}$.

N-(Benzyl)-benzyloxycarbonyl-3-aminopropyl

2-azido-3,4-di-*O*-benzyl-2-deoxy-α-D-glucopyranosyl-(1→4)-methyl

3-*O*-benzyl-*α*-L-idopyranosyluronate-(1→4)-2-azido-3-*O*-benzyl-2-deoxy-*α*-D-glucopyranosyl-(

1→4)-methyl

3-*O*-benzyl-*α*-L-idopyranosyluronate-(1→4)-2-azido-3-*O*-benzyl-2-deoxy-*α*-D-glucopyranosyl-(

1→4)-methyl

3-*O*-benzyl-*α*-L-idopyranosyluronate-(1→4)-2-azido-3-*O*-benzyl-2-deoxy-*α*-D-glucopyranosyl-(

1→4)-methyl

3-*O*-benzyl-*α*-L-idopyranosyluronate-(1→4)-2-azido-3-*O*-benzyl-2-deoxy-*α*-D-glucopyranosyl-(

1→4)-methyl 3-*O*-benzyl-*α*-L-idopyranosyluronate (**22**)

Compound **22** was prepared from compound **19** (25 mg, 0.0058 mmol) by following the general

procedure for transesterification. Purification through silica gel column (DCM/MeOH = 8/1)

provided compound **22** in 90% yield.

^{1}HNMR (500 MHz, CDCl$_3$): δ = 1.75-1.88 (m, 2H), 2.25 (br, 10H), 3.28-3.35 (m, 2H), 3.38 (s,

3H), 3.39 (s, 3H), 3.43 (s, 3H), 3.45-3.53 (m, 7H), 3.53-3.63 (m, 6H), 3.63-3.68 (m, 4H),

3.69-3.81 (m, 10H), 3.74 (s, 3H), 3.81-3.97 (m, 9H), 3.98-4.04 (m, 3H), 4.14 (s, 1H), 4.42-4.57

(m, 7H), 4.57-4.65 (m, 5H), 4.65-4.75 (m, 14H), 4.75-4.85 (m, 6H), 4.90-5.02 (m, 5H), 5.15 (s,

2H), 5.23 (s, 2H), 5.27 (s, 1H), 7.09-7.13 (m, 1H), 7.14-7.45 (m, 64H). ^{13}CNMR (125 MHz,

CDCl$_3$): δ = 17.1, 26.59, 39.83, 52.21, 52.32, 63.68, 64.06, 64.14, 64.24, 65.44, 66.29, 67.38,

67.69, 67.87, 68.13, 72.0, 72.21, 72.25, 72.66, 72.84, 72.91, 73.15, 73.95, 74.16, 74.85, 75.11,

75.88, 79.17, 79.37, 80.78, 83.98, 95.61, 95.68, 100.9, 100.97, 101.86, 127.1, 127.28, 127.31,

127.43, 127.76, 127.8, 127.98, 128.07, 128.1, 128.23, 128.26, 128.41, 128.44, 128.49, 128.53,

128.58, 128.6, 128.62, 128.65, 128.67, 128.82, 128.84, 137.08, 137.1, 137.14, 137.54, 137.72,

137.85, 140.97, 156.34, 169.58, 169.61. HRMS: m/z calc. for $C_{160}H_{182}N_{16}Na_2O_{53}$: 1610.5917; found: 1610.5923 $[M + 2Na]^{2+}$.
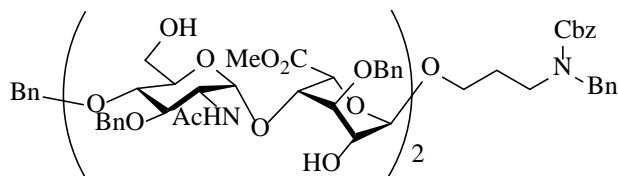
N-(Benzyl)-benzyloxycarbonyl-3-aminopropyl

2-acetamido-3,4-di-*O*-benzyl-2-deoxy-α-D-glucopyranosyl-(1→4)-methyl

3-*O*-benzyl-α-L-idopyranosyluronate-(1→4)-2-acetamido-3-*O*-benzyl-2-deoxy-α-D-glucopyrano

syl-(1→4)-methyl 3-*O*-benzyl-α-L-idopyranosyluronate (**23**)

Compound **20** (60 mg, 0.04 mmol) was dissolved in THF (4 mL), followed by the addition of Zn (104 mg, 1.6 mmol), AcOH (70 μL, 1.2 mmol) and Ac₂O (116 μL, 1.2 mmol) The reaction was stirred at room temperature overnight. Upon completion, the mixture was filtered, concentrated and purification through silica gel column (DCM/MeOH = 8/1) provided compound **23** in 99% yield.

^{1}HNMR (500 MHz, CDCl₃): δ = 1.60 (s, 3H), 1.74 (s, 3H), 1.76-1.84 (m, 2H), 3.20-3.39 (m, 4H), 3.44 (s, 3H), 3.48-3.61 (m, 4H), 3.65 (s, 3H), 3.67-3.87 (m, 8H), 3.90-4.19 (m, 7H), 4.34-4.56 (m, 6H), 4.57-4.70 (m, 5H), 4.72 (d, 1H, *J* = 11.0 Hz), 4.78 (d, 1H, *J* = 11.0 Hz), 4.82-5.02 (m, 5H), 5.08-5.20 (m, 2H), 5.31 (s, 1H), 5.96-6.18 (m, 2H), 6.73 (br, 1H), 7.05-7.45 (m, 35H). ^{13}CNMR (125 MHz, CDCl₃): δ =22.9, 22.99, 27.71, 29.73, 31.53, 36.63, 43.71, 44.26, 50.39, 50.77, 51.91, 52.17, 52.31, 52.87, 52.94, 60.95, 61.5, 66.2, 67.33, 67.35, 67.52, 67.88, 68.03, 71.59, 71.87,

72.02, 72.18, 72.33, 72.73, 72.89, 73.44, 74.36, 74.57, 74.81, 74.98, 77.41, 77.69, 78.38, 80.0, 96.18, 96.7, 100.75, 101.4, 127.2, 127.4, 127.54, 127.6, 127.69, 127.71, 127.78, 127.86, 127.88, 127.91, 127.97, 128.02, 128.05, 128.11, 128.19, 128.35, 128.44, 128.47, 128.52, 128.55, 128.6, 128.62, 136.52, 136.74, 137.39, 137.55, 137.57, 137.69, 137.71, 137.75, 138.02, 138.17, 138.24, 138.43, 156.37, 156.79, 162.97, 169.84, 170.06, 170.59, 170.82, 171.06. HRMS: m/z calc. for $C_{83}FeH_{97}N_3O_{25}$: 795.7880; found: 795.7868 $[M + Fe]^{2+}$.
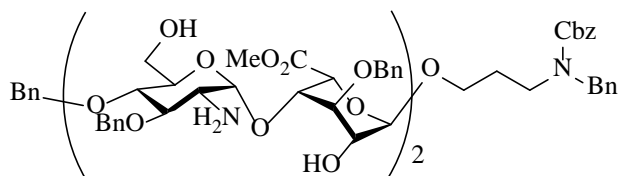
N-(Benzyl)-benzyloxycarbonyl-3-aminopropyl

2-amino-3,4-di-*O*-benzyl-2-deoxy-α-D-glucopyranosyl-(1→4)-methyl

3-*O*-benzyl-α-L-idopyranosyluronate-(1→4)-2-amino-3-*O*-benzyl-2-deoxy-α-D-glucopyranosyl-

(1→4)-methyl 3-*O*-benzyl-α-L-idopyranosyluronate (**24**)

Compound **20** (60 mg, 0.04 mmol) was dissolved in THF (4 mL), followed by the addition of Zn (104 mg, 1.6 mmol) and AcOH (70 μL, 1.2 mmol). The reaction was stirred at room temperature for 3h. Upon completion, the mixture was filtered, concentrated and purification through silica gel column (DCM/MeOH = 6/1) provided compound **24** in 88% yield.

^{1}HNMR (500 MHz, CDCl$_3$): δ = 1.75-1.87 (m, 2H), 3.11 (d, 1H, J = 10.5 Hz), 3.20 (d, 1H, J = 10.5 Hz), 3.25-3.44 (m, 3H), 3.38 (s, 3H), 3.48 (d, 2H, J = 9.5 Hz), 3.57 (t, 2H, J = 9.5 Hz), 3.62-3.73 (m, 3H), 3.65 (s, 3H), 3.79 (d, 2H, J = 11.5 Hz), 3.85 (d, 3H, J = 11.5 Hz), 3.93-4.05

(m, 4H), 4.14 (s, 1H), 4.35-4.51 (m, 4H), 4.54 (d, 1H, $J = 11.5$ Hz), 4.58-4.75 (m, 4H), 4.75-4.99 (m, 6H), 5.14 (s, 3H), 5.27 (s, 2H), 7.07-7.15 (m, 4H), 7.15-7.40 (m, 31H). ^{13}CNMR (125 MHz, CDCl$_3$): δ = 22.1, 29.76, 43.88, 44.76, 50.65, 50.93, 52.12, 52.28, 53.98, 54.33, 60.37, 60.83, 65.38, 65.53, 66.04, 66.23, 66.9, 67.02, 67.29, 67.79, 70.09, 71.04, 71.74, 72.04, 72.3, 72.53, 72.98, 74.63, 74.79, 75.17, 77.84, 78.75, 93.09, 94.4, 100.88, 101.33, 127.22, 127.28, 127.54, 127.61, 127.71, 127.83, 127.89, 127.95, 128.01, 128.12, 128.14, 128.4, 128.44, 128.47, 128.52, 128.59, 128.64, 136.68, 136.8, 137.33, 137.72, 137.83, 137.88, 156.25, 156.76, 170.19. HRMS: m/z calc. for C$_{79}$H$_{95}$N$_3$O$_{23}$: 726.8178; found: 726.8185 [M + 2H]$^{2+}$.
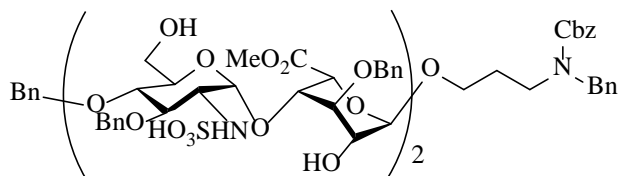
N-(Benzyl)-benzyloxycarbonyl-3-aminopropyl

3,4-di-*O*-benzyl-2-deoxy-2-sulfoamino-α-D-glucopyranosyl-(1→4)-methyl

3-*O*-benzyl-α-L-idopyranosyluronate-(1→4)-3-*O*-benzyl-2-deoxy-2-sulfoamino-α-D-glucopyran

osyl-(1→4)-methyl 3-*O*-benzyl-α-L-idopyranosyluronate (**25**)

Compound **25** was prepared from compound **24** (15 mg, 0.010 mmol) by following the general procedure for selective N-sulfation. Purification through silica gel column (DCM/MeOH = 8/1) provided compound **25** in 78% yield.

^{1}HNMR (500 MHz, CD$_3$OD): δ = 1.74-1.85 (m, 2H), 3.23 (s, 2H), 3.32-3.34 (m, 1H), 3.35 (s, 3H), 3.42-3.52 (m, 5H), 3.53 (t, 1H, $J = 10.0$ Hz), 3.63 (t, 1H, $J = (9.0$ Hz), 3.69 (s, 3H),

3.70-3.71 (m, 2H), 3.73-3.79 (m, 1H), 3.81 (s, 2H), 3.83-3.90 (m, 2H), 3.98 (s, 1H), 4.07 (s, 1H), 4.14 (s, 2H), 4.20 (s, 1H), 4.37-4.44 (m, 3H), 4.59 (d, 2H, J = 11.5 Hz), 4.66 (t, 3H, J = 10.0 Hz), 4.74 (d, 1H, J = 10.0 Hz), 4.77 (d, 2H, J = 10.5 Hz), 4.87-4.94 (m, 2H), 5.03 (d, 1H, J = 1.5 Hz), 5.06 (d, 1H, J = 10.5 Hz), 5.09-5.14 (m, 2H), 5.18 (s, 1H), 5.40-5.44 (m, 2H), 7.06-7.12 (m, 1H), 7.14-7.36 (m, 28H), 7.37-7.45 (m, 4H), 7.46-7.50 (m, 2H). ^{13}CNMR (125 MHz, CD$_3$OD): δ = 24.7, 45.2, 46.05, 48.49, 48.66, 48.83, 49.0, 49.17, 49.34, 49.51, 49.85, 51.58, 52.73, 52.97, 59.42, 59.65, 61.42, 61.74, 66.9, 67.21, 68.33, 68.54, 72.75, 72.86, 73.02, 73.16, 73.38, 73.48, 74.08, 74.4, 74.63, 75.68, 76.12, 76.25, 78.48, 79.36, 81.47, 97.4, 97.54, 101.6, 102.69, 128.13, 128.25, 128.38, 128.51, 128.58, 128.66, 128.87, 128.9, 129.07, 129.13, 129.21, 129.27, 129.39, 129.54, 129.57, 137.97, 137.99, 139.07, 139.25, 139.41, 139.6, 139.76, 139.9, 140.29, 157.91, 158.36, 171.89, 172.2. HRMS: m/z calc. for C$_{79}$H$_{91}$N$_3$O$_{29}$S$_2$: 804.7590; found: 804.7593 [M - 2H]$^{2-}$.
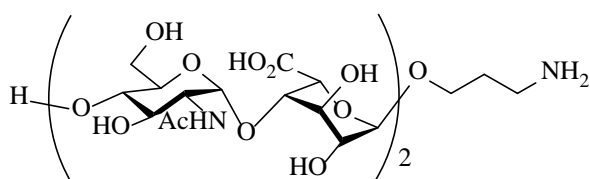
3-Aminopropyl

2-acetamido-2-deoxy-α-D-glucopyranosyl-(1→4)-α-L-idopyranosyluronate-(1→4)-2-acetamido-

2-deoxy-α-D-glucopyranosyl-(1→4)-α-L-idopyranosyluronate (**26**)

Compound **26** was prepared from compound **23** (5 mg, 0.003 mmol) by following the general

procedure for global debenzylation and methyl ester saponification, providing the final product

in 65% yield over 2 steps.

^{1}HNMR (500 MHz, D$_2$O): δ =1.80-1.89 (m, 2H), 1.84 (s, 3H), 1.86 (s, 3H), 2.98 (dt, 2H, J = 2.5, 6.5 Hz), 3.31 (t, 1H, J = 9.5 Hz), 3.45-3.50 (m, 1H), 3.50-3.61 (m, 6H), 3.61-3.74 (m, 10H), 3.75 (d, 1H, J = 4.0 Hz), 3.76-3.83 (m, 3H), 3.87 (t, 1H, J = 3.0 Hz), 3.92 (t, 1H, J = 3.5 Hz), 4.33 (d, 1H, J = 3.0 Hz), 4.58 (d, 1H, J = 3.0 Hz), 4.73 (d, 1H, J = 3.0 Hz), 4.75 (d, 1H, J = 4.0 Hz), 4.97 (d, 1H, J = 4.0 Hz), 5.03 (d, 1H, J = 3.5 Hz), . ^{13}CNMR (125 MHz, D$_2$O): δ = 21.7, 21.79, 26.2, 38.05, 53.41, 53.57, 59.46, 60.02, 66.3, 67.21, 68.12, 68.48, 69.55, 69.83, 70.95, 71.01, 71.83, 73.25, 74.19, 76.43, 94.23, 94.31, 100.29, 101.56, 174.2, 174.28, 174.81, 174.99. HRMS: m/z calc. for C31H50N3O23: 832.2835; found: 832.2836 [M - H]$^-$.
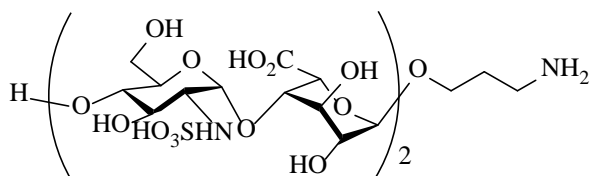
3-Aminopropyl
2-deoxy-2-sulfoamino-α-D-glucopyranosyl-(1→4)-α-L-idopyranosyluronate-(1→4)-2-deoxy-2-sulfoamino-α-D-glucopyranosyl-(1→4)-α-L-idopyranosyluronate (**27**)

Compound **27** was prepared from compound **25** (5 mg, 0.003 mmol) by following the general procedure for global debenzylation and methyl ester saponification, providing the final product in 83% yield over 2 steps.

^{1}HNMR (500 MHz, D$_2$O): δ = 1.76-1.91 (m, 2H), 2.96-3.01 (m, 1H), 3.02-3.10 (m, 2H), 3.30 (t, 1H, J = 9.5 Hz), 3.47 (t, 1H, J = 10.0 Hz), 3.50-3.60 (m, 5H), 3.60-3.76 (m, 8H), 3.85-3.89 (m,

1H), 3.90-3.96 (m, 2H), 4.01 (s, 1H), 4.31 (d, 1H, J = 2.0 Hz), 4.62 (d, 1H, J = 2.5 Hz), 4.74 (s,

1H), 4.79 (d, 1H, J = 3.0 Hz), 5.16 (d, 1H, J = 4.0 Hz), 5.23 (d, 1H, J = 3.5 Hz). ^{13}CNMR (125

MHz, D_2O): δ = 26.1, 38.24, 57.78, 57.89, 59.61, 60.11, 66.36, 67.02, 67.73, 68.1, 68.74, 69.29,

69.64, 69.66, 70.85, 71.17, 71.57, 74.41, 74.72, 76.85, 95.29, 95.72, 100.27, 101.48, 175.24,

175.29. HRMS: m/z calc. for $C_{31}H_{50}N_3O_{35}S_4$: 908.1760; found: 908.1729 [M - H]$^-$.
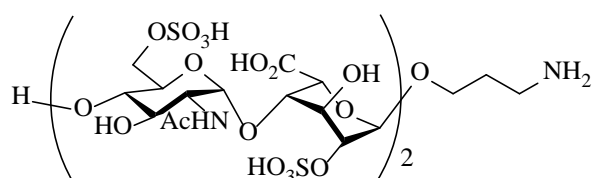
3-Aminopropyl

2-acetamido-2-deoxy-6-O-sulfonato-α-D-glucopyranosyl-(1→4)-2-O-sulfonato-α-L-idopyranosy

luronate-(1→4)-2-acetamido-2-deoxy-6-O-sulfonato-α-D-glucopyranosyl-(1→4)-2-O-sulfonato-

α-L-idopyranosyluronate (**28**)

Compound **28** was prepared from compound **23** (5 mg, 0.003 mmol) by following the general

procedure for simultaneous O, N-sulfation, global debenzylation and methyl ester saponification,

providing the final product in 83% yield over 3 steps.

^{1}HNMR (500 MHz, D_2O): δ = 1.83-1.89 (m, 2H), 1.90 (s, 3H), 1.92 (s, 3H), 3.01 (t, 2H, J = 6.5

Hz), 3.41 (t, 1H, J = 9.5 Hz), 3.49 (t, 1H, J = 9.0 Hz), 3.53-3.64 (m, 5H), 3.76-3.82 (m, 2H), 3.86

(dd, 2H, J = 3.5, 10.0 Hz), 3.91 (dd, 1H, J = 3.5, 10.5 Hz), 3.96 (t, 1H, J = 2.5 Hz), 3.98 (t, 1H, J

= 2.5 Hz), 4.07-4.11 (m, 1H), 4.11-4.20 (m, 7H), 4.76 (d, 1H, J = 2.5 Hz), 4.99 (d, 2H, J = 3.5

Hz), 5.01 (s, 1H), 5.06-5.08 (m, 2H). ^{13}CNMR (125 MHz, D_2O): δ = 22.0, 22.1, 25.96, 38.19,

53.06, 53.21, 63.01, 64.61, 66.03, 66.41, 66.5, 66.72, 66.8, 69.03, 69.63, 69.78, 70.51, 70.79, 72.08, 73.0, 73.58, 76.6, 93.98, 95.11, 98.28, 99.08, 172.54, 172.65, 174.8. HRMS: m/z calc. for $C_{31}H_{46}N_3Na_3O_{35}S_4$: 608.5245; found: 608.5258 $[M + 3Na - 5H]^{2-}$.
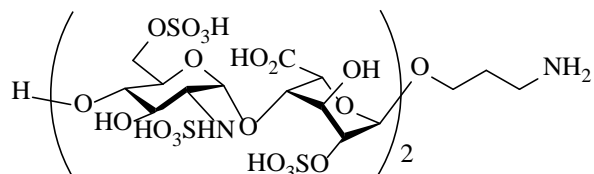
3-Aminopropyl 2-deoxy-2-sulfoamino-6-*O*-sulfonato-*α*-D-glucopyranosyl-(1→4)-2-*O*-sulfonato-*α*-L-idopyranosyluronate-(1→4)-2-deoxy-2-sulfoamino-6-*O*-sulfonato-*α*-D-glucopyranosyl-(1→4)-2-*O*-sulfonato-*α*-L-idopyranosyluronate (**29**)

Compound **29** was prepared from compound **25** (5 mg, 0.003 mmol) by following the general procedure for simultaneous *O*, *N*-sulfation, global debenzylation and methyl ester saponification, providing the final product in 81% yield over 3 steps.

^{1}HNMR (500 MHz, D$_2$O): δ = 1.80-1.90 (m, 2H), 3.02 (t, 2H, *J* = 1.5 Hz), 3.10 (dd, 1H, *J* = 3.5, 10.0 Hz), 3.13 (dd, 1H, *J* = 3.5, 10.5 Hz), 3.42 (t, 1H, *J* = 10.0 Hz), 3.50 (t, 1H, *J* = 10.0 Hz), 3.52-3.59 (m, 2H), 3.62 (t, 1H, *J* = 9.0 Hz), 3.80 (d, 2H, *J* = 7.5 Hz), 3.87 (d, 1H, *J* = 10.0 Hz), 3.93-3.99 (m, 2H), 4.02-4.15 (m, 5H), 4.18-4.27 (m, 3H), 4.40 (d, 1H, *J* = 3.0 Hz), 4.78 (d, 1H, *J* = 2.5 Hz), 4.97 (d, 1H, *J* = 3.5 Hz), 5.08 (s, 1H), 5.25 (d, 1H, *J* = 3.5 Hz), 5.27 (d, 1H, *J* = 3.5 Hz). ^{13}CNMR (125 MHz, D$_2$O): δ = 26.0, 38.31, 46.57, 57.84, 66.3, 66.57, 68.47, 68.58, 68.82,

68.87, 69.05, 69.18, 69.43, 69.93, 70.82, 75.25, 75.79, 75.92, 76.01, 76.4, 96.48, 97.34, 98.78, 99.07, 174.04, 174.26. HRMS: m/z calc. for $C_{27}H_{42}N_3Na_3O_{39}S_6$: 646.4708; found: 646.4703 [M + 3Na - 5H]$^{2-}$.
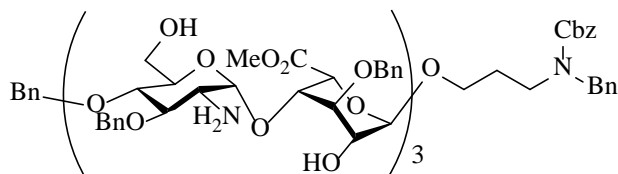
N-(Benzyl)-benzyloxycarbonyl-3-aminopropyl

2-amino-3,4-di-*O*-benzyl-2-deoxy-α-D-glucopyranosyl-(1→4)-methyl

3-*O*-benzyl-α-L-idopyranosyluronate-(1→4)-2-amino-3-*O*-benzyl-2-deoxy-α-D-glucopyranosyl-

(1→4)-methyl

3-*O*-benzyl-α-L-idopyranosyluronate-(1→4)-2-amino-3-*O*-benzyl-2-deoxy-α-D-glucopyranosyl-

(1→4)-methyl 3-*O*-benzyl-α-L-idopyranosyluronate (**30**)

Compound **30** was prepared from compound **21** (15 mg, 0.007 mmol) by following the general procedure for 1, 3-propanedithiol mediated azide reduction. Purification through silica gel column (DCM/MeOH = 6/1 with 2% Et$_3$N) provided compound **27** in 76% yield.

^{1}HNMR (500 MHz, CDCl$_3$): δ = 1.78-1.88 (m, 2H), 2.83-2.91 (m, 2H), 3.23-3.32 (m, 2H), 3.34-3.51 (m, 10H), 3.53 (s, 3H), 3.55 (s, 3H), 3.65-3.68 (m, 2H), 3.70-3.73 (m, 2H), 3.74 (s, 3H), 3.75-3.82 (m, 5H), 3.82-3.91 (m, 4H), 3.94 (s, 3H), 3.96-4.02 (m, 2H), 4.14−4.22 (m, 3H), 4.41 (d, 2H, *J* = 11.5 Hz), 4.43−4.54 (m, 4H), 4.58 (d, 2H, *J* = 11.5 Hz), 4.64 (d, 2H, *J* = 11.0 Hz), 4.66 (s, 4H), 4.72 (dd, 2H, *J* = 3.5, 11.5 Hz), 4.81 (d, 2H, *J* = 11.5 Hz), 4.86 (d, 1H, *J* = 3.0

Hz), 4.87−4.91 (m, 3H), 4.92−4.97 (m, 5H), 4.99 (d, 1H, $J = 12.0$ Hz), 5.15 (s, 2H), 5.29 (dd, 2H, $J = 3.5, 8.0$ Hz), 7.10− 7.13 (m, 1H), 7.17−7.38 (m, 44H). Comparison with literature data confirmed its identity.[25]
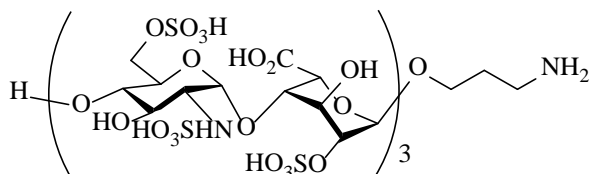
3-Aminopropyl 2-deoxy-2-sulfoamino-6-*O*-sulfonato-α-D-glucopyranosyl-(1→4)-2-*O*-sulfonato-α-L-idopyranos yluronate-(1→4)-2-deoxy-2-sulfoamino-6-*O*-sulfonato-α-D-glucopyranosyl-(1→4)-2-*O*-sulfonat o-α-L-idopyranosyluronate-(1→4)-2-deoxy-2-sulfoamino-6-*O*-sulfonato-α-D-glucopyranosyl-(1 →4)-2-*O*-sulfonato-α-L-idopyranosyluronate (**31**)

Compound **31** was prepared from compound **30** (5 mg, 0.0025 mmol) by following the general procedure for simultaneous *O*, *N*-sulfation, global debenzylation and methyl ester saponification, providing the final product in 64% yield over 3 steps.

^{1}HNMR (500 MHz, D$_2$O): δ = 1.92−2.01 (m, 2H), 3.11−3.15 (m, 1H), 3.21 (dd, 1H, $J = 3.5, 10.5$ Hz), 3.25 (dd, 2H, $J = 3.0, 10.5$ Hz), 3.54 (t, 2H, $J = 10.0$ Hz), 3.59-3.67 (m, 4H), 3.70-3.79 (m, 3H), 3.90-3.94 (m, 1H), 3.95-3.98 (m, 1H), 3.98-4.03 (m, 2H), 4.06-4.10 (m, 3H), 4.14-4.20 (m, 4H), 4.22-4.27 (m, 3H), 4.29-4.41 (m, 5H), 4.47 (d, 1H, $J = 3.0$ Hz), 4.81 (d, 1H, $J = 3.0$ Hz), 5.06 (d, 1H, $J = 3.5$ Hz), 5.19 (d, 2H, $J = 3.0$ Hz), 5.39 (d, 2H, $J = 3.5$ Hz), 5.42 (d, 1H, $J = 3.5$ Hz). Comparison with literature data confirmed its identity.[25]

3-Aminopropyl

2-deoxy-2-sulfoamino-6-O-sulfonato-α-D-glucopyranosyl-(1→4)-2-O-sulfonato-α-L-idopyranos

yluronate-(1→4)-2-deoxy-2-sulfoamino-6-O-sulfonato-α-D-glucopyranosyl-(1→4)-2-O-sulfonat

o-α-L-idopyranosyluronate-(1→4)-2-deoxy-2-sulfoamino-6-O-sulfonato-α-D-glucopyranosyl-(1

→4)-2-O-sulfonato-α-L-idopyranosyluronate-(1→4)-2-deoxy-2-sulfoamino-6-O-sulfonato-α-D-g

lucopyranosyl-(1→4)-2-O-sulfonato-α-L-idopyranosyluronate-(1→4)-2-deoxy-2-sulfoamino-6-

O-sulfonato-α-D-glucopyranosyl-(1→4)-2-O-sulfonato-α-L-idopyranosyluronate (**32**)

Compound **32** was prepared from compound **22** (5 mg, 0.0016 mmol) by following the general

procedure for 1, 3-propanedithiol mediated azide reduction, simultaneous O, N-sulfation, global

debenzylation and methyl ester saponification, providing the final product in 42% yield over 4

steps.

^{1}HNMR (500 MHz, D$_2$O): δ = 1.92-1.99 (m, 2H), 3.09-3.15 (m, 2H), 3.20 (dd, 2H, J = 3.0, 10.0

Hz), 3.25 (dd, 4H, J = 3.5, 10.5 Hz), 3.54 (t, 3H, J = 10.0 Hz), 3.58-3.66 (m, 5H), 3.68-3.79 (m,

6H), 3.92-4.02 (m, 7H), 4.08 (t, 4H, J = 3.5 Hz), 4.14-4.19 (m, 6H), 4.20-4.27 (m, 6H), 4.29-4.34

(m, 5H), 4.34-4.42 (m, 5H), 4.79-4.83 (m, 2H), 5.18 (d, 5H, J = 3.0 Hz), 5.39 (d, 5H, J = 3.0 Hz).

δ_C (values obtained from F1 dimension of HSQC spectrum) = 26.0, 38.24, 57.81, 57.82, 61.11,

65.54, 66.22, 66.23, 66.26, 66.29, 66.51, 66.52, 68.60, 69.12, 69.17, 69.24, 69.28, 69.40, 69.42,

69.66, 69.73, 70.87, 70.88, 75.66, 75.70, 75.77, 75.80, 75.81, 96.57, 99.18. HRMS: m/z calc. for

$C_{63}H_{87}N_6Na_{13}O_{96}S_{15}$: 810.4149; found: 810.4116 $[M + 13Na - 17H]^{4-}$.

APPENDIX

Product Characterization Spectra
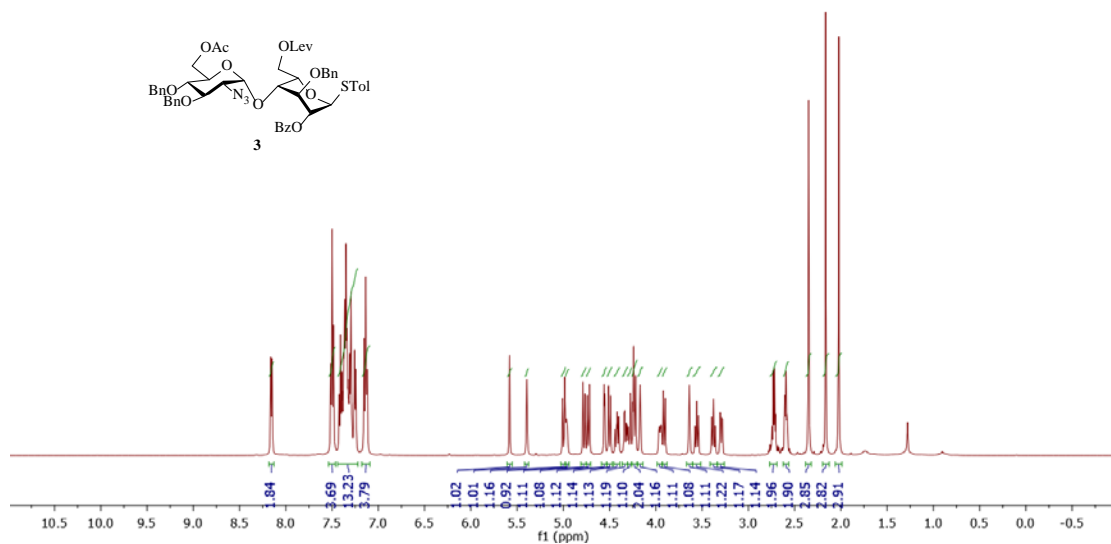
Figure 4.4. ^{1}H-NMR of **3** (500 MHz CDCl$_3$)
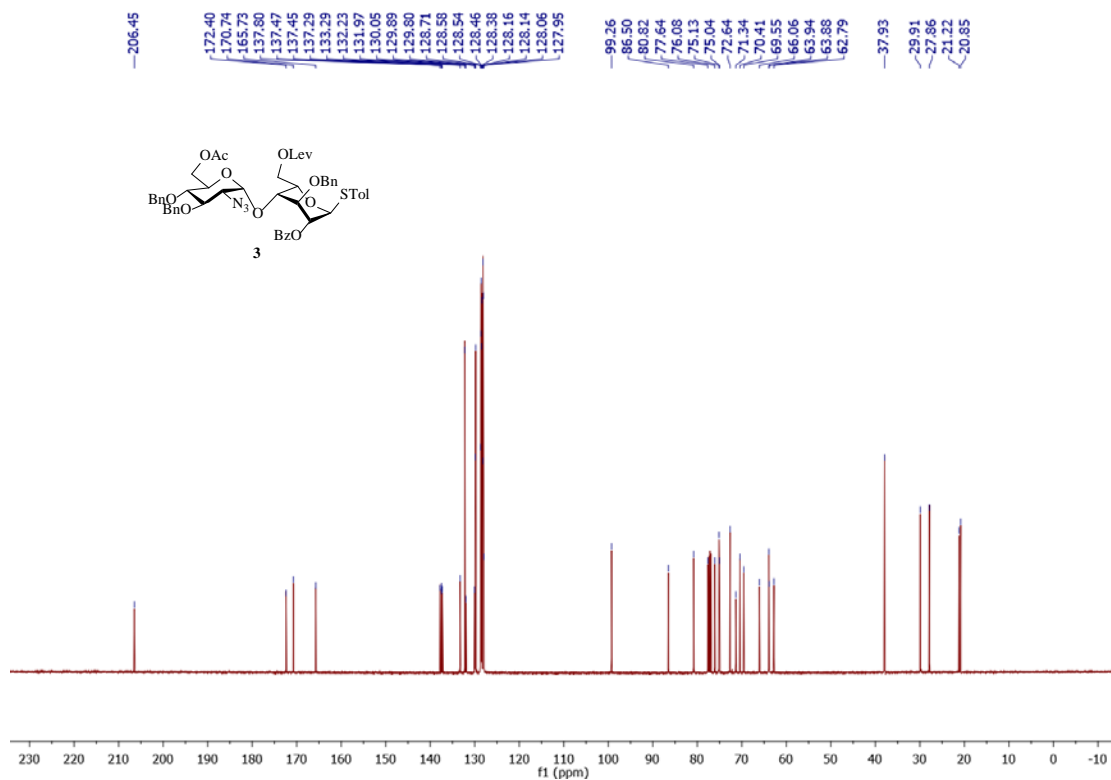
Figure 4.5. ^{13}C-NMR of **3** (125 MHz CDCl$_3$)
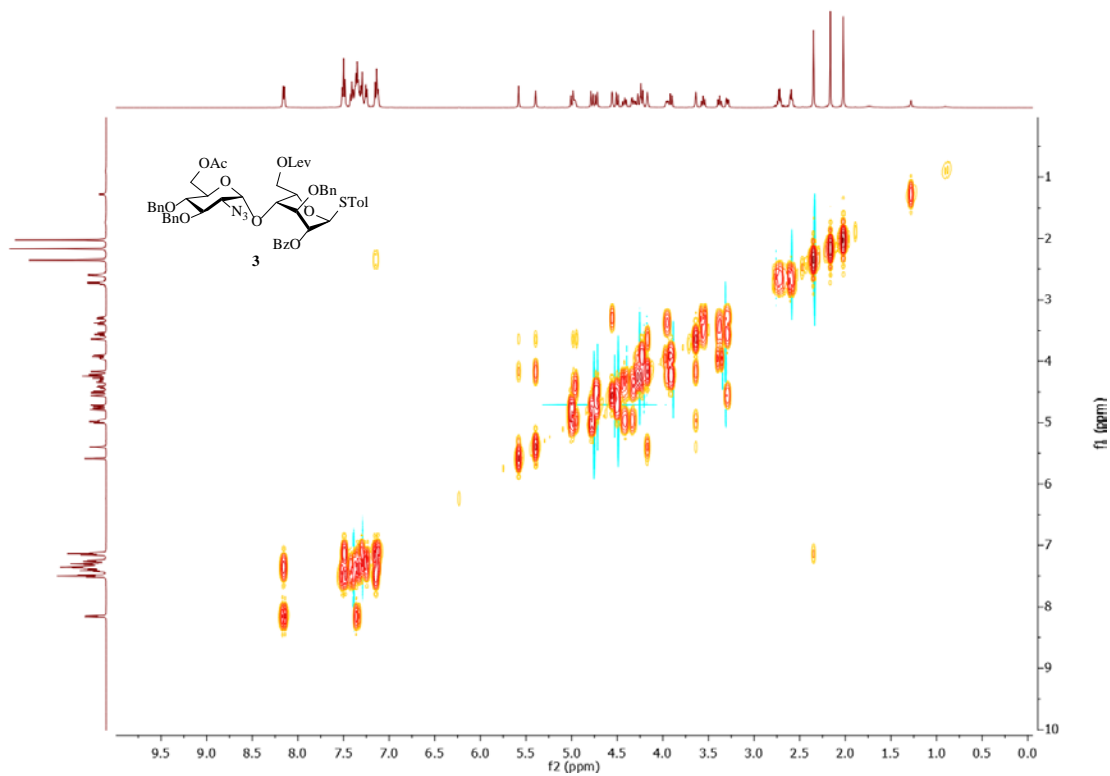
Figure 4.6. ^{1}H-^{1}H gCOSY of **3** (500 MHz CDCl$_3$)
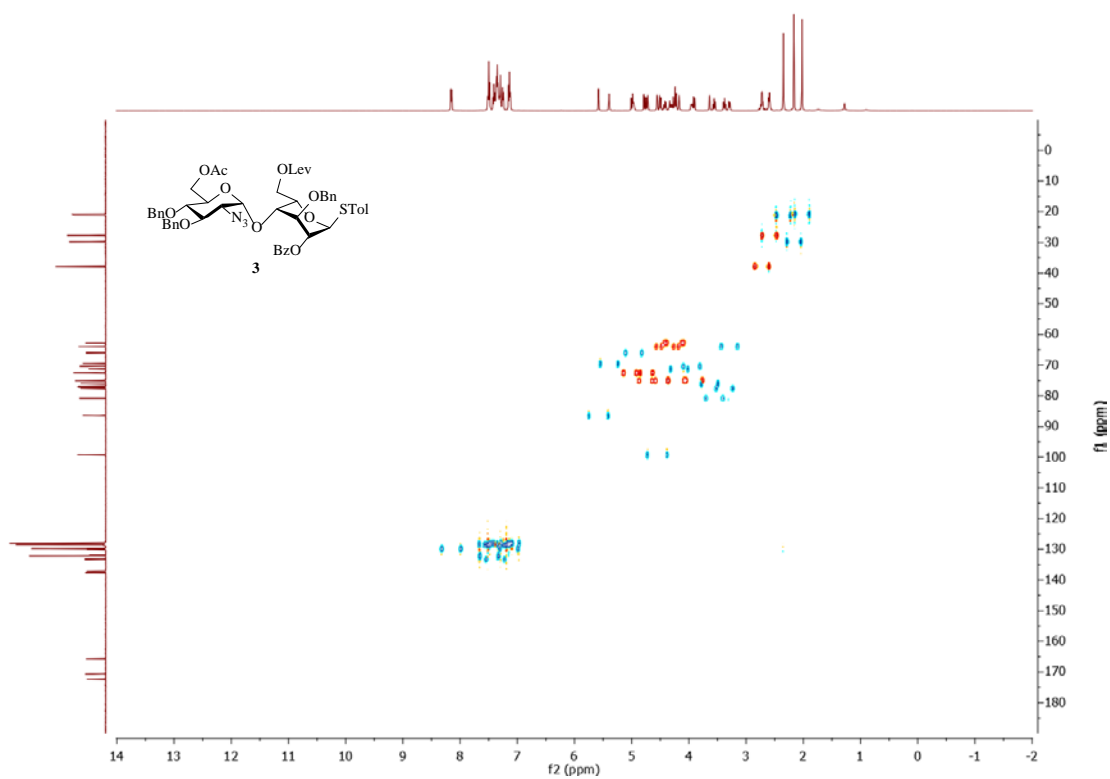
Figure 4.7. ^{1}H-^{13}C gHSQCAD of **3** (500 MHz CDCl$_3$)
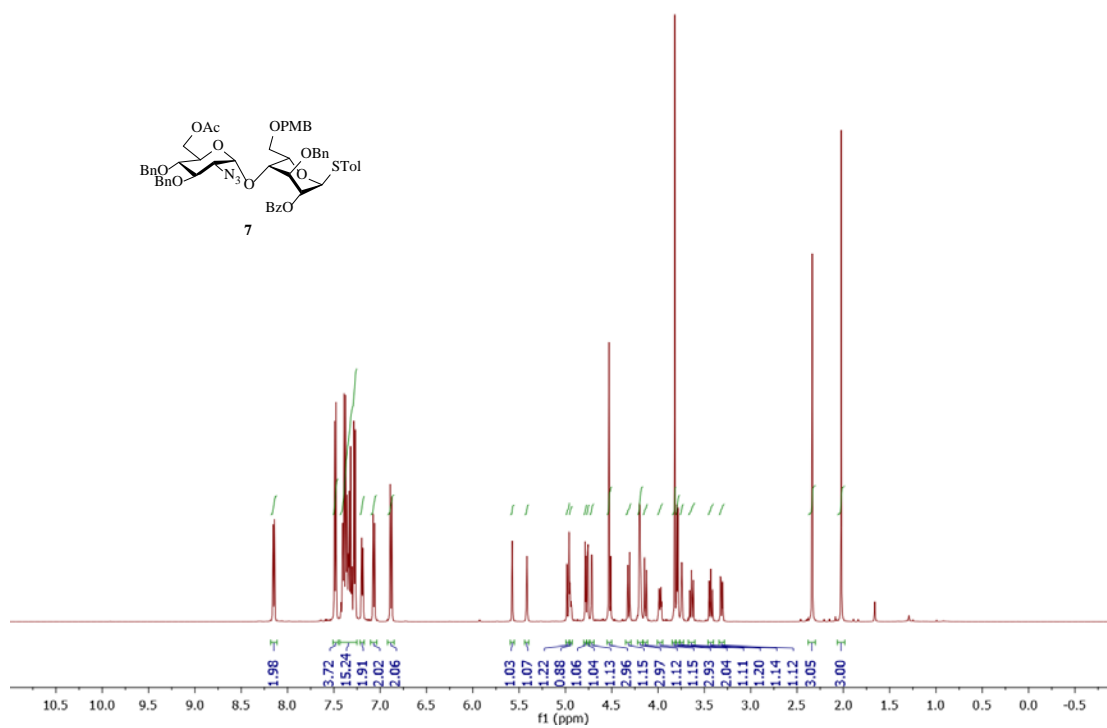
Figure 4.8. ^{1}H-NMR of **7** (500 MHz CDCl$_3$)
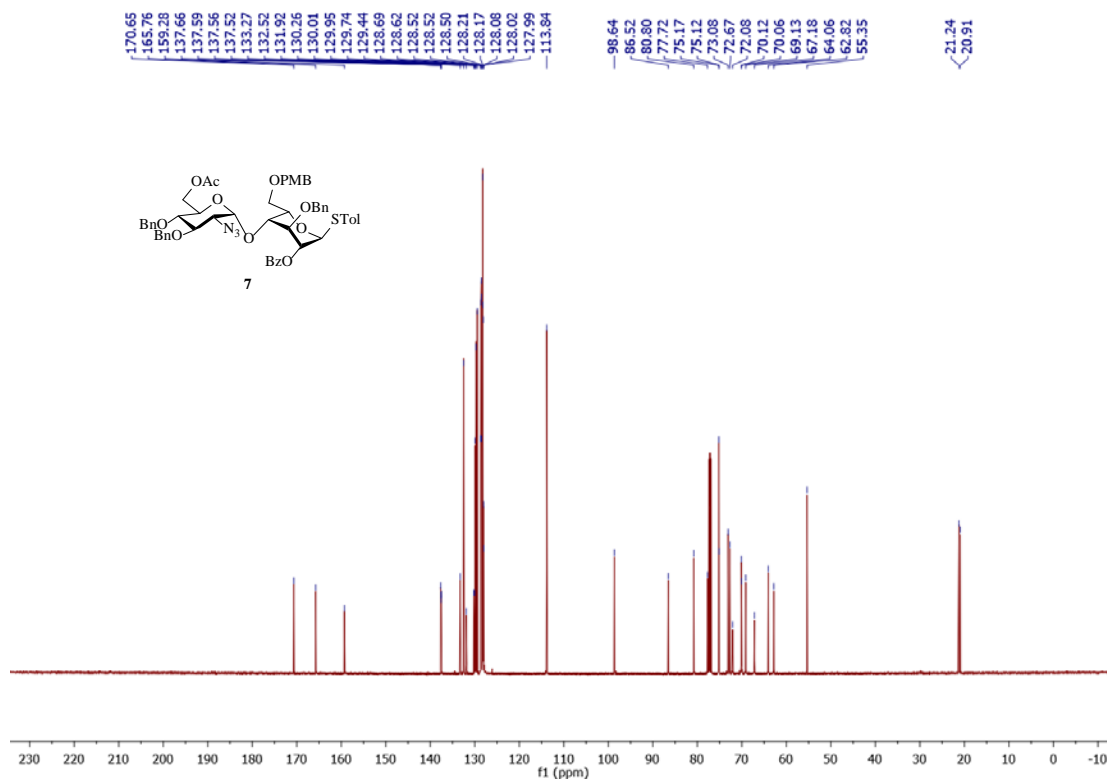
Figure 4.9. ^{13}C-NMR of **7** (125 MHz CDCl$_3$)
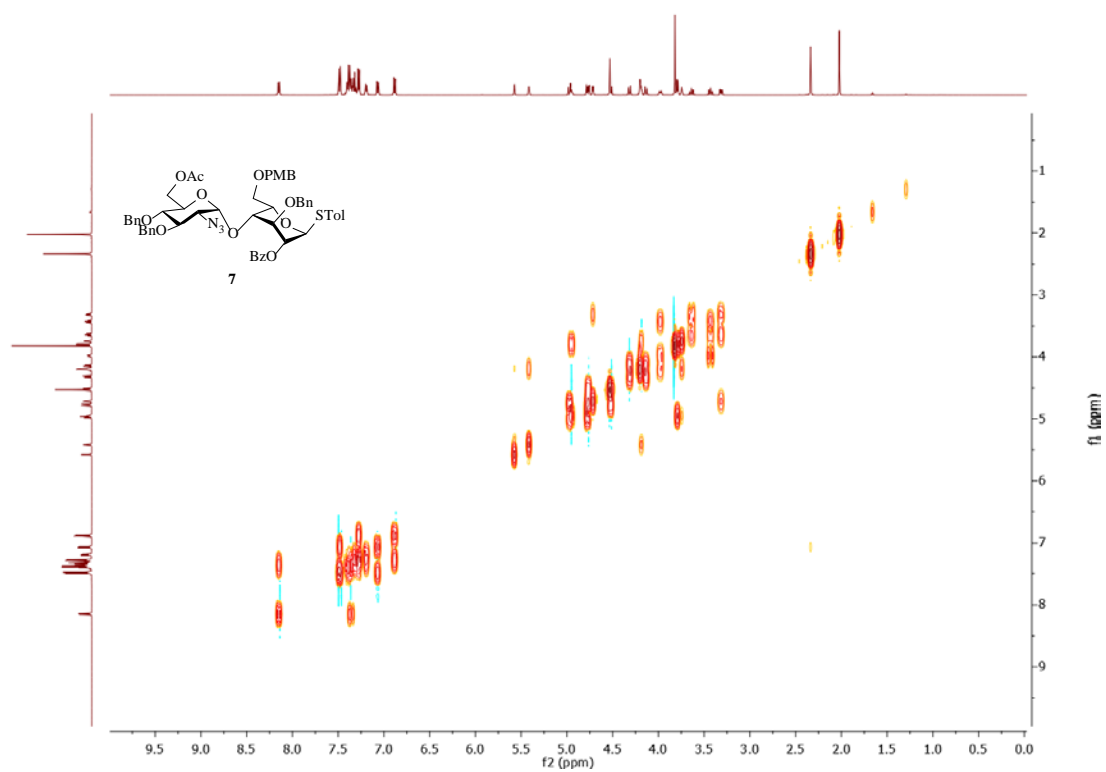
Figure 4.10. ^{1}H-^{1}H gCOSY of **7** (500 MHz CDCl$_3$)
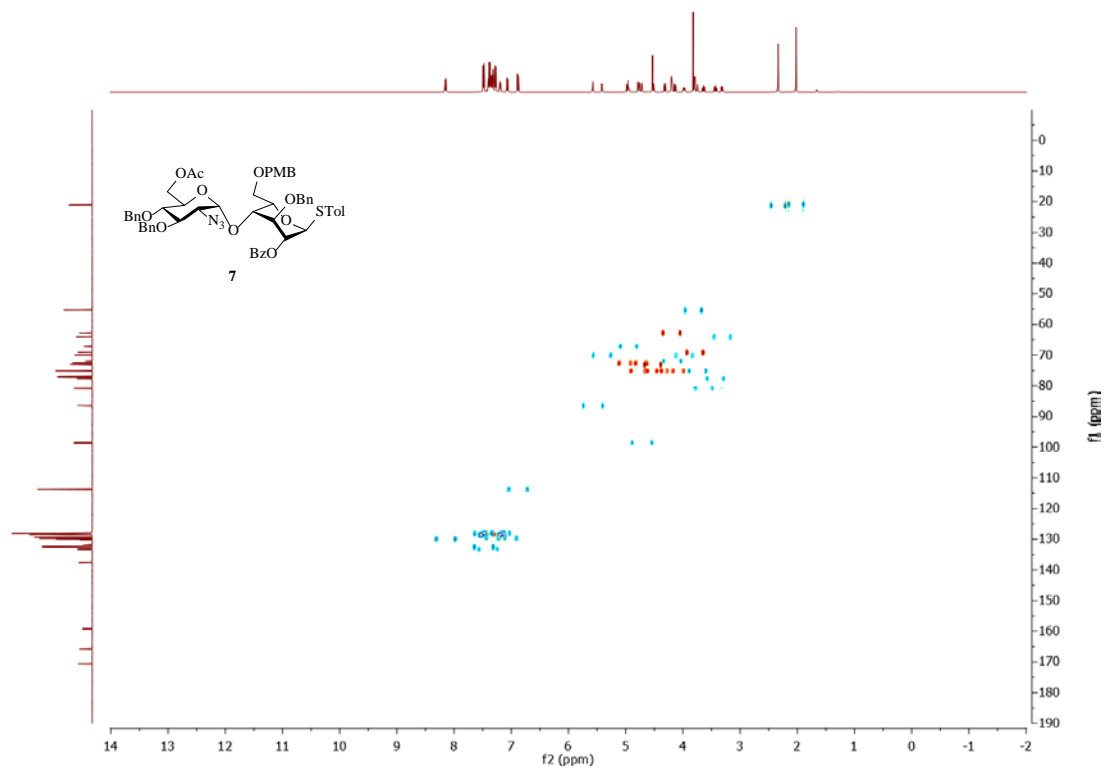
Figure 4.11. ^{1}H-^{13}C gHSQCAD of **7** (500 MHz CDCl$_3$)
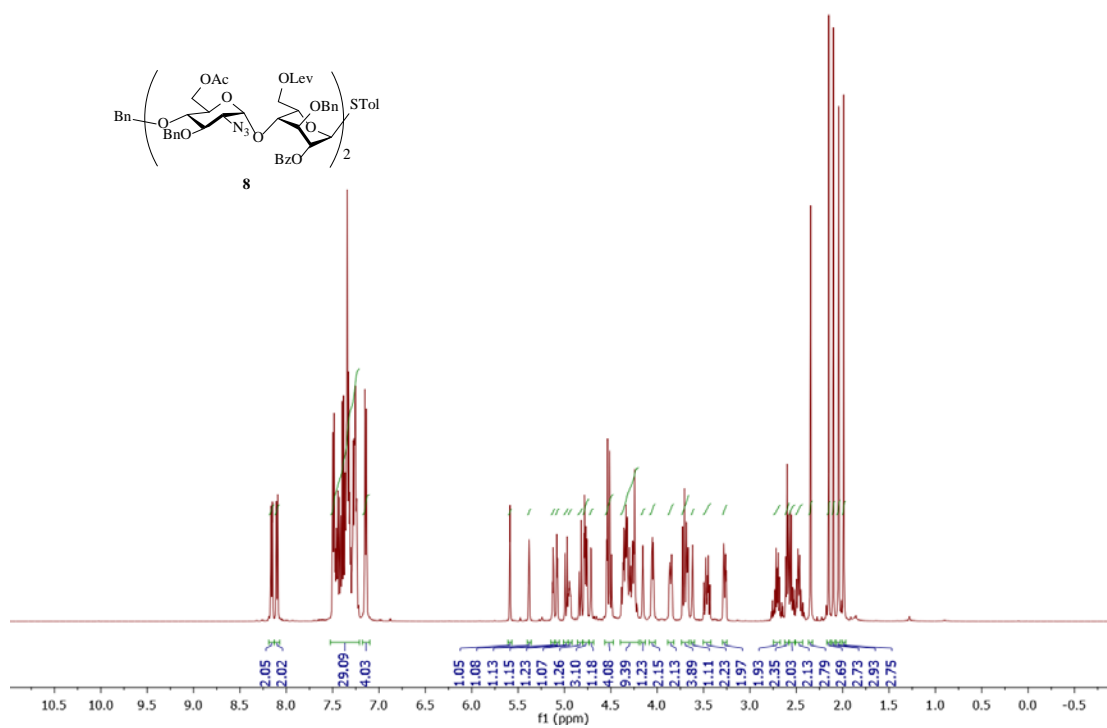
Figure 4.12. ^{1}H-NMR of **8** (500 MHz CDCl$_3$)
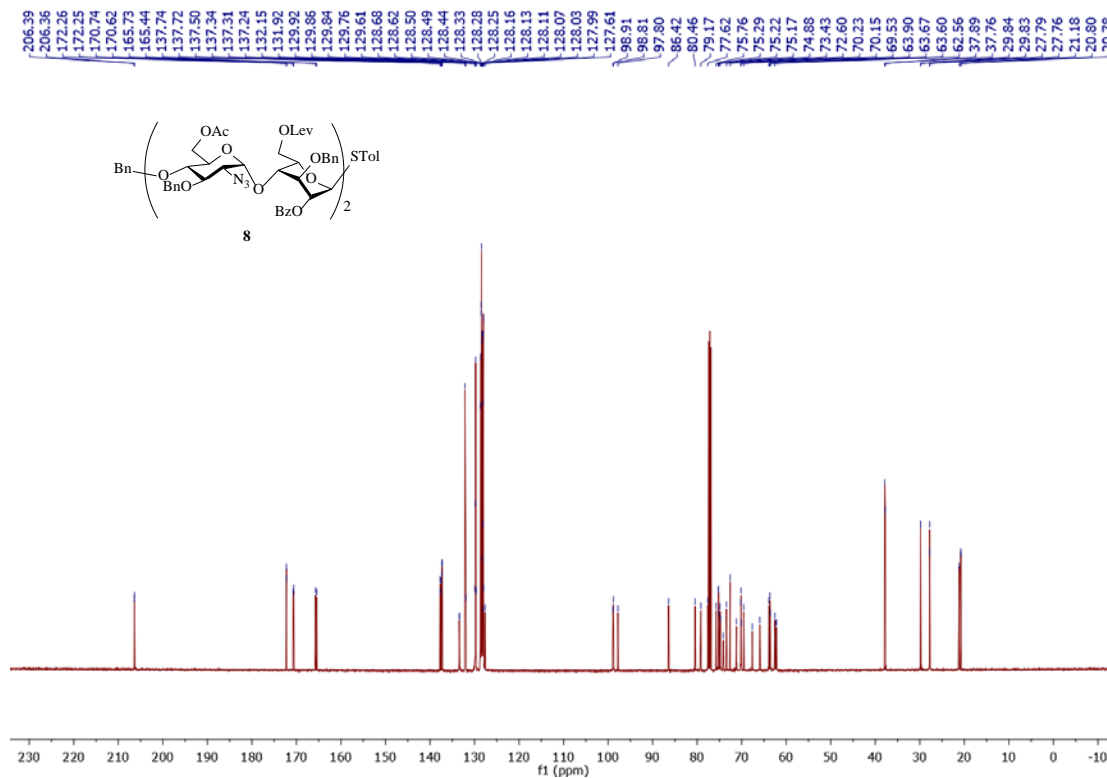
Figure 4.13. ^{13}C-NMR of **8** (125 MHz CDCl$_3$)
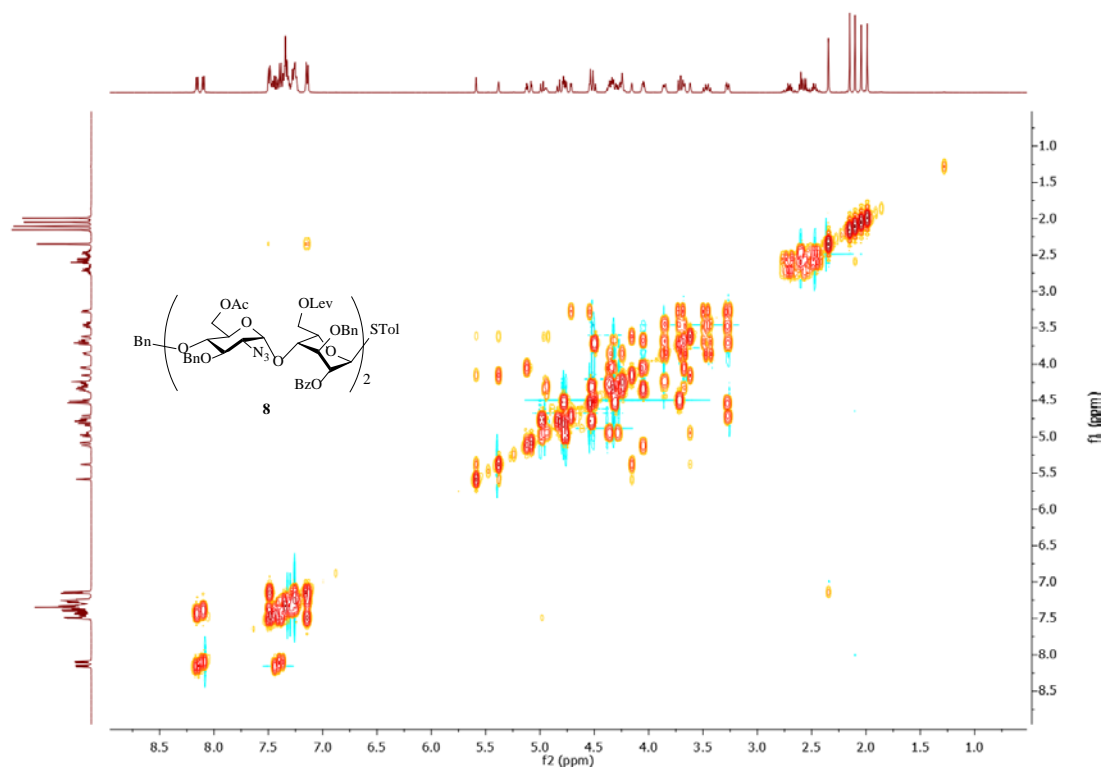
Figure 4.14. ^{1}H-^{1}H gCOSY of **8** (500 MHz CDCl$_3$)
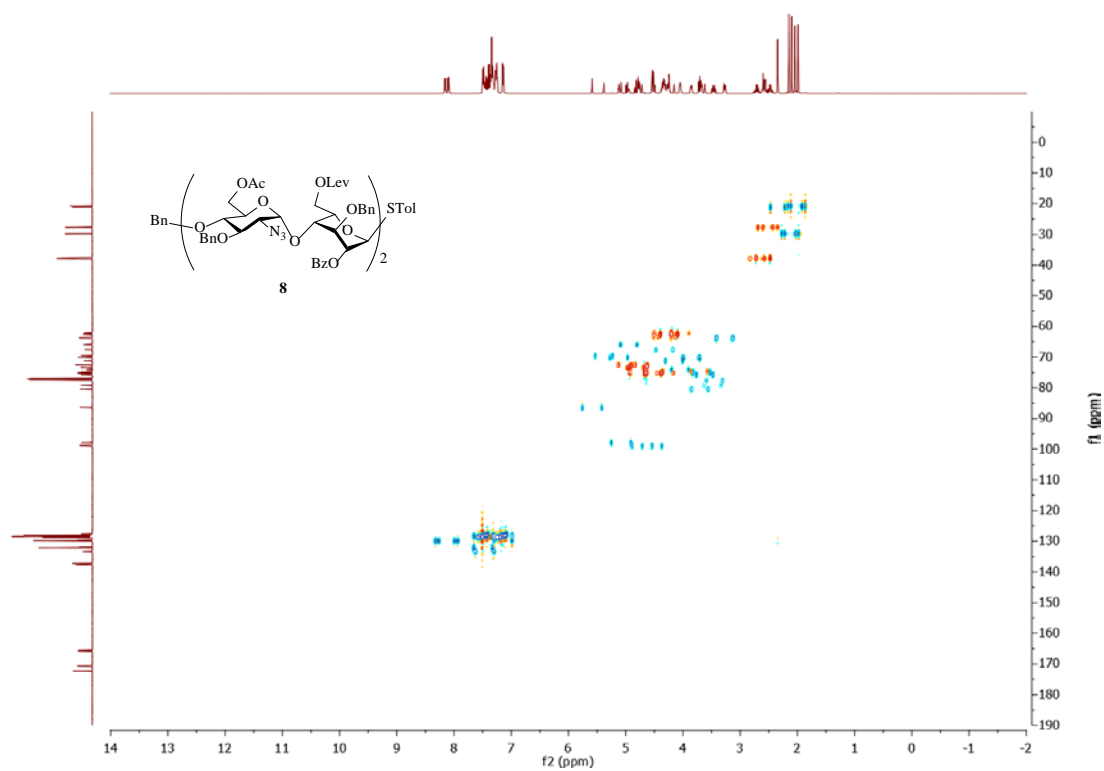
Figure 4.15. ^{1}H-^{13}C gHSQCAD of **8** (500 MHz CDCl$_3$)
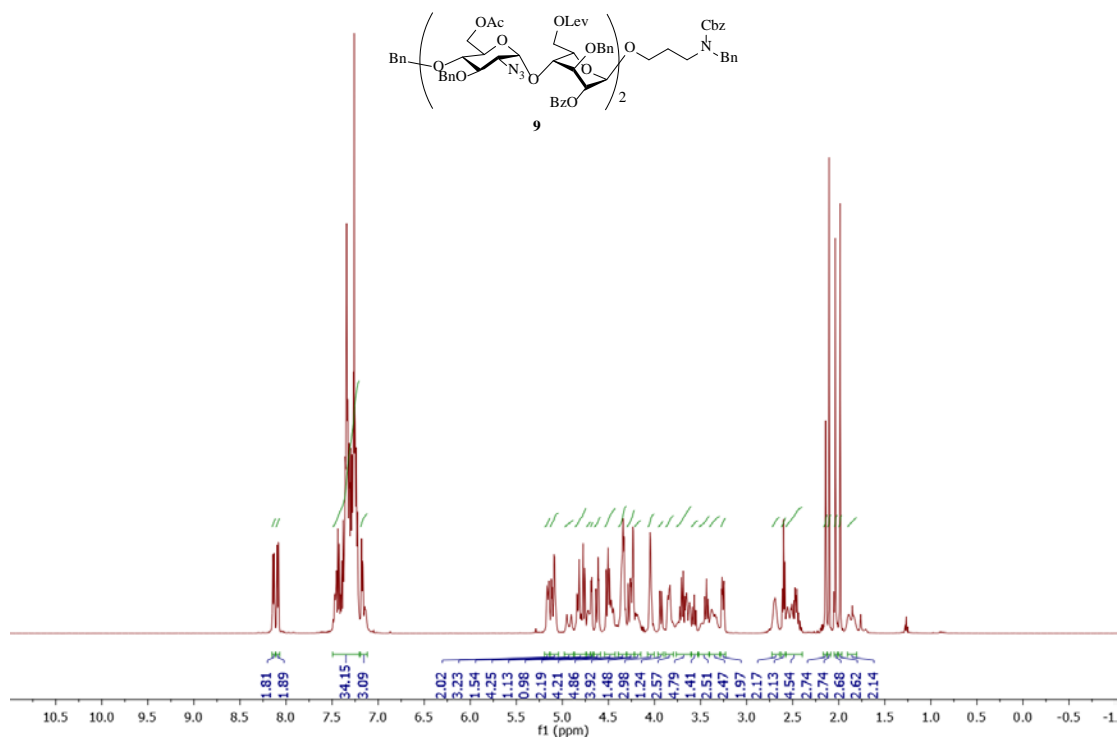
Figure 4.16. ^{1}H-NMR of **9** (500 MHz CDCl$_3$)
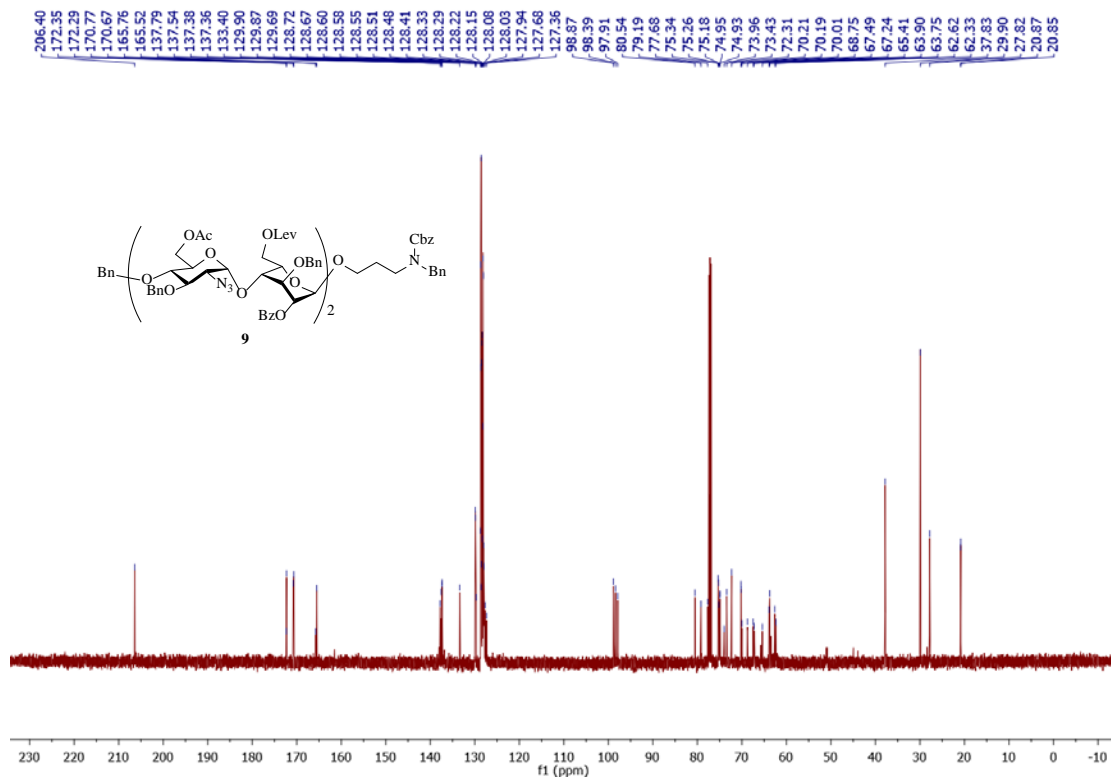
Figure 4.17. ^{13}C-NMR of **9** (125 MHz CDCl$_3$)
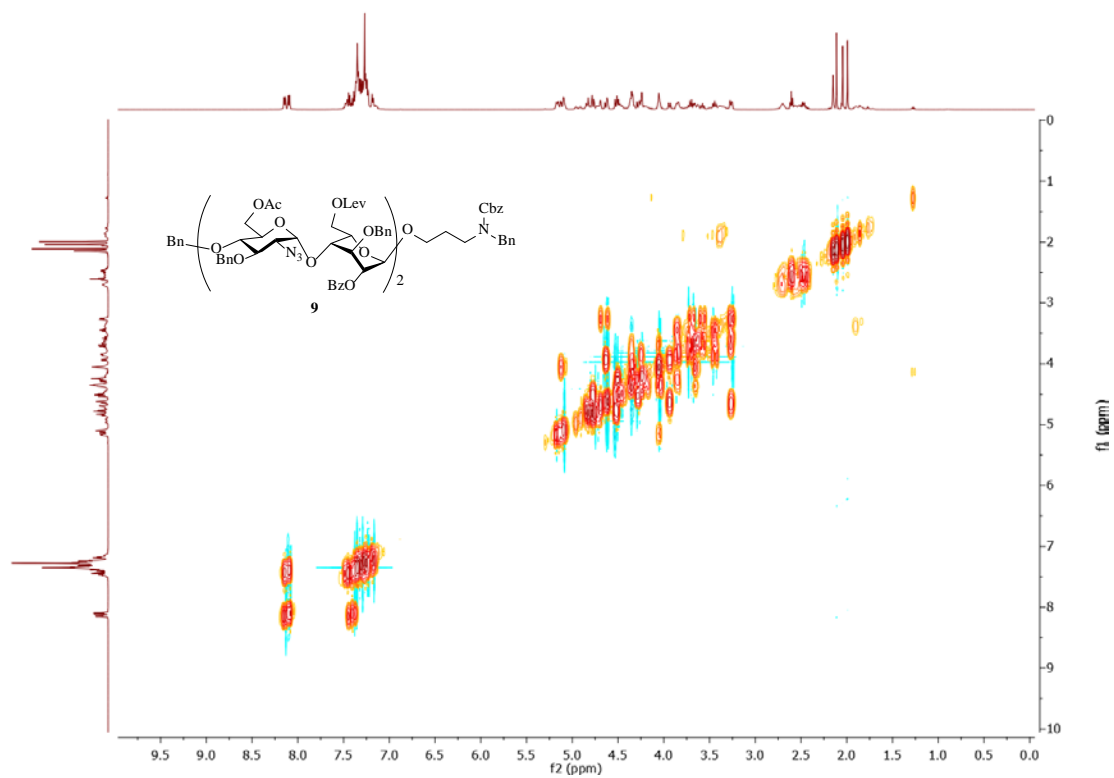
Figure 4.18. ^{1}H-^{1}H gCOSY of **9** (500 MHz CDCl$_3$)
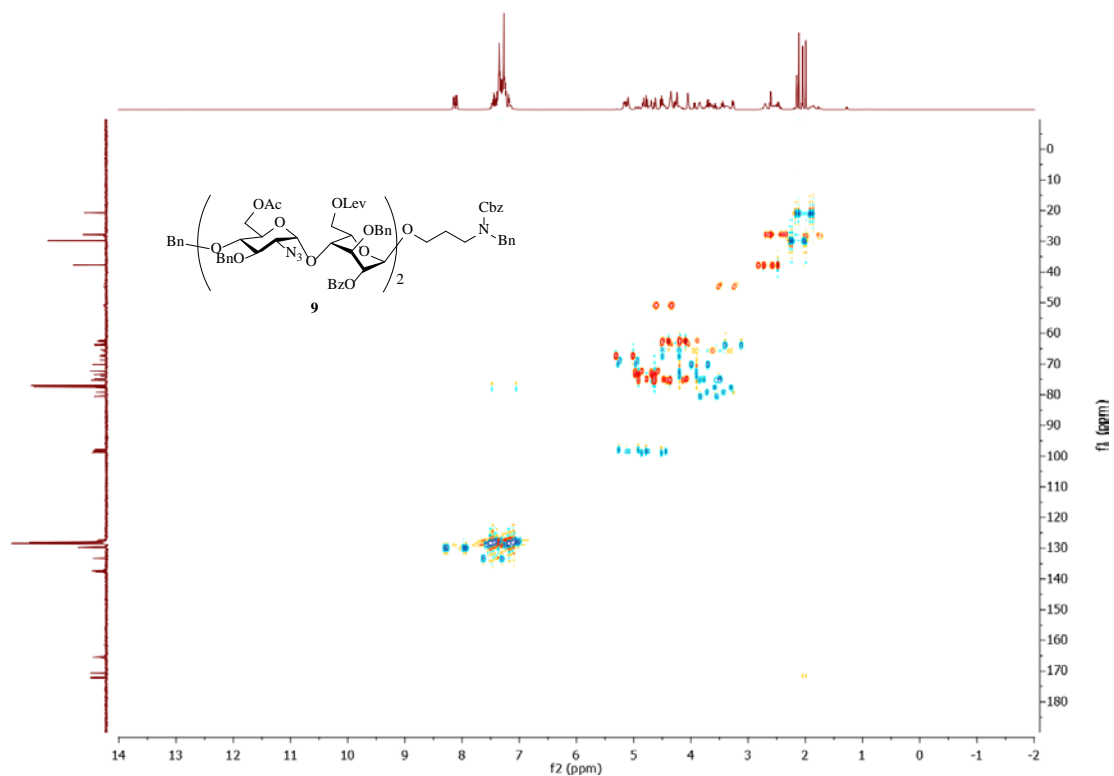
Figure 4.19. ^{1}H-^{13}C gHSQCAD of **9** (500 MHz CDCl$_3$)
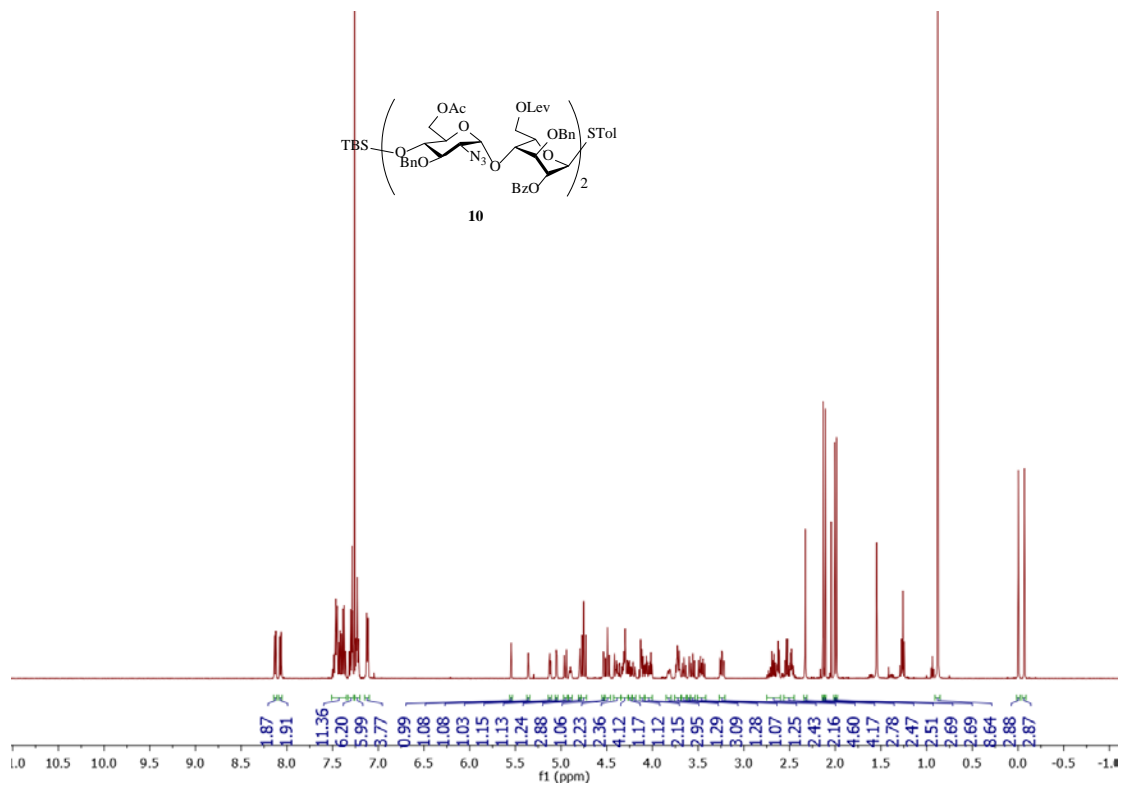
Figure 4.20. ^{1}H-NMR of **10** (500 MHz CDCl$_3$)
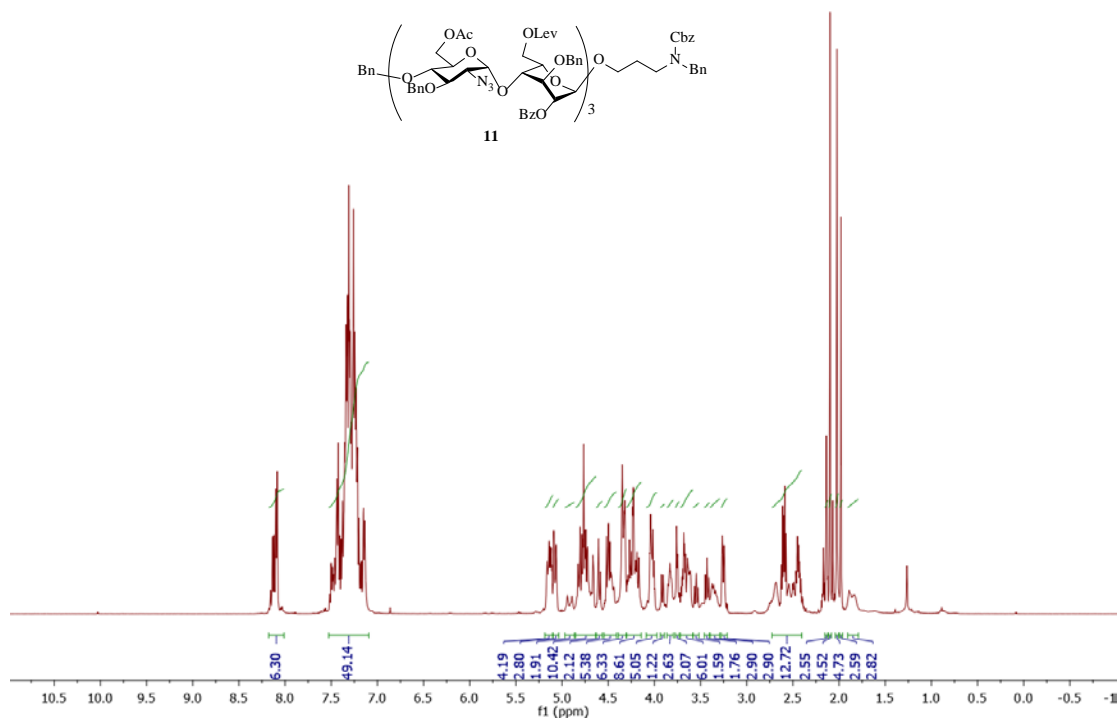
Figure 4.21. ^{1}H-NMR of **11** (500 MHz CDCl$_3$)
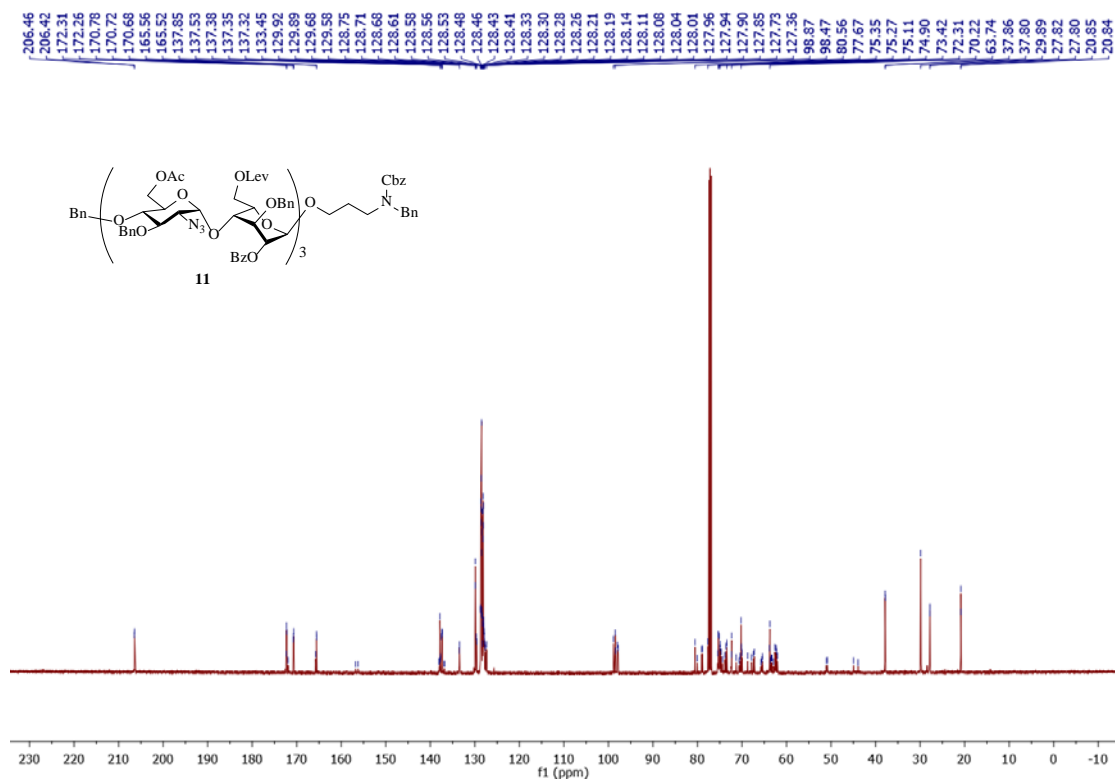
Figure 4.22. ^{13}C-NMR of **11** (125 MHz CDCl$_3$)
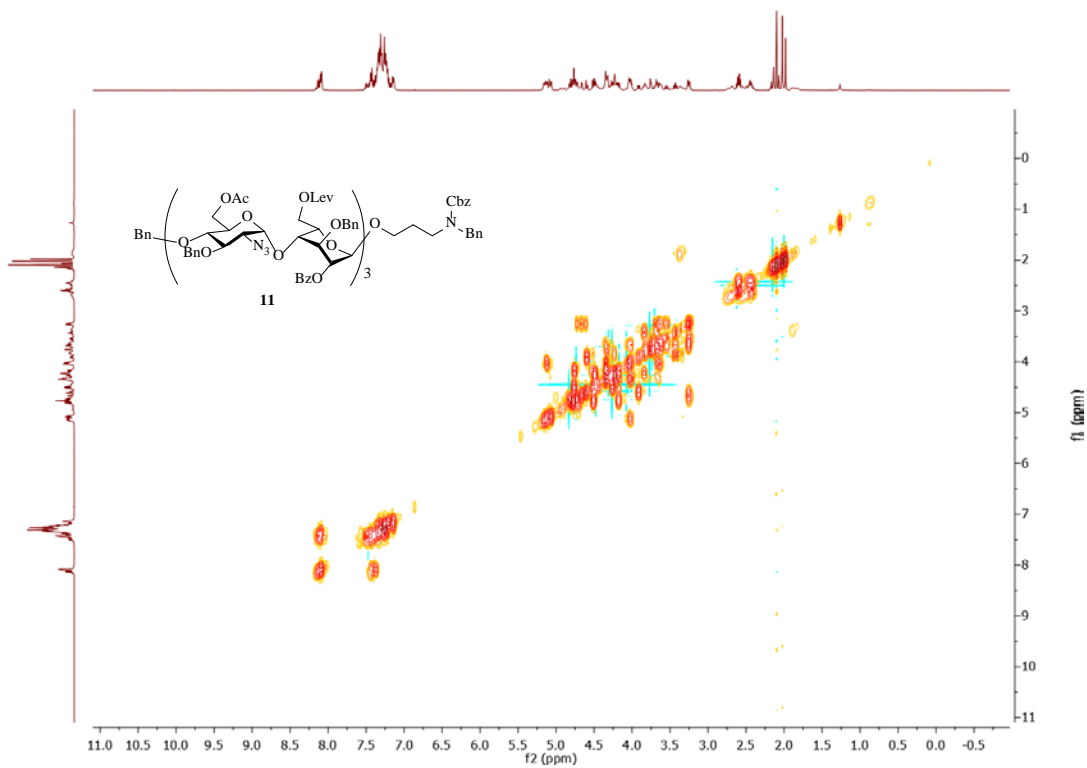
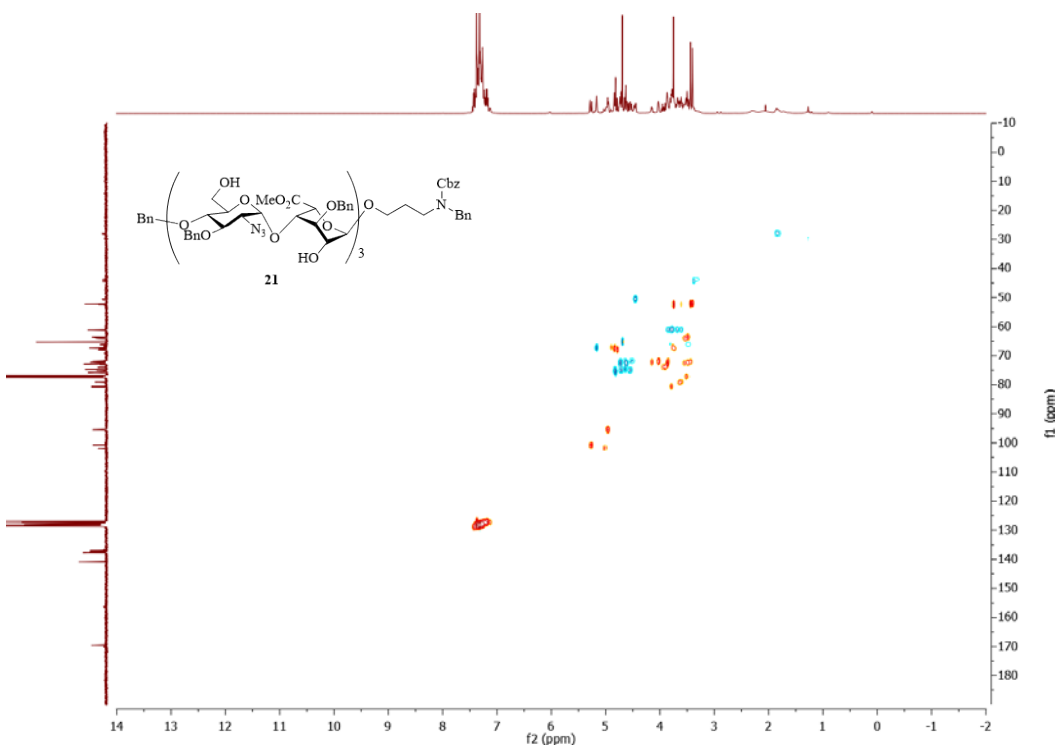**Figure 4.23.** ^{1}H-^{1}H gCOSY of **11** (500 MHz CDCl$_3$)
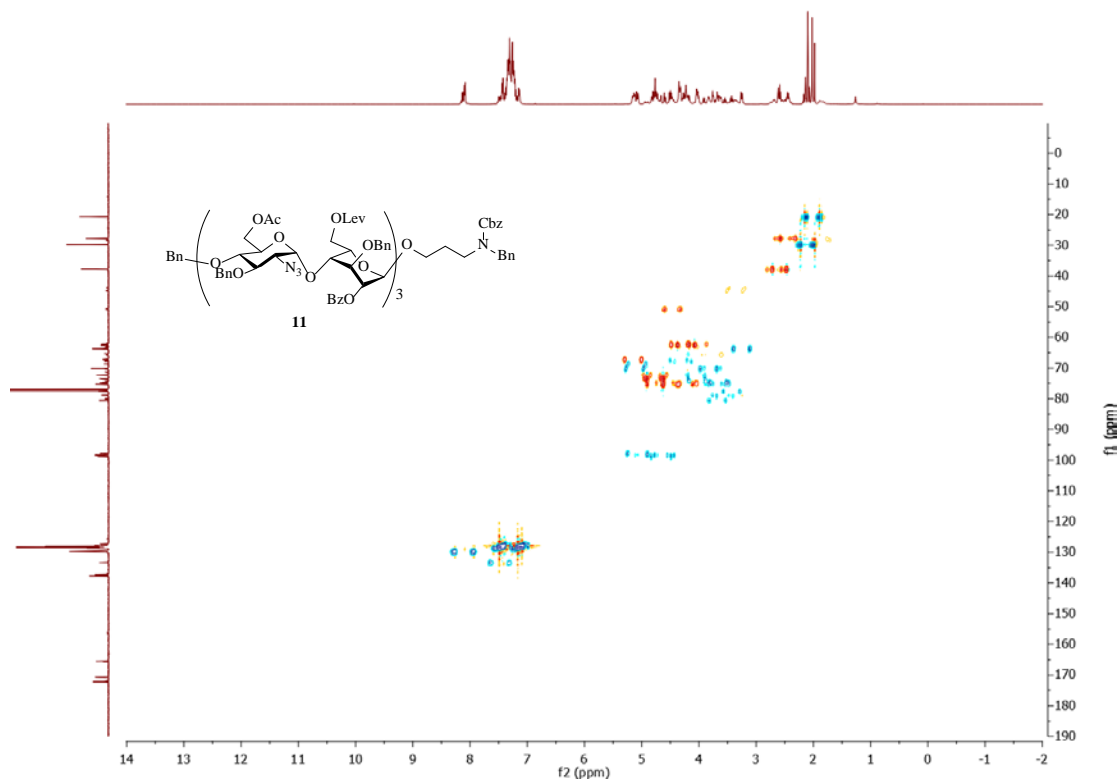
Figure 4.24. ^{1}H-^{13}C gHSQCAD of **11** (500 MHz CDCl$_3$)
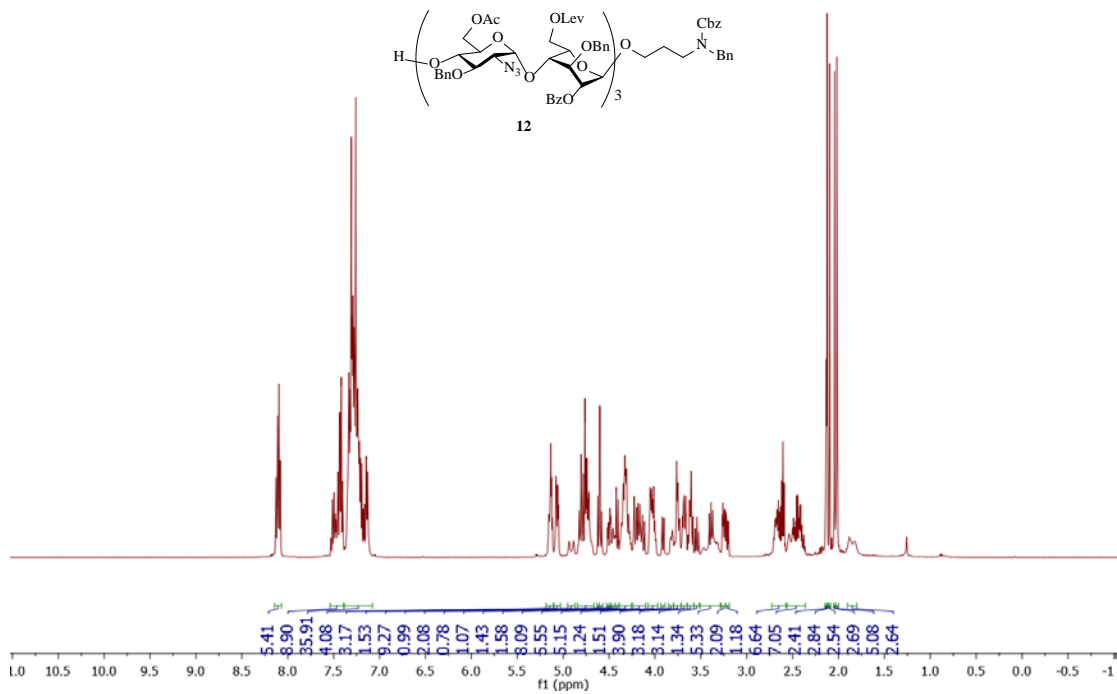
Figure 4.25. ^{1}H-NMR of **12** (500 MHz CDCl$_3$)
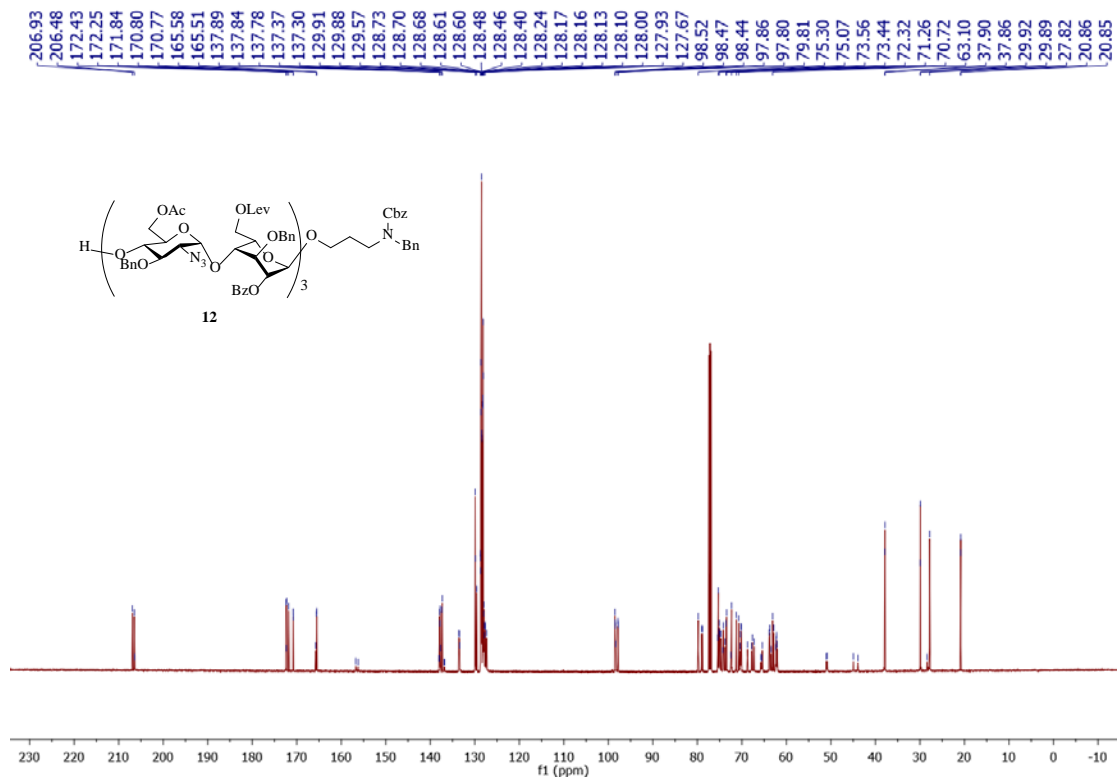
Figure 4.26. ^{13}C-NMR of **12** (125 MHz CDCl$_3$)
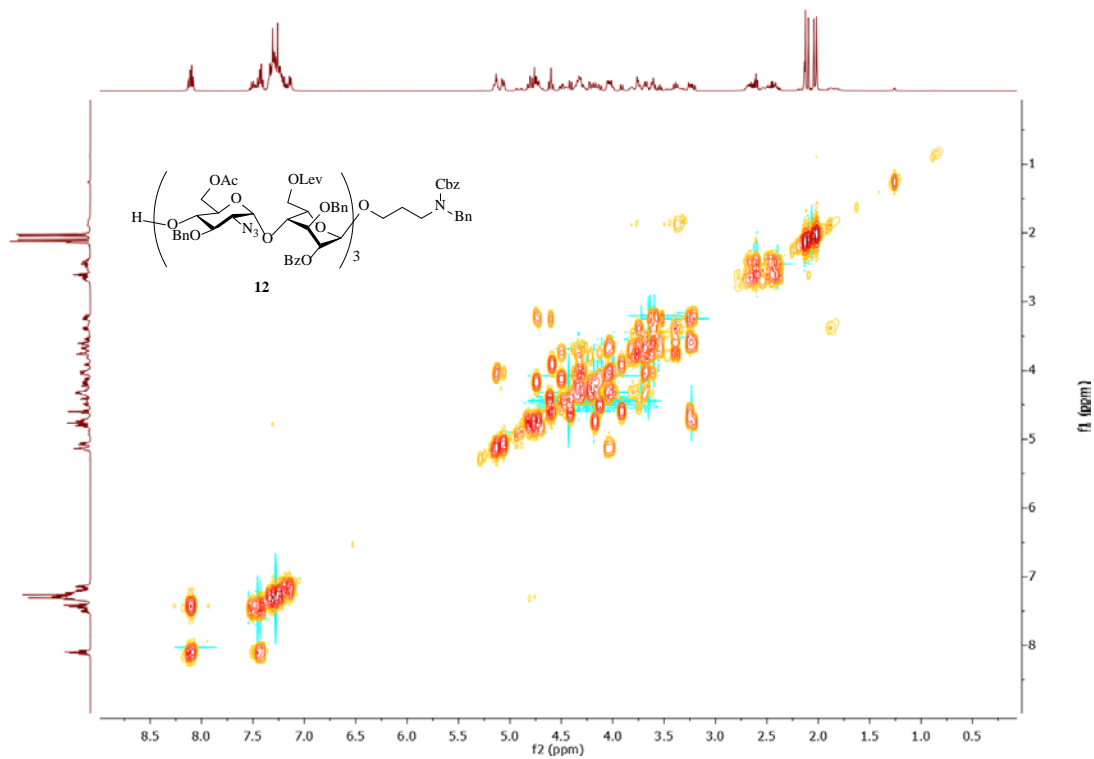
Figure 4.27. ^{1}H-^{1}H gCOSY of **12** (500 MHz CDCl$_3$)
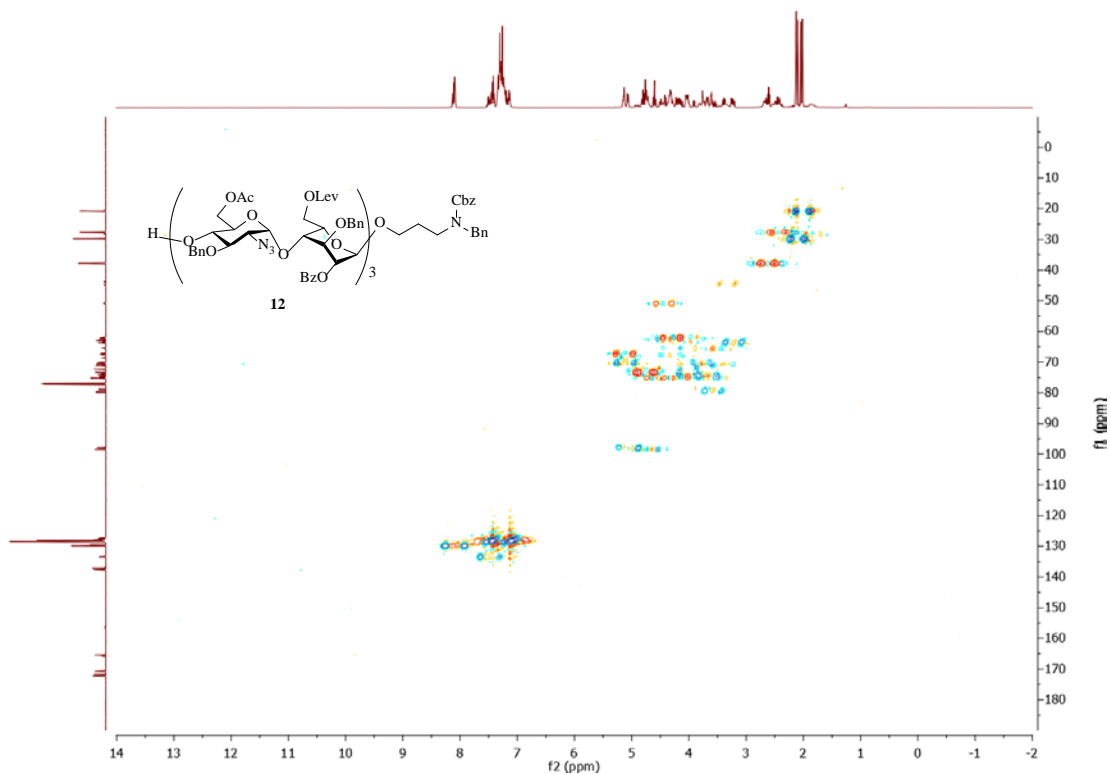
Figure 4.28. ^{1}H-^{13}C gHSQCAD of **12** (500 MHz CDCl$_3$)
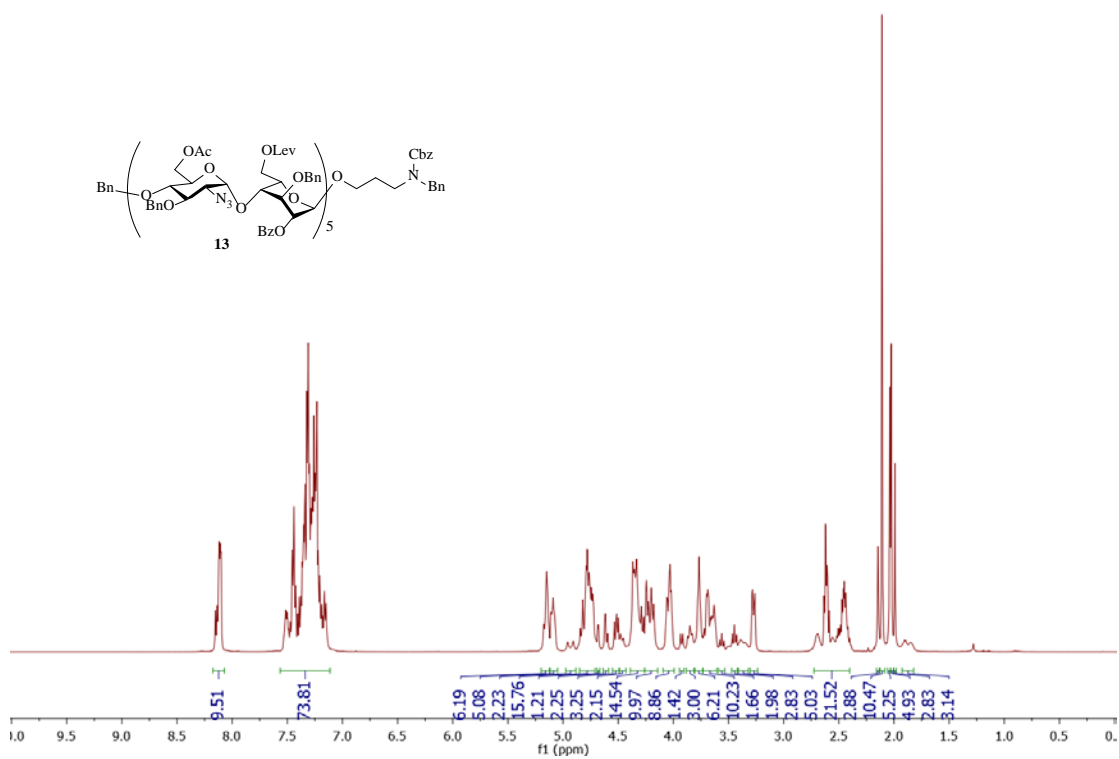
Figure 4.29. ^{1}H-NMR of **13** (500 MHz CDCl$_3$)
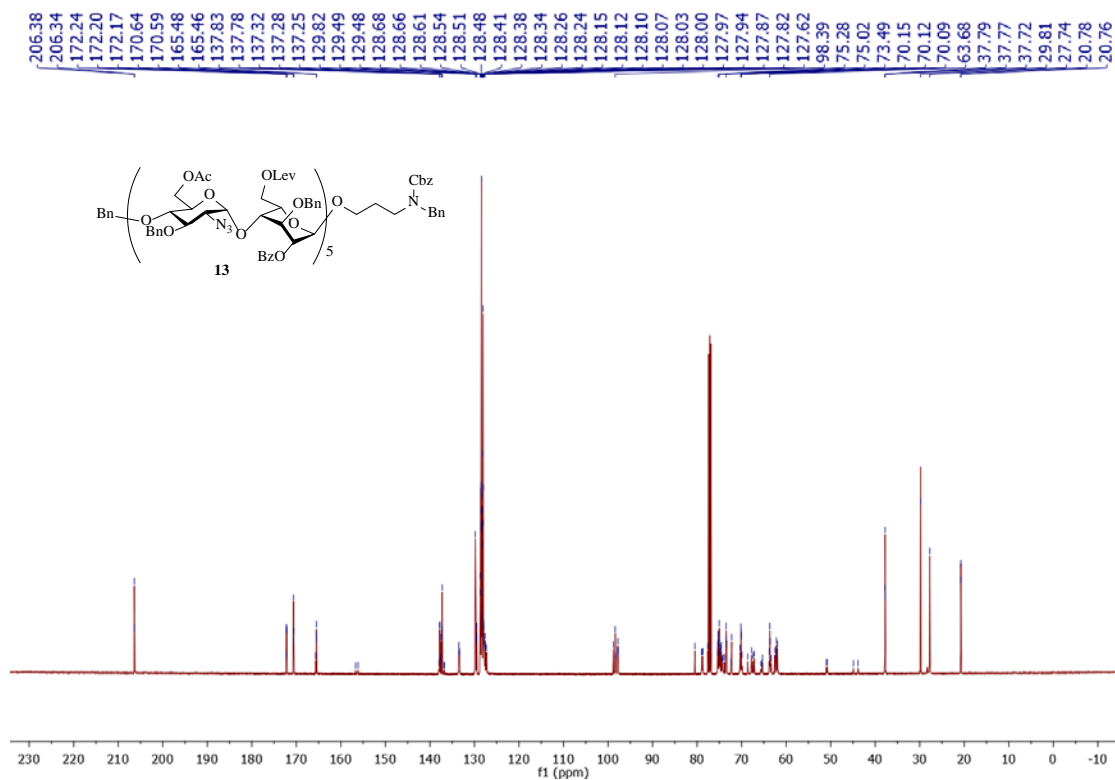
Figure 4.30. ^{13}C-NMR of **13** (125 MHz CDCl$_3$)
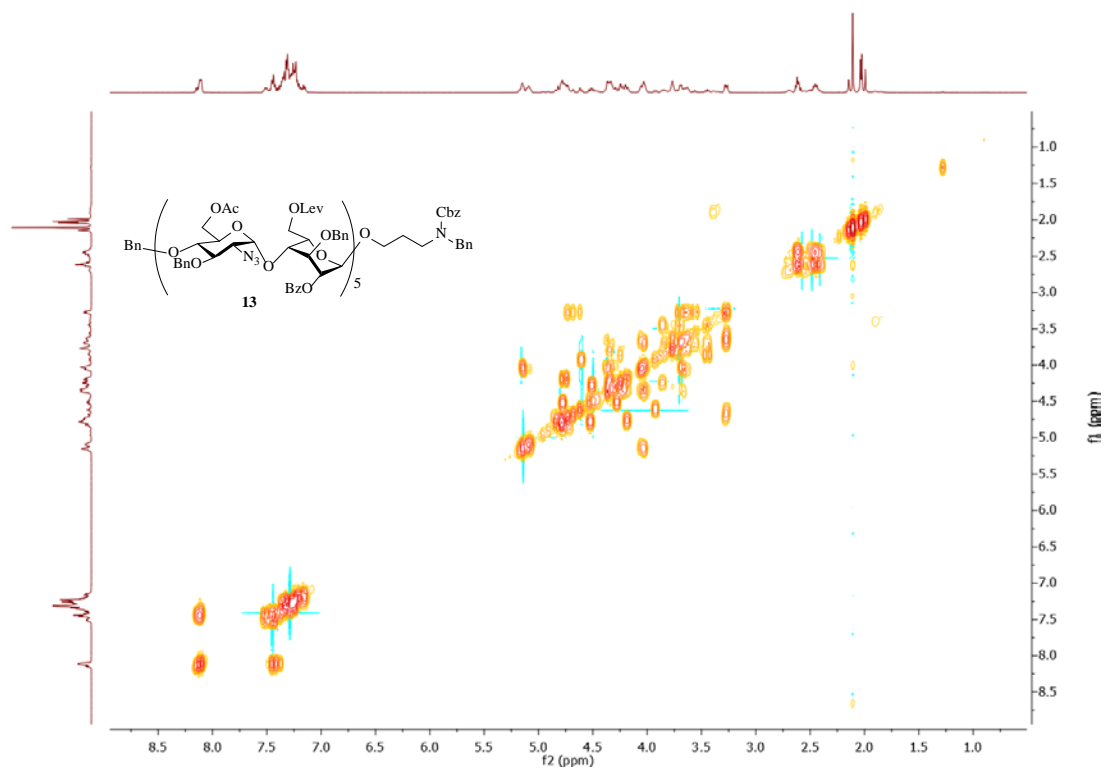
Figure 4.31. ^{1}H-^{1}H gCOSY of **13** (500 MHz CDCl$_3$)
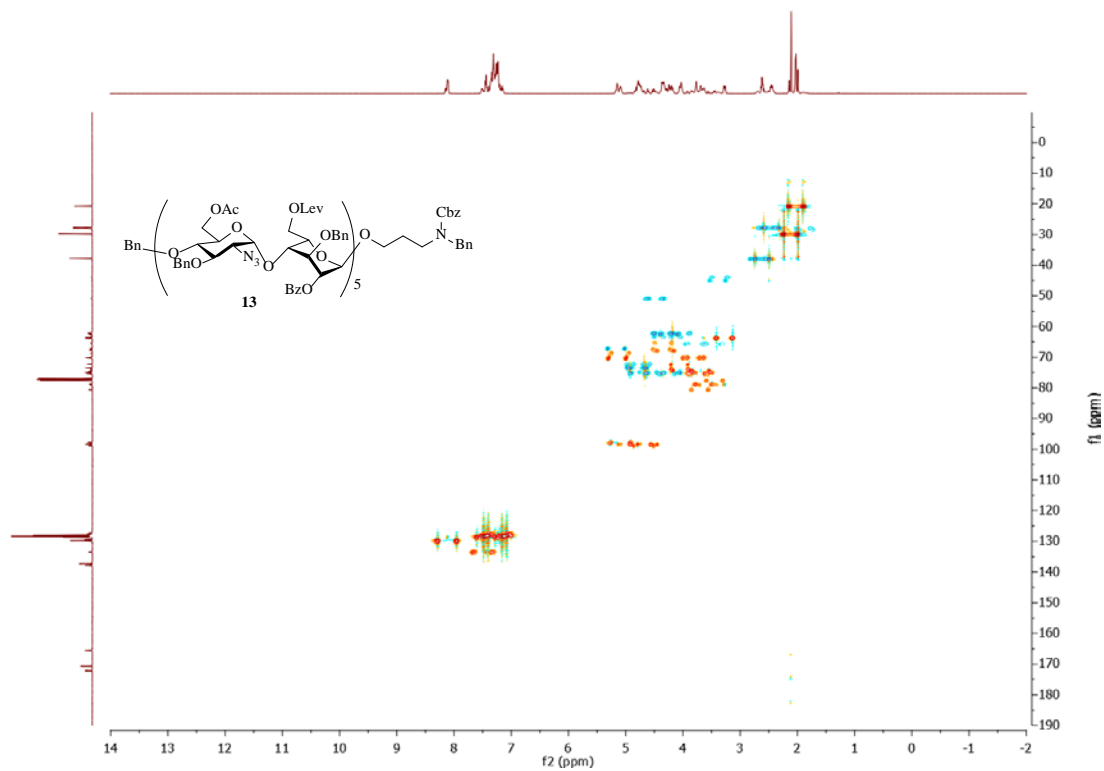
Figure 4.32. ^{1}H-^{13}C gHSQCAD of **13** (500 MHz CDCl$_3$)
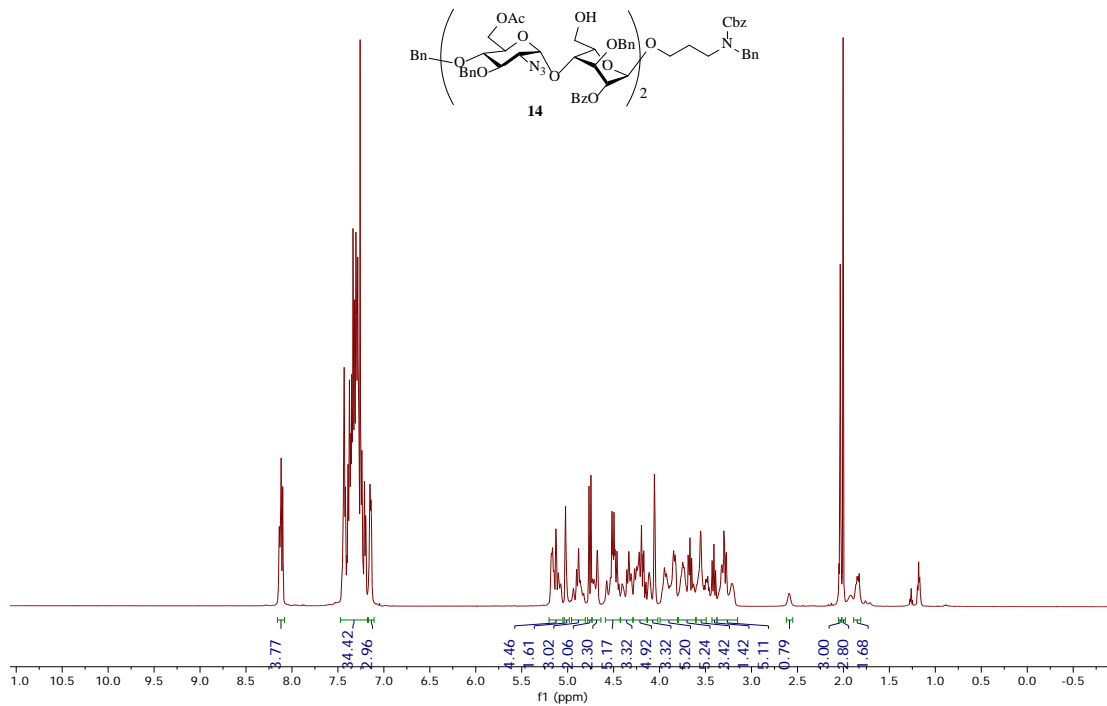
Figure 4.33. ^{1}H-NMR of **14** (500 MHz CDCl$_3$)
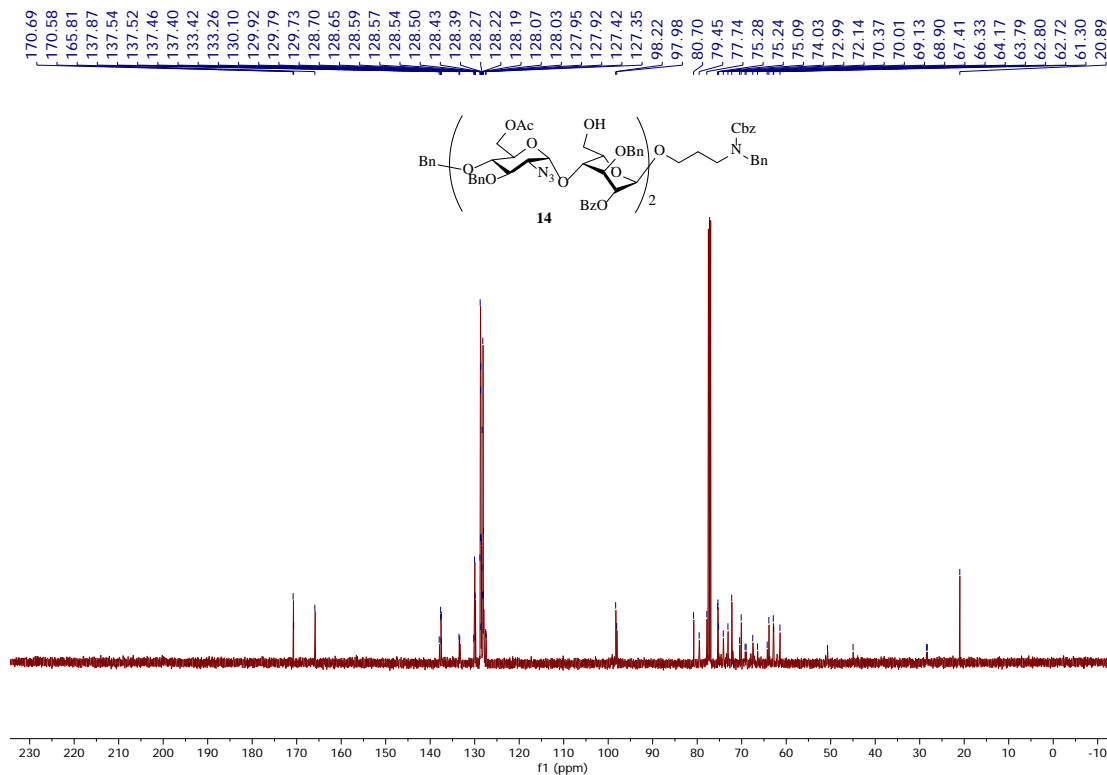
Figure 4.34. ^{13}C-NMR of **14** (125 MHz CDCl$_3$)
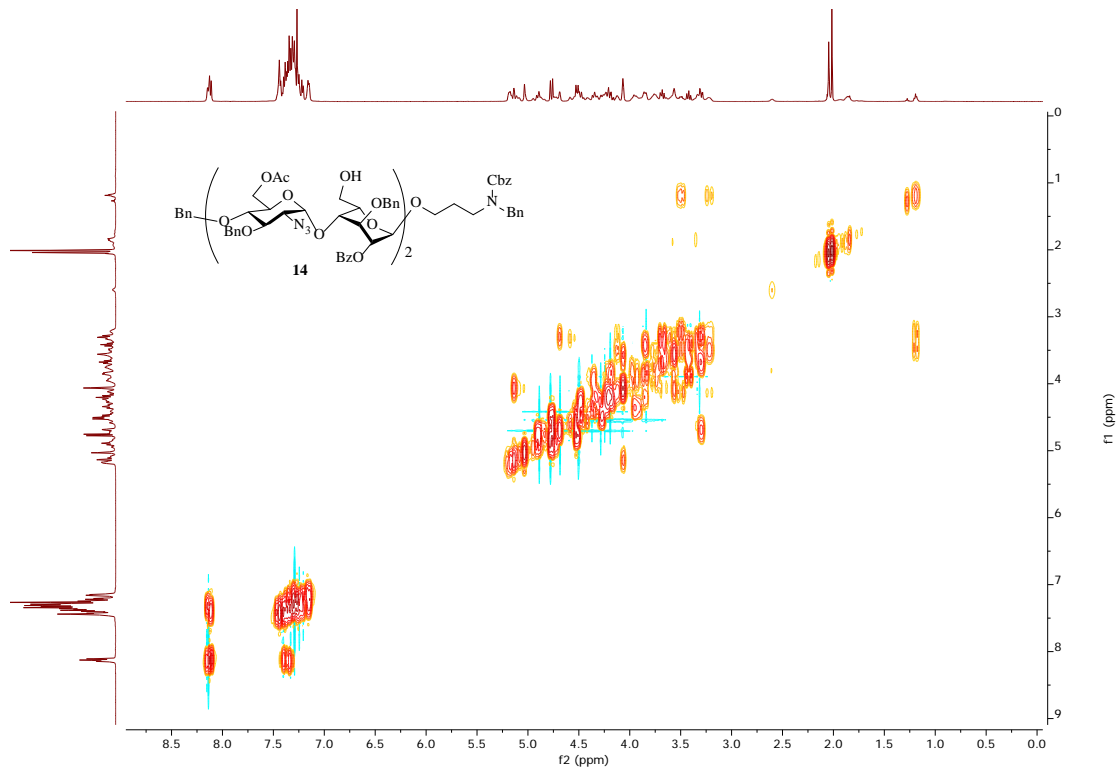
Figure 4.35. ^{1}H-^{1}H gCOSY of **14** (500 MHz CDCl$_3$)
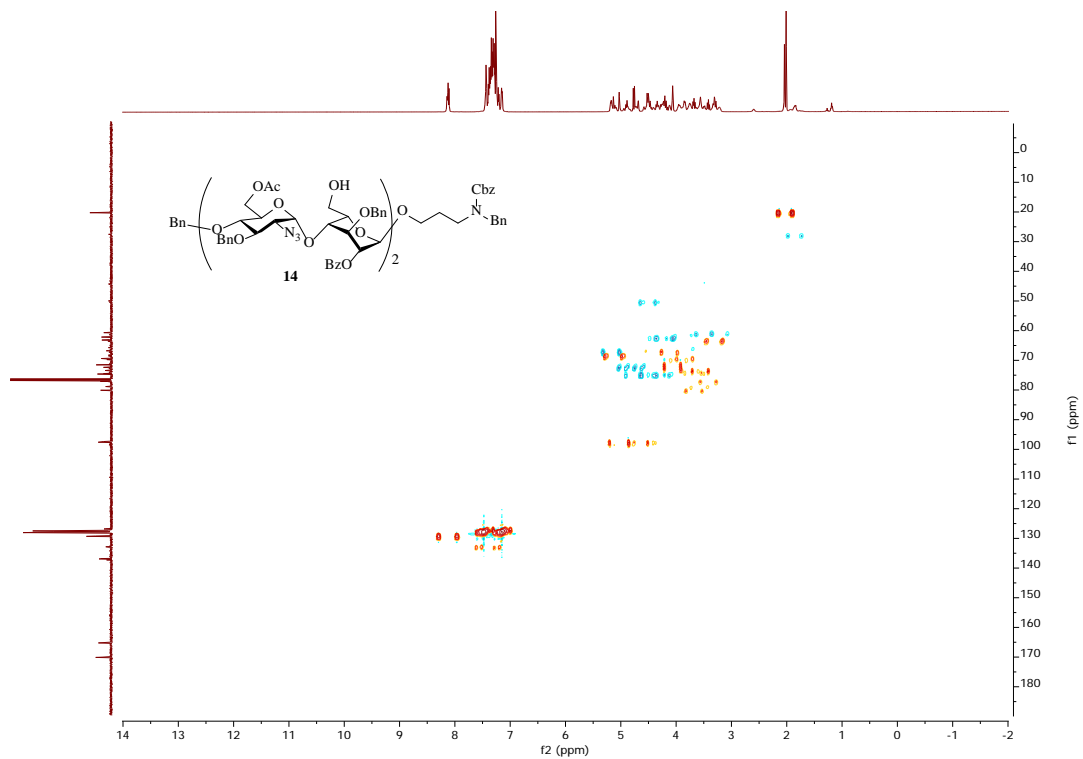
Figure 4.36. ^{1}H-^{13}C gHSQCAD of **14** (500 MHz CDCl$_3$)
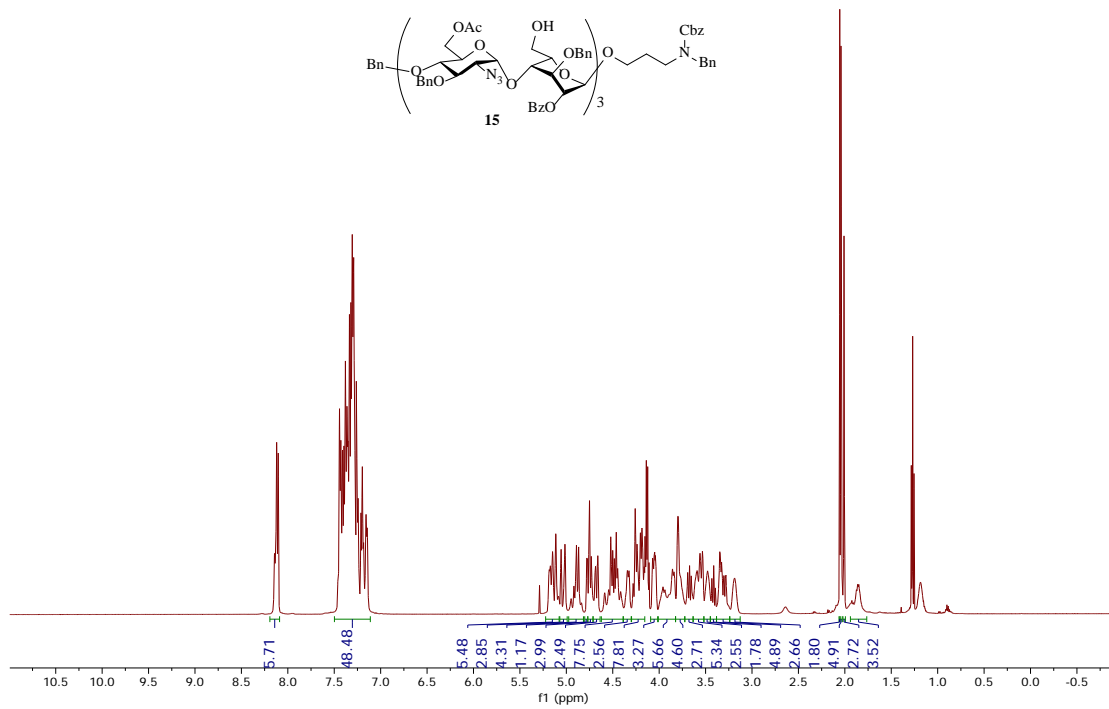
Figure 4.37. ^{1}H-NMR of **15** (500 MHz CDCl$_3$)
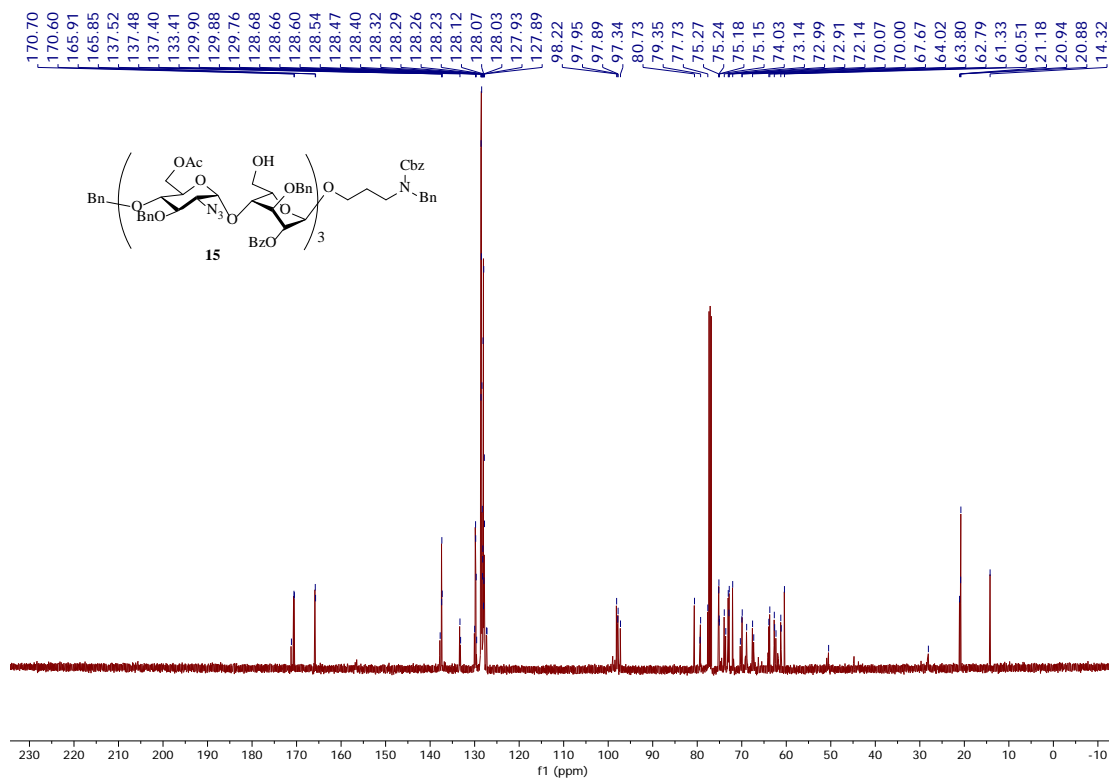
Figure 4.38. ^{13}C-NMR of **15** (125 MHz CDCl$_3$)
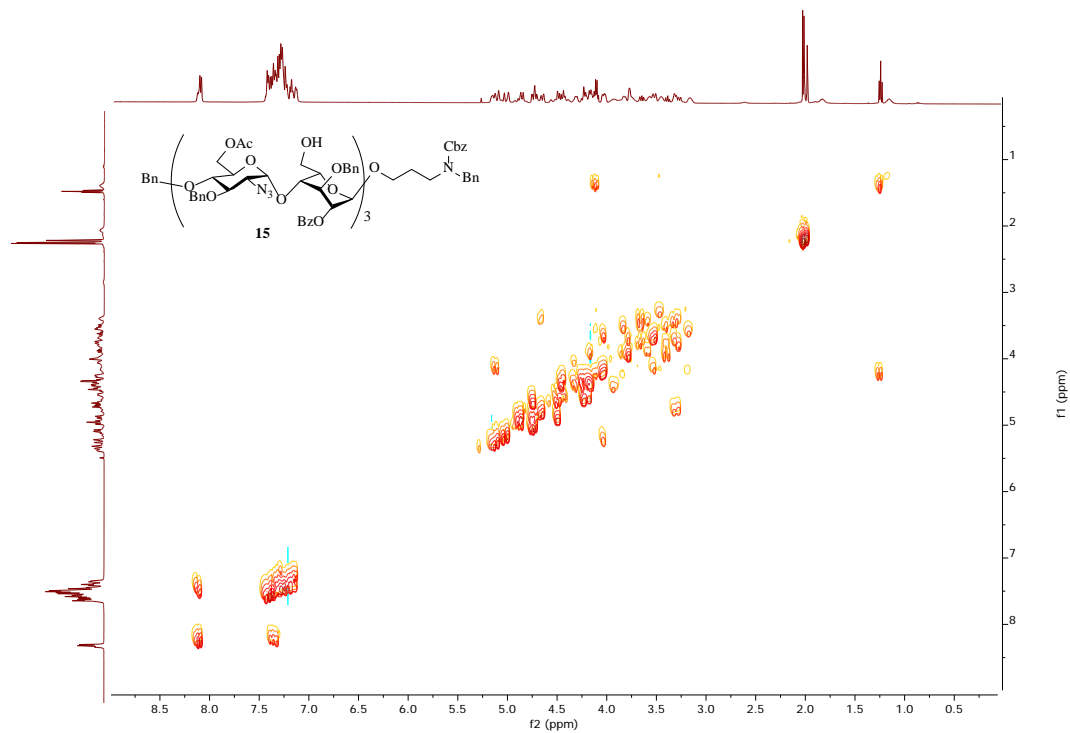
Figure 4.39. ^{1}H-^{1}H gCOSY of **15** (500 MHz CDCl$_3$)
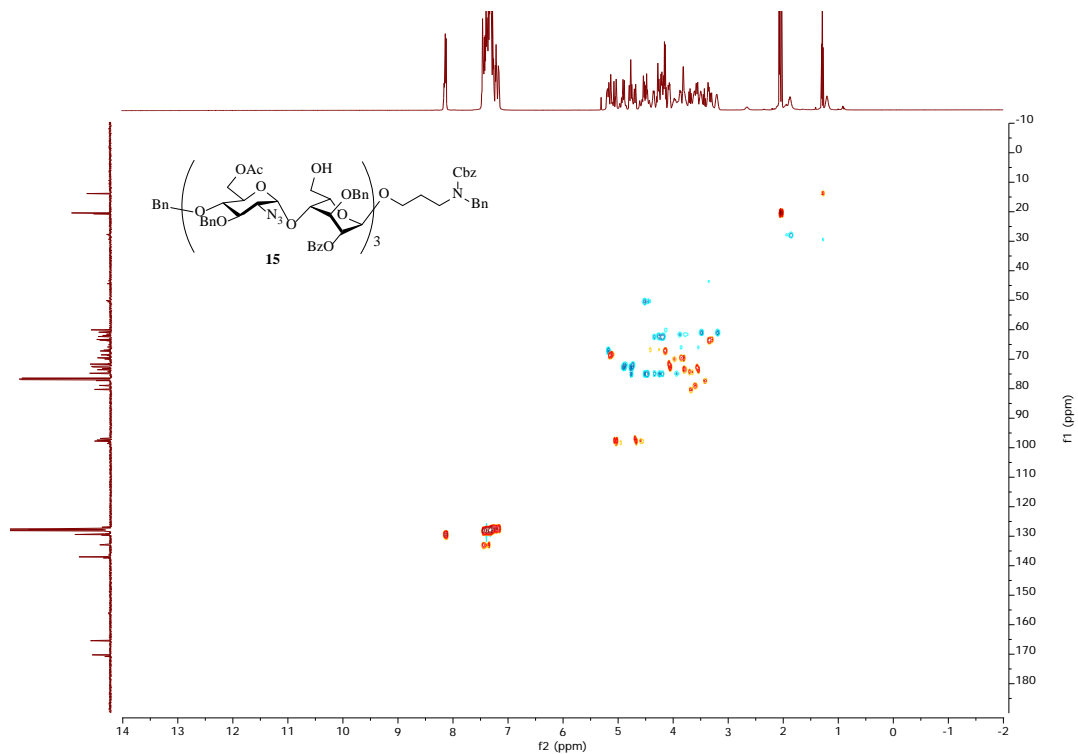
Figure 4.40. ^{1}H-^{13}C gHSQCAD of **15** (500 MHz CDCl$_3$)

Figure 4.41. ^{1}H-NMR of **16** (500 MHz CDCl$_3$)

Figure 4.42. ^{13}C-NMR of **16** (125 MHz CDCl$_3$)
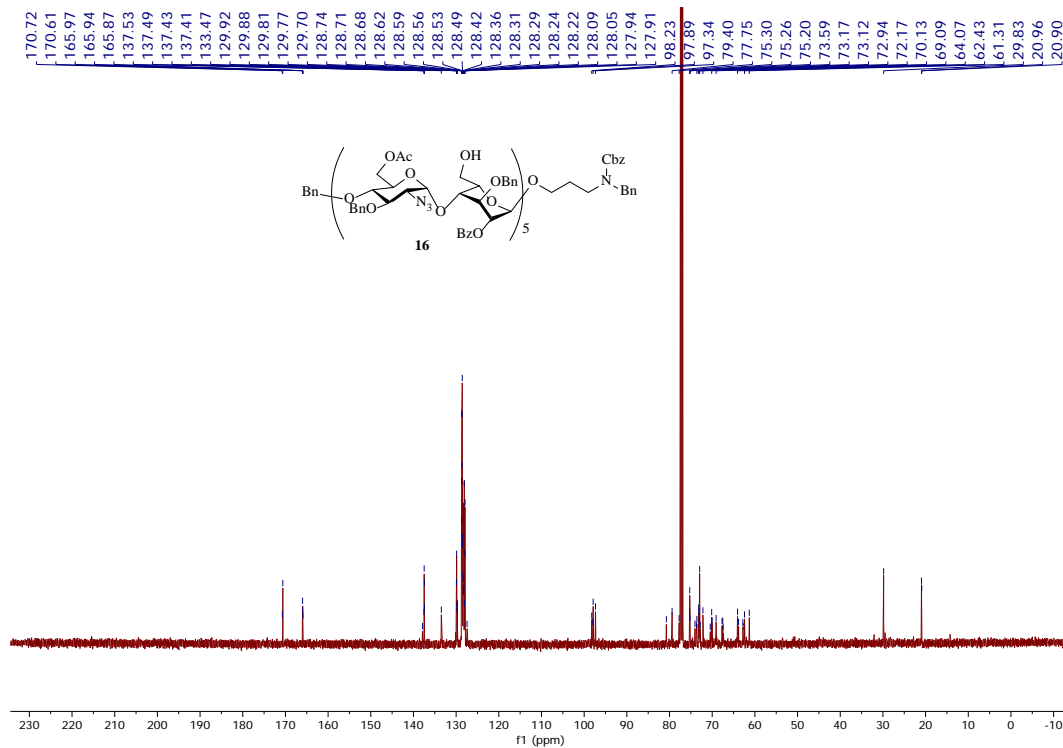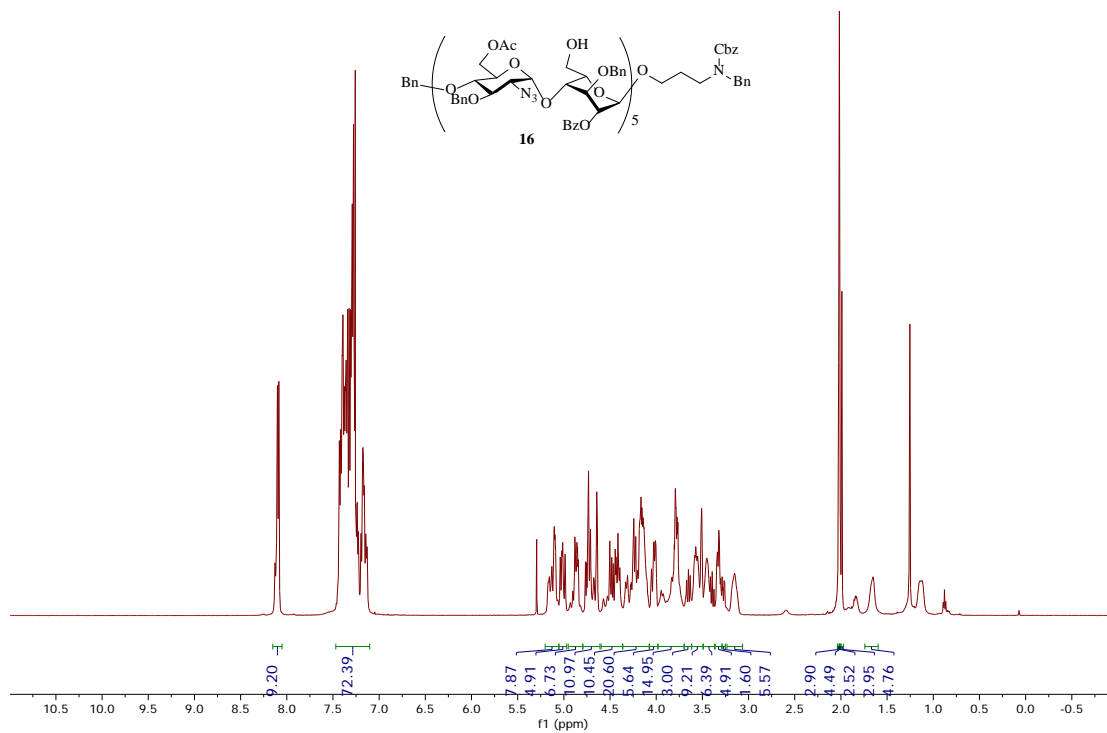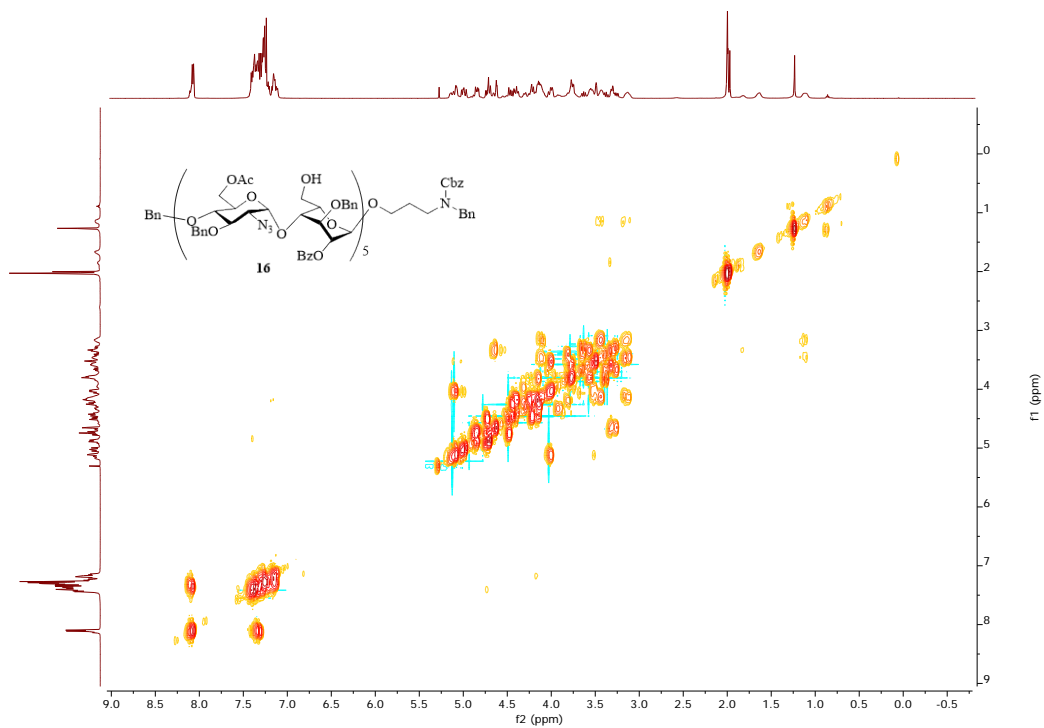
Figure 4.43. ^{1}H-^{1}H gCOSY of **16** (500 MHz CDCl$_3$)
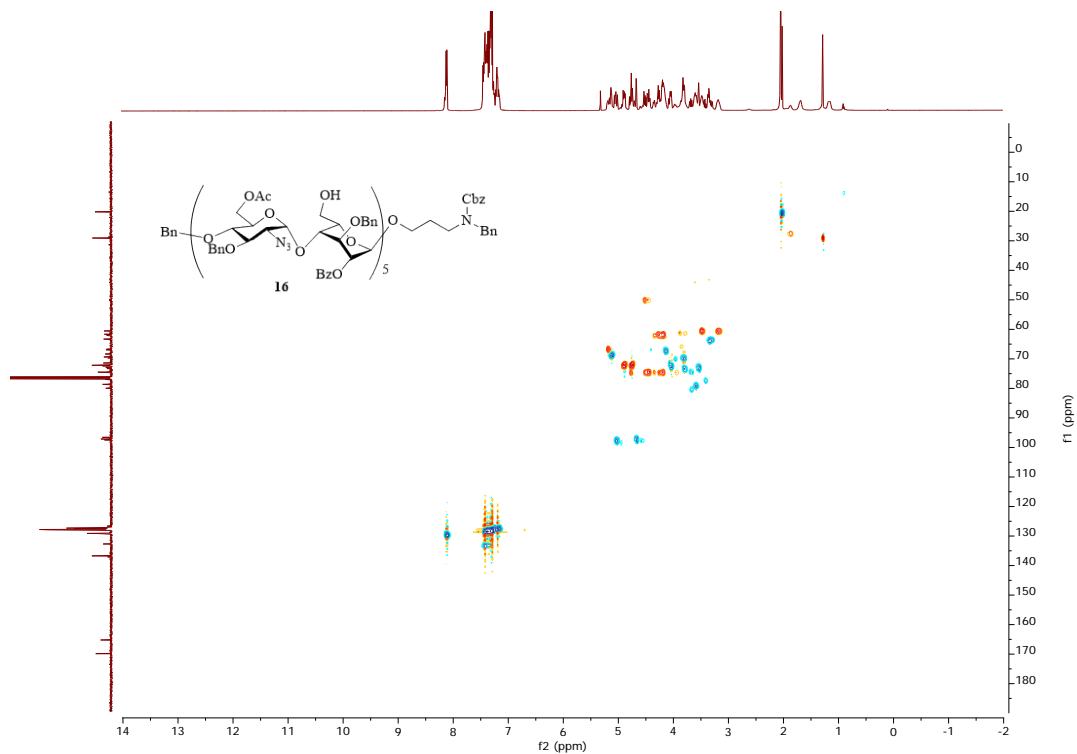
Figure 4.44. ^{1}H-^{13}C gHSQCAD of **16** (500 MHz CDCl$_3$)
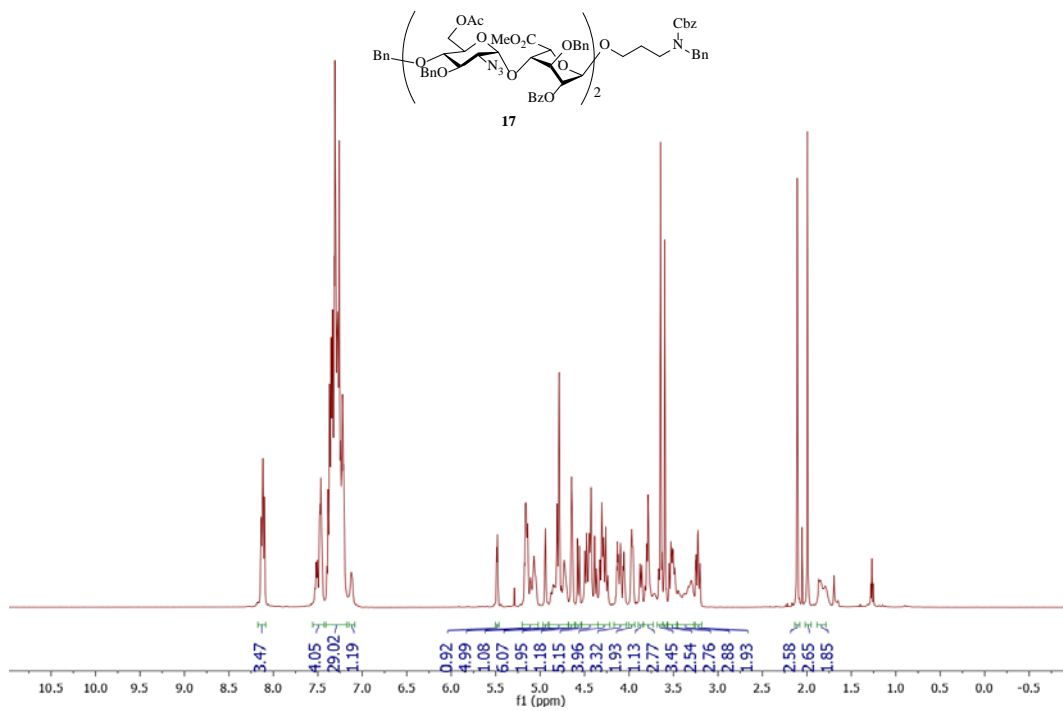
Figure 4.45. ^{1}H-NMR of **17** (500 MHz CDCl$_3$)
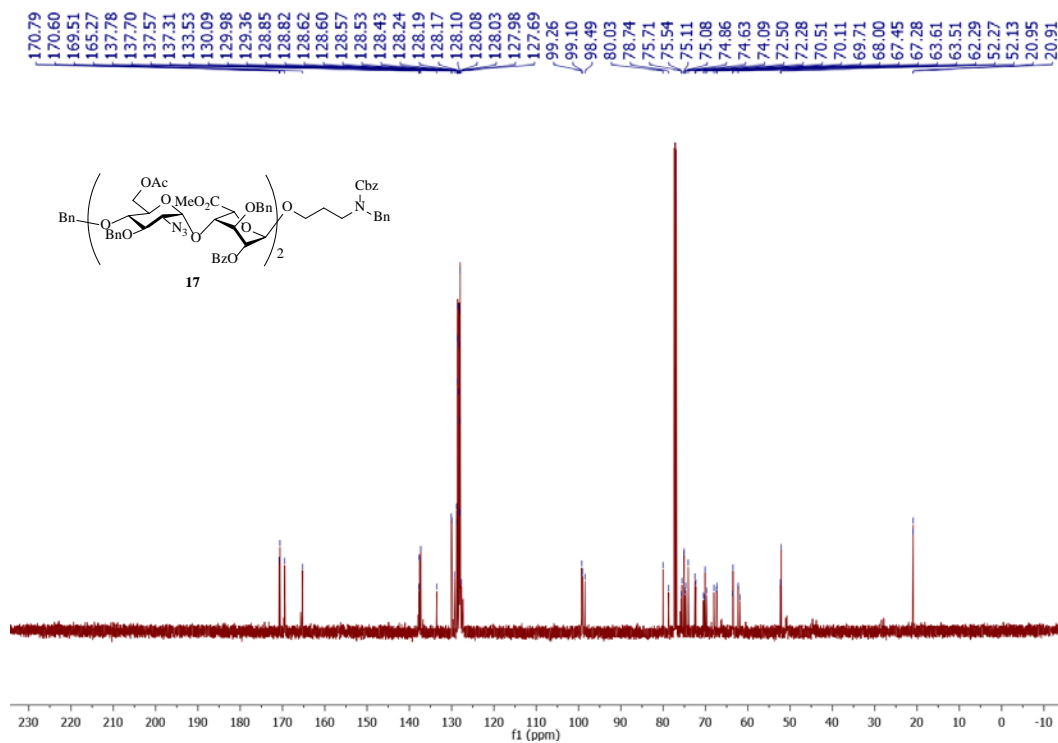
Figure 4.46. ^{13}C-NMR of **17** (125 MHz CDCl$_3$)
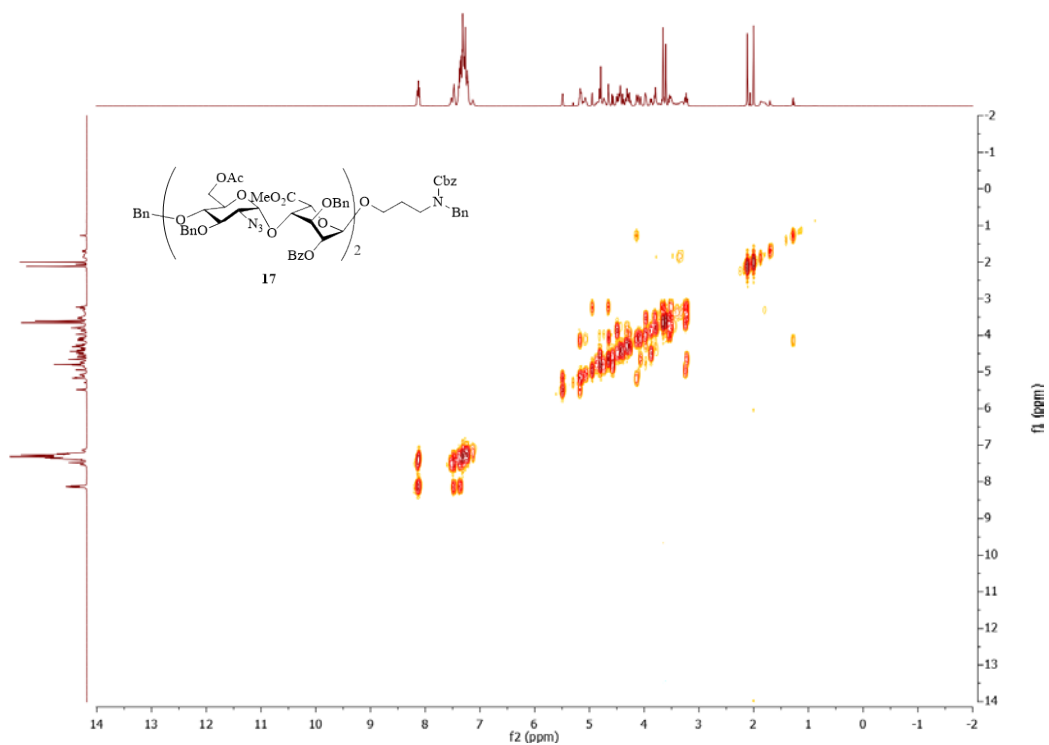
Figure 4.47. ^{1}H-^{1}H gCOSY of **17** (500 MHz CDCl$_3$)
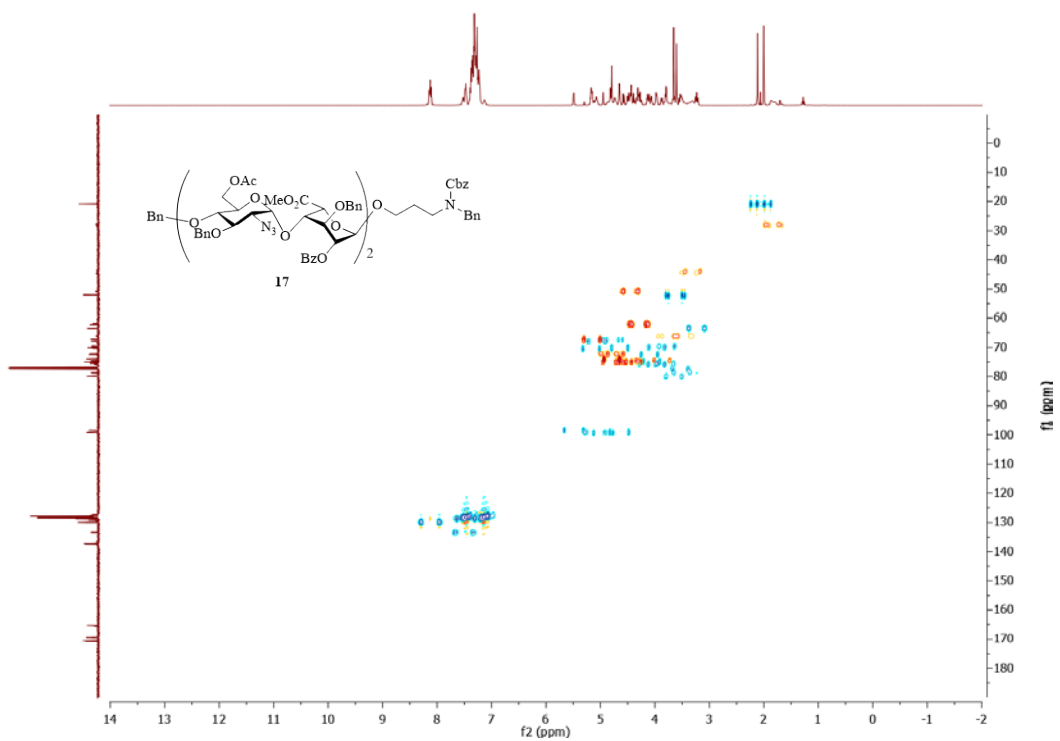
Figure 4.48. ^{1}H-^{13}C gHSQCAD of **17** (500 MHz CDCl$_3$)
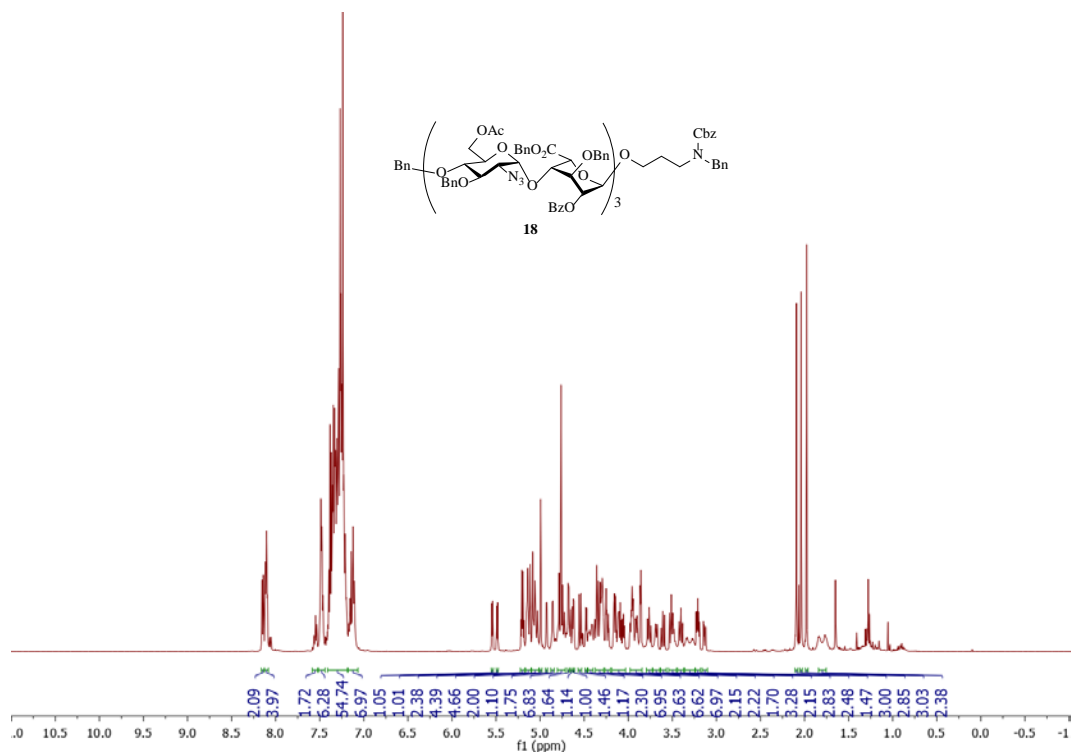
Figure 4.49. ^{1}H-NMR of **18** (500 MHz CDCl$_3$)
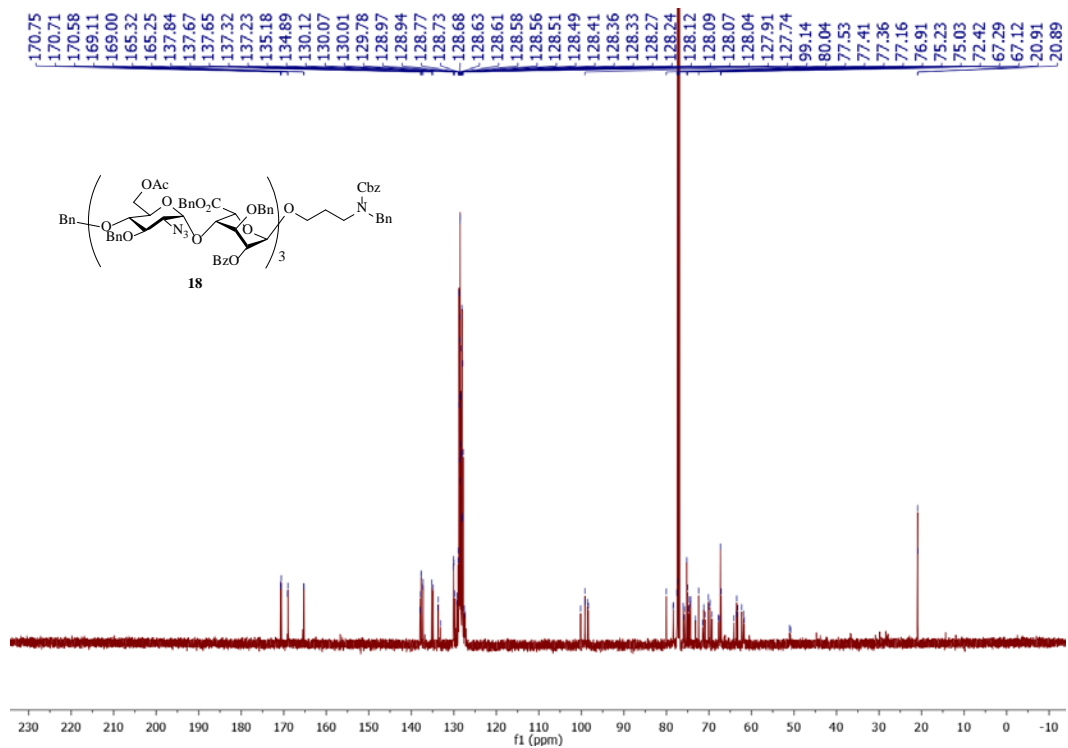
Figure 4.50. ^{13}C-NMR of **18** (125 MHz CDCl$_3$)
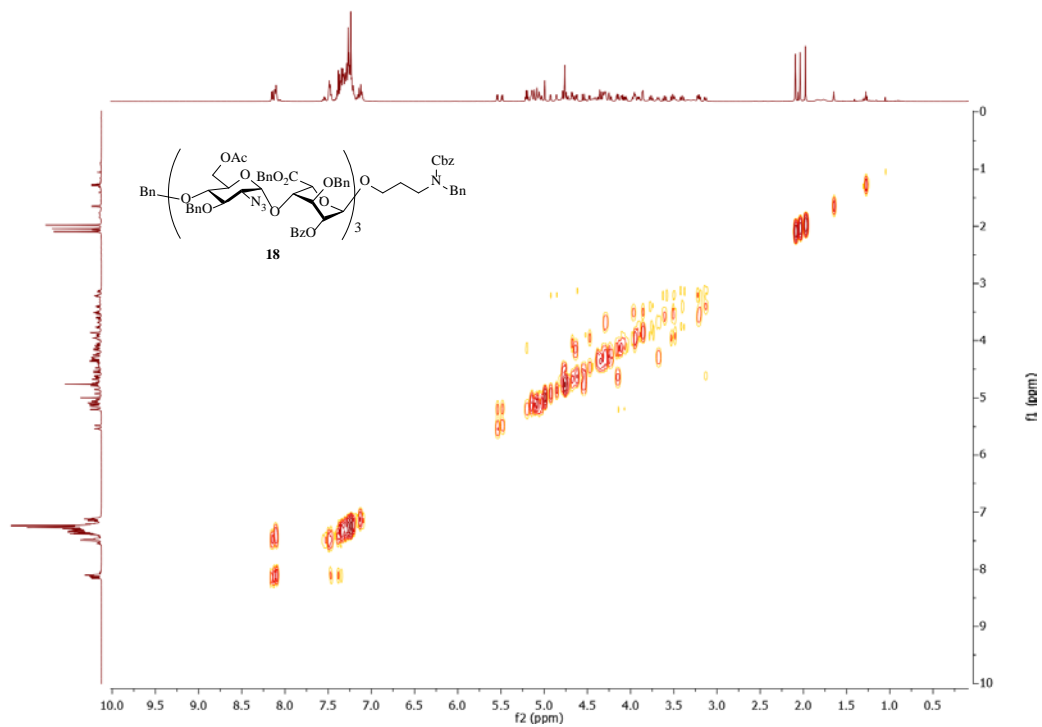
Figure 4.51. ^{1}H-^{1}H gCOSY of **18** (500 MHz CDCl$_3$)
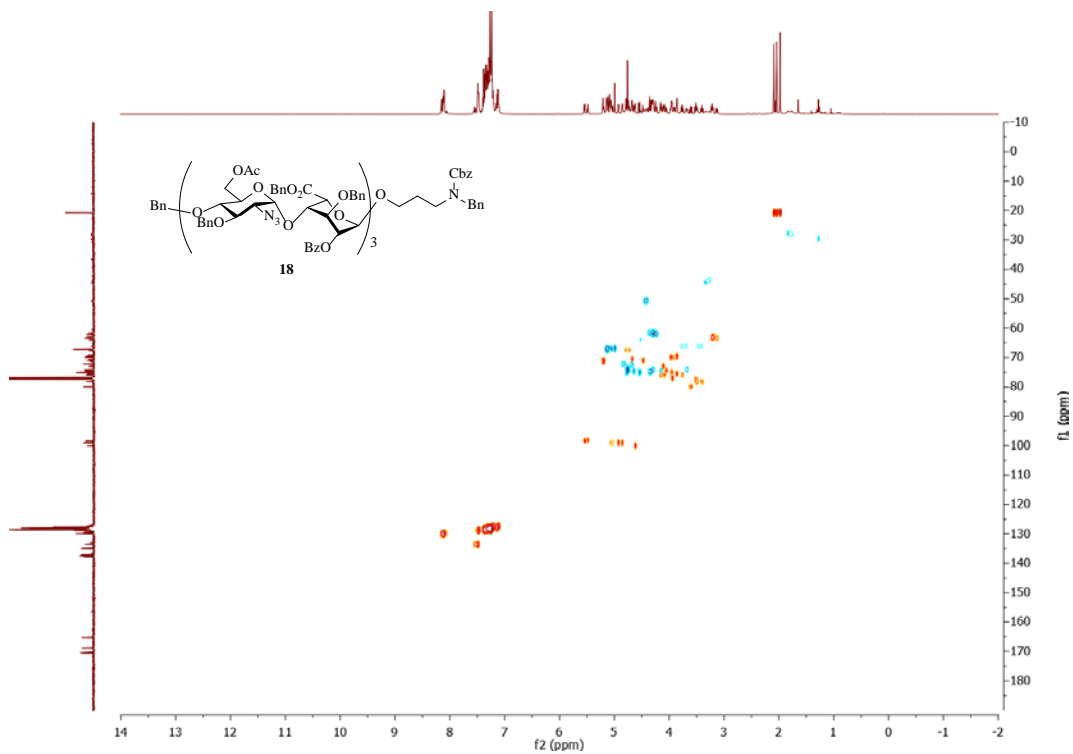
Figure 4.52. ^{1}H-^{13}C gHSQCAD of **18** (500 MHz CDCl$_3$)
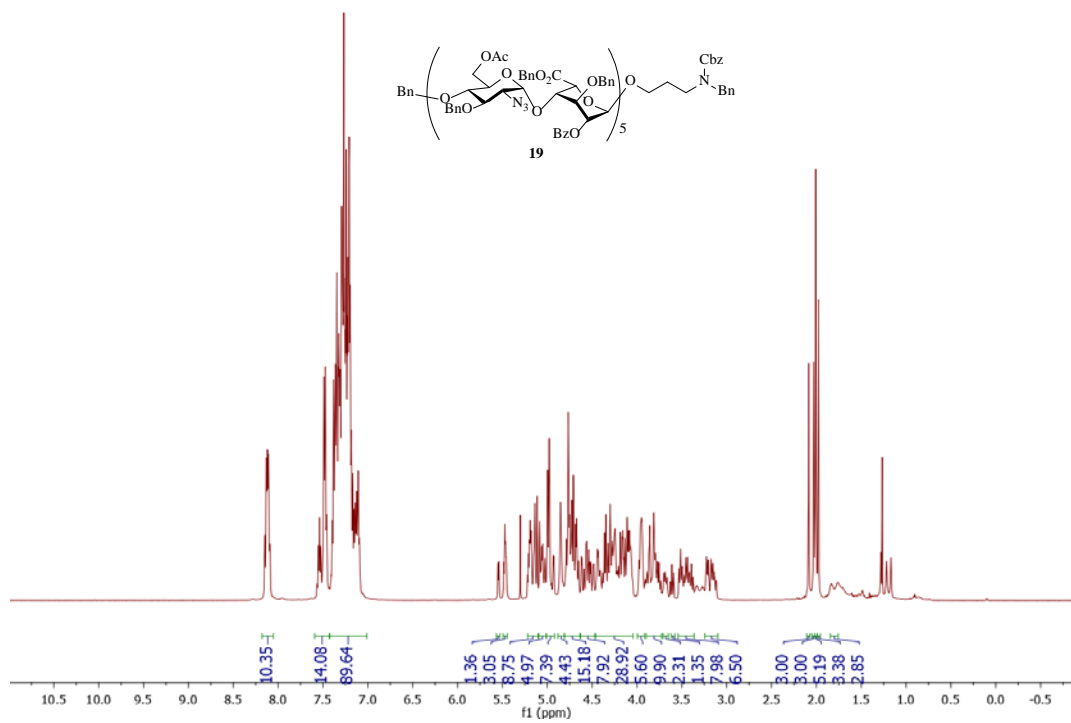
Figure 4.53. ^{1}H-NMR of **19** (500 MHz CDCl$_3$)
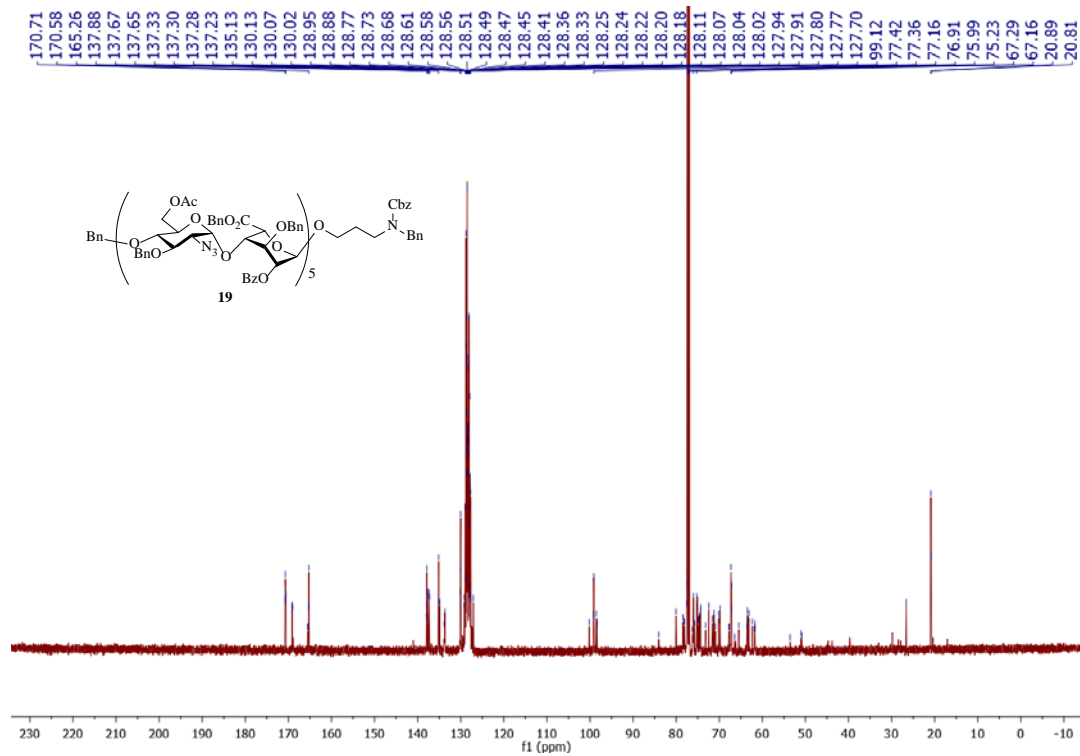
Figure 4.54. ^{13}C-NMR of **19** (125 MHz CDCl$_3$)
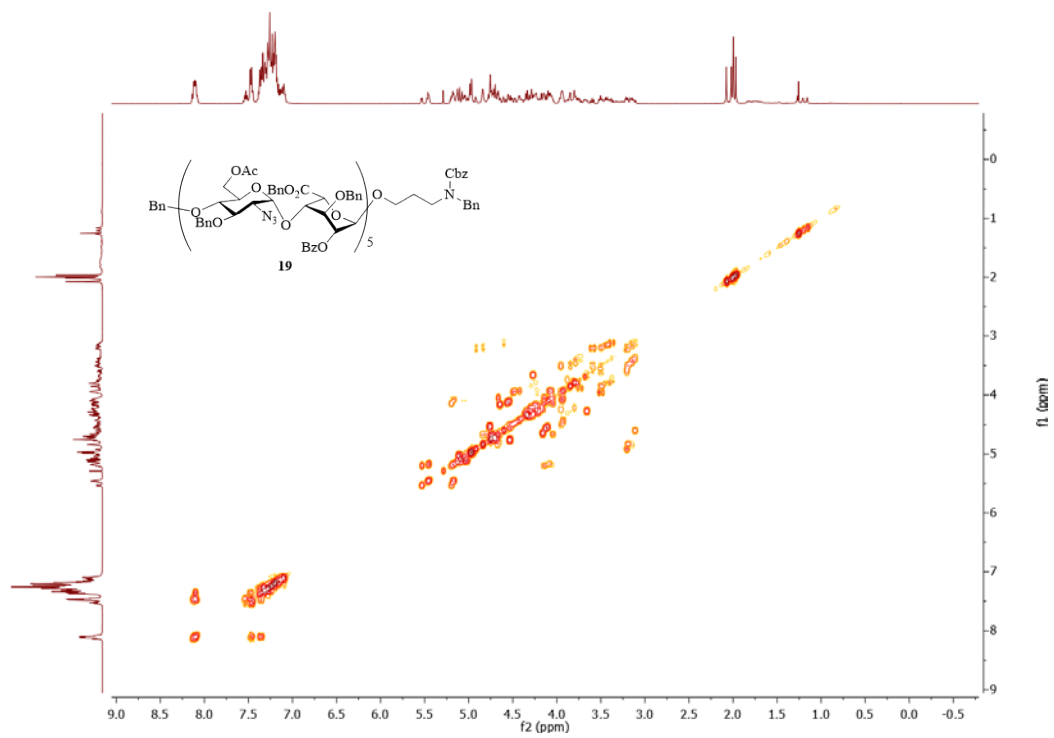
Figure 4.55. ^{1}H-^{1}H gCOSY of **19** (500 MHz CDCl$_3$)
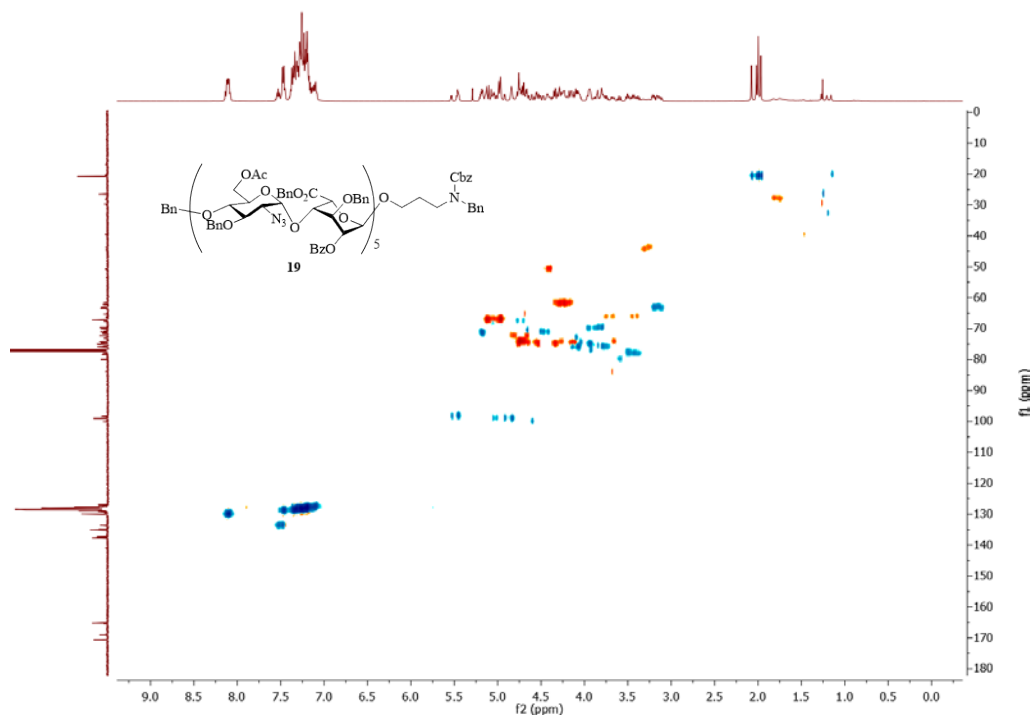
Figure 4.56. ^{1}H-^{13}C gHSQCAD of **19** (500 MHz CDCl$_3$)
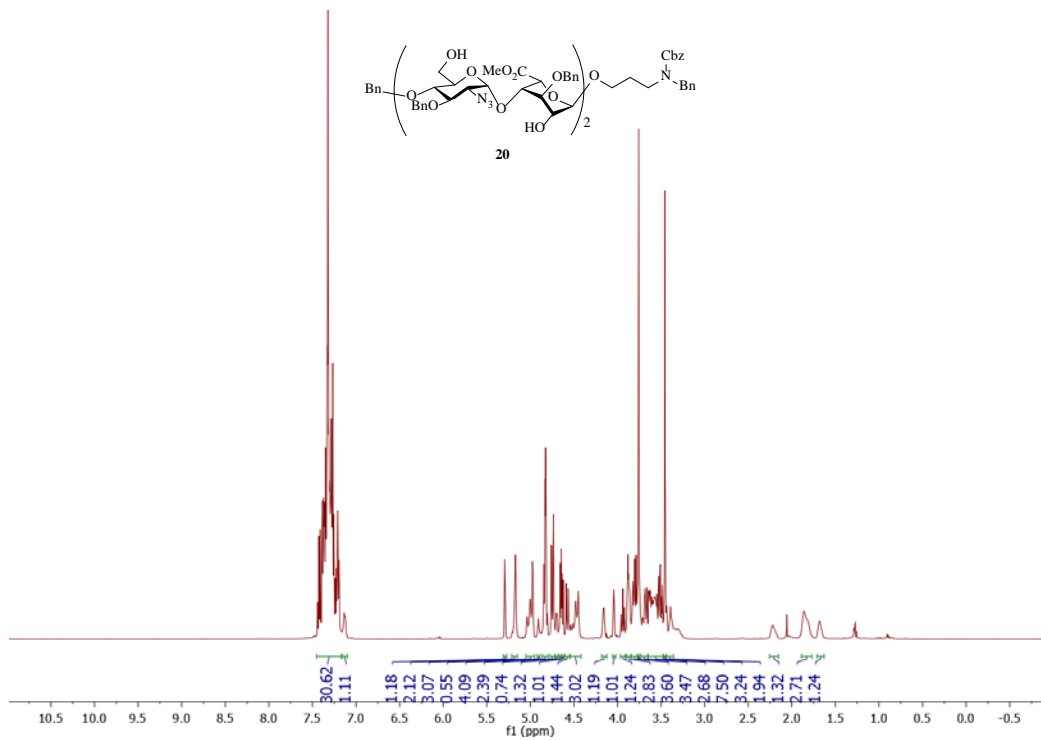
Figure 4.57. ^{1}H-NMR of **20** (500 MHz CDCl$_3$)
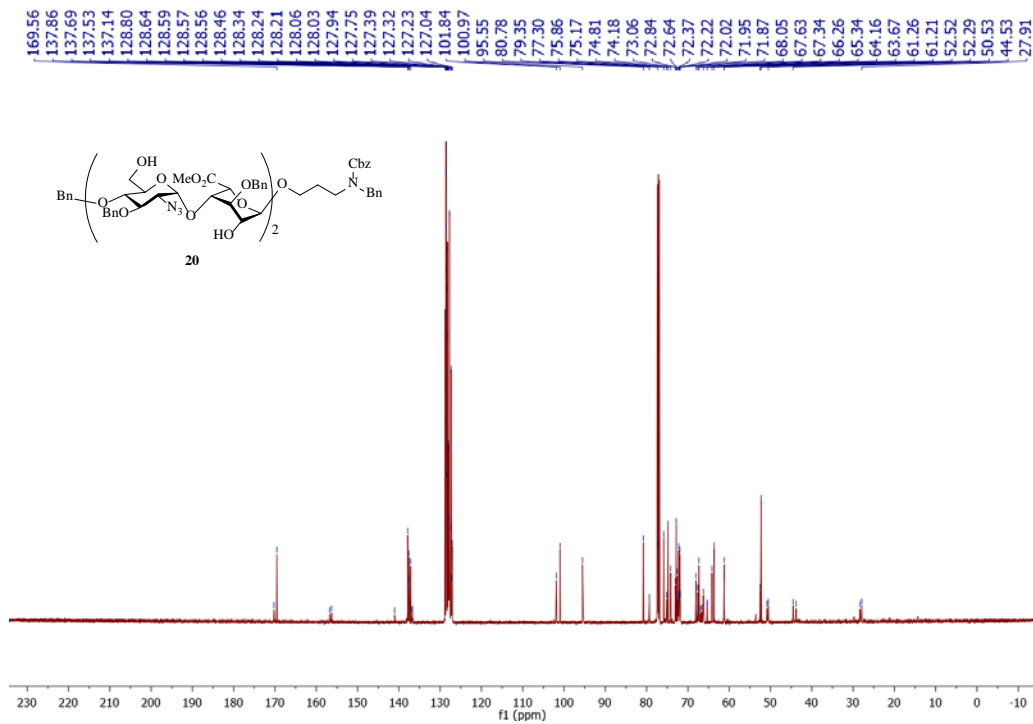
Figure 4.58. ^{13}C-NMR of **20** (125 MHz CDCl$_3$)
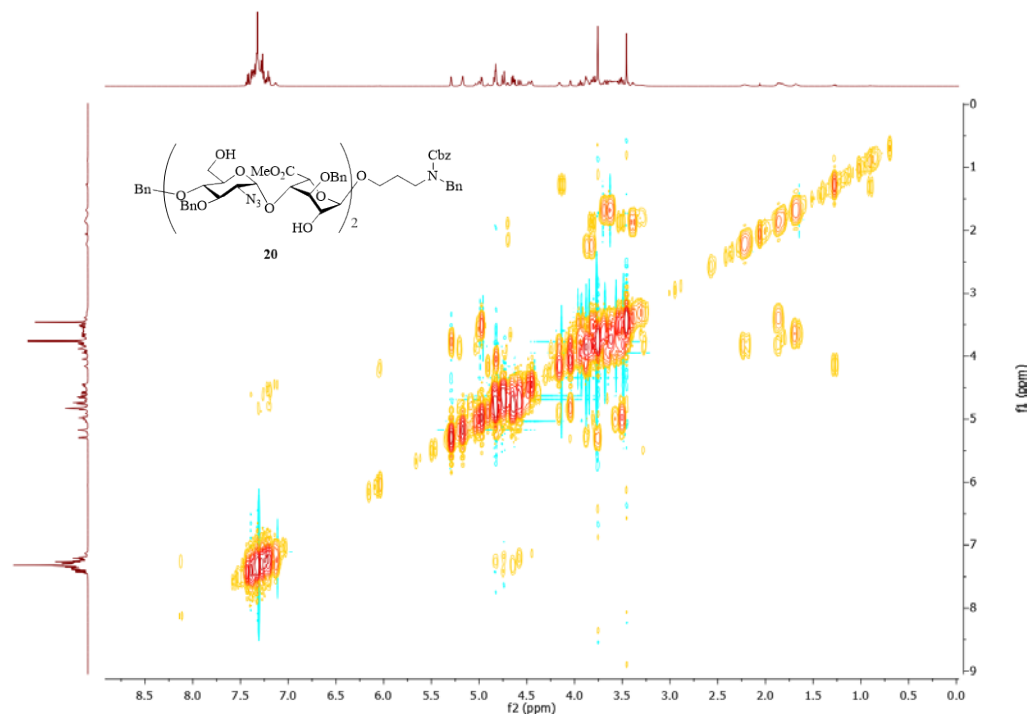
Figure 4.59. ^{1}H-^{1}H gCOSY of **20** (500 MHz CDCl$_3$)
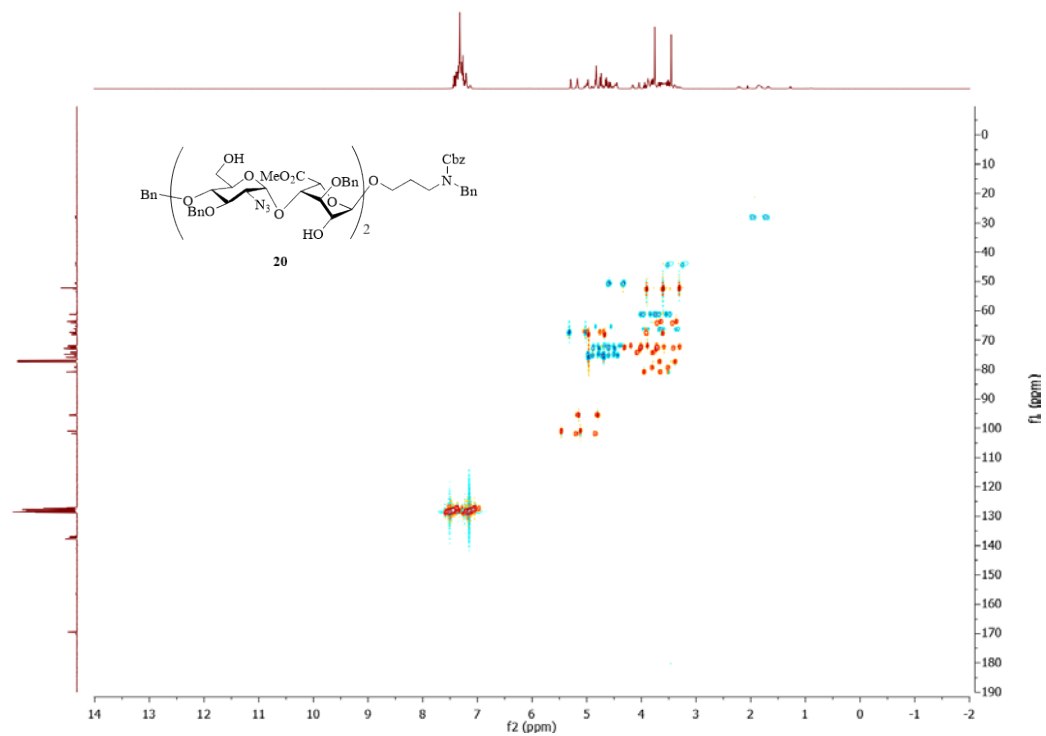
Figure 4.60. ^{1}H-^{13}C gHSQCAD of **20** (500 MHz CDCl$_3$)
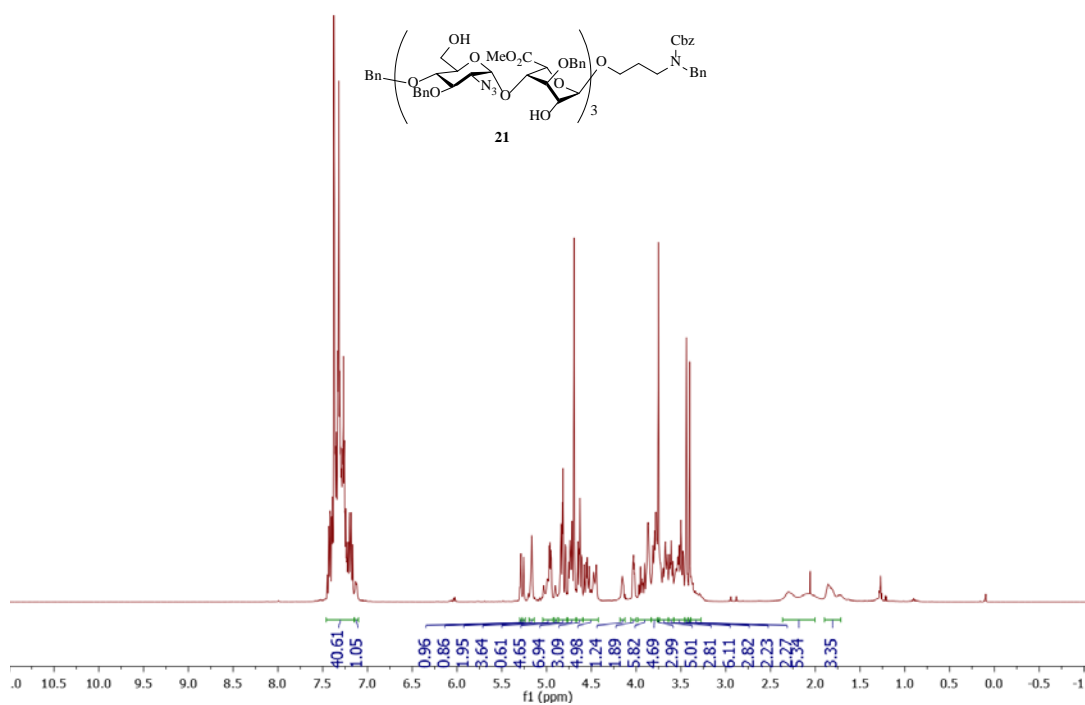
Figure 4.61. ^{1}H-NMR of **21** (500 MHz CDCl$_3$)
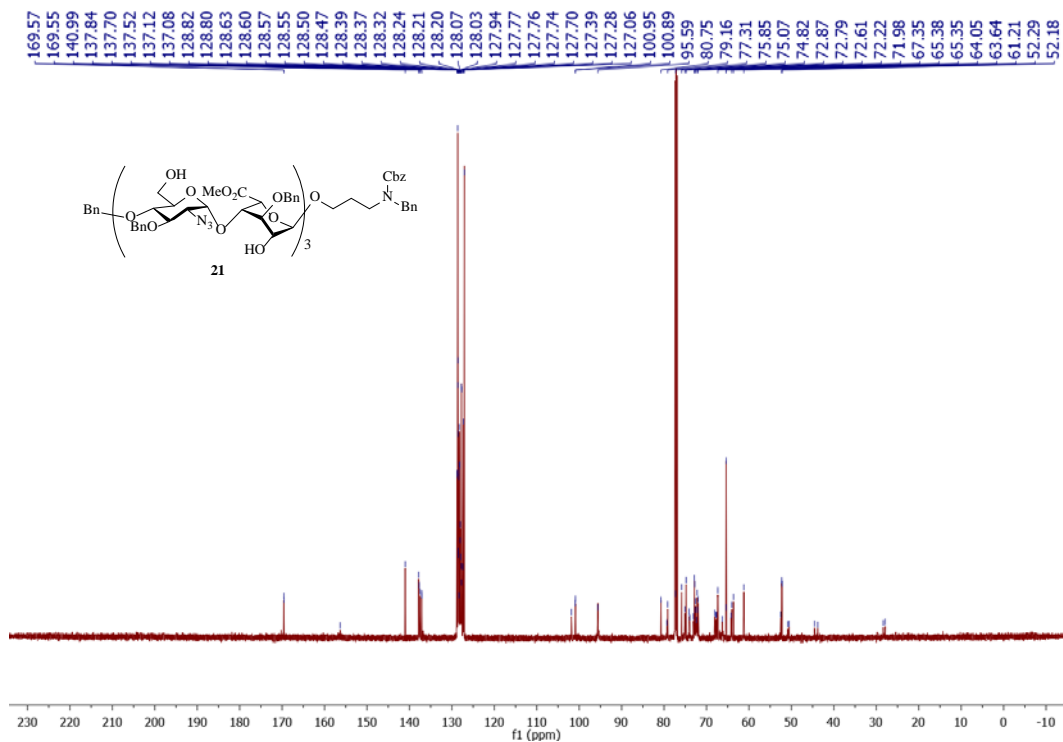
Figure 4.62. ^{13}C-NMR of **21** (125 MHz CDCl$_3$)
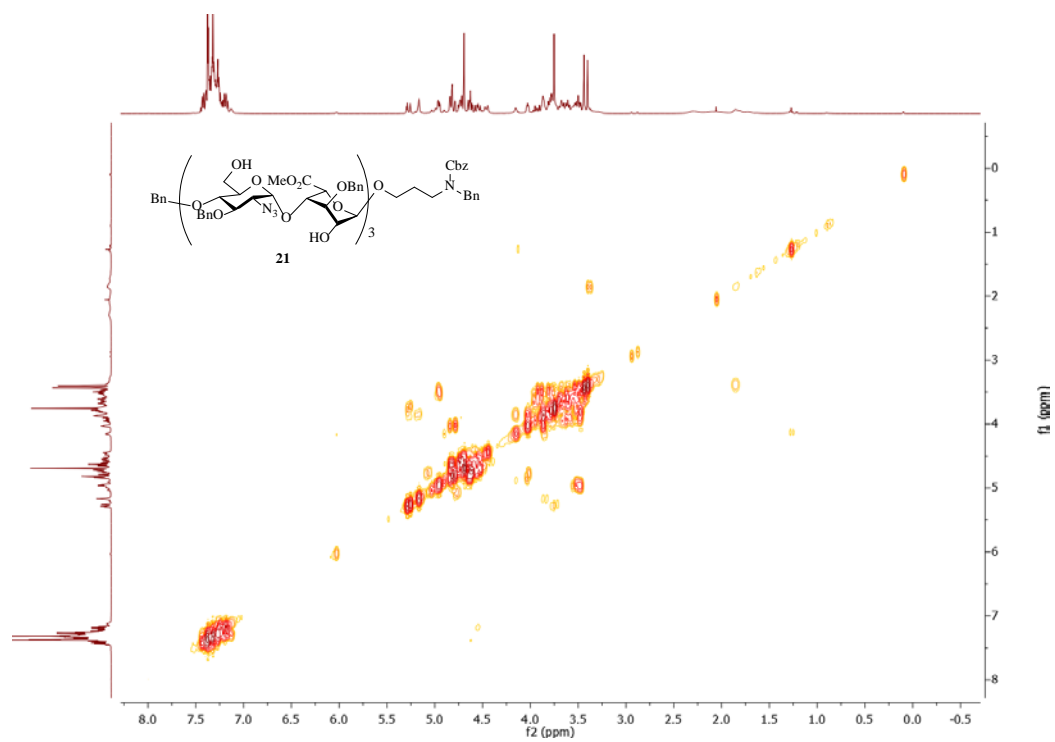
Figure 4.63. ^{1}H-^{1}H gCOSY of **21** (500 MHz CDCl$_3$)

Figure 4.64. ^{1}H-^{13}C gHSQCAD of **21** (500 MHz CDCl$_3$)
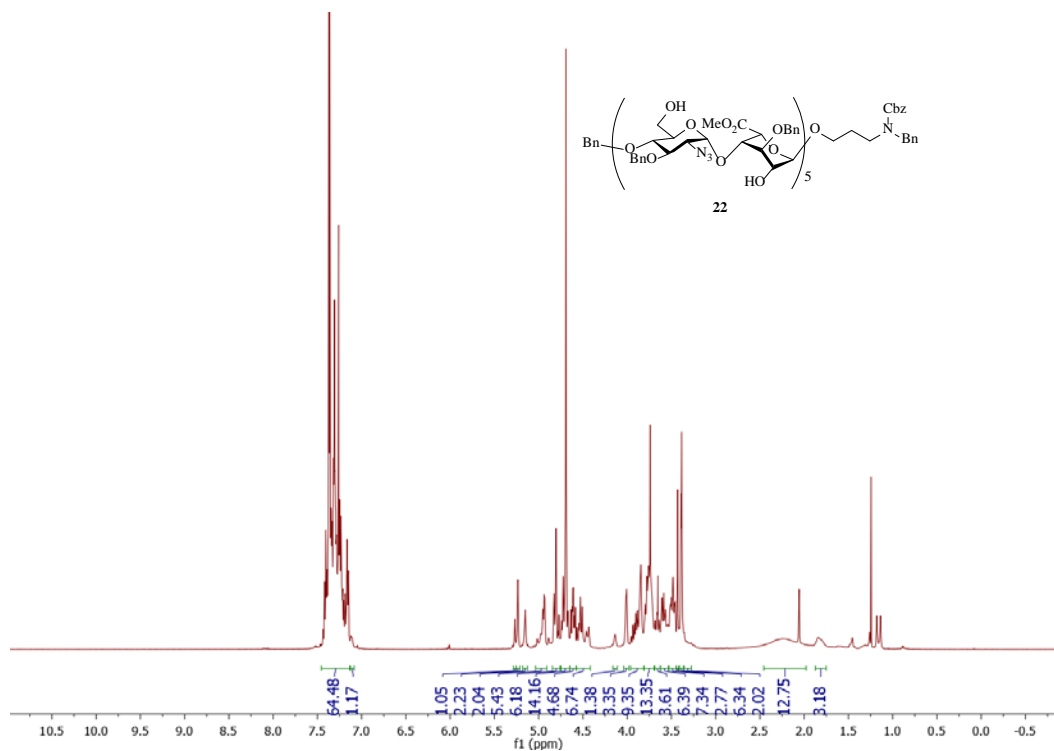
Figure 4.65. ^{1}H-NMR of **22** (500 MHz CDCl$_3$)
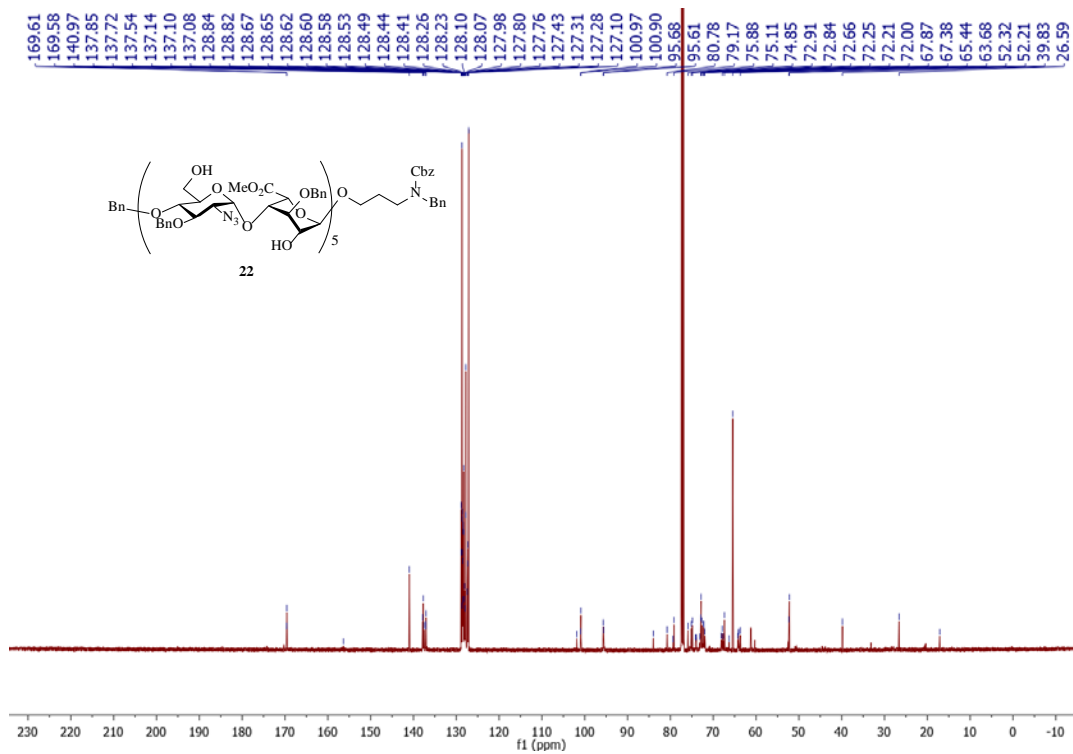
Figure 4.66. ^{13}C-NMR of **22** (125 MHz CDCl$_3$)
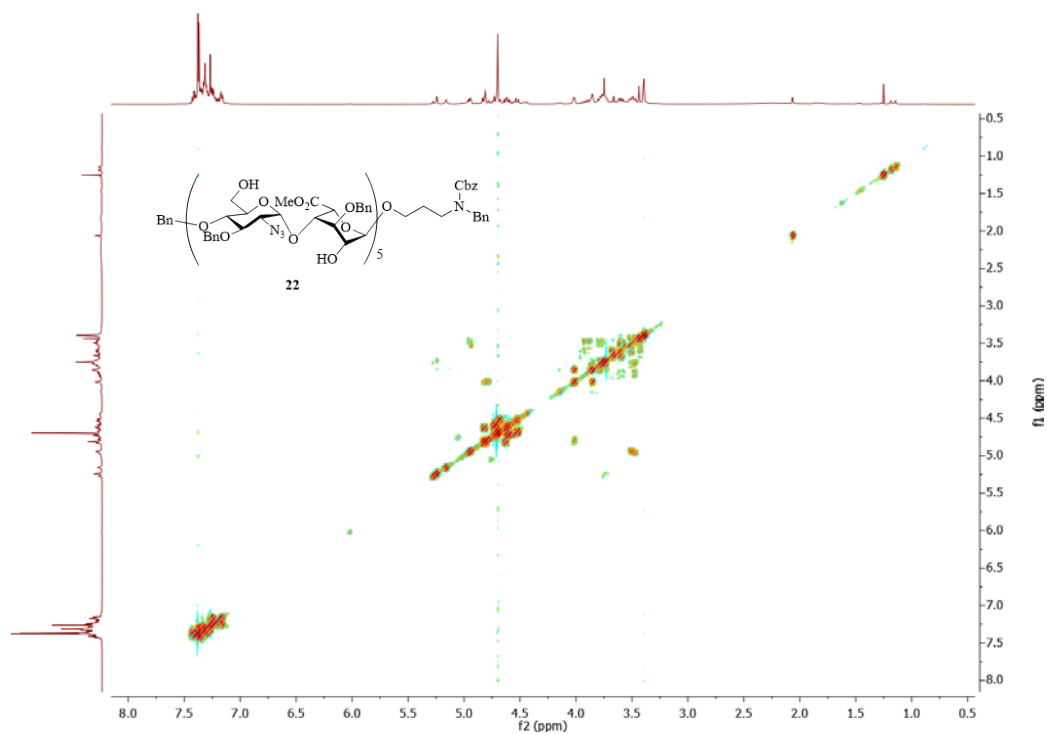
Figure 4.67. ^{1}H-^{1}H gCOSY of **22** (500 MHz CDCl$_3$)
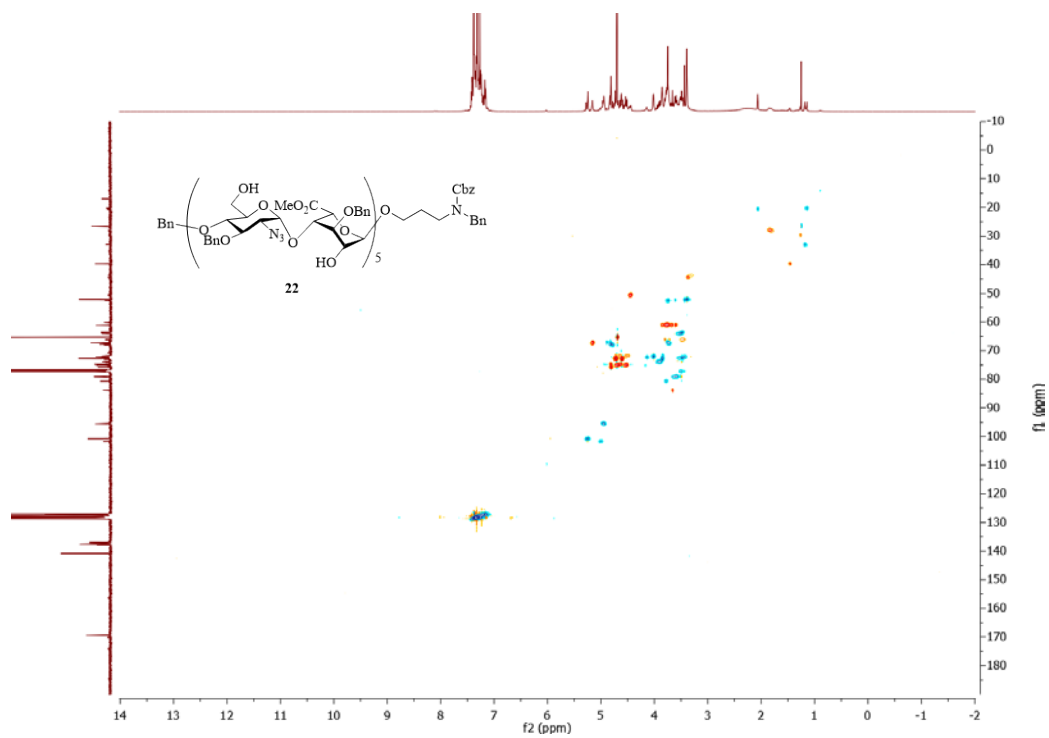
Figure 4.68. ^{1}H-^{13}C gHSQCAD of **22** (500 MHz CDCl$_3$)
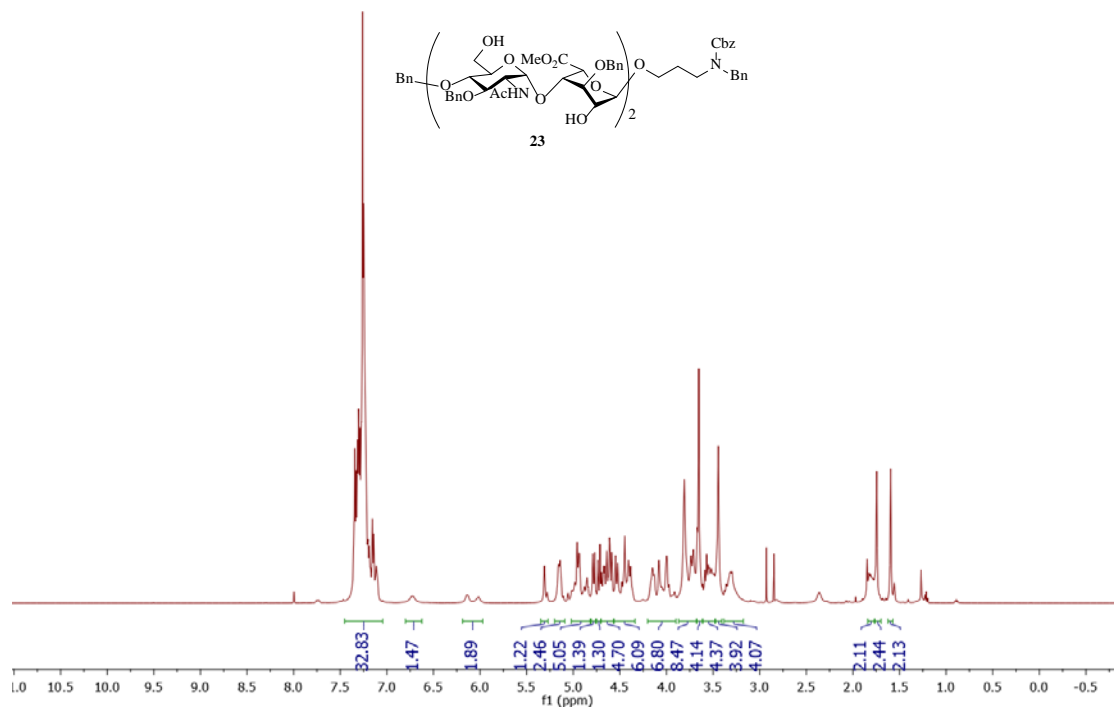
Figure 4.69. ^{1}H-NMR of **23** (500 MHz CDCl$_3$)
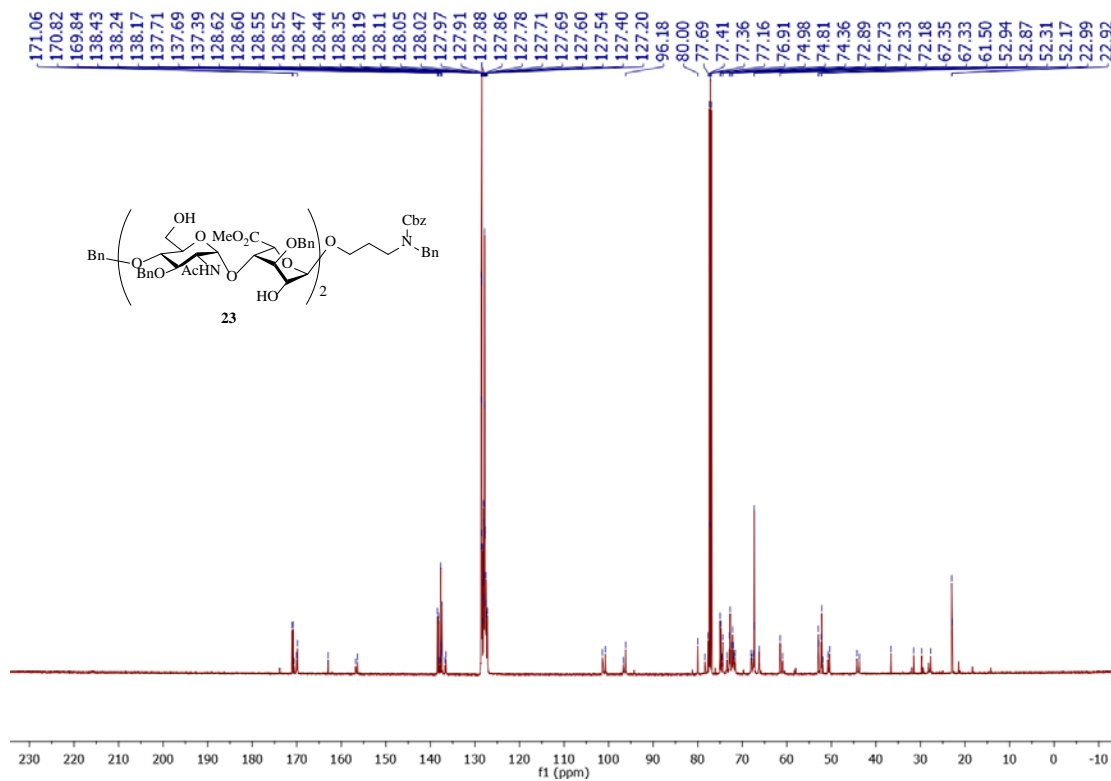
Figure 4.70. ^{13}C-NMR of **23** (125 MHz CDCl$_3$)

Figure 4.71. ^{1}H-NMR of **24** (500 MHz CDCl$_3$)

Figure 4.72. ^{13}C-NMR of **24** (125 MHz CDCl$_3$)

Figure 4.73. ^{1}H-NMR of **25** (500 MHz CD$_3$OD)
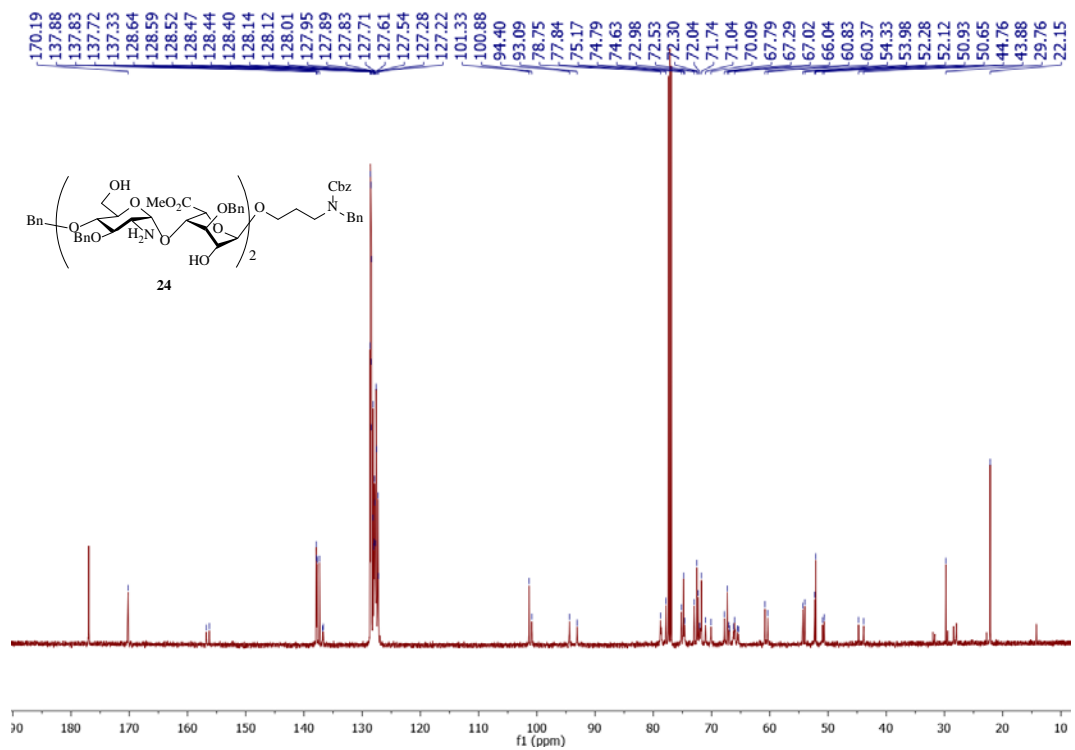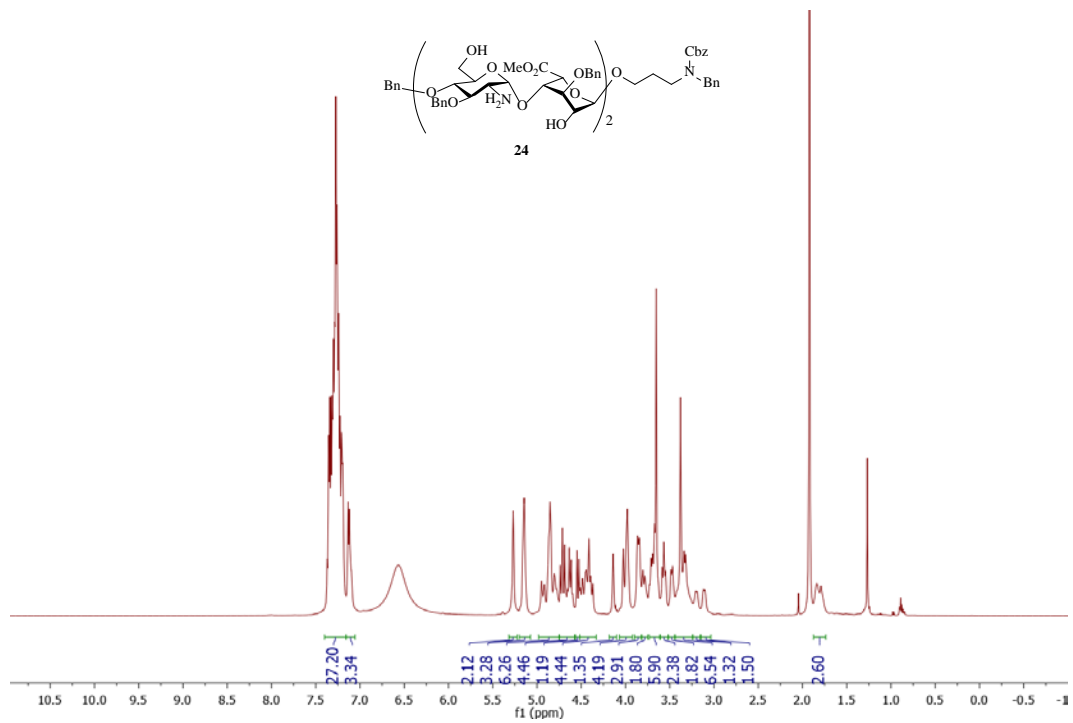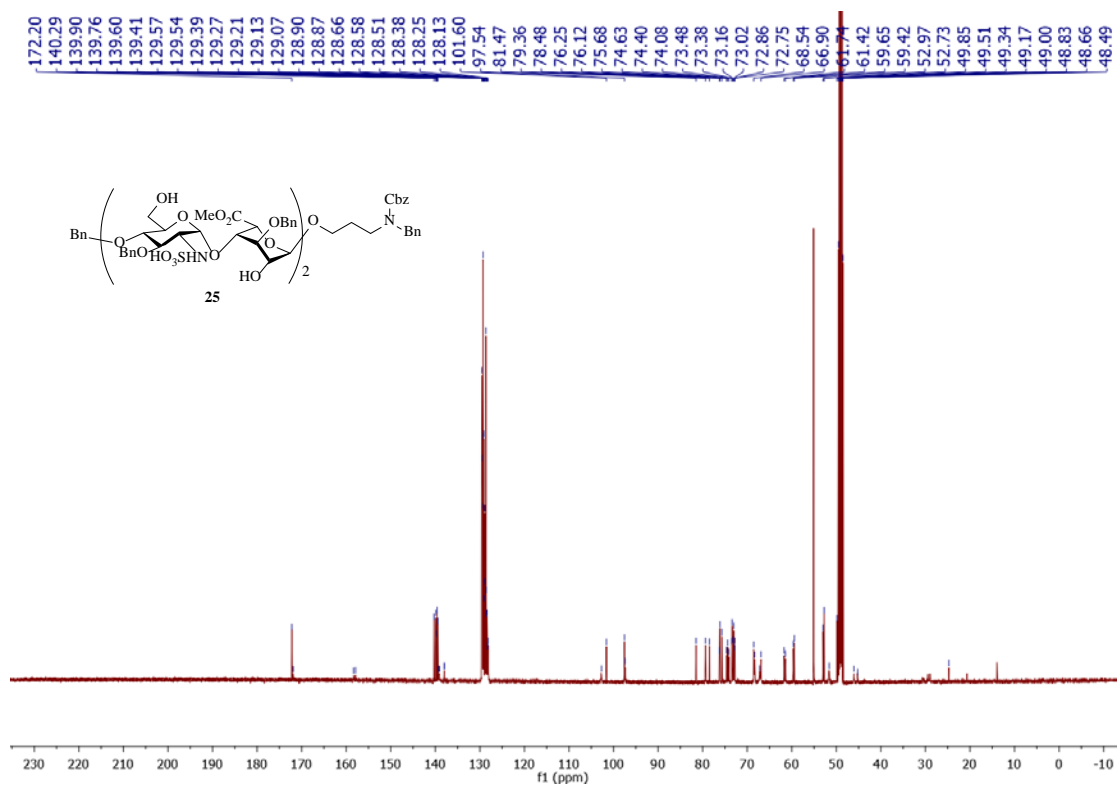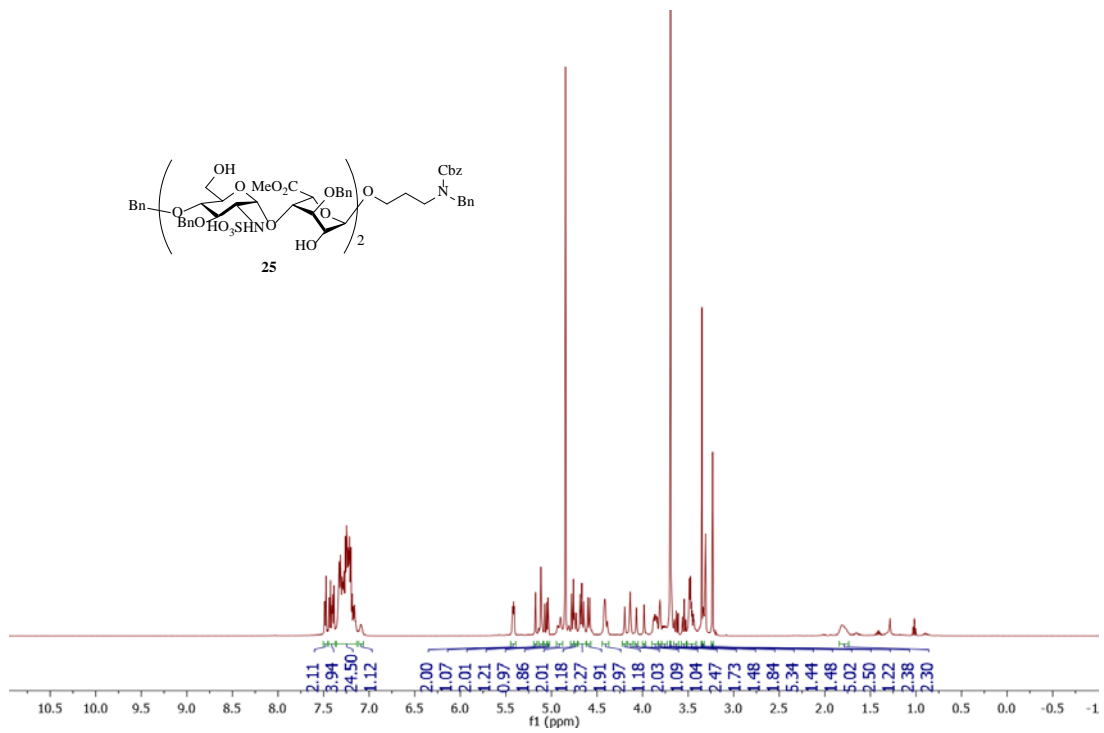
Figure 4.74. ^{13}C-NMR of **25** (125 MHz CD$_3$OD)
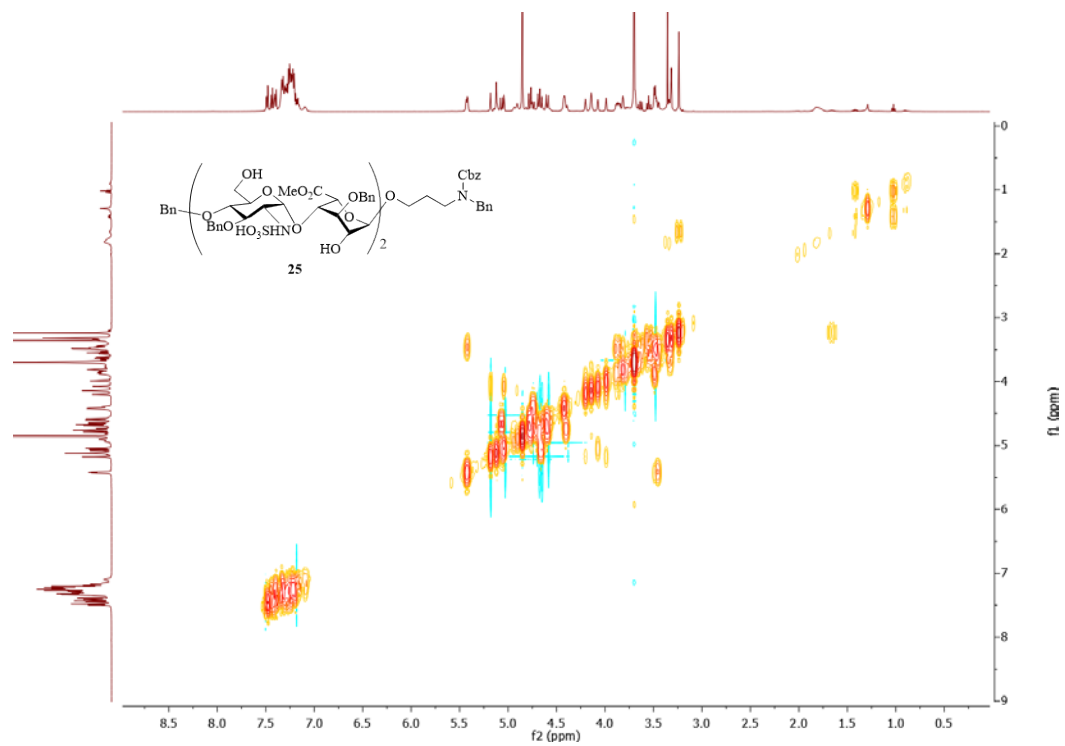
Figure 4.75. ^{1}H-^{1}H gCOSY of **25** (500 MHz CD$_3$OD)
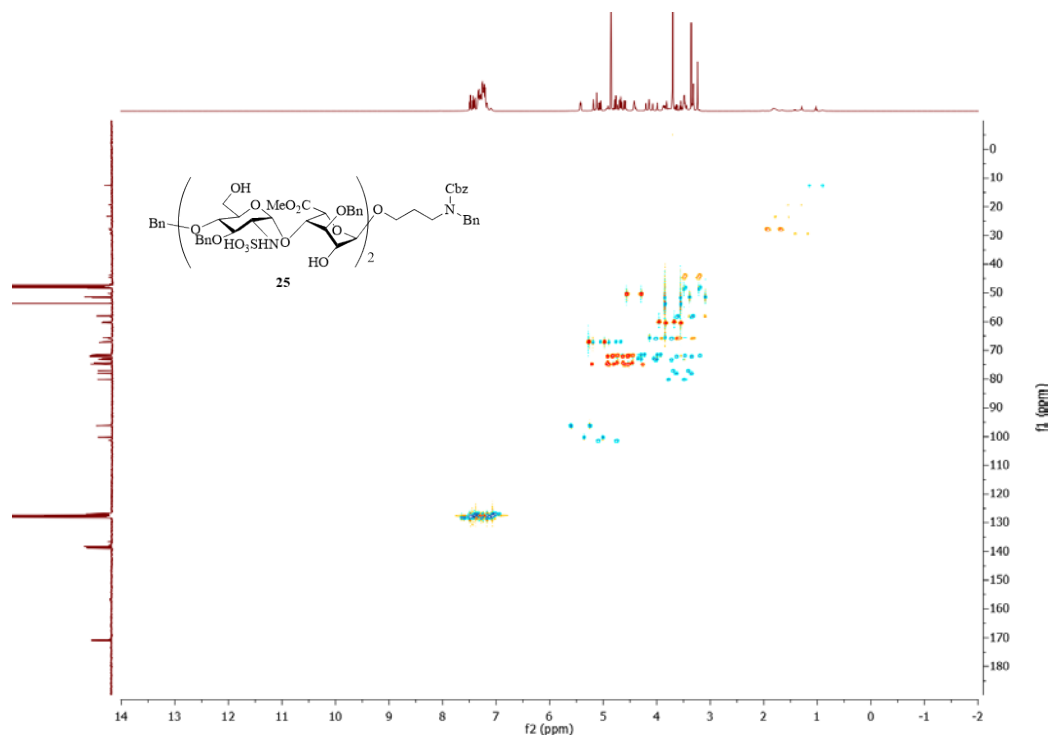
Figure 4.76. ^{1}H-^{13}C gHSQCAD of **25** (500 MHz CD$_3$OD)
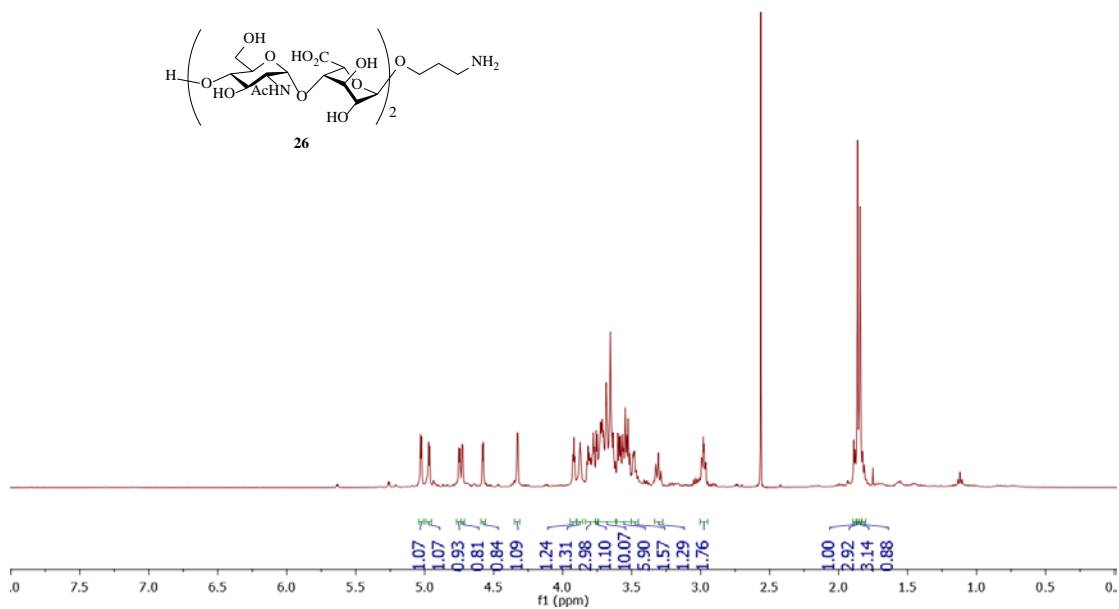
Figure 4.77. ^{1}H-NMR of **26** (500 MHz D$_2$O)
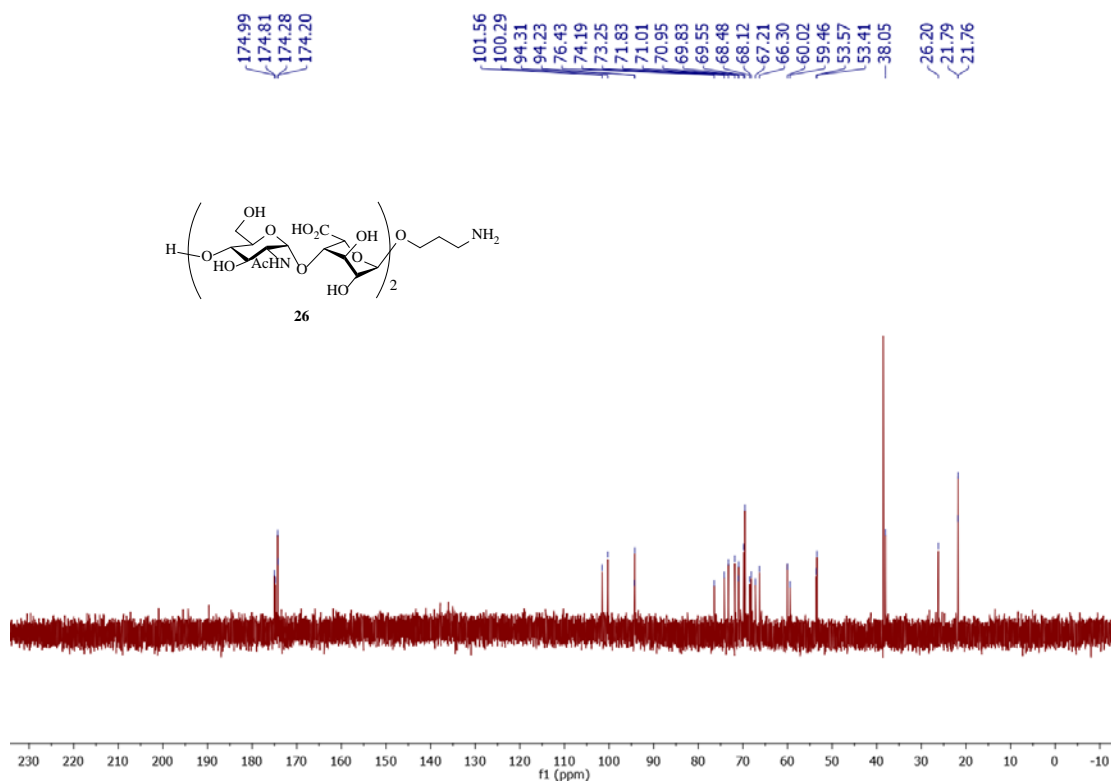
Figure 4.78. ^{13}C-NMR of **26** (125 MHz D$_2$O)
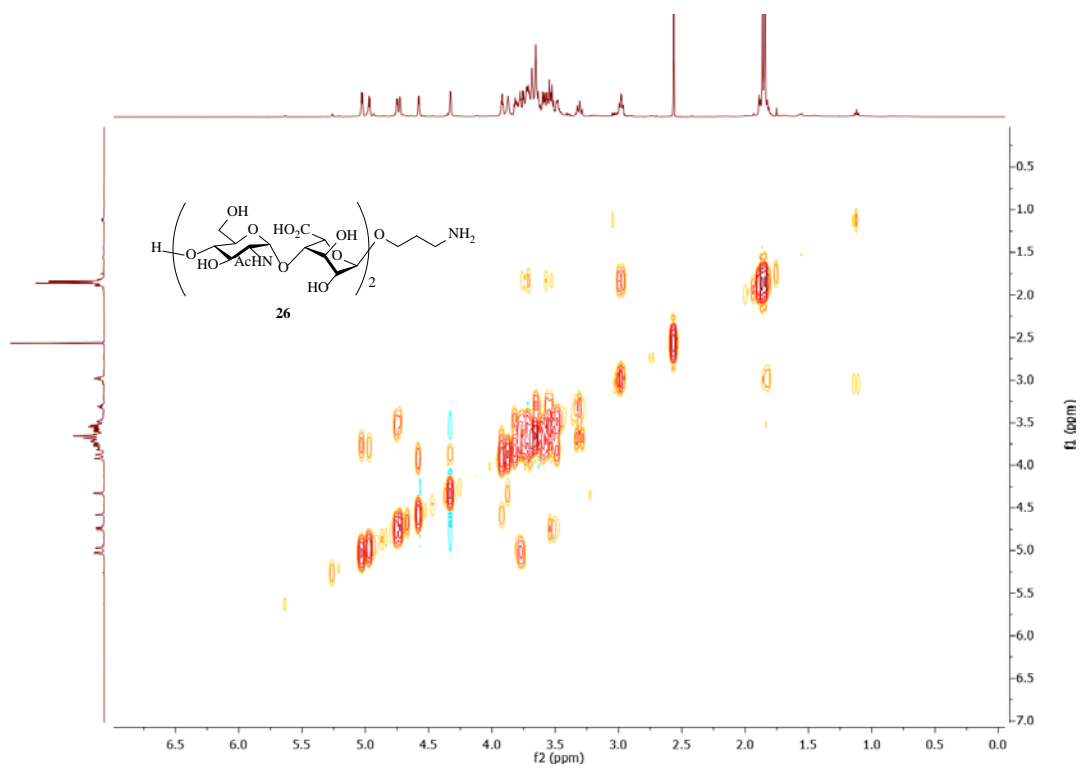
Figure 4.79. ^{1}H-^{1}H gCOSY of **26** (500 MHz D$_2$O)
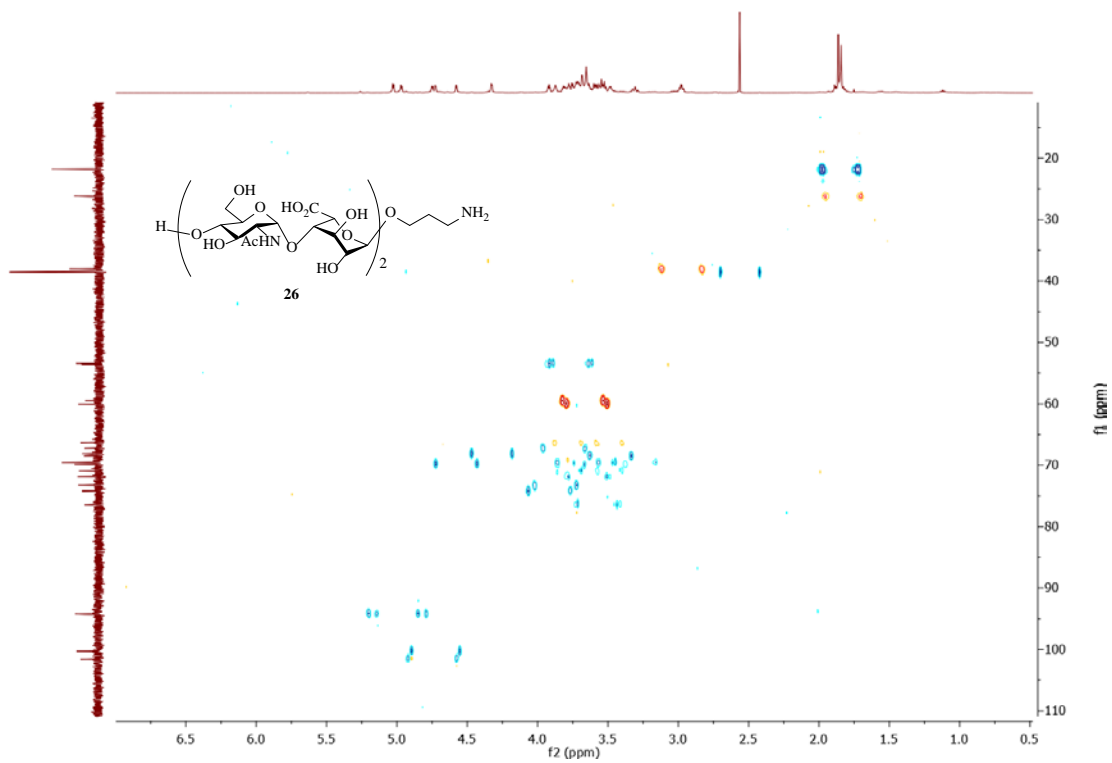
Figure 4.80. ^{1}H-^{13}C gHSQCAD of **26** (500 MHz D$_2$O)
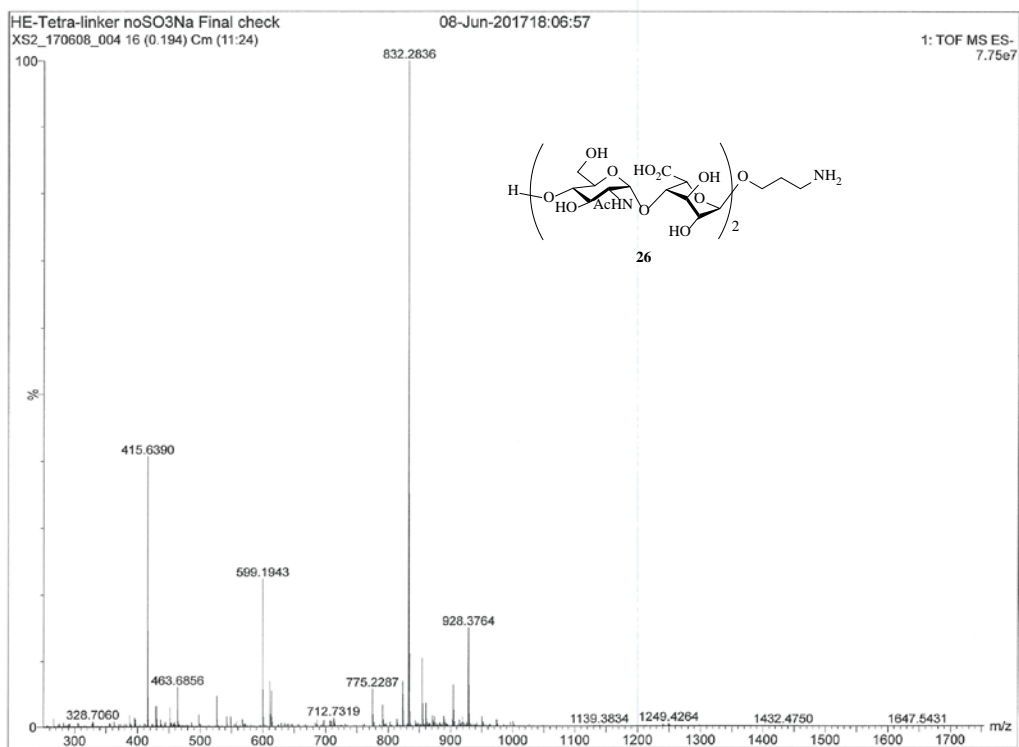
Figure 4.81. ESI-MS of **26**
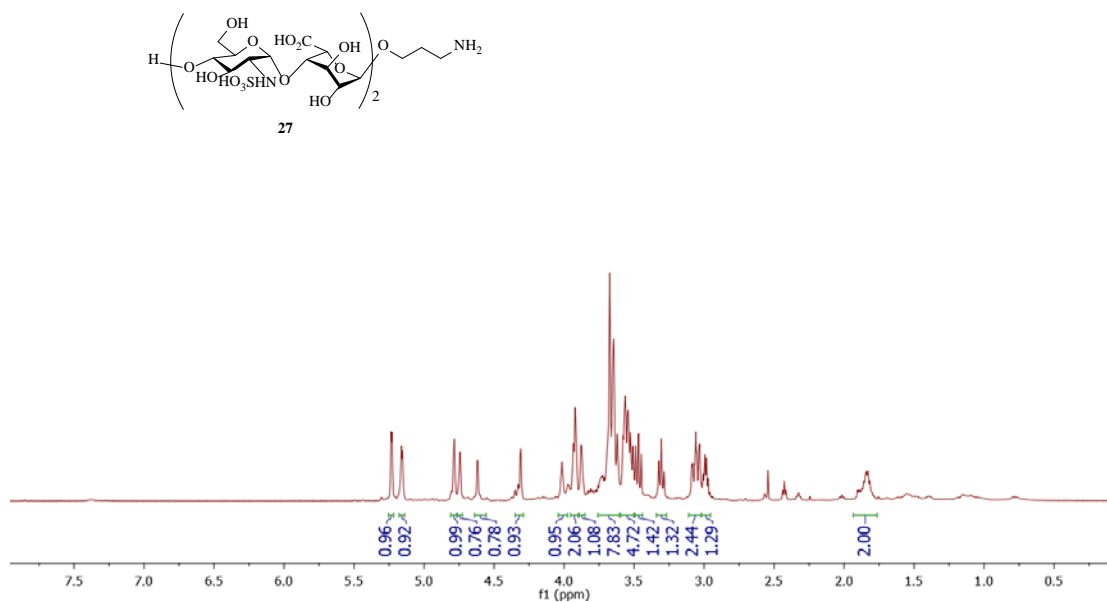
Figure 4.82. ^{1}H-NMR of **27** (500 MHz D$_2$O)
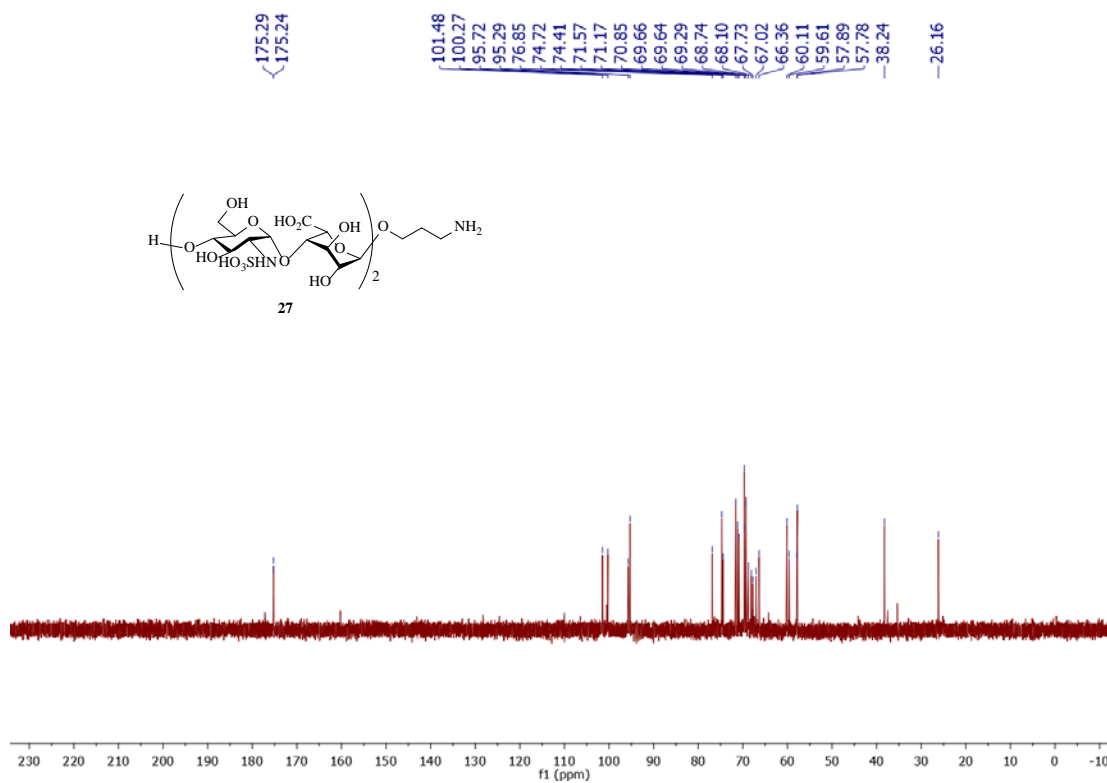
Figure 4.83. ^{13}C-NMR of **27** (125 MHz D$_2$O)
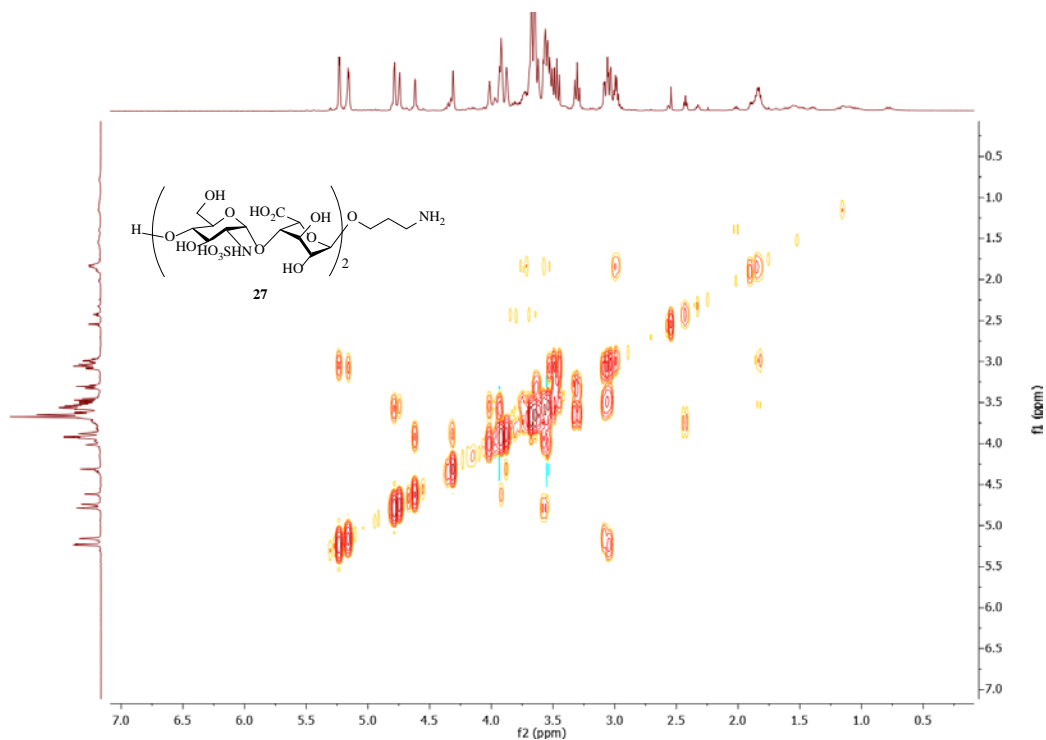
Figure 4.84. ^{1}H-^{1}H gCOSY of **27** (500 MHz D$_2$O)
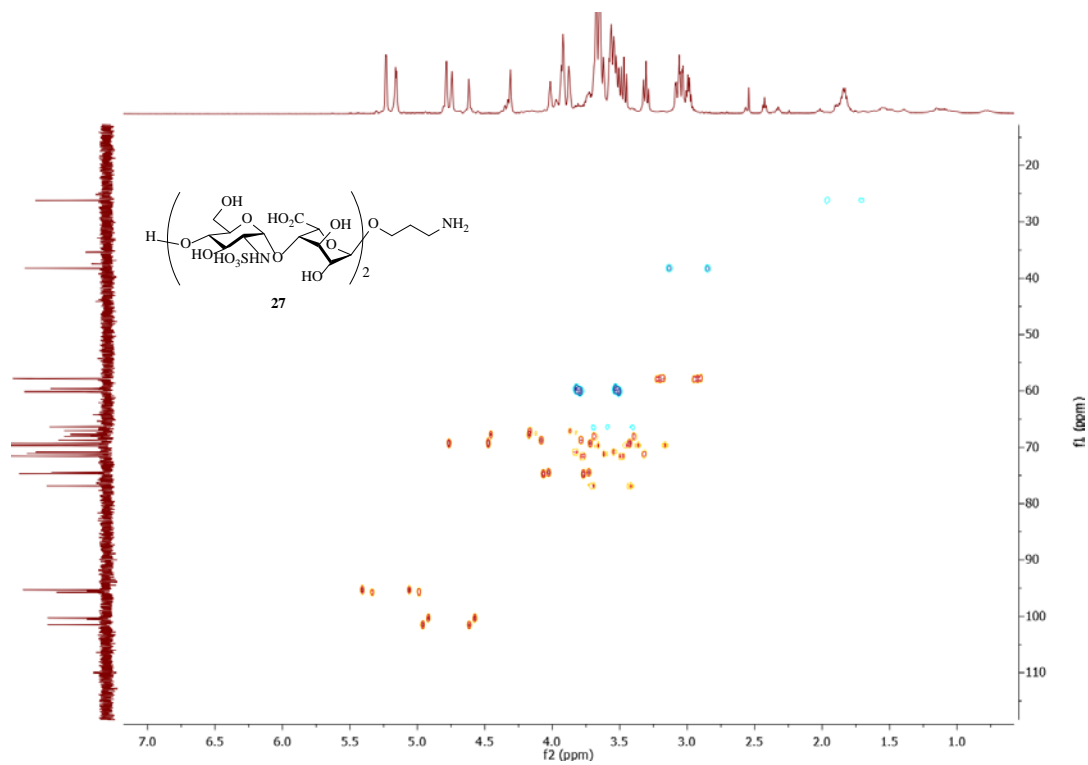
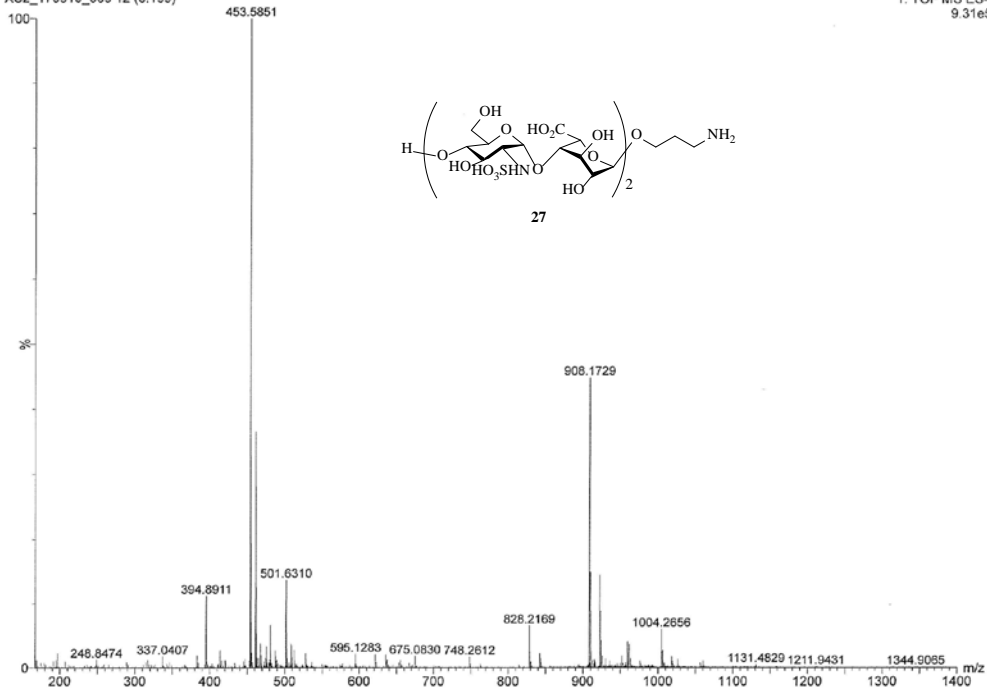**Figure 4.85.** ^{1}H-^{13}C gHSQCAD of **27** (500 MHz D$_2$O)

Figure 4.86. ESI-MS of **27**
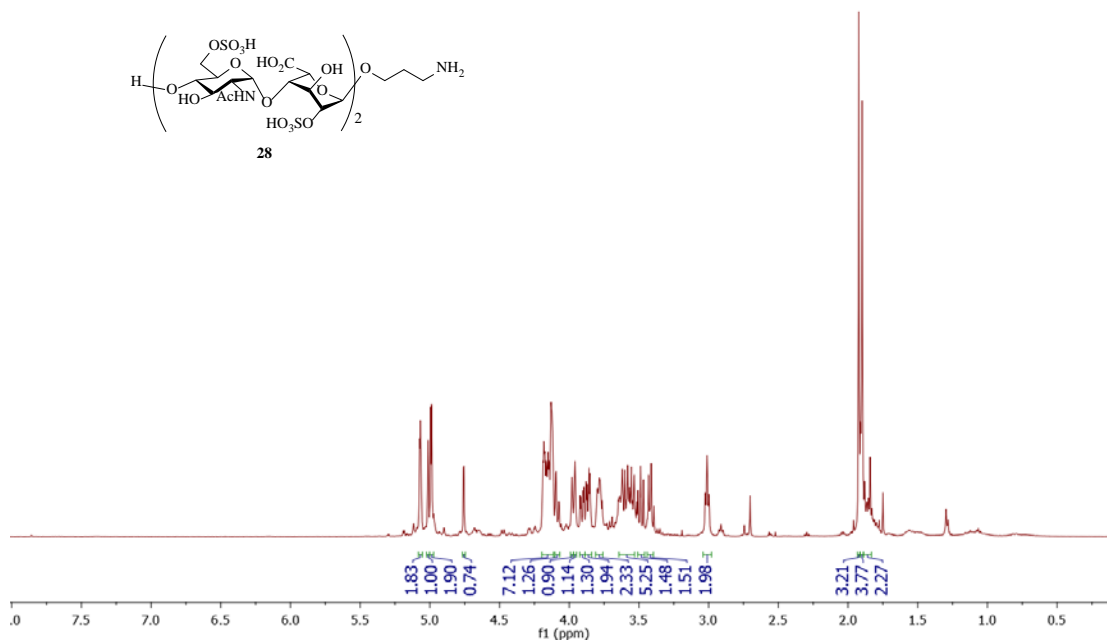
Figure 4.87. ^{1}H-NMR of **28** (500 MHz D$_2$O)
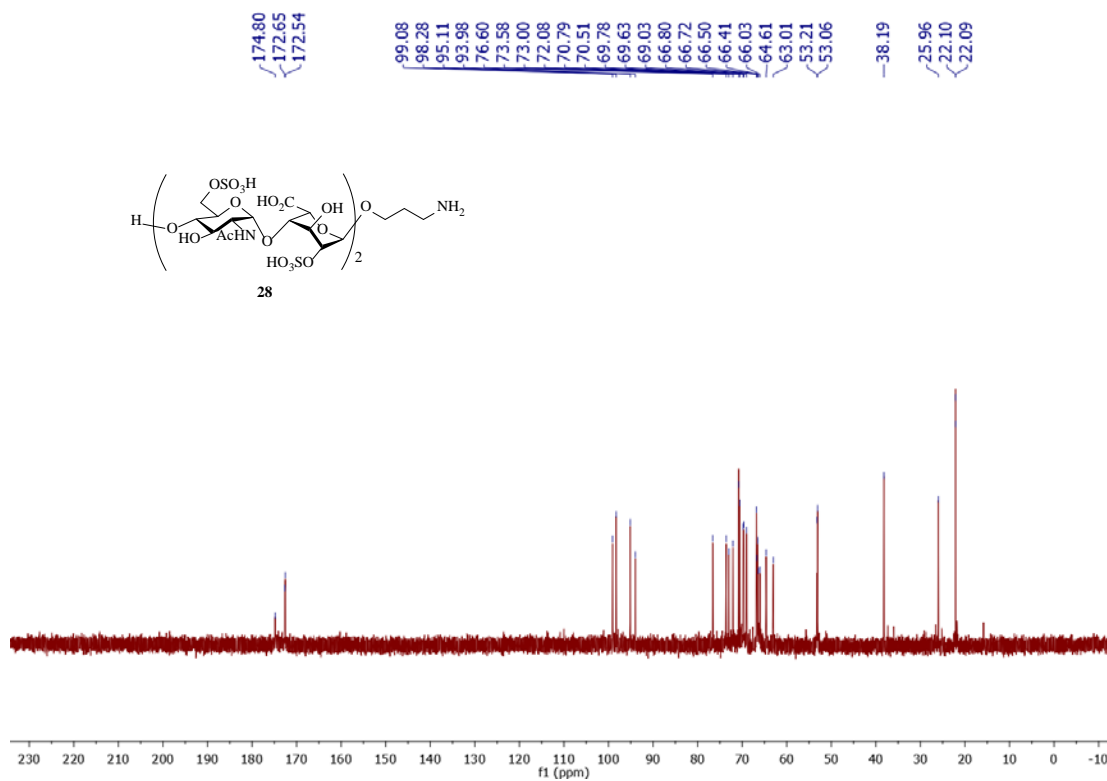
Figure 4.88. ^{13}C-NMR of **28** (125 MHz D$_2$O)
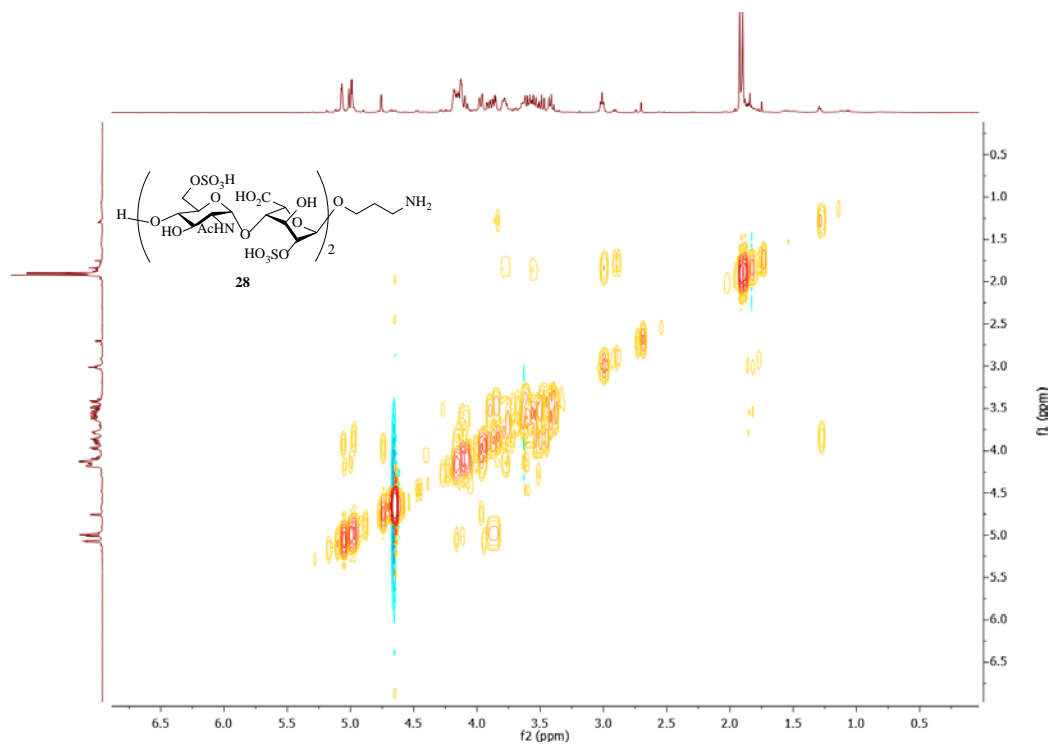
Figure 4.89. ^{1}H-^{1}H gCOSY of **28** (500 MHz D$_2$O)
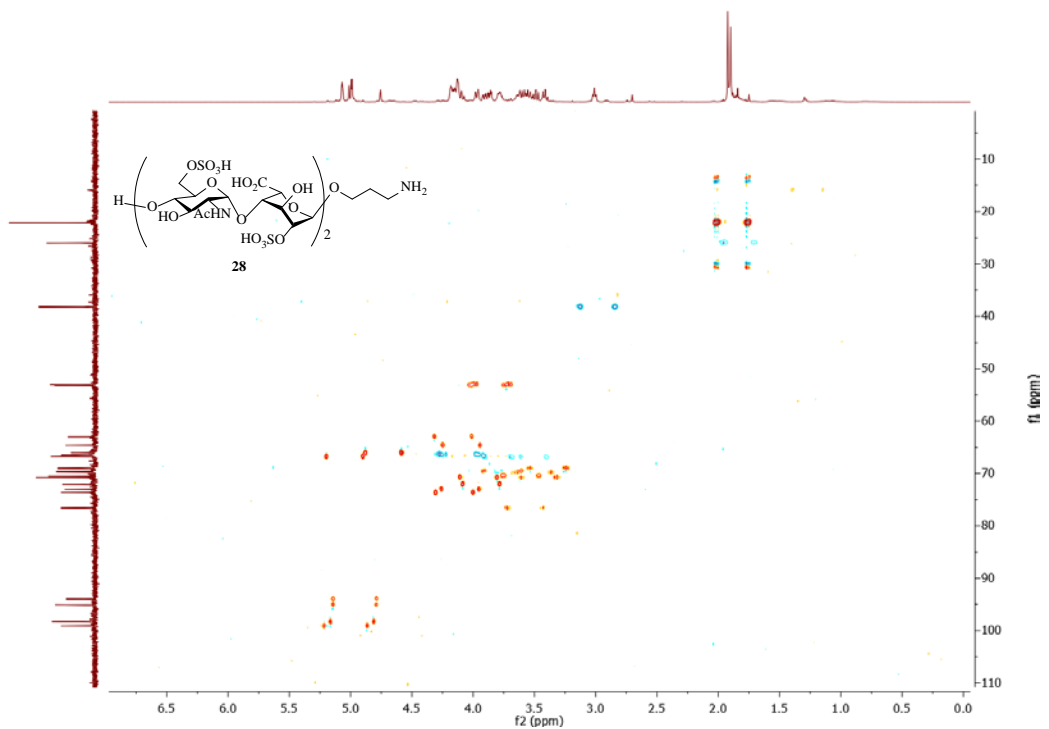
Figure 4.90. ^{1}H-^{13}C gHSQCAD of **28** (500 MHz D$_2$O)

Figure 4.91. ESI-MS of **28**

Figure 4.92. ^{1}H-NMR of **29** (500 MHz D$_2$O)
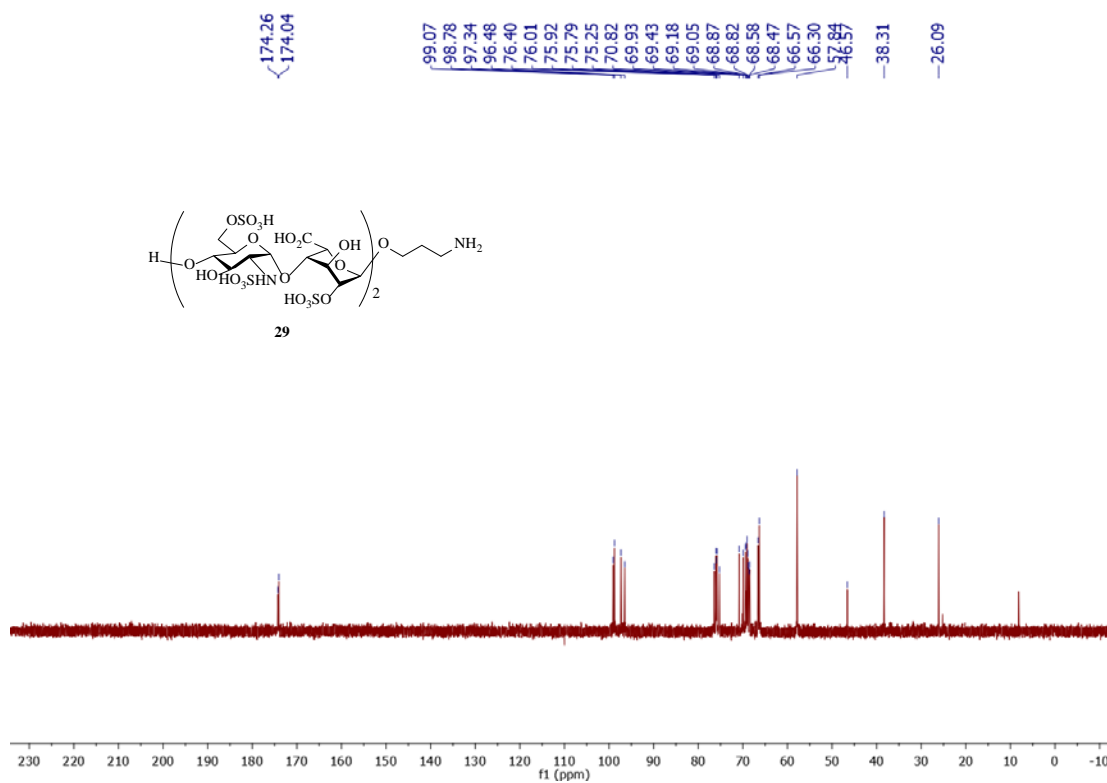
Figure 4.93. ^{13}C-NMR of **29** (125 MHz D$_2$O)

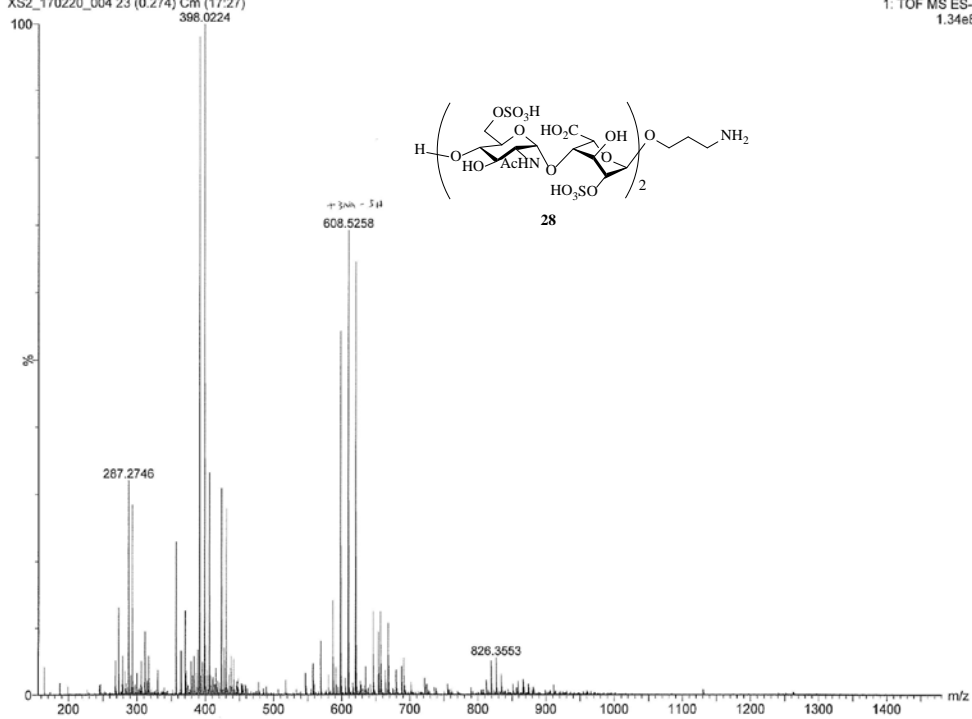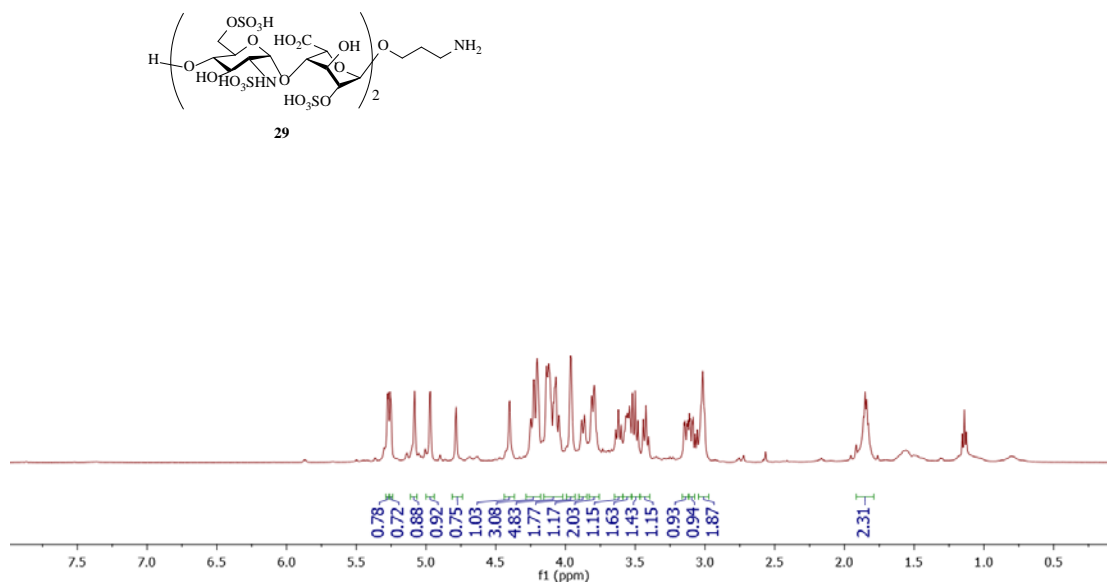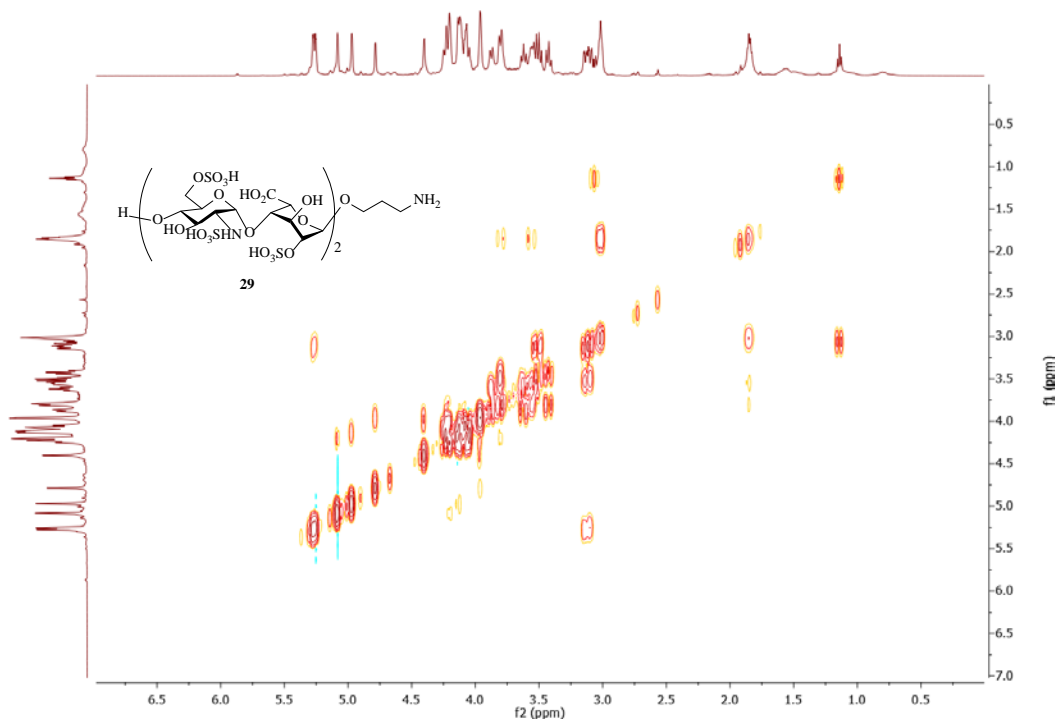**Figure 4.94.** ^{1}H-^{1}H gCOSY of **29** (500 MHz D$_2$O)

Figure 4.95. ^{1}H-^{13}C gHSQCAD of **29** (500 MHz D$_2$O)

Figure 4.96. ESI-MS of **29**

Figure 4.97. ^{1}H-NMR of **30** (500 MHz CDCl$_3$)
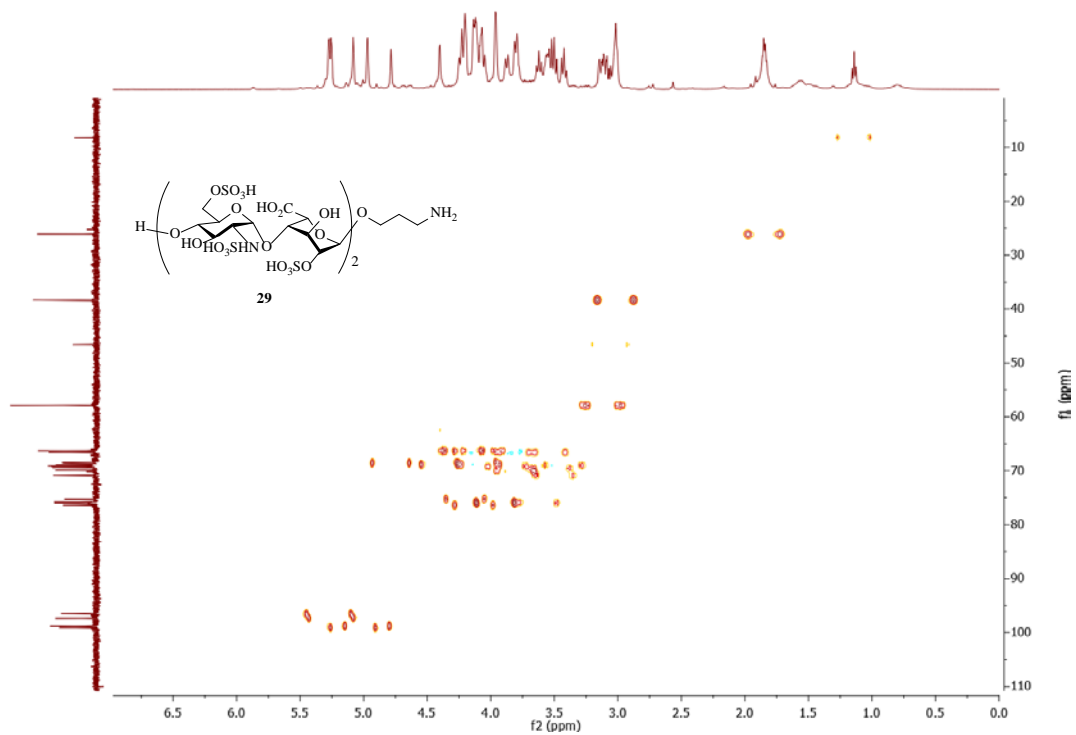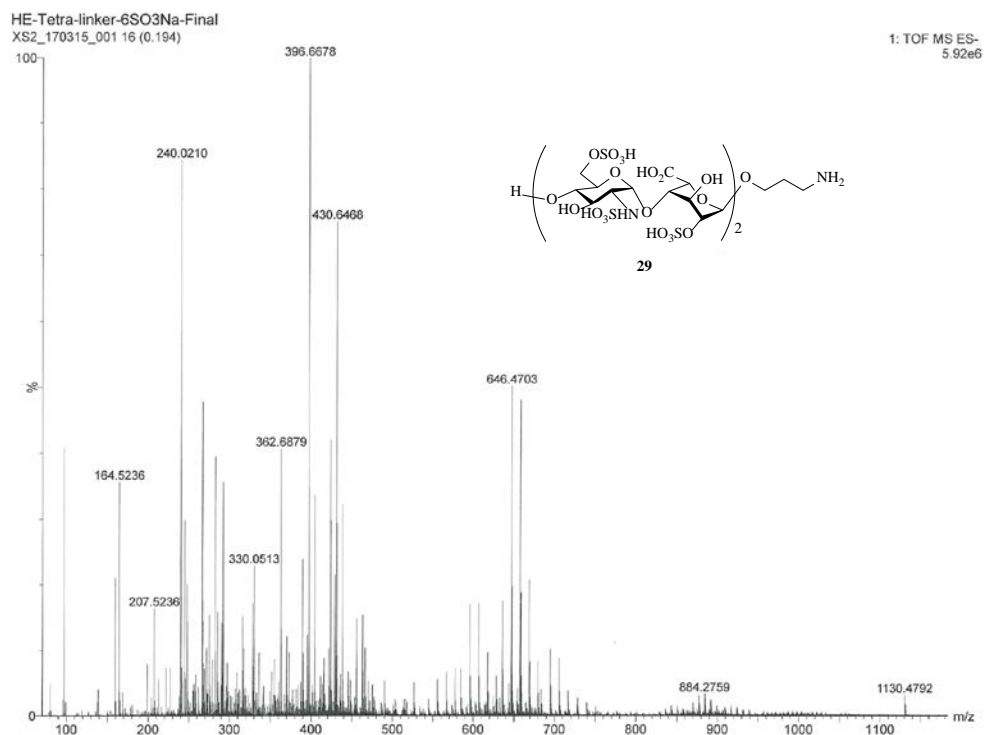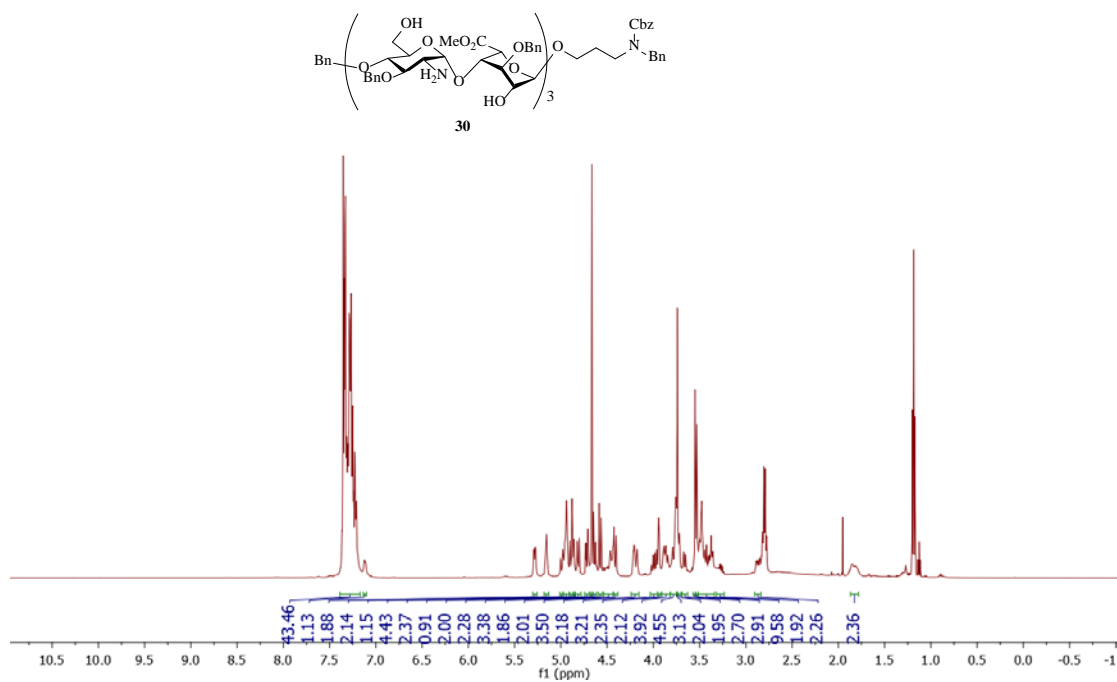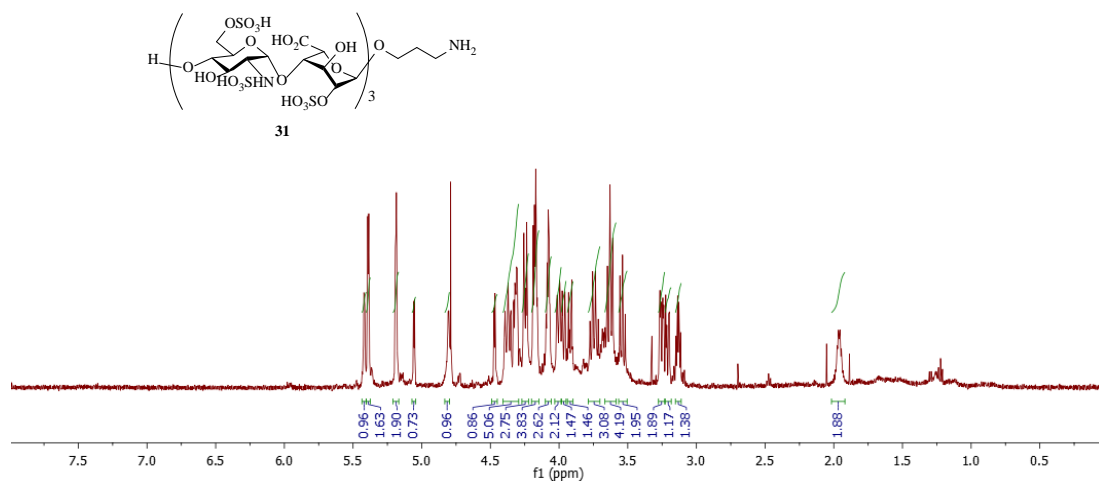

Figure 4.98. ^{1}H-NMR of **31** (500 MHz D$_2$O)
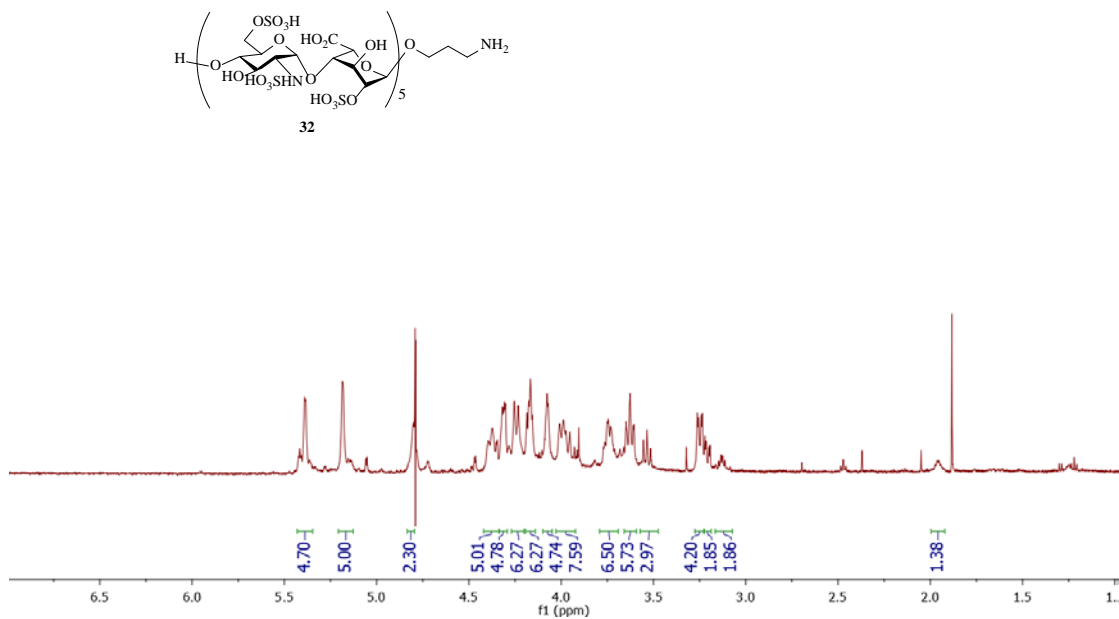
Figure 4.99. ^{1}H-NMR of **32** (500 MHz D$_2$O)

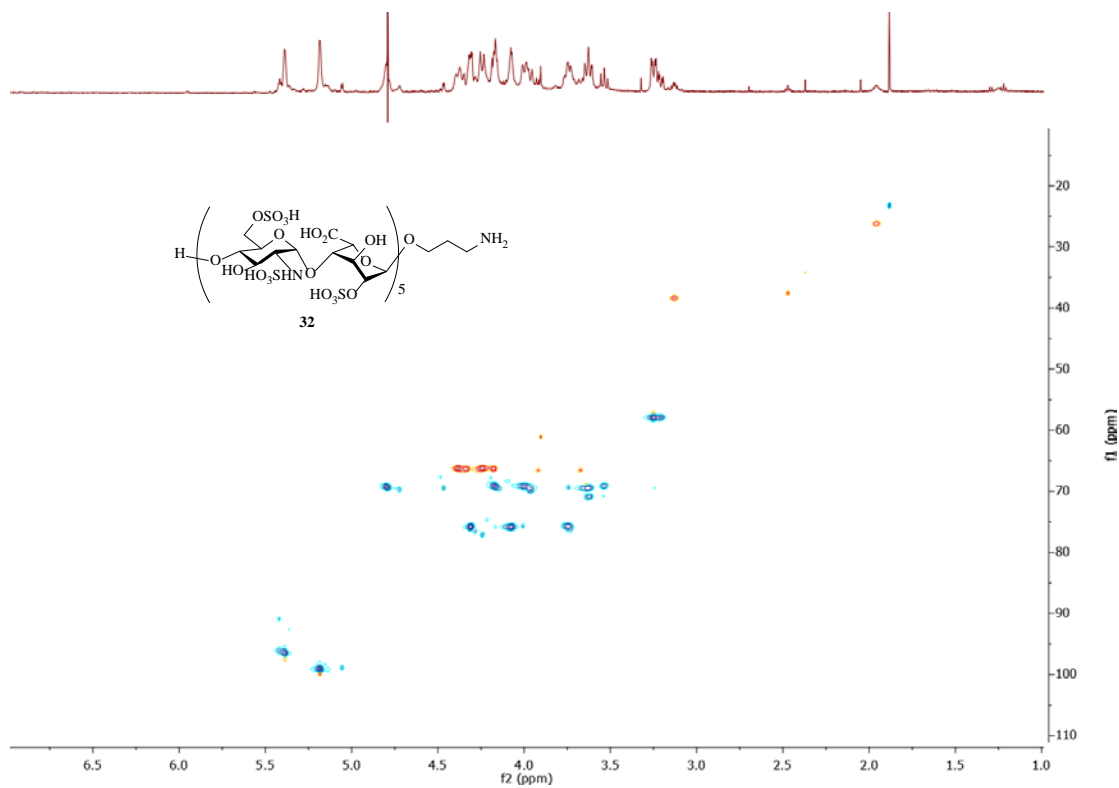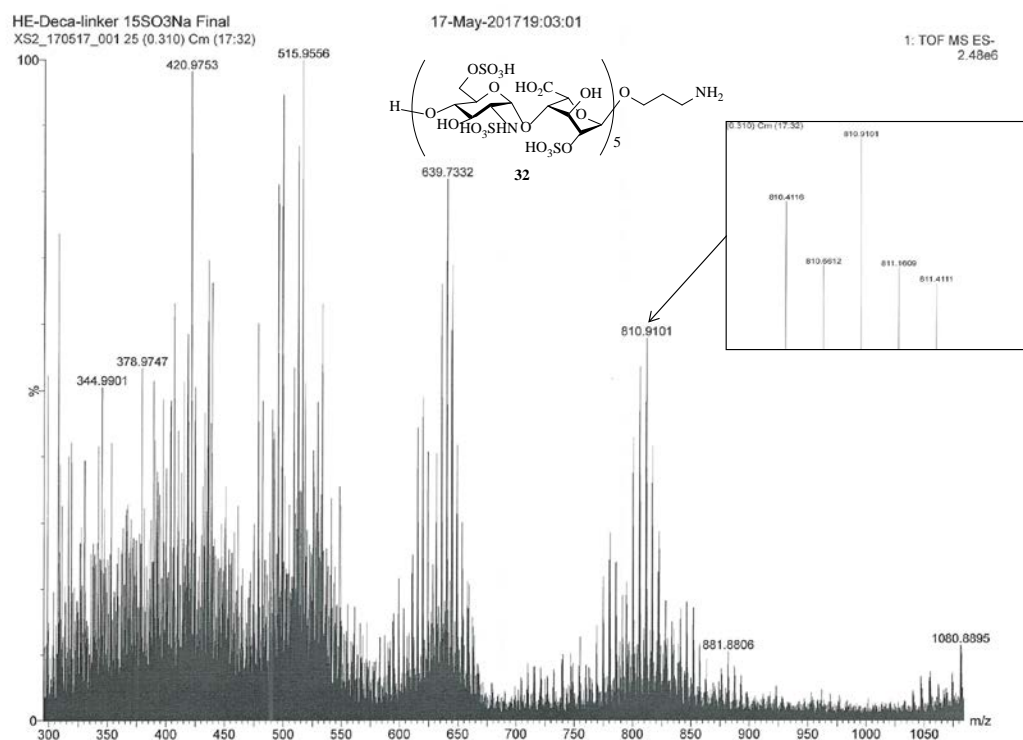**Figure 4.100.** ^{1}H-^{13}C gHSQCAD of **32** (900 MHz D$_2$O)

Figure 4.101. ESI-MS of **32**

REFERENCES

REFERENCES

1. "2017 Alzheimer's Disease facts and figures,". *https://www.alz.org/documents_custom/2017-facts-and-figures.pdf* **2017**.

2. Šimić, G.; Babić Leko, M.; Wray, S.; Harrington, C.; Delalle, I.; Jovanov-Milošević, N.; Bažadona, D.; Buée, L.; De Silva, R.; Di Giovanni, G., Tau protein hyperphosphorylation and aggregation in Alzheimer's disease and other tauopathies, and possible neuroprotective strategies. *Biomolecules* **2016,** *6* (1), 6.

3. Arriagada, P. V.; Growdon, J. H.; Hedley-Whyte, E. T.; Hyman, B. T., Neurofibrillary tangles but not senile plaques parallel duration and severity of Alzheimer's disease. *Neurology* **1992,** *42* (3), 631-631.

4. Haroutunian, V.; Davies, P.; Vianna, C.; Buxbaum, J.; Purohit, D., Tau protein abnormalities associated with the progression of alzheimer disease type dementia. *Neurobiol. Aging* **2007,** *28* (1), 1-7.

5. Kim, Y.; Choi, H.; Lee, W.; Park, H.; Kam, T.-I.; Hong, S.-h.; Nah, J.; Jung, S.; Shin, B.; Lee, H., Caspase-cleaved tau exhibits rapid memory impairment associated with tau oligomers in a transgenic mouse model. *Neurobiol. Dis.* **2016,** *87*, 19-28.

6. Cook, C.; Kang, S. S.; Carlomagno, Y.; Lin, W.-L.; Yue, M.; Kurti, A.; Shinohara, M.; Jansen-West, K.; Perkerson, E.; Castanedes-Casey, M., Tau deposition drives neuropathological, inflammatory and behavioral abnormalities independently of neuronal loss in a novel mouse model. *Hum. Mol. Genet.* **2015,** *24* (21), 6198-6212.

7. Cowan, C. M.; Quraishe, S.; Mudher, A., What is the pathological significance of tau oligomers? Portland Press Limited: 2012.

8. Gerson, J. E.; Mudher, A.; Kayed, R., Potential mechanisms and implications for the formation of tau oligomeric strains. *Crit. Rev. Biochem. Mol. Biol.* **2016,** *51* (6), 482-496.

9. Guerrero-Muñoz, M. J.; Gerson, J.; Castillo-Carranza, D. L., Tau oligomers: the toxic player at synapses in Alzheimer's disease. *Front. Cell. Neurosci.* **2015,** *9*, 464.

10. Kopeikina, K. J.; Carlson, G. A.; Pitstick, R.; Ludvigson, A. E.; Peters, A.; Luebke, J. I.; Koffie, R. M.; Frosch, M. P.; Hyman, B. T.; Spires-Jones, T. L., Tau accumulation causes mitochondrial distribution deficits in neurons in a mouse model of tauopathy and in human Alzheimer's disease brain. *Am. J. Pathol.* **2011,** *179* (4), 2071-2082.

11. Lasagna-Reeves, C. A.; Castillo-Carranza, D. L.; Sengupta, U.; Sarmiento, J.; Troncoso, J.; Jackson, G. R.; Kayed, R., Identification of oligomers at early stages of tau aggregation in

Alzheimer's disease. *FASEB J.* **2012,** *26* (5), 1946-1959.

12. Lasagna-Reeves, C. A.; Castillo-Carranza, D. L.; Sengupta, U.; Guerrero-Munoz, M. J.; Kiritoshi, T.; Neugebauer, V.; Jackson, G. R.; Kayed, R., Alzheimer brain-derived tau oligomers propagate pathology from endogenous tau. *Sci. Rep.* **2012,** *2*, 700.

13. Castillo-Carranza, D. L.; Gerson, J. E.; Sengupta, U.; Guerrero-Muñoz, M. J.; Lasagna-Reeves, C. A.; Kayed, R., Specific targeting of tau oligomers in Htau mice prevents cognitive impairment and tau toxicity following injection with brain-derived tau oligomeric seeds. *J. Alzheimer's Dis.* **2014,** *40* (s1), S97-S111.

14. Fá, M.; Puzzo, D.; Piacentini, R.; Staniszewski, A.; Zhang, H.; Baltrons, M. A.; Puma, D. L.; Chatterjee, I.; Li, J.; Saeed, F., Extracellular tau oligomers produce an immediate impairment of LTP and memory. *Sci. Rep.* **2016,** *6*, 19393.

15. Castillo-Carranza, D. L.; Sengupta, U.; Guerrero-Muñoz, M. J.; Lasagna-Reeves, C. A.; Gerson, J. E.; Singh, G.; Estes, D. M.; Barrett, A. D.; Dineley, K. T.; Jackson, G. R., Passive immunization with Tau oligomer monoclonal antibody reverses tauopathy phenotypes without affecting hyperphosphorylated neurofibrillary tangles. *J. Neurosci.* **2014,** *34* (12), 4260-4272.

16. Sarrazin, S.; Lamanna, W. C.; Esko, J. D., Heparan sulfate proteoglycans. *Cold Spring Harb. Perspect. Biol.* **2011,** *3* (7), a004952.

17. Capila, I.; Linhardt, R. J., Heparin–protein interactions. *Angew. Chem. Int. Ed.* **2002,** *41* (3), 390-412.

18. Linhardt, R. J.; Dordick, J. S.; Deangelis, P. L.; Liu, J. Enzymatic synthesis of glycosaminoglycan heparin. Semin. Thromb. Hemost. **2007**, *33* (5), 453-465.

19. Dulaney, S. B.; Huang, X., Strategies in synthesis of heparin/heparan sulfate oligosaccharides: 2000–present. *Adv. Carbohydr. Chem. Biochem.* **2012**, *67*, 95-136.

20. Zhu, H.-L.; Fernández, C.; Fan, J.-B.; Shewmaker, F.; Chen, J.; Minton, A. P.; Liang, Y., Quantitative characterization of heparin binding to tau protein implication for inducer-mediated tau filament formation. *J. Biol. Chem.* **2010,** *285* (6), 3592-3599.

21. Holmes, B. B.; DeVos, S. L.; Kfoury, N.; Li, M.; Jacks, R.; Yanamandra, K.; Ouidja, M. O.; Brodsky, F. M.; Marasa, J.; Bagchi, D. P., Heparan sulfate proteoglycans mediate internalization and propagation of specific proteopathic seeds. *Proc. Natl. Acad. Sci., U. S. A.* **2013,** *110* (33), E3138-E3147.

22. Sibille, N.; Sillen, A.; Leroy, A.; Wieruszeski, J.-M.; Mulloy, B.; Landrieu, I.; Lippens, G., Structural impact of heparin binding to full-length Tau as studied by NMR spectroscopy. *Biochemistry* **2006,** *45* (41), 12560-12572.

23. Jangholi, A.; Ashrafi-Kooshk, M. R.; Arab, S. S.; Riazi, G.; Mokhtari, F.; Poorebrahim, M.; Mahdiuni, H.; Kurganov, B. I.; Moosavi-Movahedi, A. A.; Khodarahmi, R., Appraisal of role of the polyanionic inducer length on amyloid formation by 412-residue 1N4R Tau protein: a comparative study. *Arch. Biochem. Biophys.* **2016,** *609*, 1-19.

24. Zhao, J.; Huvent, I.; Lippens, G.; Eliezer, D.; Zhang, A.; Li, Q.; Tessier, P.; Linhardt, R. J.; Zhang, F.; Wang, C., Glycan Determinants of Heparin-Tau Interaction. *Biophys. J.* **2017,** *112* (5), 921-932.

25. Dulaney, S. B.; Xu, Y.; Wang, P.; Tiruchinapally, G.; Wang, Z.; Kathawa, J.; El-Dakdouki, M. H.; Yang, B.; Liu, J.; Huang, X., Divergent synthesis of heparan sulfate oligosaccharides. *J. Org. Chem.* **2015,** *80* (24), 12265-12279.

26. Huang, X.; Huang, L.; Wang, H.; Ye, X. S., Iterative one-pot synthesis of oligosaccharides. *Angew. Chem.Int. Ed.* **2004,** *116* (39), 5333-5336.

27. van den Bos, L. J.; Codée, J. D. C.; van der Toorn, J. C.; Boltje, T. J.; van Boom, J. H.; Overkleeft, H. S.; van der Marel, G. A., Thioglycuronides: synthesis and application in the assembly of acidic oligosaccharides. *Org. Lett.* **2004,** *6* (13), 2165-2168.

28. Lasagna-Reeves, C. A.; Castillo-Carranza, D. L.; Guerrero-Muñoz, M. J.; Jackson, G. R.; Kayed, R., Preparation and characterization of neurotoxic tau oligomers. *Biochemistry* **2010,** *49* (47), 10039-10041.

29. Margittai, M.; Langen, R., Template-assisted filament growth by parallel stacking of tau. *Proc. Natl. Acad. Sci., U. S. A.* **2004,** *101* (28), 10278-10283.

30. Margittai, M.; Langen, R., Side chain-dependent stacking modulates tau filament structure. *J. Biol. Chem.* **2006,** *281* (49), 37820-37827.

31. Hernaiz, M.; Liu, J.; Rosenberg, R. D.; Linhardt, R. J., Enzymatic modification of heparan sulfate on a biochip promotes its interaction with antithrombin III. *Biochem. Biophys. Res. Commun.* **2000,** *276* (1), 292-297.

32. Kayed, R.; Head, E.; Thompson, J. L.; McIntire, T. M.; Milton, S. C.; Cotman, C. W.; Glabe, C. G., Common structure of soluble amyloid oligomers implies common mechanism of pathogenesis. *Science* **2003,** *300* (5618), 486-489.